AD A118888

REPORT DOCUMENTATION PAGE

READ INSTRUCTIONS BEFORE COMPLETING FORM

1. REPORT NUMBER: AFOSR-TR- 82-0656	2. GOVT ACCESSION NO.: AD-A118888
3. RECIPIENT'S CATALOG NUMBER:	
4. TITLE (and Subtitle): PROCEEDINGS OF THE AFOSR SPECIAL CONFERENCE ON PRIME-POWER FOR HIGH ENERGY SPACE SYSTEMS VOLUME II	5. TYPE OF REPORT & PERIOD COVERED: FINAL
	6. PERFORMING ORG. REPORT NUMBER:
7. AUTHOR(s): P.J. TURCHI	8. CONTRACT OR GRANT NUMBER(s): F49620-82-C-0008
9. PERFORMING ORGANIZATION NAME AND ADDRESS: Research & Development Associates (RDA) Rosslyn, VA 22209	10. PROGRAM ELEMENT, PROJECT, TASK AREA & WORK UNIT NUMBERS: 61102F 2301/A7
11. CONTROLLING OFFICE NAME AND ADDRESS: AFOSR/NP BOLLING AFB, DC 20332	12. REPORT DATE: 22-25 February 1982
	13. NUMBER OF PAGES: 806
14. MONITORING AGENCY NAME & ADDRESS(if different from Controlling Office)	15. SECURITY CLASS. (of this report): UNCLASSIFIED
	15a. DECLASSIFICATION/DOWNGRADING SCHEDULE

16. DISTRIBUTION STATEMENT (of this Report)

APPROVED FOR PUBLIC RELEASE; DISTRIBUTION UNLIMITED.

17. DISTRIBUTION STATEMENT (of the abstract entered in Block 20, if different from Report)

DTIC ELECTE SEP 1 1982 S H D

18. SUPPLEMENTARY NOTES

19. KEY WORDS (Continue on reverse side if necessary and identify by block number)

20. ABSTRACT (Continue on reverse side if necessary and identify by block number)

(see next page)

DTIC FILE COPY

As part of an assessment of research needs in the space prime-power area, a special conference was convened at the Omni International Hotel in Norfolk, VA, 22-25 February 1982. The intent of the Conference was to review the state-of-the-art of space prime-power technology, including new or advanced concepts, and to discuss research needed for progress toward megawatt power levels. The Conference was attended by over 190 scientists and engineers from universities, government, and private organizations. Over eighty papers were presented, including discussions of chemical, nuclear and radiant energy techniques, power conversion, heat rejection, materials, chemical and fluid physics, and also reviews of power requirements for future NASA and DoD systems.

The Special Conference on Prime-Power for High-Energy Space Systems provided a useful opportunity for research scientists and technologists to educate each other on problems and progress in space prime-power. Although the AFOSR interest is basic research, the Conference also served as a forum for description of systems, concepts, and programs with particular mission requirements, and for discussion of research in support of specific devices or needs. The proceedings of the Conference, (consisting of over 1700 pages of text and view graph copies), were compiled and distributed to Conference attendees.

PROCEEDINGS
OF THE
AFOSR SPECIAL CONFERENCE
ON
PRIME-POWER FOR HIGH ENERGY SPACE SYSTEMS

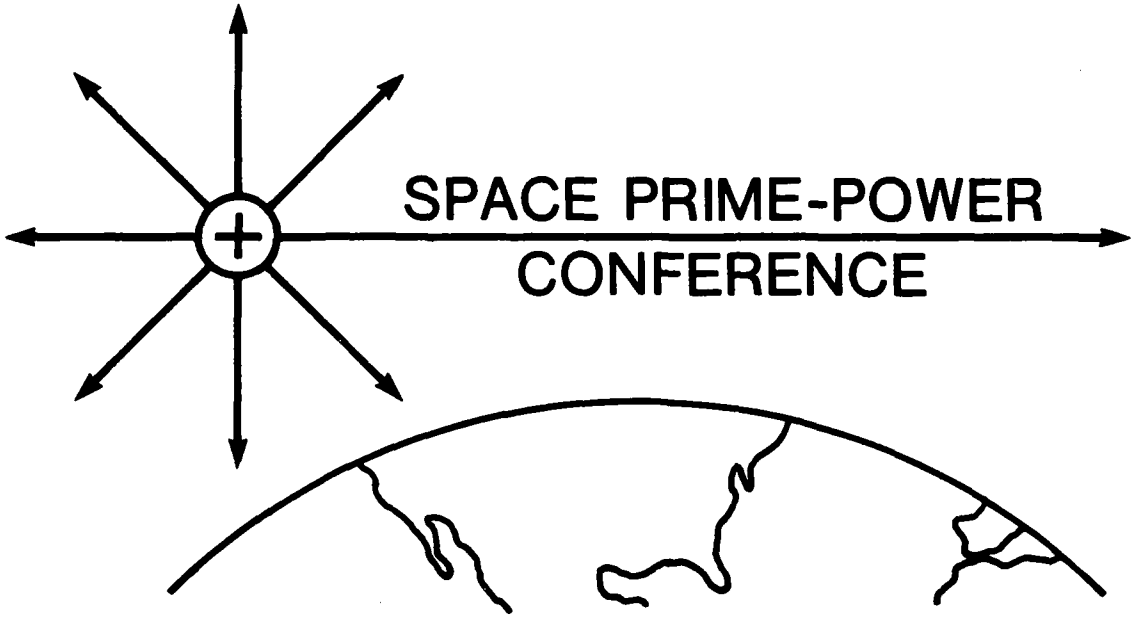

Norfolk, Virginia
22-25 February 1982

Volume II

Table of Contents

	Page
PREFACE	iii
CONFERENCE PROGRAM	vii
EXECUTIVE COMMITTEE	ix
CONFERENCE PRESENTATIONS	x
I. Prime-Power Needs	
Hartke, R. H., "Space, the Air Force, and AFOSR"	I-1 (NA)
Mullin, J., "NASA Directions for Research and Technology in Space Power"	I-2 (NA)
Cohen, M., "High Power Requirements"	I-3
Woodcock, G. R. and Silverman, S., "Power Requirements for Manned Space Stations"	I-4
Caveny, L., "Power Requirements for Orbit-Raising Propulsion"	I-5
II. Chemical Sources	
Clark, J., "Chemical Sources: Overview"	II-1 (NA)
Brown, R. A., "Batteries"	II-2
Stedman, J. K., "Alkaline Fuel Cells for Prime Power and Energy Storage"	II-3
Oberly, C. E., "Turbogenerators"	II-4 (NA)
III. Chemical/MHD	
Dicks, J. B., "MHD Power: Overview"	III-1
Smith, J. M., "NASA Lewis Research Center Combustion MHD Experiment"	III-2
Louis, J. F., "THE MHD Disk Generator as a Multimegawatt Power Supply Operating with Chemical and Nuclear Sources"	III-3
Maxwell, C. D., Bangerter, C. D. and Demetriades, S. T., "Self-Excited MHD Power Source for Space Applications"	III-4

(NA) - material not available

Massie, L., "Chemical Sources: Research Needs" III-5 (NA)

Jackson, W., "Critique of MHD Power" III-6 (NA)

Pierson, E. S., "Liquid-Metal MHD for Space Power Systems" III-7

Goswami, A., Graves, R., and Spight, C., "Solar MHD System with Two-Phase Flow with 'Magnetic' Liquid Metal" III-8

Swallom, D., "Magnetohydrodynamic Power Supply Systems for Space Applications" III-9

Seikel, G. R. and Zauderer, B., "Potential Role and Technology Status of Closed-Cycle MHD for Lightweight Nuclear Space-Power Systems" III-10

Koester, J. K., Kruger, C. H., and Nakamura, T., "MHD Generator Research at Stanford" III-11

IV. Nuclear Sources

Buden, D., "Overview of Space Reactors" IV-1

Fraas, A., "Technological Boundary Conditions for Nuclear Electric Space Power Plants" IV-2

Fitzpatrick, G. O. and Britt, E. J., "Effects of Reactor Design, Component Characteristics and Operating Temperatures on Direct Conversion Power Systems" IV-3

Parker, G. H., "Gas Cooled Reactors for Large Space Power Needs" IV-4

Elsner, N. B., "Near Term and Future Nuclear Power Conversion Systems for Space" IV-5 (NA)

Powell, J., and Botts, T./Myrabo, L., "Compact High-Power Nuclear Reactor Systems Based on Small Diameter Particulate Fuels"; "Closed-Cycle FBR/ Turbogenerator Space Power System Concept with Integrated Electric Thrusters for Orbital Transport" IV-6

Lee, J. H., Jr., "Safety Issues for Space Nuclear Power" IV-7

El-Genk, M. and Woodall, D., "Areas for Research Emphasis in Design of the Space Power Advanced Reactor" IV-8

Accession For
NTIS GRA&I
DTIC TAB
Unannounced
Justification
By
Distribution/
Availability Codes
Dist Avail and/or Special
A

DTIC COPY INSPECTED 2

(NA) - material not available

Jones, O. C., Jr., "Research Needs for Particulate Bed Nuclear Reactor Space Power Systems" IV-9

Ranken, W. A., "Selected Research Needs for Space Reactor Power Systems" IV-10

Bartine, D. E. and Engle, W. W., Jr., "Shielding Considerations for Space Power Reactors" IV-11

V. Power Conversion

Parker, G. H., "Brayton Cycle Power Conversion for Space" V-1

Peterson, J., "Rankine Cycle Power Conversion Overview" V-2

Bland, T., "Nuclear Powered Organic Rankine Systems for Space Applications" V-3

Stapfer, G. and Wood, C., "Thermoelectric Conversion" V-4

VI. Radiant Systems

English, R. and Brandhorst, H. W., Jr., "Power from Radiant-Energy Sources: An Overview" VI-1

Loferski, J. J., "High Efficiency Tandem or Cascade Photovoltaic Solar Cells" VI-2

Loferski, J., Severns, J. and Vera, E., "Thermophotovoltaic Power Sources for Space Applications" VI-3

Holt, J. F., "Solar Energy Conversion for Space Power Systems" VI-4

Conway, E. J., "Solar Pumped Lasers for Space Power Transmission" VI-5

Phillips, B. R., "A Proposed Optical Pumping System Requiring No Electric Power" VI-6

Miley, G. H., "Status, Research Requirements and Potential Application for Nuclear Pumped Lasers" VI-7

Walbridge, W. W., "Prime Power for High-Energy Space Systems: Certain Research Issues" VI-8

Britt, E. J., "Status of Thermoelectronic Laser Energy Conversion - Telec" VI-9

Finke, R. C., "Direct Conversion of Infrared Radiant Energy for Space Power Applications" VI-10

Freeman, J. W. and Simons, S., "The Phototron: A Light to R.F. Energy Conversion Device" VI-11

Lee, Ja. H. and Jaluska, N. W., "Radiation-Driven MHD Systems for Space Applications" VI-12

Freeman, J. W., "Interaction Between the SPS Solar Power Satellite Solar Array and the Magnetospheric Plasma" VI-13

VII. Materials

Saunders, N., "High-Energy Space Power Systems" VII-1

Morris, J. F., "Some Material Implications of Space Nuclear Reactors (Non-Fuel Materials)" VII-2

Yang, L., "Nuclear Fuel Systems for Space Power Application" VII-3

Rossing, B. R., "Materials for High Power MHD Systems" VII-4

Nahemow, M., "The Westinghouse High Flux Electron Beam Surface Heating Facility (ESURF)" VII-5

Cooper, M. H., "Applications of a High Temperature Radiation Resistant Electrical Insulation" VII-6

Levy, P. W., "Radiation Damage Measurements on Nonmetals Made During Irradiation with 1 to 3 MeV Electrons" VII-7

Sarjeant, W. J., Laghari, J. R., Gupta, R., and Bickford, K. J., "Charge Injection Effects Upon Partial Discharges in a DC and DC Plus AC Laminate Insulation Environment" VII-8

Sundberg, G., "Deep Impurity Trapping Concepts for Power Semiconductor Devices" VII-9

Milder, F. L., "Applications of Materials Surface Modification to Prime Power Systems" VII-10

Milder, F. L., "In Situ Monitoring of Critical System Component Erosion by Nuclear Activation Techniques" VII-11

Banks, B. A., "Growth of Diamond-like Films for Power Application" VII-12

Rice, R. W., "Ceramics for High Power Sources in Space" VII-13

Blankenship, C. P., and Tenney, D. R., "Materials Technology for Large Space Structures" VII-14

Gilardi, R., "Structural Characterization of Materials for High Energy Space Systems" VII-15

VIII. Chemical Physics

Rabitz, H., "Recent Advances in Molecular Dynamics" VIII-1

Rosenblatt, G. M., "Chemical Physics of Vaporization, Condensation and Gas-Surface Energy Exchange" VIII-2

Donovan, T./Guenther, A., "Thin Films" VIII-3

IX. Thermionics

Yang, L. and Fitzpatrick, G., "Thermionic Conversion for Space Power Application" IX-1

Huffman, F., Lieb, D., Reagan, P. and Miskolczy, G., "Thermionic Technology for Spacecraft Power: Progress and Problems" IX-2

Lawless, J. L., "A Survey of Recent Advances in and Future Prospects for Thermionic Energy Conversion" IX-3

Merrill, O. S., "Fundamental Research Areas on DoE's Thermionic Program" IX-4

X. Heat/Systems

Haslett, R., "Thermal Management of Large Pulsed Power Systems" X-1

Mattick, A. T., Hertzberg, A. and Taussig, R., "The Liquid Droplet Radiator" X-2

Bruckner, A. P., "The Liquid Droplet Heat Exchanger" X-3

Ernst, D. M. and Eastman, G. Y., "The Need for Improved Heat Pipe Fluids" X-4

Ernst, D. M. and Eastman, G. Y., "Enhanced Heat Pipe Theory and Operation" X-5

Fowle, A. A., "Two-Phase Heat Transport for Thermal Control" X-6

Teagan, W. P., "Liquid Ribbon Radiator for Lightweight Space Radiator Systems" X-7

Berry, G., "Software for Comparison and Optimization of Power Systems" X-8

Thornton, E. A., "Uncertainties in Thermal-Structural Analysis of Large Space Structures" X-9

XI. Summary

Barthelemy, R. XI-1(NA)

Vondra, R., "Power and Electric Propulsion" XI-2

Angelo, J. XI-3(NA)

Layton, J. P., "Power Conversion: Overview" XI-4

Severns, J. XI-5(NA)

Guenther, A. XI-6(NA)

English, R. XI-7(NA)

Junker, B. R. XI-8(NA)

Badcock, C., "Comments on the 'Special Conference on Prime-Power for High-Energy Space Systems' and Specifically on the Heat/Systems Session" XI-9

Hyder, A. XI-10(NA)

Bryan, H. R.

AUTHOR INDEX

LIST OF ATTENDEES

A PROPOSED OPTICAL PUMPING SYSTEM REQUIRING NO ELECTRIC POWER

BERT R. PHILLIPS

NASA-LEWIS RESEARCH CENTER

CLEVELAND, OHIO

A Proposed Optical Pumping System Requiring No Electrical Power

A method is available for optically pumping a fluid without electrical power. The method is based on utilizing the radiation from a metal-oxidant combustion reaction that is contained within a transparent tube that is immersed in the medium to be pumped. The reaction initiation and maintenance occurs by gas dynamically induced resonance within the transparent cavity. All that is required is a supply of high pressure oxidant and metallic powder. Materials that have been successfully evaluated to date include aluminum, steel, magnesium and titanium.

A Proposed Optical Pumping System Requiring No Electrical Power

Bert Phillips
NASA-Lewis Research Center
Cleveland, Ohio

Fig. 1. In the figure is shown an apparatus for generating a source of high intensity light without the need for electrical power. The principle of operation is that a source of high pressure gas, such as oxygen, is flowed into the inlet tube. The resulting large pressure ratio (30:1) in the exit flow tube generates oscillations in the underexpanded choked jet which, in turn, couples with the transparent cavity opposite the inlet tube. If particulate matter is introduced into the inlet stream, a portion of it will be trapped in the cavity and readily ignited. The combustion reaction, which will be localized in the lower part of the transparent cavity, will emit light characteristic of the particular transitions associated with the combustion reaction. No other supply of energy is needed.

Fig. 2. In this figure, light is emitted from pure aluminum/oxygen reactions. The effect is similar to a continuous photographic flash lamp. The tube in the case was uncooled quartz. Translucent alumina and vycor have also been used. In addition to aluminum the following metals have been ignited: titanium, iron, magnesium, steel. Any metal that can react with the gas will, in all probability, burn within the cavity.

Fig. 3. In this figure, a lucite resonant cavity configuration is shown. The light is from reacting aluminum. If the cavity were to be immersed in a flowing or stationary gas that could be optically pumped to a population inversion, lasing should readily occur. The optical pumping will occur as long as the gas and metallic powder is supplied.

Fig. 4. In this figure, the ignition characteristics of aluminum powders are shown as a function of inlet oxygen pressure and without use of aluminum within the tube. In the preliminary experiments shown, the particulate material was inserted within the tube prior to flow initiation. A small scale powder feeder could have been readily inserted between the inlet valve and the resonant cavity.

Fig. 5. In this figure, a comparison of analytical and experimental data is shown for the heating of the gas in the resonant cavity. The analysis is based on shock type heating with losses to the side and end walls, friction, and a coupling between the shock strength and the gas temperature. The major mechanisms operative in the tube have been identified in order to permit optimization for particular applications.

PRINCIPLE OF OPERATION

- A HIGH PRESSURE SUPPLY OF OXIDANT WHEN VENTED CAN INDUCE A GAS DYNAMIC RESONANCE IN A TRANSPARENT CAVITY
- THE RESONANCE CAN BE USED TO PROVIDE SOURCES OF IGNITION FOR PARTICULATES INTRODUCED WITHIN THE CAVITY
- RESULTING IGNITION AND COMBUSTION TAKES PLACE IN A SMALL VOLUME PROVIDING A CONCENTRATED LIGHT SOURCE
- A VARIETY OF METALS HAVE BEEN SUCCESSFULLY EVALUATED WITH VARIOUS EMISSION SPECTRA
- COMMERCIALLY AVAILABLE POWDER FEED SYSTEMS COULD BE USED TO SUPPLY POWDER CONTINUALLY - PROVIDING THE EQUIVALENT OF A CONTINUOUSLY OPERATING FLASHLAMP

RESONANCE TEE CONFIGURATION

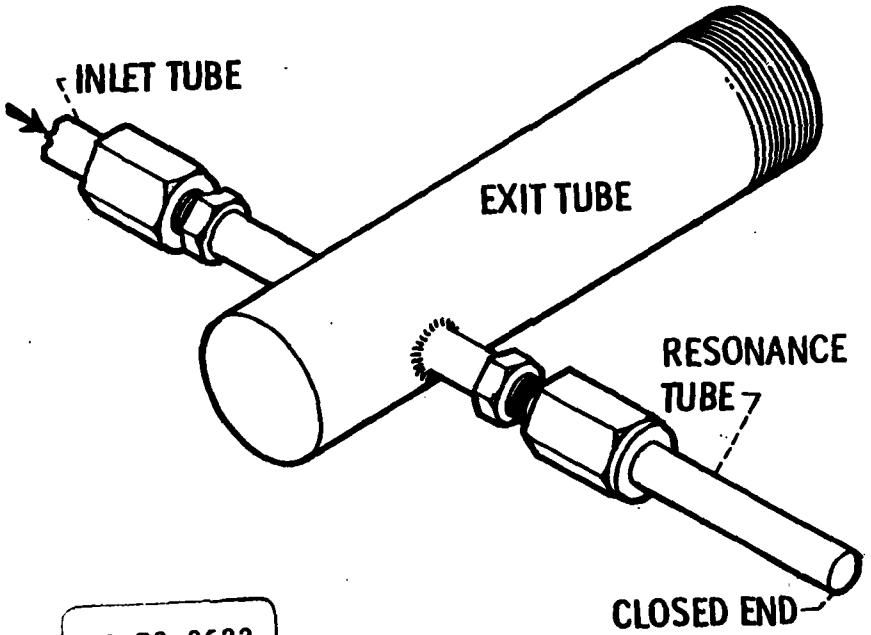

CS-78-3622

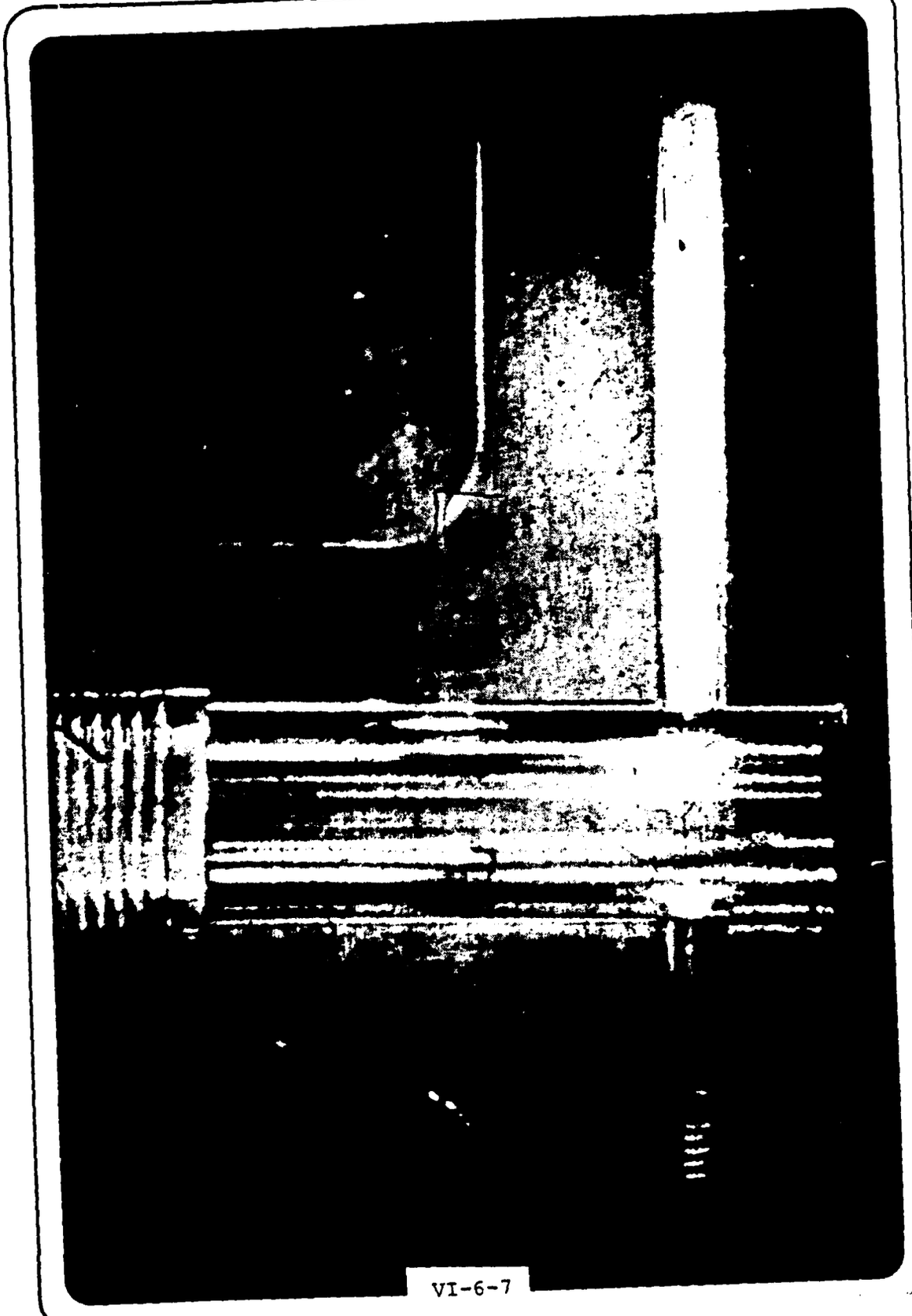

EXPLOSION OF ALUMINUM FIBER

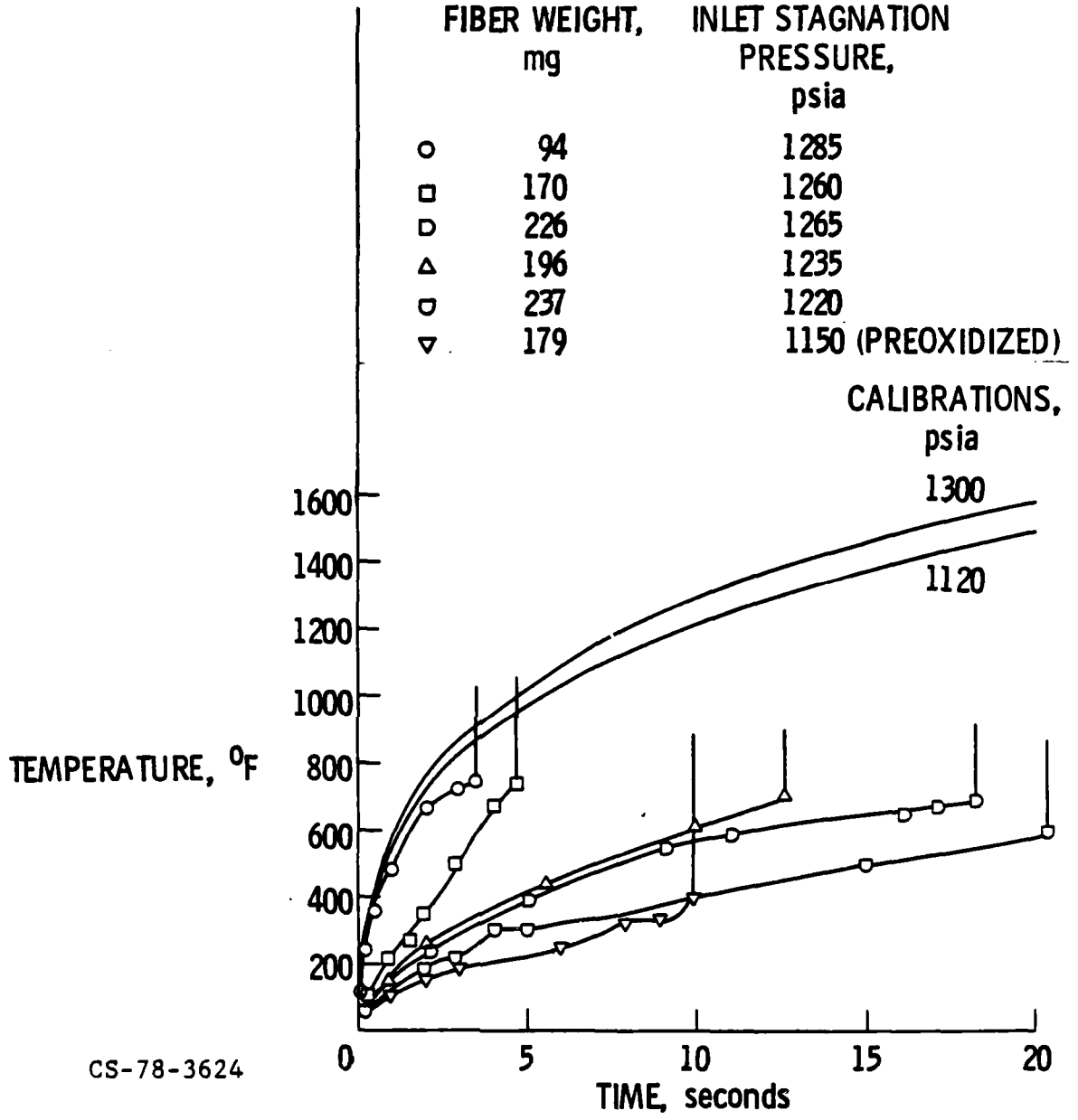

CS-78-3624

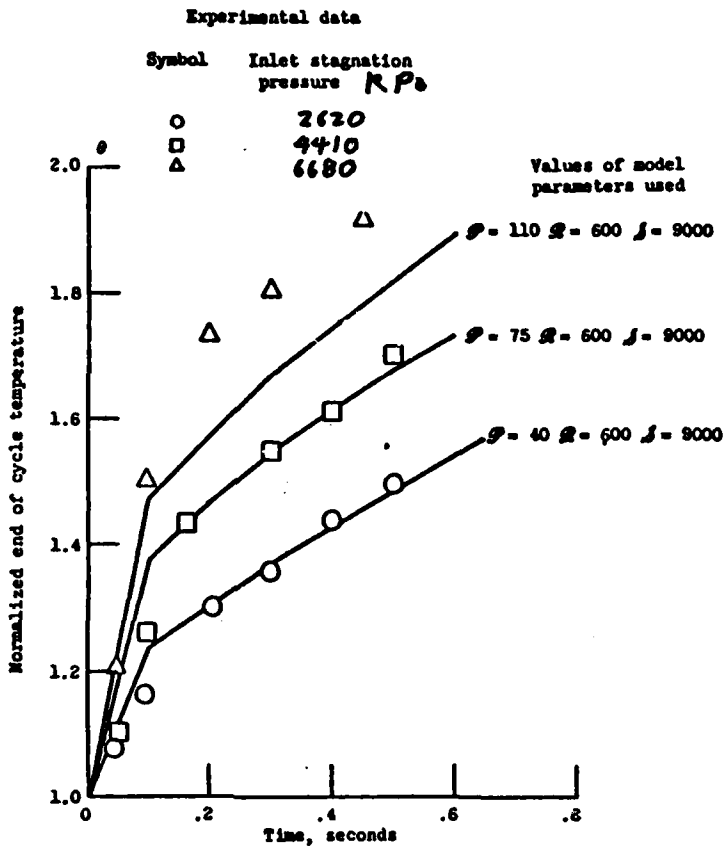

Figure 5 - Comparison of industrial mode model calculations with experimental data. Steel-quartz tube, gaseous oxygen.

SUMMARY

- CONTINUOUS SOURCE OF IGNITION FOR METALLIC PARTICULATES IN TRANSPARENT CAVITY
- METALLIC REACTANTS USED WITH OXYGEN - ALUMINUM, TITANIUM, ZIRCONIUM, STEEL
- CONTINUOUS FEED OF METALLIC PARTICULATE INTO STREAM IS FEASIBLE
- OPTICAL SOURCE CONFINED TO SMALL VOLUME
- NO ELECTRICAL POWER REQUIRED

Q & A - B. R. Phillips

From: Roy Pettis

Can this optical source be scaled to high powers for use in pumping lasers, for example I*? Comment on the limitations of this technology for high-power (peak & average) applications.

Answer:

From: P. J. Turchi, R & D Associates

What is the efficiency of radiant output power from the source: $\frac{\text{radiant power}}{(\text{chemical + mech. power used})} = \varepsilon$

Answer:

STATUS, RESEARCH REQUIREMENTS AND POTENTIAL APPLICATIONS FOR NUCLEAR PUMPED LASERS

by

George H. Miley
Fusion Studies Laboratory
University of Illinois
214 Nuclear Engineering Laboratory
103 South Goodwin Avenue
Urbana, Illinois 61801

Conference on Prime Power for
High-Energy Space System
Norfolk, VA
February 22-25, 1982

Status, Research Requirements and Potential Applications for Nuclear Pumped Lasers

by

George H. Miley
Fusion Studies Laboratory
University of Illinois
214 Nuclear Engineering Laboratory
103 South Goodwin Avenue
Urbana, Illinois 61801

Abstract

Mechanisms and various approaches to nuclear pumping of lasers are reviewed. Experimental results to date (including various noble gas lasers and more recent N_2-He-CO_2 and $O_2(^1\Delta)$-I_2 transfer lasers) are briefly noted. Both physics issues (e.g., electron energy distributions) and technology issues (e.g., coatings vs. UF_6 neutron interaction regions) are identified. Finally, considerations involved in potentially attractive applications such as space nuclear-laser systems and neutron-feedback inertial confinement fusion are outlined.

Outline

What is nuclear pumping?

Why nuclear pumping?

Status (experimental/theoretical)

Potential applications (systems studies)

Some R & D requirements

What is Nuclear Pumping?

Neutrons from a reactor or other source interact with material such as ^{10}B or ^{235}U in the laser medium causing nuclear reactions (see Fig. 1). The resulting high-energy (MeV) ions interact with the medium, producing the "pump" action.

The materials that undergo nuclear reactions can be either placed on the inner surface of the container holding the laser medium or mixed throughout the volume. The present talk will concentrate on *gas lasers* although similar techniques might be applied to liquids or solids. Radiation damage becomes a severe limitation in the latter cases. Consequently, most of the work to date has concentrated on nuclear pumped gas lasers.

Fig. 1. Methods for performing nuclear-pumped laser experiments.

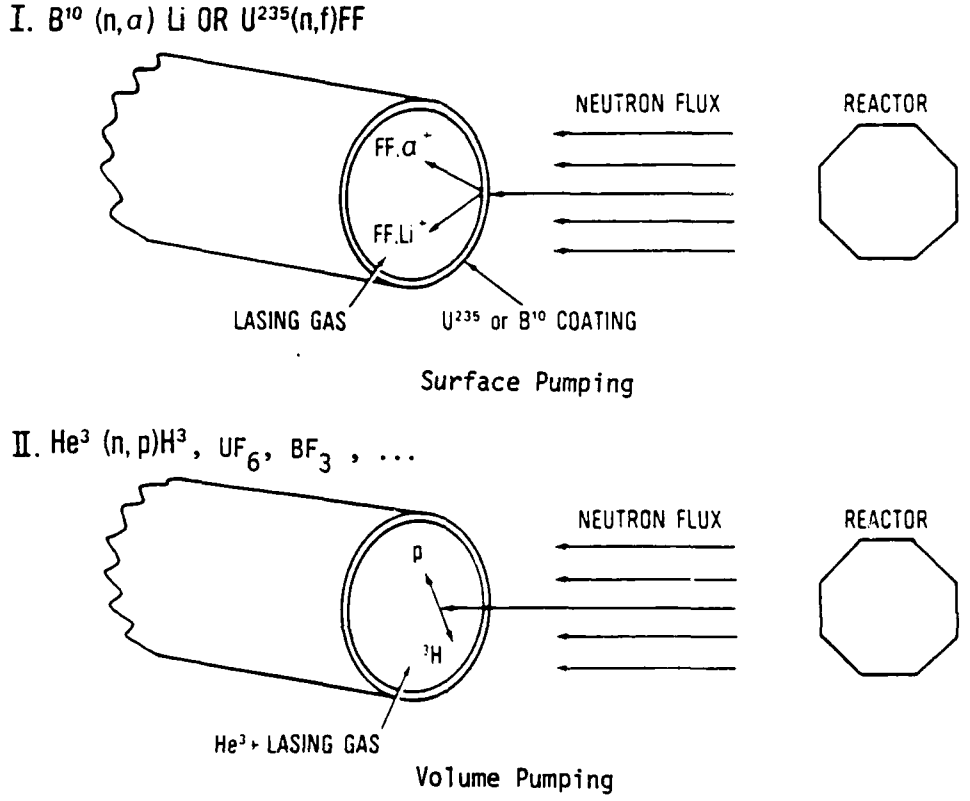

Volume sources ultimately offer ultra-large volume, high pressure excitation.

Volume sources such as UF_6, BF_3 or ^3He provide the highest pumping power density. However, since they must be compatible with the laser medium and not interfere with lasing, surface coatings of ^{10}B or U are simpler to use.

A bulk of the experiments to date have employed surface sources and modest pressures (< 1 Torr). Under these conditions the energy deposition rate in the laser medium during a pulse is typically < 1 kW/cm^3 (Fig. 2), a fairly modest value compared to some electron beam experiments. As indicated in Fig. 2, next stage experiments using volume source techniques shou'd achieve 10's of kW/cm^3. Also, high pressure experiments (> 5 atm) in princip'e, should be able to achieve multi MW/cm^3 provided that suitable laser media can be developed which won't deteriorate at high deposition levels. In addition, the energy deposition for nuclear pumping can be very large for pulsed lasers. Steady-state operation at lower powers however, is possible for selected lasers. Thus, as seen later in the discussion on applications, the use of an energy storage medium [e.g., O_2 ($^1\Delta$)] can, in principle, lead to nuclear-pumped lasers with "record" energy output per pulse.

Figure 2

Typical Peak Deposition Rates For ^{3}He and ^{235}U

Sources Coupled to a Fast Burst Reactor

Situation	Peak Power Deposition, kW/cm^3
^{3}He-Ar Laser Experiment at 4 atm Volume Source	~1 kW/cm^3
Conceptual reactor design, CO at 1 atm, U-coated plates Surface Source	~20 kW/cm^3 (~2 kJ/ℓ per pulse)
Conceptual mixture with 150 Torr ^{235}U Volume Source	~90 kW/cm^3 (~9 kJ/ℓ per pulse)

- Very large power densities possible with high pressure volume sources, e.g., > 1 MW/cm^3 for p > 5 atm.
- Uniquely suited to large energy densities per pulse.

Why Nuclear Pumping?

In situations where the source (e.g. a nuclear reactor or even a radioisotope) and the laser medium are naturally combined, nuclear pumping offers a direct conversion from nuclear to laser energy, bypassing the need for intermediate conversion to electricity. This offers the opportunity for compact, efficient systems with a high energy output (Fig. 3). The elimination of electrical conditioning/switching gear offers improved reliability while the nuclear source implies a self-contained, long lifetime system.

Figure 3

WHY NUCLEAR PUMPING ?

1. HIGH ENERGY DENSITY } HIGH ENERGY LASER
   LARGE LASER VOLUME }

2. INTEGRAL LASER → COMPACT
   AND ENERGY SOURCE → HIGH SYSTEM EFFICIENCY

What mechanisms are involved in the pumping? Is it unique?

Generally, most of the excitation of the laser gas is due to secondary electrons produced by interaction with the MeV ions. As indicated by the calculated electron energy distribution shown in Figure 4, a characteristic feature is the "high-energy" tail combined with a large thermalized (Maxwellian) electron population. In some cases, e.g., pumping of O_2 ($^1\Delta$), the high-energy tail plays a key role by providing a source of electrons in the ~ 10 eV range. In other cases, e.g., the Ne-N_2 laser, the large cold Maxwellian population leads to excited states via recombination. A third possible route to utilization of nuclear pumping takes advantage of the relatively large ion density in the plasma created under irradiation and operates on charge-exchange. An example is the He-Hg laser, the first nuclear pumped laser operating with visible output.

While the mechanisms involved in nuclear pumping share many features with electron and ion beam pumping, considerable effort is necessary to create a situation where the latter can fully simulate the electron distribution created in nuclear pumping. Indeed, when all the variables (distribution, energy and power density, etc.) are considered, the use of a pulsed research reactor appears to be the best approach for such studies, although supplemental e and i - beam kinetics studies may still be helpful.

Figure 4. The unique electron energy distribution created by nuclear pumping.

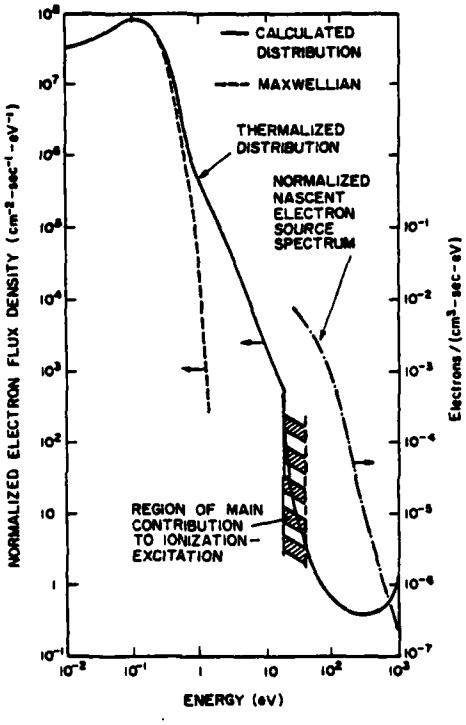

- Pumping largely associated with unique secondary electron distribution.

Reactors for Nuclear Pumping Studies

Both fast burst and pulsed TRIGA reactors have been used for NPL experiments and characteristics for both reactors are compared in Fig. 5. The fast burst reactor gives a higher peak flux, while the TRIGA is more accessible and can provide more pulses (hence more data) per day. The TRIGA's flux is adequate in the sense that it is roughly equivalent to that expected in a practical system. In addition, the energy per pulse from the TRIGA, which is equally important to nuclear pumping, is actually larger than from a fast burst reactor.

Figure 5. Characteristics of Reactors Used for NPL Studies

	TRIGA	Fast Burst
type reactor	thermal	fast
core materials	^{235}U, ZrH, H_2O	^{235}U alloy
pulse FWHM	$\tilde{<}$ 10 msec	$\tilde{>}$ 50 μsec*
peak neutron flux	~5×10^{15} n/cm^2-sec	~10^{18} n/cm^2-sec*
energy/pulse	~30 MW-sec	~3 MW-sec

*After thermalization, as required for DNPL studies, the peak flux is reduced by an order of magnitude and the FWHM increased by ~3 or more. In present experiments, thermalization is accomplished using a thin polyethylene cylinder around the laser tube.

TRIGA offers more data/day, larger energy/pulse lower neutron flux.

Current Status

Most nuclear pumped lasers reported to date are summarized in Fig. 6 However, NPL research was severely cut back in the past year since major funding th:ough NASA-Langley was stopped. (This decision by NASA was based on the lack of a near-term mission rather than concern about progress.) A majority of the experiments have been done by NASA-Langley (R. DeYoung), U. of Florida (R. Schneider) and U. of Illinois (G. Miley). A few experiments were also carried out at Sandia and Los Alamos.

The maximum power output achieved to date is ~ 1 kW from a ^{3}He-Ar "box" laser developed by NASA which demonstrated the volume scaleability of nuclear pumped lasers. Since, most studies have concentrated on the kinetics of a certain system rather than attempting to produce high power/energy outputs, greater power outputs have not been obtained. In addition, the noble gas mixtures, which have been extensively studied, are not good candidates for high power/energy lasers.

The scale-up to high power/energy will require larger volumes and special geometries in order to intercept large fractions of the neutron flux. This implies an expensive apparatus (and is a technology issue vs a reaction kinetics issue) which no one has been commissioned to undertake thus far. Consequently, the listing of lasers studied to date, while important, has little relevance to the topic of high power which is of interest in this conference. A new dedicated program would be necessary to attack this issue.

Figure 6. LASERS TO DATE

Laser	Pumping Reaction	Wavelength	Thermal Neutron Flux Threshold (n/cm^2-sec)	FWHM of Pulse	Peak Power
He-Hg (1)	$^{10}B(n,\alpha)^7Li$	6150 Å	$\sim 1 \times 10^{16}$	.400 msec	$\sim$ 1 mW
CO (1)	$^{235}U(n,f)ff$	5-1-5.6 μm	$\sim 5 \times 10^{16}$	.05 msec	> 2 W
He^3-CO (2)	$^3He(n,p)T$	5-1-5.6 μm	"	"	> 30 W
He-Xe (1)	$^{235}U(n,f)ff$	3.5 μm	$\sim 3 \times 10^{15}$	.15 msec	> 10 mW
Ne-N_2 (1)	$^{235}U(n,f)ff$ $^{10}B(n,\alpha)^7Li$	8629 Å 9393 Å	1×10^{15}	6 msec	> 10 mW
^{3}He-Xe (3)	$^3He(n,p)T$	2.027, 3.508, 3.652 μ	$\sim 1 \times 10^{16}$	.3 msec	< 10 W
He,Ne, Ar-CO_2 (4)	$^{10}B(n,\alpha)^7Li$	1.45 μm	2×10^{14}	6 msec	$\sim$ 100 mW
He,Ne-CO (4)	"	"	"	"	"
^{3}He-Ne (7)	$^3He(n,p)T$	6328 Å	10^{11}	cw	> 10 mW
^{3}He-Ar (5)	$^3He(n,p)T$	1.79 μm	1×10^{16}	.12 msec	> 1 KW
^{3}He-Xe (3)	$^3He(n,p)T$	2.63 μ	3×10^{16}	$\sim$ .05 msec	> 200 W
He-N_2-CO_2 (6)	$^{10}B(n,\alpha)^7Li$	10.6 μm	10^{14}	1-3 msec	> 100 W

- Verified scientific feasibility.
- Concentration thus far on kinetics and <u>not</u> on power/energy demonstration.

Ref.

1. G. H. Miley, Laser Int. and Related Plasma Phen. Vol. 4A (1976) pp. 181-228.

2. N. W. Jalufka, F. Hohl, 1980 IEEE Internat. Conf. on Plasma Sci. Madison, Wisc. May (1980) 5C5.

3. N. W. Jalufka, 1981 IEEE Internat. Conf. on Plasma Sci, Santa. Fe, N. M., May (1981) 6B1.

4. M. A. Prelas, J. H. Anderson, F. P. Boody, S. J. S. Nagalingam, and G. H. Miley, Radiation Energy Conversion in Space, Vol. 61, Progress in Astronautics and Aeronautics (1978).

5. R. J. DeYoung, Appl. Phys. Left. 38(5), 1 March 1981, pp. 297-298.

6. M. J. Rowe, R. H. Liang, and R. T. Schneider, 1981 IEEE Conf. on Plasma Sci., Santa, Fe, N.M. May (1981) 6B6-7.

7. B. D. Carter, M. J. Rowe and R. T. Schneider, Appl. Phys. Lett., Vol. 36 (2), p. 115 (Jan. 1980).

Current Studies

With the shutdown of the NASA program, the number of laboratories in the U.S. working on NPLs is very limited as seen from Fig. 7. Some NPL studies are in progress in Europe. Also, the Russians have worked in this area for a number of years but little is known about their efforts. (To illustrate the importance placed on NPL's in Russia, we note that members of the original research team subsequently received the Lenin prize for their work). The two Russian studies listed in the table are based on abstracts submitted for the May 1982 IEEE Plasma Sciences Conference in Ottawa, Canada.

The remaining studies in the U. S. are largely directed at the dual medium approach (i.e., nuclear pumping is carried out in one medium and the energy transferred to a second medium). In the U. of Illinois studies, for example, O_2 is pumped to form $O_2(^1\Delta)$ which flows out of the irradiation zone and is subsequently mixed with iodine. In other work, the first medium effectively serves as a flash lamp, photolytically pumping the second medium. An advantage of the dual media approach is that it avoids input radiation (and in the case of volume pumping, additives such as UF_6) in the laser medium itself which can result in quenching of lasing action. In the specific case of O_2-I_2, the $O_2(^1\Delta)$ and the transit flow time provide a very effective energy storage mechanism between reactor pulses.

Figure 7. Current Studies

Laser Systems	Wavelength	Place	Approach	Comments
$O_2(^1\Delta)$-I_2	1.31μm	U.of Ill. (U.S.AFWL)	modeling experiments (TRIGA)	Both modeling and experiments suggest efficient operation. Energy storage in $O_2(^1\Delta)$. Production efficiency measurements in progress
N_2-CO_2	10.6μm	U.of Ill.	modeling experiments (TRIGA)	Lasing originally demonstrated by U.of Fla.. Vibrational states efficiently pumped. Energy storage in $N_2(v=1,8)$. Laser studies in progress.
Rare Gas Halide Fluorescer	—	U.of Mo.-Columbia	modeling experiments (MURR)	Steady state data for RGH systems. Modeling of photon transport for energy focussing, and chemical synthesis.
RGH		U.S. Army Huntsville	simulations (accelerator)	Study of mechanisms
XeF(C-A)	460nm	Wayne State U.S. Army	modeling	Direct gamma ray pumping and gamma ray pumped liquid Xe fluorescer for photolytic pumping of XeF_2
RGH and Metal Halides		NPL Corp.	modeling	Modeling of RGH flourescer coupling to RGH laser or metal halide laser with energy focussing. Photolytic driver pumped by ^{235}U dust.
CO,CO_2	5.1-10.6μm	Academy of Science Kazakh,USSR	experiments (steady state reactor)	Nuclear enhanced discharge work.
He-Xe	2.69μm	Academy of Science Lenningrad USSR	experiments (pulsed reactor)	Pumping with ^{235}U coatings. Power output exceeds 250W
RGH,$O_2(^1\Delta)$		Academy of Sci. Moscow USSR	experiments (accelerator)	Work in progress
NeN_2	8629,9393Å	U.of Paris Orsay	experiments (accelerator, steady state)	Simulated NPL with proton beam.
Noble gases		U.of Stuttgart	experiments (accelerator)	Simulated NPL

Advanced Work (cf Figure 8)

Thus far, little effort has been expended on systems that would potentially lead to high power/energy systems of interest here. Some "advanced work" that might fall into this category is shown in Fig. 8. If high power/energy lasers are truly the goal, a dedicated program is needed to first sort out directions and then develop a data base. Some possible routes are already apparent however. For example, energy storage in a medium such as $O_2(^1\Delta)$ followed by a "Q-switched" laser is one approach. Another is to use a very effective volume source (e.g., uranium "dust" pellets) in the flash lamp pump region in order to obtain a high specific power deposition and then use optical focussing techniques in order to further increase the energy density in the second (laser) medium. An ultimate goal might be to develop a self-critical UF_6 reactor that would also represent the laser medium.

Figure 8. ADVANCED WORK

- Energy Transfer Lasers

  Continued studies of $O_2(^1\Delta)$-I_2 system and N_2-CO_2 systems. Search for a suitable laser species compatible with $N_2(A^3\Sigma)$ metastable state.

- Photolytic Pumping

  RGH and Metal Halide systems to be photolytically pumped by RGH Fluorescer with ^{235}U dust as pumping source.

- Excimer Lasers

  Saturation of trimers at high power depositions may allow excimers to be nuclear pumped.

Need a dedicated program to search out best route to high power/energy.

Status of Theoretical Studies (cf Figure 9)

Theoretical studies have two key aspects: prediction of the electron energy distribution (cf Fig. 4 shown earlier) and study of the reaction kinetics. While several distribution function calculations have been reported, more work is required in this area to handle general cases of mixtures with molecular gases. Also, an experimental verification would be desirable.

Kinetics studies for nuclear pumping are, of course, similar to those of interest for all lasers. Fairly extensive studies have been reported for various nuclear pumped lasers including the noble gases and most recently $O_2(^1\Delta)$. A key point is that due to the unique conditions (source energy distribution, pressure, power density, zero electric field, etc.) some reactions neglected in other studies may become important and visa versa. For example, in our study of the formation of O_2 $(^1\Delta)$, super elastic electron collisions with metastable O_2 states and three body atomic recombination into O_2 $(^1\Delta)$ appear to be important but were neglected in previous studies of chemical or electrical lasers.

Figure 9. STATUS OF THEORETICAL STUDIES

Two Aspects:

- Calculation of unique electron energy distribution

  Thus far restricted to simple cases

- Reaction kinetics

  Need to identify important reactions under unique NPL conditions

Figure 10. SOME POTENTIAL APPLICATIONS

- Self-contained reactor-laser space unit
- Multipurpose electrical generator - laser unit
- Neutron-feedback laser fusion
- Stripping unit for negative ion beam injector for fusion devices.

As indicated above, potential applications in space include high power/energy directed energy applications and also lower power CW communication uses. In addition, there appear to be several potentially important applications to fusion, but these will not be discussed further here.

Status of System Studies

System studies to date (Fig. 11) are too fragmentary to properly access the potential applications or the technological problems. Perhaps the most complete study for high-power space applications is the 1979 study by Naff and French of a reactor-driven laser. Because solid fuel elements were assumed, heat dissipation required a large radiator which limited the power to weight ratio. However, improvements in the concept appear possible and should be investigated. Further, the Naff-French study showed that even with the radiator restrictions imposed, the nuclear pumped approach would be superior as the number of output pulses required becomes large.

The other systems studies noted are very sketchy. However, it is instructive, for purposes of illustrating near term system sizes, to review the 1-MJ laser design by McArthur, reported in 1975. Again, this design would need much study to refine it but the results are interesting from a conceptual point of view. As illustrated in the next figure, this laser uses a subcritical uranium-plate driver region surrounding a conventional fast burst reactor. A device (representing the combined power supply and laser) with only a 85-cm outside radius and 150-cm height would deliver 1.17 MJ (see Fig. 12). This design is considered to be "off of the shelf" in the sense of building on an existing pulsed reactor and adding driver technology based on experimental lasers.

In contrast to McArthur's concept that employs a driven region pumped by neutrons from a separate reactor, advanced conceptual designs generally assume a unified reactor-laser using a UF_6-laser-gas mixture. Rodger's 1979 study of a "self-critical" laser examined the neutronics in some detail and reports a 3.2 m^3 lasing volume containing 4.9 kg of U^{235} in the form of UF_6. A problem in this and related studies, however, is that an appropriate lasing mixture with UF_6 has not yet been identified. Thus, pressure conditions, optical components, etc. remain at best, a guess.

Figure 11. STATUS OF SYSTEM STUDIES

- Study of space application by W. T. Naff and F. W. French (IEEE Plasma Sciences Conf., Montreal, 1979)

- Fragmentary studies
  - 1-MJ laser - pulsed reactor, D. McArthur, et al., 1975
  - UF_6 reactor - laser, K. Thom, et al., 1976
  - Self-Critical Nuclear Pumped Laser System, R. J. Rodgers, et al., 1979.
  - Neutron feed-back ICF, G. Miley, et al., 1980.

Fragmentary -- need extensive systems studies to provide insight regarding directions and problems

Figure 12. DEMONSTRATION CO-LASER REACTOR

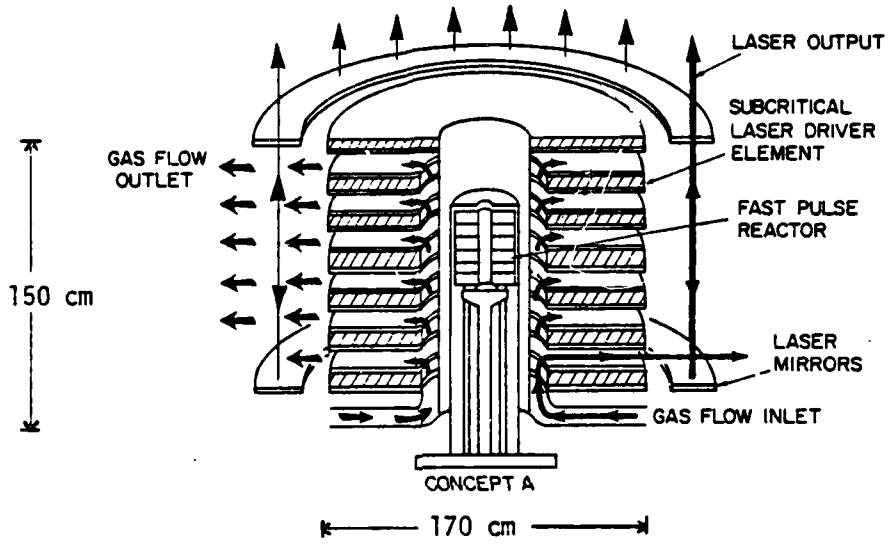

An example of a possible near-term experiment.

1.2 MJ Laser

2980 ℓ. driver

100 J/cm^2 out

371 J/ℓ-atm

FIGURE 13. SOME R & D REQUIREMENTS

- General

  Identification of candidate high power/energy systems with desired wavelengths; candidate energy storage media

- Experimental

  Study of production mechanisms and kinetics under unique NPL conditions

  Demonstration of scaling to large volumes in specialized geometries

  Identification and study of compatible volume sources (UF_6, BF_3, ^3He, Li compounds, U dust, etc)

  Development of long-lived plate sources

  Flow dynamics of transfer lasers under unique conditions

  Study of radiation effects on optics and materials

  Ultimately develop integrated reactor-laser

- Theoretical

  Electron source distribution calculations

  Continued kinetic modeling for specific systems, including medium with volume pumping

  Mixing under transfer laser conditions

- Systems Studies

  Series of dedicated studies needed to explore new directions, establish potential advantages, identify problem areas, establish directions for R & D.

Figure 14. CONCLUSION

- The scientific feasibility of nuclear pumping has been established.

- In principal applications to high power/energy systems seem feasible and attractive but to verify this a dedicated program is needed consisting of:
  - systems studies to identify directions and problem areas
  - identification and study of selected candidate laser media to establish kinetics and scaling
  - supporting R & D on components, including reactor-laser coupling, radiation damage, and flow dynamics.

- A first step goal would be a demonstration reactor-laser system, perhaps along the lines of the 1-MJ device noted in this paper.

Q & A - G. H. Miley

From: Roy Pettis

Could you forsee an integrated system in which a gas-core reactor is used to pump a laser, and the two fluids move in the same duct system?

A.

This is possible but difficult. The UF_6 used may quench lasing, but UF_6 + some excimer laser mixtures have a possibility of working (theoretically, but not demonstrated). Transmitting the energy from the core, either by flow or by radiation, to a second lasing fluid is more assured of working but a little more complex system.

From: P. J. Turchi, R & D Associates

What kind of efficiencies appear feasible:

$$\eta = \frac{\text{laser power}}{\text{waste heat power}}$$

A.

The most concrete example would be based on the 1 MJ demo reactor-laser study by David McArthur (Sandia-1975).

$$\text{Laser output} = 1 \text{ MJ}$$

$$\text{Driver + Reactor input} = 11 \text{ MJ} + 13 \text{ MJ}.$$

$$\text{Overall system efficiency} = \frac{\text{laser energy/pulse}}{\text{reactor energy /pulse}} = \frac{1}{24} \sim 4\%$$

Some References

1. G. H. Miley, "Direct Nuclear Pumped Lasers - Status and Potential Applications," in Laser Interaction and Related Plasma Phenomena, Vol 4A, Plenum Publishing Corp. 1977.

2. K. Thom and R. T. Schneider, "Nuclear Pumped Gas Lasers," AIAA Journal, 10, 400 (1972).

3. D. H. Nguyen and A. E. Fuhs, Nuclear Pumped Lasers: Report of Workshop on Direct Nuclear Pumping of Lasers, Naval Postgraduate School, Monterey, CA (April 1976).

4. Proceedings of International Symposium on Nuclear Induced Plasmas and Nuclear Pumped Lasers, May 23-25, 1978, Orsay, France.

5. Proceedings, NASA Workshop on Nuclear Pumped Lasers, NASA-Langley Research Center, July 1979.

6. See Sessions on Nuclear Pumped Lasers in:
   1979 IEEE International Conference on Plasma Science, Montreal, Canada;
   1981 Conference, Santa Fe, NM;
   1982 Conference, Ottawa, Canada.
   Radiation Energy Conversion in Space, Vol. 61, Progress in Astronautics and Aeronautics (1977).
   Also, see NPL papers in
   International Conference on Lasers '79, Orlando, FL.
   International Conference on Lasers '80, New Orleans, LA.
   International Conference on Lasers '81, New Orleans, LA.

7. Compilation of Data Relevant to Nuclear Pumped Lasers, Vols I-III, Technical Report H-78-1, US Army Missile R & D Command, Redstone Arsenal, Ala.

8. G. H. Miley and M. S. Zediker, "Nuclear Pumping $O_2(^1\Delta)$ for an $O_2(^1\Delta)$-I_2 Laser," XIIth International Quantum Electronics Conference 1982, Munich, Germany, June 22-25, 1982.

9. G. H. Miley, E. Greenspan, and J. Gilligan, Atomkernenergie/ Kerntechnik, Vol. 36, No. 3 (1980) pp. 182-187.

10. $O_2(^1\Delta)$-I_2 studies are described in:
    M. S. Zediker and G. H. Miley, Topical Meeting on Infrared Lasers, University of S. California, December 1980.
    M. S. Zediker and G. H. Miley, International Conference on Lasers '81, New Orleans, LA, December 1981.
    M. S. Zediker, T. R. Dooling, and G. H. Miley, 1981 IEEE International Conference on Plasma Science, Santa Fe, NM.

PRIME POWER FOR HIGH-ENERGY SPACE SYSTEMS: CERTAIN RESEARCH ISSUES

Edward W. Walbridge
Argonne National Laboratory
9700 South Cass Avenue
Argonne, Illinois 60439
(312) 972-3262

ABSTRACT

The most fundamental issue is: to what extent can high power space systems be hardened against directed energy attack. If they cannot be so hardened the result will be greater strategic instability. For large satellites Alfvén wave drag and induced magnetic moment effects (drag and torque) may be significant. These need to be better assessed. The physical mechanisms underlying Alfvén wave drag and induced magnetic moment effects are described. An expression, not hitherto published, for the induced magnetic moment of a (ring-shaped) satellite is presented. Several other issues requiring attention are also pointed out. These include, in particular, the need to avoid a demise like that of Skylab, how to obtain high heat engine thermal efficiency, what to do about the damaging effects of Van Allen belt radiation, and the need for storing energy over long periods but having it quickly available on short notice.

PRIME POWER
FOR HIGH-ENERGY SPACE SYSTEMS:
CERTAIN RESEARCH ISSUES

EDWARD W. WALBRIDGE
ARGONNE NATIONAL LABORATORY

Figure 1

PRESENTED TO THE

SPECIAL CONFERENCE ON PRIME POWER
FOR HIGH -ENERGY SPACE SYSTEMS

FEBRUARY 22 -25, 1982
OMNI INTERNATIONAL HOTEL
NORFOLK, VA.

Figure 2 One issue is fundamental: whether or not a directed energy (DE) space weapon system can be hardened against DE attack. If it can be there exists the possibility of a DE system in space which could defend against intercontinental ballistic missile attack, but which would itself be invulnerable. This promotes strategic stability. If such a system cannot be hardened the result is a strategic instability, since: (1) a concerted DE attack against the space system would come without warning at very high speed and, (2) the first attacker would win. To avoid premature and uncontrolled descents from orbit such as occurred with Skylab, it will be necessary to have a capability for boosting large space platforms into higher orbits and/or a dependable capability for making controlled descent from orbit to a preselected splashdown point. Two magnetic effects, Alfvén wave drag and induced magnetic moment drag, may contribute significantly to the total drag on a large space satellite. These effects need to be better assessed. For a solar powered system, the concentrating mirror will be large, will have low mass/meter^2, and may be deformed by mechanical oscillations, electrostatic surface charging, and electric currents driven by a uniform or time-varying magnetic field. Other important issues for a satellite which generates large amounts of power, whether from the sun or otherwise, are (see Walbridge [1980], [1982] for a more detailed discussion of these): how to obtain high heat engine thermal efficiency, the need to take into account angular momentum internal to the satellite, and the effects of Van Allen belt radiation on materials and maintenance personnel. If the satellite-generated electric power were to be used to power laser or particle beam weapons, then it would be necessary to store energy in the satellite for years, but be capable of using essentially all of the energy up within several minutes. Clearly energy storage is a crucial issue.

A FUNDAMENTAL ISSUE	CAN A DIRECTED ENERGY (DE) SPACE SYSTEM BE HARDENED AGAINST DE ATTACK	IF YES IDEAL DEFENSIVE WEAPON IF NO STRATEGIC INSTABILITY	SYSTEM NEEDS "HARDNESS" DESIGNED IN

OTHER IMPORTANT ISSUES

- AVOID SKYLAB - TYPE DEMISE
- MAGNETIC EFFECTS
  - ALFVÉN WAVE DRAG
  - INDUCED MAGNETIC MOMENT ($\vec{m}$)
- SHAPE MAINTENANCE FOR SUNLIGHT COLLECTING MIRROR
- HEAT ENGINE EFFICIENCY
- ANGULAR MOMENTUM OF FLOWS, TURBINE ETC.
- VAN ALLEN BELT RADIATION
- ENERGY STORAGE

Figure 2

Figure 3 Schematic of the Lockheed Laser Satellite Power System (SPS). This system is described in detail in Walbridge [1980, 1982] and Lockheed Missiles and Space Co., Inc. [1978]. Problem areas for this system a[illegible] magnetic drag (due to Alfvén wave radiation or to an induced magnetic moment), maintenance of the shape of the large (2.8 km diameter) sunlight collecting mirror, efficiency of the heat engine, angular momentum of internal fluid flows and of the turbine and other rotating machinery, and inner Van Allen belt radiation. These, and other, problem areas for the Lockheed laser SPS could be problem areas for any space satellite having a capability for generating large amounts of electrical power.

Figure 3

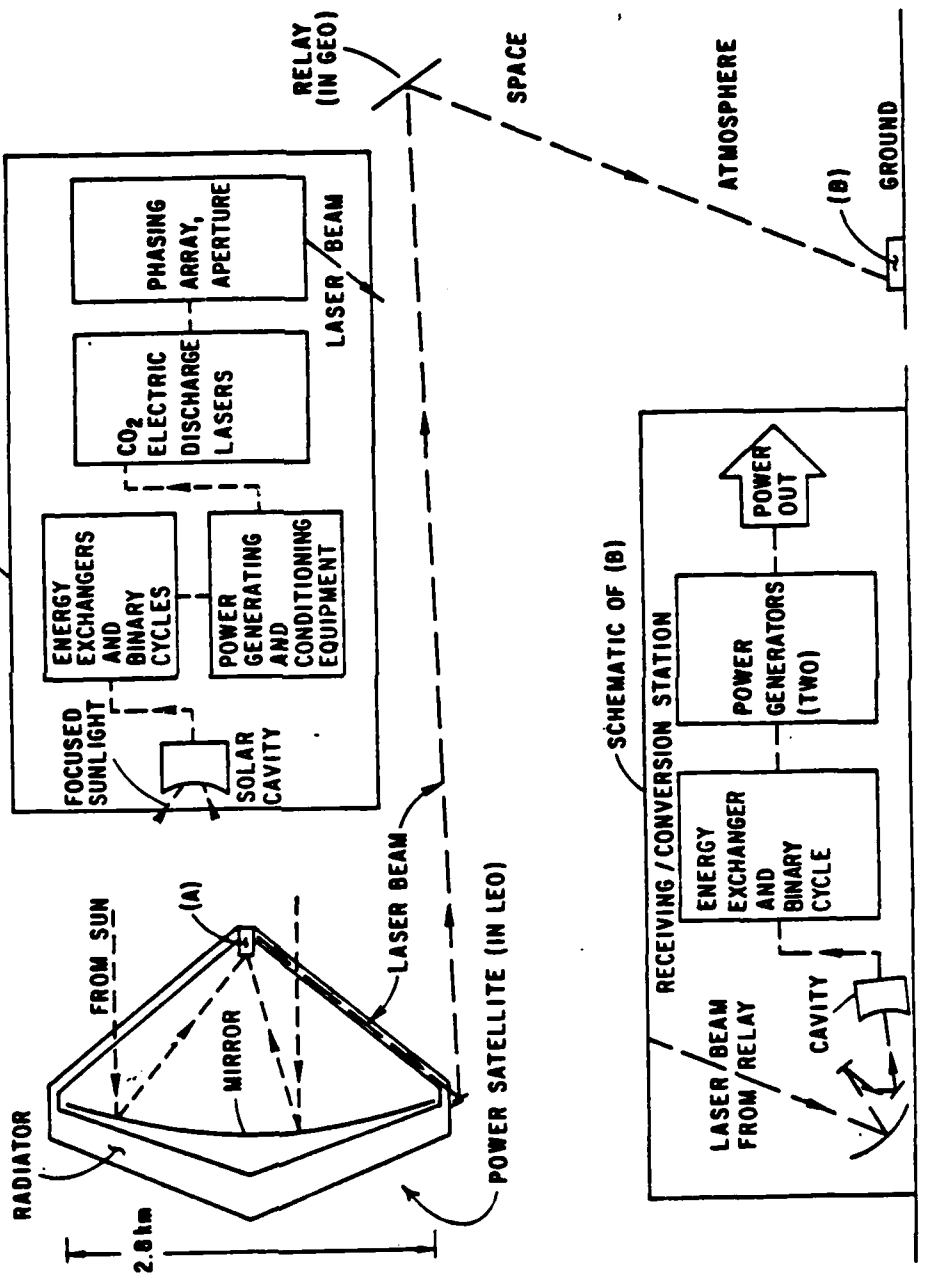

THE LOCKHEED LASER SPS

Figure 4 As shown by Drell, Foley, and Ruderman [1965] an electrically conducting satellite moving through the magnetosphere will radiate energy in the form of Alfvén waves provided an internal source of electric power is not employed to counteract this effect. The result is a "magnetic drag" on the satellite. An internal power source can reverse this effect to create an Alfvén propulsion engine. This figure illustrates the case of no internal source of electric power used to reverse the effect. The satellite is not drawn to scale. The drawing on the left shows the magnetic field perturbed by the Alfvén wave, while the drawing on the right shows the current loop associated with that wave. Electric charge moves across magnetic field lines in the lower ionosphere where there are sufficient ion-neutral and electron-neutral collisions to permit this, along field lines at higher levels where the perpendicular-to-field-line-conductivity is zero, and across field lines within the satellite. The potential difference in the satellite, shown by the + and - minus signs, maps down the (equipotential) field lines to the lower ionosphere. The current is driven by an electromotive force (EMF) acting in the satellite and due to the motional electric field, of magnitude $V_s B_o/c$, seen by the satellite. Here B_o is the unperturbed geomagnetic field in gauss, c is the speed of light in cm/sec, and the satellite speed, V_s, is in cm/sec. In the expression for p, h is in gauss, r in cm, and V_a in cm/sec. In sunlight, the Echo 1 satellite radiates energy via Alfvén waves at the rate of 0.5 watts. When Echo 1 is in the earth's shadow electrons cannot be photoemitted from the satellite's surface, the current cannot flow, and no Alfvén wave energy is radiated. Since the satellite is in sunlight about half the time, on the average it radiates 0.25 watts via Alfvén waves. To account for the observed degradation in the orbit of Echo 1, an energy loss rate of 0.33 watts is required [Drell, Foley, and Ruderman, 1965]. Thus, the 0.25 watts loss rate by Alfvén radiation is of the right order of magnitude to account for all, or most of, the observed energy loss rate. Alfvén waves are described in Spitzer [1956].

ALFVÉN WAVE DRAG

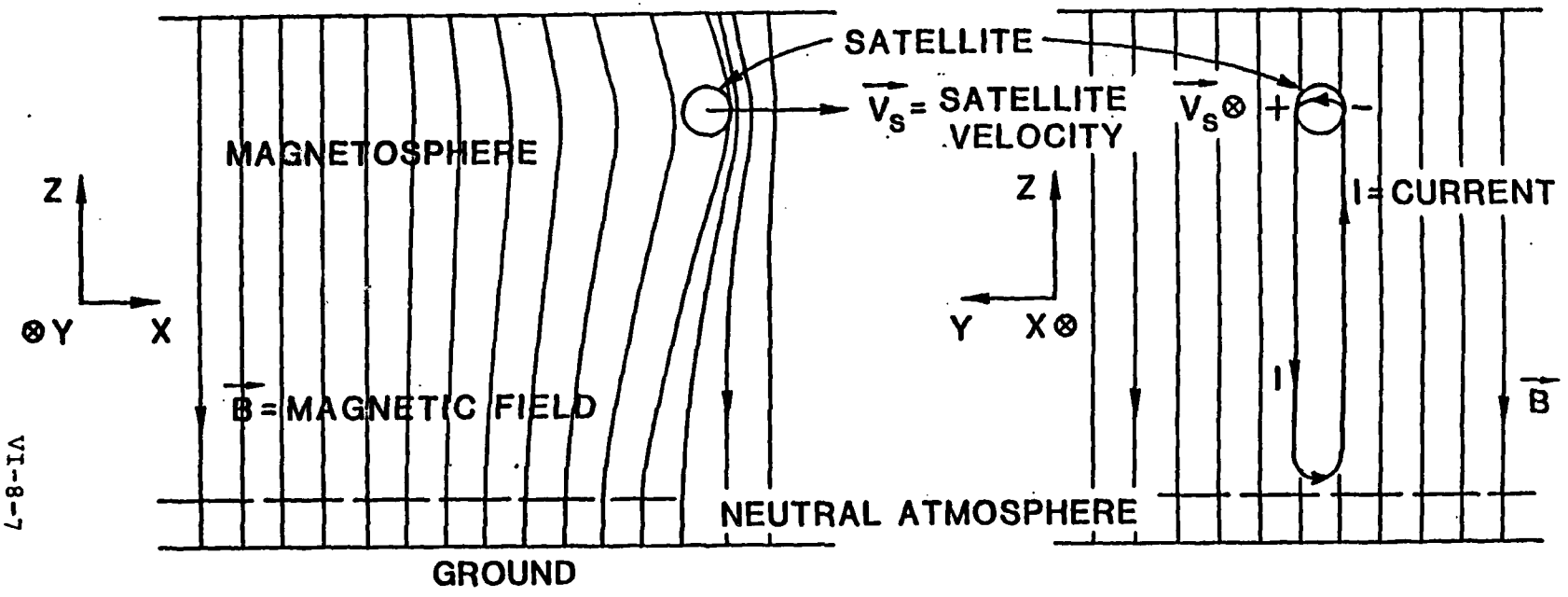

Figure 4

ALFVÉN WAVES CARRY ENERGY AWAY FROM THE SATELLITE AT THE RATE $p(\text{ERGS/SEC}) = (h^2/4\pi)2\pi r^2 V_a$, WHERE h = ALFVÉN FIELD STRENGTH, r = SATELLITE RADIUS, AND V_a = ALFVÉN SPEED.

EXAMPLE: FOR THE ECHO 1 SATELLITE

(r = 15M, ALTITUDE = 1600KM, $V_a = 10^4$ KM/SEC)

$p = 0.5 \times 10^7$ ERGS/SEC = 0.5 WATT

Figure 5 A magnetic moment is induced in a satellite when the magnetic flux, ϕ, (number of magnetic field lines in a certain direction) through a directed cross-sectional area of the satellite (which area is to be understood as being rigidly fixed in the satellite, so that it rotates with the satellite) changes with time, t. The change of ϕ with t can occur when: (i) the satellite is rotating in a uniform magnetic field, (ii) the satellite is not rotating but moves through a spatially non-uniform magnetic field, (iii) i and ii occur simultaneously. In Figure 5, the two drawings on the left (one above the other) illustrate case i. Case ii is illustrated by two subcases, one shown in the two middle drawings and one in the two drawings on the right. The expression for $\dot{\phi} = d\phi/dt$ is given for cases i and ii. By Maxwell's equations a non-zero $\dot{\phi}$ induces a current, i, in the satellite, the current loop being contained entirely within the satellite, in contrast to the Figure 4 case where the current loop extends through, and outside of, the satellite. It is simplest to calculate i when the satellite is ring-shaped. Hence such a satellite was assumed in deriving the expression shown for the induced magnetic moment (i.e., the induced magnetic dipole moment) $\vec{m} = i\vec{A}$. The induced magnetic moment will interact with the geomagnetic field to produce a torque and/or a force on the satellite. The equations for the torque and force on a magnetic moment in the presence of a magnetic field are presented in Peck [1953]. The expressions for $\vec{\tau}$ and $\vec{F}$ assume gaussian-cgs units. Symbols are as follows: $c = 3 \times 10^{10}$cm/sec, a(cm) and r(cm) are radial distances, as shown below, δ(cm) = average skin depth, i.e. the average depth in the satellite's metal surface to which the induced electric field penetrates, σ = conductivity (esu), the area, $\vec{A}$, is in cm^2, the magnetic field $\vec{B}$ is in gauss, ∇ denotes the gradient operator, and $\vec{V}_s$ is in cm/sec.

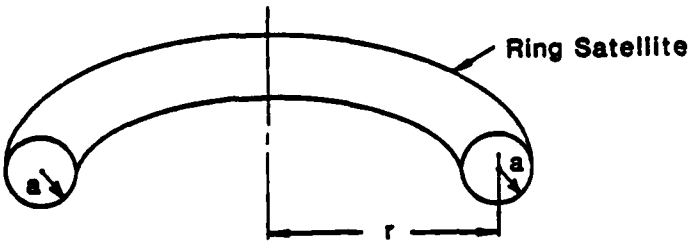

INDUCED MAGNETIC MOMENT ($\vec{m}$)

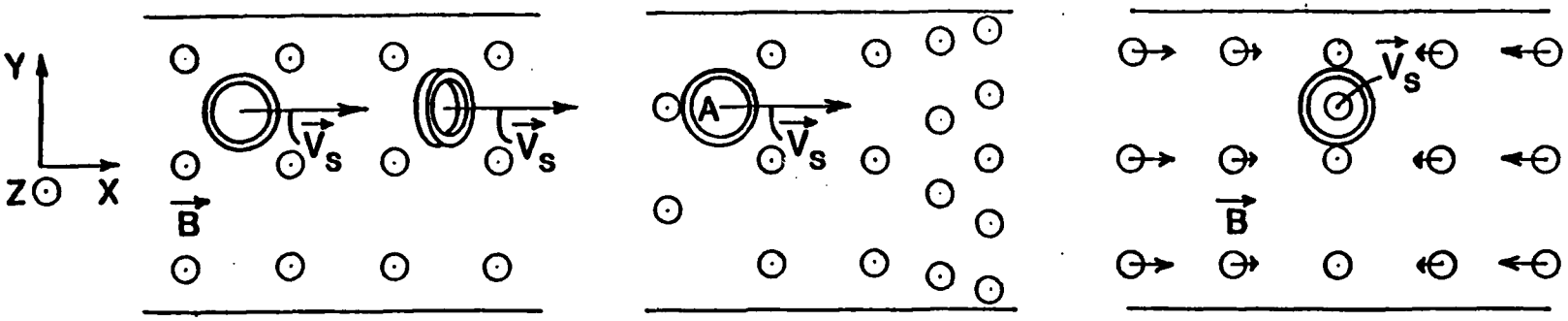

$\vec{V}_S$ = SATELLITE VELOCITY, $\vec{B}$ = MAGNETIC FIELD, $\vec{A}$ = (DIRECTED) AREA OF SATELLITE

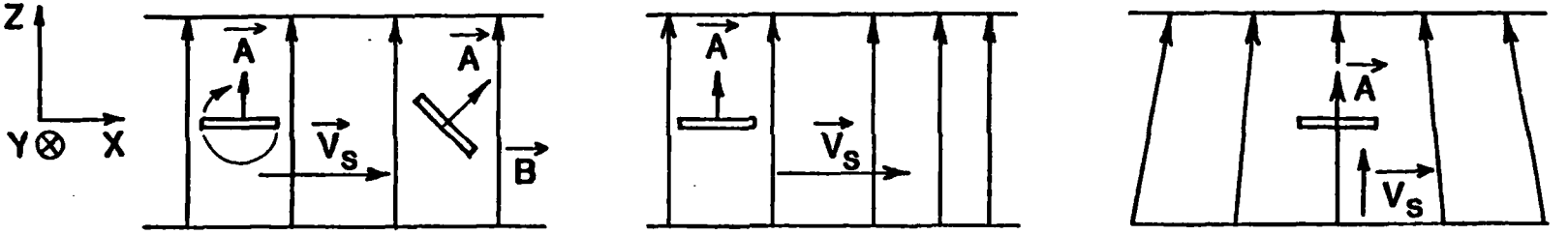

UNIFORM $\vec{B}$ FIELD, SATELLITE ROTATING

$$\dot{\phi} = \vec{B} \cdot \partial\vec{A}/\partial t$$

NONUNIFORM $\vec{B}$ FIELD, SATELLITE NOT ROTATING

$$\dot{\phi} = \vec{A} \cdot (\vec{V}_S \cdot \nabla)\, \vec{B}$$

NONUNIFORM $\vec{B}$ FIELD, SATELLITE NOT ROTATING

$$\dot{\phi} = \vec{A} \cdot (\vec{V}_S \cdot \nabla)\, \vec{B}$$

$\vec{m}$ = INDUCED MAGNETIC MOMENT

$$\text{INDUCED TORQUE ON SATELLITE} = \vec{\tau} = -\frac{a\sigma\delta}{c^2 2r}\left[\vec{B}\cdot\frac{\partial\vec{A}}{\partial t} + \vec{A}\cdot(\vec{V}_S\cdot\nabla)\,\vec{B}\right]\vec{A}\times\vec{B}$$

$$\text{INDUCED FORCE ON SATELLITE} = \vec{F} = (\vec{m}\cdot\nabla)\,\vec{B}$$

Figure 5

REFERENCES

Drell, S.D., H.M. Foley, and M.A. Ruderman, Drag and Propulsion of Large Satellites in the Ionosphere: An Alfvén Propulsion Engine in Space, J. Geophys. Res., Vol. 70, No. 13, p. 3131, July 1, 1965.

Lockheed Missiles and Space Co., Inc., *Laser Power Conversion Systems Analysis, Vol. II*, September 1978.

Peck, E.R., *Electricity and Magnetism*, McGraw-Hill, 1953.

Spitzer, L., Jr., *Physics of Fully Ionized Gases*, Interscience Publishers, 1956.

Walbridge, E.W., Laser Satellite Power Systems, Argonne National Laboratory Formal Report ANL/ES-92, January 1980.

Walbridge, E.W., Laser Satellite Power Systems: Concepts and Issues, *Space Solar Power Review*, Vol. 3, No. 1, 1982.

STATUS OF

THERMOELECTRONIC LASER ENERGY CONVERSION - TELEC

BY

E. J. BRITT

A novel concept known as a Thermo-Electronic Laser Energy Converter (TELEC), has been studied as a method of converting a 10.6 μm CO_2 laser beam into electric power. The calculated characteristics of a TELEC seem to be well matched to the requirements of a spacecraft laser energy conversion system.

The TELEC is a high power density plasma device which absorbs an intense laser beam by inverse bremsstrahlung with the plasma electrons. In the TELEC process, electromagnetic radiation is absorbed directly in the plasma electrons producing a high electron temperature. The energetic electrons diffuse out of the plasma striking two electrodes which are in contact with the plasma at the boundaries. These two electrodes have different areas: the larger one is designated as the collector, the smaller one is designated as the emitter. The smaller electrode functions as an electron emitter to provide continuity of the current. Waste heat is rejected from the collector electrode.

An experiment was carried out with a high power laser at Lewis Research Center using a cesium vapor TELEC cell with 30 cm active length. Laser supported plasma were produced in the TELEC device during a number of laser runs over a period of several days. Electric power from the TELEC was observed with currents in the range of several amperes and output potentials of less than 1 volt. The magnitudes of these electric outputs were smaller than anticipated but consistent with the power levels of the laser during this experiment.

RASOR ASSOCIATES, INC.

FEBRUARY 1982

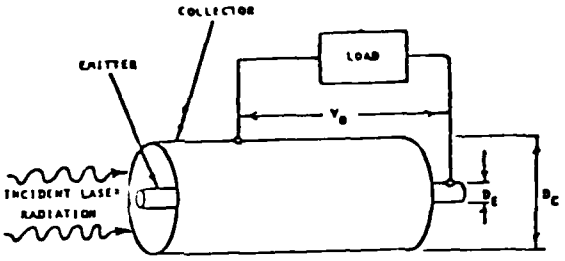

Elementary TELEC configuration

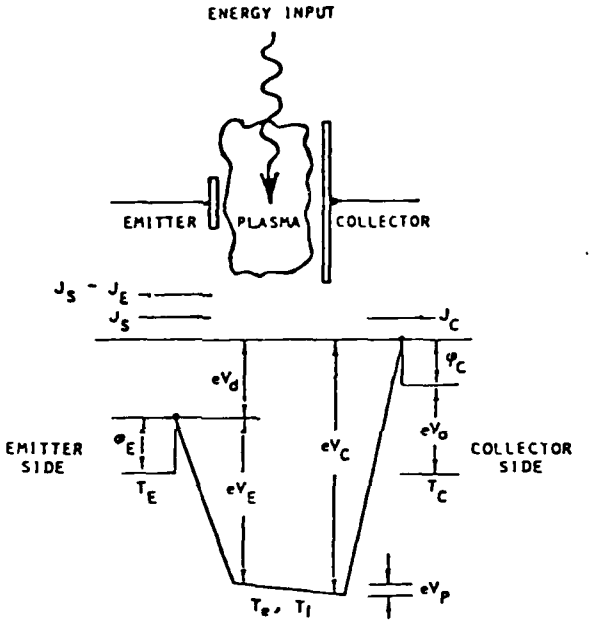

TELEC plasma motive diagram

A conceptual TELEC configuration is shown in the upper figure. The motive diagram for electrons in a TELEC device is shown in the lower figure. Most of the electrons diffusing out of the plasma strike the surrounding collector surface causing it to become negatively charged. Although the current density at the collector is smaller, the total current into the collector is higher because of the larger collector area. This generates an EMF in the external circuit. The TELEC output voltage arises from the difference between the heights of the plasma sheaths, V_E and V_C. Positively charged ions also flow out of the plasma and those striking the collector neutralize part of the output current. However, because the mobility of the ions is much smaller than the mobility of the electrons (for cesium $\mu_i = 1/500\ \mu_e$), and because of ion reflection at the boundaries, the ion currents are small and do not constitute a serious loss.

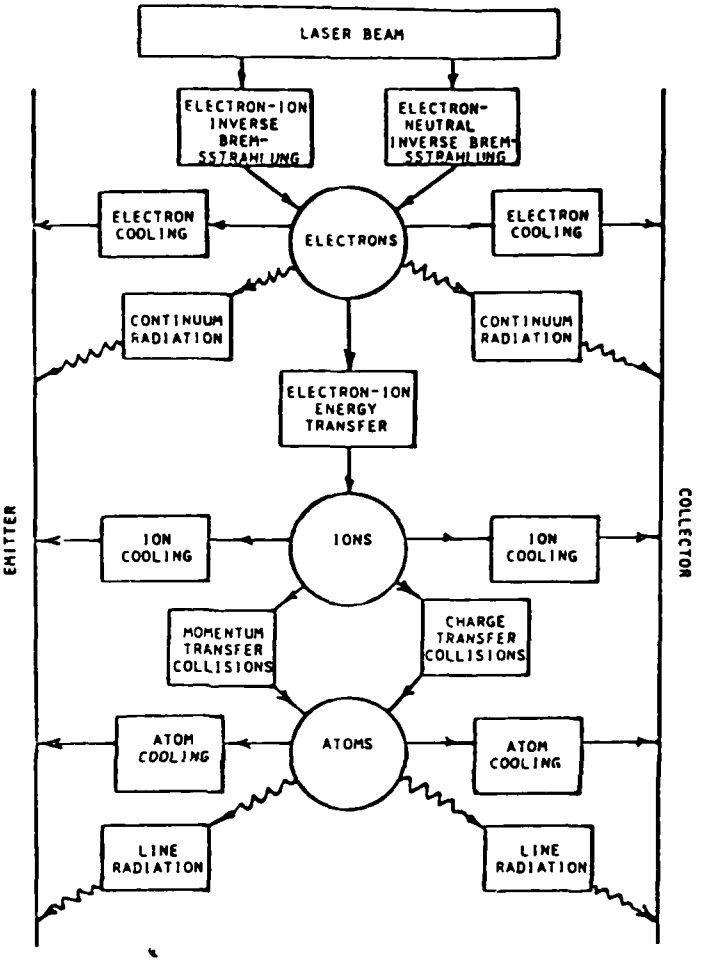

TELEC plasma model

The complete energy balance model which is used in the TELEC calculations is shown diagramatically in the figure. Although all of the energy in the laser beam is first transferred to the plasma electrons, portions of the energy are subsequently transferred to other species of the plasma. The ion temperature rises and reduces power transferred from electrons until an energy balance is reached for the ions. It is necessary to simultaneously calculate an energy balance for all species of the particles in the plasma to determine the ion and electron temperatures. The energy balance also includes losses of particles to the walls. As shown in the figure, the plasma energy balance includes several types of radiation and particle losses. The energy deposited in the emitter is not immediately lost since this energy is returned to the plasma in the form of electron cooling and black body radiation from the emitter. Thermal energy deposited in the collector is a loss which must be removed. The collector would most likely be cooled with a liquid metal loop to the radiator. Waste heat can be removed at ~1000° K.

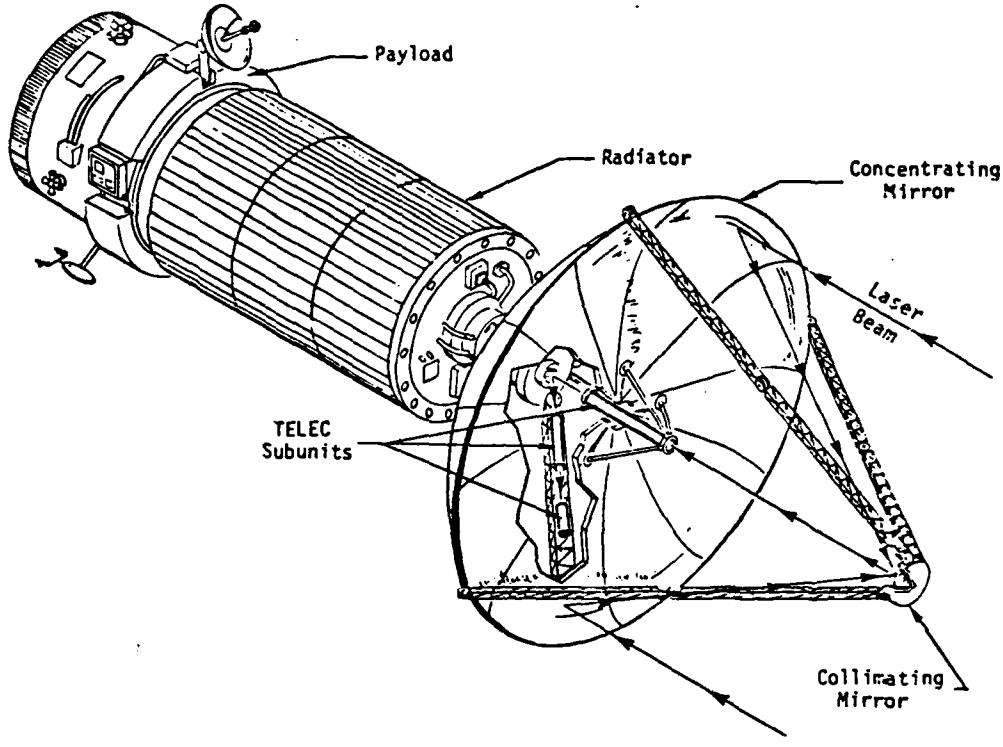

ARTIST'S CONCEPT FOR A TELEC POWERED SPACECRAFT

Characteristics of Series Connected 1 Megawatt TELEC System with Eccentric Emitters

Total Length = 24.5 m
Emitter/Area/Unit Length = .1 cm^2
Collector Area/Unit Length = 2 cm^2
Inner Diameter = 2 cm^2
Outer Diameter = 3 cm^2
Busbar Diameter = 1 cm
Pressure = 800 torr

Number of Subunits = 3
ϕ_C = 1.5 eV
Collector Temperature = 1000°K
Laser H = 0 watt/cm^2
Ion Loss = 0%
Input Beam Power = 1 x 10^6 watts

	SUBUNIT 1	SUBUNIT 2	SUBUNIT 3
Length of Cell (cm)	50	50	50
Number of Cells	30	13	5
Length (m)	15.3	6.6	2.6
Emitter Temperature (°K)	2500	2525	2575
Average Laser Q (W/cm^2)	$2x10^5$	$7.2x10^4$	$2.6x10^4$
Voltage (volts)	890	330	105
Current (A)	310	310	310
Power Absorbed From Beam (W)	$6.3x10^5$	$2.4x10^5$	$9.3x10^4$
Output Power (W)	$2.9x10^5$	$1.0x10^5$	$3.2x10^4$
Waste Heat Flux at Collector (W/cm^2)	37	34	39
Conversion Efficiency (%)	50.4	47.9	37.9

Total Output Power = $4.2x10^5$ W
Overall Efficiency = 42%

Total Current = 310 A
Total Voltage = 1330 V

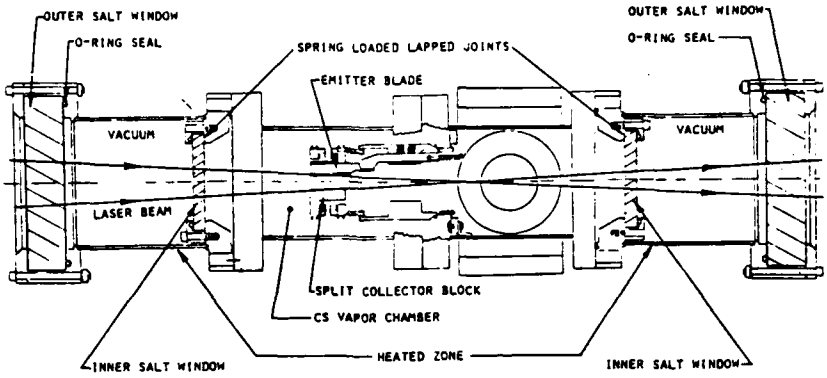

DRAWING SHOWING LOCATION OF TELEC ELECTRODES IN TEST CHAMBER

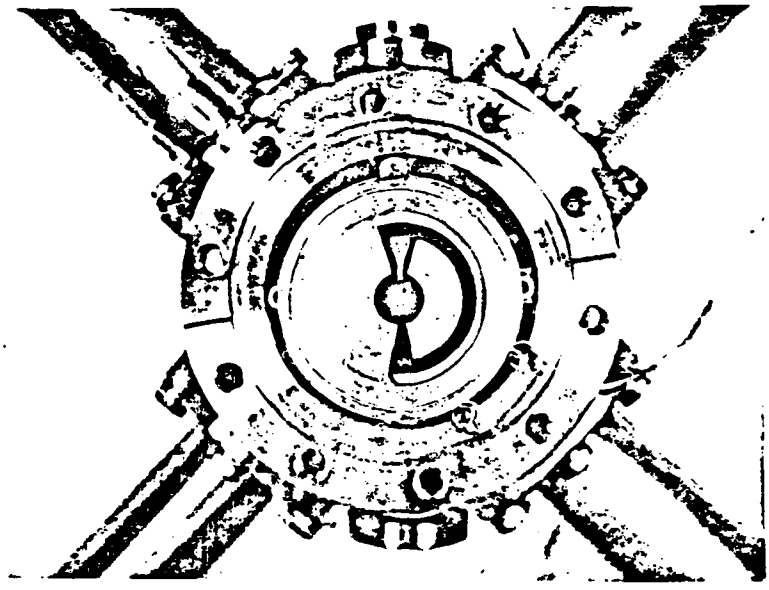

TELEC ELECTRODES (seen from beam input end)

The test chamber and the electrodes of the cesium TELEC experiment at NASA-Ames are shown in these figures. The laser beam entered and exited the device through differentially pumped dual salt optical windows necessitated by an inability to attain a high vacuum seal between NaCl and the support flanges. The beam was focused ($f/12$ optics) into the electrode region which was filled with cesium vapor in the pressure range 2-5 Torr. The electrodes were of 1-cm inner diameter and 2.5 cm in axial length. The emitter was a tungsten blade, 1 mm thick at the tip which protruded 1.1 mm into the 1-cm annular opening. The molybdenum collector presented a greater effective surface area to the plasma by approximately a factor of 10.

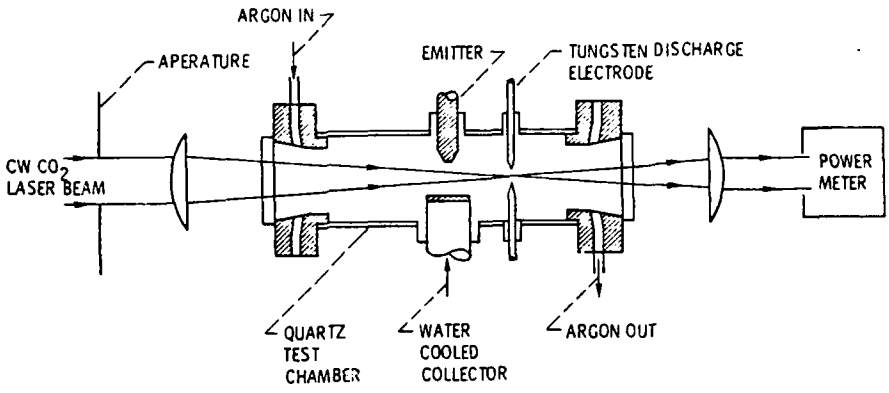

EXPERIMENTAL SET-UP SHOWING CHAMBER ASSEMBLY AND OPTICS

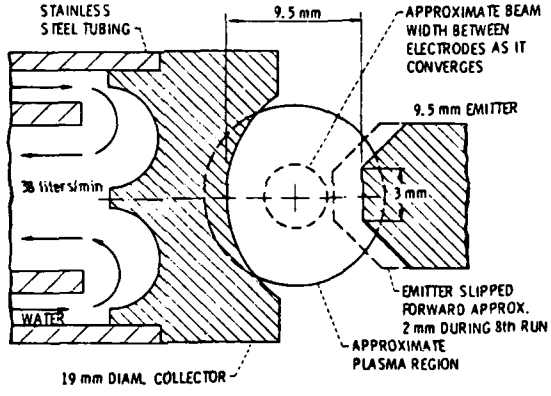

ENLARGED SECTIONAL VIEW OF EMMITER AND COOLED COLLECTOR

The test chamber and electrodes for an Ar gas TELEC experiment, performed at LeRC, are shown in these figures. The electrodes are two opposed rods: one with a pointed end, and the other with a concave end, which is water cooled. the argon pressure during operation was 800 Torr. The plasma was initiated by a spark between the tungsten discharge electrodes and sustained by the laser beam. A "tear drop shaped" plasma volume, 1.2 to 1.5 cm in diameter and 4 to 5 cm long, was formed. The lenses were then moved to transport the plasma between the emitter and the collector.

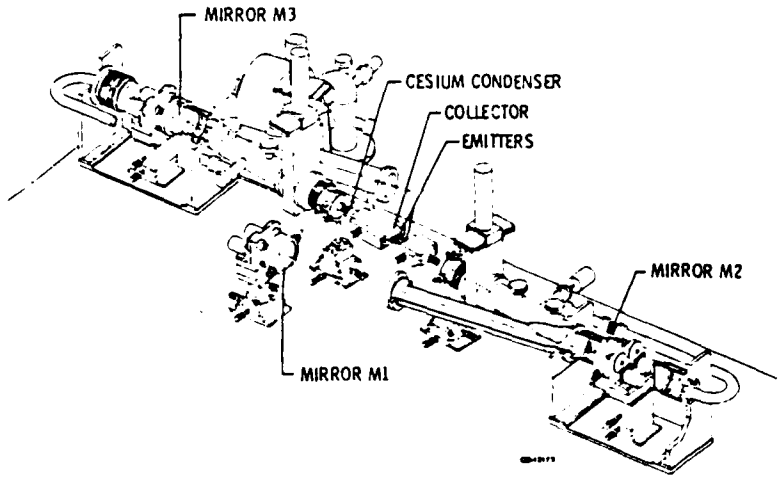

THE SYSTEM USED IN THE LeRC TELEC EXPERIMENT

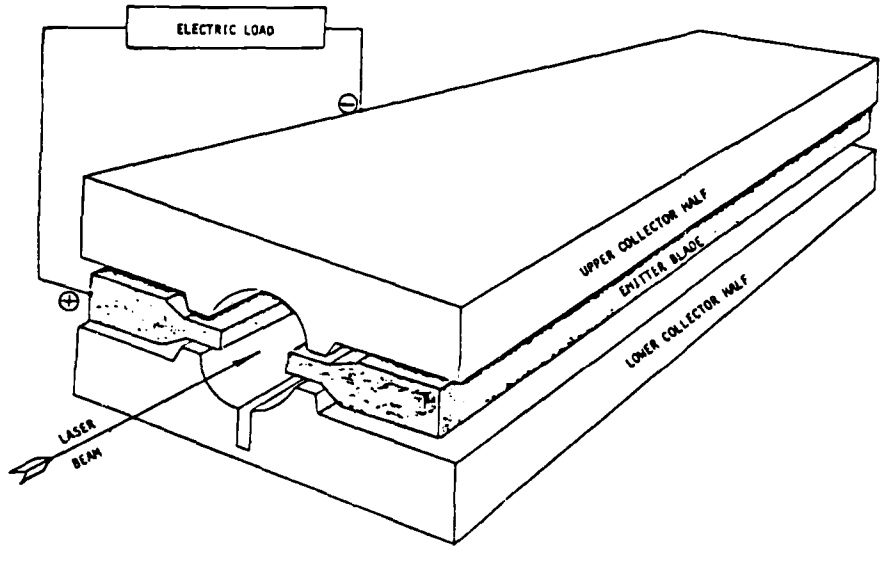

SCHEMATIC REPRESENTATION OF THE ELECTRODES IN THE LeRC TELEC EXPERIMENT

The optical system and the electrodes used in the NASA-LeRC TELEC experiment are shown in these figures. The optical set-up produces a narrow,parallel laser beam and directs it through the TELEC apparatus. The TELEC active section is coupled between two inert gas filled end chambers, which have high power laser mirrors at each end. There are zinc selenide windows on the ends of oblique mounted tubes which permit the laser beam to enter and exit the test apparatus.

TELEC EXPERIMENTS

- AMES EXPERIMENT WITH Cs VAPOR
  - -Cs REACTION "FROSTED" NaCl WINDOWS
  - -ELECTRIC OUTPUTS OBSERVED (2-8 AMPERES AT 1 TO 4 VOLTS)
  - -DATA UNCERTAIN
- LeRC EXPERIMENT WITH Ar GAS
  - -SMALL ELECTRIC OUTPUT (0.1 AMPERE AT 1/2 VOLT)
  - -FOCUSED LASER BEAM (5 kW) PRODUCED STABLE PLASMA
  - -NON-OPTIMUM GEOMETRY AND PLASMA GAS
- LeRC EXPERIMENT WITH Cs VAPOR
  - -PARALLEL LASER BEAM (8-10 kW)
  - -GAS BUFFERED HEAT PIPE WINDOWS
  - -ELECTRIC OUTPUT (SEVERAL AMPS AT <1 VOLT) CONSISTENT WITH CALCULATED PREDICTIONS FOR LOW POWER LASER INPUT
  - -GREATER LASER POWER NEEDED TO OPERATE AT DESIGN CONDITIONS

TELEC CURRENT PERSPECTIVE

- GOOD CALCULATED PERFORMANCE AS A LASER ENERGY CONVERTER
  - -CALCULATED EFFECIENCIES >40%
  - -HIGH HEAT REJECTION TEMPERATURE
- ALL EXPERIMENTS TO-DATE HAVE YIELDED POSITIVE, BUT NOT DEFINITIVE RESULTS
- FURTHER EXPERIMENTATION WITH HIGHER LASER POWER NEEDED TO DEFINITIVELY CHARACTERIZE THE TELEC PERFORMANCE POTENTIAL
- OPERATION WITH LASER BEAM ABSORBTION MECHANISMS OTHER THAN INVERSE BREMSSTRAHLUNG SHOULD BE STUDIED
  - -Cs_2 DIMER ABSORBTION
  - -SUPERELASTIC COLLISIONS (SELEC)
  - -CESIUM LINE RADIATION ABSORPTION

LASER TRANSMITTER

- HIGH POWER LASER NEEDED
- LASER WAVELENGTH WITH TRANSMISSION THROUGH SAPPHIRE WINDOWS DESIRABLE (1 TO 5 μ)

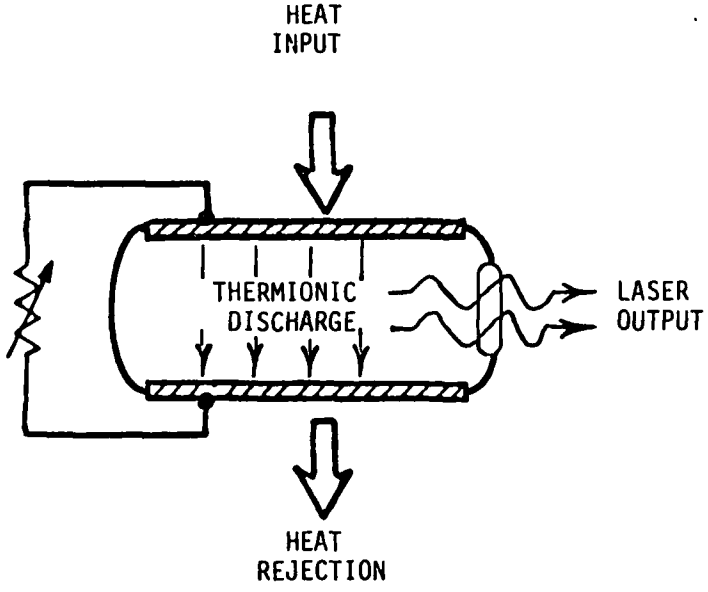

CESIUM THERMIONIC LASER

-DIRECT HEAT TO LASER OUTPUT

-POTENTIALLY HIGH POWER DENSITY AND HIGH EFFECIENCY

-NO CONSUMABLES

-HIGH HEAT REJECTION TEMPERATURE

-LASER BEAM EASILY ABSORBED BY A CESIUM TELEC RECEIVER

Q & A - W. J. Britt

From: P. J. Turchi, R & D Associates

I don't believe you mentioned the actual mechanism of converting hot electrons in electricity. Is the basic effect ∇T or ∇N_e or does it require $\nabla N_e \times \nabla T$?

A.

TELEC works because one electrode emits electrons and is small so it collects very few electrons. The other electrode is cooled (heat rejection) and cannot emit electrons; it has a large area and collects a large current of elelectrons from the plasma. In the interior of the plasma ∇N and ∇T controlled by ambipolar diffusion and heat balance.

From: D. Woodall, University of New Mexico

Inverse bremsstrahlung absorption is not 100% efficient, but depends on density profile, etc. in plasma. Have you calculated total absorption efficiency for your parameters?

A.

Inverse Bremsstrahlung (IB) calculated by methods of J. W. Stallcup and K. I. Bellman. Both electron-ion and electron-atom IB is active. Plasma density $\approx 10^{16}$ cm^{-3}

$T_e \approx 20{,}000$ K

DIRECT CONVERSION
OF INFARED RADIANT ENERGY
FOR SPACE POWER APPLICATIONS

R. FINKE

ABSTRACT

Conventional solar array and battery systems impose severe system design considerations and mass penalties on spacecraft, especially those designed for operation in low earth orbits.

The earth reradiates a preponderance of the solar energy it receives as infrared radiation principally at 10 microns.

A proposed technology to convert the earth radiant energy for spacecraft power is presented. The resultant system would eliminate energy storage requirements and simplify the spacecraft design.

This effort is based on prior work which demonstrated conversion of R.F. energy to D.C. power at 10 cm wavelength with an efficiency of 85%.

TYPICAL POWER SYSTEM

A typical power system for earth orbital space craft consists of a solar array system, fixed in inertial space, pointed towards the sun, a rotary power transfer device which conducts the array power across a rotating point to the space craft, power processing for load power conditioning and battery charging and a battery system for energy storage. Since the solar array must stay fixed pointing towards the sun, the space craft body must be rotated to maintain earth orientation and be controlled by a propulsive system to maintain its and the solar array's attitude.

TYPICAL SPACE POWER SYSTEM

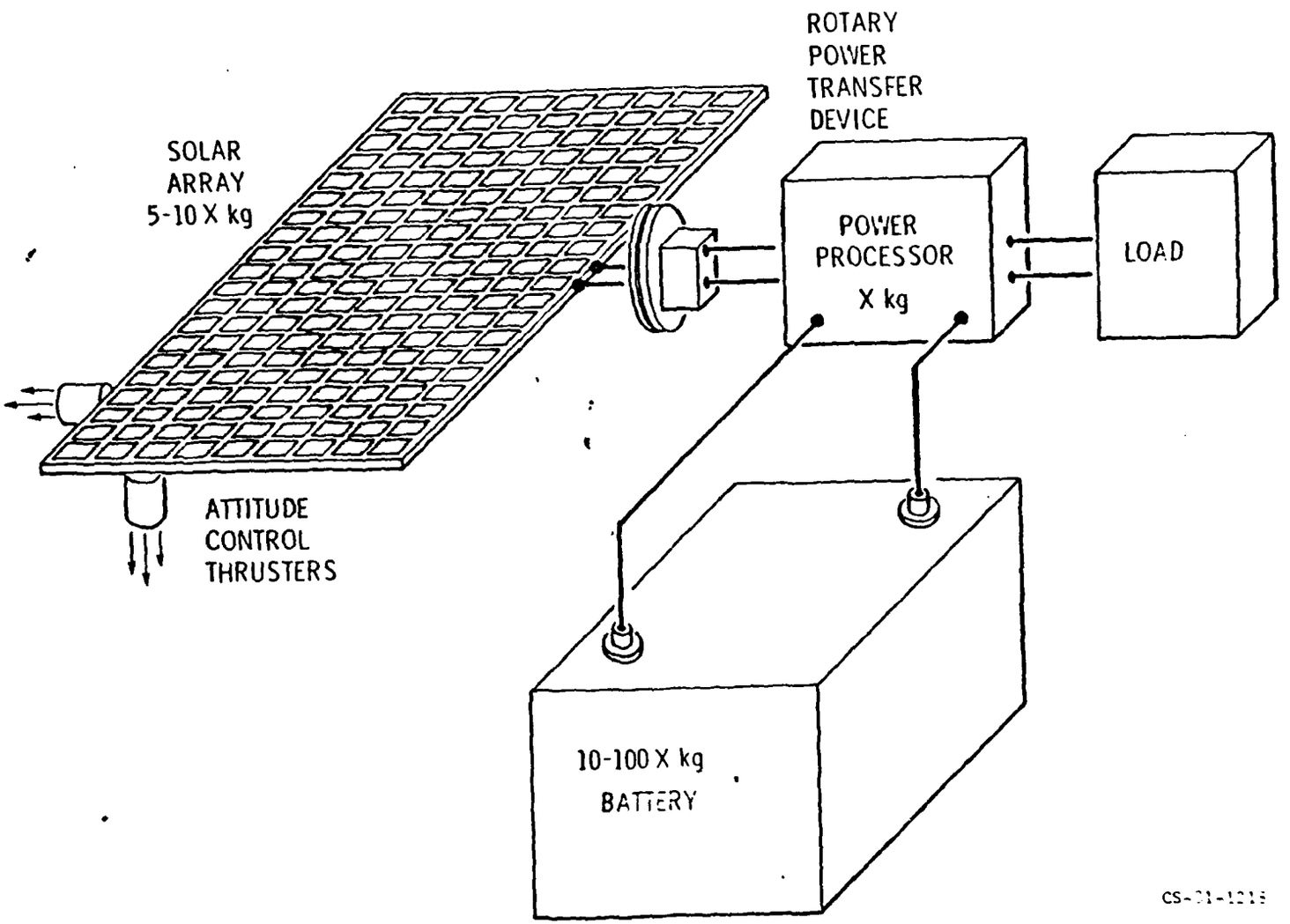

RELATIVE WEIGHTS ON A SPACE POWER SYSTEM

In almost all contemporary space power systems, except those in sun synchronous orbits, the energy storage system, the batteries, are the single heaviest component and often times drive the system with respect to life, duty cycle and maximum power available.

RELATIVE WEIGHTS ON A SPACE POWER SYSTEM

*BATTERIES	- 50kg/kw
*SOLAR ARRAYS	- 10kg/kw
*POWER PROCESSING	- 5kg/kw
*LOADS	- 1-10kg/kw

CS-81-1197

THE SUN AS A POWER SOURCE

The curve on the facing page is an idealized one, assuming the sun to be an $8000^{0}K$ blackbody. Applying Wein's displacement law a peak at 0.36 microns is obtained. Actual data from ground and airplane tests have indicated that the suns intensity at the center of its disk could be approximated by a smooth $7200^{0}K$ continuum with superimposed Fraunhofer absorbtion. For the longer wavelengths the solar irradiance is effectively that of a $6000^{0}K$ blackbody. For the purpose of this presentation, however, this idealized curve will serve to illustrate the general output characteristic of the sun.

THE SUN AS A POWER SOURCE

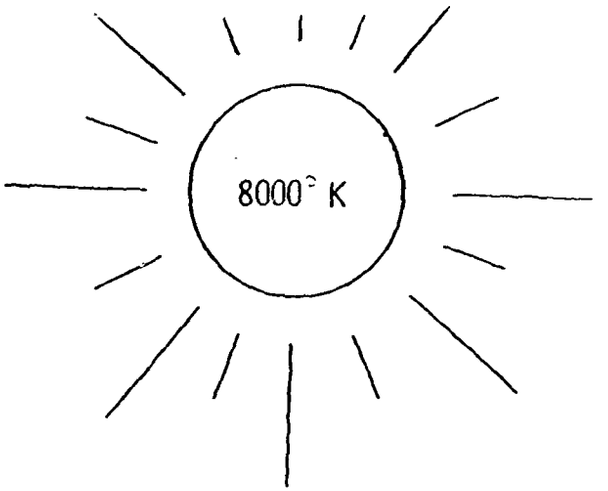

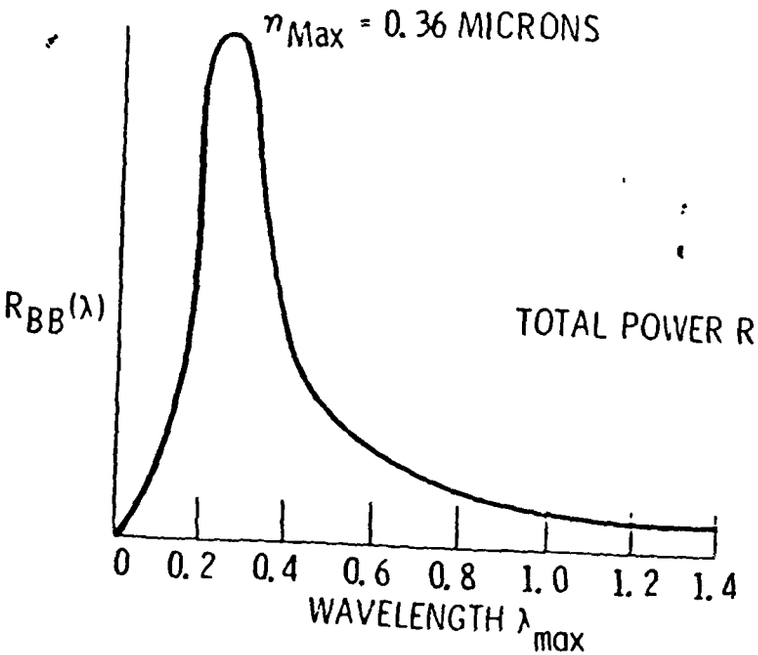

TOTAL POWER $R_{BB} \cong 0.14$ WATTS/cm^2 AT 1 AU

CS-71-1322

REDISTRIBUTION OF SUN'S ENERGY ON EARTH

Since the earth is in thermal equilibrium all the incident energy falling on it from the sun must either be converted or reradiated back to space. Some of the solar energy is simply reflected back to space, visual albedo, the rest is absorbed and reradiated at a much lower wave length, uniformly from the entire surface of the earth. In a near equatorial orbit around the earth, this reradiated energy is remarkably constant from the sun lit to the dark side of the earth.

REDISTRIBUTION OF SUN'S ENERGY ON EARTH

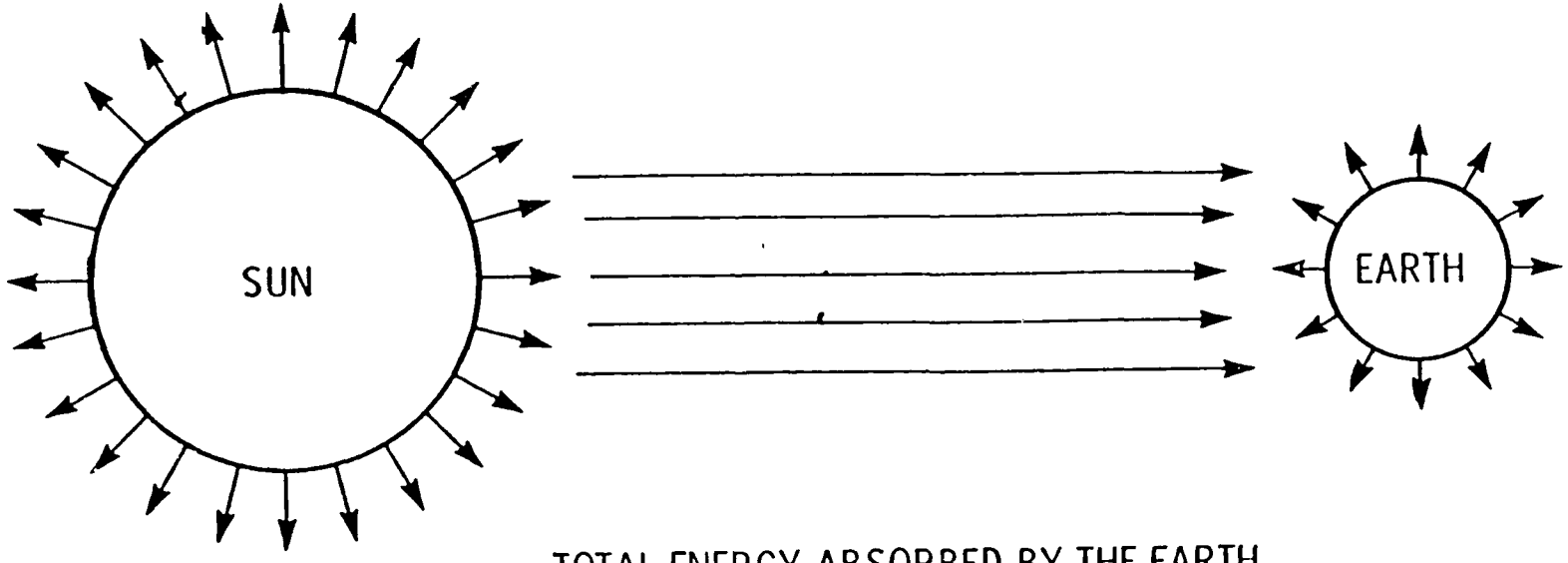

TOTAL ENERGY ABSORBED BY THE EARTH
≅ TOTAL ENERGY RADIATED (EARTH ALBEDO)

$$\pi R_E^2 I_{SUN} = 4\pi R_E^2 I_{ALBEDO}$$

$$I_{ALBEDO} \approx \frac{I_{SUN}}{4}$$

EARTH ALBEDO INFRARED SPECTRUM

This again is an idealized curve of reradiated energy from the earth. The earth is an approximately 290^{0}K blackbody. Again using the Wein displacement law, an energy distribution is calculated with a peak occurring at approximately 10 microns. To first order the power reradiated from the earth's surface is approximately 400 watts/m^{2}. Actual measurement have shown that there is absorbtion of some of this energy by the earths atmosphere, but again, this curve is adequate to illustrate that a surprising amount of energy is available as reradiated energy from the earth.

EARTH ALBEDO INFRARED SPECTRUM

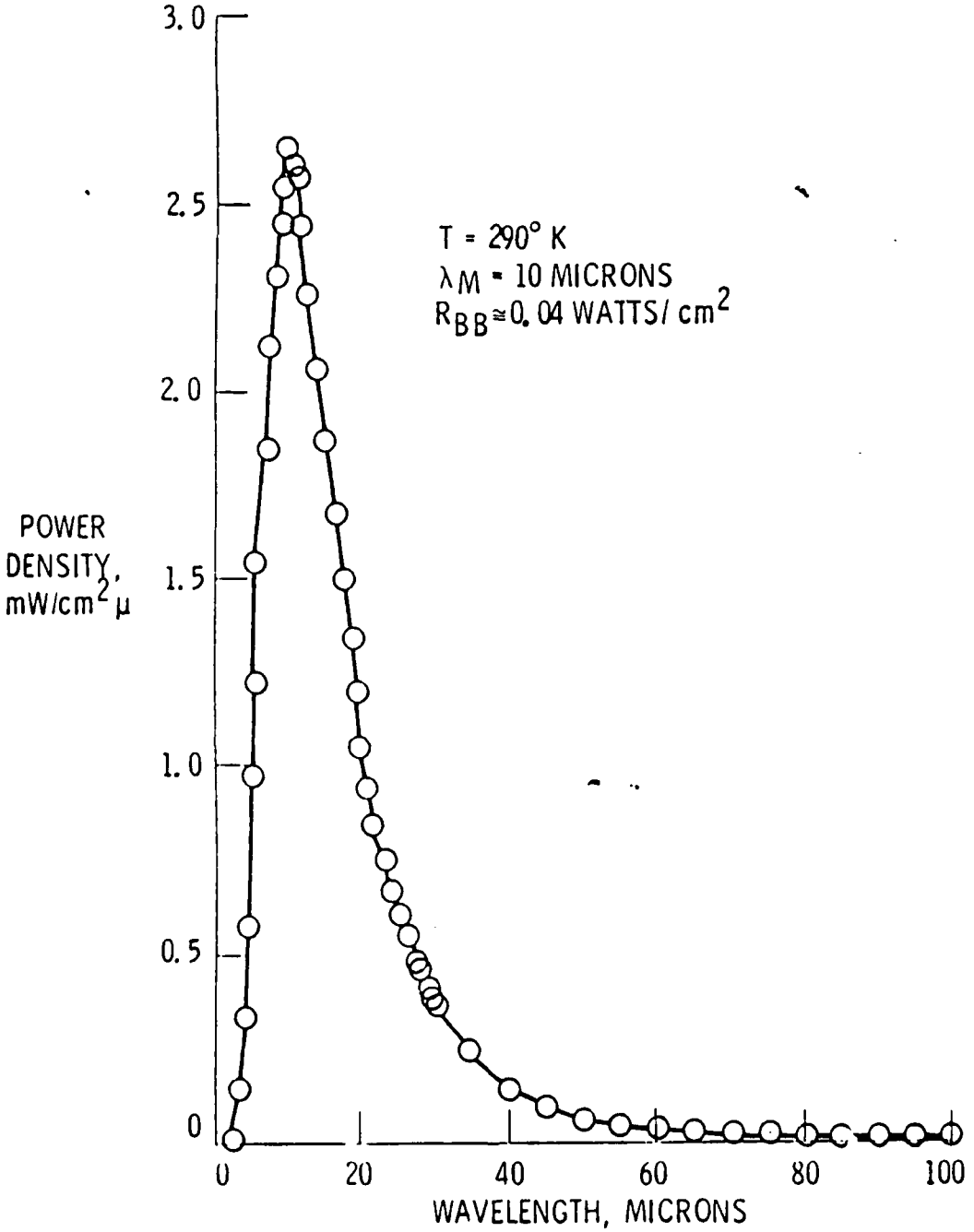

CS-81-1323

SPACECRAFT CONFIGURATION

Most earth orbital spacecraft maintain their attitude to point one surface toward the earth. Photovoltaic power sources require tracking the sun with the solar array panels. Using energy radiated from the earth's surface allows a simplification of the design of the spacecraft. Since the energy conversion devices always point towards the earth below, no articulation, tracking or drive systems are required, simple gravity gradiant stabilization techniques will suffice. Since the energy available is constant, no energy storage is required, eliminating batteries, charging equipment, etc.

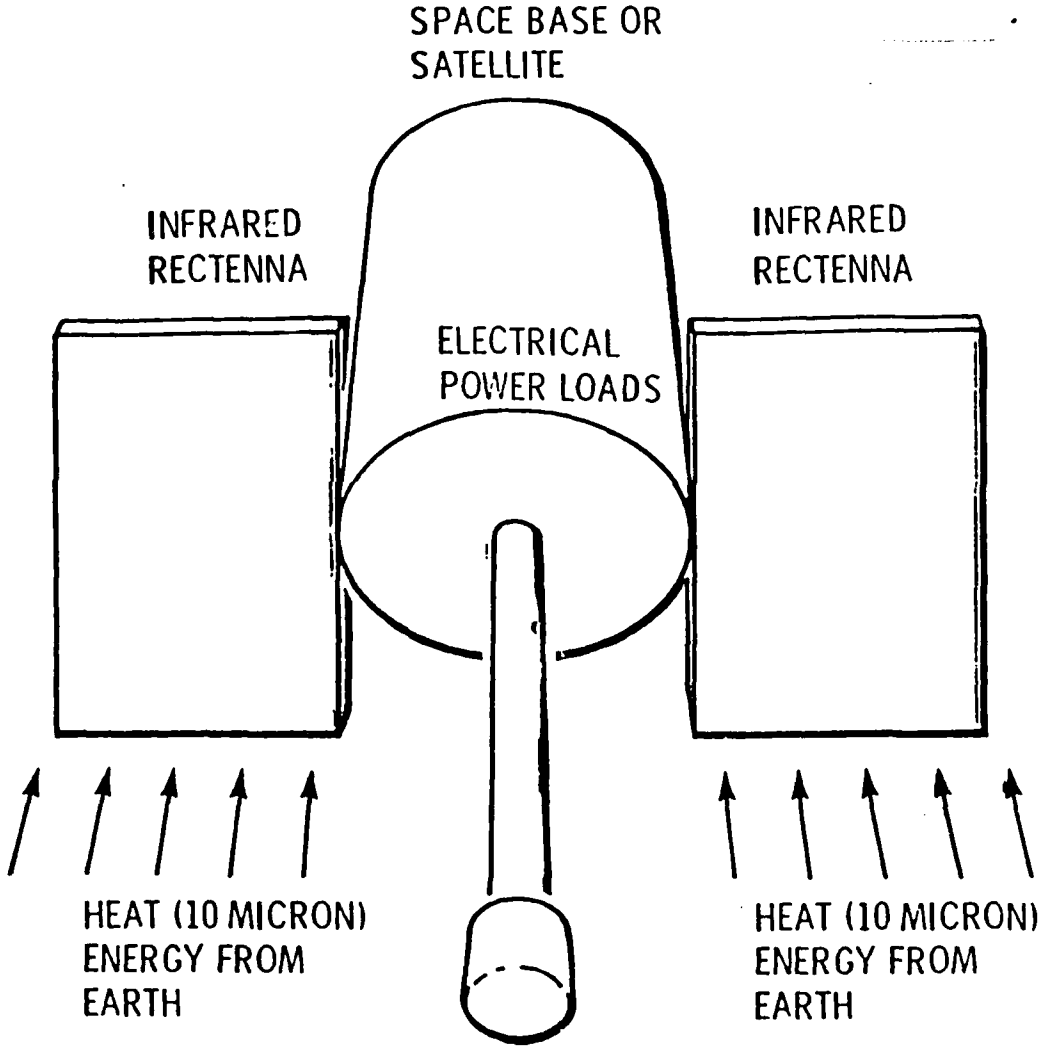

CS-31-1217

VI-10-13

POWER SYSTEMS WEIGHT ESTIMATE

Elimination of energy storage requirement permits marked reduction in over all spacecraft system mass. The comparison shown typifies the savings that could result.

POWER SYSTEM WEIGHT ESTIMATE COMPARISON BETWEEN SOLAR ARRAY/BATTERY SYSTEMS AND EARTH ALBEDO/RECTENNA SYSTEMS

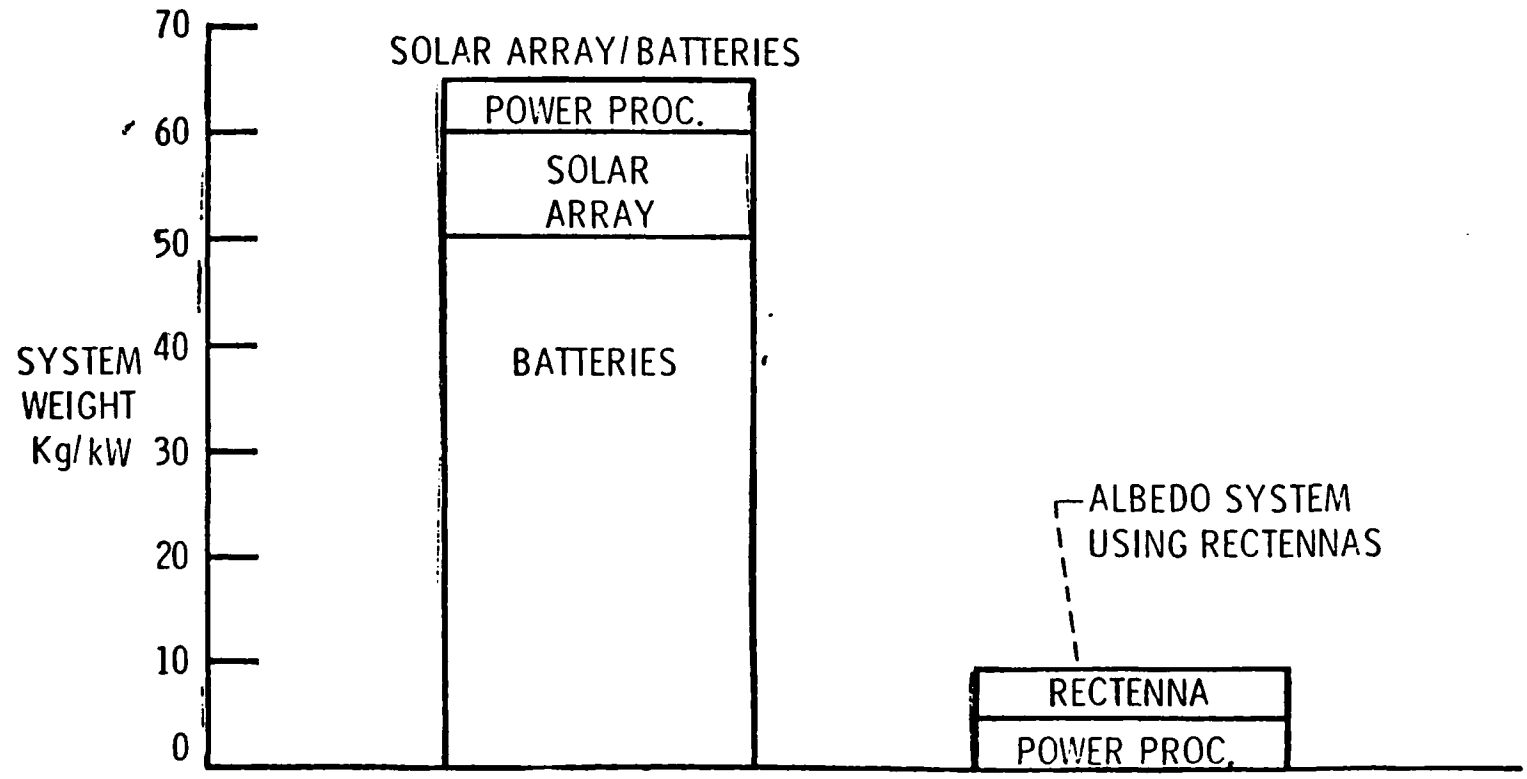

VI-10-15

CS-81-132

SIMPLIFIED ELECTRICAL SCHEMATIC FOR THE RECTENNA ELEMENT

The device shown, a rectenna, was built originally for a ground based array to convert 2.5 ghz power beamed down from a spacecraft in geosynchonous orbit. It is essentially a half wave dipole with associated filters and rectification to convert the R.F. energy to a D.C. output. Measurements of system efficiency indicated a conversion of 85% of incident R.F. energy to D.C. output. Recent developments have demonstrated that this technology can be produced as light weight, deployable printed circuit arrays with no loss of conversion efficiency.

SIMPLIFIED ELECTRICAL SCHEMATIC FOR THE RECTENNA ELEMENT

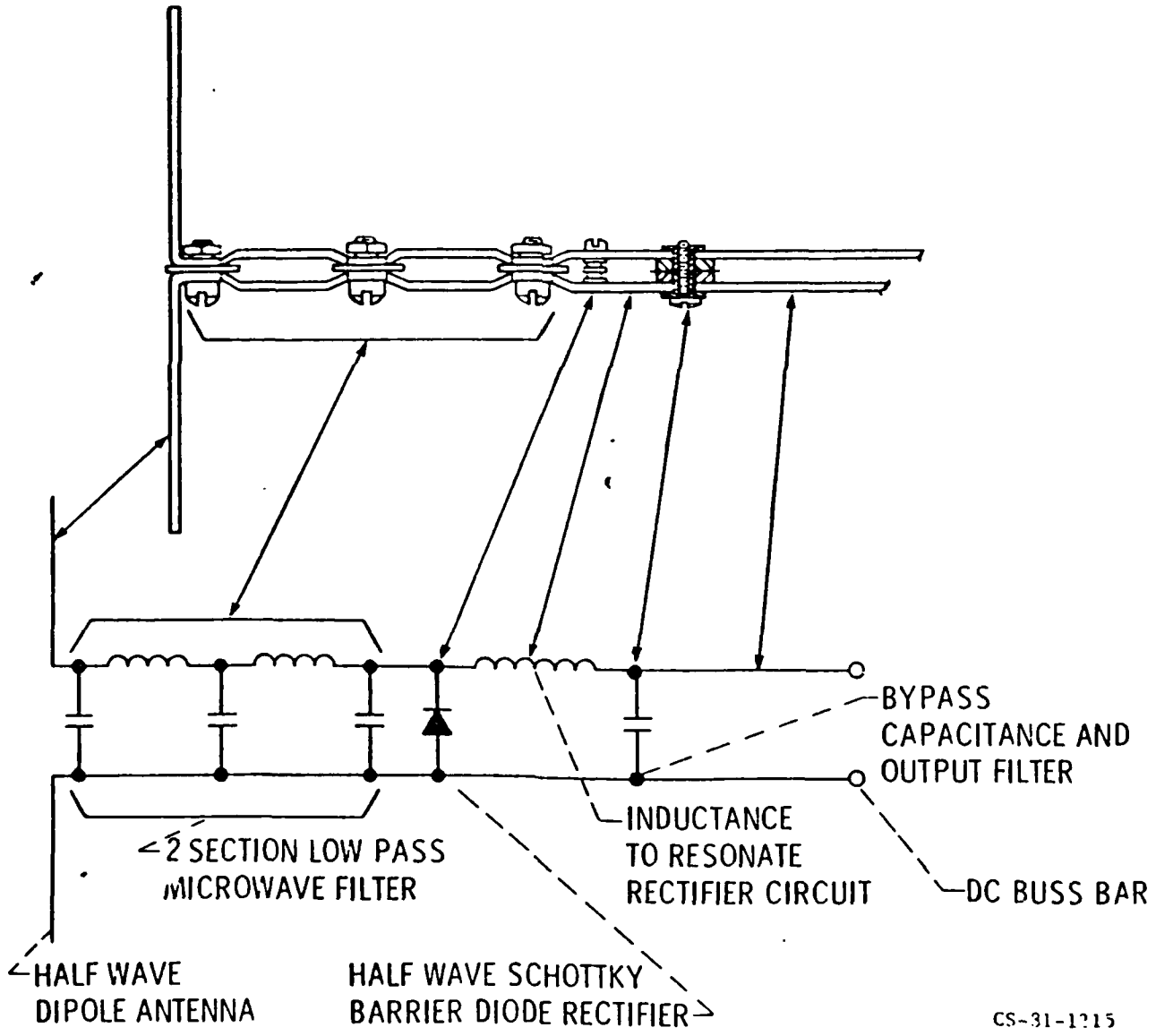

CS-31-1215

IR RECTENNA

A rectenna, designed to operate at 10 microns wavelength, could convert the earth's thermal radiant energy to D.C. power for spacecraft.

Since the technology under development is not that of a heat engine it does not depend on the temperature differential between the source and receiver to achieve its performance. As long as the rectenna is not radiating energy at the same frequency that it is receiving, then the device will produce power. An operating rectenna, one producing power, will be cooler than one orbiting quiescently, since energy is being removed and transferred to the load.

IR RECTENNA ENERGY BALANCE

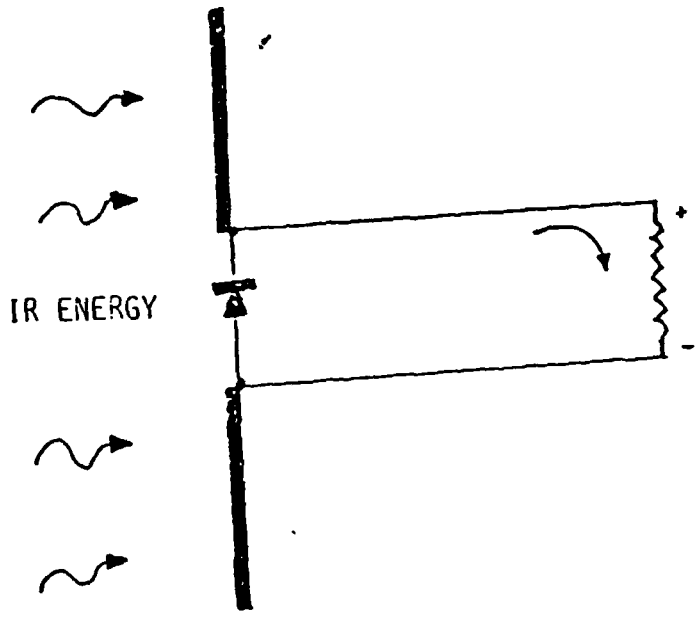

- DIRECT CONVERSION (RECTIFICATION) OF ELECTROMAGNETIC ENERGY INTO ELECTRICAL ENERGY.
- NOT A THERMAL ENGINE (NO CARNOT LIMIT ON EFFICIENCY).
- OBEYS FIRST LAW OF THERMODYNAMICS (CONSERVATION OF ENERGY).

IR RECTENNA ENERGY BALANCE (Cont'd)

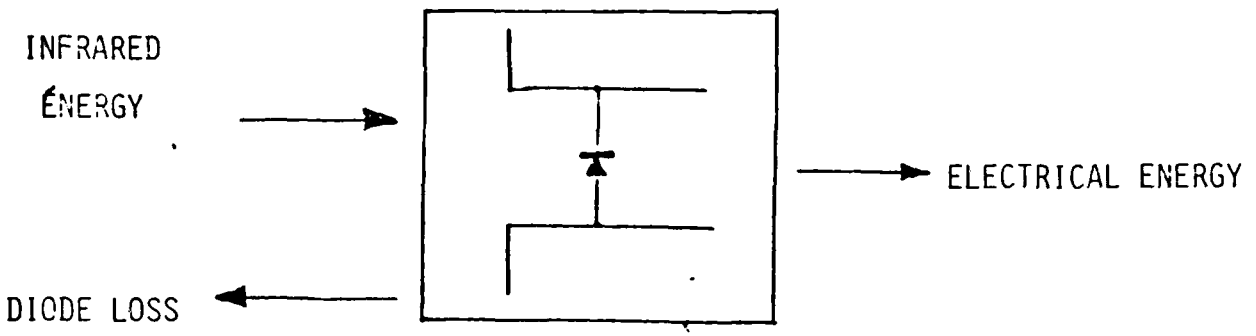

- SINCE ENERGY IS CONSERVED, THE RECTENNA IS COOLED BY THE REMOVAL OF ELECTRICAL ENERGY.

- A COOLER RECTENNA SATISFIES THE SECOND LAW OF THERMODYNAMICS (HEAT FLOWS FROM HOT TO COLD).

- THEREFORE THE INFRARED ANTENNA IS NOT A PERPETUAL MOTION DEVICE.

TECHNOLOGY STATUS

- o FERTILE TECHNOLOGY BASE AVAILABLE.
- o ELECTRON BEAM LITHOGRAPHY TECHNIQUES ARE AVAILABLE WITH THE RESOLUTIONS OF THE RIGHT ORDER OF MAGNITUDE.
- o SEMICONDUCTORS ARE AVAILABLE WITH APPARENT SENSITIVITIES WITHIN ONE ORDER OF MAGNITUDE (1975 TECHNOLOGY BACK DIODES).
- o EXTENSIVE DOD EFFORTS IN INFRARED OPTICS.
- o NO INSURMOUNTABLE TECHNICAL PROBLEMS EVIDENT AT THIS TIME.

Q & A - R. C. Finke

From: P. J. Turchi, R & D Associates

What is the effect of the random phase distribution of the 10μ radiation from earthshine (vs the coherent radiation from a 10μ laser) on rectenna operation?

A.

Rectification of Coherent Radiation from a 10μ laser should be easier and done more efficiently than that of earth radiation. A rectenna to convert earth radiation will have to be broad band, as omni directional as possible, coupled, hopefully, with high gain.

From: Steve Wax, AFOSR

What is the power (at 85% efficiency) that can be produced? Also, does a cloudy region over the earth cause a significant decrease in available power?

A.

The power level is limited by heating of the recifier diode. We have not calculated what maximum powers could be converted by cooling the devices with heat pipes or cooling fluids.

Clouds do not have an appreciable effect on the total radiation output.

THE PHOTOTRON: A LIGHT TO R.F. ENERGY CONVERSION DEVICE

BY

JOHN W. FREEMAN AND SEDGWICK SIMONS

DEPARTMENT OF SPACE PHYSICS AND ASTRONOMY
RICE UNIVERSITY, HOUSTON, TX 77251

ABSTRACT

THE PHOTOTRON IS A PHOTOELECTRIC DEVICE THAT CONVERTS LIGHT TO RADIO FREQUENCY ENERGY. IT IS A VACUUM TUBE, FREE ELECTRON, DEVICE THAT IS MECHANICALLY SIMILAR TO A REFLEX KLYSTRON WITH THE HOT FILAMENT CATHODE REPLACED BY A LARGE AREA PHOTOCATHODE. THE DEVICE CAN OPERATE EITHER WITH AN EXTERNAL VOLTAGE SOURCE USED TO ACCELERATE THE PHOTOELECTRONS OR WITH ZERO BIAS VOLTAGE; IN WHICH CASE THE PHOTOKINETIC ENERGY OF THE ELECTRONS SUSTAINS THE R.F. OSCILLATIONS IN THE TUNED R.F. CIRCUIT.

TO DATE, WE HAVE TESTED ONE BASIC DESIGN OF THE PHOTOTRON. WE HAVE OBTAINED FREQUENCIES AS HIGH AS ABOUT 1 GHz AND AN OVERALL EFFICIENCY OF ABOUT 1% IN THE BIASED MODE. IN THE UNBIASED MODE, THE FREQUENCIES OF OPERATION AND EFFICIENCIES ARE CONSIDERABLY LOWER. SUCCESS WITH TEST MODEL SUGGESTS THAT CONSIDERABLE IMPROVEMENTS ARE POSSIBLE THROUGH DESIGN REFINEMENTS. ONE SUCH DESIGN REFINEMENT IS THE REDUCTION OF THE LENGTH OF THE ELECTRON FLIGHT PATH. TESTS ON SUCH A REDUCED SCALE DEVICE ARE UNDERWAY.

THE PHOTOTRON

- A DEVICE THAT CONVERTS SUNLIGHT OR LASER LIGHT DIRECTLY TO R.F.
- IT IS A VACUUM TUBE, PHOTOELECTRIC, FREE ELECTRON DEVICE.
- SIMILAR IN CONCEPT TO A REFLEX KLYSTRON WITH THE HOT FILAMENT REPLACED BY A PHOTOCATHODE.
- OPERATES EITHER BIASED OR UNBIASED.
- APPLICATIONS: LIGHT TO R.F. ENERGY CONVERSION OR COMMUNICATIONS VIA MODULATED LASER BEAM DECODING.

FIGURE 1

SCHEMATIC DIAGRAM OF THE PHOTOTRON LARGE DIMENSION PHOTOTRON. PHOTOELECTRONS EJECTED FROM THE PHOTOCATHODE PASS THROUGH THE GRIDS ON WHICH AN R.F. FIELD EXISTS. (THE CAPACITANCE OF THE GRIDS AND AN EXTERNAL INDUCTOR OR RESONANT CAVITY FORM A RESONANT CIRCUIT). A R.F. FIELD EXISTS IN ALL THREE REGIONS OF THE TUBE, HENCE THE ELECTRONS ARE CONTINUALLY EXCHANGING ENERGY WITH THE FIELD. THE DIMENSIONS AND VOLTAGES CAN BE ADJUSTED SO THAT THERE IS A NET ENERGY TRANSFER FROM THE ELECTRONS TO THE FIELD, THUS PROVIDING THE ENERGY TO SUSTAIN FREE OSCILLATIONS. THERE ARE TWO PRINCIPAL MODES OF OPERATION IN WHICH THIS ENERGY TRANSFER IS MAXIMIZED, THESE ARE CALLED THE MULTI-PASS MODE AND HALF-CYCLE MODE.

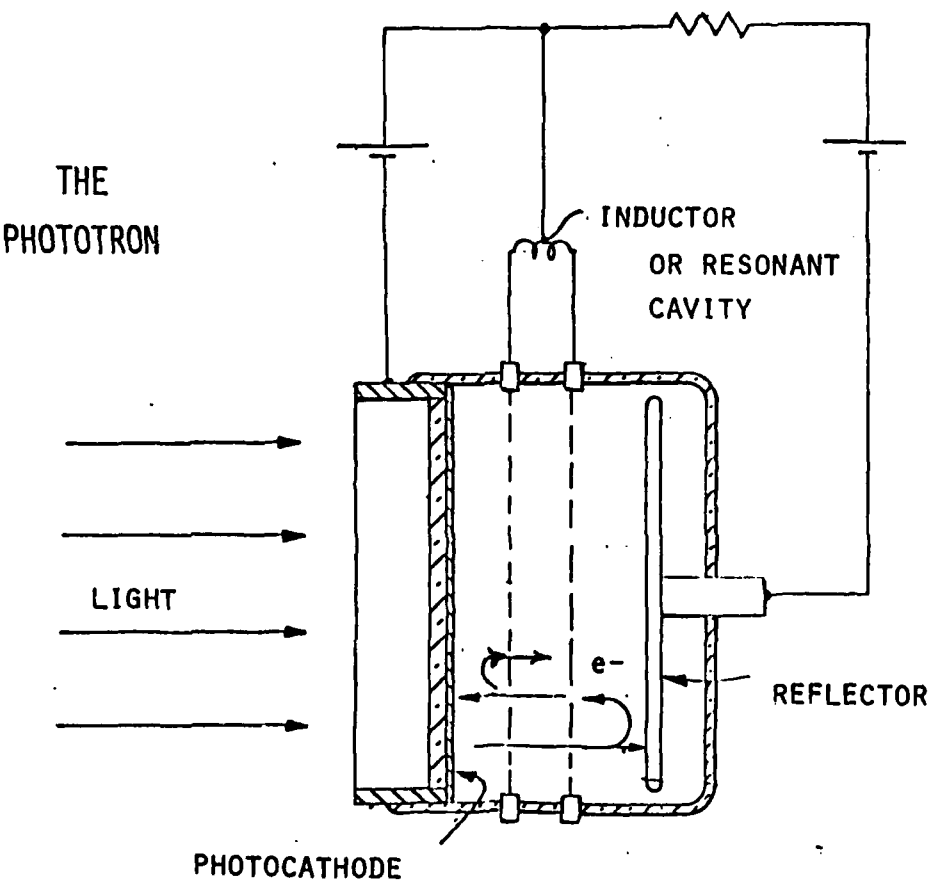
THE
PHOTOTRON
INDUCTOR
OR RESONANT
CAVITY
LIGHT
e-
REFLECTOR
PHOTOCATHODE

Figure 1

OPERATING MODES

- MULTI-PASS MODE: THIS MODE IS CHARACTERIZED BY MULTIPLE OSCILLATIONS OF THE ELECTRONS BACK AND FORTH THROUGH THE GRIDS. IT REQUIRES HIGHER BIAS VOLTAGES, ABOUT 50 VOLTS, AND RESULTS IN HIGHER OUTPUT FREQUENCIES.

- HALF-CYCLE MODE: THIS MODE EXHIBITS ELECTRON BUNCHING AND IN SOME CASES ELECTRON REFLECTION. IT OCCURES AT ZERO OR LOW BIAS VOLTAGES AND RESULTS IN LOWER FREQUENCIES. THE HALF-CYCLE MODE OCCURES DURING SELF-OSCILLATION, IE. WHEN ELECTRON PHOTOKINETIC ENERGY ALONE SUSTAINS THE R.F. OSCILLATIONS.

FIGURE 2

FIGURE 2 IS A COMPUTER GENERATED APPLEGATE DIAGRAM OF THE MULTI-PASS MODE. THE CENTRAL CURVES ARE THE POSITIONS VERSES TIME IN CYCLES OF EIGHT SAMPLE ELECTRONS DEPARTING FROM THE PHOTOCATHODE AT DIFFERENT TIMES. NOTE THAT FIVE OF THE EIGHT ELECTRONS STRIKE THE REFLECTOR OR PHOTOCATHODE ON THE FIRST CYCLE. THE REMAINING THREE ELECTRONS LOSE ENERGY TO THE R.F. FIELD AND CONTINUE TO OSCILLATE WITH DECREASING AMPLITUDE. THESE THREE ARE THE FAVORABLE ELECTRONS AND THEIR CONTINUED OSCILLATION RESULTS IN A NET ENERGY TRANSFER FROM THE ELECTRON BEAM TO THE R.F. FIELD.

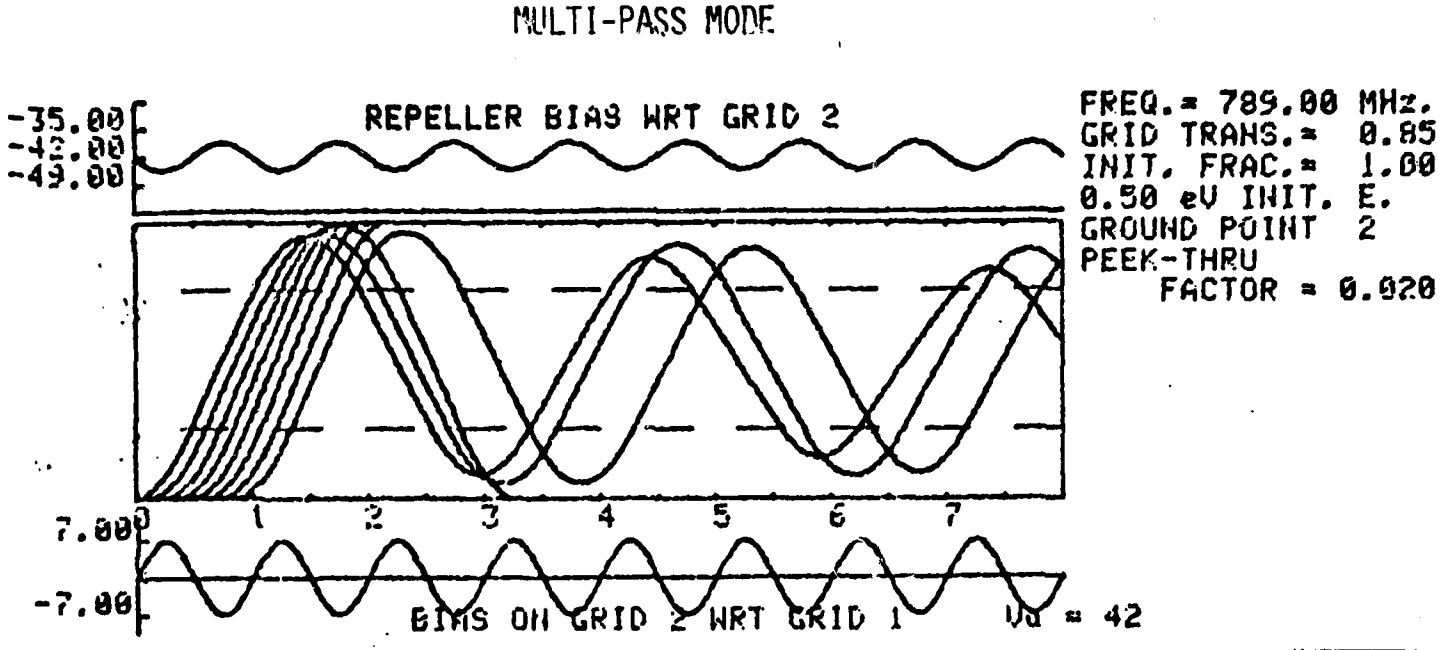
MULTI-PASS MODE
REPELLER BIAS WRT GRID 2
-35.00
-42.00
-49.00
FREQ.= 789.00 MHz.
GRID TRANS.= 0.85
INIT. FRAC.= 1.00
0.50 eV INIT. E.
GROUND POINT 2
PEEK-THRU
FACTOR = 0.020
0
1
2
3
4
5
6
7
7.00
-7.00
BIAS ON GRID 2 WRT GRID 1
Vd = 42

Figure 2

FIGURE 3

A COMPUTER GENERATED APPLEGATE DIAGRAM OF A "FAVORABLE" ELECTRON IN THE MULTI-PASS MODE. THE HORIZONTAL DASHED LINES REPRESENT THE TWO GRIDS AND THE TOP AND BOTTOM-LINES THE REPELLER ELECTRODE AND PHOTOCATHODE RESPECTIVELY. THE UPPER SINE WAVE IS THE REPELLER ELECTRODE VOLTAGE WITH RESPECT TO THE UPPER GRID, GRID 2, AND THE LOWER SINE WAVE IS THE VOLTAGE ON GRID 2 WITH RESPECT TO GRID 1. THE LOWER SINE WAVE ALSO GIVES THE VOLTAGE OF THE PHOTOCATHODE WITH RESPECT TO GRID 1. NOTICE THAT AS THE ELECTRON MOVES THROUGH EACH REGION OF THE TUBE THE INSTANTANEOUS POLARITY OF THE R.F. FIELD IN THAT REGION IS SUCH AS TO DECELERATE THE ELECTRON. THE DEVICE PARAMETERS ARE ADJUSTED SO THAT ZERO CROSSINGS OF THE R.F. OCCUR: 1. AS THE ELECTRON CROSSES A GRID; AND 2. AS THE ELECTRON REVERSES DIRECTION IN THE REFLECTION REGIONS. ALSO NOTICE HOW WELL THE ELECTRON MAINTAINS ITS PROPER PHASE RELATIONSIPS TO THE R.F. AS IT LOSES ENERGY. AN ELECTRON DEPARTING THE PHOTOCATHODE A HALF CYCLE LATER WILL BE ACCELERATED AND HIT THE REPELLER ELECTRODE IMMEDIATELY.

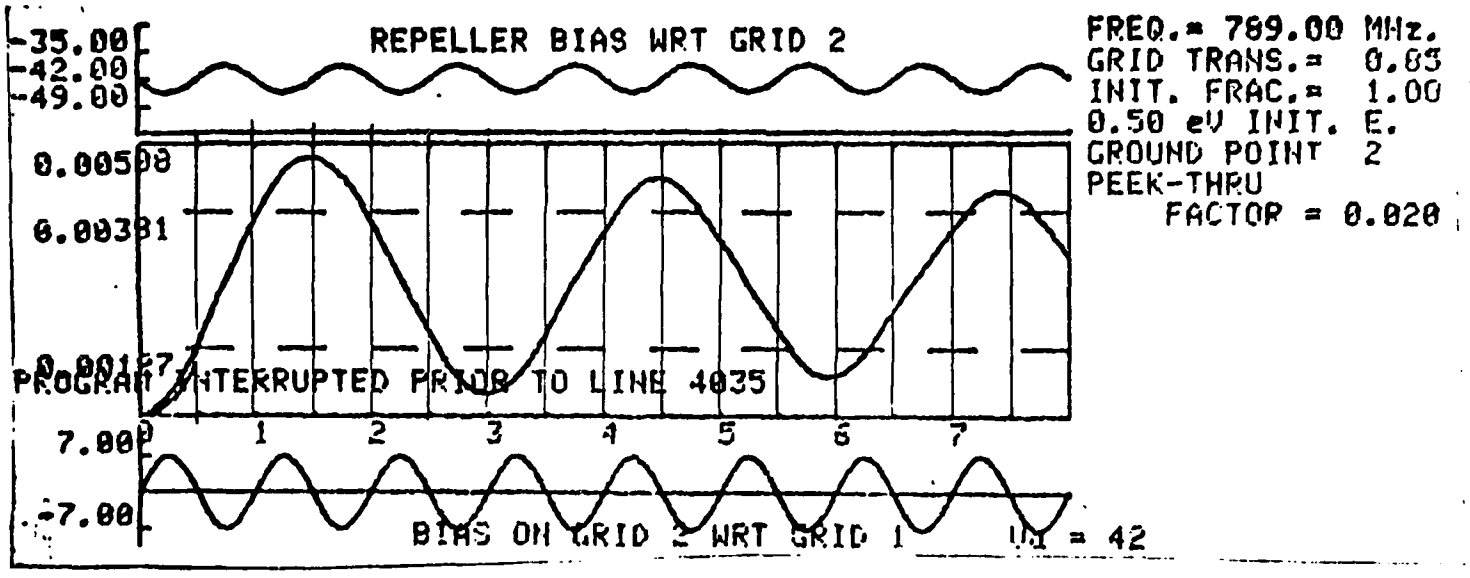
REPELLER BIAS WRT GRID 2
-35.00
-42.00
-49.00
0.00508
0.00381
0.00127
PROGRAM INTERRUPTED PRIOR TO LINE 4035
0
1
2
3
4
5
6
7
7.00
-7.00
BIAS ON GRID 2 WRT GRID 1
FREQ.= 789.00 MHz.
GRID TRANS.= 0.83
INIT. FRAC.= 1.00
0.50 eV INIT. E.
GROUND POINT 2
PEEK-THRU
FACTOR = 0.020

Figure 3

FIGURE 4

THIS FIGURE ILLUSTRATES HOW THE ELECTRON CYCLE TIME P IN UNITS OF THE R.F. PERIOD CHANGES ONLY SLIGHTLY OVER A WIDE RANGE OF ELECTRON ENERGIES ABOVE ABOUT 1 EV. THIS IS BECAUSE AS THE ELECTRON LOSES ENERGY TO THE R.F. FIELD ITS TRANSIT TIME BETWEEN THE GRIDS INCREASES BUT ITS TURN AROUND TIME IN THE TWO REFLECTION REGIONS DECREASES. THESE TWO EFFECTS NEARLY COMPENSATE FOR ONE ANOTHER. THIS CAN BE SEEN IN FIGURE 3. THIS EFFECT ALLOWS FAVORABLE ELECTRONS TO REMAIN IN PROPER PHASE WITH THE R.F. FOR A NUMBER OF CYCLES THUS MAXIMIZING THE ENERGY THEY CAN TRANSFER TO THE R.F. FIELD.

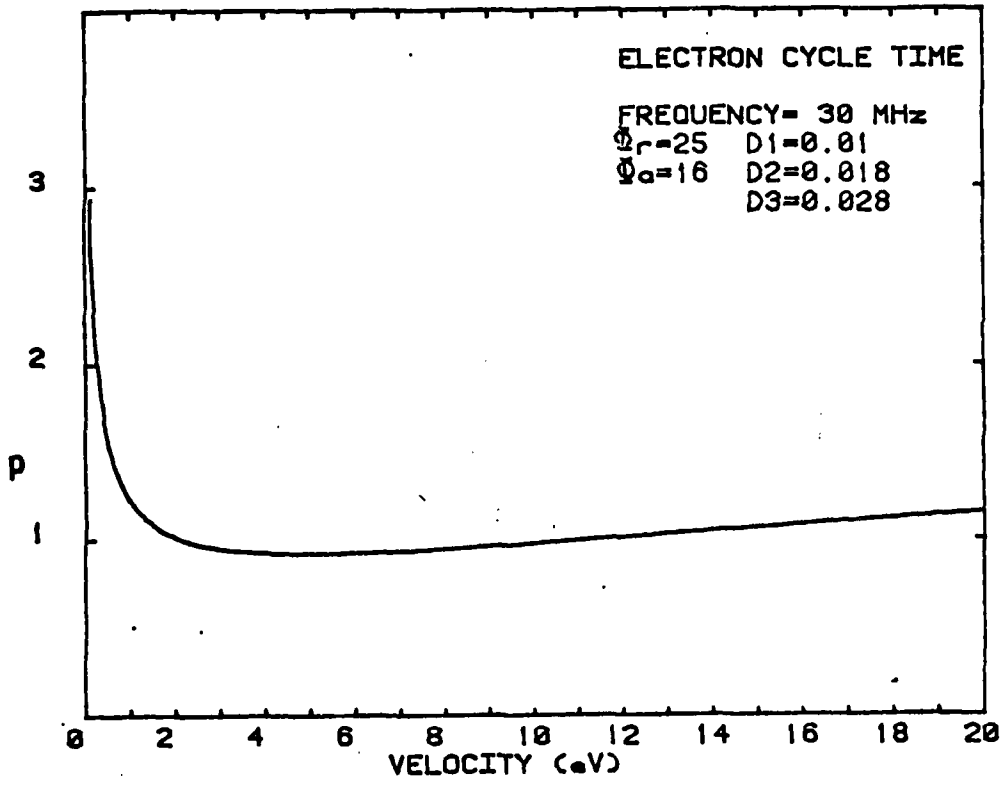

Plot of electron cycle time (in cycles) vs. electron velocity.

Figure 4

FIGURE 5

THIS IS AN APPLEGATE DIAGRAM THAT ILLUSTRATES THE HALF-CYCLE MODE WITH ZERO BIAS VOLTAGE FOR ACCELERATING THE ELECTRONS. ELECTRON BUNCHING IS CLEARLY VISIBLE AS THE ELECTRONS APPROACH THE REFLECTOR ELECTRODE. BASED ON THIS COMPUTER SIMULATION, THE NET ELECTRON ENERGY TRANSFERED TO THE R.F. FOR THIS CONFIGURATION IS ABOUT 10%.

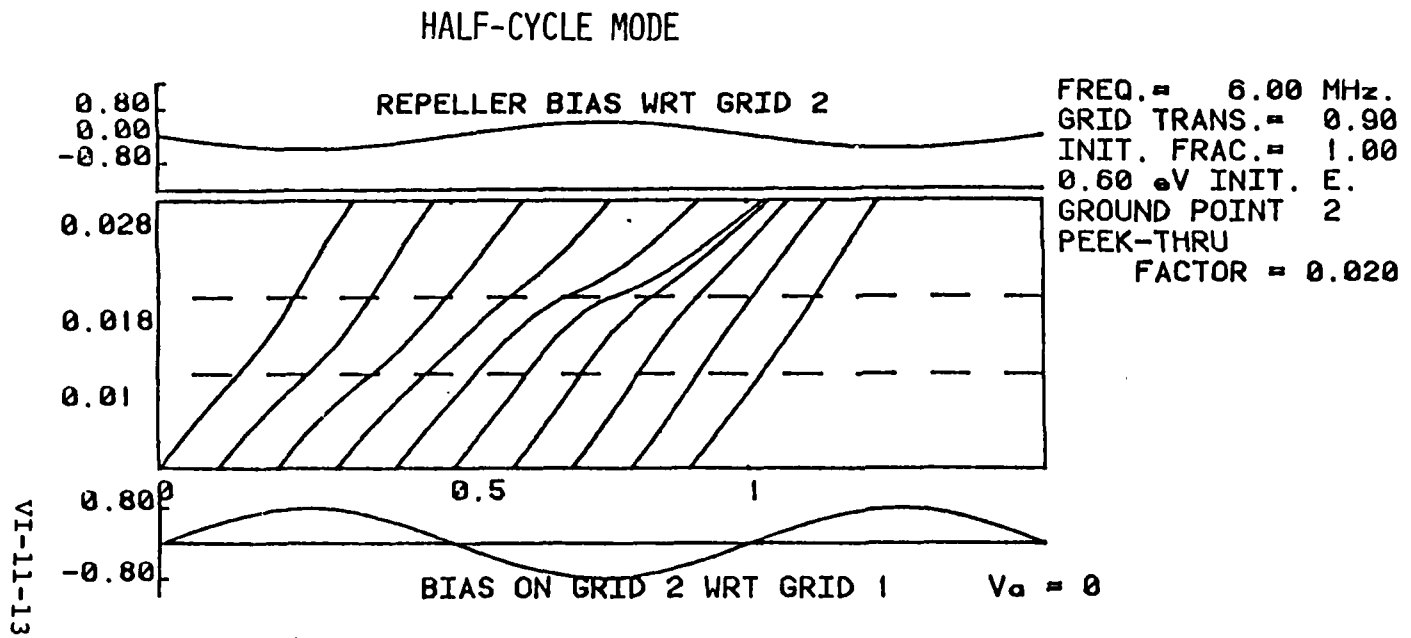
HALF-CYCLE MODE
REPELLER BIAS WRT GRID 2
0.80
0.00
-0.80
0.028
0.018
0.01
0
0.5
1
0.80
-0.80
BIAS ON GRID 2 WRT GRID 1
Va = 0
FREQ.= 6.00 MHz.
GRID TRANS.= 0.90
INIT. FRAC.= 1.00
0.60 eV INIT. E.
GROUND POINT 2
PEEK-THRU
FACTOR = 0.020
VI-11-13

Figure 5

TEST RESULTS *

MULTI-PASS BIASED MODE	HALF-CYCLE, LOW OR UNBIASED MODE
FREQUENCY RANGE: 1 TO ABOUT 1300 MHz	1 TO ABOUT 12 MHz
EFFICIENCY: ABOUT 1 % @ 227 MHz	.0006 TO 0.3 %

* BASED ON SIX TEST MODELS OF SIMILAR DESIGN.
A NEW 1/4 SCALE MODEL HAS JUST BEEN RECEIVED. TEST DATA IS NOT YET AVAILABLE ON THIS MODEL.

PHOTOTRON ADVANTAGES

- EXTREME SIMPLICITY AND THEREFORE RELIABILITY
- NO HOT CATHODE TO BURN OUT
- IT IS A LOW VOLTAGE R.F. OSCILLATOR
- CONSISTS ONLY OF PASSIVE ELEMENTS
- HIGH POWER ACHIEVED THROUGH LARGE ARRAYS

SUMMARY

THE PHOTOTRON SHOWS PROMISE AS A DIRECT OPTICAL ENERGY TO R.F. ENERGY CONVERTER IN THE MHz TO MICROWAVE REGIME.

Q & A - J. W. Freeman

From: P. J. Turchi, R & D Associates

Have you considered using a magnetic field to couple via electron cyclotron frequency?

A.

We have fooled around with a magnetic field perpendicular to the tube axis. We found several new modes but we have not tried to understand them. One would need to start with a new, perhaps flatter tube designed to be used with a B field.

We have used a magnetic field parallel to the tube axis to decrease beam spreading.

References

1. J. W. Freeman, W. B. Colson, S. Simons, "New Methods for the Conversion of Solar Energy to Radio Frequency and Laser Power," Space Manufacturing Facilities 3, AIAA, New York, N. Y., 1979.

2. J. W. Freeman, S. Simons, W. B. Colson, F. Brotzen and J. Hester, "The Photoklystron," Spa. Sol. Pwr. Rev., 1, pp. 145-154, 1980.

3. J. W. Freeman and S. Simons, "Direct Conversion of Light to Radio Frequency Energy," Proceedings of the 16th Intersociety Energy Conversion Conference, Altanta, GA., August 1981, 1, pp. 95-97, 1981, ASME, N. Y., N. Y.

Acknowledgments

Work described herein has been supported by NASA (NAG3-29), and The Brown Foundation of Houston, Texas.

We acknowledge cooperation from Bud Ambler and Bruce Johnson of the ITT Electro-optical products division, manufacturer of the test model Phototrons.

RADIATION-DRIVEN MHD SYSTEMS FOR SPACE APPLICATIONS

JA H. LEE
VANDERBILT UNIVERSITY

AND

NELSON W. JALUFKA
NASA LANGLEY RESEARCH CENTER

ABSTRACT

High-power radiation such as concentrated solar or high-power laser radiation is considered as a driver for magnetohydrodynamic (MHD) systems which could be developed for efficient power generation and propulsion in space. Eight different systems are conceivable since the MHD systems can be classified in two: plasma and liquid-metal MHD's. Each of these systems is reviewed and solar- (or laser-) driven MHD thrusters are proposed.

RADIATION SOURCES IN SPACE

- SUN
- LASERS FROM SPACE PLATFORM

MHD SYSTEMS

- PLASMA MHD
- LIQUID METAL MHD

APPLICATIONS

- ELECTRIC POWER GENERATION
- PROPULSION

RADIATION-DRIVEN MHD SYSTEMS

	STATUS	REFERENCES
SOLAR-DRIVEN PLASMA MHD GENERATOR	PE	PALMER (1978) LAU & DECHER (1978)
SOLAR-DRIVEN LIQUID METAL MHD GENERATORS	CS	LEE & HOHL (1978)
SOLAR-DRIVEN PLASMA MHD THRUSTER	NO	N/A
SOLAR-DRIVEN LMMHD THRUSTER	NO	N/A
LASER-DRIVEN PLASMA MHD GENERATORS	PE	TAUSSIG ET AL (1978) JALUFKA & LEE (1981)
LASER-DRIVEN LMMHD GENERATORS	CS	LEE & HOHL (1978)
LASER-DRIVEN PLASMA MHD THRUSTERS	NO	N/A
LASER-DRIVEN LMMHD THRUSTERS	NO	N/A

STATUS:

- PE PROOF-OF-PRINCIPLE EXPERIMENT
- CS CONCEPTUAL STUDIES ONLY
- NO NO STUDY

LASER DRIVEN MHD GENERATOR

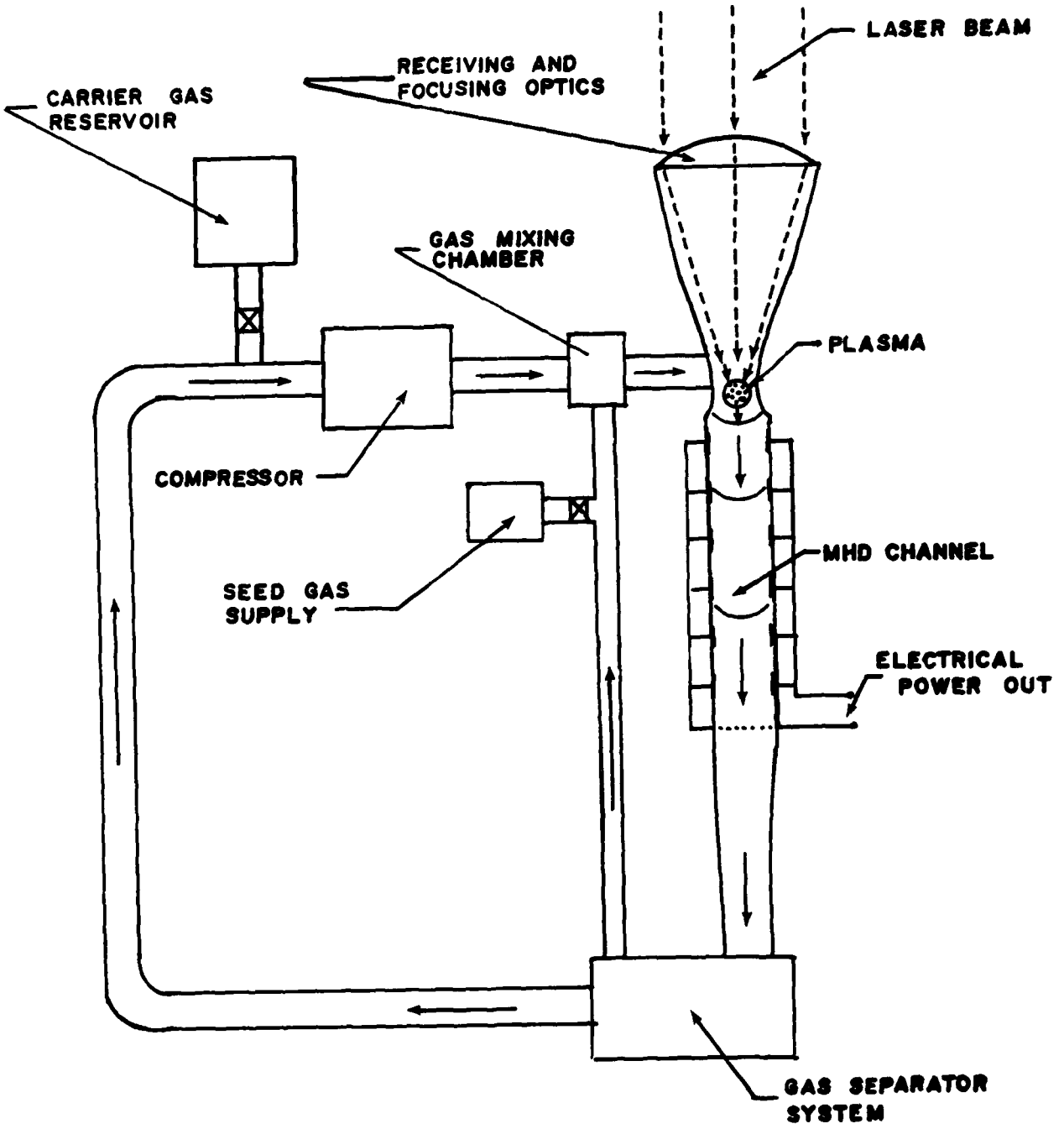

SOLAR-DRIVEN LIQUID METAL MHD GENERATOR

A space application of the liquid metal MHD generator was originally proposed for power production from a nuclear reactor in space (D. G. Elliott, 1968). Vugraph 4 illustrates a solar-driven LMMHD generator which utilizes a specially designed solar oven as the heat source and which enables large-scale power production in space at a high efficiency. This two-phase MHD generator can capitalize on its advantages over the plasma MHD system which requires extremely high temperatures (> 3000°K). For more detailes, see the reference by J. H. Lee and F. Hohl, 1978.

NASA
L-81-10,198

Solar-Driven Liquid Metal MHD Generator

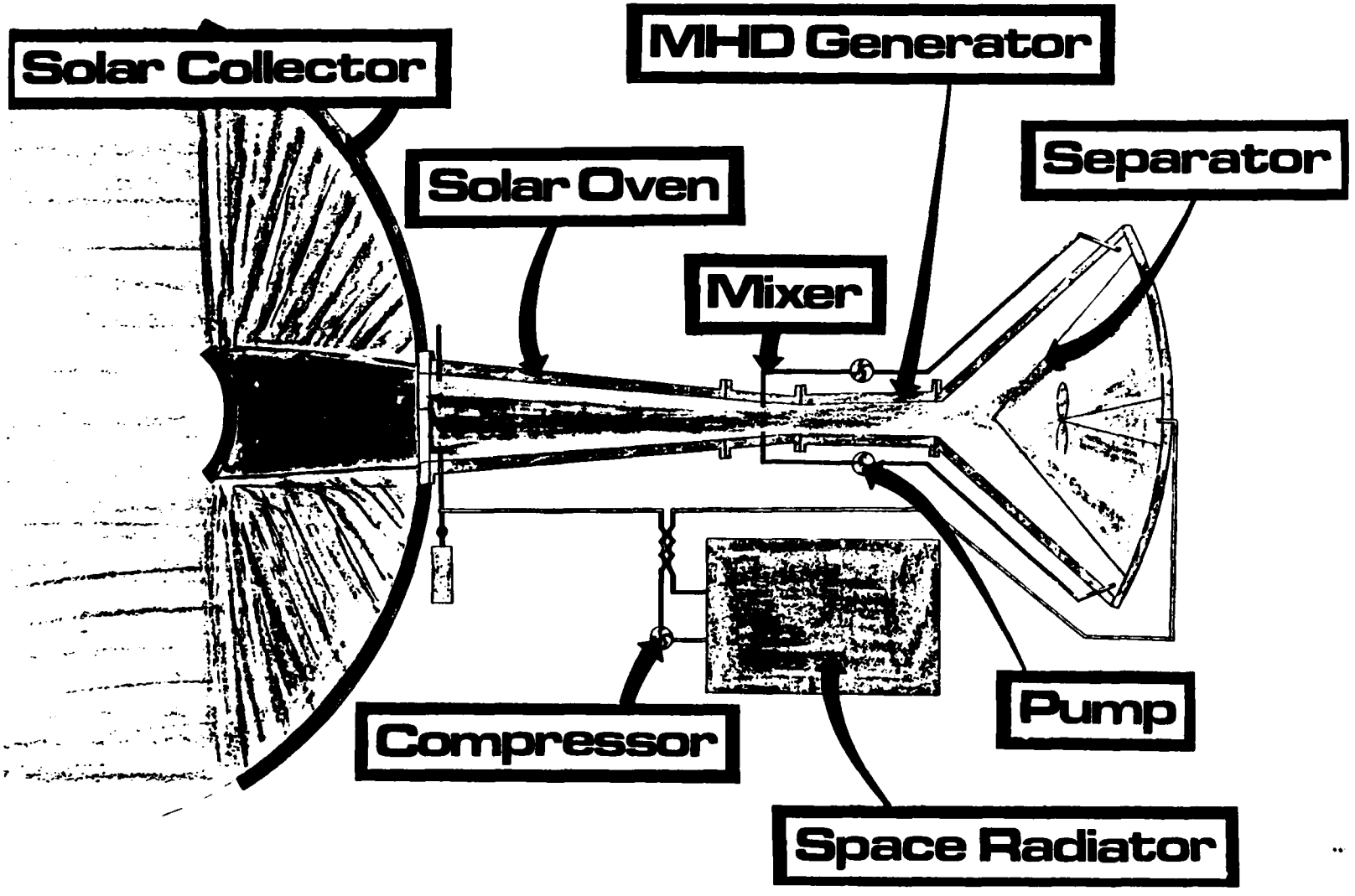

SOLAR-DRIVEN MHD THRUSTER

High-power radiation such as concentrated solar or high-power laser radiation can be utilized for aerospace propulsion. Vugraph 5 shows a concept of a solar-driven MHD thruster. Solar radiation is used in two modes, namely radiative production of a high-temperature plasma and photovoltaic power generation to provide electricity for MHD accelerators. The solar concentrator may be made dichroic so that the solar panel could be integrated behind the reflective surface. Advantages are (1) more efficient production of plasma in comparison with the arc-jet heater necessary for an all-electric thruster, and (2) increase and easy control of the thrust by the MHD system.

SOLAR-DRIVEN MHD THRUSTER

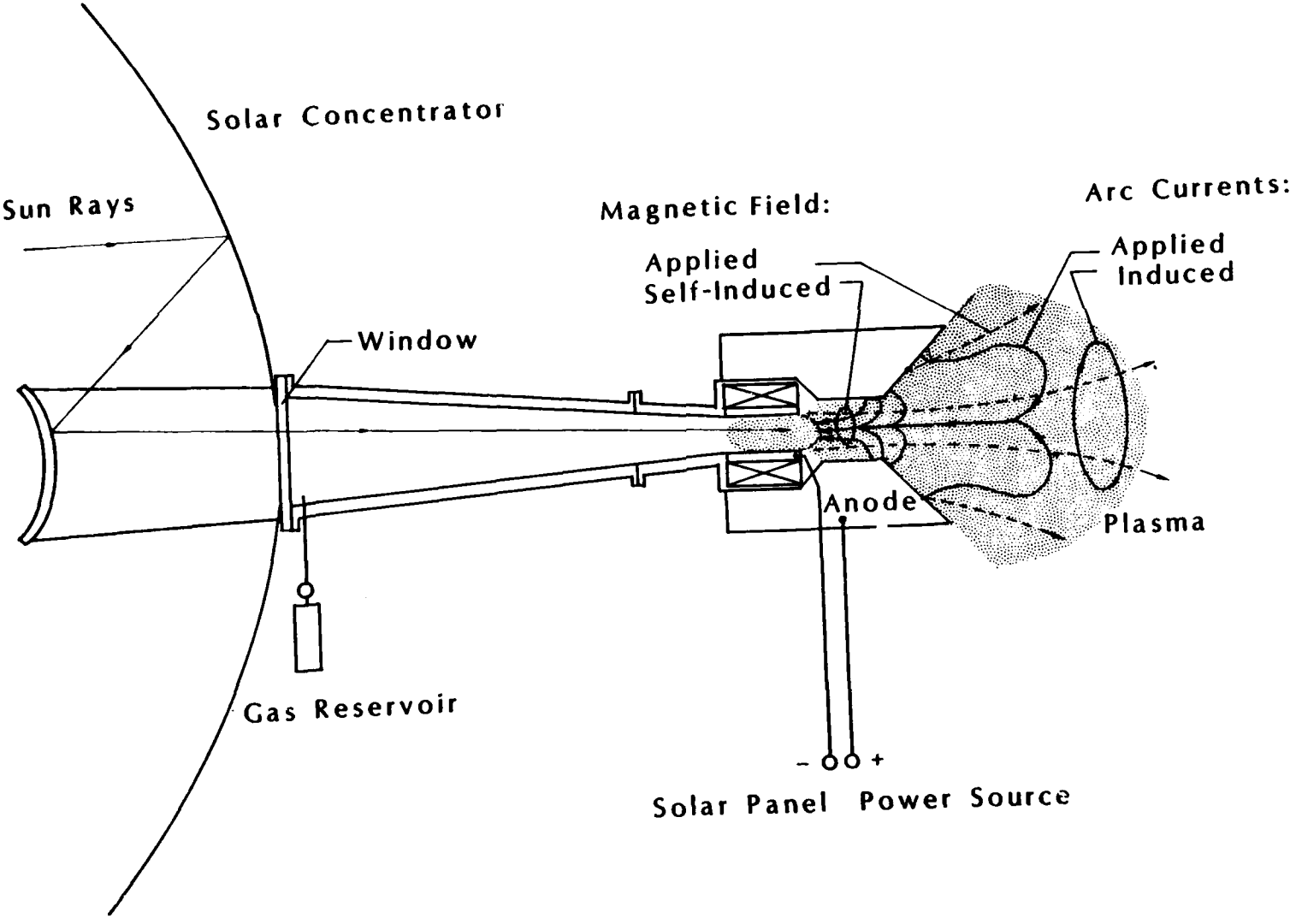

SUMMARY

- EIGHT TYPES OF MHD SYSTEMS COULD BE CONSIDERED FOR PROPULSION AND POWER GENERATION IN SPACE.

- ELECTRIC THRUSTERS MAY GAIN A BETTER EFFICIENCY BY USING SOLAR- OR LASER-PRODUCED PLASMAS AS THE WORKING FLUID.

Q & A - Ja H. Lee

From: P. J. Turchi, R & D Associates

Isn't specific energy per particle contribution of solar radiation input to solar-MHD thruster limited to sun temperature? Rest of energy must come from solar-electric (or other electric) and will be much greater than radiation input.

A.
Yes. Radiation-plasma coupling can be made at high efficiency > .9. Therefore better than

$$(\text{Rad} \rightarrow \text{electric} \rightarrow \text{plasma} \rightarrow \quad)$$
$$\eta=.10 \qquad \eta=.5 \qquad \eta_{net}=.05$$

From: Steve Wax, AFWL

What, if any, are the problems of coupling radiant energy to the MHD thruster concepts? i.e., Has the physics been solved?

A.
No. Physics of laser/solar plasma production is wide open. At Langley we just started to look for the plasma properties at 10^9 w/cm^2 beam intensity much below the laser fusion plasma range.

From: D. Woodall, University of New Mexico

How much <u>flexibility</u> is there in Solar-driven MPD thruster with respect to <u>angle</u> of motion <u>away</u> from sun? (Driving only directly into sun seems unrealistic)

A.
Yes. However in practice you can devise optics such that thruster can be directed in different directions.

References

A. F. Carter, W. R. Weaver, D. R. McFarland, and G. P. Wood, "Development and Initial Operating Characteristics of the 20-Megawatt Linear Plasma Accelerator Facility." NASA TN D-6547, December 1971.

D. G. Elloitt, "Performance Characteristics of Liquid-Metal MHD Generators." SM 107/41, IAEA, Vienna, July 1968.

N. W. Jalufka and J. H. Lee, "Laser-Driven MHD Generator for Conversion of Laser Energy to Electricity." Invention Disclosure, NASA Case No. LAR 12859-1, 1981.

C. V. Lau and R. Decher, "MHD Conversion of Solar Radiant Energy" in Radiation Energy Conversion in Space, (K. W. Billman, Ed.). AIAA 1978, p. 201.

J. H. Lee and F. Hohl, "Solar-Driven Liquid Metal MHD Power Generator." Invention Disclosure, NASA Case No. LAR 12495-1, 1978.

A. J. Palmer, "Radiatively Sustained Cesium Plasmas for Solar Electric Conversion" in Radiation Energy Conversion in Space, (K. W. Billman, Ed.). AIAA 1978, p. 201.

R. T. Taussig, P. Cassady, and J. Zumbieck, "Study, Optimization, and Design of a Laser Heat Engine," in Radiation Energy Conversion in Space, (K. W. Billman, Ed.). AIAA 1978, p. 498.

INTERACTION BETWEEN THE SPS SOLAR POWER SATELLITE SOLAR ARRAY AND THE MAGNETOSHERIC PLASMA

BY

JOHN W. FREEMAN
DEPARTMENT OF SPACE PHYSICS AND ASTRONOMY
RICE UNIVERSITY, HOUSTON, TX 77251

ABSTRACT

THIS PAPER SUMMARIZES THE RESULTS OF STUDY TO DETERMINE THE EFFECTS OF SPACE PLASMAS ON A LARGE GaAs SOLAR CELL ARRAY USING SOLAR REFLECTORS AT A CONCENTRATION RATIO OF 2 IN GEOSTATIONARY ORBIT. THE CONFIGURATION STUDIED WAS AN EARLY ROCKWELL INTERNATIONAL SPS. IT WAS CONCLUDED THAT THE SYSTEM COULD FUNCTION IN THE GEO ENVIRONMENT IF CERTAIN DESIGN CHANGES WERE IMPLEMENTED. THESE INCLUDED CONDUCTIVE COATINGS ON THE SOLAR CELLS, CHANGING THE REFLECTOR MATERIAL FROM KAPTON TO A HIGHER CONDUCTIVITY MATERIAL AND OVERSIZING THE ARRAY TO COMPENSATE FOR A 0.7% PARASITIC LOAD DUE TO LOSSES FROM THE AMBIENT MAGNETOSPHERIC PLASMA. THE STUDY ALSO LOOKED AT THE OPERATION OF THE SOLAR POWERED EARTH ORBIT TRANSFER VEHICLE IN LEO AND CONCLUDED SEVERE ARCING WOULD TAKE PLACE ON ALL HIGH VOLTAGE NEGATIVE PORTIONS OF THE ARRAY. THE PARASITIC LOAD LOSS AT LEO WAS ESTIMATED AT 3%. OPERATION OF A HIGH VOLTAGE ARRAY A_4^t LEO REPRESENTS A MAJOR PROBLEM. CHARGE EXCHANGE ION FEEDBACK FROM ARGON ION THRUSTERS LOCATED NEAR THE EOTV SOLAR ARRAY WAS ALSO EXAMINED AND ALL PROBLEMS FOUND WERE BELIEVED TO BE SOLVABLE BY THE PLACEMENT OF PROTECTIVE GROUND SCREENS.

OBJECTIVES

The objective of this portion of the study is to examine the ambient plasma environment at the geostationary orbit and calculate the resulting currents to and voltages on various parts of the solar power satellite. For purposes of this study the SPS design employed is the January 25, 1978 MSFC baseline study with supporting documentation provided by Rockwell International.

FIGURE 1
SOURCES OF CHARGING

ANY BODY EXPOSED TO SUNLIGHT AND/OR SPACE PLASMAS ACQUIRES A CHARGE ON IT'S SURFACE. THE CHARGE DUE TO SUNLIGHT IS POSITIVE AND ARISES BECAUSE THE PHOTO-ELECTRONS ARE EJECTED FROM THE SURFACE. ORDINARILY THE CHARGE DUE TO A PLASMA IS NEGATIVE AND ARISES BECAUSE MORE ELECTRONS HIT THE SURFACE THAN POSITIVE IONS. THIS IS BECAUSE THE ELECTRONS HAVE A HIGHER THERMAL VELOCITY THAN THE IONS. THUS A SUNLIT BODY IN A PLASMA CAN BE EITHER POSITIVE OR NEGATIVE DEPENDING ON THE PLASMA TEMPERATURE. THE NIGHTSIDE OF THE BODY WILL ALWAYS CHARGE NEGATIVELY.

A BODY IN MOTION IN A PLASMA EXPERIENCES MORE POSITIVE IONS IN THE DIRECTION OF MOTION DUE TO THE RAM EFFECT. THIS DECREASES THE NEGATIVE CHARGE AND INCREASES THE ION CURRENT TO THE SPACECRAFT. THIS EFFECT IS IMPORTANT IN LEO.

CHARGING PROCESSES FOR A
BODY IN A PLASMA

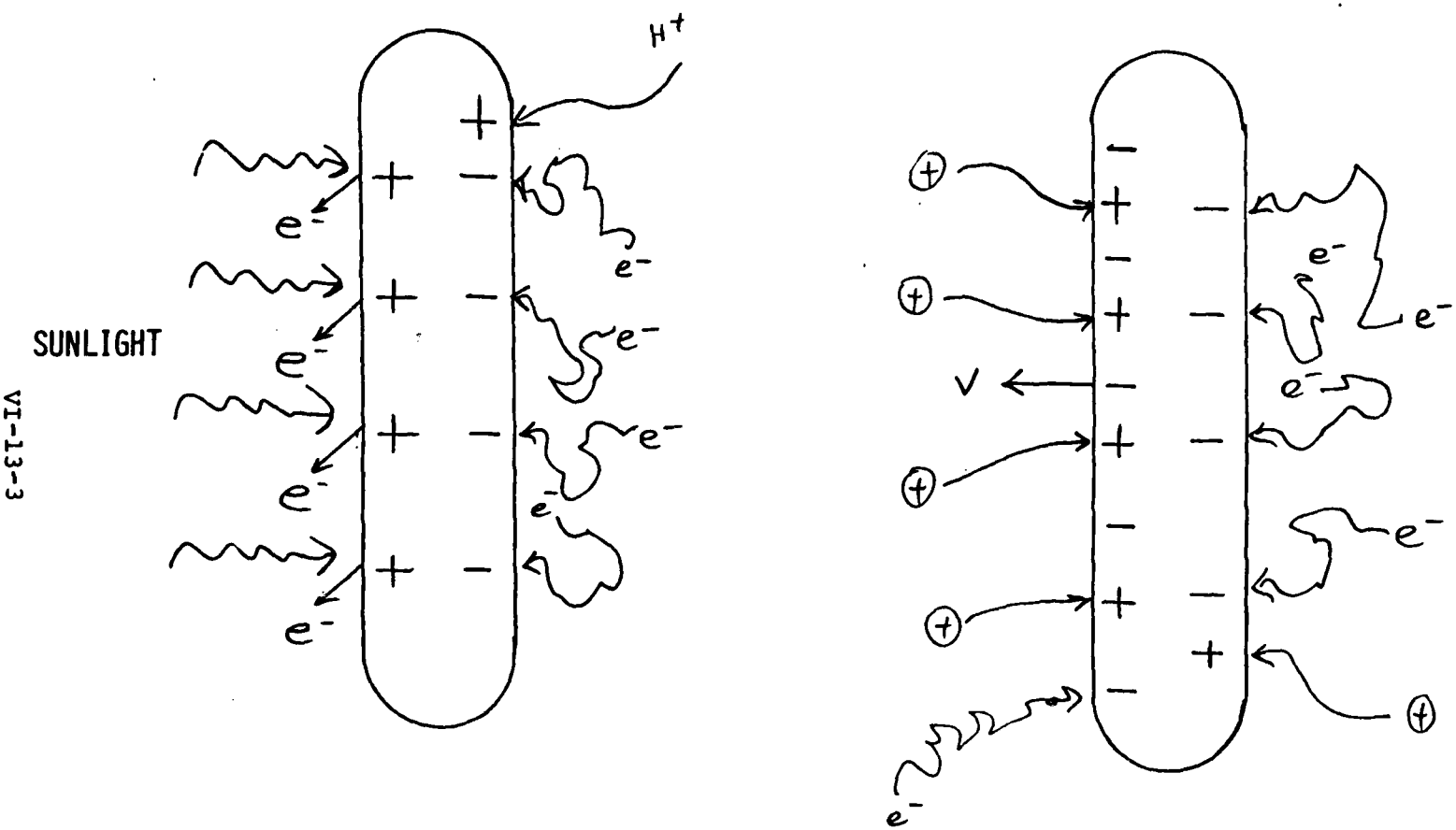

VI-13-3

FIGURE 1

FIGURE 2

PLASMA REGIONS IN THE MAGNETOSPHERE

THE EARTH'S MAGNETOSPHERE CONTAINS A VARIETY OF DIFFERENT PLASMA REGIONS. THE VAN ALLEN RADIATION BELTS AND THE PLASMA SHEET ARE TWO PLASMA REGIONS WHICH AFFECT A SPACECRAFT IN GEOSTATIONARY ORBIT. THE RADIATION BELTS ARE NOT IMPORTANT FOR THIS STUDY, HOWEVER, THEY MAY CONTRIBUTE TO RADIATION DAMAGE EFFECTS.

THE PLASMA SHEET IS A SOURCE OF INTENSE HOT PLASMA WHICH IS KNOWN TO OCCASIONALLY INTERSECT THE GEOSTATIONARY ORBIT AND CHARGE SATELLITES TO 10,000 VOLTS OR HIGHER.

AT LEO THE IONOSPHERE IS A SOURCE OF PLASMA.

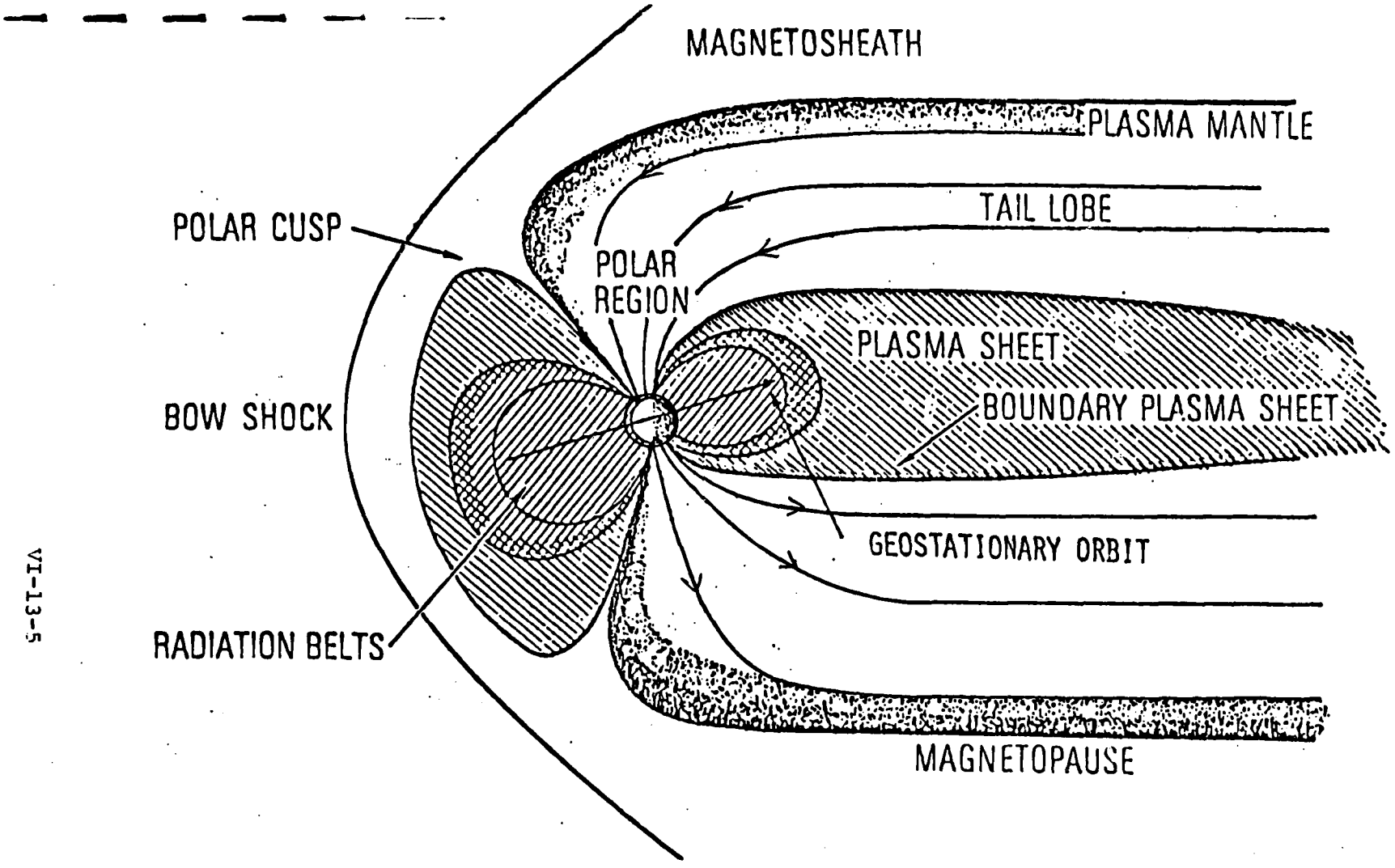

THE EARTH'S MAGNETOSPHERE

FIGURE 2

POSSIBLE EFFECTS OF PLASMA CHARGING:

1. ARC GENERATION DUE TO EXCEEDING THE BREAKDOWN VOLTAGES.
2. DIRECT ELECTRICAL DAMAGE TO COMPONENTS FROM THE TRANSIENT.
3. EMI DISRUPTION OF LOGIC AND SWITCHING CIRCUITS.
4. CHANGE OF REFLECTIVE OR THERMAL CONTROL SURFACES DUE TO OUTGASSING AND PITTING.
5. SHOCK HAZARD FOR EVA AND DOCKING ACTIVITIES.

STUDY STEPS

1. DEFINE "WORST CASE" PLASMA ENVIRONMENT
2. CALCULATE PLASMA AND PHOTOELECTRON CURRENTS ON VARIOUS SURFACES
3. IDENTIFY VULNERABLE AREAS
4. CALCULATE PARASITIC CURRENT LOADS
5. SUGGEST DESIGN CHANGES WHERE NECESSARY

"WORST CASE"

PLASMA CONDITIONS

KT (ELECT) = 5 KEV

KT (PROT) = 10 KEV

$N_E = N_P$ = 2 CM^{-3}

FIGURE 3 The Baseline Design

This figure illustrates the basic configuration and solar cell layout for the MSFC January 25, 1978 baseline design.

All surfaces on the satellite are divided into two categories, active or passive, depending on whether or not voltages appear on the surfaces as a result of the satellite's own power supply. Passive surfaces include the solar reflectors, structural members etc. Active surface include the solar cells, interconnects and bus bars. Active surfaces may attract or repel the ambient ions or electrons depending on the polarity of the surface voltage. Currents reach the passive surfaces only by the thermal motion of the plasma ions or electrons.

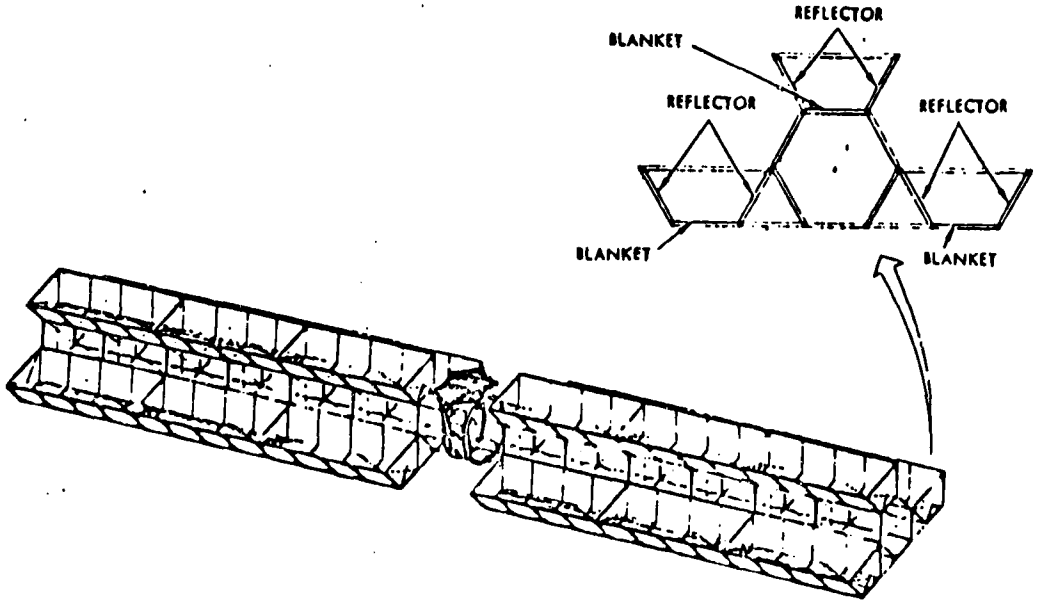

Figure 3. Photovoltaic Structure Model

FIGURE 4. SUMMARY OF VOLTAGE CALCULATIONS.

THE MAJOR HIGH VOLTAGE AREAS ARE THE KAPTON REFLECTORS AND THE BACK SIDES OF THE SOLAR CELL BLANKETS.

SUMMARY OF VOLTAGES:

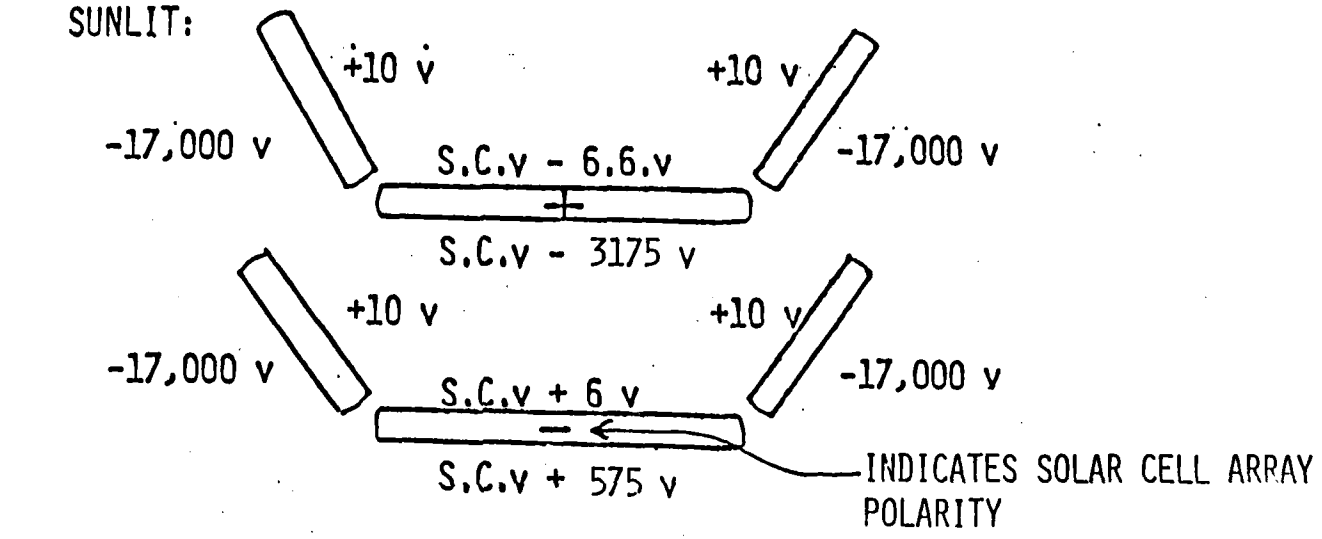

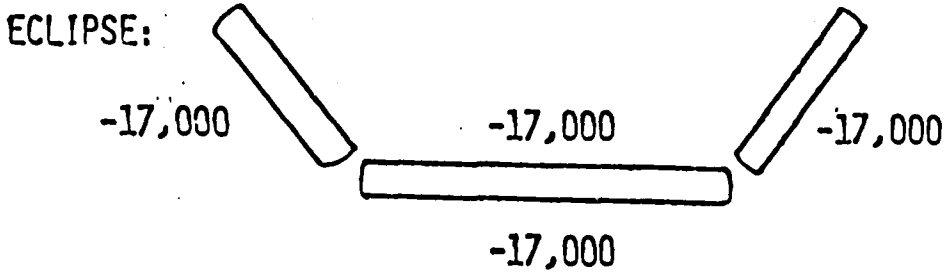

FIGURE 4

THE VARIOUS CURRENT DENSITIES ARE:

$J_{PHE} = 3 \times 10^{-9}$ AMP/CM^2 (FOR SAPPHIRE)

J_E (PLASMA) $= 3 \times 10^{-10}$ AMP/CM^2

J_I (PLASMA) $= 1 \times 10^{-11}$ AMP/CM^2

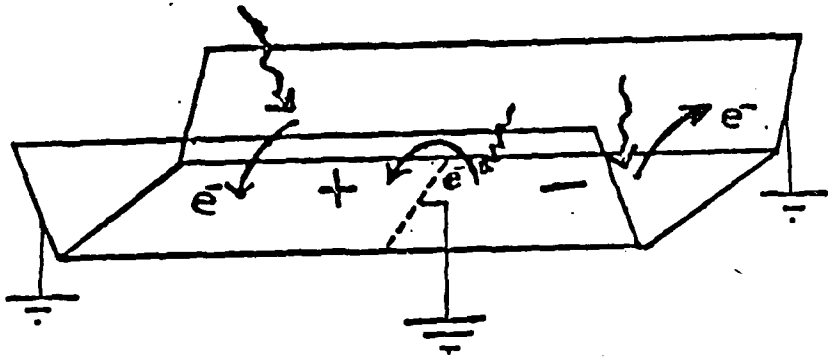

PHOTOELECTRON FLOW DIRECTIONS

TOTAL PARASITIC CURRENT:

$I_P \cong 3000$ AMPS

$\bar{V} = 11{,}375$ V

THE PARASITIC POWER IS:

$P_P \cong 34$ MW

(0.7% OF OUTPUT POWER)

CONCLUSIONS FOR GEO

1. BREAKDOWN WILL OCCUR ON THE SOLAR REFLECTOR BACKSIDES

2. BREAKDOWN MIGHT OCCUR ON THE SOLAR CELL KAPTON BLANKET.

3. THE PARASITIC LOAD WILL BE ABOUT 34 MW (FOR GEO ONLY)

4. THE OPTIMUM GROUND POINT TO THE STRUCTURE IS THE MIDDLE OF EACH SOLAR CELL VOLTAGE STRING IE. WANT + 22.75 KV TO -22.75 KV

5. TESTS SHOULD BE RUN ON SOLAR CELL AND KAPTON SAMPLE MATERIALS IN A SUBSTORM TEST FACILITY

THE EOTV AT LEO

FOR A 400 KM ORBIT THE CURRENTS ARE:

J_I (RAM) = 2×10^{-7} AMPS/CM^2

J_I (THERMAL) = 7×10^{-9} AMPS/CM^2

J_E (THERMAL)=3×10^{-7} AMPS/CM^2

J_{PHE} (PHOTO ELECTRON) = 3×10^{-9} AMPS/CM^2

USING THE CURRENT BALANCE EQUATION,

$$A^-(\Sigma J_I + J_{PHE}) - A^+(\Sigma J_E + J_{PHE}) = 0$$

GIVES $A^+ = 0.3\ A^-$

FOR A 8300 VOLT SYSTEM WE HAVE

+2490 V AND -5810 V

THE PARASITIC LOAD AT LEO DUE TO IONOSPHERIC PLASMA

THE TOTAL AREA THAT IS HIGH VOLTAGE NEGATIVE IS 7×10^9 CM^2

I_{TOT} (PARASITIC) = $7 \times 10^9 \times 2 \times 10^{-7} = 1.4 \times 10^3$ AMPS

THE AVERAGE VOLTAGE = $\frac{8300}{2}$ = 4150 V

P_{PAR} = 5.8 MW

OR 1.7% OF THE
335.5 MW S/C OUTPUT

IF THE ARRAY IS RUN ALL POSITIVE

P_{PAR} = 10.5 MW

OR 3.1% OF THE 335.5 MW S/C OUTPUT

CONCLUSIONS FOR LEO

1. THE ION CURRENT IS SUFFICIENTLY HIGH THAT ANOMALOUS ARCING IS EXPECTED.

2. THE PARASITIC LOAD MAY BE BETWEEN 2% AND 3%.

3. HIGH VOLTAGE ARRAYS SHOULD NOT BE CONSIDERED FOR LEO.

References

1. Reiff, P. H., J. W. Freeman and D. L. Cooke, Environmental Protection of the Solar Power Satellite, Space Systems and their Interactions with Earth's Space Environment, H. B. Garrett and C. P. Pike, ed. Vol. 71, Progress in Astronautics and Aeronautics, 1979.

2. Freeman, J. W., Electrostatic Protection of the Solar Power Satellite and Rectenna, Final report for NASA Contract NAS8-33023, Marshall Space Flight Center, 1979.

3. Kennerud, K. L., Final Report High Voltage Array Experiments, Boeing Aerospace Report No. CR121280, NASA Contract No. NAS3-14364, NASA Lewis Research Center, 1979.

Acknowledgments

This research was supported by NASA grant NAS8-33023.

SESSION VII. MATERIALS

OVERVIEW
OF
HIGH-TEMPERATURE MATERIALS
FOR
HIGH-ENERGY SPACE POWER SYSTEMS

NEAL T. SAUNDERS
NASA - LEWIS RESEARCH CENTER
CLEVELAND, OHIO

AFOSR SPECIAL CONFERENCE ON
PRIME POWER FOR HIGH-ENERGY SPACE SYSTEMS
NORFOLK, VIRGINIA
FEBRUARY 22-25, 1982

ABSTRACT

This presentation discusses the current state-of-technology and some of the more-pressing research needs and challenges associated with the possible use of high-temperature materials in future high-energy space power systems. Particularly, emphasis is on the need to improve and quantify the fundamental understanding of the effects of the following: (1) fast-neutron radiation on the properties and behavior of nuclear reactor fuels and claddings; and (2) long-term, high-temperature, space (vacuum) exposure on the properties of refractory metals considered for use as structural materials in various power conversion systems. The data presented were abstracted from published papers prepared by numerous authors from several different organizations.

BACKGROUND OF PRESENTER

Neal Saunders has spent most of his 24-year career with the NASA-Lewis Research Center conducting and managing research and technology efforts directed at developing and applying advanced materials for various aerospace systems. Much of his early efforts involved high-temperature materials for nuclear space power systems. He currently serves as Chief of the Materials Division at NASA-Lewis.

PURPOSES OF PRESENTATION

- TO SUMMARIZE THE CURRENT STATE-OF-TECHNOLOGY OF HIGH-TEMPERATURE MATERIALS CONSIDERED FOR FUTURE HIGH-ENERGY SPACE POWER SYSTEMS
  - NUCLEAR FUELS/CLADDINGS
  - REFRACTORY METALS

- TO HIGHLIGHT SOME RESEARCH NEEDS FOR FUTURE USE OF THESE MATERIALS

The previous presentations at the Conference has discussed a wide diversity of system technology needs for various combinations of heat sources and energy conversion systems being considered for high-energy, space-power generation systems. But one common theme in many of these presentations is the need for higher operating temperatures to improve efficiency of the energy conversion systems. And in most cases, materials limitations are currently the most difficult technology-barriers to increasing system temperatures. Thus, the need for improved high-temperature materials presents many fruitful areas for future research.

I personally believe that the most challenging materials problems are associated with the fuel element materials (fuel and cladding) in nuclear reactor heat sources and refractory metals that could be used as high-temperature structural materials in Thermionic, Brayton, or Rankine systems. So these materials are the subjects of this presentation.

HIGH-ENERGY POWER GENERATION SYSTEMS

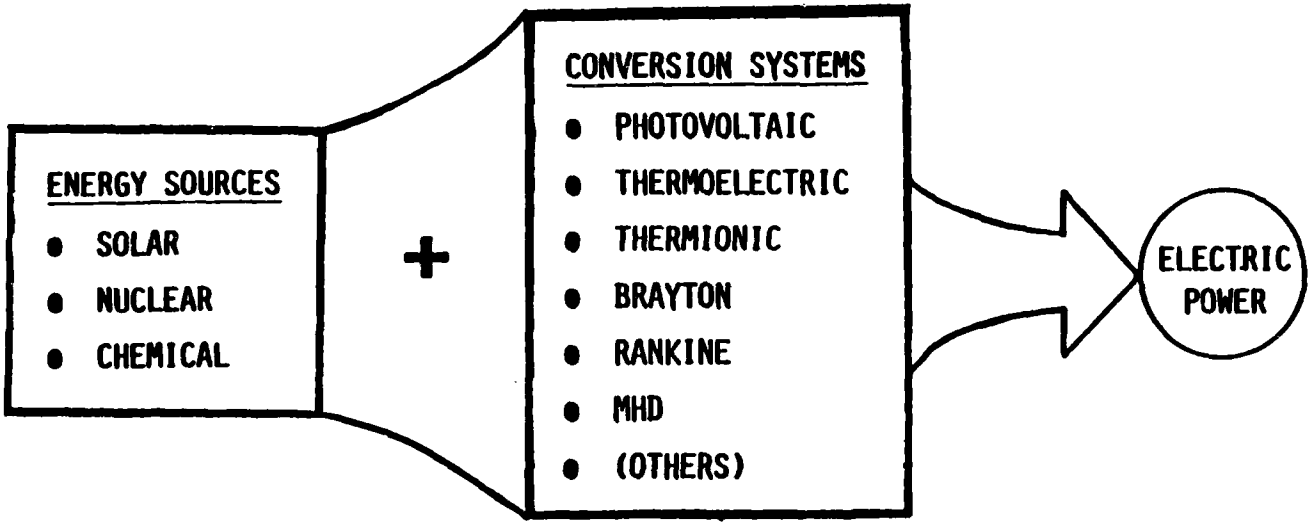

THE COMMON DENOMINATOR —

CONVERSION EFFICIENCY = f (TEMPERATURE)

Since future space power reactors are expected to operate in the temperature range of about 1200° to 1600°C, the choice of nuclear fuels is very limited. The three prime candidates for this use are uranium dioxide (UO_2), uranium nitride (UN), and uranium carbide (UC). None of these three candidates is a clear-cut choice since each of them present some advantages and disadvantages for this application. UO_2 is attractive because it is the most chemically stable at high temperatures and an extensive technology-base has been generated for this fuel through its wide-spread use in terrestrial reactors. However, the uranium density of UO_2 is much less than that for either UN or UC. Thus, reactors fueled with either UN or UC could be designed more compactly and significantly lighter than a reactor fueled with UO_2.

COMPARISON OF HIGH-TEMPERATURE NUCLEAR FUELS

	UO_2	UN	UC
URANIUM DENSITY, G/CM^3	9.70	13.50	12.97
MELTING POINT, ^oC	2800	2850	2375
THRESHOLD TEMP. FOR FISSION GAS SWELLING, ^oC	~1100	~1200	~1050

Uranium dioxide also has a much lower thermal conductivity than either UN or UC. In fact, UO_2 really acts as a thermal insulator while UN and UC conduct heat in a more metallic-like nature. This thermal insulator nature of UO_2 tends to aggravate dimensional instability problems in UO_2 fuel elements because the interior sections of these fuel elements operate at much higher temperatures than the fuel element surface temperature. So fuel vaporization can occur at the higher-temperature regions (because of relatively high vapor pressure of UO_2), and this vaporized fuel can migrate within the fuel element and deposit in lower-temperature regions. Thus, some attempts have been made to artificially increase the thermal conductivity of UO_2 by dispersing fuel particles in a metallic matrix of either molybdenum or tungsten. This cermet approach is highly effective in increasing thermal conductivity, but it also reduces the effective uranium density of the fuel to even lower levels.

Although UN and UC are attractive on the basis of uranium density and thermal conductivity, these fuels also have some drawbacks for this use. UN has the highest vapor pressure of these three fuels. So its upper use-temperature is limited by the allowable vapor pressure within a fuel element. For example, if a high-temperature fuel element is designed for fission gas venting, some of the UN fuel could be lost during operation through vaporization and subsequent venting to space. Conversely, UC has the lowest vapor pressure of these three refractory fuel materials, but UC is the least chemically stable of the three. At high operating temperatures, UC will decompose to uranium and carbon, and these can chemically attack refractory metal claddings.

HIGH-TEMPERATURE PROPERTIES OF NUCLEAR FUELS

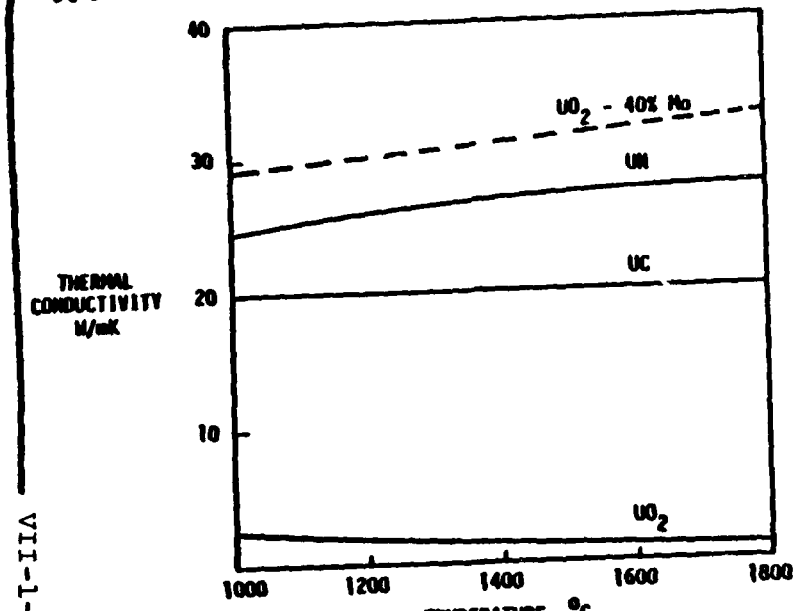

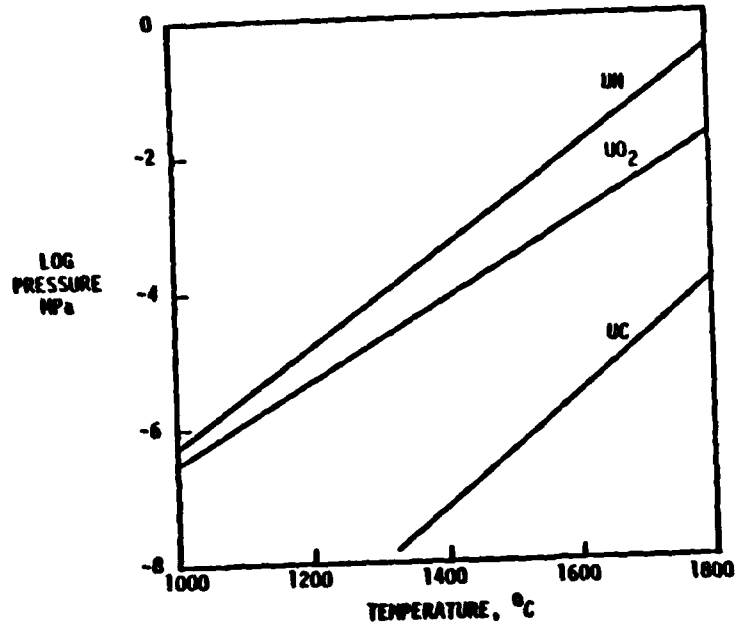

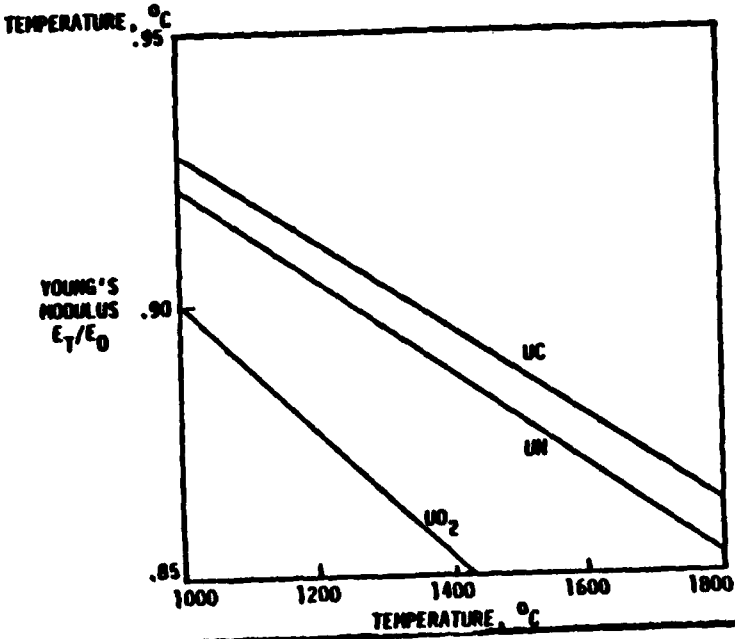

NASA

The most difficult problem associated with nuclear fuel elements is their dimensional growth during long-term reactor operation. The five major contributors to this dimensional instability problem are listed in this figure. The most significant of these are:

- the effects of fission gas swelling in the nuclear fuel material as a result of the fission gas bubbles generated by the nuclear reaction process; and

- the effects of fast-neutron irradiation on the refractory metal cladding as a result of the clustering of interstitial atoms and vacancies generated by the high-energy fission process.

These effects are becoming reasonably-well quantified for the fuel and cladding materials used in lower-temperature nuclear reactors for terrestrial power-generation systems. But the level of understanding for the materials and temperatures required for high-energy space power systems is still relatively meager.

CONTRIBUTORS TO DIMENSIONAL INSTABILITY OF NUCLEAR FUEL ELEMENTS

- FISSION GAS SWELLING OF FUEL
  - GAS BUBBLE GENERATION
- SOLID-STATE SWELLING OF FUEL
  - 2 FISSION PRODUCT ATOMS/ATOM FISSIONED
- FAST NEUTRON EFFECTS ON CLADDING
  - INTERSTITIAL AND VACANCY CLUSTERING
- THERMAL CYCLING EFFECTS ON FUEL/CLADDING
  - DIFFERENCES IN THERMAL EXPANSIVITIES
- CHEMICAL REACTIONS ON FUEL AND CLADDING
  - FUEL/CLADDING/COOLANT COMPATIBILITY

The available irradiation-swelling data for the three nuclear fuel candidates, tested under similar irradiation conditions, are compared in this figure. Based on these "averaged" swelling rates, UN is the most resistant to swelling, UC is the least resistant, and UO_2 has an intermediate swelling rate.

Also, some very limited swelling data have been obtained on cermets of 40% UO_2 dispersed in a molybdenum matrix. Based on these limited data, this cermet fuel had significantly greater resistance to irradiation swelling than any of the three refractory fuels in bulk form. So this concept represents an attractive approach to reducing fuel swelling. However, the tests on this cermet fuel were run under significantly different reactor test conditions. So the resulting data may not be directly comparable. Additional irradiation tests of this fuel form are needed to verify the attractiveness of this approach.

AVERAGE SWELLING RATES FOR NUCLEAR FUELS

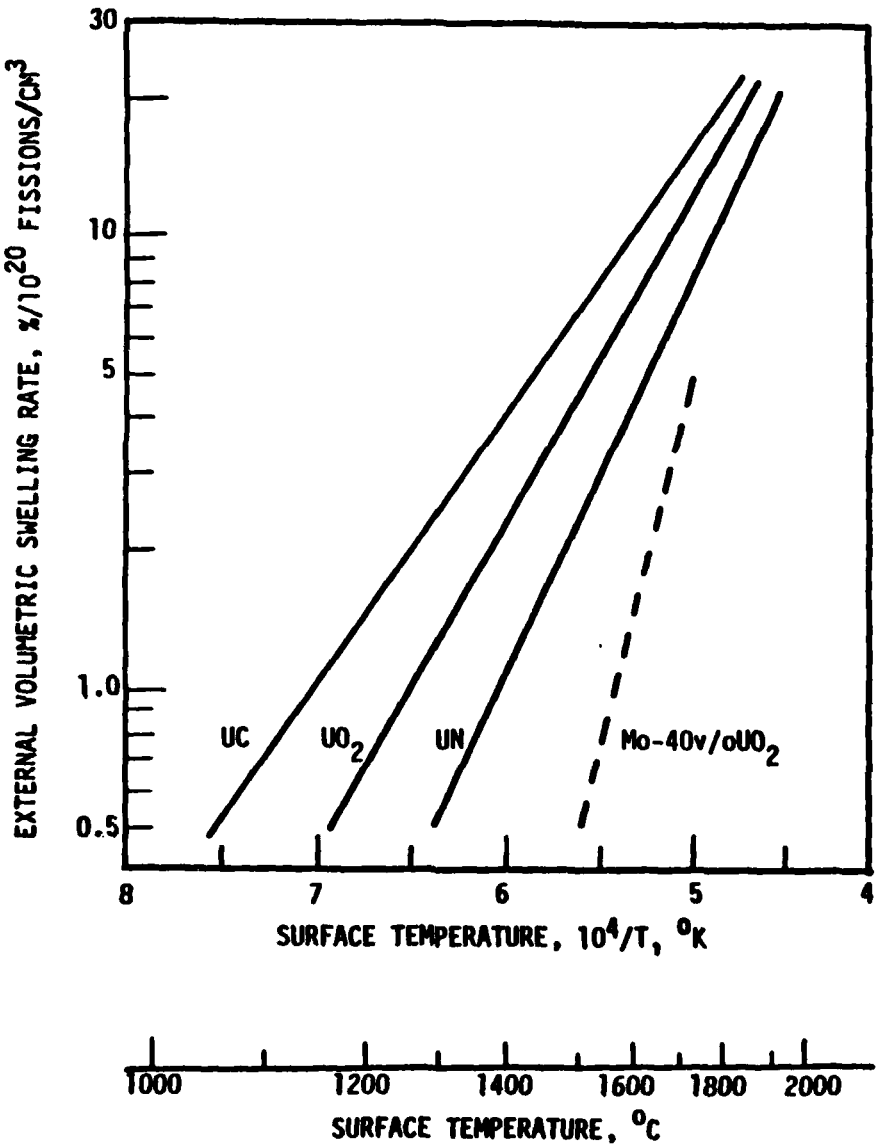

NASA

These figures illustrate the actual fuel swelling data that were used to develop the "average" swelling rates shown in the previous figure. It is apparent that a considerable amount of scatter exists in the available data. In some cases, the difference in measured swelling rates at a given cladding temperature varies as much as an order of magnitude. This large variation is hardly an acceptable level of uncertainty to permit design of nuclear reactors for future space power systems. Thus, considerably more irradiation swelling data must be obtained under closely-controlled test conditions to establish a design base for future systems.

IRRADIATION SWELLING OF NUCLEAR FUELS

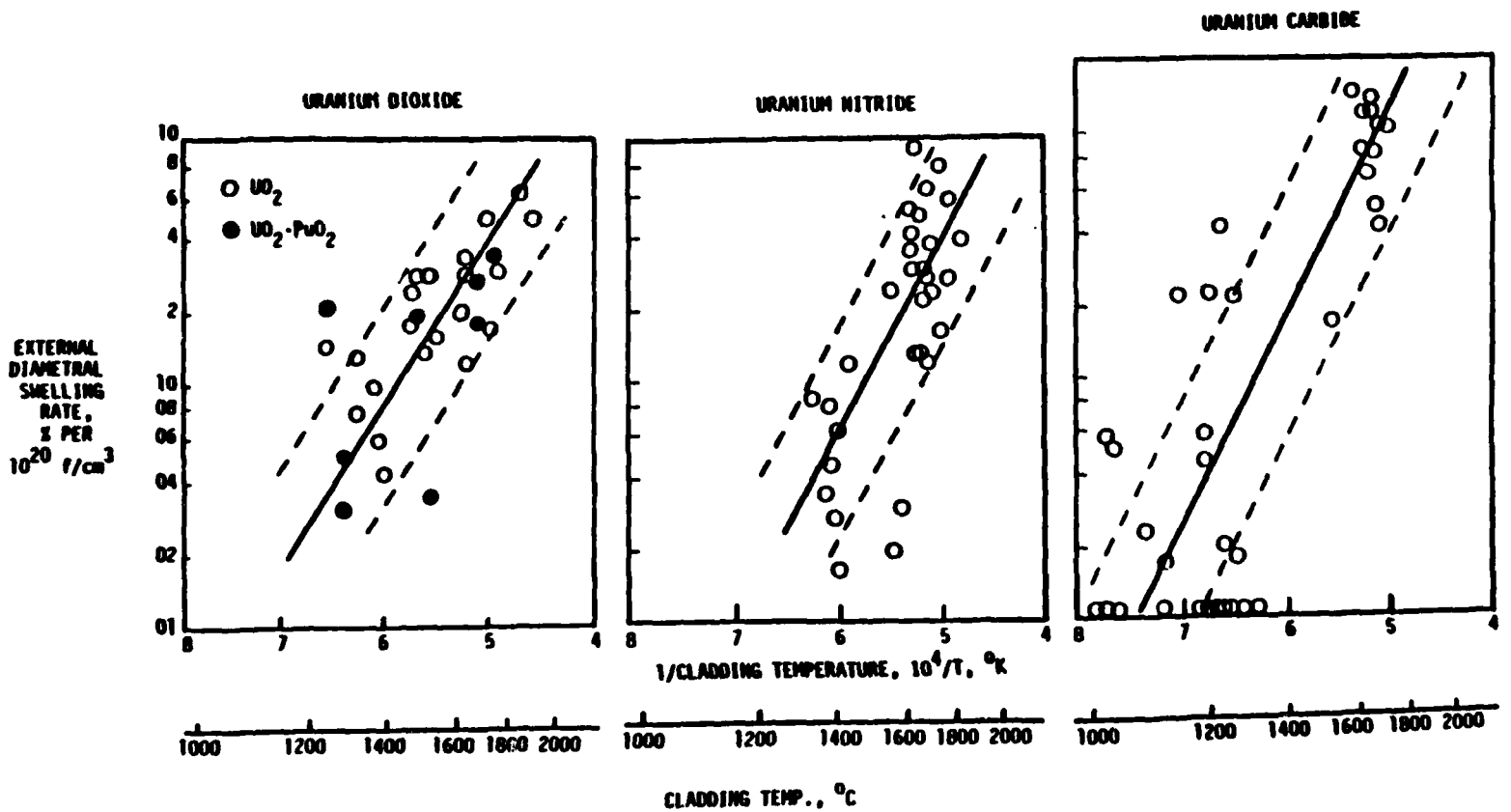

Based on the limited state of knowledge for these nuclear fuel materials, this field offers several opportunities for both basic and applied research. These include modification of the compositions of the various fuels to improve specific properties. For example, the use of metal-matrix with dispersed UO_2 particles to improve the effective thermal conductivity of UO_2 is representative of this approach. Also, some limited data show promise for the alloying of UC with WC to improve its chemical stability. Similar alloying approaches should be tried with UN to try to reduce its vapor pressure at the high reactor operating temperatures.

Further research is needed to improve the understanding of the long-term high-temperature operating effects on the properties of the various fuel candidates in contact with refractory metal claddings. Some compositional changes and interactions will likely occur, and these could have significant effects on the mechanical and physical properties of each material.

The most pressing research need is for developing a better state of knowledge for the effects of irradiation on the various materials. Certainly, better understanding of fuel swelling is needed. But also needed are the effects of irradiation on the chemical compatibility of the fuel and cladding and on the behavior and properties of the refractory metal cladding candidates.

RESEARCH NEEDS FOR NUCLEAR FUEL MATERIALS

- MODIFY FUELS TO IMPROVE CRITICAL PROPERTIES
  - THERMAL CONDUCTIVITY OF UO_2
  - VAPOR PRESSURE OF UN
  - CHEMICAL STABILITY OF UC
- CHARACTERIZE OPERATIONAL BEHAVIOR OF FUEL/CLADDING CANDIDATES
  - MECHANICAL & PHYSICAL PROPERTIES (TEMP./TIME EFFECTS)
  - CHEMICAL COMPATIBILITY OF FUEL/CLADDING/COOLANT
- DETERMINE IRRADIATION EFFECTS ON FUEL ELEMENT MATERIALS
  - FUEL SWELLING
  - FISSION EFFECTS ON CHEMICAL COMPATIBILITY
  - FAST-NEUTRON EFFECTS ON CLADDING

The properties of refractory metals and alloys are known to degrade under the thermal and irradiation conditions typically encountered in space nuclear power systems. Of major significance are the changes in physical and mechanical properties listed in this figure. For example, swelling occurs as material dimensions and volume increase with continued neutron irradiation. The swelling is generally accompanied by a decreased electrical conductivity and an embrittlement of mechanical properties. This latter effect can be observed as increased strength, hardness, and/or ductile-brittle transition temperature and also decreased elongation. All of these effects vary as a function of the fast-neutron fluence. So a range of fluence levels needs to be examined in future research on these effects.

FAST-NEUTRON EFFECTS ON REFRACTORY METAL CLADDINGS

SWELLING

- INCREASED VOLUME

EMBRITTLEMENT

- INCREASED STRENGTH AND HARDNESS
- DECREASED DUCTILITY (ELONGATION, DUCTILE-BRITTLE TRANSITION)

RESISTIVITY

- DECREASED ELECTRICAL CONDUCTIVITY

$$\text{EFFECTS} = f(\text{FLUENCE})$$

A general idea of the damage during neutron irradiation as a function of temperature can be obtained from this figure. This shows a schematic representation of swelling effects to be observed at various irradiation temperatures. For convenience, temperature is normalized by the melting point so that, for example, 0.4 is approximately 600°C for niobium, 850°C for molybdenum, and about 1200°C for tungsten. In the low temperature range (below about 0.3), the radiation damage generally consists of small vacancy and interstitial clusters which together produce little volume change or swelling. However, in the intermediate temperature range (between about 0.3 and 0.5), the small vacancy clusters give way to large-scale clusters or voids which can have pronounced effects on material dimensions. In the high temperature regime (above 0.5), the thermal energy is high enough to eliminate or anneal out intrinsic defects. This leaves only transmutation products, such as helium bubbles, which produce little swelling effects in these body-centered-cubic refractory metals. Thus, swelling problems are confined primarily to the intermediate temperature range where voids are the major damage source.

SWELLING EFFECTS IN REFRACTORY METALS

(FLUENCE ~10^{22} N/CM^2)

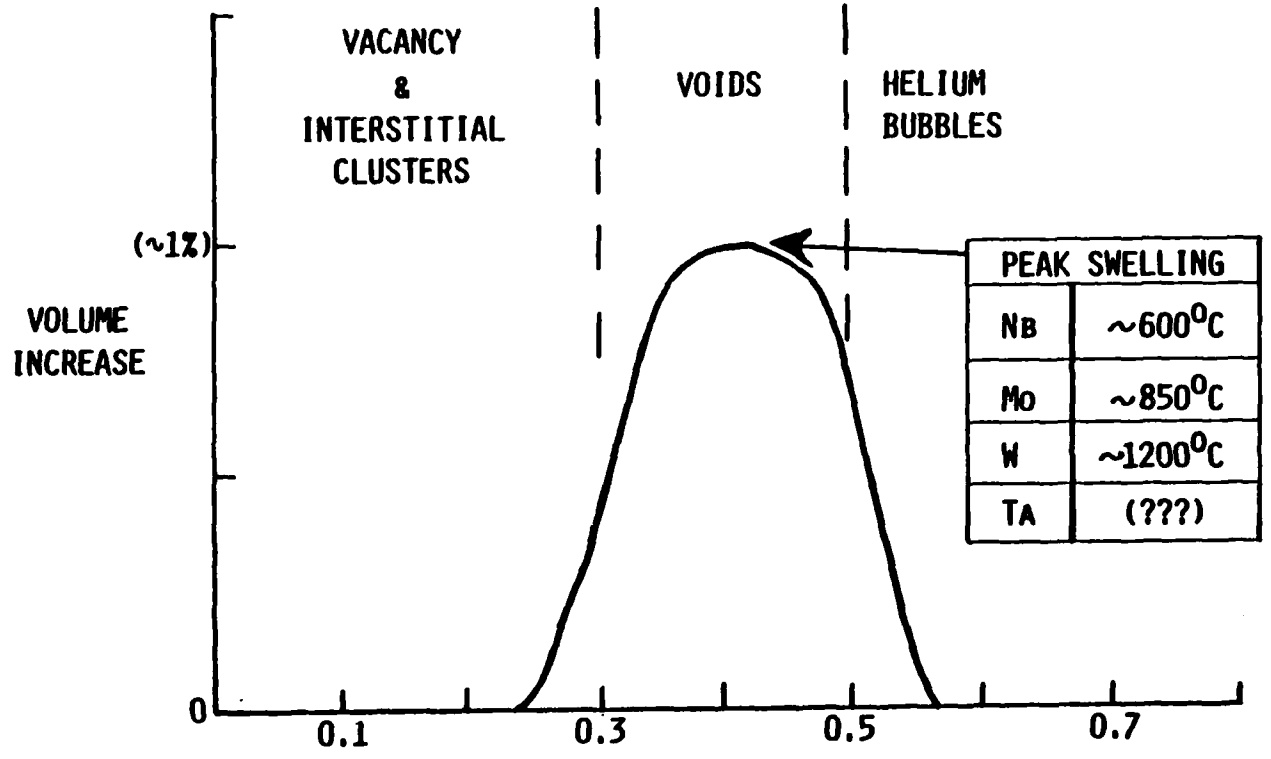

PEAK SWELLING	
Nb	~600°C
Mo	~850°C
W	~1200°C
Ta	(???)

This figure schematically shows some of the principal mechanical property changes caused by fast-neutron irradiation. In this case, the increase in both the ductile-brittle transition temperature and the ultimate tensile strength are plotted as a function of normalized irradiation temperature (at a fluence of about $10^{22} n/cm^2$). Whereas vacancy and interstitial clusters have little effect on material dimensions, they can strongly hinder dislocation motion, thereby producing a significant embrittling effect on mechanical properties. For example, in the low temperature range the ductile-brittle transition temperature of molybdenum has been observed to increase by about 550°C, and the ultimate tensile strength has been observed to increase by about 70 ksi. At the intermediate temperatures where voids are formed, the embrittling effects are still evident but not as serious. Finally, at the high temperatures, the mechanical effects due to intrinsic defects essentially disappear. But for some metals and alloys, some embrittlement may continue to exist due to the effects of the helium bubbles generated as a transmutation product.

MECHANICAL EFFECTS IN REFRACTORY METALS

(FLUENCE ~10^{22} N/CM^2)

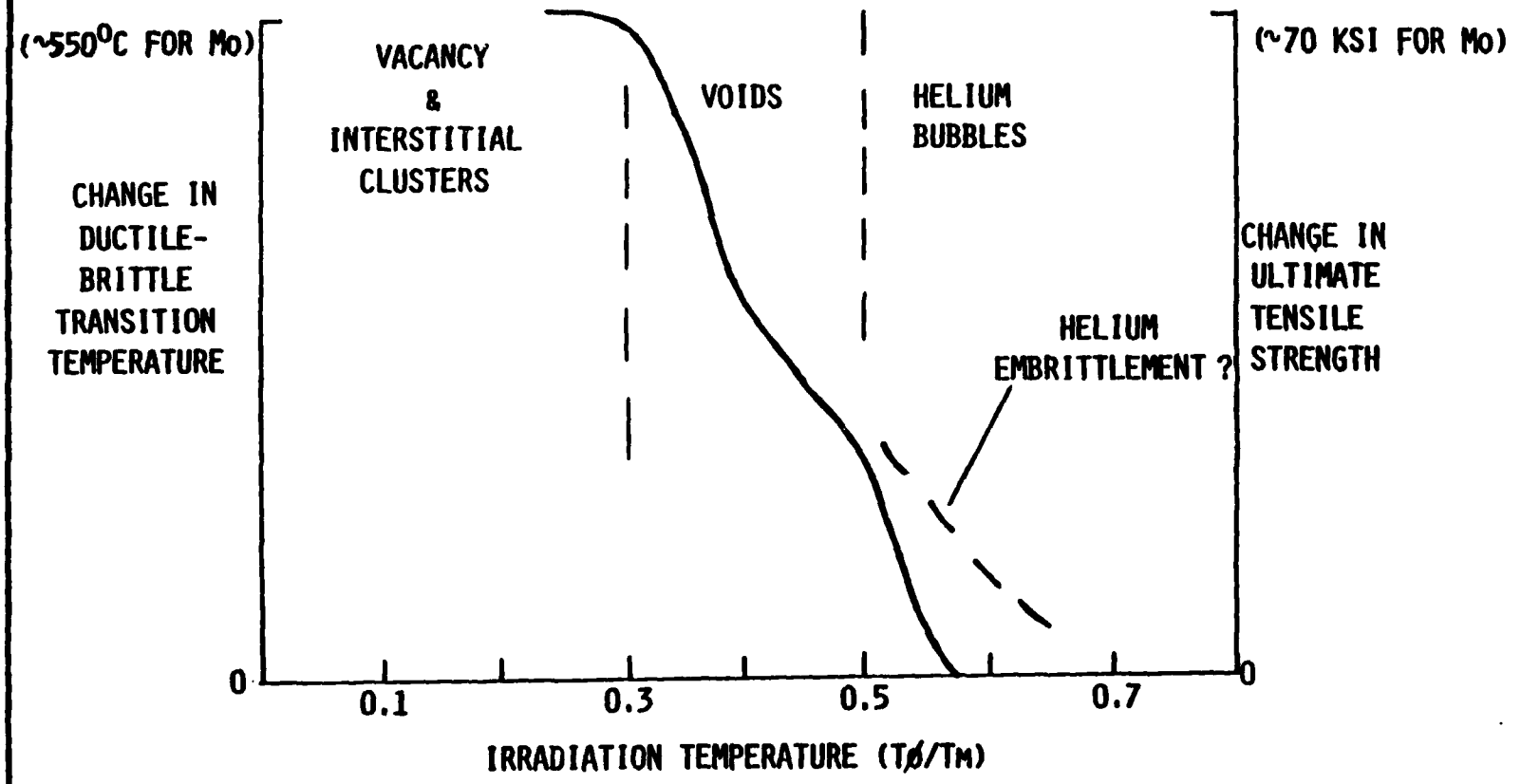

The schematic curves previously presented for swelling and mechanical embrittlement were obtained from very limited data in the literature. Unfortunately, only a meager amount of research has involved refractory metals irradiated at high temperatures with subsequent property testing. Considerably more research, both applied and basic, must be performed before adequate knowledge can be gained of the physical and mechanical effects to be expected for refractory metals in space nuclear power systems.

This figure lists some of the basic research that is still needed. For example, the effects of various irradiation temperatures must be examined, the effects of flux and fluence, of alloying and impurity elements, of thermal cycling, of transmutation elements and helium bubbles, of void formation, of flux and thermal gradients, and in-situ damage by annealing. The effects of each of these variables on critical properties of the candidate refractory metal cladding materials must be more quantitatively defined before design of a reactor system can be seriously considered. And since irradiation tests of this type are lengthy in nature, this type of study must be considered as a long lead-time research need.

RESEARCH NEEDS FOR IRRADIATION EFFECTS ON REFRACTORY METALS

- DETERMINE EFFECTS OF IRRADIATION VARIABLES
  - TEMPERATURE/TIME
  - FLUX/NEUTRON SPECTRUM/FLUENCE
  - THERMAL GRADIENTS
  - THERMAL CYCLING

- DETERMINE EFFECTS OF MATERIAL VARIABLES
  - ALLOYING ELEMENTS
  - IMPURITIES
  - PROCESSING/MICROSTRUCTURE
  - IRRADIATION PRODUCTS (TRANSMUTATION ELEMENTS/HELIUM)

DEFINITIVE EFFECTS ON CRITICAL PROPERTIES

If we direct our attention outside the reactor shield to the power conversion system, it is still apparent that high-temperature materials are one of the key requirements for high-energy systems. For the power conversion systems most likely to be used for high energy systems (i.e., Brayton, Rankine, or Thermionics), refractory metals will be required as the structural material in the primary heat-transfer system.

During the 1960's, a considerable amount of effort was directed at the technology of refractory metals. But much of this effort ended in the early 1970's with termination of several major government-sponsored efforts. So only minimal progress has been made in this field during the past decade. As a result, the nation's facilities and capabilities for conducting this work have greatly diminished during this period of relative inactivity. So much of the nation's capabilities for this type of research must be rebuilt.

This figure compares the long-term creep strengths of some of the more highly-developed refractory metals. The alloys shown represent each of the four classes of refractory metals:

Niobium alloys:	CB-1Zr and FS-85
Tantalum alloys:	T-111 and ASTAR-811C
Molybdenum alloys:	TZM and TZC
Tungsten alloys:	Unalloyed Tungsten, W-25Re, and W-25Re-30Mo

Each of these alloys are candidates as structural materials for various power conversion systems.

CREEP STRENGTH OF SOME REFRACTORY METALS & ALLOYS

(1% CREEP IN 10,000 HRS.)

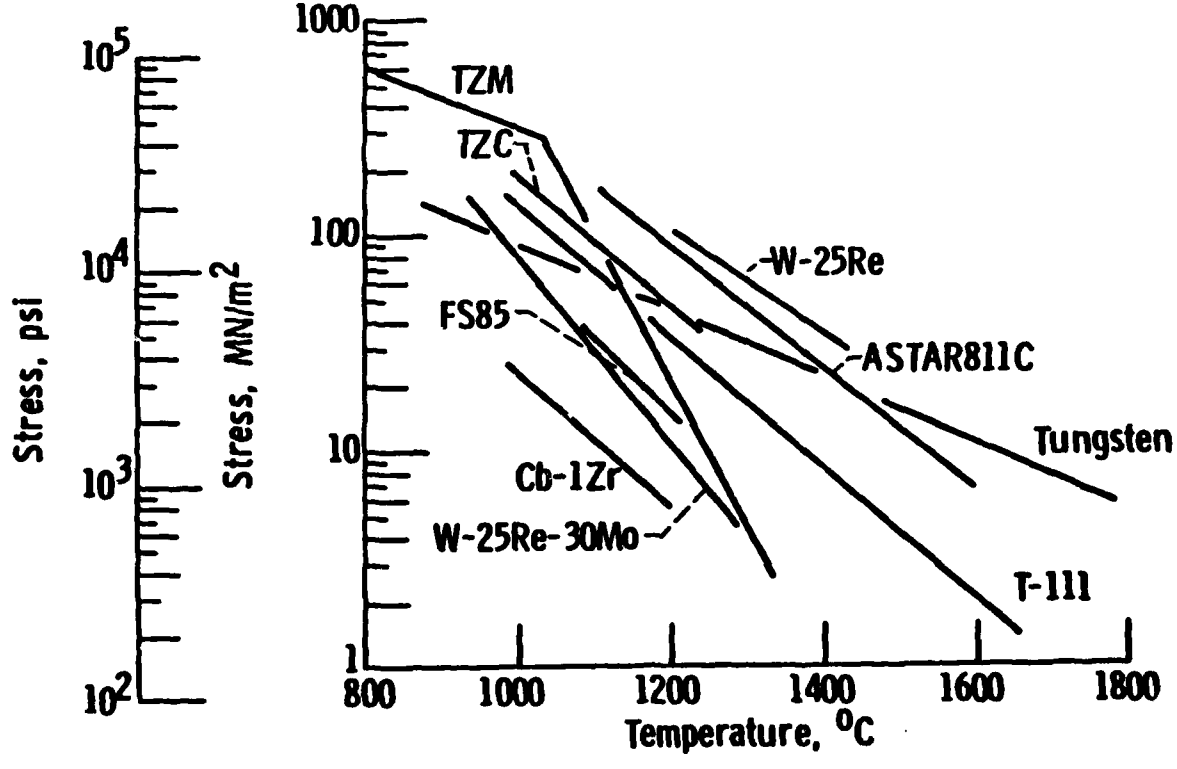

The previous plot showed averaged values for the creep strengths of the various refractory metal alloys, and several of the plots were based on long-term extrapolations from short-term creep data. Considerably more long-term creep data are needed for most of these alloys to develop a more meaningful data-base for future design of power conversion systems.

This figure shows the results of some long-term creep tests that were previously run on the strongest of the tantalum-base alloys (ASTAR-811C). The solid line shows the average values of the data, and the dashed line indicates the amount of data scatter encompassed in a 2-sigma variation. Since the latter values are typically used for systems design purposes, creep-strength plots like this are needed for each of the refractory alloy candidates. And each of these long-term data points must be obtained in tests conducted in ultra-high vacuum (better than 10^{-9} Torr) systems to minimize the effects of interstitial impurities (e.g., oxygen and nitrogen) on the properties. Also, better understanding is needed of the creep mechanisms involved in each of these candidate alloys.

CREEP STRENGTH TO LIMIT STRAIN TO 10,000 HOURS

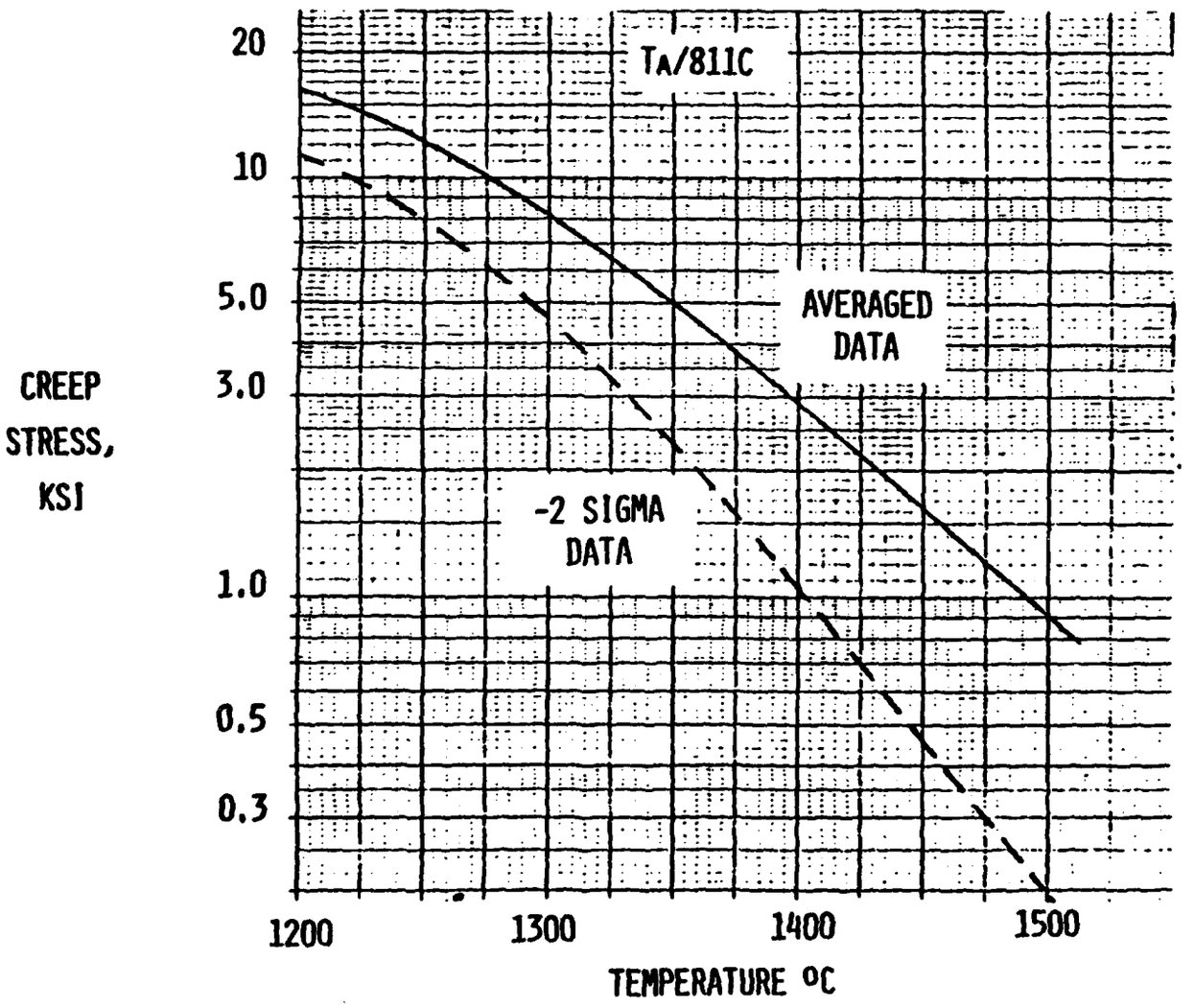

Similarly, other mechanical property data are needed for each of these refractory alloys. For example, in the dynamic power conversion systems (Brayton and Rankine), fatigue may well be the life-limiting property. But only minimal fatigue data are included in the open literature. This figure is representative of the limited data available. Shown here are some low-cycle fatigue data for two tantalum-base alloys (T-111 and ASTAR-811C) and some high-cycle fatigue data for T-111 and a molybdenum alloy (TZC). These data were obtained for specific combinations of cyclic and temperature conditions, and they cannot be generalized to other possible operating conditions. So analytical means of predicting the fatigue performance of refractory alloys at high temperatures is a fertile area of research in structural mechanics.

FATIGUE PROPERTIES OF SOME REFRACTORY METAL ALLOYS

LOW-CYCLE FATIGUE

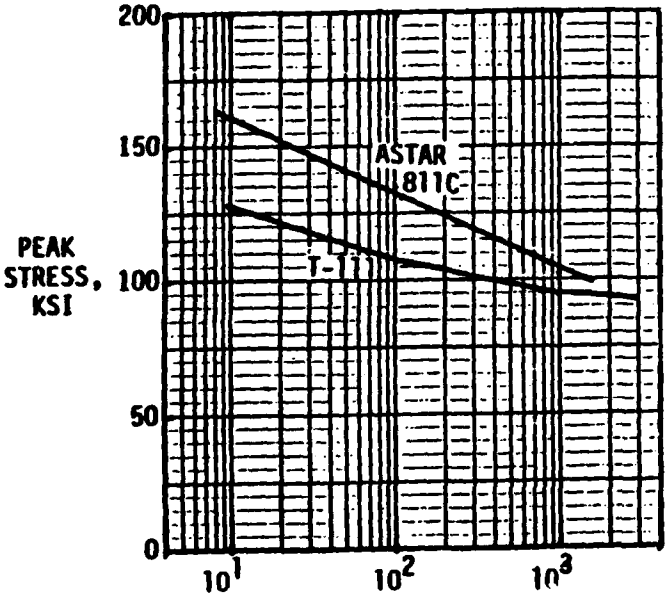

FATIGUE TESTED AT 0.0065 Hz AND 1150°C

HIGH-CYCLE FATIGUE

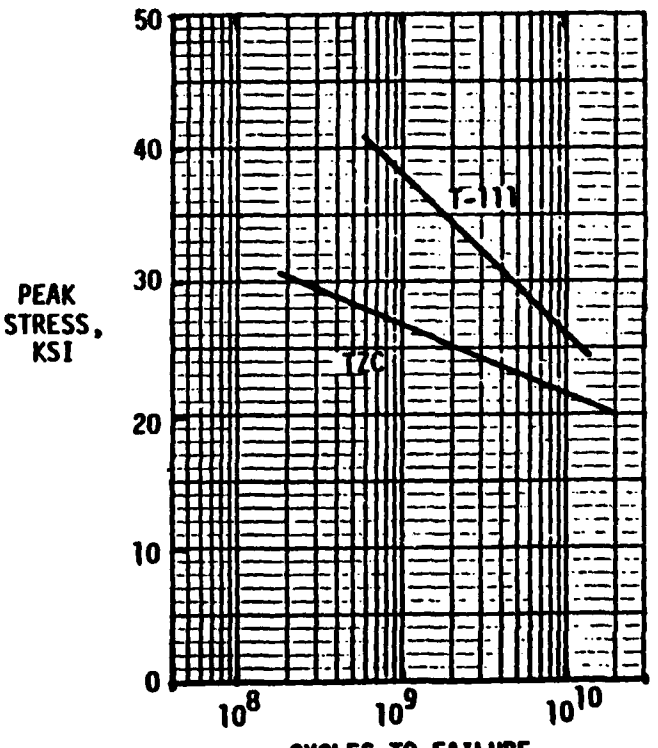

FATIGUE TESTED AT 20. KHz AND 1100°C

Another high-potential research area is the field of refractory alloy synthesis. Although several alloy candidates exist, most of these are rather simple alloys that were largely the result of empirical technology efforts. Very limited knowledge is available on the roles of various alloying elements, and most of the existing knowledge is for simple binary or ternary alloys. Examples of the available data are shown in this figure. These plots illustrate the effects of rhenium alloying in either molybdenum or tungsten. The rhenium additions have a rather dramatic effect on the low-temperature ductility of these alloys -- particularly on alloys in the recrystallized condition.

Since considerable gains have been made in materials science knowledge during the past decade, this knowledge should now be applied to refractory metals. This research may well lead to the future development of more complex refractory alloys that can offer significant improvements in properties over the alloys currently available.

EFFECTS OF RHENIUM IN MOLYBDENUM & TUNGSTEN

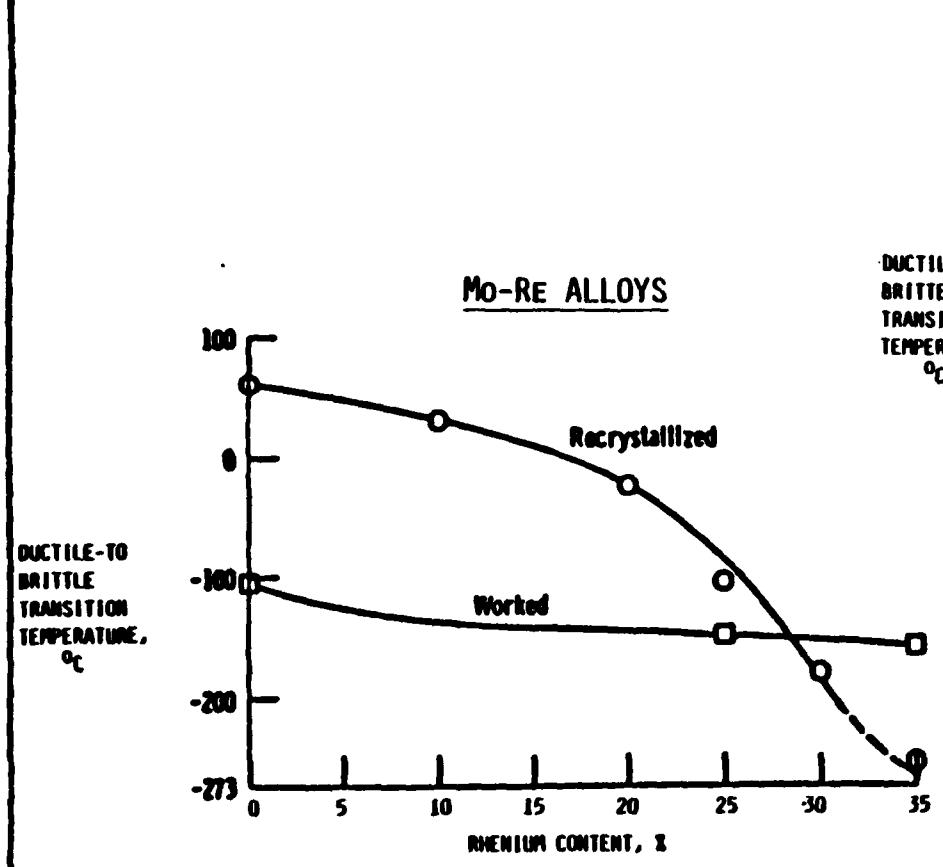

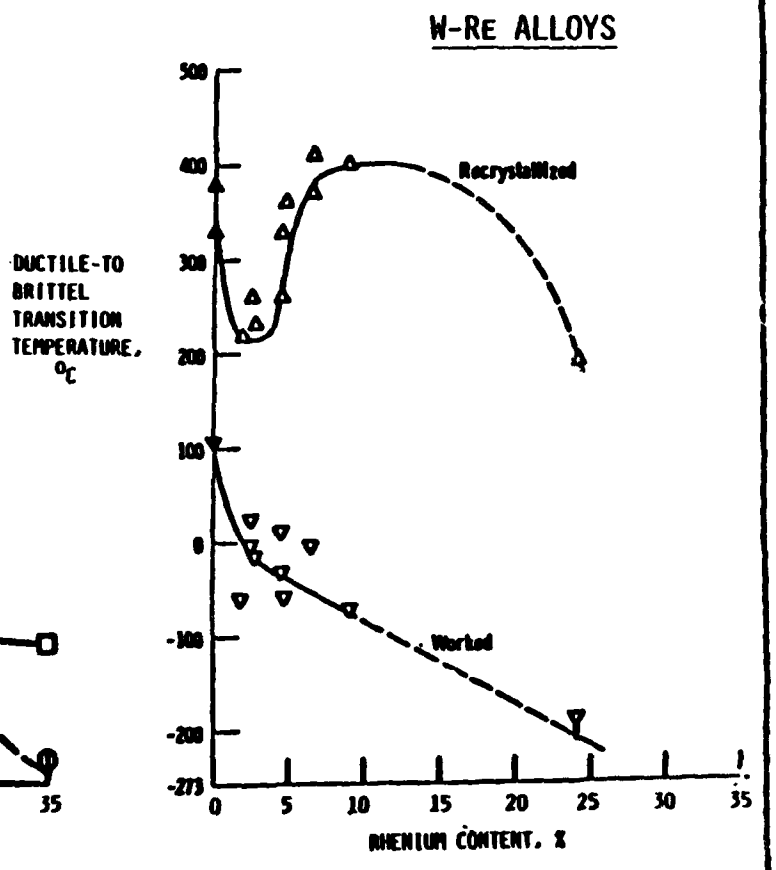

NASA

In the synthesis and development of new refractory alloys, the potential effects of long-term operation in the space environment must be considered. An example of long-term operating effects on properties of refractory alloys is illustrated in this figure. These plots show the effects of high-temperature aging on the low-temperature ductility of weld-zones in the tantalum alloy T-111. The upper section of this figure indicates that long-term operation (up to 10,000 hours) at temperatures above 800°C causes significant increases in the ductile-brittle transition temperature of the weld zones produced by tungsten-inert-gas (TIG) welding. However, the lower section of the figure indicates that weld zones produced by electron-beam (EB) welding were not as sensitive to this aging effect. The prime differences in these two types of welds are the greater purity and smaller grain size resulting from the EB welds. Long-time, high-temperature operation permits diffusion of interstitial impurities within the weld zones and migration to the grain boundaries. This can cause embrittlement of this ductile alloy.

Long-term studies such as these will be required on any new refractory alloys considered for future power systems.

EFFECTS OF AGING ON THE DUCTILITY OF A TANTALUM ALLOY (T-111)

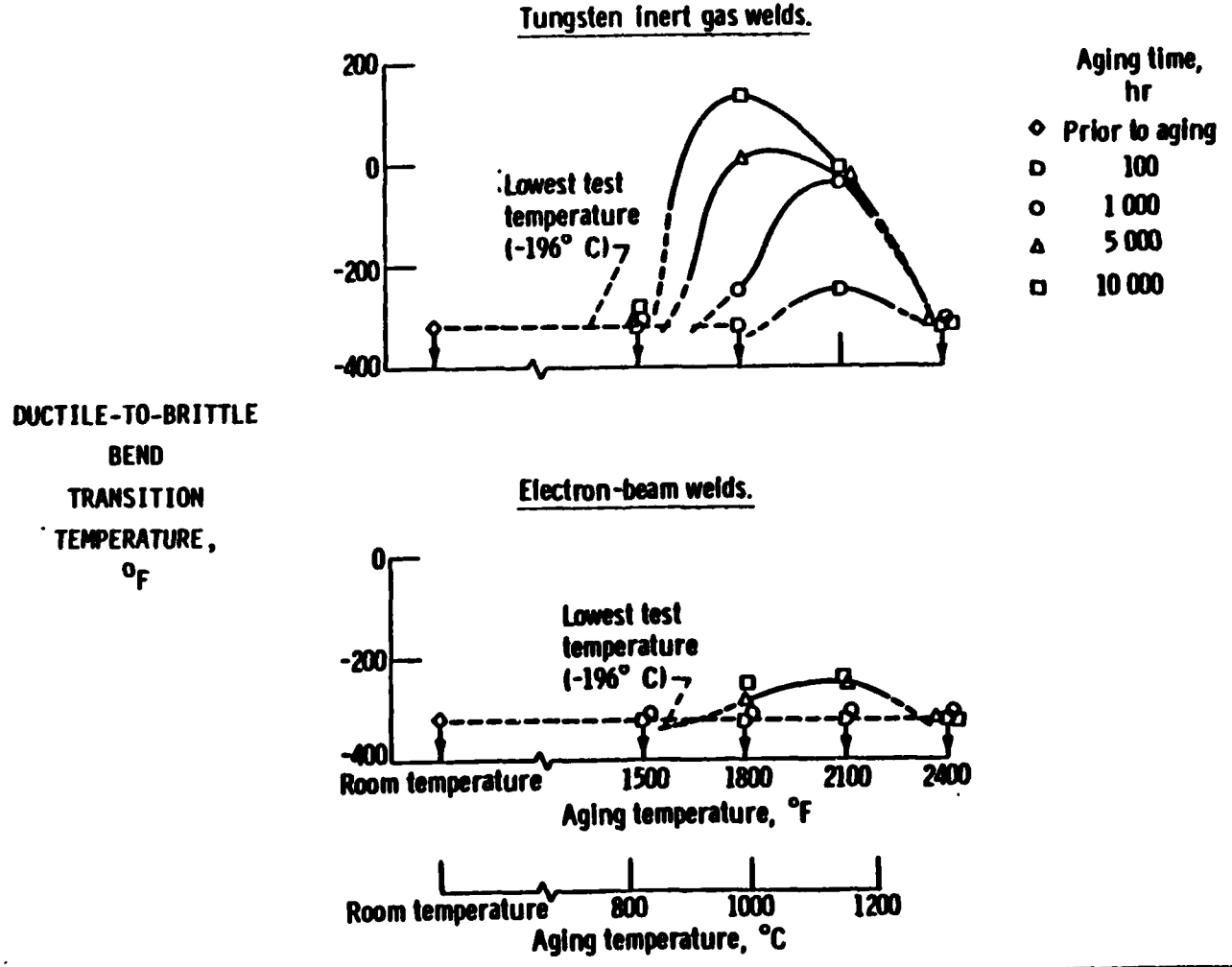

This figure lists some of the current research needs for future use of refractory metals as structural materials in high-energy power conversion systems. The more basic research needs are associated with alloy modification and synthesis. But just as important are the applied research aspects of the other three topics listed (i.e., mechanical property characterization, environmental resistance studies, and hardware fabrication technology).

Many of these research needs involve very long-term tests in unique high-vacuum facilities. So considerable lead-time is required to rebuild the national research capabilities for this effort and then to conduct the required research. So effort should be started in these areas as soon as possible in order to permit adequate research time prior to any future national commitment to a systems development effort.

RESEARCH NEEDS FOR REFRACTORY METAL STRUCTURES

- ALLOY MODIFICATIONS
  - LONGER-TERM, HIGH-TEMPERATURE STABILITY
  - IMPROVED WELDABILITY IN W OR Mo ALLOYS
  - IMPROVED RESISTANCE TO FAST-NEUTRON EFFECTS
- MECHANICAL PROPERTY CHARACTERIZATION
  - LONG-TERM CREEP
  - CREEP-FATIGUE
  - THERMAL FATIGUE

  } DESIGN DATA BASE
- ENVIRONMENTAL RESISTANCE
  - COMPATIBILITY WITH HEAT-TRANSFER/WORKING FLUIDS
  - LONG-TERM SPACE (VACUUM) EXPOSURE
- HARDWARE FABRICABILITY
  - FORMABILITY
  - WELDABILITY
  - REPRODUCIBILITY/RELIABILITY/INSPECTABILITY

This presentation has attempted to indicate the relatively meager state-of-technology associated with high-temperature materials being considered for future high-energy space power systems. The research and technology needs in this field are considerable, and this presents many opportunities for both fundamental and applied research. Fulfilling these research needs is likely to be the pacing item in considering future commitments to a high-energy space power system.

A prime concern is that very little effort has been conducted during the past decade on the high-temperature materials of greatest interest for these advanced power systems. As a result, much of the nation's unique facilities and capabilities for conducting this research have waned. So significant investments of capital and time will be required to rebuild this capability. Because of the long lead-time required for this, these investments must be started in the very near future.

CONCLUSIONS

- HIGH-TEMPERATURE MATERIALS FOR SPACE POWER USE REQUIRE CONSIDERABLE ADVANCES IN TECHNOLOGY
  - MANY FERTILE AREAS FOR USEFUL RESEARCH
- THE CURRENT U.S. CAPABILITIES FOR THIS RESEARCH ARE VERY LIMITED
  - LONG TIME AND LARGE CAPITAL INVESTMENTS REQUIRED TO REBUILD CAPABILITIES

THE POTENTIAL IS HIGH!
IS THERE A NATIONAL WILL?

NASA

Q & A - N. Saunders

From: P. J. Turchi, R & D Associates

Why is there such scatter in fuel swelling data at same temperature with the same fuel? Is it manufacturing statistics, operating differences?

A.

The currently-available nuclear fuel swelling data includes a large amount of scatter for a variety of reasons. But the major contributor to this scatter is probably associated with the severe difficulties involved in in-pile testing of materials. In this type of testing, it is very difficult (if not impossible) to control the major test variables, particularly temperature and neutron flux. Thus, each test specimen will likely see variations in these variables as a function of testing time and they may also be subjected to gradients of temperature and fluence along the axial length of a specimen at any particular time. Thus, all published data are really an averaging of the projected operating variables.

SOME MATERIAL IMPLICATIONS OF SPACE NUCLEAR REACTORS (NON-FUEL MATERIALS)

SPECIAL CONFERENCE
ON
PRIME POWER FOR HIGH-ENERGY SPACE SYSTEMS
FEBRUARY 22 TO 25, 1982

AIR FORCE OFFICE OF SCIENTIFIC RESEARCH

JAMES F. MORRIS
MECHANICAL AND ENERGY SYSTEMS ENGINEERING
ARIZONA STATE UNIVERSITY

ABSTRACT

As the title states this presentation points to non-fuel materials for space nuclear reactors: high-temperature alloys and electric isolators. Because the charts for the ten-minute talk are reasonably self-explanatory, no further explanations attend them. But a selectively underlined manuscript for "Tungsten, Rhenium Alloys in Space Nuclear Reactors" accompanies this handout package. That text will appear soon in Air Force TM form.

SOME MATERIAL IMPLICATIONS OF SPACE NUCLEAR REACTORS (NON-FUEL MATERIALS)

SPECIAL CONFERENCE
ON
PRIME POWER FOR HIGH-ENERGY SPACE SYSTEMS
FEBRUARY 22 TO 25, 1982

AIR FORCE OFFICE OF SCIENTIFIC RESEARCH

JAMES F. MORRIS
MECHANICAL AND ENERGY SYSTEMS ENGINEERING
ARIZONA STATE UNIVERSITY

"IF THERE IS A SINGLE GENERAL TREND THAT APPLIES TO THE VARIOUS COMBINATIONS OF HEAT SOURCES AND CONVERSION METHODS, IT IS THE ONE TOWARD HIGHER SOURCE TEMPERATURE AND HIGHER SINK TEMPERATURE--AND CONSEQUENTLY LIGHTER WEIGHT SYSTEMS. FOR THIS REASON, THE WORKSHOP FELT THAT HIGH-TEMPERATURE-MATERIALS DATA WAS OF PRIME IMPORTANCE...."

W. A. RANKEN, LOS ALAMOS NATIONAL LABORATORY: "FUTURE ORBITAL POWER SYSTEMS TECHNOLOGY REQUIREMENTS," NASA CP-2058 (CONFERENCE), SEPTEMBER 1978.

"...TOWARD HIGHER SOURCE TEMPERATURE..."

HEAT-PIPE-COOLED REACTORS (HPCR'S):

"OUR CHOICE OF A REACTOR DESIGN TEMPERATURE DEPENDS MAINLY ON THE CONVERTER ELEMENT. TO MINIMIZE (SIC) POWER PLANT MASS AND SIZE, A TEMPERATURE OF 1400K IS NEEDED. HOWEVER, TO ACCOMMODATE ANTICIPATED FUTURE IMPROVEMENTS IN CONVERTERS, THE ABILITY (SIC) TO OPERATE AT SEVERAL HUNDRED DEGREES HIGHER TEMPERATURE SHOULD BE DEVELOPED."

LANL: "SELECTION OF POWER PLANT ELEMENTS FOR FUTURE REACTOR SPACE ELECTRIC POWER SYSTEMS," LA-7858, SEPTEMBER 1979

"SEVERAL:" "MORE THAN TWO OR THREE, BUT NOT MANY"
THE AMERICAN HERITAGE DICTIONARY OF THE ENGLISH LANGUAGE

1800 TO 2000K: "...SEVERAL HUNDRED DEGREES HIGHER TEMPERATURES SHOULD BE DEVELOPED."

"...TOWARD HIGHER SOURCE TEMPERATURE..."

ROTATING BED REACTORS (RBR'S) AND OTHER NUCLEAR ULTRAVERSIONS: 2000 TO 3000K EFFLUENTS

RBR'S OR OTHER ULTRAVERSIONS WITH MAGNETOHYDRODYNAMICS (MHD): 2000 TO 2100K EFFLUENTS

"...TOWARD HIGHER SOURCE TEMPERATURE..."

"...THE WORKSHOP FELT THAT HIGH-TEMPERATURE-MATERIAL DATA WAS OF PRIME IMPORTANCE...."

FOR SPACE NUCLEAR REACTORS IN GENERAL, THE MINIMAL"... HIGHER SOURCE TEMPERATURE..." APPEARS TO FALL

BETWEEN 1800K AND 2100K

NIOBIUM AND TANTALUM ALLOYS FAIL BECAUSE OF NUCLEAR-FUELS COMPATABILITY PROBLEMS, AS OBSERVED BY LANL IN LA-7858, AND OTHER SIGNIFICANT DISADVANTAGES.

IN ADDITION TO STRENGTH AND CREEP PROBLEMS, MOLYBDENUM VAPORIZES AT ABOUT ONE MIL A YEAR AT 1900K.

THUS TUNGSTEN ALLOYS APPEAR TO OFFER THE LOGICAL APPROACH "...TOWARD HIGHER SOURCE TEMPERATURE..."

PROBABLY WITH RHENIUM TO IMPROVE DUCTILITY AS WELL AS TO INHIBIT RECRYSTALLIZATION AND

POSSIBLY WITH VERY LOW LEVELS OF GETTERING ELEMENTS LIKE THORIUM TO BE CONSUMED IN CLEANING UP THE TUNGSTEN ALLOY.

"...TOWARD HIGHER SOURCE TEMPERATURE..."

AFTER SKIMMING THROUGH NUMEROUS CHARTS ON REFRACTORY-ALLOY CHARACTERISTICS ONE OBSERVATION SEEMS OBVIOUS:

TUNGSTEN AND RHENIUM ARE REFRACTORY METALS OF PRIMARY QUALITY.

MOLYBDENUM IS A REFRACTORY METAL OF SECONDARY, PERHAPS TERTIARY QUALITY.

MIXING RHENIUM WITH MOLYBDENUM AS AN ALLOY APPROACH "...TOWARD HIGHER SOURCE TEMPERATURE..." WOULD BE AN UNFORTUNATE DIVERSION FROM WORK ON TUNGSTEN, RHENIUM ALLOYS THAT CAN SERVE SPACE NUCLEAR REACTORS IN GENERAL--- INCLUDING LOW-POWER HEAT-PIPE-COOLED REACTORS.

CAN TUNGSTEN ALLOYS SERVE AT THE
"...HIGHER SOURCE TEMPERATURE...?"

"IT HAS BEEN CONCLUDED THAT W-26RE/LI HEAT PIPES PROMISE LIFETIMES OF MANY YEARS AT 1600°C."
BUSSE ET AL. (EURATOM): "LIFE-TIME BEHAVIOR OF HIGH-TEMPERATURE TUNGSTEN-RHENIUM HEAT PIPES WITH LITHIUM OR SILVER AS WORKING FLUID. "PAPER 4-4, INTERNATIONAL HEAT PIPE CONFERENCE 1973, STUTTGART.

"THE LC-9 CONVERTER CONFIRMED TEC STABILITY WITH OVER 5.3 YEARS (TERMINATED BY PROJECT CESSATION) OF CONSTANT OUTPUT AND EFFICIENCY FROM A 1973K EMITTER AND A 1073K COLLECTOR."

MORRIS: "THERMIONIC ENERGY CONVERSION (TEC) AND SPACE NUCLEAR REACTORS (SNR'S)," TO BE PUBLISHED IN THE 1982 IEEE COPS RECORD, OTTAWA, CANADA, MAY 1982.

HIGH-TEMPERATURE ELECTRICAL ISOLATION (OFTEN WITH REQUIRED HEAT TRANSMISSION)

DEFINITE DIFFERENCES (OR GRADIENTS) IN CHEMICAL POTENTIAL PROMOTE DIFFUSION AND CHEMICAL REACTIONS.

BOTH DIFFUSION AND CHEMICAL-REACTION ACTIVATIONS INCREASE EXPONENTIALLY WITH TEMPERATURE.

CHEMICAL-POTENTIAL DIFFERENCES ACROSS SOLID INTERFACES (AS BETWEEN CONTACTING CONDUCTORS AND INSULATORS--OR AS IN COUPLES IN GENERAL) OR CHEMICAL-POTENTIAL GRADIENTS TEND TO DEGRADE MORE AND MORE RAPIDLY AS TEMPERATURES INCREASE--PARTICULARLY WHEN ACCELERATED BY ELECTRIC-POTENTIAL DIFFERENCES.

SIMPLIFIED DIFFUSION THEORY

$\partial n/\partial t = - AD_c \partial c/\partial x$ (Fick, 1855)

$\partial n/\partial t$ = atom transport rate, A = area, D_c = concentration diffusion coefficient, $\partial c/\partial x$ = concentration gradient

FICK'S FIRST AND SECOND LAWS FAIL TO EXPLAIN DIFFUSION THAT INCREASES CONCENTRATION.
ATOMS MIGRATE TO REDUCE OVERALL FREE ENERGY AND APPROACH SYSTEM EQUILIBRIUM.
THUS DIFFERENCES IN CHEMICAL POTENTIAL CAUSE DIFFUSION.
ATOM FLOW RATE IS PROPORTIONAL TO THE CHEMICAL-POTENTIAL GRADIENT ($\partial\mu/\partial x$):

$\partial n/\partial t = - AD\mu \, \partial\mu/\partial x$ where D_μ = chemical potential diffusion coefficient

$D_\mu = cD_c \partial \ln c/\partial\mu$

$\mu = \mu^o + RT\ln a$ where activity $a = \gamma c$ replaces c in reality; $\mu^o = \mu$ for pure component

$D_c = D_o e^{- \Delta H/RT}$ Arrhenius diffusion-constant expression

D_o = frequency factor; ΔH = effective activation enthalpy

$D_\mu = cD_o e^{- \Delta H/RT} \partial \ln c/\partial\mu$

CHEMICAL-POTENTIAL-DIFFUSION EFFECTS INCREASE EXPONENTIALLY WITH TEMPERATURE.

SIMPLIFIED CHEMICAL-REACTION THEORY

$$iI + jJ \rightleftarrows yY + zZ$$

FREE-ENTHALPY CHANGE

$$dG = -SdT + VdP + \mu_I dn_I + \mu_J dn_J + \mu_Y dn_Y + \mu_Z dn_Z$$

$$dG_{T,P} = \mu_I dn_I + \mu_J dn_J + \mu_Y dn_Y + \mu_Z dn_Z = (n_1 + n_2)(-i\mu_I - j\mu_J + y\mu_Y + z\mu_Z)\, d\alpha$$ WHERE THE

RIGHT HAND EXPRESSION RESULTS FROM REACTION CONSTRAINT RELATIONS

IF THE REACTION GOES COMPLETELY TO THE RIGHT $\alpha \to 1$ AND $d\alpha > 0$

IF THE REACTION GOES COMPLETELY TO THE LEFT $\alpha \to 0$ AND $d\alpha < 0$

FOR SPONTANEOUS REACTION $dG_{T,P} < 0$

TO REACT SPONTANEOUSLY TO THE RIGHT $i\mu_I + j\mu_J > y\mu_Y + z\mu_Z$

TO REACT SPONTANEOUSLY TO THE LEFT $i\mu_I + j\mu_J < y\mu_Y + z\mu_Z$

AT EQUILIBRIUM $G_{T,P}$ *IS A MINIMUM;* $dG_{T,P} = 0$ AND

$$i\mu_I + j\mu_J = y\mu_Y + z\mu_Z$$

WITH $\mu = \mu^o + RT\ln a$

$$RT\ln \frac{a_Y^y \times a_Z^z}{a_I^i \times a_J^j} = RT\ln K = (i\mu_I^o + j\mu_J^o) - (y\mu_Y^o + z\mu_Z^o) = -\Delta G^o \quad \text{OR} \quad K = e^{-\Delta G^o/RT}$$

WHERE K IS THE EQUILIBRIUM CONSTANT

CHEMICAL-POTENTIAL DIFFERENCE DETERMINES REACTION TENDENCIES

HIGH-TEMPERATURE ELECTRICAL ISOLATION (OFTEN WITH REQUIRED HEAT TRANSMISSION)

USE VACUUM OR INERT-GAS GAPS RATHER THAN SOLID INSULATORS WHEN POSSIBLE--AS ADVOCATED IN THE MAY 1978 IEEE COPS PRESENTATION "OPTIMIZE OUT-OF-CORE THERMIONIC ENERGY CONVERSION FOR NUCLEAR ELECTRIC PROPULSION."

MORRIS: NASA TM-73892, FEBRUARY 1978, CITING "HIGH-THERMAL-POWER-DENSITY HEAT TRANSMISSION WITH ELECTRICAL ISOLATION AT HIGH TEMPERATUES," NASA LERC DISCLOSURE LEW-12950-1, JULY 1977.

USE COOLED SOLID INSULATORS WITH HEAT-CHOKE CONNECTIONS TO HIGH-TEMPERATURE CONDUCTORS.

SOME MATERIAL IMPLICATIONS OF SPACE NUCLEAR REACTORS (NON-FUEL MATERIALS)

ASIDE FROM CLEVER MECHANICAL AND GEOMETRIC INNOVATIONS TO AVOID HIGH-TEMPERATURE MATERIAL PROBLEMS, PERHAPS THE MAJOR RECOMMENDATION IS FOR AN INTENSIVE PROGRAM ON HIGH-TEMPERATURE CHARACTERISTICS OF ALLOYS FROM THE TUNGSTEN, RHENIUM, ADDITIVE SYSTEM.

NUCLEAR FUEL SYSTEMS FOR SPACE POWER APPLICATION

L. Yang

ABSTRACT

Work carried out during 1960 to 1972 on in-core thermionic fuel-cladding development has indicated that the uranium carbide-tungsten and the uranium oxide-tungsten fuel systems are promising candidates. Materials and fabrication techniques were developed to meet the requirements of the thermionic fuel elements. Out-of-pile and in-pile studies of fuel-cladding compatibility, dimensional stability, and thermionic performance stability were performed for both fuel systems. Accelerated irradiation tests have attained a burnup of 3×10^{20} fissions/cm^3 for both the carbide and the oxide fueled emitters at 1900°K, which is equivalent to that for 40,000 hours of operation of a 120 ekw thermionic reactor. Prototypical carbide and oxide fueled emitters have been tested for 8000 hours at 1740 - 1840°K. Comparatively speaking, the carbide-fueled system exhibited greater dimensional stability than the oxide-fueled system, while the oxide-fueled system exhibited better thermionic performance stability than the carbide-fueled system. Any future efforts on in-core thermionic fuel-cladding development should be directed toward seeking solutions in these technological areas.

Some recent space power concepts of high power levels use coated fuel particles as nuclear heat source. The experiences gained in the development of coated fuel particles for the high-temperature-gas-cooled reactor at General Atomic will be described and the potential of such coated fuel particles for space power application will be discussed.

PART I.

FUEL SYSTEMS FOR

IN-CORE THERMIONICS

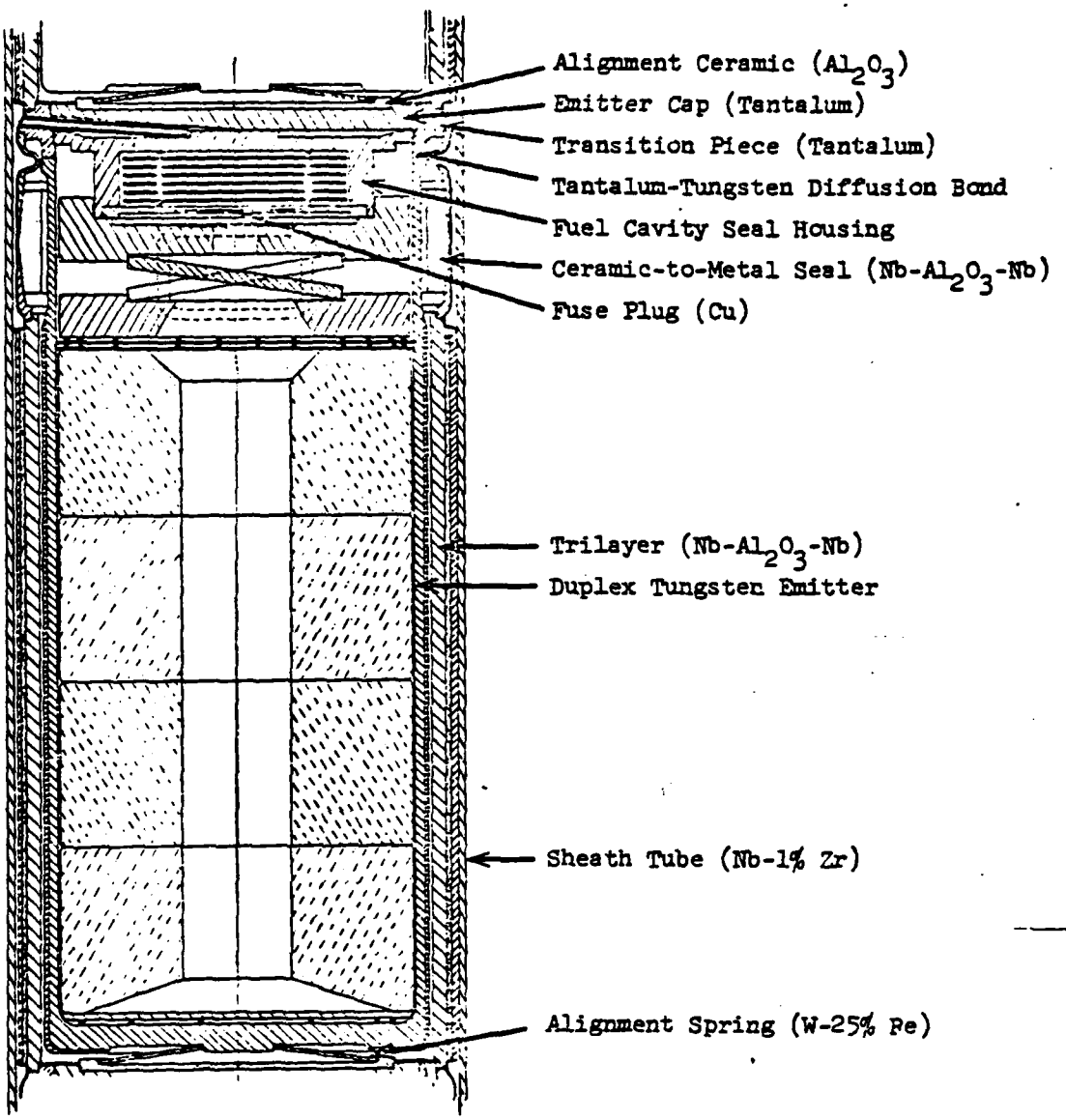

COMPONENT	OPERATING TEMPERATURE, °K	
Duplex Emitter	1881	(Average)
Trilayer	983	(Collector Average) 710°C
Tantalum-Tungsten Diffusion Bond	1262	
Ceramic-to-Metal Seal	1078	(Ceramic Maximum)
Emitter Cap	1213	(Center)
Transition Piece	1153	(Average)
Sheath Tube	973	
Alignment Spring	1773	(Maximum)

Arrangement of Components and Operating Temperatures for F Series Cells

THERMIONIC FUEL-CLADDING SYSTEMS

1. TUNGSTEN – URANIUM CARBIDE

2. TUNGSTEN – URANIUM OXIDE

TUNGSTEN CLADDING

1. PREPARED BY CVD PROCESS

2. DUPLEX STRUCTURE

FLUORIDE TUNGSTEN SUBSTRATE – 28 MIL THICK, 10-20 PPM FLUORINE

CHLORIDE TUNGSTEN EMITTING LAYER – 12 MIL THICK, 4.9-5.0 eV VACUUM WORK FUNCTION

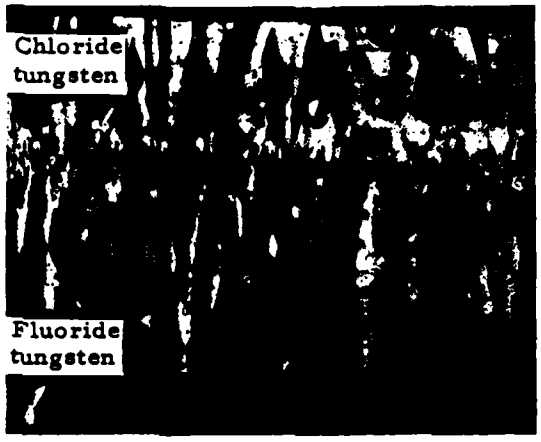

(a) As deposited

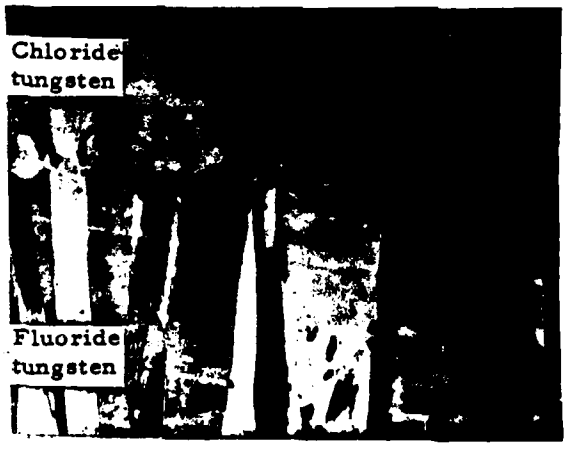

(b) After 10,000 hours at 1923°K out-of-pile

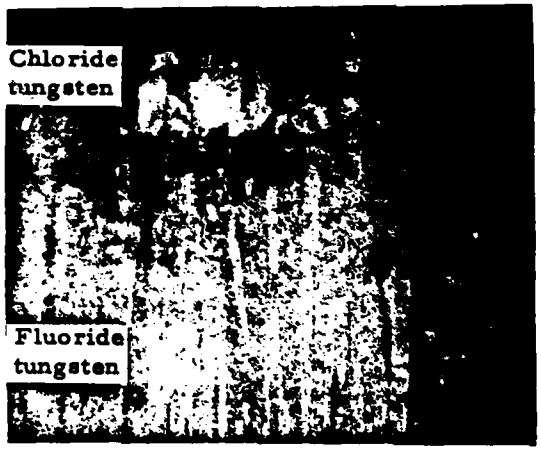

(c) After 3661 hours at 1773°K in-pile

Microstructures of chloride-fluoride duplex tungsten, showing stability of fluoride tungsten grain structure.

CARBIDE FUELS

1. UC AND 90UC-10ZrC

2. HIGH DEGREE OF OPEN POROSITY – 75 - 79% DENSE

3. TUNGSTEN ADDITION – 4 WT %

4. C/U ATOM RATIO - 1.01 - 1.02

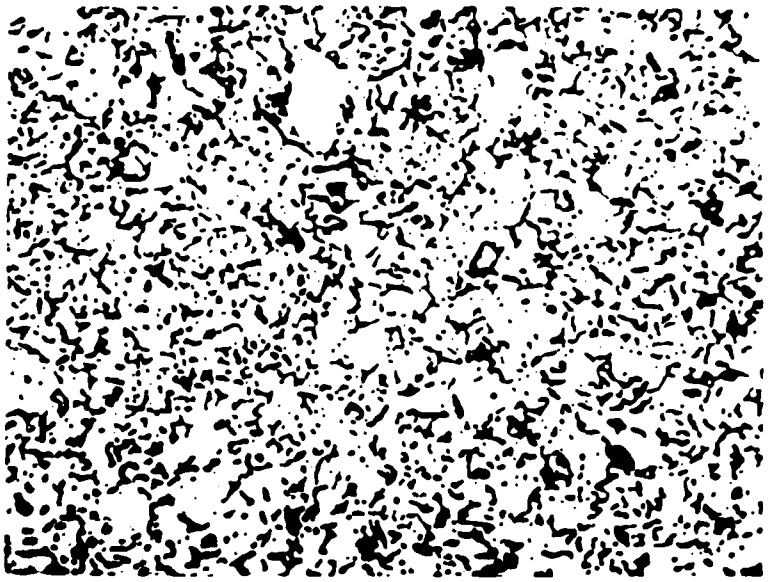

M 31488-1

(a) Unetched .004"

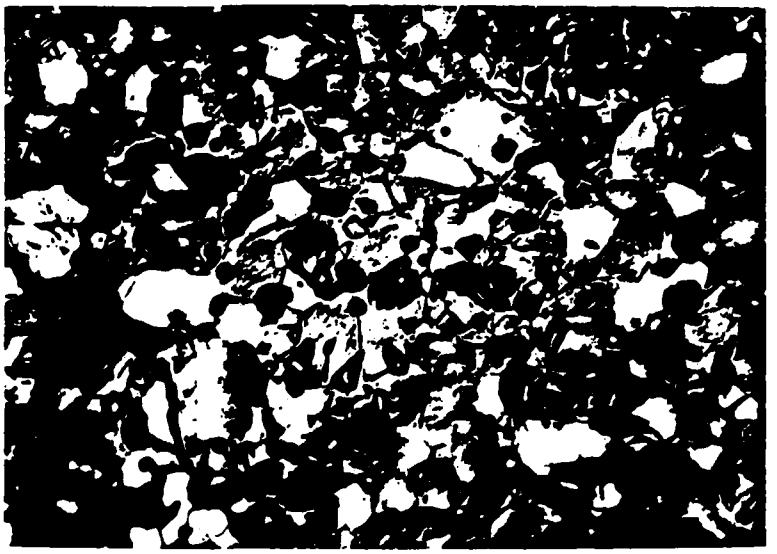

M 21488-2

(b) Etched .001"

Microstructure of 90UC-10ZrC, showing porosities and W and UWC_2 secondary phase

Irradiated carbide-fueled emitter, showing fuel swelling and fuel-cladding interaction

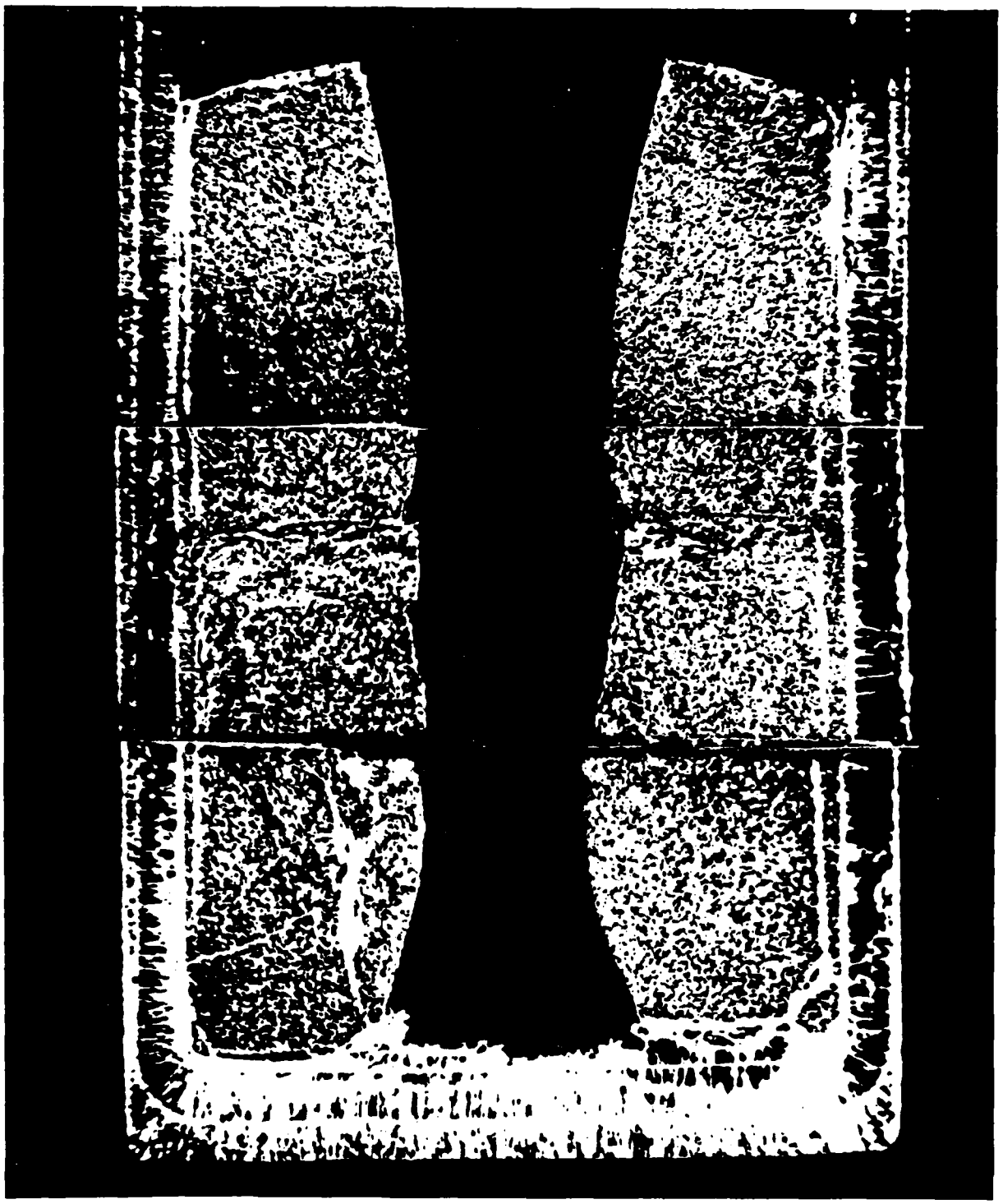

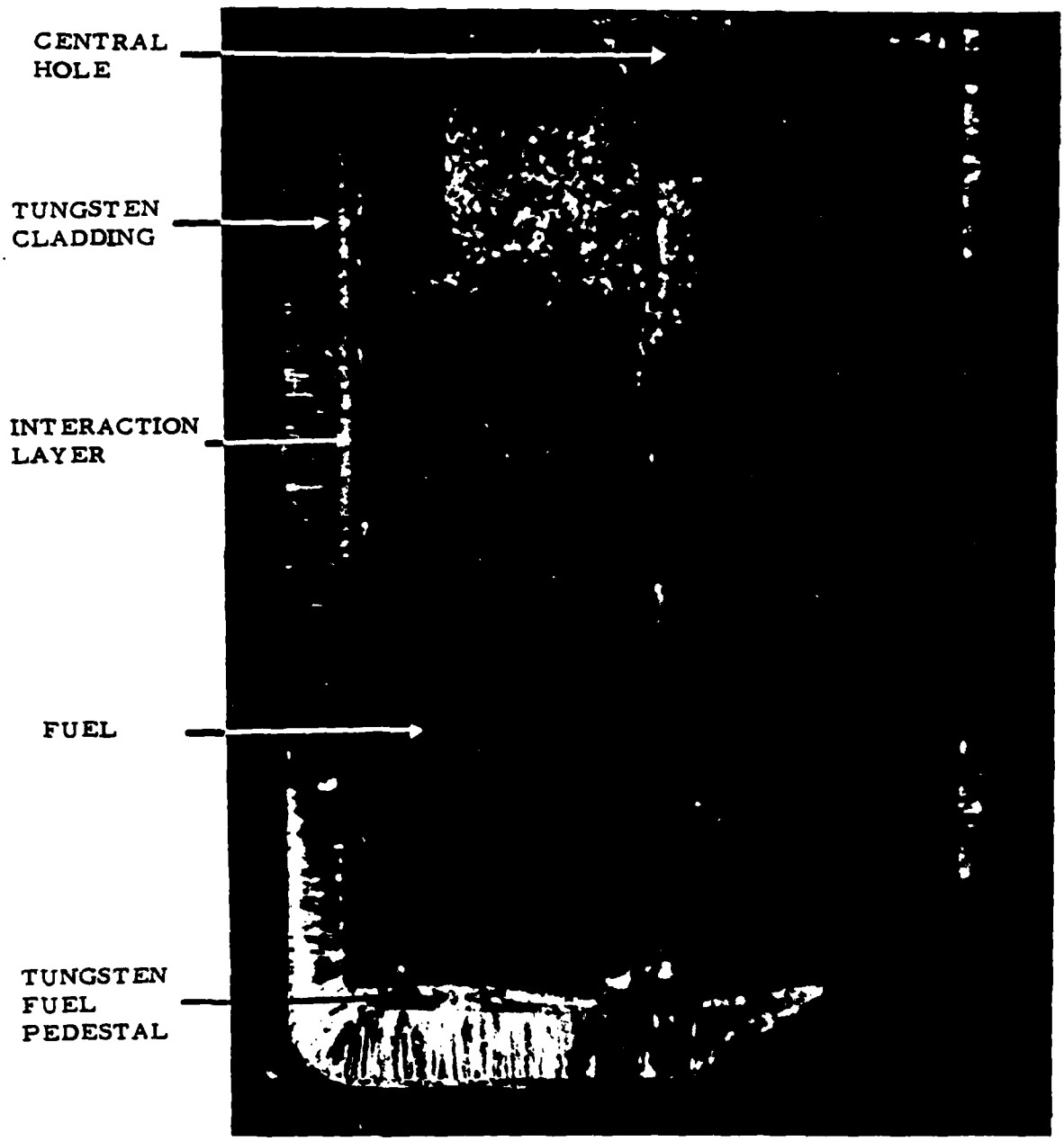

Irradiated carbide-fueled emitter, showing fuel swelling and fuel-cladding interaction

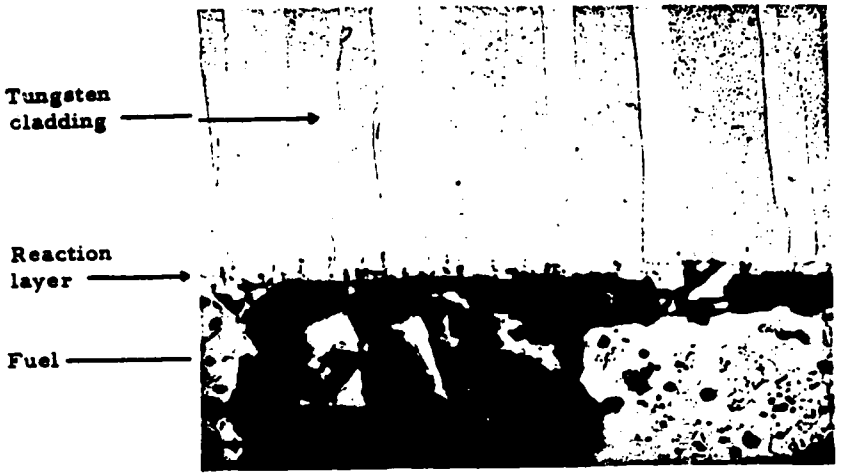

M33291-6

(a) Out-of-pile, 10,000 hours at 1923°K

.004"

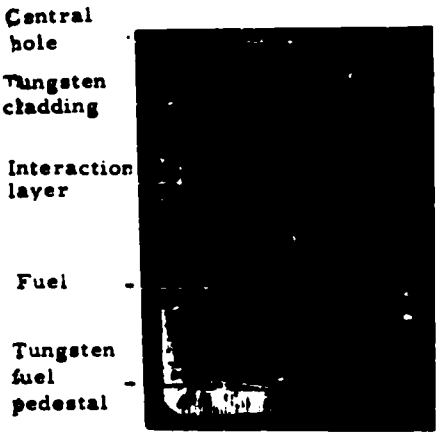

(b) In-pile, 4395 hours at 1950°K, 93% enrichment.

0.3"

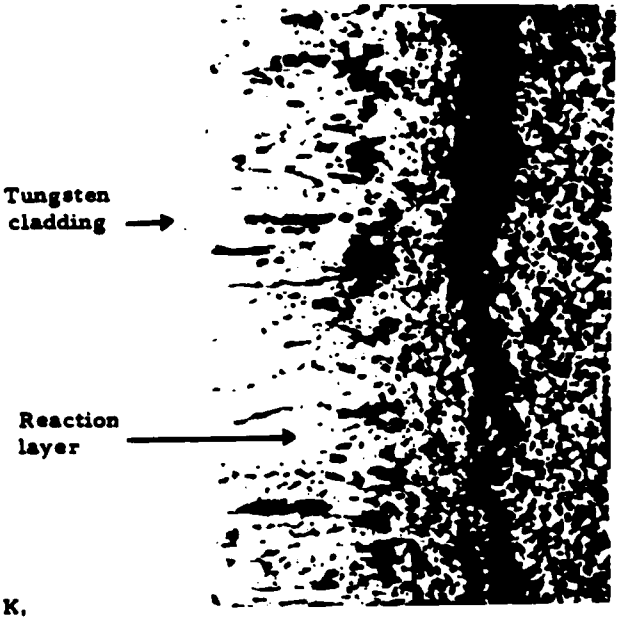

(c) Magnified view of (b)

.010"

Compatibility study of 90UC-10ZrC with tungsten cladding, showing interaction layer

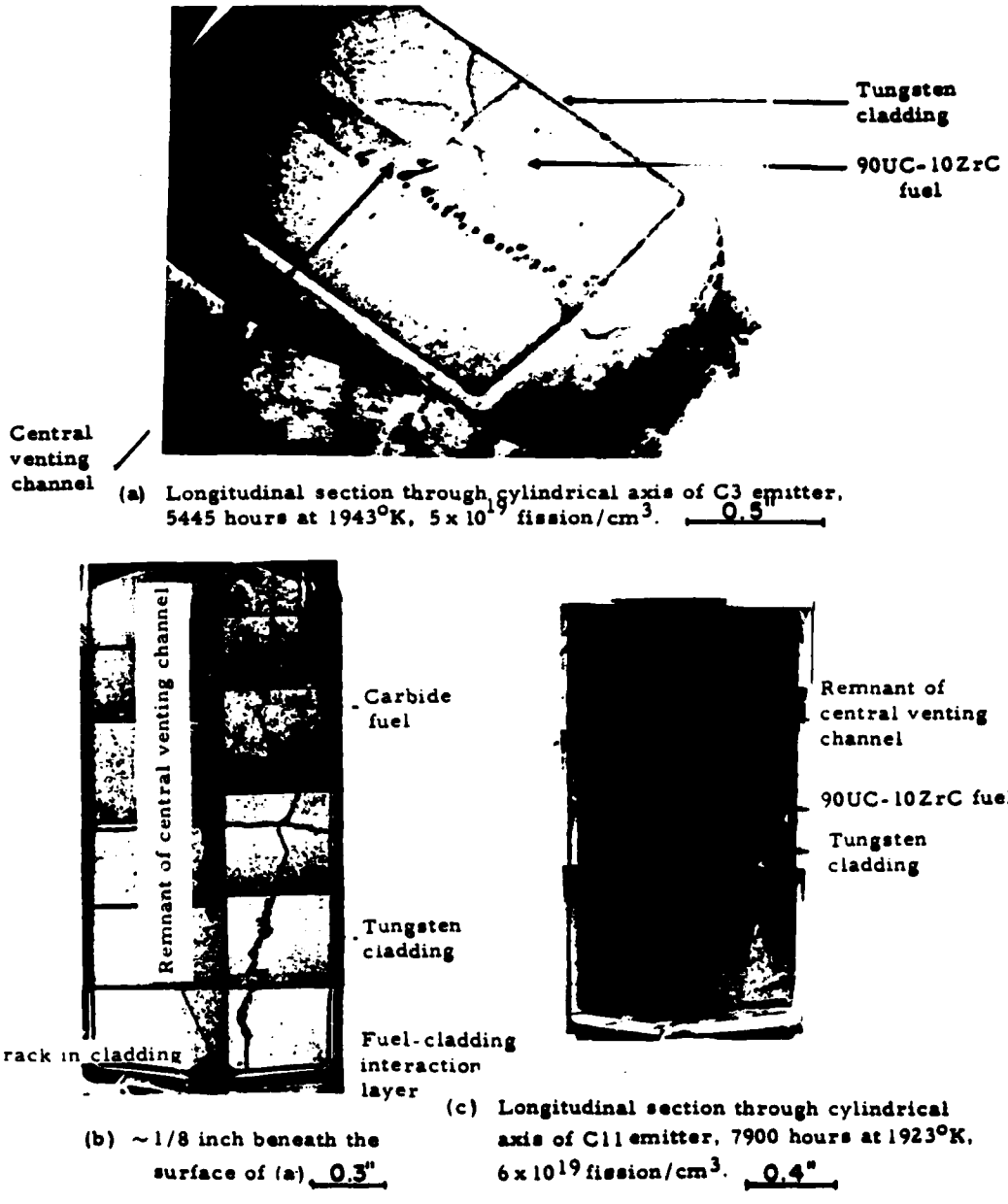

(a) Longitudinal section through cylindrical axis of C3 emitter, 5445 hours at 1943°K, 5×10^{19} fission/cm^3. 0.5"

(b) ~1/8 inch beneath the surface of (a) 0.3"

(c) Longitudinal section through cylindrical axis of C11 emitter, 7900 hours at 1923°K, 6×10^{19} fission/cm^3. 0.4"

90UC-10ZrC fueled prototypical fluoride tungsten emitter (1.1 inch, 40 mil cladding thickness) after in-pile irradiation, showing fuel swelling, fuel-cladding interaction, and cladding cracking

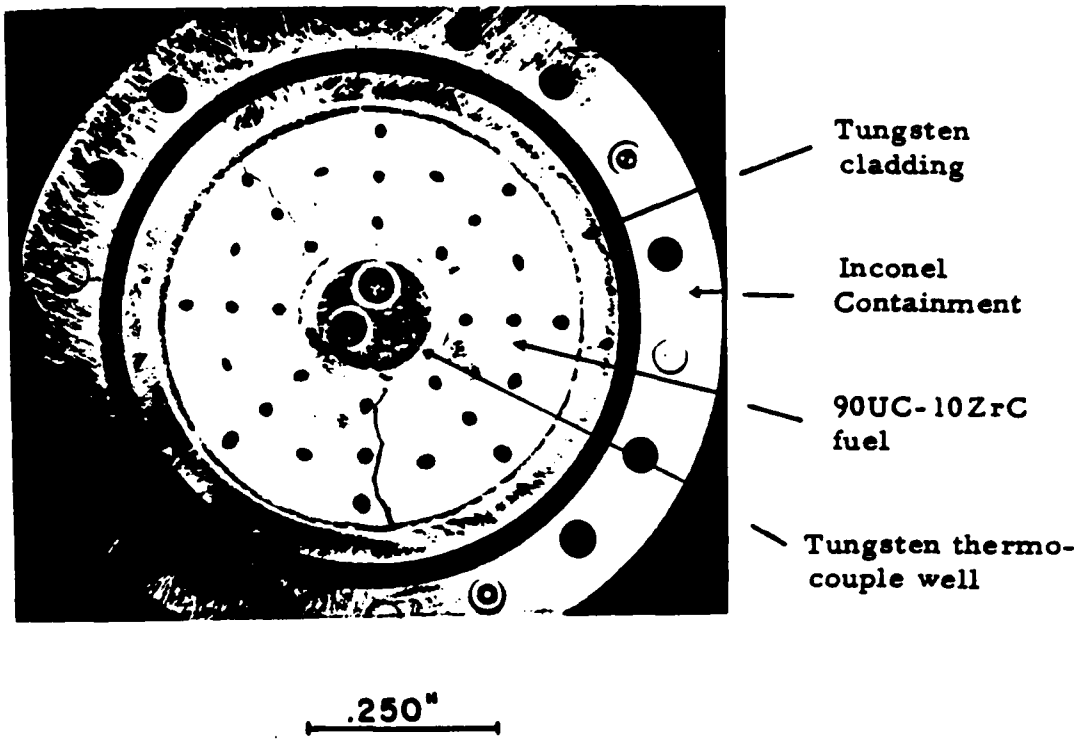

Transversal section of fluoride tungsten (40 mil thick, 0.625 inch diameter) clad 90UC-10ZrC irradiated at a fuel temperature of 1873°K for 11,000 hours to an average burnup of 3×10^{20} fission/cm^3, showing low swelling due to the presence of well distributed venting holes

OXIDE FUEL

1. UO_2

2. O/U = 2.002 - 2.007

3. 90 - 95% DENSE

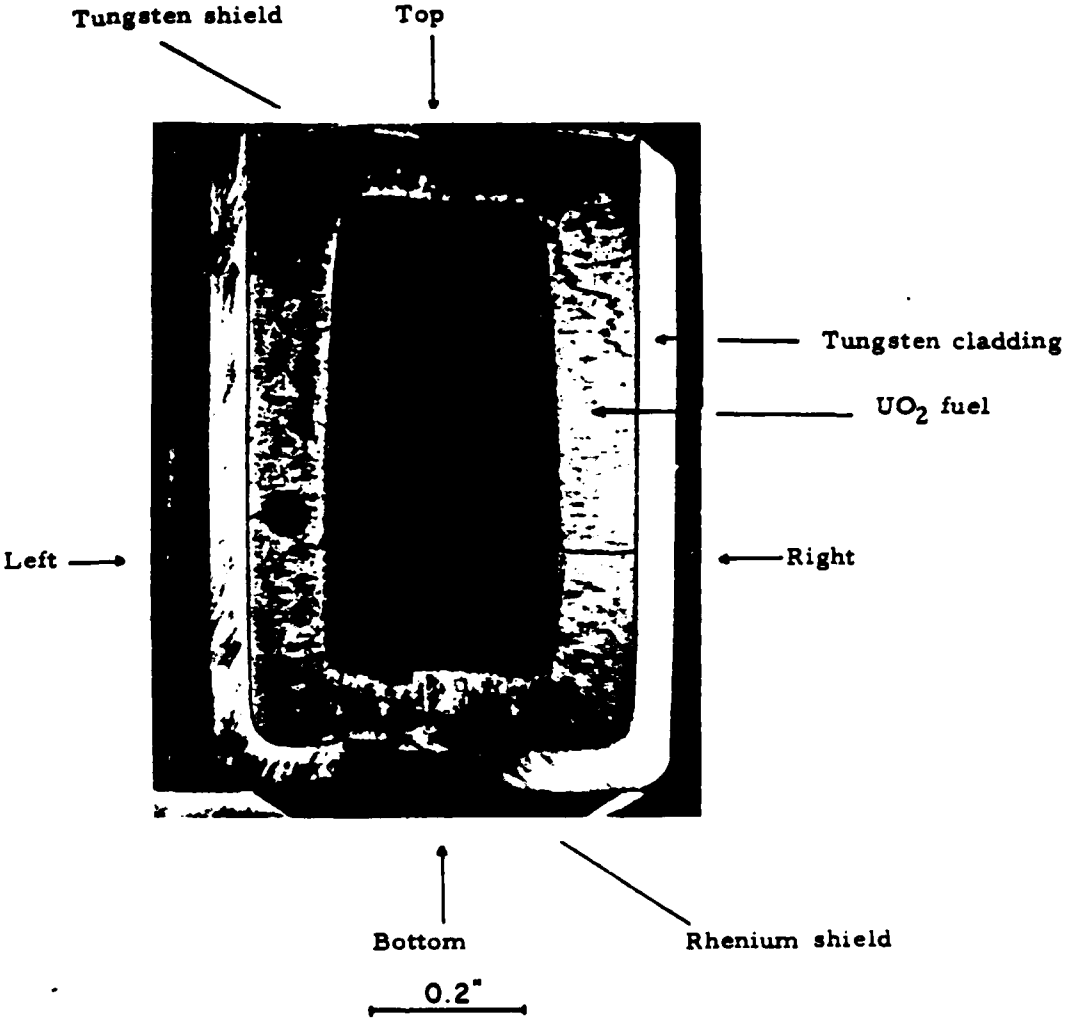

Longitudinal section of UO_2 fueled I4 fluoride tungsten emitter (5/8 inch diameter, 50 mil thickness) irradiated at 1900°K for 9875 hours to 3 x 10^{20} fission/cm^3, showing UO_2 fuel redistribution

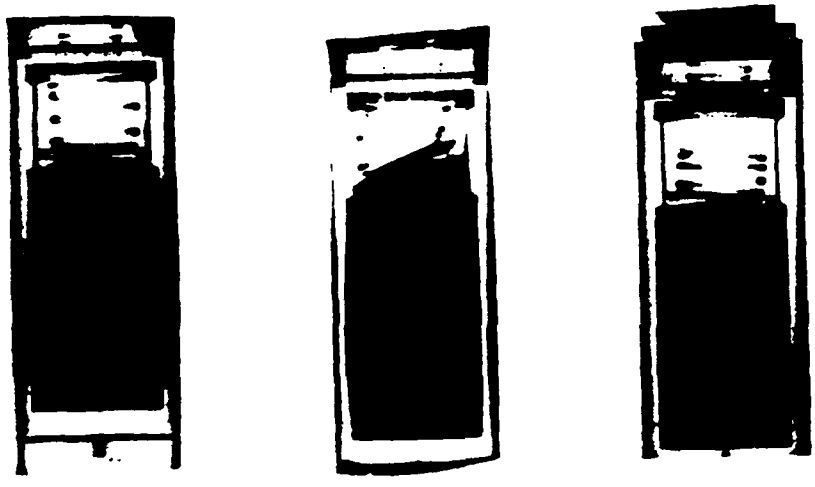

Neutron radiograph of FC-1 samples (4632 hours), showing cladding deformation

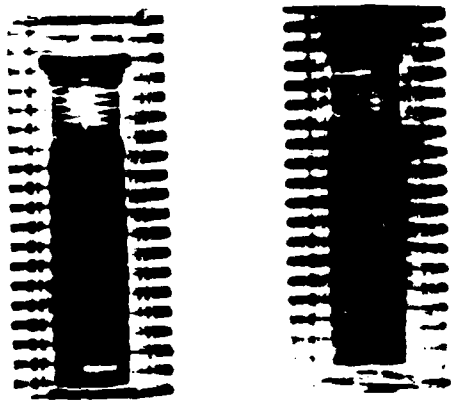

Neutron radiograph of 2E-1 emitters (8644 hours), showing less cladding deformation in smaller emitters

PART II.

COATED FUEL PARTICLES

ASSUMPTIONS IN THE COATED PARTICLE STRESS MODEL

1. LOW-DENSITY BUFFER PYROCARBON DOES NOT POSSESS MECHANICAL STRENGTH.
2. AN INTERNAL PRESSURE IS GENERATED IN THE VOID VOLUME OF THE BUFFER DUE TO GASEOUS FISSION PRODUCTS. SOLID AND CONDENSED FISSION PRODUCTS DECREASE THE AVAILABLE VOLUME.
3. STRESSES ARE GENERATED IN THE COATINGS DUE TO:
   - A. DIFFERENTIAL THERMAL EXPANSION BETWEEN SiC AND DENSE CARBON LAYERS
   - B. THE INTERNAL FISSION GAS PRESSURE
   - C. RADIATION-INDUCED DIMENSIONAL CHANGES IN THE DENSE CARBON.
4. SILICON CARBIDE IS DIMENSIONALLY STABLE UNDER IRRADIATION AND UNDERGOES NO CREEP.
5. FAST-NEUTRON-INDUCED CREEP IN THE DENSE PYROLYTIC CARBON TENDS TO RELIEVE THE STRESSES GENERATED IN THE CARBON COATINGS.

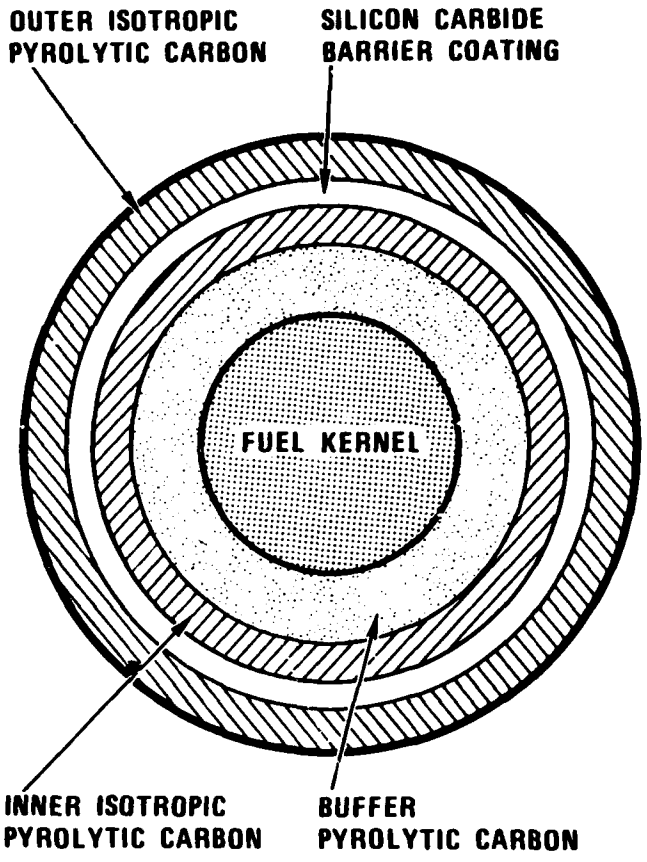

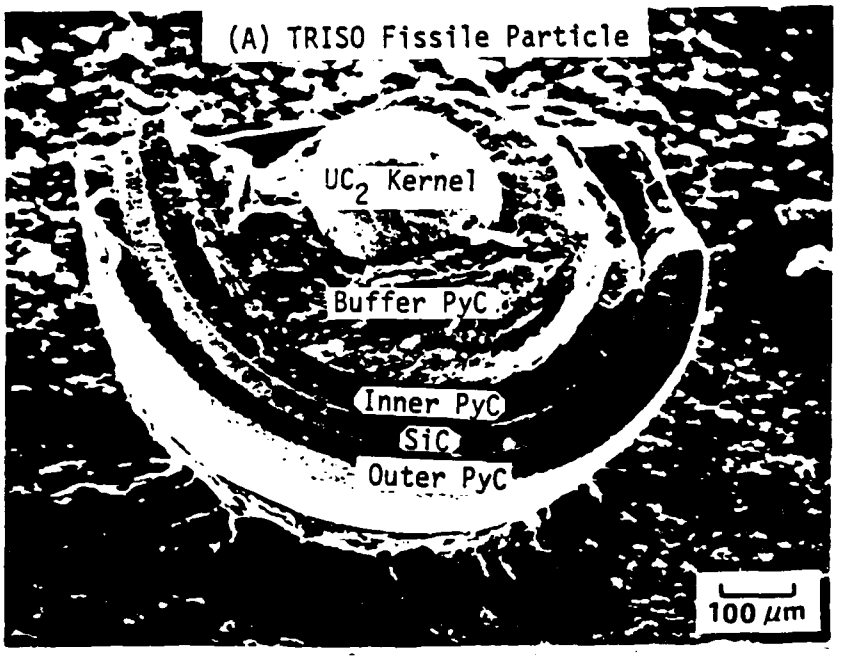

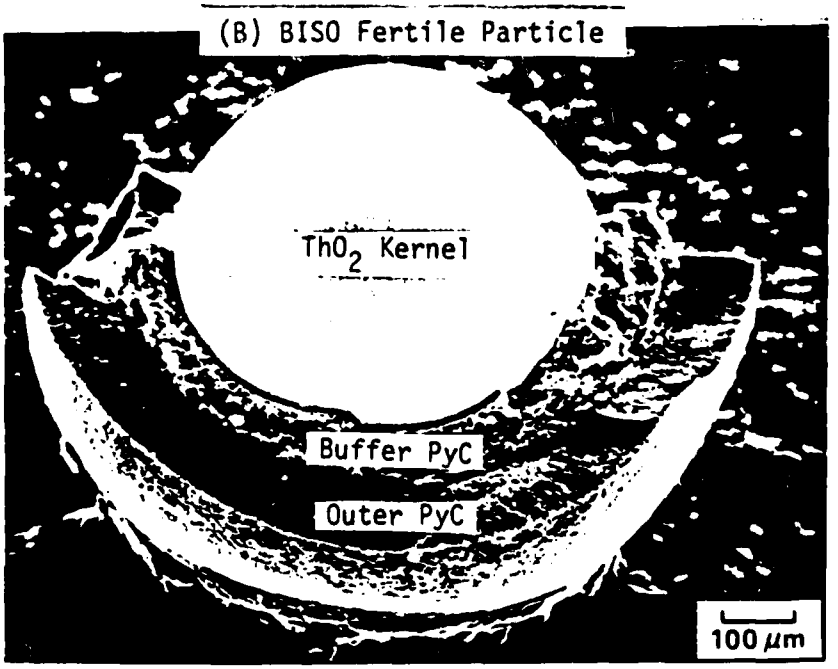

Coated fuel particles as seen under scanning electron microscope

COATED FUEL PARTICLES

1. Fuel Kernels
   - UC_2
   - UO_2
   - UC_xO_y

2. Coating
   - Carbon (porous)
   - Carbon (isotropic)
   - SiC
   - ZrC

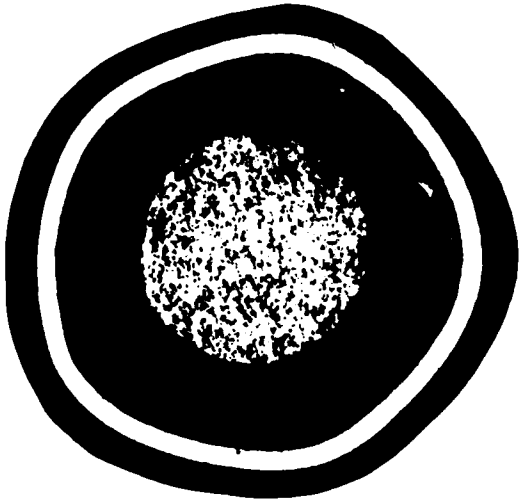

FISSILE PARTICLE

DESIGN

FUEL KERNEL	200 μm UC_2
BUFFER	85 μm
INNER PyC	25 μm
SIC	25 μm
OUTER PyC	35 μm

IRRADIATION CONDITIONS

1350°C

~70% FIMA

8.0×10^{21} n/cm^2 (E > 0.18 MeV)

FERTILE PARTICLE

DESIGN

FUEL KERNEL	500 μm ThO_2
BUFFER	85 μm
PyC	75 μm

IRRADIATION CONDITIONS

1250°C

14.3% FIMA

10.2×10^{21} n/cm^2 (E > 0.18 MeV)

Irradiated coated fuel particles, showing no coating breakage or coating-fuel interaction

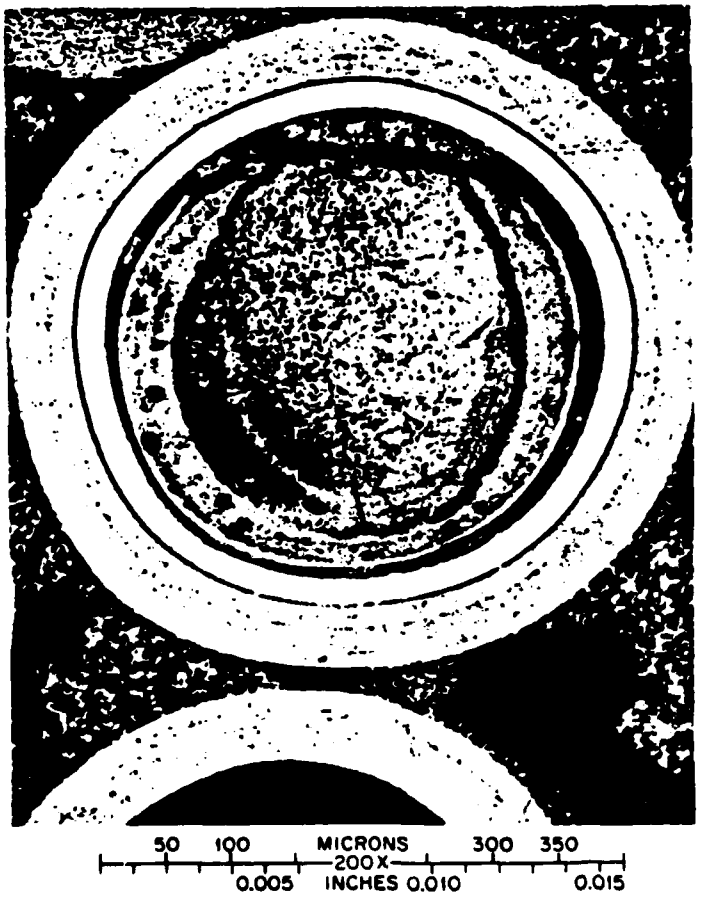

ZrC TRISO-I fuel particle with VSM UC_2 kernel irradiated to 80% FIMA/1500°C/6 x 10^{21} n/cm^2. Particle location 740 μm from rod O.D. Note no reaction between ZrC coating and kernel even though kernel has penetrated through buffer coating and touched ZrC coating. All of the particles (about 200) examined showed this resistance to fission product attack and no broken coatings were observed.

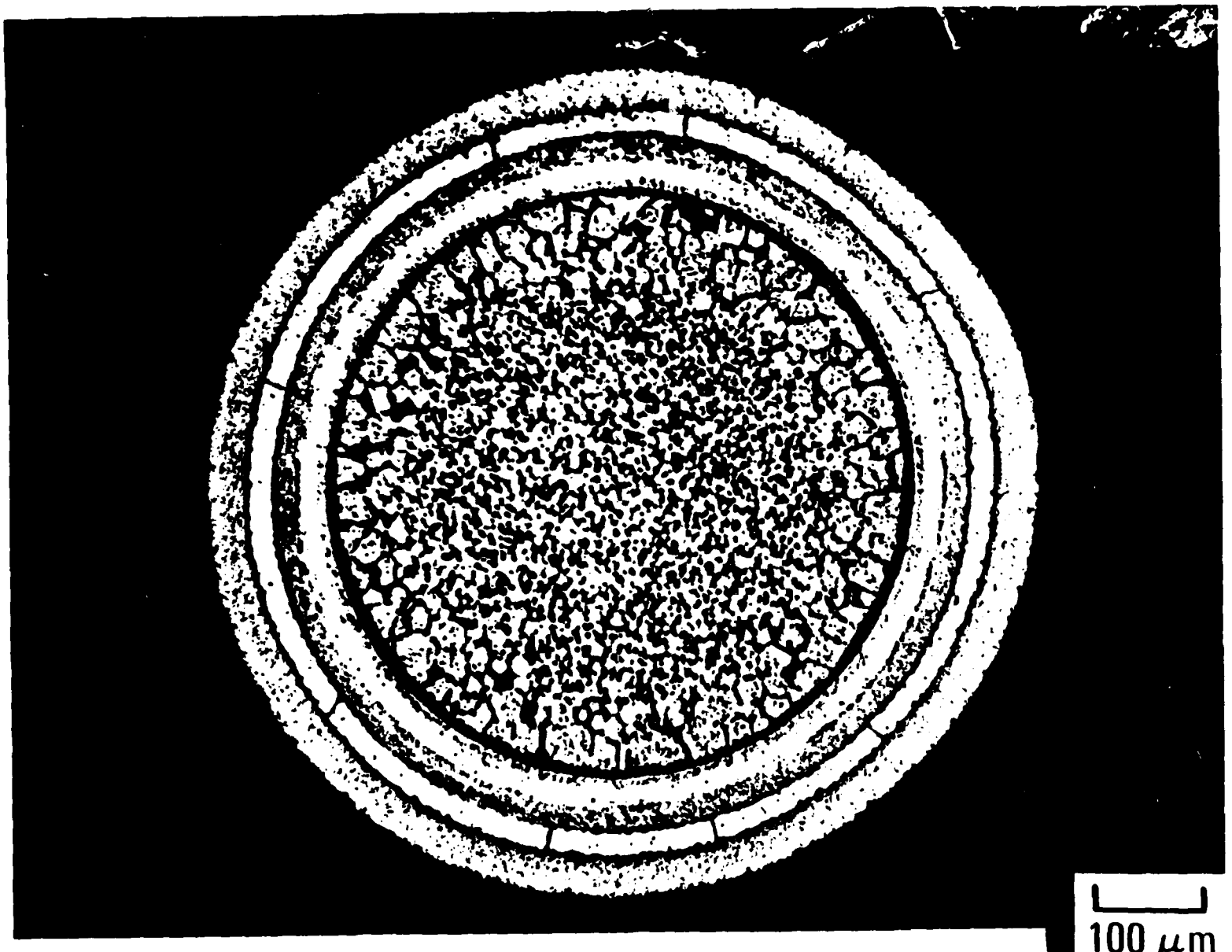

Coated ThO_2 particle heated at 2160°C for 2 hours after irradiation to 4% FIMA, showing no failure of outer pyrocarbon

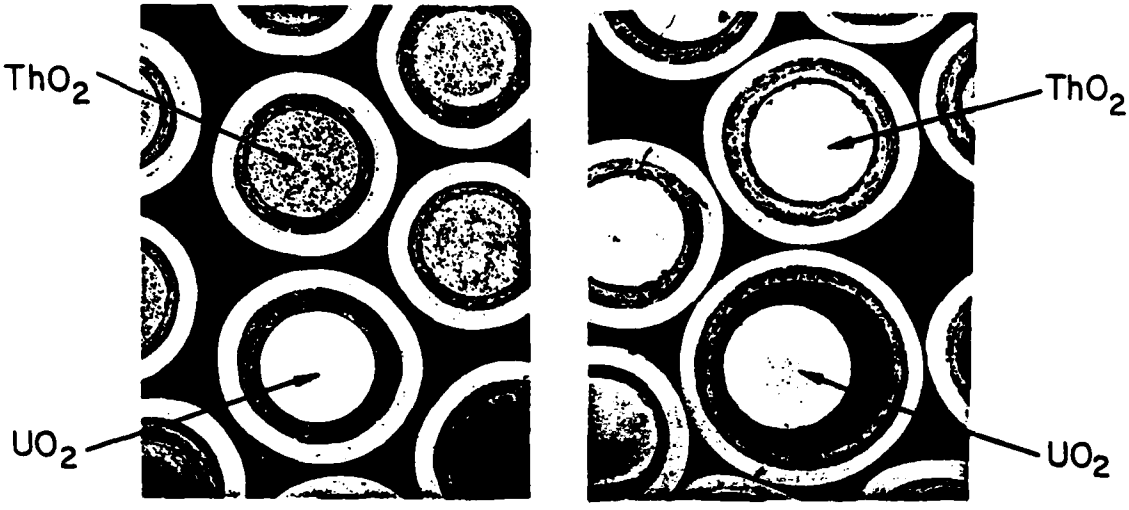

BRIGHT FIELD

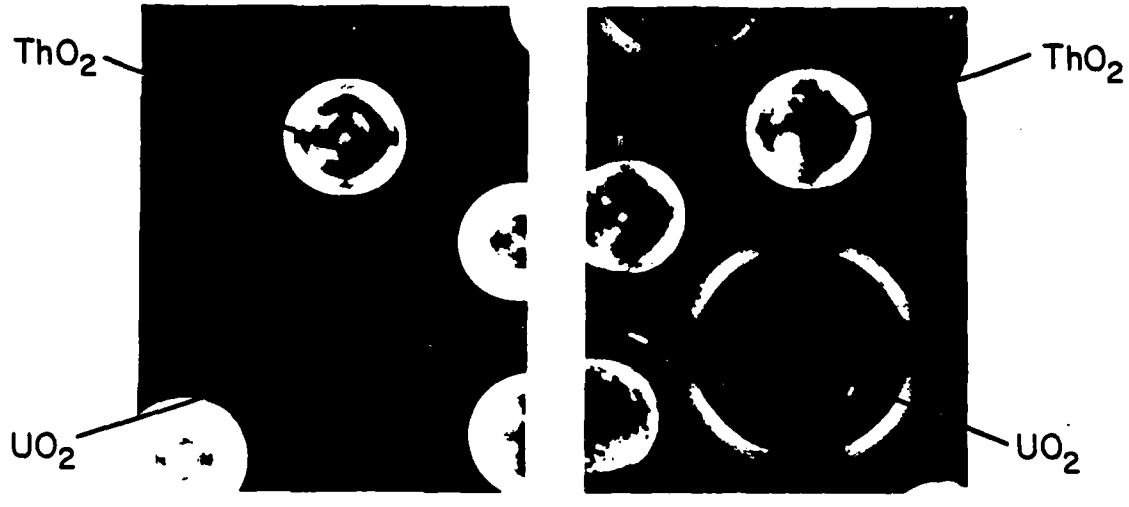

POLARIZED LIGHT

AS COATED

AFTER HEAT TREATMENT 2500 °C 10 min

Comparison of Microstructure of Coated ThO_2 and UO_2 Microspheres Before and After Heat Treatment at 2500 °C for 10 min (100 x).

The carbon coating around UO_2 particle swells due to high CO pressure produced by reaction between UO_2 and C. (ORNL-4036)

RECOMMENDED WORK

- Investigation of means for reducing fuel swelling, emitter deformation, fuel-cladding interaction, and fuel component diffusion through cladding in carbide-fueled systems.

- Investigation of means for reducing fuel swelling and emitter deformation in oxide-fueled systems.

- Design and testing of coated fuel particles for space power application.

Answer to a question by T. Nakamura of Stanford University on the paper "Reactor Materials" by Ling Yang, Session VII

Question:

Problems of High-Temperature-Gas-Cooled reactor (HTGR) core material such as (i) slow migration of fuel element, so called Amoeba Effect, (ii) containment of radioactive cesium, have been limiting factors in the development of HTGR. Are they still so? What is the maximum gas temperature available for HTGRs for space application?

Answer:

This paper is not proposing the use of HTGR as a space power system. It is aimed at pointing out the potential of coated fuel particles which have been tested extensively under the HTGR program, for fueling the high power rotating fluidized bed and the fixed bed core concepts of Jim Powell of Brookhaven National Laboratory for space application. These concepts require coated fuel particles capable of being pulsed to temperatures from 1500°K (for fixed bed core) to 3000°K (for rotating bed core) in a few seconds. It is doubtful standard HTGR coated fuel particles can meet these requirements. Better particle design and coating materials which are being developed under the advanced HTGR fuel program at General Atomic may meet these requirements but high temperature performance of these advanced particles have to be tested. Standard HTGR delivers helium gas of about 700°C temperature but it has the potential of delivering helium of much higher temperatures (e.g. 950°C), as demonstrated by the German pebble bed AVR. By using the right system design and coating and fuel materials, amoeba effect and diffusive cesium release are not considered as the life limiting factors for standard HTGR coated fuel particles.

Bibliography for "Reactor Materials", Ling Yang, Session VII

1. "Material Development for Thermionic Fuel-Cladding Systems", L. Yang, R. G. Hudson, H. Johnson, H. Horner and D. Allen; Proceedings of the 3rd International Conference on Thermionic Electrical Power Generation, p 873 - 893. Julich, Federal Republic of Germany, June 5 - 9, 1972.

2. "Developmental Status of Thermionic Materials", L. Yang and J. Chin; Proceedings of the 7th Intersociety Energy Conversion Engineering Conference, p 1041 - 1049. San Diego, California, 1972.

3. "Development of a Thermionic Reactor Space Power System, Final Summary Report'; Contract AT(04-3)-840, Gulf-GA-A12608, June 30, 1973.

4. "Development and Irradiation Performance of LHTGR Fuel", D. P. Harmon and C. B. Scott, GA-A13173, October 31, 1975.

5. "Design and Performance of Coated Particle Fuels for the Thorium Cycle HTGR", T. D. Gulden, D. P. Harmon, and O. M. Stansfield. GA-A12628, January 24, 1974.

6. "Irradiation Behavior of Experimental Fuel Particles Containing Chemically Vapor Deposited Zirconium Carbide Coatings", G. H. Reynolds, J. C. Janvier, J. L. Kaae, and J. P. Morlevat.

7. "Fuel Particle Behavior Under Normal and Transient Conditions", C. L. Smith. GA-A12971, October 1, 1974.

8. "Gas-Cooled Reactor Program Semi-Annual Program Report for the Period Ending September 30, 1966", ORNL-4036, February 1967.

MATERIALS FOR HIGH POWER MHD SYSTEMS

B. R. Rossing
Westinghouse Research and Development Center
Pittsburgh, PA 15235

MATERIALS FOR HIGH POWER MHD SYSTEMS

Magnetohydrodynamic power generation offers two possible options for space power; open cycle power generation using a chemical heat source for short burst applications or closed cycle power generation using a nuclear heat source for continuous long duration power generation. Two basic generator configurations are possible: the linear generator which has been brought to an advanced state of development and the disk generator to which limited effort has been applied but which offers several possible advantages in construction and operation. Each of these options, open cycle/linear, open cycle/disk, closed cycle/linear and closed cycle/disk present differing material requirements. In addition specific generator designs will further define material requirements. Due to the limited time for this presentation only the material requirements for linear generators will be discussed. A few comments will be made in regard to disk generator materials at the end of this discussion.

Electrode material requirements are shown in SLIDE 2. Open cycle generators would utilize refractory oxide electrodes and insulators operating at surface temperatures above 2000K. The chemical requirements, which are

most severe in commercial long duration open cycle MHD power generation, would be relatively unimportant in short burst applications. However, the goal of extracting the maximum power in a minimum of volume increases the severity of electrical and mechanical stresses on materials. These stresses are very demanding for ceramics used in open cycle systems. These same requirements placed upon metallic closed cycle electrodes, even for very long durations, are much less severe. Especially critical to open cycle electrodes is the development of ceramic based electrode structures that could pass up to 10 amp/cm^2 between cold copper and the plasma.

First, low electrode resistance (to avoid joule heating) and a small temperature dependence of resistivity (to avoid current channeling) are desired. Two classes of oxide ceramics are the primary candidate materials for open cycle electrodes, the refractory rare earth chromites such as $LaCrO_3$ or $YCrO_3$ doped with various alkaline earth oxides and very refractory ZrO_2-or HfO_2-based compositions. As shown in SLIDE 3 the electrical properties of the perovskites are superior to those of ZrO_2-or HfO_2-based compositions. Since resistivities must be less than 5 ohm-cm to avoid joule heating, the refractory ZrO_2-based compositions can function as the current carrier at only the highest temperatures (>1600K). To utilize these compositions electrode structures (SLIDE 4) have been developed that use intermediate materials

such as highly conducting spinel (or perovskite) layers, refractory metal pins (or mesh) and graded cermet structures to produce electrodes with low resistance. It should be pointed out that closed cycle electrode materials such as molybdenum, zirconium diboride and graphite possess very low resistivities at all temperatures (see SLIDE 3).

Electrode materials should be electronic conductors to avoid electrolysis. The reduction of Y_2O_3 stabilized ZrO_2 is shown in SLIDE 5. The formation of finely dispersed $Zr_{\wedge}^{at}$ grain boundaries produces a loss of structural integrity in Y_2O_3 stabilized ZrO_2. Even materials that are electronic conductors are subject to decomposition at high current densities if they are not thermodynamically stable over a wide range of electrochemical conditions (SLIDE 6).

Electrode development for high power, short burst systems has been minimal. However, test results on a light weight 200kW linear MHD channel (Ref. 22) were encouraging. Electrodes of the design shown in SLIDE 7 survived 250 cycles at 2-4 amp.cm^2.

Insulator requirements (SLIDE 8) are the same as electrodes except that the electrical functions are quite different. Electrical conductivities of less than 10^{-3} ohm-cm are required. As shown in SLIDE 9 a number of oxides and nitrides meet this requirement at 2000K and above. Although the nitrides will oxidize above 1000°C in open cycle systems,

are attractive candidates in closed cycle systems because of their superior thermal stress resistance. Insulator high temperature breakdown may be a critical requirement in these systems. As shown in SLIDE 10 the critical breakdown voltage decreases exponentially with reciprocal temperature. It appears that to avoid dielectric breakdown by thermal runaway it may be necessary to limit insulator surface temperatures.

To achieve the desired goals for space MHD systems in terms of kW/kg will require the development of light weight MHD magnets. In turn, this will require the substitution of high performance, light weight materials for existing conventional materials (SLIDE 11).

The final SLIDE outlines critical research efforts that would be needed to support the development of electrodes and insulators for open cycle, short burst MHD generators. Closed cycle materials studies would be directed toward long duration corrosion studies on electrodes and insulators.

The disk generator offers the attractions of much simpler electrode designs and lower electrode current densities. However, the higher electric fields and the need for very good insulation between anode and cathode structures places a more critical requirement on insulator materials and structures.

High Power MHD Systems

Options

Linear	vs	Disk Generators
Open Cycle	vs	Closed Cycle Systems
'High Performance'	vs	'Very High' Performance Designs

SLIDE 1

Electrode Requirements
(High Power Linear MHD Generator)

Electrical

Most Pass Currents up to 10 amp/cm^2

- Low Electrode Resistance
- Small Temperature Dependence of Resistivity
- Electronic Conduction
- Adequate Thermionic Emission

Chemical

Not reactive with
- Cesium and/or Cesium Compounds
- Plasma Gases (O_2, N_2, CO, H_2O, etc.)
- Adjacent Insulators

Mechanical

Resistant to
- Action of high velocity, high temperature gases (erosion)
- Thermo-mechanical stresses (thermal shock)

Practical

Must be realistic in terms of ease of fabrication and cost.

Slide 2

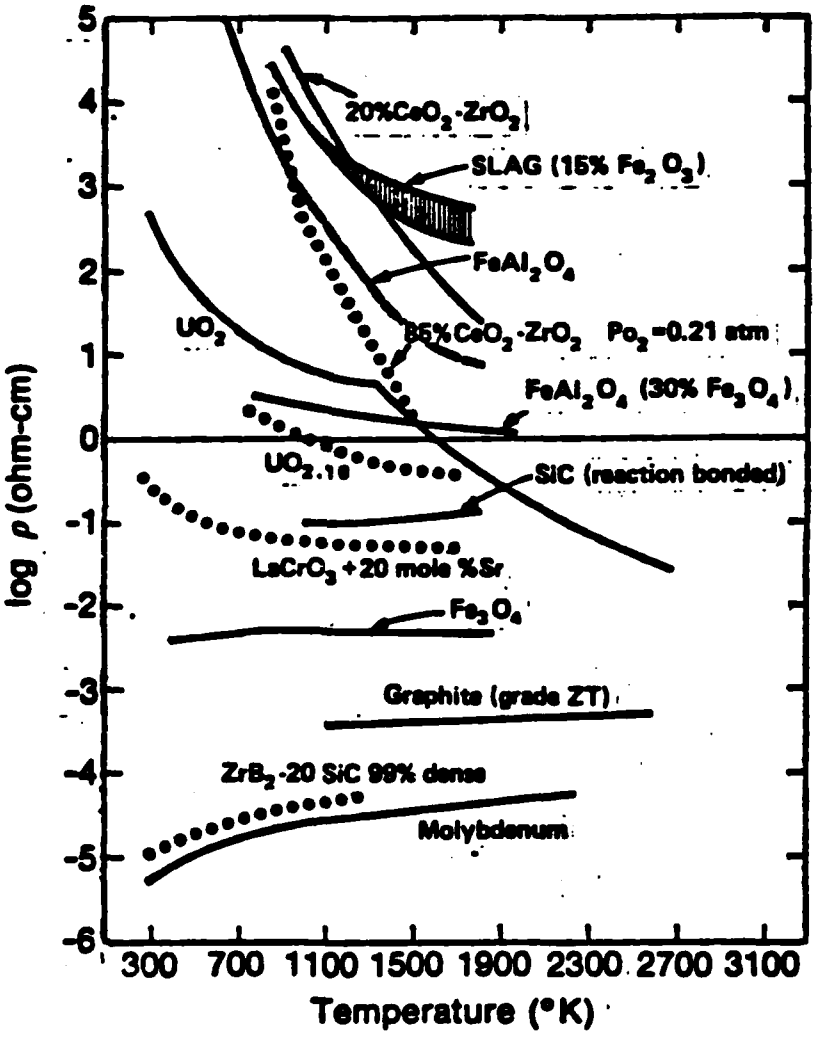

Figure 4 Resistivity-temperature plot of MHD electrode materials. (Ref. 2)

SLIDE 3

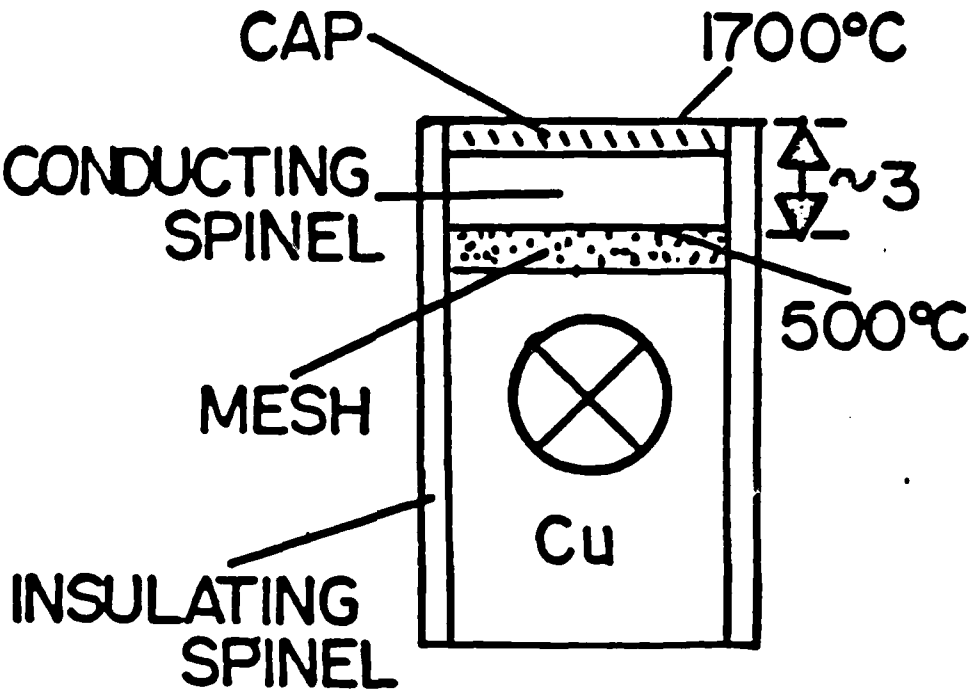

Fig. 4. High Heat Flux Electrode.

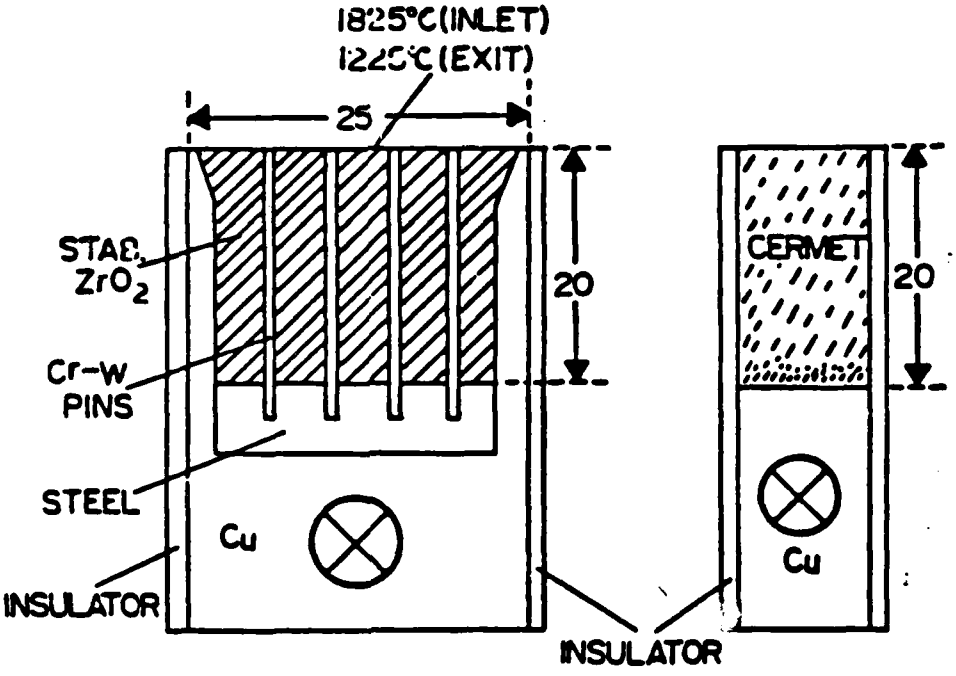

Fig. 5.
Pin Structure.

Fig. 6.
Cermet Electrode.

SLIDE 4

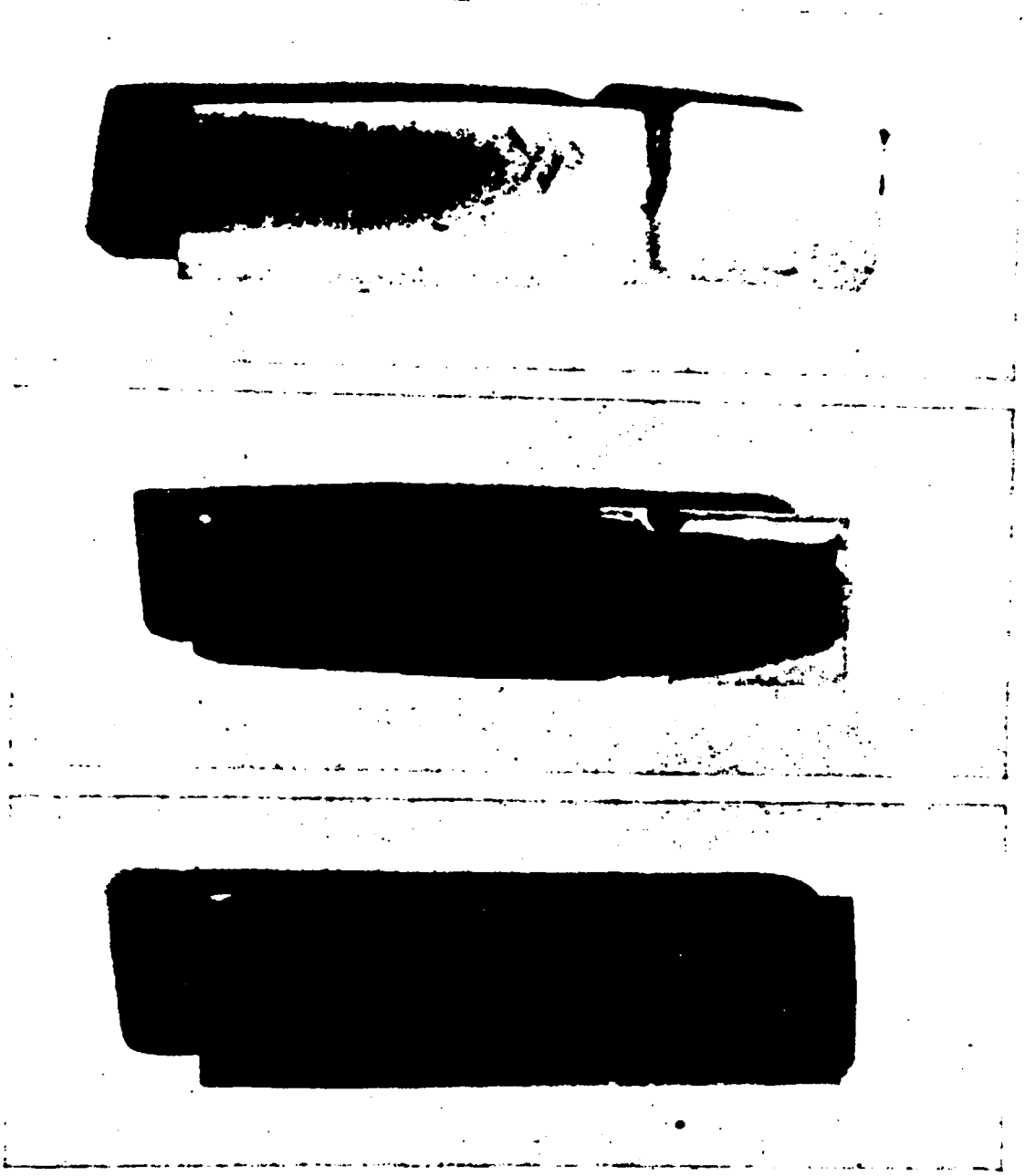

(d)

FIG. 7.13. Potential distribution at 1653°K across a cylindrical 12 mole % Y_2O_3:ZrO_2 sample for various oxygen partial pressures, and current densities of: (a) 12·9 A m^{-2}; (b) 1·29 kA m^{-2}; (c) 12·9 kA m^{-2}. (d) Photographs of small quenched samples corresponding to curves in (c) showing blackened zone at the cathode; top sample $p_{O_2} = 2 \times 10^{-2}$ atm, middle sample $p_{O_2} = 5 \times 10^{-3}$ atm, bottom sample $p_{O_2} = 10^{-3}$ atm. (Ref. 1)

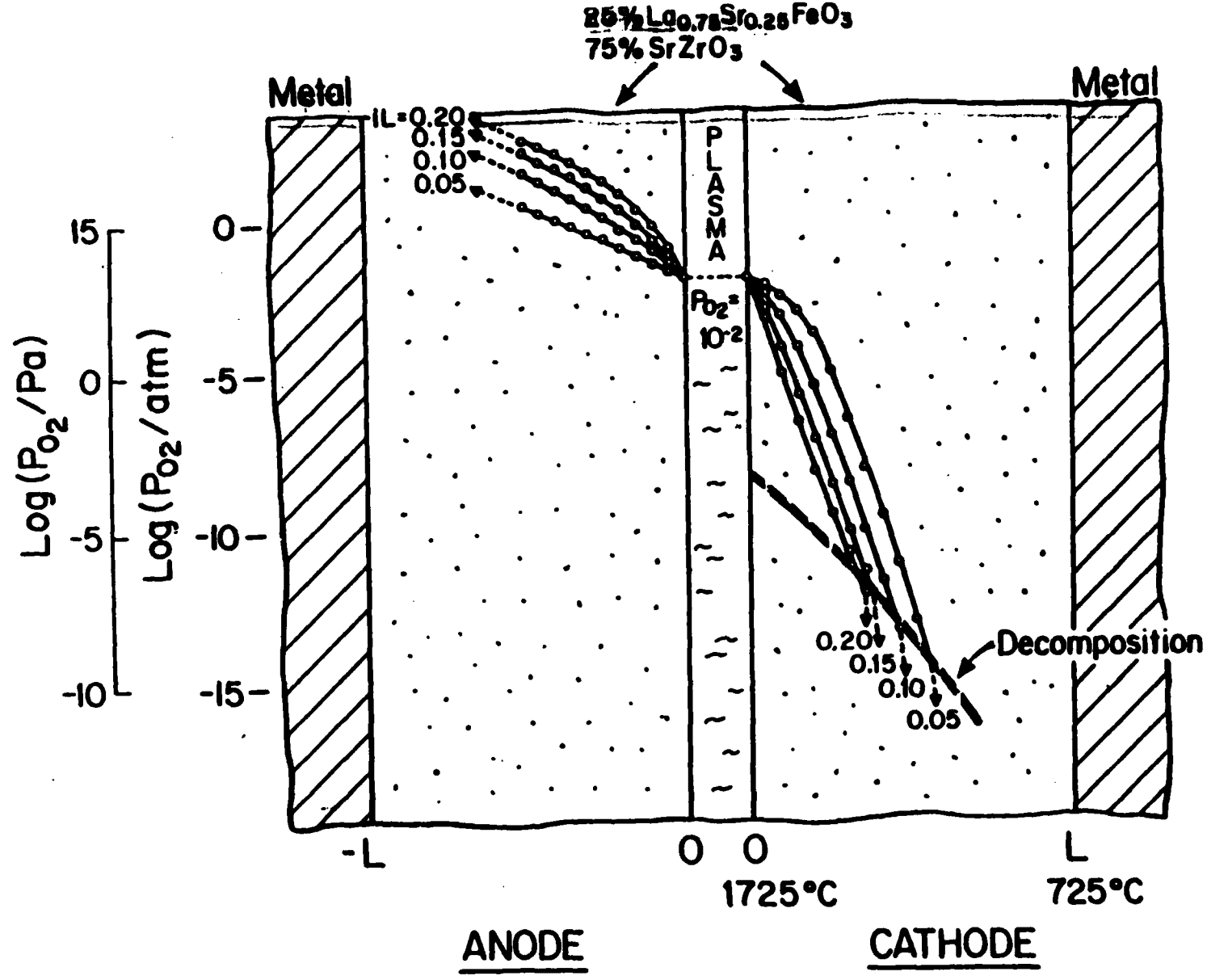

VII-4-11

SLIDE 6

Ca[illegible]ate[illegible]O_2 t[illegible]ugh [illegible]rZr[illegible], [illegible]a0.[illegible]0.2[illegible]O_3 [illegible] tro[illegible]

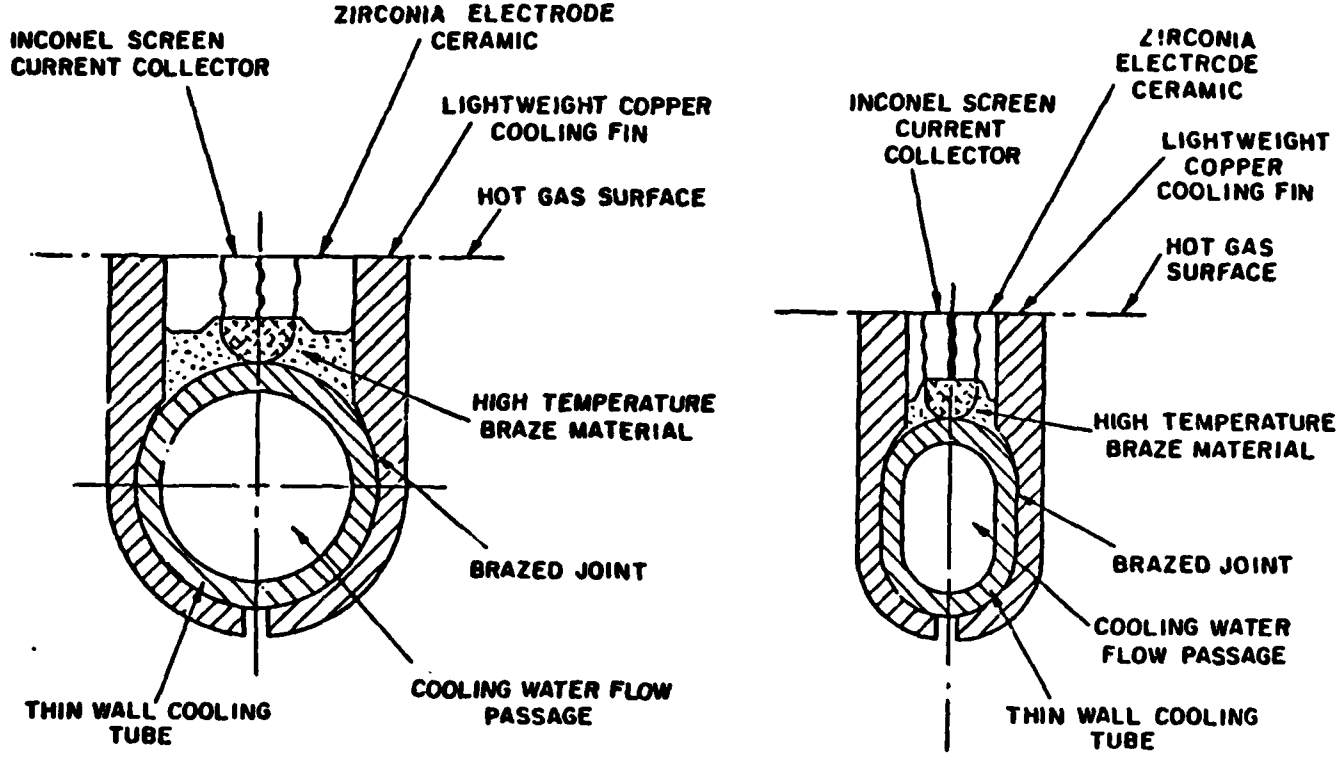

Proposed Electrode Design. (from Ref. 22)

Insulator Requirements
(High Power Linear MHD Generator)

Electrical

Must Provide Insulation Between Electrodes in the Presence of High Electric Fields

- Electrical Resistivities 100X that of the plasma
- Dielectric Breakdown, > 4kv/m

Chemical, Mechanical, Practical

Same as Electrodes

SLIDE 8

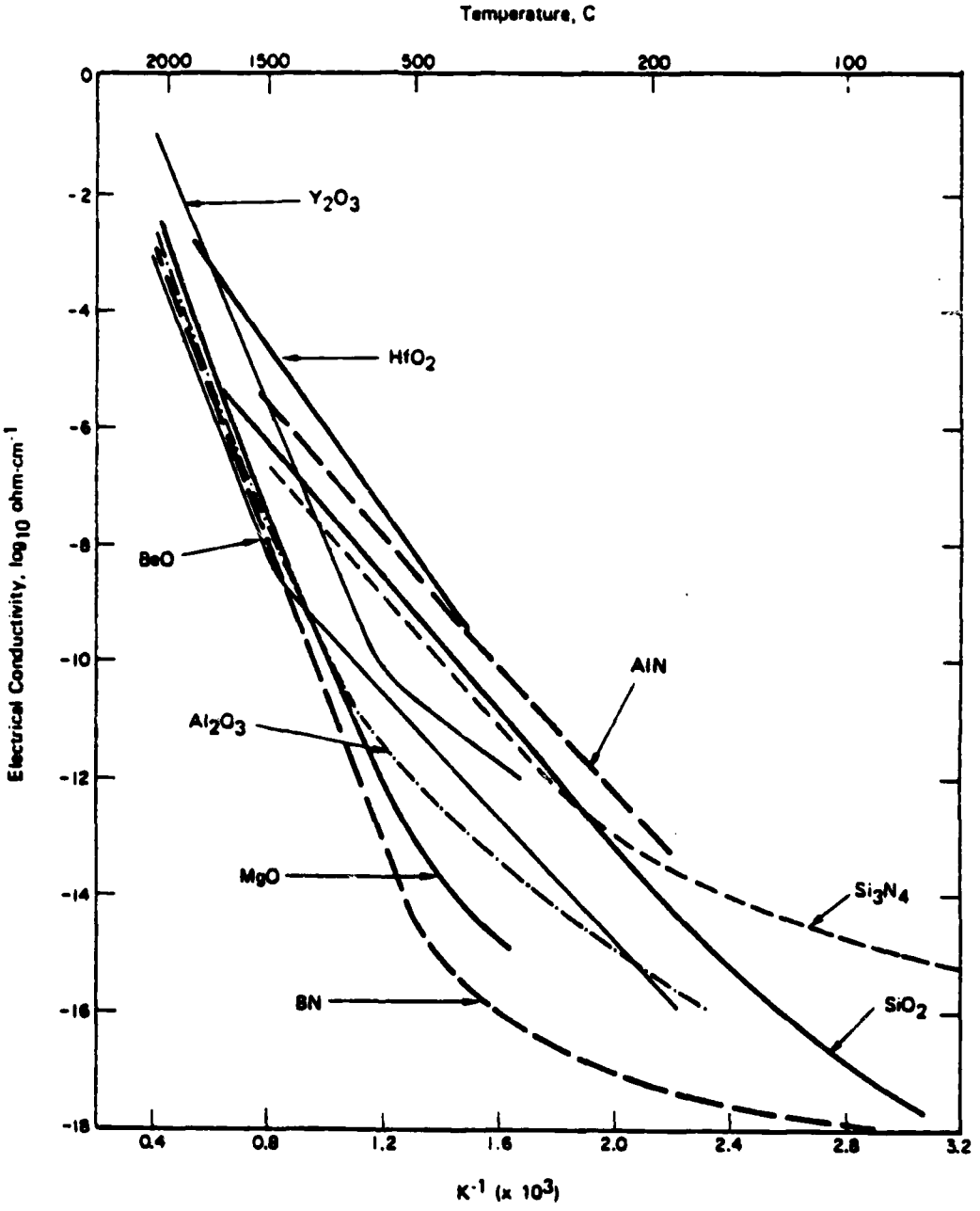

FIGURE . ELECTRICAL CONDUCTIVITY OF INSULATING MATERIALS (Ref. 23)

SLIDE 9

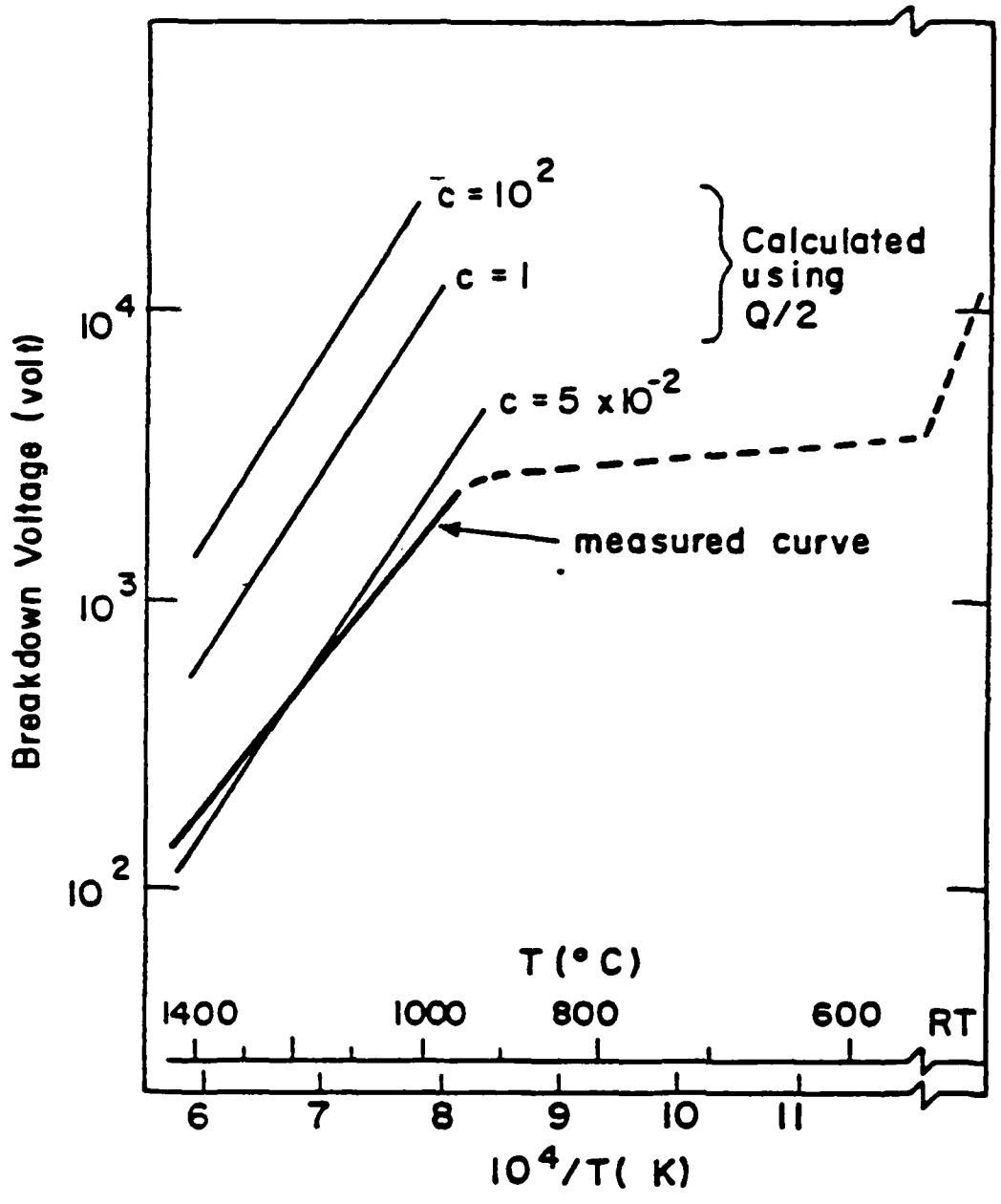

Fig. . Calculated and observed critical breakdown voltage as a function of temperature. The value of $Q/2$ used in the calculations is 135 kJ/mol (1.43 eV); Q for the measured curve is 106 kJ/mol (1.1 eV). (from Ref. 21)

MHD MAGNET MATERIALS

NEED TO REDUCE PAYLOADS MAY REQUIRE SUBSTITUTION OF LOWER DENSITY MATERIALS FOR CONVENTIONAL MATERIALS.

FOR EXAMPLE

- ALUMINUM STABILIZED CONDUCTORS
- HIGH PERFORMANCE FIBER-COMPOSITES AS STRUCTURAL MATERIALS

MHD Materials R & D Activities

Development Activities	Supportive Research Activities
Electrodes Operating at High Current Densities (1-10 amp/cm^2)	• Electrode to Plasma Current transport Studies • Electrolysis of Ceramic Electrode Materials • Current Transport in Ceramic Electrode Materials
Insulators for High Electric Fields (> 2 kv/m)	High Temperature Dielectric Breakdown Studies
Ceramic Structures under High Heat Fluxes (> 100w/cm^2)	Thermal Stress Resistance of Ceramics and Ceramic/ Metal Composites

SLIDE 12

BIBLIOGRAPHY

1. J. B. Heywood, W. T. Norris and A. C. Warren, "Electrodes and Insulators" in Open Cycle MHD Power Generation Ed. by J. B. Heywood and G. J. Womack, Pergamon Press, Oxford, 1969.

2. H. K. Bowen, "MHD Channel Materials Development Goals," Proceedings of NSF-OCR Engineering Workshop on MHD Materials Edited by A. L. Bement, Cambridge, MA, Nov. 1974, pp. 85-112.

3. S. J. Schneider, H.P.R. Frederikse, G. P. Telegin, A. I. Ramonov, "Materials" in Open Cycle Magnetohydrodynamic Electrical Power Generation Edited by M. Petrick and B. Ya. Shumyatsky Argonne Nation Laboratories, Argonne, IL, 1978.

4. B. R. Rossing and H. K. Bowen, "Materials for Open Cycle Magneto-hydrodynamic (MHD) Channels," in Critical Materials in Energy Production, Edited by C. Stein, Academic Press, New York, 1977.

5. J. Mizusaki, W. R. Cannon and H. K. Bowen, "Electrochemical Degradation of Ceramic Electrodes," J. Am. Cer. Soc., 63 391-7 (1980).

6. B. L. Pober, W. R. Cannon, H. K. Bowen and J. F. Louis, "Development of Super-Hot-Wall Electrodes," 7th Int. Conf. on MHD Electrical Power Generation, Cambridge, MA, June 1980, pp. 278-286.

7. B. R. Rossing, L. H. Cadoff and T. K. Gupta, "The Fabrication and Properties of Electrodes Based On Zirconium Oxide," 6th Int. Conf. on MHD. Electrical Power Generation, Cambridge, MA, June 1975, Vol. II, pp. 105-117.

8. W. D. Jackson et al., "Joint Test of a U.S. Electrode System in the U.S.S.R. U-02 Facility," Proc. of 16th Sym. on Eng. Aspects of MHD, Philadelphia, PA, May, 1976, p.I. 1. 1-12

9. G. Rudins et al., "The Second Joint Test of a U.S. Electrode System in the U.S.S.R. U-02 Facility," Proc. of 16th Sym. on Eng. Aspects of MHD, Pittsburgh, PA, May 1977, pp. IV, 1.1-12.

10. H.P.R. Frederiskse and W. R. Hosler, "Electrodes and Insulators: Design and Materials Considerations," Proc. of 16th Sym. on Eng. Aspects of MHD, Pittsburgh, PA, May 1977, pp. IV, 4.22-28

11. B. R. Rossing, et al., "Evaluation of Phase III Proof Test Materials," Proc. of 17th Sym. of Eng. Aspects of MHD, Stanford, CA, March 1978, pp. G.2.1-8.

12. J. W. Sadler, et al., "Design, Test and Evaluation of Refractory MHD Electrodes," Proc. of 17th Sym. of Eng. Aspects of MHD, Stanford, CA, March, 1978, pp. G.3.1-9.

13. ANL-77-21, Conference on High Temperature Sciences Related to Open Cycle, Coal Fired MHD Systems, Argonne National Laboratory, Argonne, IL, April, 1977.

14. A. M. George, "Improved $LaCrO_3$ Ceramics For High Temperature Electrodes in Open Cycle MHD Systems, 15th Sym. on Eng. Aspects of MHD, Philadelphia, PA, May 1976.

15. G. P. Telegin, et al., "Investigation of Thermophysical Properties of Refractory Materials Used in MHD Generator Channels," High Temperatures-High Pressures, 8, 199-208 (1976).

16. D. D. Marchant and J. L. Bates, "Development of Yttrium Chromites and Rare Earth Doped Halnia for MHD Generator Applications," 18th Sym. on Eng. Aspects of MHD, Butte, MT, June 1979, pp. P.1.5.1-8.

17. J. L. Bates, et al., "Performance of U.S. Electrodes-Insulators Tested in the U.S.S.R. U-02: Phase III, 18th Sym. on Eng. Aspects, Butte, MT., June 1979, pp. P-1.6.1-10.

18. T. Negas, W. R. Hosler and L. P. Domingues, "Preparation and Properties of Yttrium Chromite Ceramics," 4th Int. Meeting on Modern Ceramic Technologies, St. Vincent, Italy, May 1979.

19. D. D. Marchant and J. L. Bates, "Hafnia-Rare Earth Oxides for High Temperature MHD Electrodes," 7th Int. Conf. on MHD Electrical Power Generation, Cambridge, MA, June 1980, pp. 287-291.

20. Jiang Dong-liang, et al., "A Composite Electrode Material Study and Its Performance in a MHD Test Unit," 7th Int. Conf. on MHD Electrical Power Generation, Cambridge, MA, June 1980, pp. 292-299.

21. M. Yoshimura and H. K. Bowen, "Electrical Breakdown Strength of Alumina at High Temperatures," J. Am. Cer. Soc. 64, 404-410 (1981).

22. D. W. Swallom, et al., "High Power Magnetohydrodynamic Sytem," AFAPL-TR-78-51.

23. A. A. Bouer and J. L. Bates, "An Evaluation of Electrical Insulators For Fusion Reactors, BMI-1930, July 1974.

The Westinghouse High Flux Electron Beam Surface Heating Facility (ESURF)

M. D. Nahemow
Westinghouse R&D Center
1310 Beulah Rd.
Pittsburgh, Pennsylvania 15235

The ESURF facility is located at the Westinghouse Electric Corp., Research and Development Center, Pittsburgh, Pennsylvania. It has been operational since March, 1980. It was first used to test cathodes for a BNL designed negative ion source.[1,2] The water cooled copper cathodes were operated at a loading of 2 KW/cm^2 steady state loading. Divertor collector targets for the MIT divertor program were subject to transient conditions. These molybdenum tubes were subject to up to 500 2 kW/cm^2 transients.[3] The facility is currently being used in a first wall/blanket/shield engineering test program for the Argonne National Labs.

The ESURF uses a 50 KW 150 KeV electron beam as a heat source. The beam can be rastored at .5 cm/μs in both the x and y axis. The beam spot size is variable from .02 to 1.5 cm. The scan logic permits a wide variety of transient and steady state thermal effects to be modeled. Samples can have heated sections up to 28 cm by 18 cm. The system cooling loop has a maximum operating pressure of 1000 psi. The pumps have an operating range from 7 gpm at a 700 ft head to 30 gpm at a 500 ft head. 40 KW of preheat and 100 KW of subcooling are provided. Temperature, pressure, flow, strain, etc. are measured and controlled. The system has a TI microprocessor control system linked to a LSI/11 computer system for control, data acquisition, and data processing. An infrared (2μ) TV camera and video recorder, are used to monitor surface conditions and are being interfaced to the LSI/11.

---

1. M. D. Nahemow, et al., The Design of a Nucleated Boiling Water Cooled Cathode for the BNL Negative Ion Source. Proceedings of the 8th Symposium on Engineering Problems of Fusion Research, San Francisco, November 13-16, 1979.

2. J. R. Easoz and M. D. Nahemow, Testing of Water-Cooled Cathodes on the Westinghouse High Surface Heat Flux Test Facility. Proceedings of 9th Symposium on Engineering Problems of Fusion Research, Chicago, IL, October 26-29, 1981.

3. A. Y. Lee, R. B. Chianese and J. R. Easoz, Thermal and Structural Analyses of Solid Divertor Targets for E-Beam Testing. Proceedings of the 9th Symposium on Engineering Problems in Fusion Research, Chicago, IL, October 26-29, 1981.

M. D. Nahemow (W) ESURF

Figure Captions

Fig. 1. The table lists the general system specifications of the ESURF facility. The beam voltage is variable. The x or y scan distances refer to D.C. bias within the limits of the x-y raster plan. The beam size can be varied from 10^{-3} cm^2 to 1 cm^2 giving a maximum flux of 5 x 10^4 MW/m^2. The vacuum pressure is with the beam running. The base pressure is lower.

Fig. 2. The characteristics of the two pumps referred to in Fig. 1 are given in Fig. 2. The actual flow possible will depend on the headering loss for a specific device.

Fig. 3. The deflection coil is a ferrite core orthogonal magnetic device. The sin of θ is proportional to the coil current to .1%. The coil is driven by two 600 watt current amplifiers that operate from D.C. to 20 KHz. The logic permits the beam to scan the x-y plane or move to any spot and dwell. The power to the target is determined integrating the current through R_1, R_2, and R_3 and subtracting it from the peak current through R_4.

Fig. 4. Only pump A is shown is the loop schematic. Pump B is valved parallel to pump A with its own flow control.

Fig. 5. The two peaks in a are the beam currents through 2 1 mm^2 pinholes 5 cm apart. They show the sin effect in flux due to deflection. b is an expanded view of the first peak a showing a true gaussian profile with a full width half max of 1 mm. c shows the central peak and ring which develops when the beam is expanded to 1 cm.

Fig. 6. A 3 mm beam was allowed to dwell for 5 x 10^{-3} sec on a thick walled stainless tube to produce the damage shown in 6-(4,5,6). Spot 4 was produced by one 11 KW shot, spot 5 by ten 11 KW shots, and spot 6 by one 22 KW shot. Note that spot 5 is a deep hole.

ESURF SPECIFICATIONS

Heat Source	Electron Beam; 150 kV and 5-330 ma
Maximum e-beam Power Output	50 kW
Maximum Scan:	20 cm x or y -- 28 cm x and 18 cm y
Scan Speed	1 cm/s to 1 cm/μs
Target Area	1 cm^2 to 500 cm^2
Peak Surface Heat Flux	∿ 300 MW/m^2 to < 1 MW/m^2
Rep Rate:	20 Hz to 20 kHz
Heat Sink Coolant	Water
Maximum Working Pressure:	400 psi* → 1014 psi**
Maximum Head:	700 ft. H_2O
Working Temperature:	300°F* → 500°F**
Maximum Temperature:	350°F → 600°F**
Maximum Flow Rate:	7 gpm (at 700 ft. head rise)* 30 gpm (at 550 ft. head rise)**
Pre-Heater Power	40 kW
Heat Removal	72 kW Air Controlled Heat Exchanger
Control	Texas Instrument Programmable Control System
Vacuum Tank Working Space	3 ft. Diameter x 4 ft. Long
Vacuum Pressure	$<10^{-4}$ torr

Pump Limited *Pump A -- **Pump B

Nahemow Figure 1

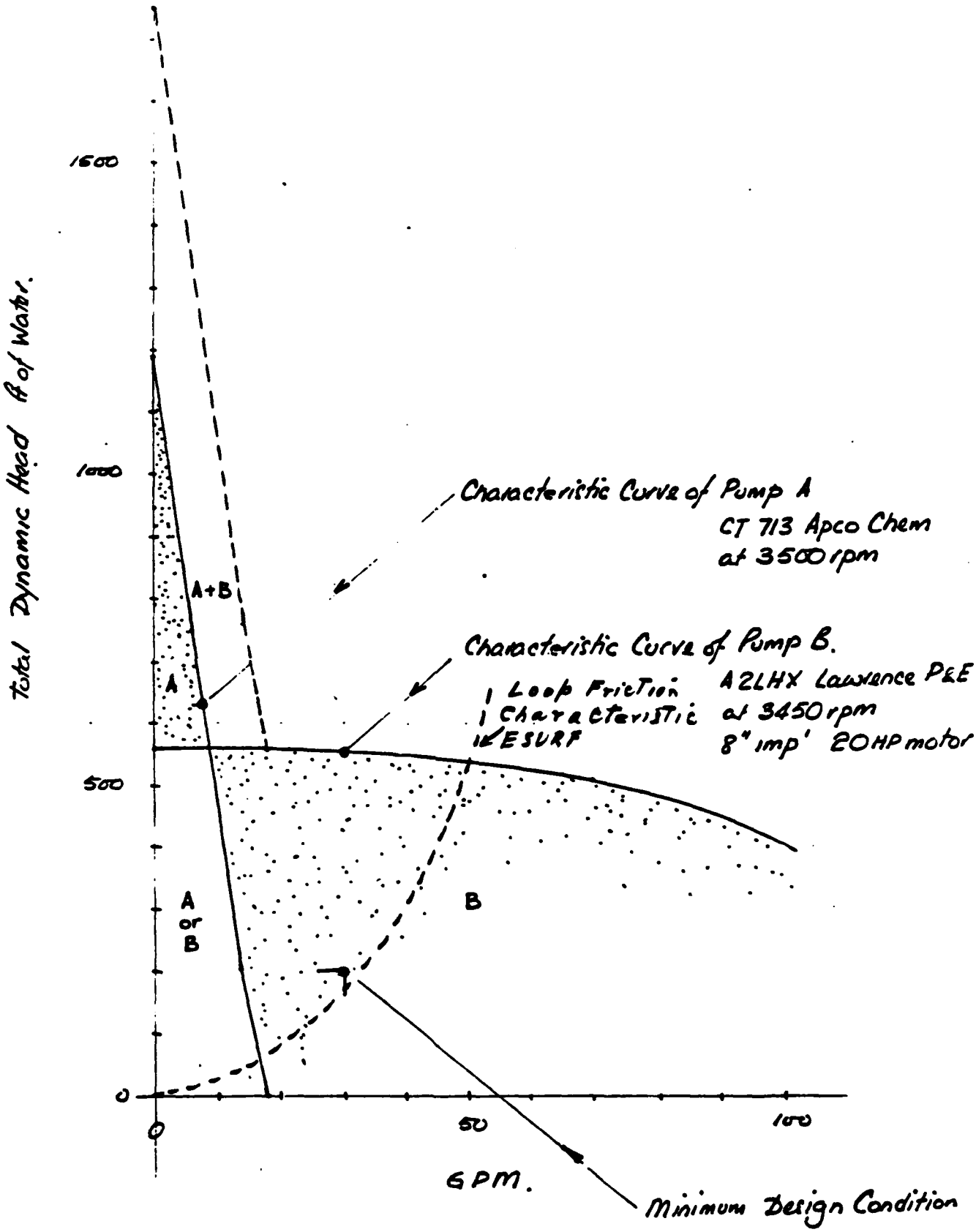

Nahemow Figure 2

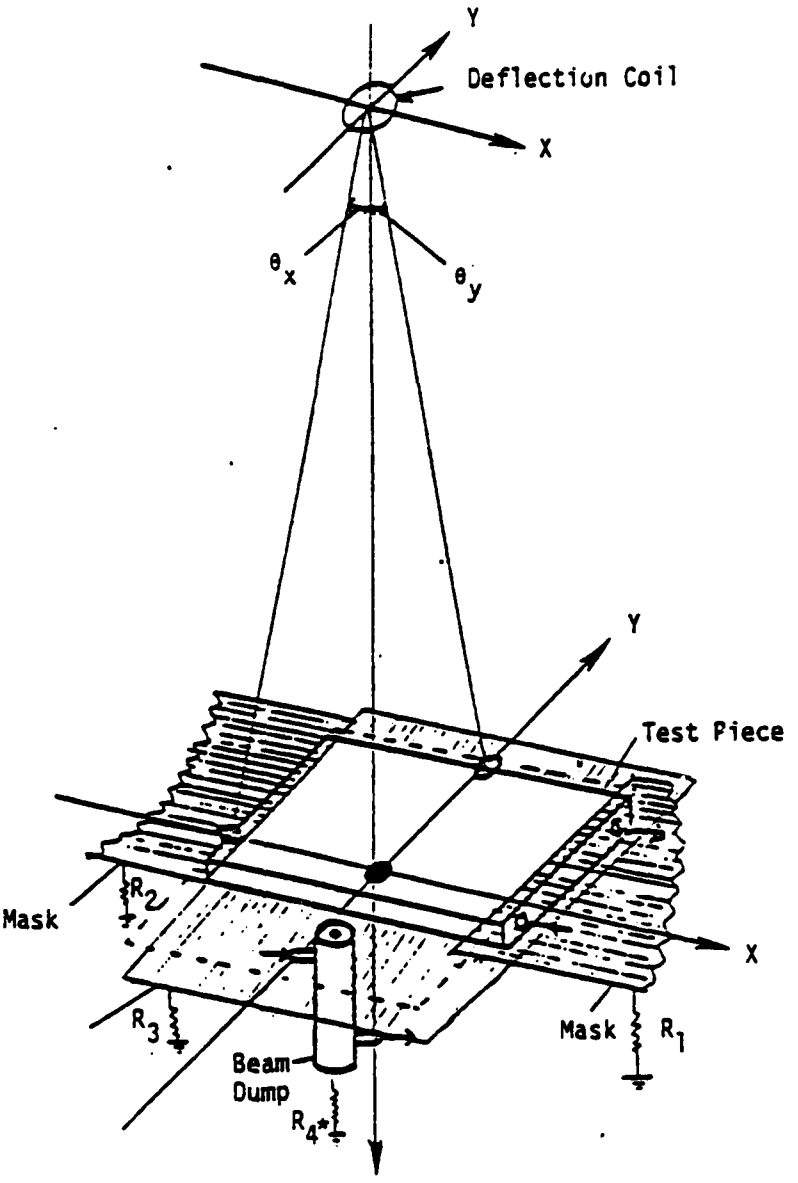

* R_4 measures beam current

ESURF E-Beam Scan System

Nahemow Figure 3

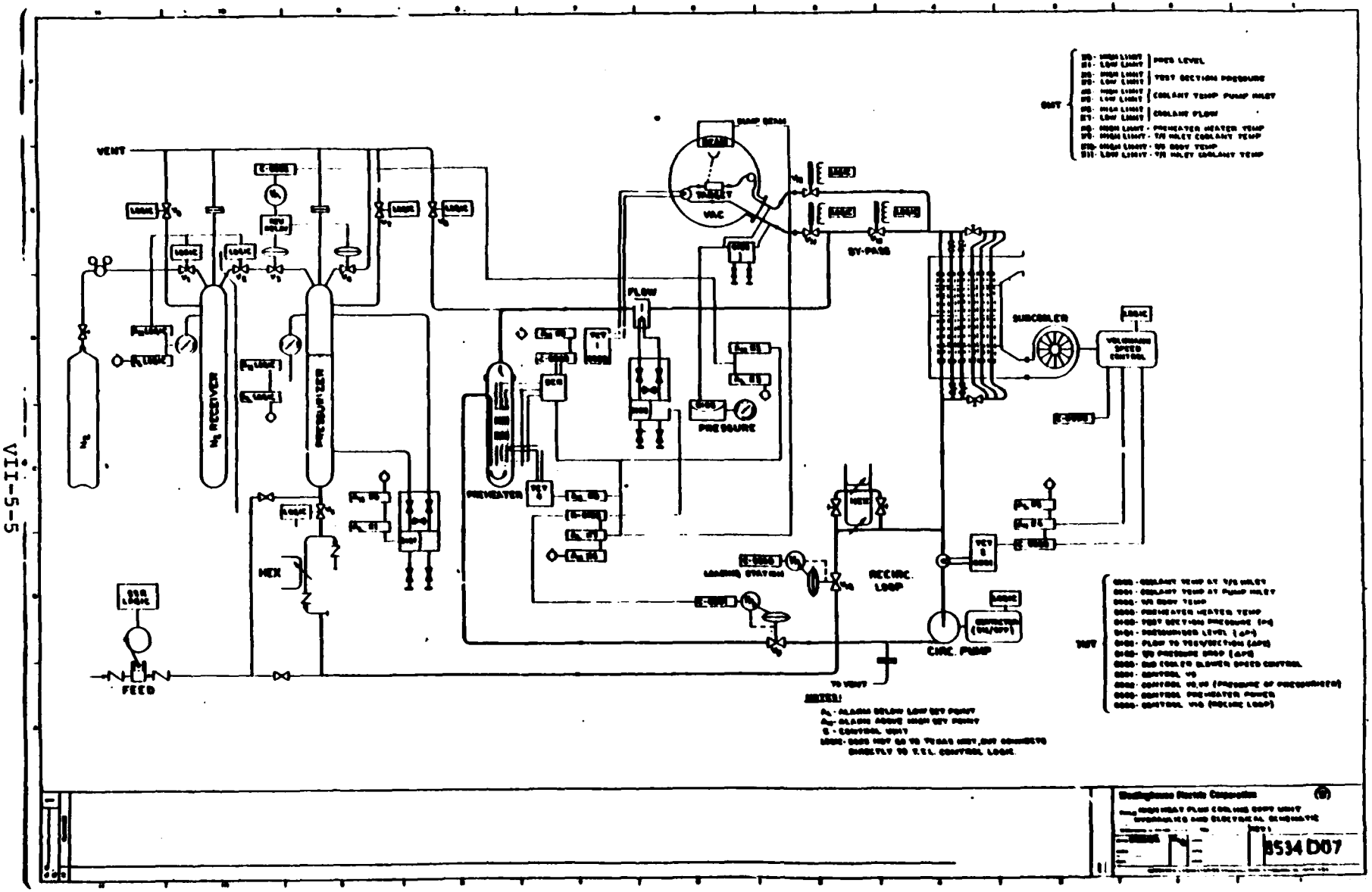

Nahemow Figure 4

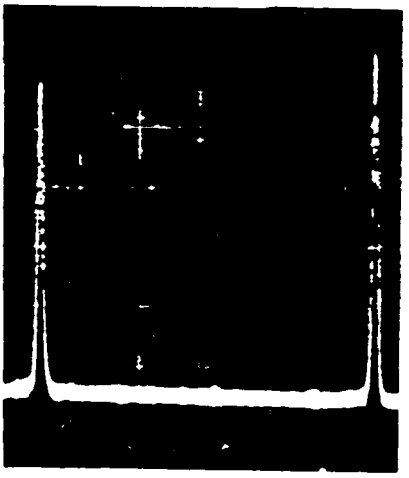

a

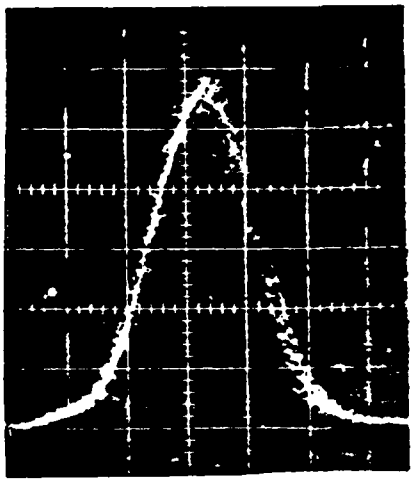

1 mm

b

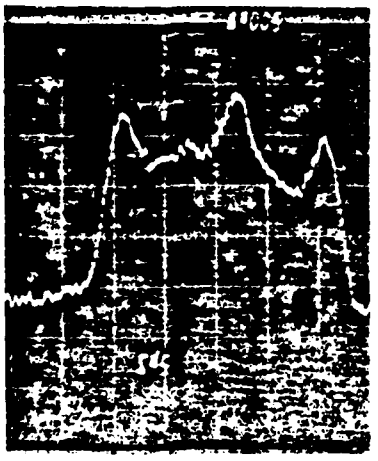

1 cm

c

Nahemow Figure 5

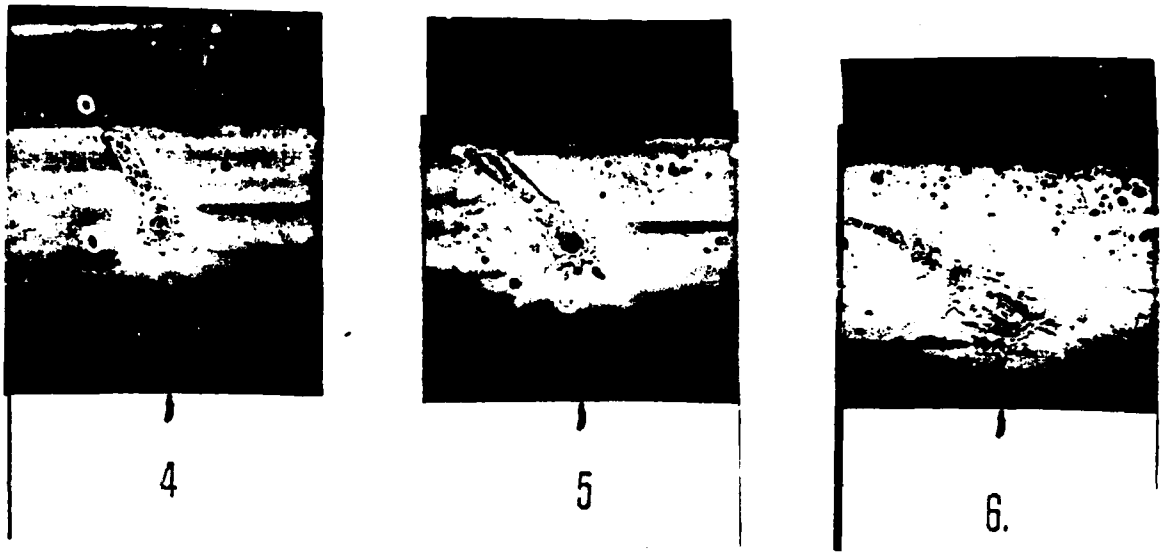

Nahemow Figure 6

Applications of a High Temperature Radiation Resistant Electrical Insulation

M. H. Cooper
Westinghouse Electric Corporation
Advanced Reactors Division
Madison, PA 15663

Abstract

Electrical components are being developed for service inside the reactor vessel of Fast Breeder Reactors. These components will function in an exceptionally hostile environment combining high temperature (1000°F), chemical activity (liquid sodium), and nuclear radiation (fast neutron fluences to 10^{21} n/cm^2). Two components which are being developed are an electromagnetically actuated shutdown system and an induction motor. The successful development of a glass-alumina insulation which is suitable for operation at high temperature and in high radiation fields is the key technological advance that has resulted in the development of these components. The insulation is applied by a dipping process similar to conventional enamel insulation utilizing a slurry of glass-alumina in an organic binder. Drying at modest temperature results in a "green" flexible coating that is adherent to the wire. After the wire is formed into the desired component, the wire is fired at high temperature to eliminate the binder and to fuse the glass mixture to the wire. Electromagnetic coils thus fabricated have been operated for more than 18 months in sodium systems from 850 to 1100°F.

This insulation is especially suited for application to space energy systems because its high temperature capability permits design of electrical components without cooling. In addition, the fabrication process includes a thorough high temperature, vacuum outgassing operation. Thus, outgassing of organic materials from conventional insulations in space can be avoided. Several potential space energy system applications of this insulation are:

- Radiative-cooled electric motors/generators
- Operators for valves that can be completely sealed within the valve body (eliminates seal leakage or unreliable bellows seals)
- Instrumentation and control systems.

Summary of Viewgraph Material

"Applications of a High Temperature Radiation Resistant Electrical Insulation"

M. H. Cooper
Westinghouse Electric Corporation
Advanced Reactors Division

Viewgraph 1

The presentation will consist of a review of the background and history of the development of high temperature, radiation resistant electrical insulation; a description of its use in two nuclear reactor applications, reactor shutdown system and high temperature motor, and several potential applications in space power systems.

Viewgraph 2

Development of a high temperature electrical insulation began in the 1960's to provide a motor capable of operation at 1000°C. A glass-alumina oxide insulation was successfully demonstrated and a small motor fabricated and delivered to NASA. This technology remained dormant until 1977 when the need for a high temperature coil for use in a nuclear reactor shutdown system was identified. This high temperature electromagnetic system has been successfully developed and development of a high temperature, hermetically sealed induction motor was initiated in 1980.

Viewgraph 3

The temperature sensitive electromagnet supports a neutron absorber bundle above the reactor core. Upon a high temperature approaching the Curie point of a specifically developed nickel-iron alloy, the magnetic reluctance increases which reduces the magnetic flux providing the holding force for the neutron absorber. The key component in this system is the high temperature, radiation resistant electrical coil, which consists of 700 turns of 0.040 inch diameter nickel clad copper wire insulated with glass-alumina.

Viewgraph 4

A high temperature coil with its hermetic can is shown prior to assembly. Twenty-six coils have been fabricated for testing to determine the reliability and life of the coil.

Viewgraph 5

A miniature "coilette" is being irradiated in the core of EBR-II, a fast experimental reactor being operated in Idaho. The electrical properties of this coilette after exposure to a neutron fluence of 4×10^{21} n/cm^2 will be compared with the pre-irradiation electrical properties.

Viewgraph 6

Results of breakdown voltage tests on twisted wire pairs after exposure to temperatures of 600 to 750°C indicate that the breakdown voltage increases with both time and temperature. Since the breakdown voltages were measured at room temperature after exposure to high temperature, this increase in breakdown voltage could result from either more complete elimination of the organic binder or relaxation of contact because of creep of the wires. Hence, in-situ resistance measurements are being made on the twisted wire pairs.

Viewgraph 7

As part of the coil reliability program, twisted pairs of insulated wires are being tested to characterize the insulation resistance as a function of temperature and time. Resistances are periodically measured for twisted wire pairs while they are at temperature using the arrangement shown. This method will eliminate the thermal cycling relaxation problem encountered with the breakdown voltage tests.

Viewgraph 8

In 1980, development of a 1/2 hp induction motor designed to operate in a nuclear reactor (1000°F, under sodium, neutron fluence) was initiated. This motor is based upon its use to power an in-vessel fuel handling machine.

Viewgraph 9

The high temperature motor design is complete, fabrication of components is complete, and room temperature operational tests are in progress prior to installation of hermetic can.

Viewgraph 10

This photograph shows the rotor prior to welding its hermetic can.

Viewgraph 11

This photograph shows the stator prior to installation of the windings. The winding consists of three phases, six 0.040-inch diameter wires per coil, operating at 96 volts. The motor has been designed for a low speed of 450 rpm to facilitate gearing in the refueling application.

Viewgraph 12

There are several military and space applications of this high temperature insulation. Use of glass-alumina insulation for motors in mobile applications would reduce cooling requirements and enhance system reliability. The higher temperature capability would reduce cooling requirements permitting natural convection to replace forced convection or air cooling to replace water cooling. In space systems, outgassing of organic insulating materials in vacuum would be eliminated and cooling requirements would be reduced, permitting simpler heat rejection systems utilizing thermal radiation. This material will also eliminate insulation degradation resulting from exposure to high radiation fields.

OVERVIEW

- BACKGROUND AND HISTORY
- NUCLEAR REACTOR SHUTDOWN SYSTEM
- HIGH TEMPERATURE MOTOR
- POTENTIAL SPACE/DOD APPLICATIONS

- HIGH TEMPERATURE MOTOR DEVELOPED BY W R&D FOR NASA IN MID 1960's
- TECHNOLOGY DORMANT UNTIL 1977
- INITIATED DEVELOPMENT OF HIGH TEMPERATURE COIL FOR NUCLEAR REACTOR SHUTDOWN SYSTEM
- INITIATED DEVELOPMENT OF HIGH TEMPERATURE, HERMETICALLY SEALED MOTOR IN 1980

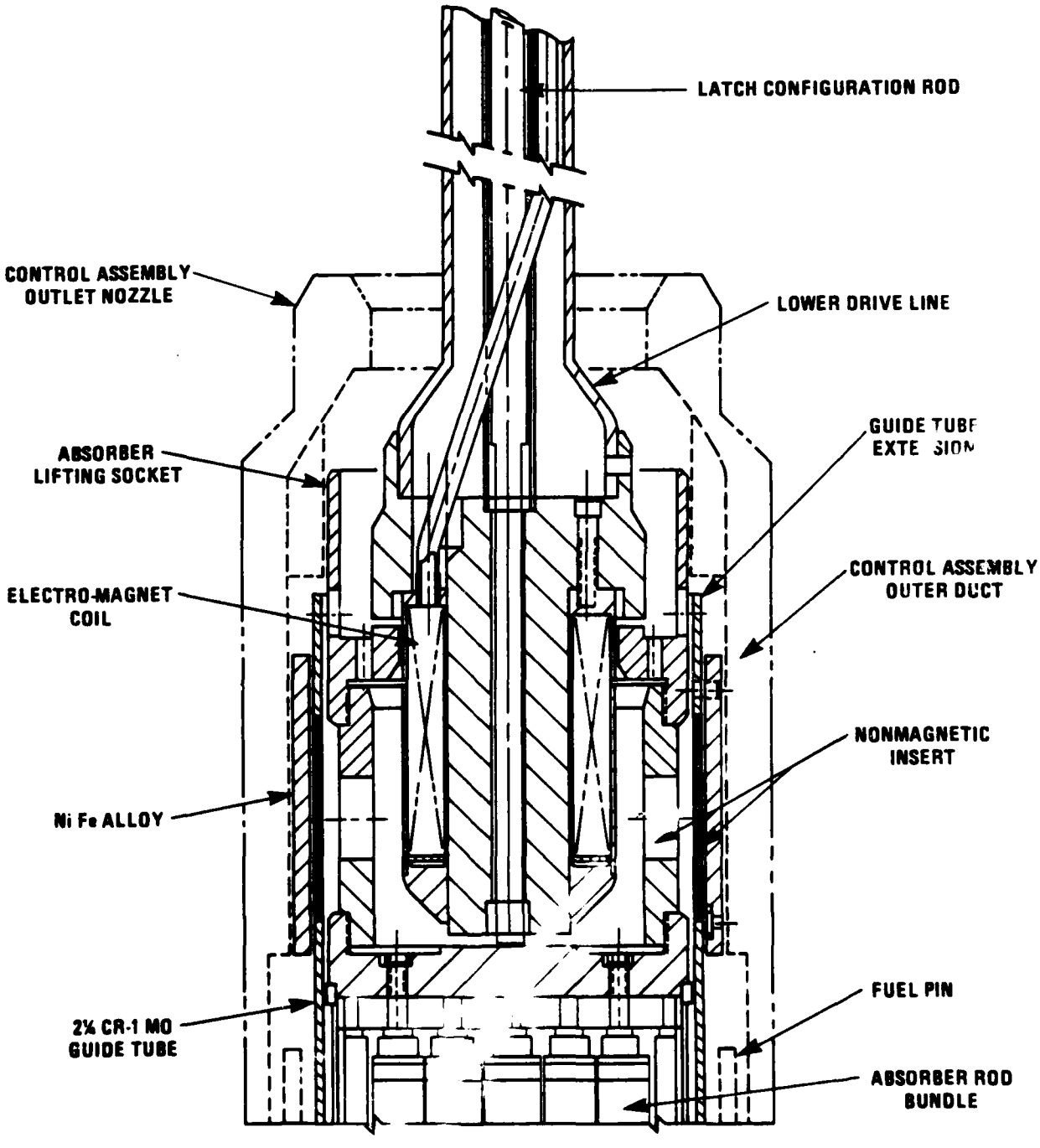

Revised TSEM Geometry

1976-7

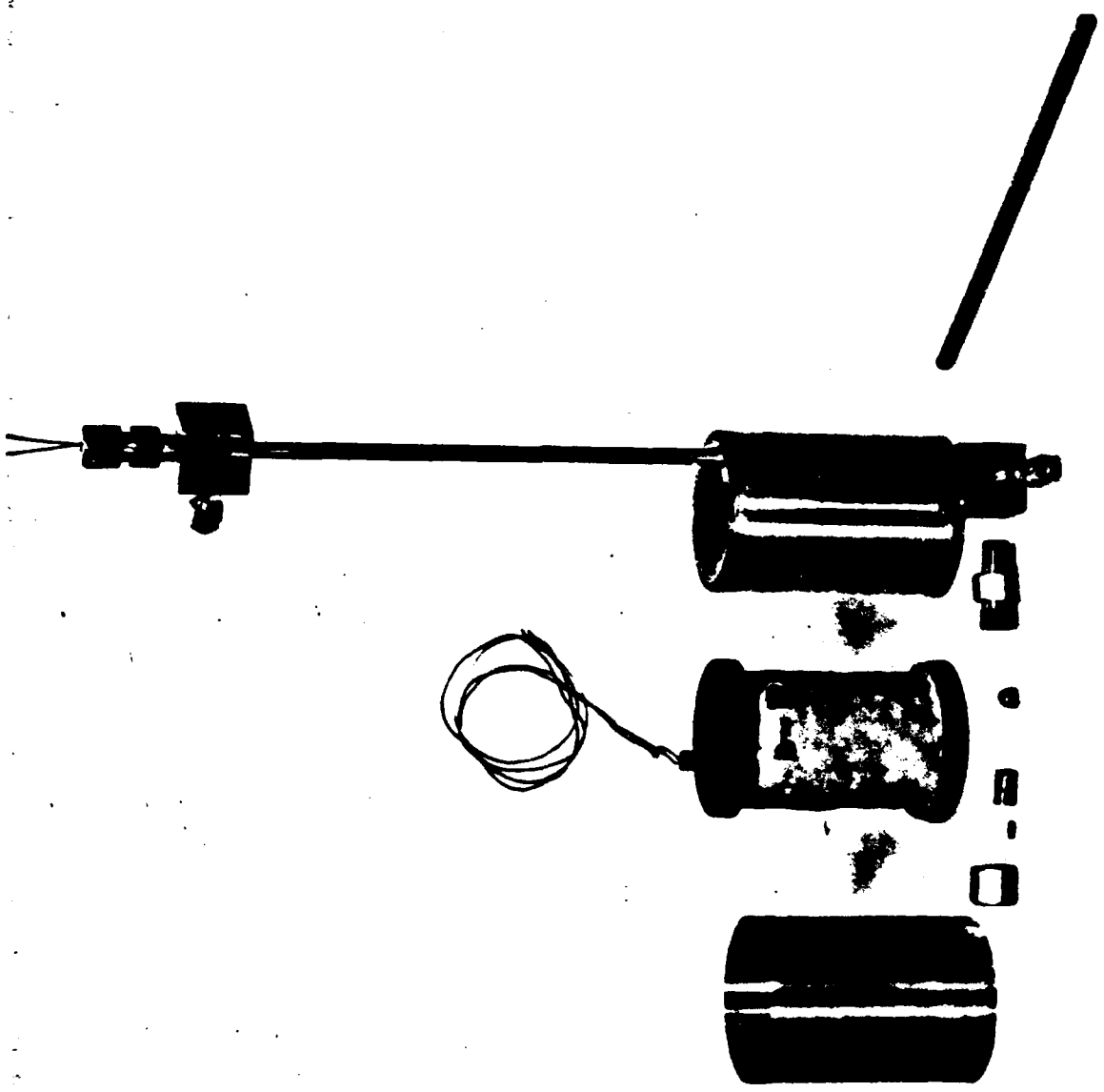

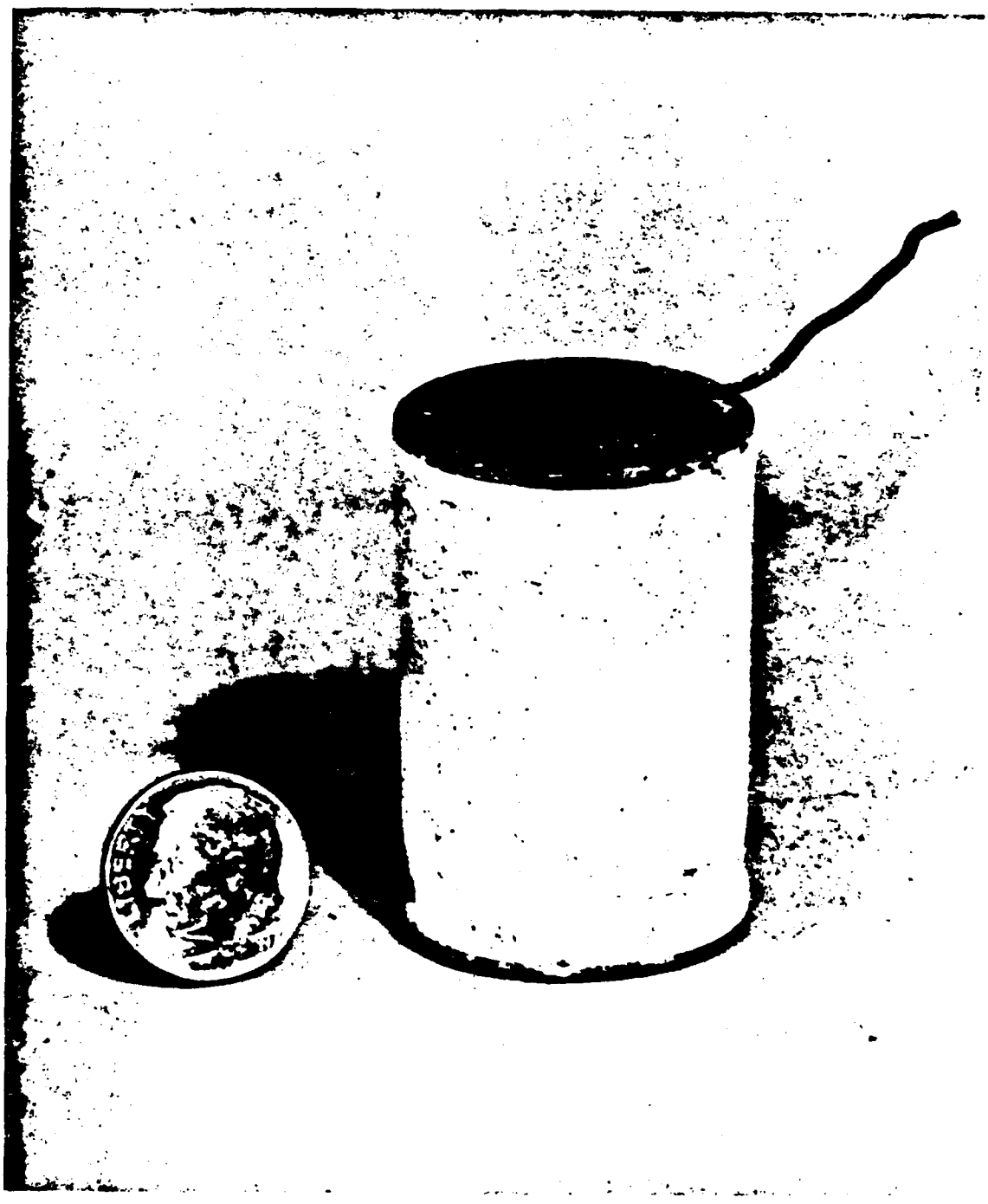

High Temperature Coil Used in the EBR-II Irradiation Test

4988-24

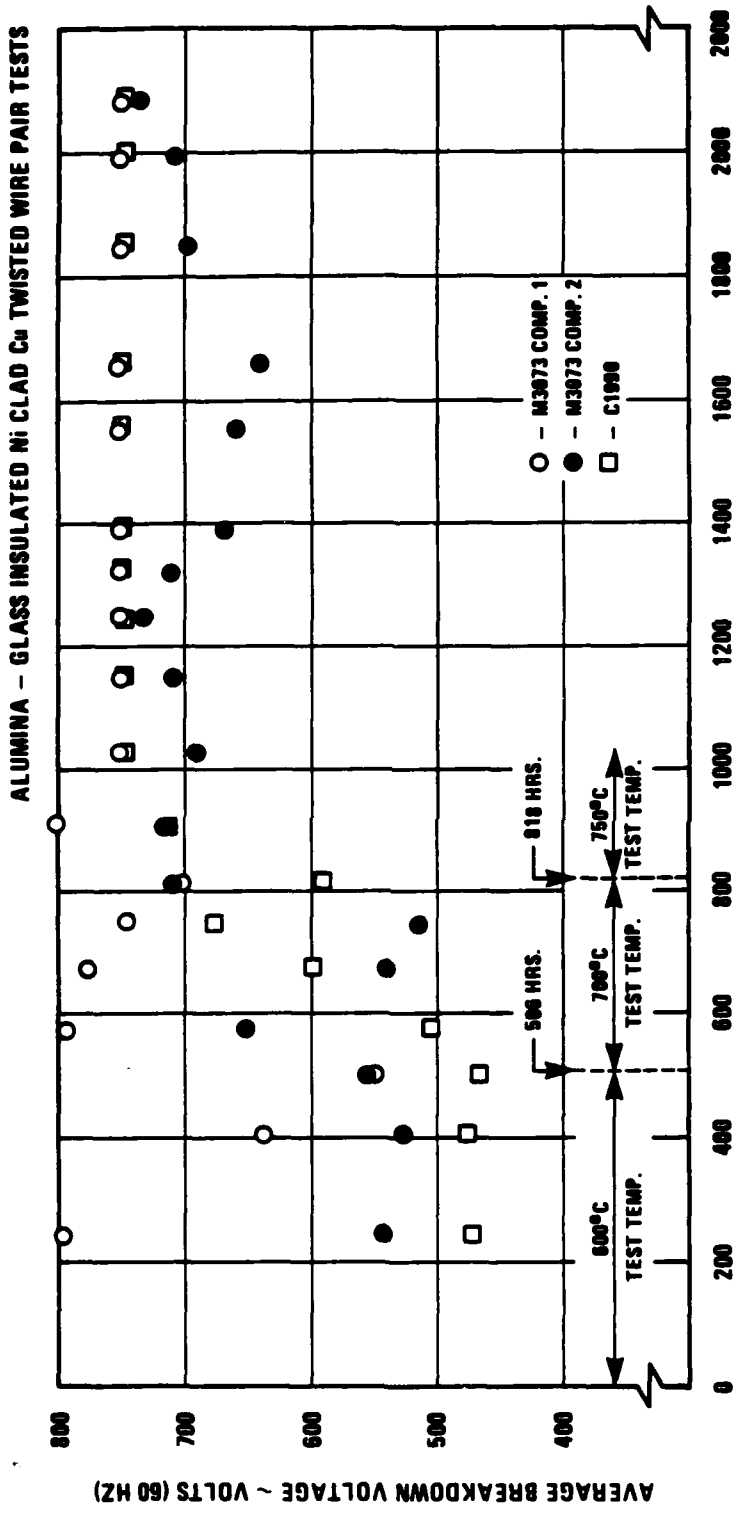

Figure 6-1 Breakdown Voltage Tests (600°C/700°C/750°C)

6127-2

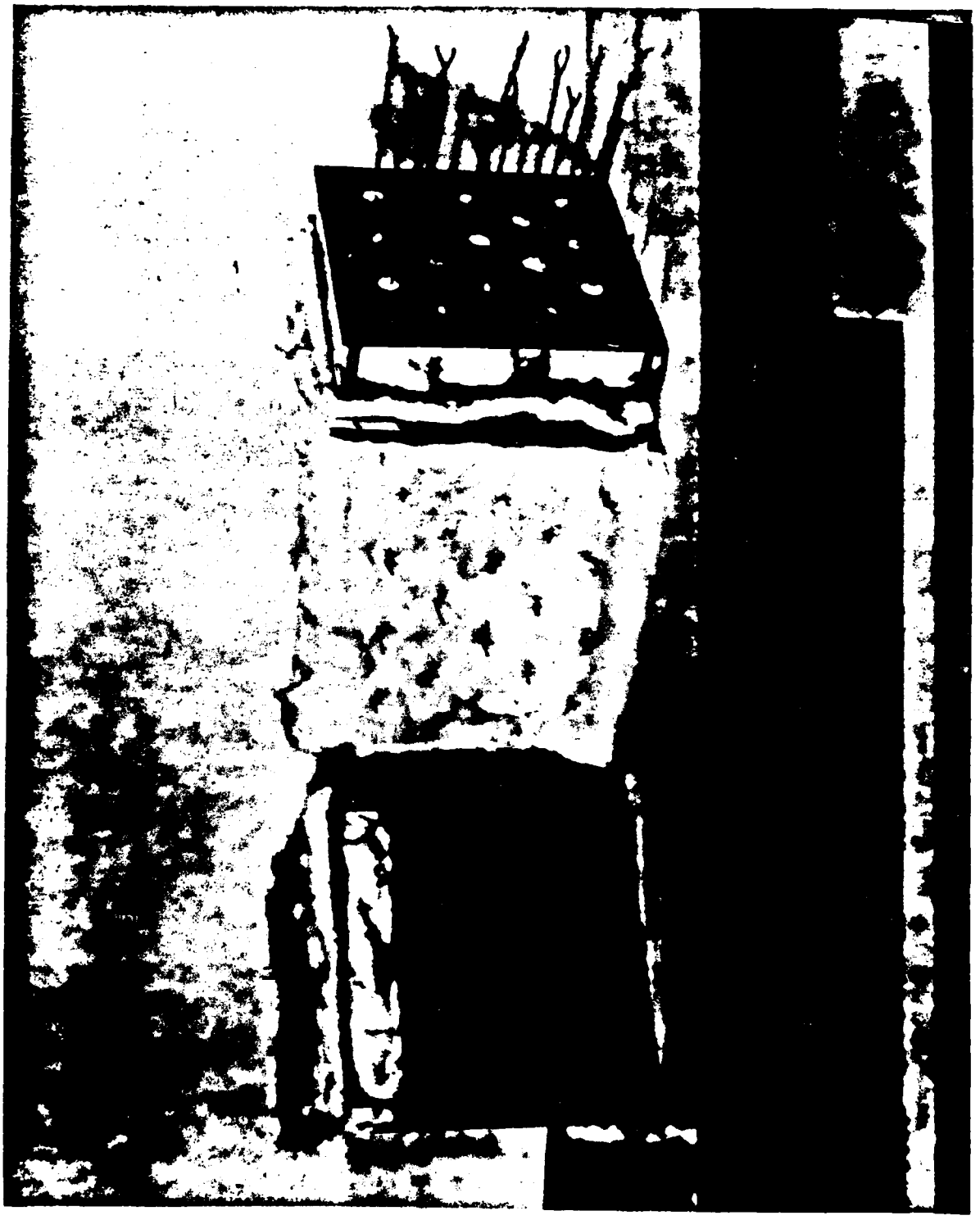

DEVELOPMENT OF HIGH TEMPERATURE MOTOR

OBJECTIVES

- DESIGN, FABRICATE AND TEST 1/2 HP MOTOR TO OPERATE IN LMFBR ENVIRONMENT (1000°F, UNDER SODIUM, NEUTRON FLUENCE)
- MOTOR TO BE USED TO POWER IN-VESSEL REFUELING MACHINE

STATUS OF MOTOR DEVELOPMENT

- DESIGN COMPLETE
- FABRICATION OF COMPONENTS COMPLETE
- OPERATIONAL TESTS AT ROOM TEMPERATURE IN PROGRESS
- HIGH TEMPERATURE TESTS SCHEDULED LATER THIS YEAR

Stator

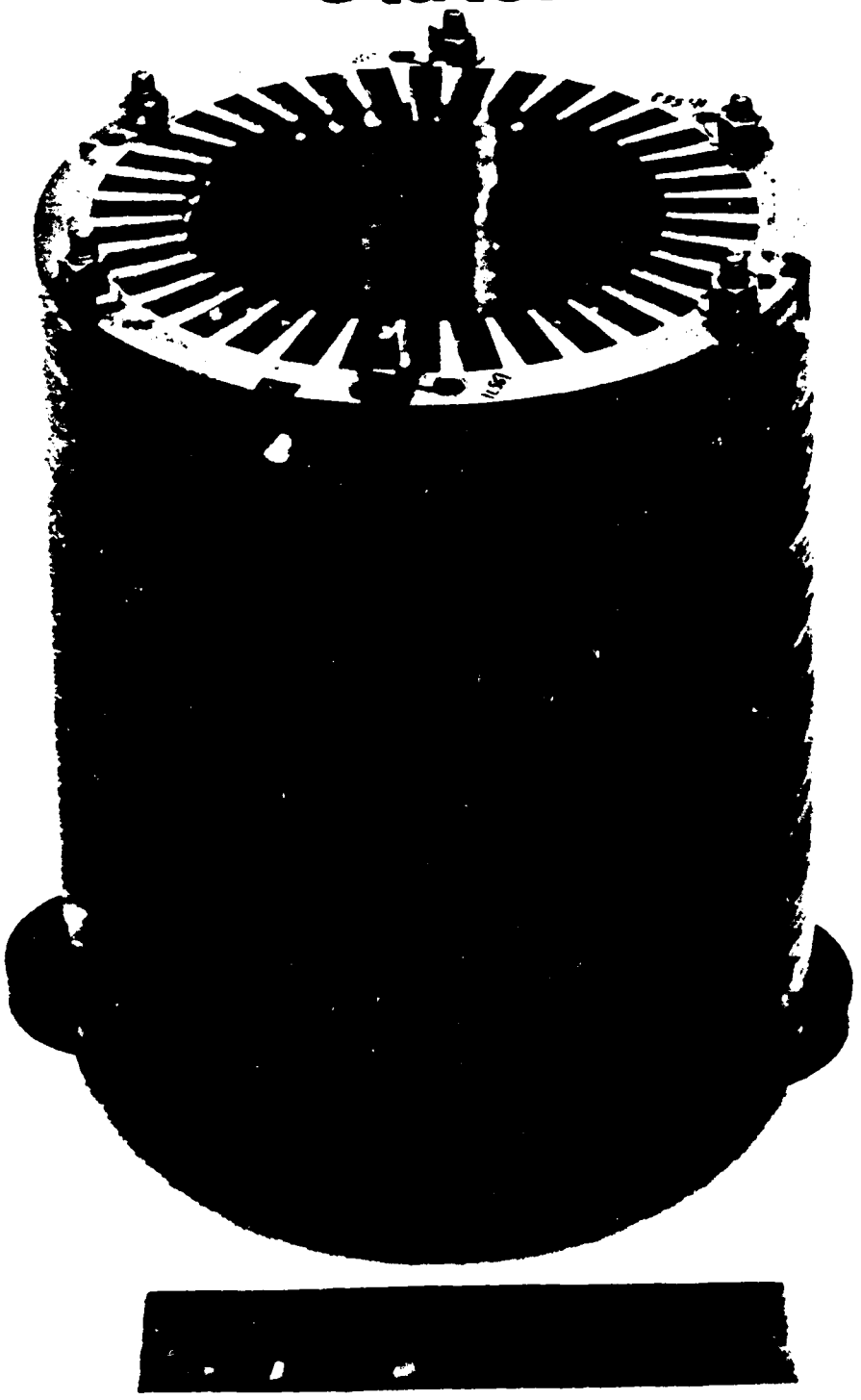

APPLICATIONS OF HIGH TEMPERATURE INSULATION

- MOBILE SYSTEMS
  - REDUCE COOLING REQUIREMENTS

    FORCED CONVECTION → NATURAL CONVECTION

    WATER COOLED → AIR COOLED
  - INCREASE RELIABILITY

    LARGER MARGIN TO INSULATION BREAKDOWN
- SPACE SYSTEMS
  - ELIMINATES OUTGASSING OF ORGANIC INSULATING MATERIALS IN VACUUM
  - REDUCTION IN COOLING REQUIREMENTS; REJECT HEAT BY THERMAL RADIATION
- ELECTRICAL SYSTEMS EXPOSED TO RADIATION FIELDS

Bibliography

"Inherently Safe Core Design Program Annual Summary Report, July 1, 1976 through September 30, 1977", WARD-IS-3045-6, June 1980.

R. B. Tupper and M. H. Cooper, "Inherently Safe Core Design Program Annual Summary Report, October 1, 1977 through September 30, 1978", WARD-IS-3045-4, June 1980.

R. B. Tupper, M. H. Cooper and C. E. Swenson, "Nuclear Safety and Reliability Engineering, Self-Actuated Shutdown System Development, Annual Progress Report, for the Period Ending September 30, 1979", WARD-SR-94000-4, March 1980.

R. B. Tupper, C. E. Swenson, W. C. Frank, "Nuclear Safety and Reliability Engineering, Self-Actuated Shutdown System Development, Annual Progress Report for the Period Ending September 30, 1980", WARD-SR-94000-25.

R. B. Tupper, A. M. Bernard, W. C. Frank, "Nuclear Safety and Reliability Engineering, Self-Actuated Shutdown System Development, Annual Progress Report for the Period Ending September 30, 1981", WARD-SR-94000-30.

RADIATION DAMAGE MEASUREMENTS ON NONMETALS MADE DURING IRRADIATION WITH 1 TO 3 MeV ELECTRONS*

Paul W. Levy
Brookhaven National Laboratory, Upton, New York 11973

To investigate the fundamental processes producing radiation damage in nonmetals a unique facility has been developed for making optical absorption, luminescence and other measurements during irradiation with 1 to 3 MeV electrons. Measurements are made with a 13 meter long double beam spectrometer arranged so that all sensitive components, e.g. phototubes, are outside of the irradiation chamber. A computer provides automatic control and data recording. A 256 point absorption and a 256 point luminescence spectra are recorded as often as every 40 seconds in either the 200-400 or 400-800 mm wavelength range. Samples are irradiated, at temperatures between 20 and 900°C, in an electronically controlled chamber containing He exchange gas and equipped with thin Havar windows to transmit the electron beam and high purity fused silica windows for the spectrophotometer beams. Radiation induced luminescence and absorption in the chamber windows, etc. is eliminated by the double beam spectrophotometer.

Studies made with this equipment demonstrate clearly that many of the processes occurring during damage formation are transient. For example, in NaCl irradiated at 300°C F centers are present during irradiation but disappear when the irradiation is terminated. Also, when NaCl containing colloids is irradiated at 150°C lowering the dose rate immediately decreases the F-center concentration and increases the colloid particle concentration. In contrast, the F-center and colloid concentrations change very slowly after the irradiation terminates. Thus, in principal, by making measurements during irradiation one can determine both the transient and stable defects introduced and, in turn, determine the damage formation kinetics.

*Research supported by the DOE Division of Basic Energy Sciences and the DOE Office of Nuclear Waste Isolation, operated by Battelle Institute-Columbus, Ohio, under contract DE-AC02-76CH00016.

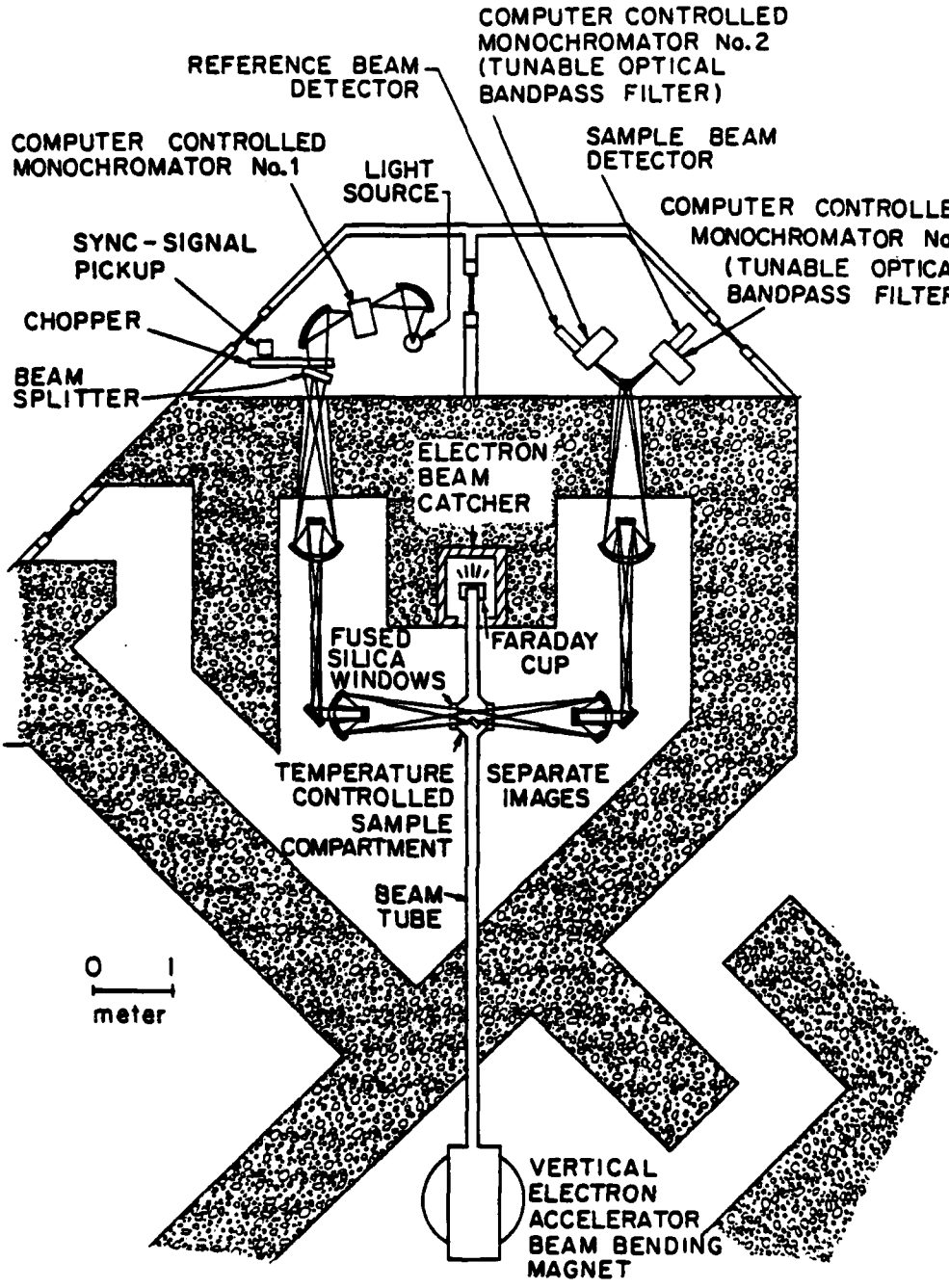

Fig. 1 -- The equipment developed at Brookhaven National Laboratory for studying radiation damage in nonmetals by making optical absorption, luminescence and other measurements on samples at controlled temperatures during irradiation by 1-3 MeV electrons. Measurements are made with a 13 meter long double beam spectrophotometer with all sensitive components outside of the irradiation chamber. A computer is used for both experiment control and data recording.

Fig. 2 — The temperature controlled irradiation chamber for studying radiation damage at temperatures between 20 and 900°C. It is equipped with thin Havar windows to transmit the electron beam, high purity fused silica windows for the spectrophotometer light beams and is operated with a He atmosphere to facilitate precise electronic temperature control.

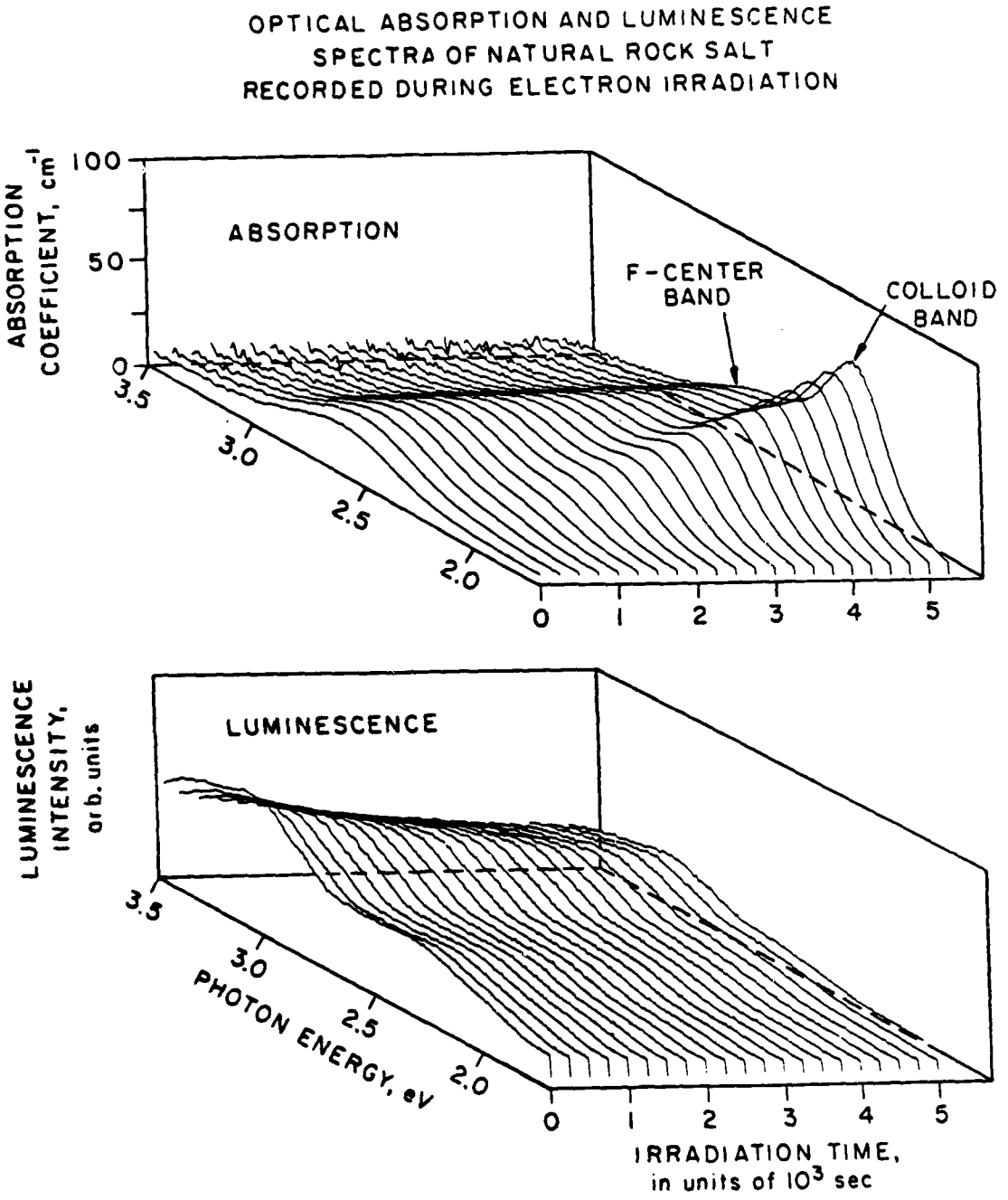

Fig. 3 -- Growth of the radiation induced F centers, i.e. Cl^- ion vacancies, Na metal colloid particles and the luminescence emitted by natural rock salt measured during electron irradiation. The natural salt is similar to that occurring in bedded salt deposits which could be used for a radioactive waste repository.

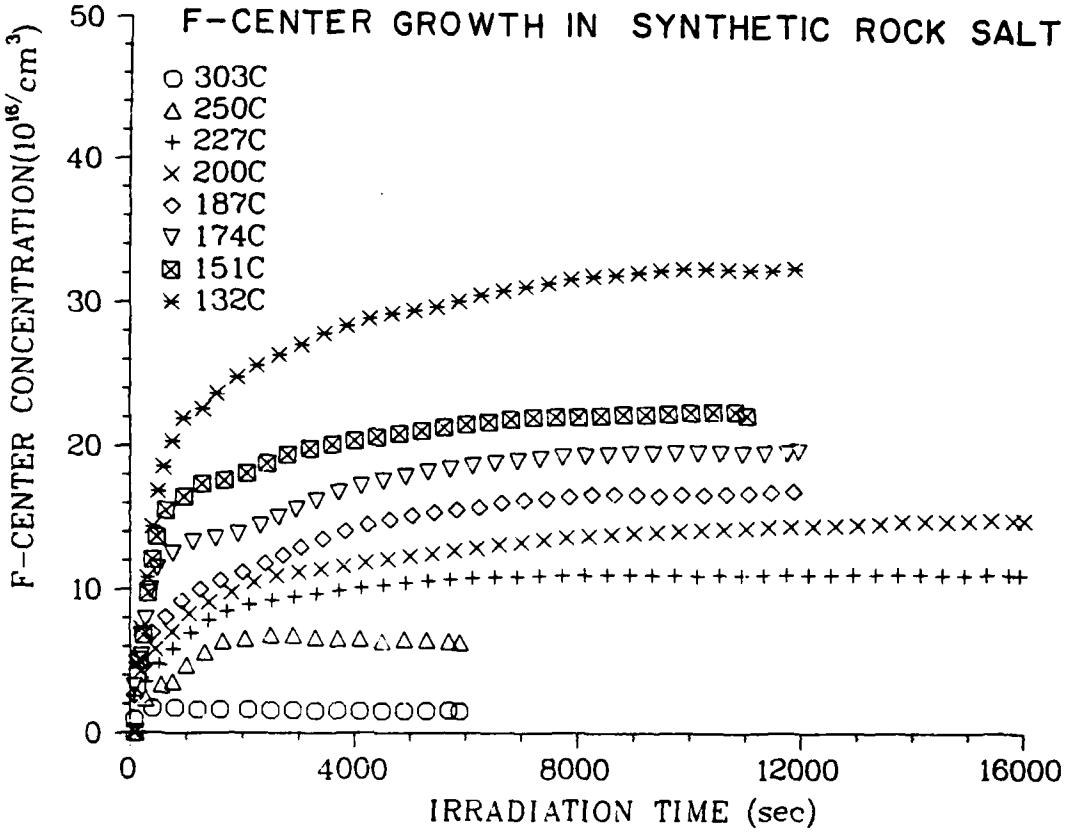

Fig. 4 -- Growth of radiation induced F centers in NaCl measured during irradiation at various temperatures. These curves were obtained from data similar to that shown in Fig. 3. The F-center decay occurring after the measurements were terminated is shown in Fig. 5

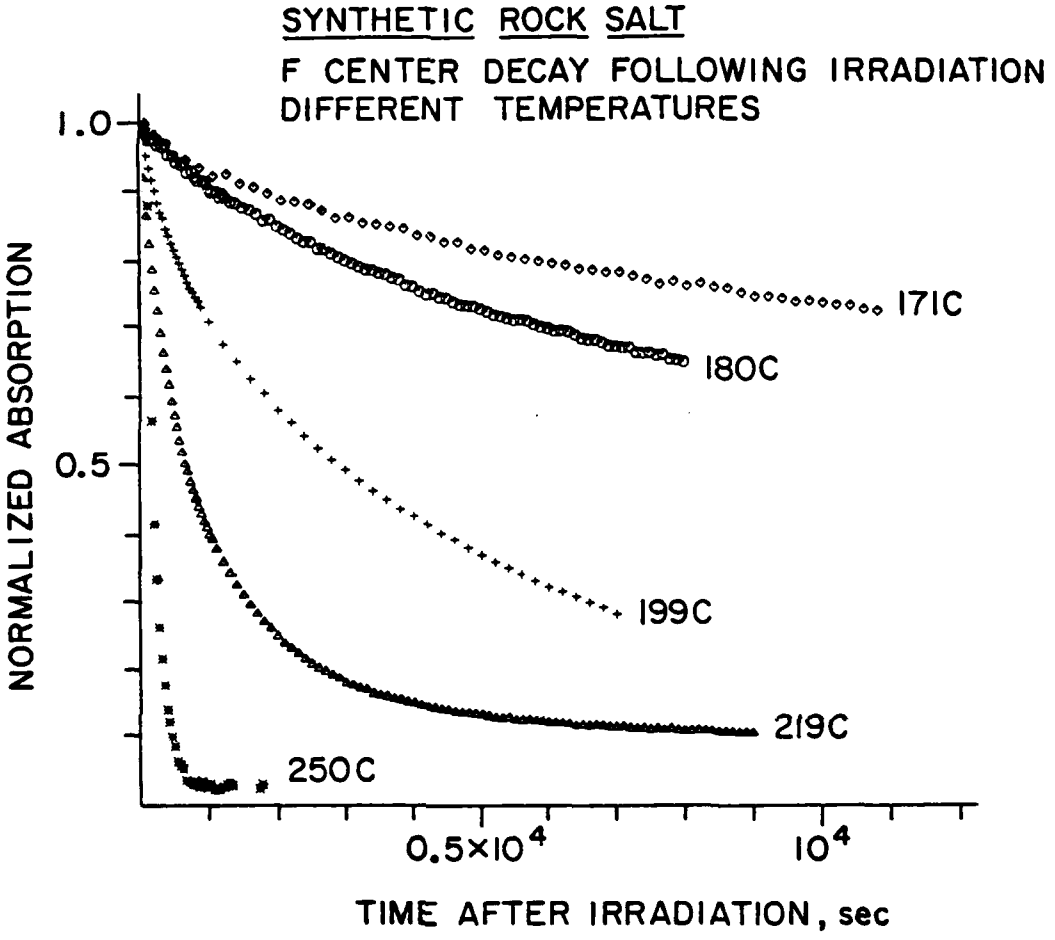

Fig. 5 -- Decay of radiation induced F centers in NaCl recorded after the irradiation was terminated.

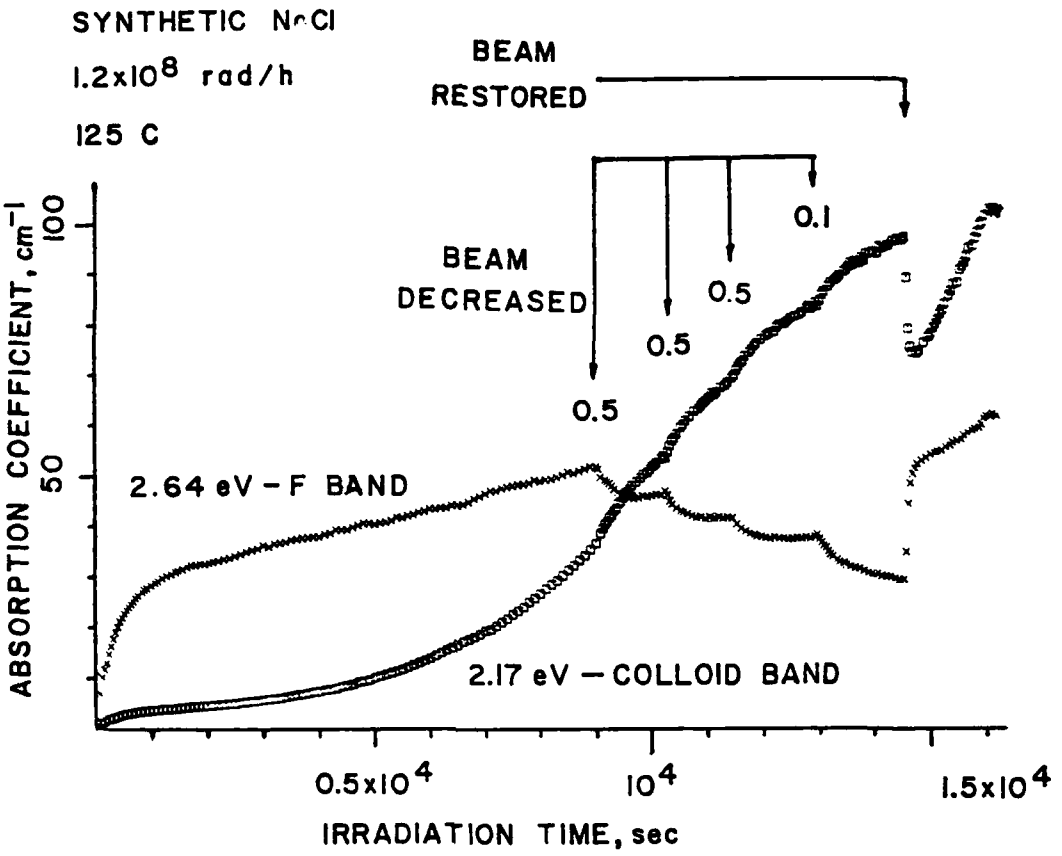

Fig. 6 -- NaCl F center and colloid absorption changes produced in natural rock salt by changing the dose rate during irradiation. Decreasing the dose rate causes the F centers to decrease and the colloids to increase by large amounts. The reverse happens when the dose rate is increased. Most importantly, the changes which occur when the irradiation is terminated are much smaller than those which occur when the dose rate is changed. These measurements show that at least one defect is present and/or mobile only during irradiation.

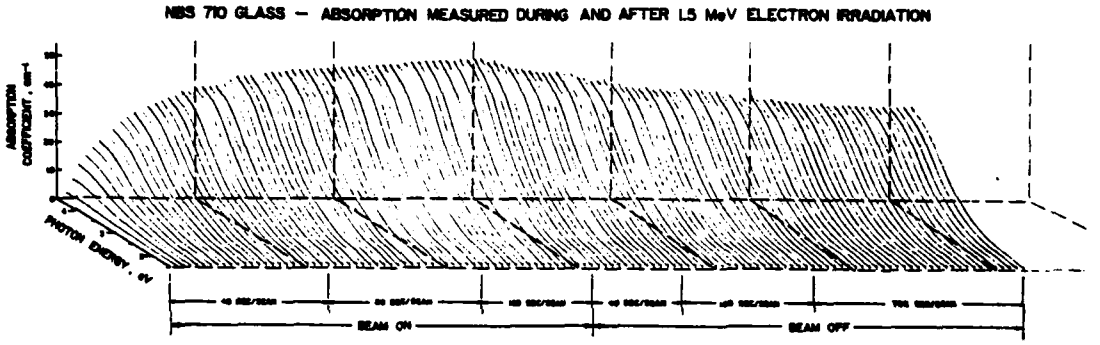

Fig. 7 -- Growth of radiation induced defects in glass, measured during electron irradiation, and the decay occurring after the irradiation is terminated.

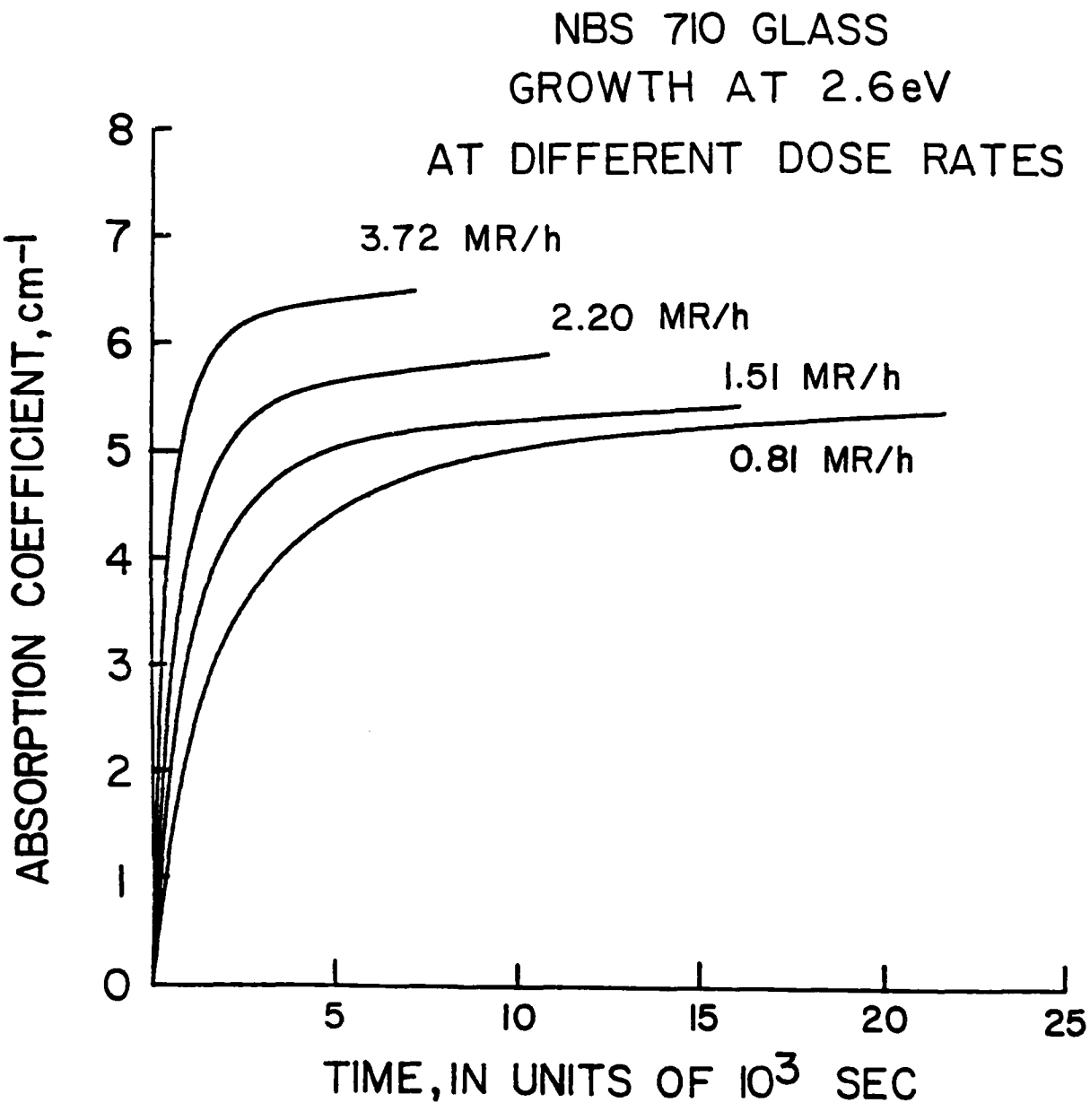

Fig. 8 -- Growth of radiation induced defects in glass measured during irradiation at different dose rates. The decay recorded after the irradiation was terminated is shown in Fig. 9.

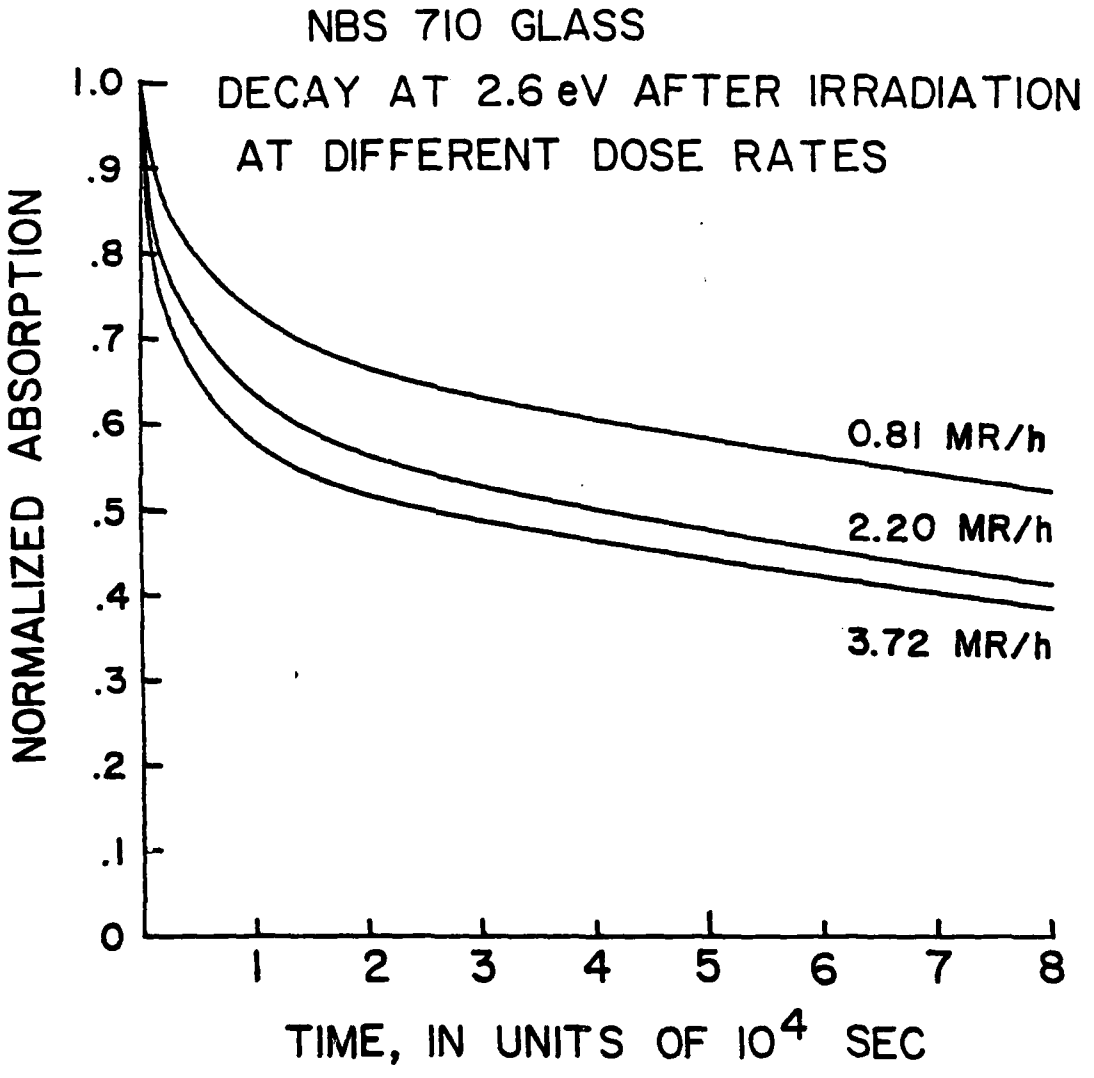

Fig. 9 -- Decay of the radiation induced defects in glass occurring after the growth curves shown in Fig. 8 were recorded.

SELECTED REFERENCES ON RADIATION DAMAGE STUDIES

P. W. Levy. The Use of Color Centers for the Detection and Measurement of Radiation Induced Defects, Symposium on the Chemical and Phys. Effects of High Energy Radiation on Inorganic Substances, ASTM Tech. Pub. No. 359, p. 3, 1964.

P. W. Levy, P. L. Mattern and K. Lengweiler. Studies on Non-metals During Irradiation: I. The Growth and Decay of F-centers in KCl at 20°C, Phys. Rev. Letters 24, 13 (1970).

P. L. Mattern, K. Lengweiler and P. W. Levy. Studies on Non-metals during Irradiation: II. The Formation and Post-irradiation Growth and Decay of F-centers in NaCl at 20°C, Solid State Comm. 9, 935 (1971).

K. Lengweiler, P. L. Mattern and P. W. Levy. Studies on Non-metals during Irradiation. III. The Growth of F-centers in KCl at 85°K, Phys. Rev. Letters 26, 1375 (1971).

P. W. Levy, P. L. Mattern, K. Lengweiler and M. Goldberg. Studies on Non-metals during Irradiation. IV. The Effect of Strain Applied during Irradiation on the Gamma-ray Induced F-center Coloring of KCl at Room Temperature, Solid State Comm. 9, 1907 (1971).

P. W. Levy, P. L. Mattern, K. Lengweiler and A. M. Bishay. Studies on Non-metals during Irradiation: V. Growth and Decay of Color Centers in Barium Aluminoborate Glasses Containing Cerium, J. Amer. Ceramic Soc. 57, 176 (1974).

P. W. Levy, M. Goldberg and P. J. Herley. Kinetics of Defect and Radiolytic Product Formation in Single Crystal $NaBrO_3$ Determined from Color Center Measurements, J. Phys. Chem. 76, 3751 (1972).

P. W. Levy, M. Goldberg and P. J. Herley. Formation of Color Centers in Ammonium Perchlorate by X-ray Irradiation at 21°C, Radiation Effects 38, 231 (1978).

K. J. Swyler and P. W. Levy. Radiation Induced Coloring of Glasses Measured during and after Electron Irradiation and Studies on Color-center Formation in Glass Utilizing Measurements Made during 1 to 3 MeV Electron Irradiation. 1975 IEEE Annual Conf. on Nuclear and Space Radiation Effects, Arcata/Eureka, California, July 1975. IEEE Nucl. Trans. NS22 2259-64 (1975); Proc. Princeton University on Partially Ionized and Uranium Plasmas. National Aeronautics and Space Administration, Washington, D. C., Sept. 1976, p. 160-169, Princeton University, Princeton, New Jersey, June 1976.

K. J. Swyler, R. W. Klaffky and P. W. Levy. Radiation Damage Studies on Synthetic NaCl Crystals and Natural Rock Salt for Waste Disposal Applications, Scientific Basis of Nuclear Waste Management, Vol. 1, G. J. McCarthy, editor (Plenum, New York), p. 349

P. W. Levy, K. J. Swyler and R. W. Klaffky. Radiation Induced Color Center and Colloid Formation in Synthetic NaCl and Natural Rock Salt, Third Europhysics Topical Conf., Lattice Defects in Ionic Crystals, J. de Physique 41, Supplement-Colloque C6, pp. 344-347.

K. J. Swyler, R. W. Klaffky, and P. W. Levy. Recent Studies on Radiation Induced Color Centers and Colloid Formation in Synthetic NaCl and Natural Rock Salt for Waste Disposal Applications, Int. Sym. on the Sci. Basis for Nuclear Waste Management, Vol. II, C.J.M. Northrup, editor (Plenum, New York, 1980) p. 553.

P. W. Levy, J. M. Loman, K. J. Swyler, and R. W. Klaffky. Radiation Damage Studies on Synthetic NaCl Crystals and Natural Rock Salt for Radioactive Waste Disposal Applications, to be published in: Advances in the Science and Technology of the Management of High Level Nuclear Waste, P. L. Hofmann, ed.

J. M. Loman, P. W. Levy, and K. J. Swyler. Radiation Induced Sodium Metal Colloid Formation in Natural Rock Salt from Different Geological Localities, to be published in Proc. 4th Materials Res. Soc. Symp. on the Scientific Basis of Nuclear Waste Mgmt., Boston, MA, 1981.

CHARGE INJECTION EFFECTS UPON PARTIAL DISCHARGES IN A DC AND DC PLUS AC LAMINATE INSULATION ENVIRONMENT

W. J. Sarjeant, J. R. Laghari and R. Gupta
State University of New York at Buffalo
4232 Ridge Lea Road
Amherst, New York 14226

and

K. J. Bickford
MS 566
Los Alamos National Laboratory
Los Alamos, New Mexico 87545

ABSTRACT

Foil-edge partial discharge phenomena in liquid impregnated laminate structures have been investigated. A partial discharge dependency on $\dot{V}$ has been found to exist. Experiments support the hypothesis that electric charges are injected into the dielectric regions near the conductor edge by field-controlled charge injection during impressed voltage transients. The resulting conduction current space charge can establish equilibrium by reduction of the electric field intensity below the partial discharge inception threshold. A temporal characterization of this space charge injection is discussed relative to the effect on partial discharge inception at the foil edge. The significance of these effects in general insulation configurations having a combination of solid-liquid-gas-vacuum interfaces will be discussed in some detail.

CHARGE INJECTION EFFECTS...

INTRODUCTION

Evolving power conditioning system requirements in many important technological areas will place severe demands upon long-lived, repetitive pulse-power components. A major pacing system component in this high reliability, repetitive pulse-power technology is the energy storage capacitor. Recently, increasing availabilities of quality plastic films, especially polypropylene, and the discovery of the excellent properties of perfluorocarbon liquids for impregnation fluids make spirally-wound, plastic film/liquid impregnated capacitors a leading candidate for high energy density, repetitively operated pulse discharge energy storage devices. The dominant lifetime-limiting mechanism is this type of high energy density capacitor is a direct result of partial discharge activity at the buried foil edges, where the electric field is maximum. Objectives of ongoing research programs include the characterization and understanding of the mechanisms of this and related partial discharge phenomenon.

CHARGE INJECTION EFFECTS...

A sharp and microscopically irregular foil edge defines the inner boundary of a capacitor margin. The electric field intensity at these buried foil edges can be very high, especially for unaligned foils, a configuration that exists in all real capacitor geometries. Extended foil designs, because of inherently better inductive, peak current and heat-sinking characteristics, will be considered as the model for this discussion. Figure 1 is a cross-sectional view of a hypothetical foil edge, the section taken parallel to the axis of the capacitor winding. This model embodies only the effects of field enhancement caused by the dielectric permittivities interacting with the geometries of the dielectric and foil edge; intrinsic, extrinsic and charge-injection conductivities are not incorporated. The permittivities are assumed to be homogeneous and of an electronic and/or ionic nature (no rotational orientation polarization), so no frequency dependence in the permittivities exists below microwave frequencies. Under these assumptions, the electric field intensities at the foil-edge surfaces in the figure are representative of the behavior during the risetime of a fast voltage transient impressed on the foils. The particular foil-edge shapes are conservate representations relative to real foil edges formed by commercial shearing processes. The tendency to large field enhancements can be seen to be extreme. An enhancement factor of slightly greater than 7 occurs at the point where the foil edge radius is minimum (0.01 mil); hence for this shape a field of 7800 volts per mil per kilovolt is hypothesized during a voltage transient. For extremely well degasified and filtered perfluorocarbons, the thin-film breakdown strength has been measured to be in the range 11 kV - 13 kV per mil. As shown in Figure 1, for an impressed transient voltage less than 2 kV, the breakdown threshold of the liquid impregnant is exceeded and partial discharges occur characteristically in the form of low intensity (< 20 pc) impulse streamers at the foil edge.

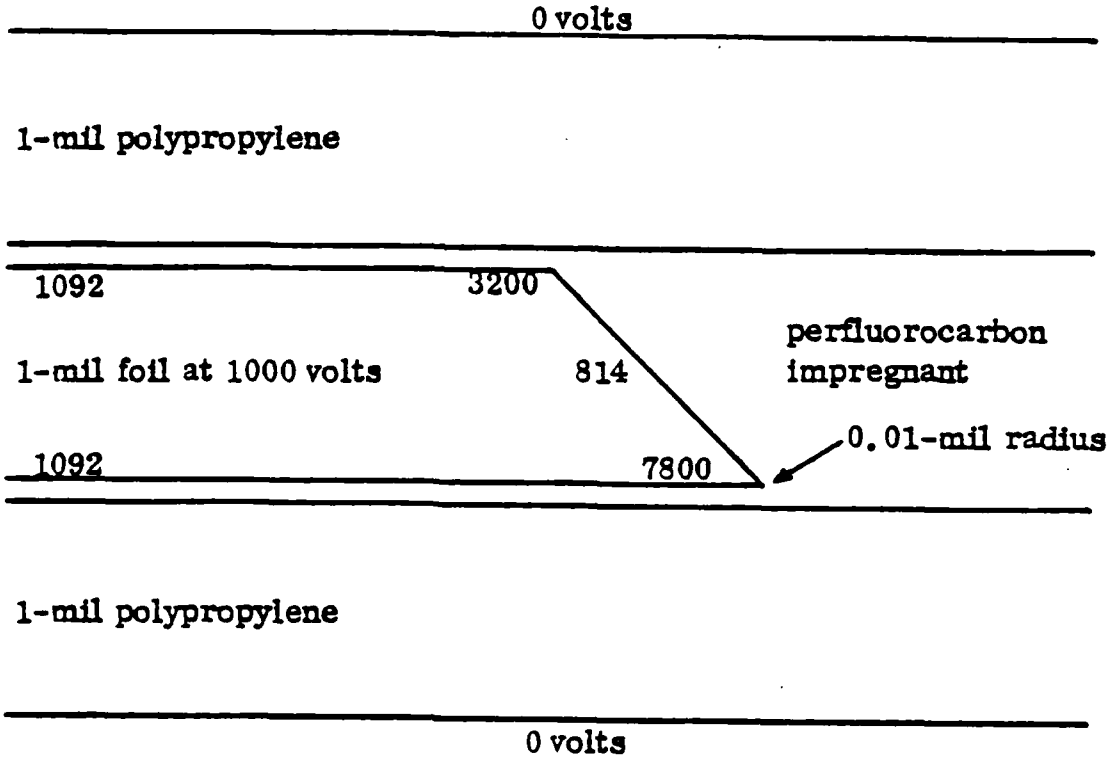

Figure 1. Electric field strength in volts per mil at a bogey foil-edge surface for 1000 volts applied to the liquid-impregnated laminate structure.

CHARGE INJECTION EFFECTS...

PARTIAL DISCHARGE INCEPTION VS DIELECTRIC CONDUCTIVITY

Considering only the effects of the dielectric permittivities and conductivities interacting in a laminar capacitor geometry of large area and small thickness, a two-component dielectric system can be modeled as shown in Figure 2. The value of the ratio permittivity/conductivity (rearrangement time) is on the order of minutes for polypropylene and perfluorocarbons (10^{-11} F m^{-1}/10^{-15} Ω^{-1} m^{-1}) such that the effect of the dielectric conductivities on the electric field intensities is negligible for angular frequencies exceeding fractional radians per second. The model shown in Figure 2 is, therefore, appropriate for describing the electric field at the surfaces of the foil edges when considering only the contributions from dielectric permittivity and conductivity. The breakdown threshold of the impregnant at the locus of maximum electric field intensity is again theoretically exceeded by voltages less than 2 kV with rise times approaching dc values.

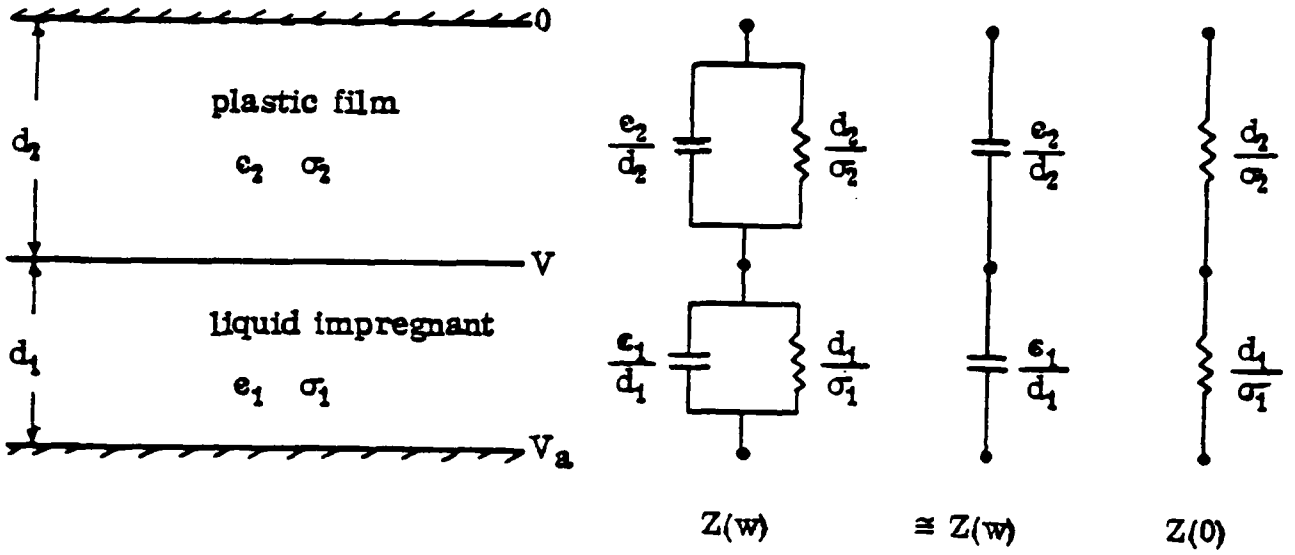

Figure 2. Model of a two-component dielectric system impedance as a function of frequency.

CHARGE INJECTION EFFECTS...

PARTIAL DISCHARGE INCEPTION VS INJECTED SPACE CHARGE

Charge carriers under the influence of an electric field can be injected into a dielectric material from the surface of an electrode. These carriers are transported through the dielectric, and are captured at the opposing electrode. Charge injection is not an impulse breakdown process like partial discharges, but is a continuous conduction phenomenon similar to intrinsic or extrinsic conduction except the origin of the carriers is entirely external to the dielectric, and the current is hyperlinear with the electric field. Two types of injection processes that have been specifically identified and described are Schottky and tunnel injections: Regardless of the physics at the electrode/dielectric interface, the result is a current density in the dielectric that can approach a space charge limited condition, where the electric field at the injection site is reduced to a small value by the proximity of the space charge. Because charge injection is a field-controlled process, the current density will be maximum at the high field sites on the foil edges. The conduction path follows the electric field vector and injected current flows from the foil edge to the opposing foils through the multiple layers of the dielectric, a distance approximating 1 mil. If the charge injection process can become established during the rise or fall times of voltage transients across the conductive foils, the reduction of the electric field at the foil edge would increase the partial discharge inception voltage. Although the time constants for the distribution of space charge duing field-controlled injection are significantly shorter than the ε/σ ratio discussed above, the values are large compared to the millisecond charge times and nanosecond discharge times of pulse discharge service.

CHARGE INJECTION EFFECTS...

Using the transport time for a slow electron under the influence of a 1-kV per mil field to travel a distance of 1 mil as a measure of the injected space charge formation time,

$$t_f = \frac{d}{E \cdot \mu} \qquad (1)$$

where μ is the effective carrier mobility, d is the dielectric carrier thickness, E is the electric field near the foil edge (spatial average), and t_f is an estimate of the space charge formation time. The mobility is known to be in the range 10^{-12} - 10^{-6} m^2 V^{-1} s^{-1} for most dielectrics and is relatively low because the carriers spend most of the time in shallow traps so the mobility is an effective value. The range of t_f is then calculated to be $6 \times 10^{-7} < t_f < 6 \times 10^{-1}$ s.

The hypothesis that space charge associated with field-controlled injection reduces the electric field intensity at the high field sites on the foil edges and hence increases the partial discharge inception voltage has been supported by the laboratory experiments being reported herein.

CHARGE INJECTION EFFECTS...

Mock-ups of laminar foil-edge structures were constructed using 1-mil mylar film and 0.5-mil foil, vacuum impregnated with vacuum degasified mineral base transformer oil. DC partial discharge measurements were performed with a Biddle corona test set coupled to a multichannel analyzer. Pulse height and multichannel scaling signatures of the partial discharge activity shown in Figure 3 were recorded as a function of the voltages applied to the foil-edge structures. Pulse height histograms exhibited approximately Maxwellian distributions with most of the partial discharge impulses below 20 pC in magnitude. The multichannel scaling signatures were approximately Maxwellian distributions in time, with most of the activity decaying to zero in less than 10 s. The partial discharge inception dependency on dV/dt, and the apparent time constants are in reasonable agreement with the hypothesis that space charge from field-controlled injection controls the partial discharge inception voltage at the foil edges.

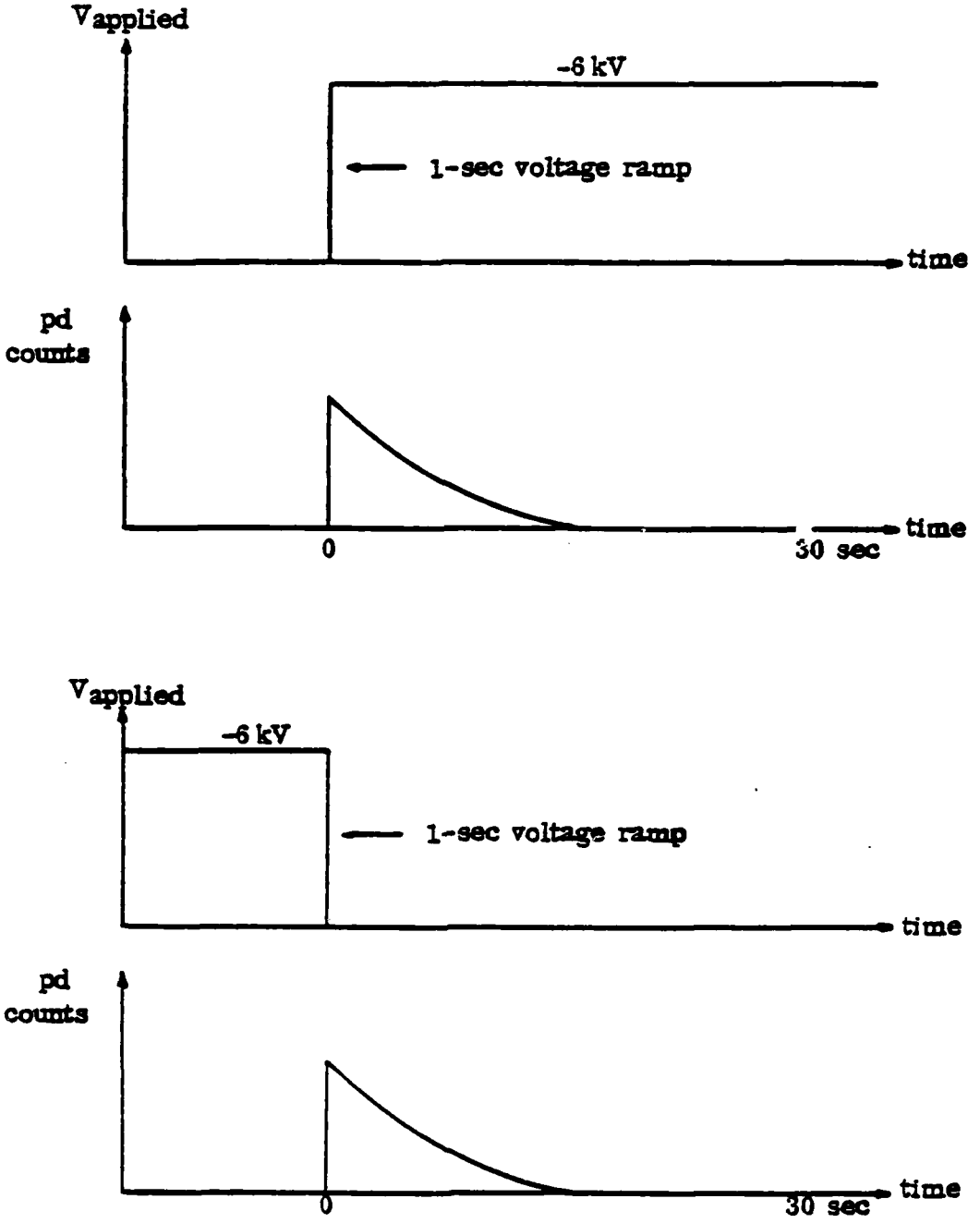

Figure 3. Partial discharges at the foil-edge structure as a function of time and applied voltage. The decrease in pd (partial discharge) counts to zero by 15 seconds after voltage step is predicted by the space-charge injection model herein presented.

CHARGE INJECTION EFFECTS...

Impregnated 2-mil mylar/0.5-mil foil samples were observed to exhibit no partial discharges when the applied voltages were increased from 0 to ± 15 kV during intervals of 1-minute risetimes. The pd distribution in time shown in Figure 4 exnibited a marked peaking and a minor tendency to narrow in time for faster risetimes of applied voltage. It is hypothesized that when voltage is applied across the foils faster than space charge can form and reduce the field at the foil edge, partial discharges occur and create an impulsed, spatial distribution of charges in the regions near the foil edge, reducing the electric field below the partial discharge inception threshold. For conditions where dV/dt is negative (decreasing voltage), if the transient voltage is fast enough in fall time so the conduction current cannot establish a reversal, the charges trapped in the dielectric by the low mobility create an electric field by proximity with the foil edge that exceeds breakdown and partial discharges occur in the opposite direction, dissipating the excess space charge.

Because space charge formation due to charge injection is limited temporally by the magnitude of the free carrier mobility in the dielectric, a theoretically ideal impregnant would possess the electrical properties of high dielectric strength, low intrinsic/extrinsic carrier concentrations, and a high value for free carrier mobility so space-charge formation times would be comparable or faster than the transient voltages applied to the foil edges.

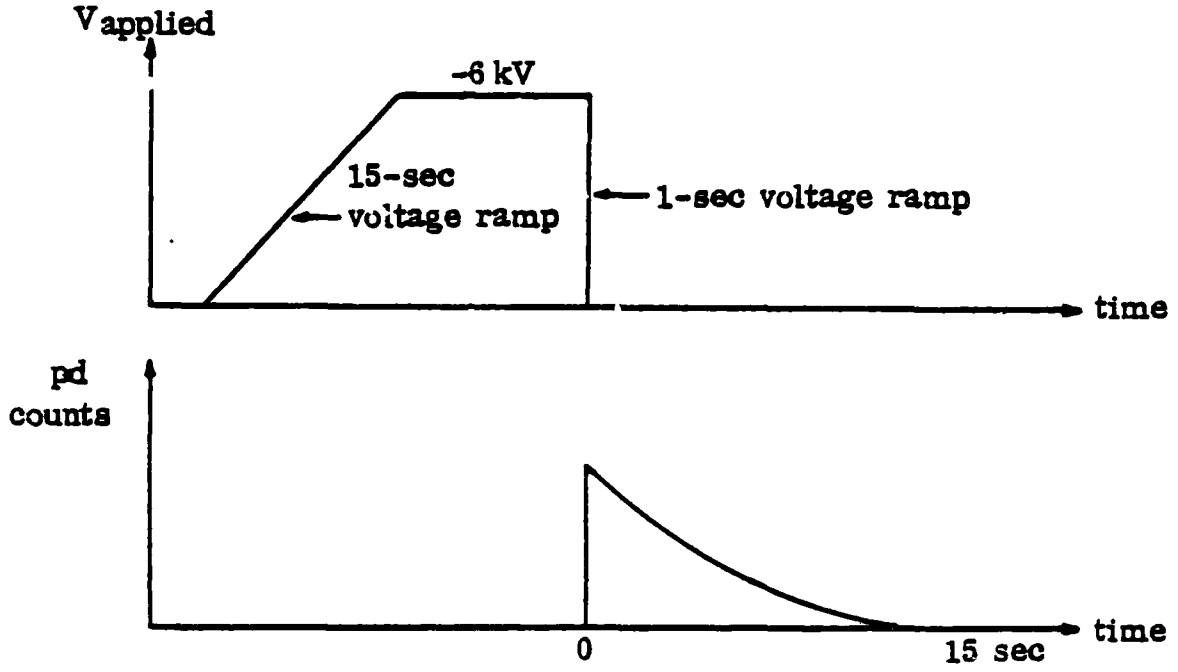

Figure 4. Partial discharge activity at a foil-edge structure as a function of time and applied voltage; voltage risetime was below the + dV/dt threshold.

ELECTRIC FIELD GRADING TECHNIQUES AND MODEL STRUCTURES TO MINIMIZE PARTIAL DISCHARGE ACTIVITY IN LIQUID-IMPREGNATED POLYMER LAMINATE STRUCTURES

INTRODUCTION

This section describes some of the results of modeling electric fields in the margin of a bogey plastic film liquid impregnated laminate structure in which effects of foil edge shape, different impregnants, and grading wires are examined. It will be concluded that placement tolerance and connection problems make grading wires impractical and that folded foil edges remain a very good solution to edge field grading.

In order to develop higher reliability laminate structures. it appeared appropriate initially to carry out a modeling study of maximum fields developed for various foil edge shapes with various impregnants in an otherwise specific bogey laminate structure.

BOGEY LAMINATE MODELS

The bogey laminate geometry that was selected had a solid dielectric thickness of 1 mil, representing two 0.5 mil polypropylene films, and a 0.1 mil impregnant layer next to the foil. The foil thickness was fixed at 1 mil, which should represent a single cut foil or a 0.5 mil folded foil. Thus, in the bulk structure there was a 1.2 mil spacing between foils of opposite potentials.

Foils are presently cut by such techniques as shearing, melting with lasers or with electrical discharges. Figure 5 shows six shapes for foil edges selected as representative of most possible configurations. Each corner was rounded to a known radius to allow exact specification of the electric field on the foil edge, as perfectly shape corners lead to singularities in the surface field. Radii of 0.01 and 0.05 mils were used and the functional variation of field with continuously changing radius on the corners was also determined. At the horizontal coordinate of 0 mils, the field was forced to be vertical. At 30 mils, the potential was set to zero along the vertical boundary, representing the grounded connection. The potential was zero well before 30 mils, so the solution is applicable to longer margin widths.

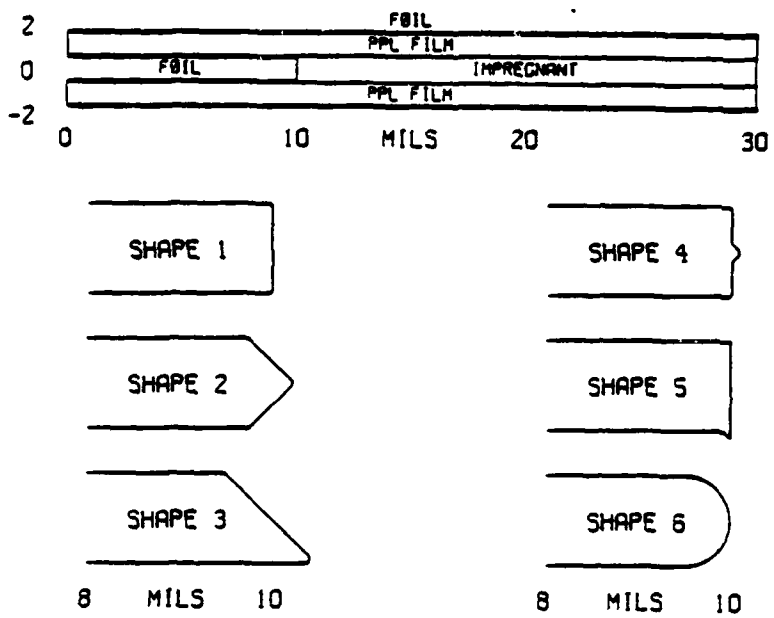

Figure 5. Bogey laminate structure with dimensions. Below it are representative foil edge geometries utilized in calculating the electric field distributions. These edges would be located at the 10 mil distance in the laminate structure.

CHARGE INJECTION EFFECTS...

Fortunately in a problem such as this, containing multiple regions with uniform permitivity in each region, extensive experience to date indicated the maximum field in such region must occur on the boundary. Thus, it was only necessary to compute the electric field along the foil edges and along the interface between the impregnant and plastic film.

The solution to the Laplace equation yielding the potential and electric fields inside the capacitor section was obtained using Green's third formula, which gives the potential, in closed regions as a function of the potential and its normal derivative around the boundary.

CHARGE INJECTION EFFECTS...

EFFECTS OF DIFFERENT FOIL EDGES AND IMPREGNANTS

To visualize explicitly the effects of different foil edges and different impregnants in a film laminate, polypropylene film of 1 mil total thickness was used with 1 mil foil thickness and 0.1 mil impregnant between film and foil. Impregnant also filled the margin.

For each choice of impregnant there is an assumed dielectric strength that the maximum field should not exceed, or breakdown occurs. This limit sets the electric field in the polypropylene film, wherein the bulk of the energy is stored.

Figure 1 shows the potentials of Shape 3, the 45° shear with 0.01 mil corner radii, around the foil edge for 1000 V across the opposite foils. The field enhancement factor at the foil edge is defined as the ratio of the maximum field to the field in the impregnant in the parallel section. Figure 6 shows how moving to a much higher dielectric constant impregnant significantly reduces the electric field in the laminate margins. The use of such impregnants would be controlled by their thermal stability, chemical compatibility and ability to permit complete impregnation of the structure. Their role remains to be determined.

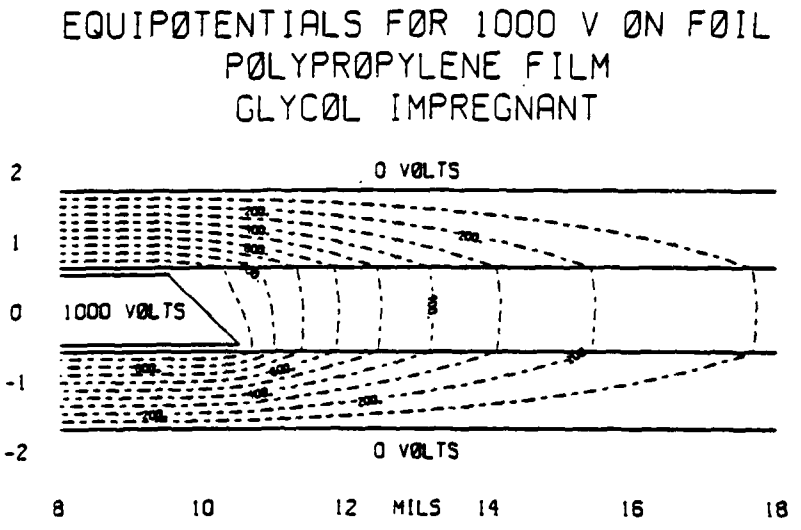

Figure 6. Electric field distributions in a glycol-impregnated laminate structure.

CHARGE INJECTION EFFECTS...

Calculations similar to those illustrated in Figure 1 were executed for the six foil edge shapes with two different corner radii and for six representative impregnants: fluorinert, transformer oil, MIPB, silicone oil, castor oil, and glycol. The Tables in Figures 7 and 8 show the bulk field in the polypropylene and energy density including foil mass but excluding margin container mass when the maximum impregnant field is equal to the assumed dielectric strength, D_s, indicated in the tables.

The bulk energy density, W, can be shown to be given by:

$$W = \frac{1/2\ \varepsilon_p E_p^2\ [t_p + \{\varepsilon_p/\varepsilon_I\}\ t_I]}{\rho_p\ t_p + \rho_I t_I + \rho_f t_f} \qquad (2)$$

where the subscripts refer to p - polypropylene, I - impregnant, and f - foil; ε is the permitivity; t the thickness; and E the field. The dielectric strength of certain impregnants is a strong function of thickness. For example, recent experiments utilizing fluorinert yield data consistent with around 11000 v/mil breakdown strength in impregnant thicknesses of less than 1 mil decreasing to 500 v/mil in 10 cm thickness. Standard dielectric strength tests with 1 inch spheres at 1 cm spacing are not applicable for thicknesses less than 1 mil. The data used for dielectric strengths is what was currently available.

Figure 7. Bulk insulating film field for various electrode edge shapes, liquid impregnant and impregnant breakdown field, Ds. Estimates of maximum laminate energy density are also tabulated.

SHAPE		RADIUS	FLUORINERT K = 1.89 D_s = 11000 V/mil PPL BULK FIELD V/mil	FLUORINERT ENERGY DENSITY J/kg	TRANSFORMER OIL K = 2.20 D_s = 1000 V/mil PPL BULK FIELD V/mil	TRANSFORMER OIL ENERGY DENSITY J/kg	MIPB K = 2.66 D_s = 400 V/mil PPL BULK FIELD V/mil	MIPB ENERGY DENSITY J/kg
	1	.01	1580.	14.0	159.9	.146	73.1	.030
		.05	2646.	39.2	267.9	.410	122.4	.083
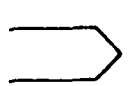	2	.01	1844.	19.1	177.7	.180	76.5	.032
		.05	3112.	54.3	299.9	.513	129.1	.092
	3	.01	1143.	7.3	113.2	.073	50.3	.014
		.05	2261.	28.7	224.2	.287	99.7	.055
	4	.01	1609.	14.5	163.0	.152	74.7	.031
		.05	2669.	39.9	270.5	.418	123.8	.085
	5	.01	1164.	7.6	121.8	.085	58.0	.019
		.05	N/A	N/A	N/A	N/A	N/A	N/A
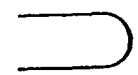	6		5297.	157.2	548.2	1.715	256.0	.362

SHAPE		RADIUS	SILICONE OIL K = 2.8 D_s = 350 V/mil		CASTOR OIL K = 3.7 D_s = 330 V/mil		GLYCOL K = 38. D_s = 500 V/mil	
			PPL BULK FIELD V/mil	ENERGY DENSITY J/kg	PPL BULK FIELD V/mil	ENERGY DENSITY J/kg	PPL BULK FIELD V/mil	ENERGY DENSITY J/kg
	1	.01	66.	.024	80.5	.034	528.1	1.29
		.05	111.	.067	134.5	.095	812.7	3.07
	2	.01	68.	.025	76.1	.030	302.1	.42
		.05	115.	.073	128.4	.087	509.4	1.20
	3	.01	45.	.011	52.7	.015	254.4	.30
		.05	90.	.044	104.0	.057	476.3	1.05
	4	.01	68.	.025	82.5	.036	554.3	1.43
		.05	112.	.069	136.4	.098	849.3	3.35
	5	.01	53.	.016	68.5	.025	529.7	1.30
		.05	N/A	N/A	N/A	N/A	N/A	N/A
	6		232.	.294	265.9	.372	1032.2	4.94

Figure 8. Bulk insulating film field for various electrode edge shapes, liquid impregnant and impregnant breakdown field, D_s. Estimates of maximum laminate energy density are also tabulated.

CHARGE INJECTION EFFECTS...

ENERGY DENSITY AND DIELECTRIC STRENGTH

From the results of Figures 7 and 8, the importance of a high dielectric strength for the impregnant is clearly evident. Even with the best impregnant and the rounded Shape 6, the ultimate dielectric strength of 9600 V/mil in polypropylene is not exceeded. Note also that differences between 0.01 and 0.05 mil radii of curvature on corners on the different shapes can affect the energy density by factors of 2.7 to 3.9. The folded foil, as was pointed out by Mandelcorn and Parker, has a substantial improvement in energy density over bare cut edges.

The energy densities in the Tables of Figures 7 and 8 are on the order of one hundred times greater for fluorinert than for the other impregnants because of the high dielectric strength assumed (11,000 V/mil).

Since effective dielectric strengths for other impregnants in thin sections may be substantially higher than bulk stengths, the effects of foil edges and dielectric constant were analyzed several other ways. In the Table in Figure 9 the field in the PPL film was taken to be 1000 V/mil, as used in many high-repetition-rate plastic-film liquid-impregnated capacitors.

MAXIMUM FIELD IN IMPREGNANT
V/mil
(for 1000 V/mil in PPL, K_{IMP} = 2.55)

SHAPE	K_{IMP} = 1.89	2.2	2.66	2.8	3.7	39.
1 .01	6961	6253	5471	5278	4345	947
.05	4157	3733	3267	3152	2602	615
2 .01	5965	5627	5230	5128	4599	1655
.05	3535	3334	3099	3038	2725	981
3 .01	9622	8835	7953	7732	6647	1965
.05	4864	4460	4013	3903	3365	1050
4 .01	6835	6133	5358	5167	4243	902
.05	4122	3697	3231	3117	2567	589
5 .01	9454	8210	6891	6574	5107	944
.05	N/A	N/A	N/A	N/A	N/A	N/A
6	2077	1824	1563	1509	1316	484

RADIUS MILS

Figure 9

CHARGE INJECTION EFFECTS...

Here in Figure 9 we see how the maximum field in the impregnant varies with the different shapes and with different dielectric constants. Several conclusions may be drawn. The highest field for a given dielectric constant occurs at the 45° angle of Shape 3. Shape 2 acts to reduce the maximum field from that of a square cut (Shape 1). The maximum field on Shape 2 occurs in the 90° corner in the center. The projection at the center of the foil edge in Shape 4 extending 0.1 mil at 45° and meeting in a 90° corner, serves to slightly shield the charge build-up on the two corners as the projection itself is shielded by the surrounding edge. Thus, the peak field, though still at the outside corners, is reduced from that of Shape 1 and the PPL energy density is slightly higher. The 45° projection at the lower corner in Shape 5 makes the maximum field higher than on 90° corner in Shape 1 but less than the 45° corner of Shape 3 where there are no nearby concave corners to shield the tip. As expected, Shape 6 allows the highest energy density.

ENHANCEMENT FACTORS AND MAXIMUM FIELDS

The Table in Figure 10 shows the enhancement factor, the ratio of maximum impregnant field to bulk impregnant field, for the various shapes.

For a given dielectric constant, this factor serves well to compare effects of foil edge shape; however, it gives a distorted view of effects of different dielectric constants relative to the plastic film since the higher dielectric constant tends to suppress the impregnant field more in the bulk than around the foil edge. As the impregnant dielectric constant is increased relative to that of the film, the field in the impregnant is suppressed. Thus, for a given dielectric stress, a higher impregnant dielectric constant will allow higher energy densities.

While maximum fields in the impregnant have been presented for two radii of curvature and for several specific dielectric constants, in examining the results for other radii and dielectric constants, the maximum field, E_{max}, for Shapes 1 to 5 could then be approximately expressed as a function

$$E_{max} = A \left[\frac{K_{imp}}{K_{film}} \right]^{-B} \cdot \left[\frac{r}{0.01} \right]^{-\alpha} \qquad (3)$$

ENHANCEMENT FACTOR

SHAPE	K_{imp} = 1.89	2.2	2.66	2.8	3.7	39.
1	.01	5.16	5.39	5.71	5.80	6.30	14.5
	.05	3.08	3.22	3.41	3.46	3.78	9.4
2	.01	4.42	4.85	5.46	5.63	6.67	25.3
	.05	2.62	2.88	3.23	3.34	3.95	15.0
3	.01	7.13	7.62	8.30	8.49	9.64	30.1
	.05	3.61	3.85	4.19	4.29	4.88	16.1
4	.01	5.07	5.29	5.59	5.67	6.16	13.8
	.05	3.06	3.19	3.37	3.42	3.72	9.0
5	.01	7.01	7.08	7.19	7.22	7.41	14.4
	.05	N/A	N/A	N/A	N/A	N/A	N/A
6		1.54	1.57	1.63	1.66	1.91	7.4

RADIUS MILS

Figure 10.

Here K_{imp}/K_{film} is the impregnant to film dielectric constant ratio and r is the radius of curvature in mils. The Table in Figure 11 gives values of A, B, and α for the five shapes. The fields on the 45° projection of Shapes 3 and 5 have a stronger inverse dependence on radius ($\alpha \approx 0.42$) than on the 90° projections of Shapes 1, 2, and 4 ($\alpha \approx 0.32$).

While a high permittivity impregnant will grade the field at a foil edge, such impregnants may not have other necessary characteristics. Glycol, for instance, does not wet or impregnate the capacitor well (refer to Figures 11 and 12).

Figure 11. Parameter Values for Equation 3

Shape	A (V/mil)	B	α
1	4682	0.623	0.32
2	4409	0.386	0.325
3	6773	0.488	0.424
4	4593	0.633	0.314
5	5986	0.728	0.431

WIRE GRADING

The effect of placing a conducting wire whose diameter equaled the foil thickness in the margin parallel to the edge was computed for Shapes 1 and 3 in fluorinert. The Table in Figure 12 gives the maximum field on the foil edge or wire as a function of distance from the edge of the center foil to wire edge. Note that it would be necessary to position the wire with a tolerance of a few tenths of a mil to insure limiting the maximum field.

The potential of the wire was held to the center foil potential of 1000 V in these calculations. If the wire is allowed to electrically float, the potential drops to a much lower value, increasing the field stress. A 1 mil diameter wire placed 0.25 mil from the edge of Shape 1 foil will have, then, a floating potential of 530 V and will allow a maximum field of 5851 V/mil, up from 3288 V/mil. Unfortunately, the wire cannot be held at the foil potential during a transient current flow since the current flows at right angles to the wire in the foil, and must be constrained to follow the wire to a connection to the foil.

It is concluded that wires are an impractical solution to field grading, both from position tolerance and from electrical connection aspects. While high dielectric constant impregnants will grade the field, no suitable material is known at present. Thus, folded foils are one of the best solutions presently available to minimize partial discharge activity in highly-stressed insulating laminate structures.

MAXIMUM FIELD WITH 1 MIL GUARD WIRE
RADIUS = 0.01

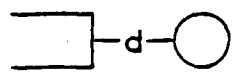

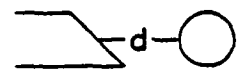

d(mils)	E_{max} (V/mil)	E_{max} (V/mil)
0.25	3288	----
0.5	3623	3074
0.75	3916	3659
1.0	4189	4238
1.25	4436	4801
1.5	4649	5311
2.5	5243	6775
0.0	5637	7792

Figure 12.

REFERENCES

1. W. G. Dunbar and J. W. Seabrook, "High Voltage Design Guide for Airborne Equipment," Air Force Aero Propulsion Laboratory Technical Report No. AFAPL-TR-76-41, June 1976 (NTIS Reference No. AD-A-29-268).

2. K. C. Kao and J. P. C. McMath, "Time-Dependent Pressure Effect in Liquid Dielectrics," IEEE Trans. on Elec. Insulation, Vol. EI-5, No. 3, September 1970.

3. F. Tse, W. Bell, M. Mulcahy and P. Bolin, "Liquid Insulation," High Voltage Technical Seminar, Ion Physics Corp., Boston, Massachusetts, September 1969.

4. E. Kuffell and M. Abdullah, "High Voltage Engineering," Pergamon Press, 1970.

5. J. C. Martin, "Comparison of Breakdown Voltages for Various Liquids Under One Set of Conditions," AWRE Report, 1965.

6. G. McDuff, K. Rust, W. J. Sarjeant and P. N. Mace, "Development of High Reliability, Multikilohertz Repetition-Rate Components," Proc. Fourteenth Pulse Power Modulator Symposium, Orlando, Florida, June 3-5, 1980, pp. 122-124.

7. G. H. Mauldin, "The Application of Perfluorocarbons as Impregnants for Plastic Film Capacitors," to be published in the Proc. of the NASA Symposium, Huntsville, Alabama, February 14, 1981.

8. "Development of a High Energy Density Capacitor for Plasma Thrusters," Air Force Rocket Propulsion Laboratory, Air Force Systems Command Technical Report AFRPL-TR-80-35, October 1980.

9. W. J. Sarjeant, "Energy Storage Capacitors," submitted for publication in the Proc. IEEE Plasma Science Pulse Power Course, Santa Fe, New Mexico, May 18-22, 1981.

10. Proceedings of the "Special Symposium on High-Energy-Density Capacitors and Dielectric Materials," at the 1980 Conference on Electrical Insulation and Dielectric Phenomena, Boston, Massachusetts, October 26-28, 1980, National Academy Press, Washington, DC.

11. T. E. Springer, W. J. Sarjeant, "Field Grading in Capacitor Margins," Proc. IEEE 3rd International Pulsed Power Conference, Albuquerque, New Mexico, June 1-3, 1981, to be published.

12. R. D. Parker, "Technological Development of High Energy Density Capacitors," NASA Lewis Research Center, Cleveland, Ohio, NASA CR12496, February 1976.

13. R. D. Parker, "Effect of Foil Edge Modifications and Configurations Charges on Energy Storage Capacitor Weight," IEEE Trans. on Parts, Hybrids, and Packaging, Vol. PHP-13, 3, September 1979.

14. L. Mandelcorn, T. W. Dakin, R. L. Miller and G. E. Mercier, "High Voltage Power Capacitor Dielectrics: Recent Developments," Proc. of the 14th Electrical/Electronics Conference, Boston, Massachusetts, October 9-11, 1979.

DEEP IMPURITY TRAPPING CONCEPTS FOR POWER SEMICONDUCTOR DEVICES

by Gale R. Sundberg
NASA Lewis Research Center, Cleveland, OH

ABSTRACT

High voltage semiconductor switches using deep impurity doped silicon now appear feasible for high voltage (1-100 kV), high power (>10 kW) switching and protection functions for future space power applications. Recent discoveries have demonstrated several practical ways of gating deep impurity doped silicon devices in planar configurations and of electrically controlling their characteristics, leading to a vast array of possible circuit applications. A new family of semiconductor switching devices and transducers are possible based on this technology. New deep impurity devices could be simpler than conventional p-n junction devices and yet use the same basic materials and processing techniques. In addition, multiple functions may be possible on a single device as well as increased ratings.

THIS PRESENTATION WILL DESCRIBE A NEW FAMILY OF SEMICONDUCTOR ELECTRONIC DEVICES USING DEEP IMPURITY TRAPPING CONCEPTS RATHER THAN CONVENTIONAL p-n JUNCTION EFFECTS.

DEEP IMPURITY TRAPPING CONCEPTS

FOR

POWER SEMICONDUCTOR DEVICES

WE WILL EXAMINE BRIEFLY THE DEVICE PHYSICS, LOOK AT A WIDE RANGE OF POTENTIAL APPLICATIONS AND DEMONSTRATE THE BENEFITS OF THIS TECHNOLOGY IN TERMS OF EXPANDED POWER RANGES, LOWER SIZE, WEIGHT AND COST, AND INTEGRATED CIRCUIT COMPATIBILITY. THIS WORK DEFINES A UNIQUE MATERIAL STUDY REPRESENTING A DEPARTURE FROM CONVENTIONAL JUNCTION SEMICONDUCTOR EFFECTS. ACTUALLY, WE ARE CAPITALIZING ON A PHENOMENON CAUSED BY DEEP IMPURITIES IN THE BAND GAP THAT THE JUNCTION PEOPLE SHY AWAY FROM. I REFER TO THESE DEVICES AS A FAMILY BECAUSE OF THE LARGE NUMBER OF DEVICES EMERGING FROM THE STUDY.

A NEW SEMICONDUCTOR FAMILY

DEVICE PHYSICS

- BULK EFFECTS
- DEEP ENERGY TRAPS
- VERSATILE, EFFICIENT GATING

POTENTIAL APPLICATIONS

- GATE CONTROLLED SWITCHING DEVICES
- VOLTAGE CONTROLLED OSCILLATORS
- SENSITIVE, MINIATURE TRANSDUCERS
- PULSE WIDTH MODULATORS
- MEMORY DEVICES IMMUNE TO RADIATION

BENEFITS

- INEXPENSIVE HOMOGENEOUS MATERIALS
- SIMPLE FABRICATION PROCESSES
- EXPANDED POWER RANGES
- INTEGRATED CIRCUIT COMPATIBILITY

IN UNDERSTANDING HOW DEEP IMPURITY DEVICES WORK, WE WILL BE LOOKING AT BULK EFFECTS IN SILICON (OR SOME OTHER SEMICONDUCTOR MATERIAL) RATHER THAN TYPICAL p-n JUNCTION CHARACTERISTICS. WE ARE INTERESTED IN WHAT HAPPENS IN SILICON DOPED WITH A DEEP IMPURITY SUCH AS GOLD BETWEEN CHARGE INJECTING ELECTRODES.

BY DEEP ENERGY LEVELS, WE ARE INVESTIGATING ADDING IMPURITIES TO SILICON THAT ADD ONE OR MORE ENERGY LEVELS AT OR VERY NEAR THE CENTER OF THE ENERGY BAND. THE CENTER LIES AT 0.55 ev FROM BOTH THE CONDUCTION AND VALENCE BANDS IN SILICON. WE USE SHALLOW IMPURITIES TO COMPENSATE THE MATERIAL (THAT IS, TO ADJUST THE FERMI LEVEL), BUT DO NOT FORM CONVENTIONAL p-n JUNCTIONS.

THREE TYPES OF GATING ARE POSSIBLE AND HAVE BEEN EXPLORED IN THIS WORK. SWITCHING CAN BE ACCOMPLISHED BY LIGHT GATING, INJECTION GATING (THE ADDITION OF AN INJECTION TYPE GATE IN THE SPACE BETWEEN ANODE AND CATHODE) OR MOS-VOLTAGE GATING (METAL-OXIDE-SEMICONDUCTOR GATE).

DEVICE PHYSICS

- BULK EFFECTS VS P-N JUNCTION EFFECTS

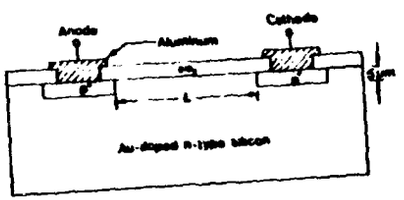

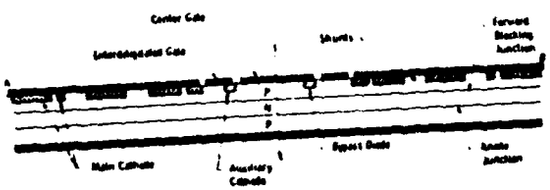

- DEEP ENERGY TRAPS VS SHALLOW IMPURITIES AND JUNCTIONS

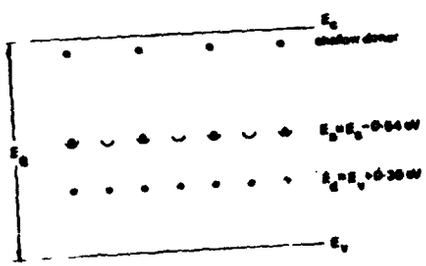

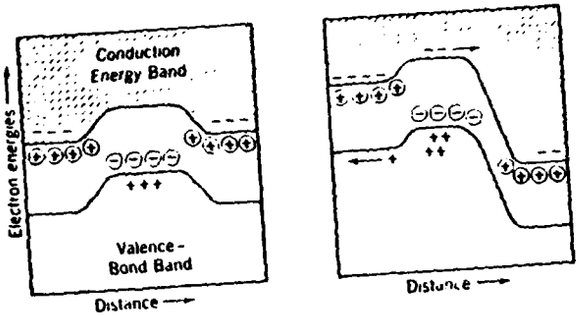

- VERSATILE, EFFICIENT GATING

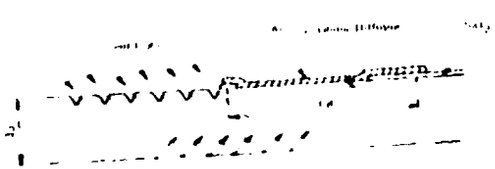

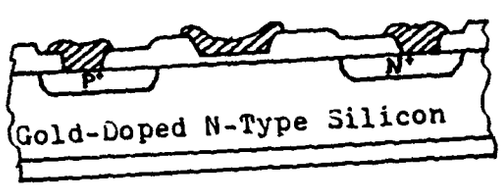

THIS CHART LISTS FIVE MAIN APPLICATIONS THAT HAVE MUCH INTEREST FOR FURTHER DEVELOPMENT. SWITCHING DEVICES AND TRANSDUCERS ARE THE AREAS IN WHICH MOST OF THE EFFORT TO DATE HAVE BEEN FOCUSED.

THE PRIMARY INTEREST NOW IS SWITCHING DEVICES WITH GATE CONTROLLED THRESHOLD VOLTAGES (LIMITED ONLY BY THE BREAKDOWN VOLTAGE OF SILICON), CONTROLLABLE HOLDING VOLTAGE GIVING EVIDENCE OF ZERO FORWARD VOLTAGE DROP, AND THYRISTOR-LIKE SWITCHING WITH BOTH TURNON AND TURNOFF CAPABILITY.

OF SECONDARY INTEREST HAS BEEN THE DEMONSTRATION OF SEVERAL VERY SENSITIVE, MINIATURE TRANSDUCERS. THE GAS FLOW METER IS A HOT WIRE ANEMOMETER TYPE, BUT ONLY 0.2 mm ON A SIDE, RESPONSE TIMES OF A SECOND AND MUCH GREATER SENSITIVITY THAN A p-n JUNCTION DEVICE. THE MULTIPLE INTERNAL REFLECTION EXTRINSIC INFRARED DETECTORS HAVE DEMONSTRATED QUANTUM EFFICIENCES GREATER THAN 34%, A FLAT DETECTIVITY CURVE OUT TO 160^{o}K AND MULTIPLE FREQUENCY RANGES USING SILICON-GERMANIUM ALLOYS.

THE CAPABILITY OF VOLTAGE CONTROLLED OSCILLATORS AND DETECTORS, VOLTAGE CONTROLLED PULSE WIDTH MODULATORS AND DELAY LINES, AND A TEMPERATURE TO FREQUENCY THERMOMETER ARE BASED ON PRE- AND POST-BREAKDOWN OSCILLATIONS IN DEVICES WITH CERTAIN DOPING CHARACTERISTICS. BECAUSE OF THE POSSIBILITY OF CHARGE STORAGE IN THE DEEP LEVELS, THERE HAS BEEN PREDICTED AN EXCITING

POSSIBILITY FOR VERY SMALL, VERTICALLY INTEGRATABLE MEMORY DEVICES HAVING AN EXCELLENT IMMUNITY TO RADIATION. HOWEVER, THIS HAS NOT YET BEEN DEMONSTRATED IN THE LABORATORY.

POTENTIAL APPLICATIONS

GATE CONTROLLED SWITCHING DEVICES

- THYRISTOR-LIKE SWITCHING
- ZERO VOLTAGE DROP DIODES
- LOGIC FUNCTIONS
- PWM CONTROLLERS
- DISCRIMINATORS
- OPTICAL SWITCHES

VOLTAGE CONTROLLED OSCILLATORS

- VOLTAGE TO FREQUENCY CONVERTER
- AM AND FM OSCILLATOR/DETECTORS

SENSITIVE, MINIATURE TRANSDUCERS

- GAS FLOW METERS
- MAGNETIC FIELD - HALL TYPE PROBE
- TEMPERATURE TO FREQUENCY THERMOMETER
- INFRA RED DETECTORS

PULSE WIDTH MODULATOR

- VOLTAGE CONTROLLED DELAY LINE
- VOLTAGE CONTROLLED PULSE WIDTH

MEMORY DEVICES IMMUNE TO RADIATION

- CHARGE STORAGE IN DEEP LEVELS
- SMALL SIZE, VERTICALLY INTEGRATEABLE

THE PRIMARY BENEFITS SUMMARIZED ON THIS CHART ARE THE POSSIBILITY OF VERY HIGH SWITCHING VOLTAGES IN THE TENS OF KILOVOLTS AND POSSIBLE POWER SWITCHING AT MEGAWATT LEVELS. THE FEASIBILITY OF VERY LOW OR ZERO FORWARD VOLTAGE DROP WITH VERY LOW ON STATE POWER REQUIREMENTS COULD GIVE EXTREMELY GOOD EFFICIENCY FOR THE HIGH POWER SWITCHING. IC COMPATIBILITY OF THE DEVICES USING CONVENTIONAL MATERIALS, PLANAR TOPOLOGIES AND CONVENTIONAL SEMICONDUCTOR PROCESSING TECHNOLOGIES GIVES THE VERY REAL POSSIBILITY OF LOW COST AND STRAIGHTFORWARD TRANSFER OF THE TECHNOLOGY FROM A UNIVERSITY LABORATORY TO INDUSTRY.

BENEFITS

INEXPENSIVE HOMOGENEOUS MATERIALS

- SILICON, GERMANIUM, GALLIUM-ARSENIDE
- CONVENTIONAL DOPANTS
- ALUMINUM OR OTHER METALLIZATIONS

SIMPLE FABRICATION PROCESSES

- CONVENTIONAL SEMICONDUCTOR TECHNOLOGY
- PLANAR SURFACE TOPOLOGIES

EXPANDED POWER RANGES

- UP TO 50 KILOVOLTS
- POSSIBLE MEGAWATT POWER SWITCHING

INTEGRATED CIRCUIT COMPATIBILITY

- PLANAR TOPOLOGY
- MICROCIRCUIT SIZE
- USES LSI, VLSI TYPE PROCESSES

ON THE LEFT PORTION OF THIS FIGURE IS SHOWN THE BAND GAP OF INTRINSIC SILICON WHERE E_C REPRESENTS THE CONDUCTION BAND EDGE, E_V IS THE VALENCE BAND EDGE, AND THE DOTTED LINE THE FERMI LEVEL. SHOWN NEAR E_C ARE FOUR TYPICAL SHALLOW DONORS THAT GIVE n-TYPE SILICON. NEAR E_V ARE SEVERAL SHALLOW ACCEPTORS THAT YIELD p-TYPE SILICON. ALSO SHOWN IN THE MID-GAP ARE DEEP IMPURITY ACCEPTORS DUE TO GOLD AND ZINC, WHICH HAVE BEEN STUDIED MOST EXTENSIVELY. THE FIRST LABORATORY DEMONSTRATION OF THE TRAPS-FILLED-LIMIT BEHAVIOR AT LIQUID NITROGEN TEMPERATURE WAS MADE USING A NEUTRON INDUCED 'A' CENTER AT 0.17 ev FROM E_C. THALLIUM AT 0.26 ev FROM E_V WAS ALSO EXAMINED AS A POSSIBLE CANDIDATE.

THE TWO ENERGY LEVEL DIAGRAMS TO THE RIGHT SHOW THE EFFECT OF DOUBLE DOPING OR ADDING AN n-TYPE IMPURITY OR A p-TYPE IMPURITY TO MOVE THE FERMI LEVEL TO ONE OF THE DEEP TRAP LEVELS. THIS COMPENSATES THE TRAP IN SUCH A MANNER THAT IT WILL ACCEPT AND HOLD AN ELECTRON OR A HOLE AND EMPTY ONLY WHEN GATED OR DUE TO HIGH INDUCED FIELDS RATHER THAN THERMALLY.

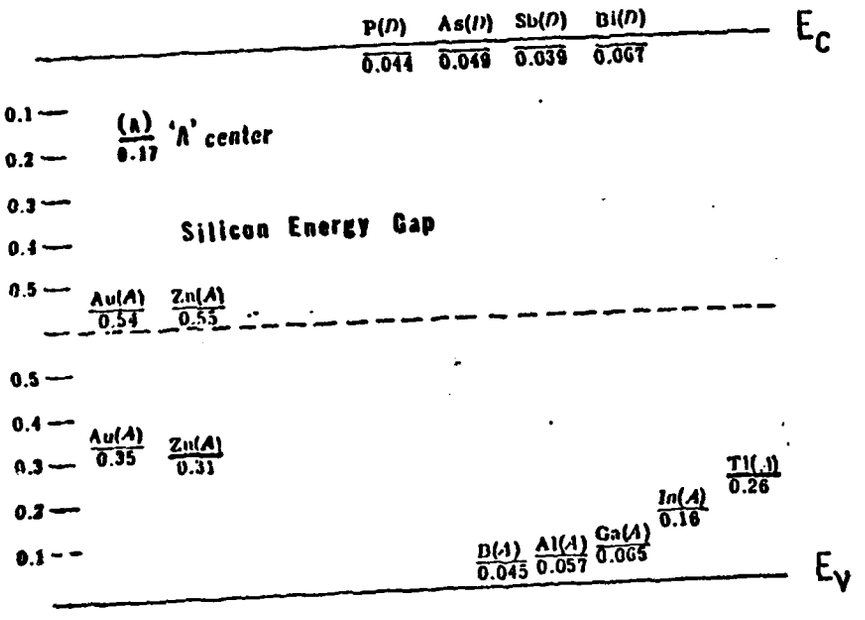

IMPURITY ENERGY LEVELS IN SILICON

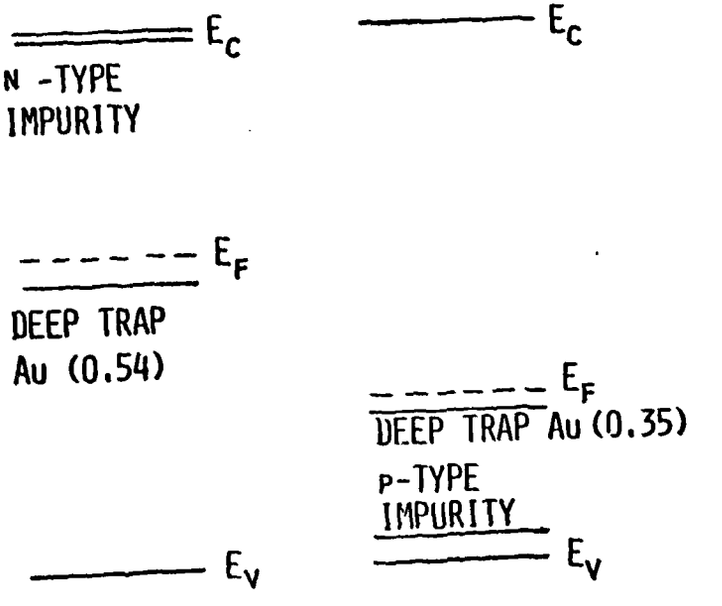

MODIFICATION OF FERMI LEVEL IN DOPED SILICON (WITH DEEP TRAPS)

THE UPPER PART OF THIS FIGURE SHOWS A CROSS-SECTION OF A DOUBLE INJECTION, DEEP IMPURITY DEVICE. THE BULK MATERIAL IS GOLD DOPED SILICON COMPENSATED BY A SHALLOW DONOR SUCH AS PHOSPHORUS. THE ENERGY LEVEL DIAGRAM IS SHOWN BELOW AS A REMINDER. THE GOLD ACCEPTOR LEVEL AT 0.54 ev IS THE LEVEL ACTIVATED AND PREDOMINATES IN THE DEVICE BEHAVIOR.

ALSO SHOWN IN THE UPPER PORTION ARE THE ANODE AND CATHODE FORMED BY DIFFUSING p+ AND n+ REGIONS INTO THE BULK MATERIAL. THESE REGIONS PROVIDE EFFICIENT OHMIC CONTACTS AND THE APPROPRIATE BAND BENDING AT THE SURFACE TO PROMOTE HIGH LEVEL INJECTION OF HOLES AND ELECTRONS. THUS, THIS IS CALLED A DOUBLE INJECTION DEVICE. IF ONLY AN n+ REGION WERE PRODUCED THEN THE DEVICE WOULD BE A SINGLE INJECTION DEVICE WITH CHARACTERISTICS FOLLOWING MURRAY LAMPERT'S TRAPS-FILLED-LIMIT BEHAVIOR AS SHOWN IN THE NEXT FIGURE.

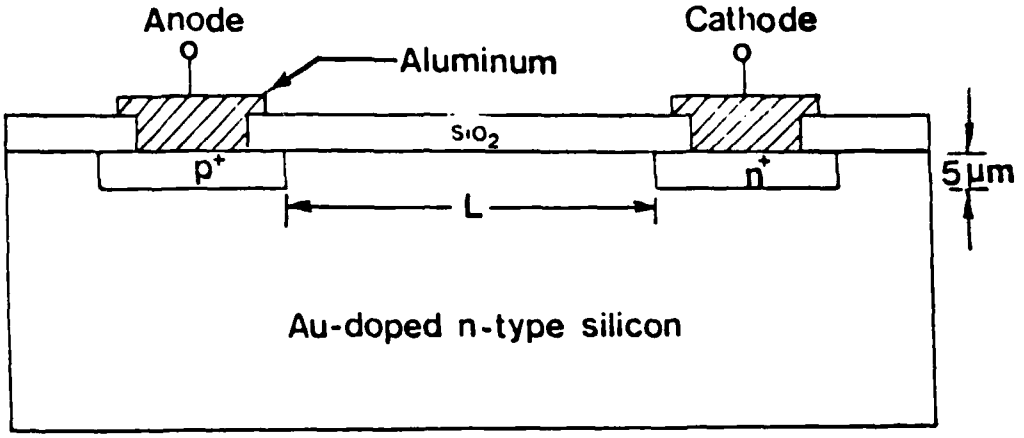
Anode
Aluminum
Cathode
SiO_2
p^+
n^+
5 μm
L
Au-doped n-type silicon

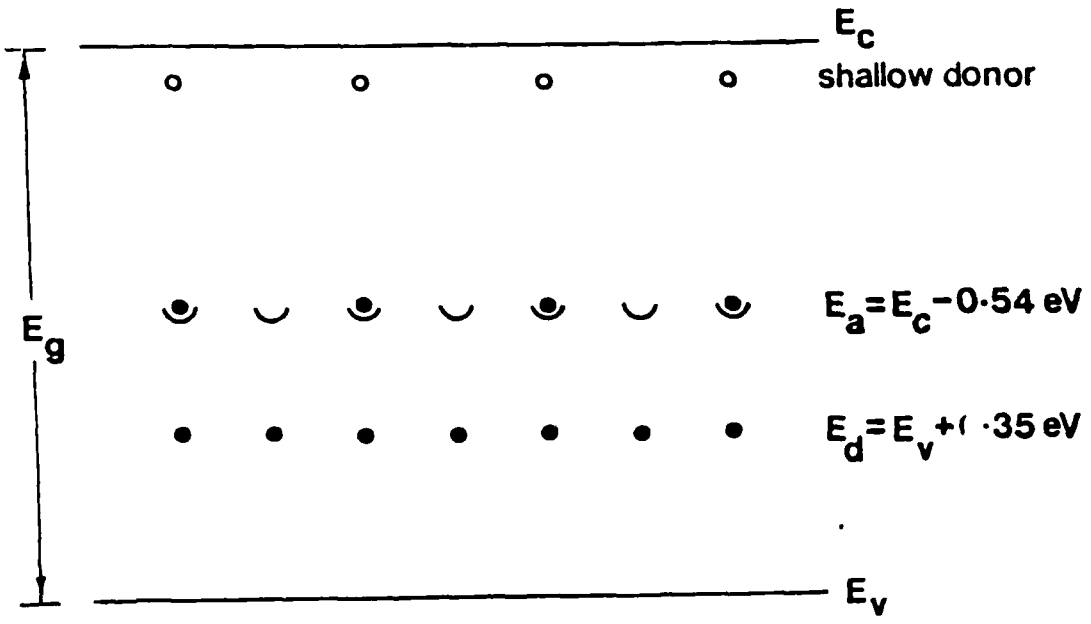
E_c
shallow donor
E_g
$E_a = E_c - 0.54$ eV
$E_d = E_v +$ (·35 eV
E_v

ON THE LEFT WE HAVE A LOG-LOG PLOT OF A NEUTRON IRRADIATED SILICON DIODE WITH A SINGLE INJECTING ELECTRODE. AS VOLTAGE WAS INCREASED ACROSS THE DIODE, CURRENT INCREASED FOLLOWING AN OHM'S LAW DEPENDENCE OUT TO ABOUT 100 VOLTS WHERE IT SUDDENLY JUMPED 4 TO 5 ORDERS OF MAGNITUDE UP TO POINT B WHERE IT FOLLOWS A TYPICAL SQUARE LAW BEHAVIOR. THIS JUMP WAS FIRST DESCRIBED IN THEORY BY LAMPERT WHO CALLED IT THE TRAPS-FILLED-LIMIT AND IS DESIGNATED V_{TFL}. TO THE RIGHT IS A TYPICAL OSCILLOSCOPE TRACE OF THE BREAKDOWN PHENOMENON. IN PRINCIPLE, IT LOOKS VERY MUCH LIKE A ZENER DIODE WITH A VERY SHARP KNEE.

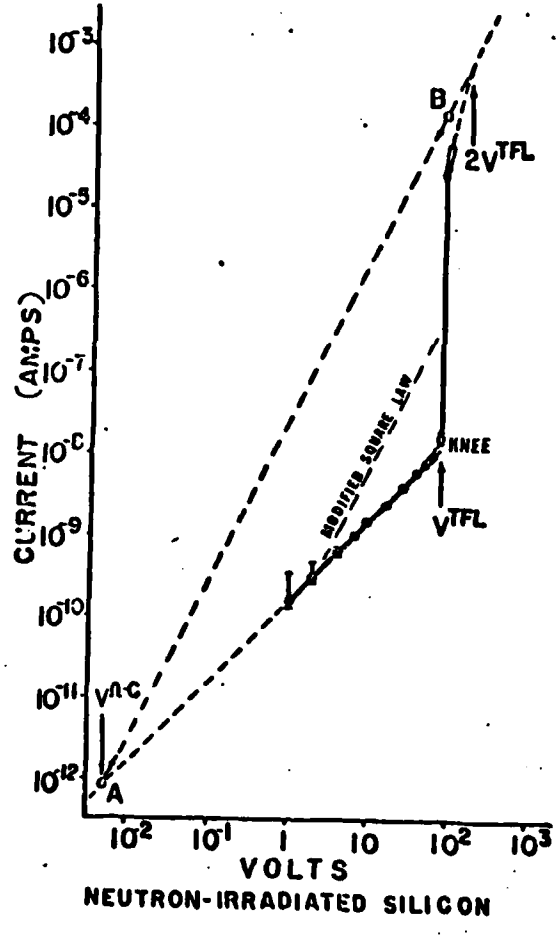

LOG-LOG PLOT OF TFL DIODE

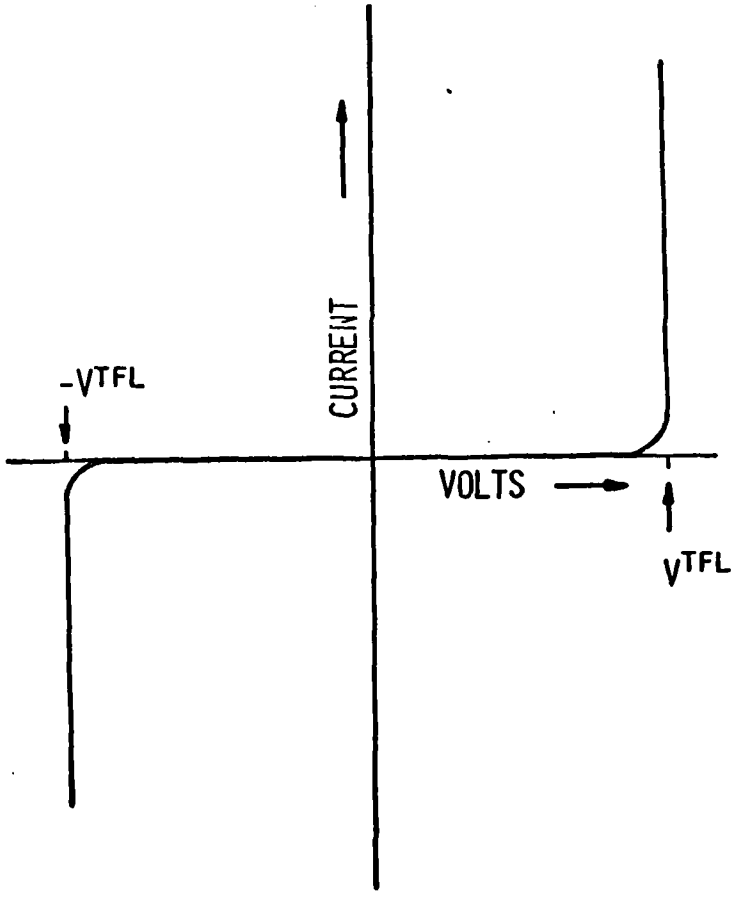

LINEAR CURVE-TRACER PLOT

THIS FIGURE SHOWS THE SWITCHING CHARACTERISTICS OF A DOUBLE INJECTION DIODE USING GOLD DOPED n-TYPE SILICON. ON THE LOG-LOG PLOT OF CURRENT VS. VOLTAGE TO THE LEFT IS THE TYPICAL SWITCHING CHARACTERISTICS, THE S-TYPE CURVE CHARACTERISTIC OF A THYRISTOR. THE VARIOUS REGIONS OF THE DISCHARGE ARE LABELED. V_o INDICATES THE TRANSITION VOLTAGE WHERE THE DIODE MOVES FROM OHM'S LAW TO A SPACE-CHARGE-LIMITED SQUARE LAW BEHAVIOR UNTIL IT REACHES A THRESHOLD VOLTAGE, V_{TH}, WHERE IT BREAKS DOWN INTO A HIGH CURRENT CONDUCTION REGION. V_M INDICATES THE HOLDING VOLTAGE SOMETIMES REFERRED TO AS THE FORWARD VOLTAGE DROP. IN MANY OF THE EARLY DEVICES, V_M WAS OF THE ORDER OF 10% OF V_{TH}. HOWEVER, IMPROVEMENTS ARE BEING MADE IN THIS RATIO.

ON THE RIGHT IS SHOWN A DRAWING OF THE DOUBLE INJECTION SWITCHING CURVE AS IT WOULD APPEAR ON AN OSCILLOSCOPE.

DOUBLE INJECTION CHARACTERISTICS

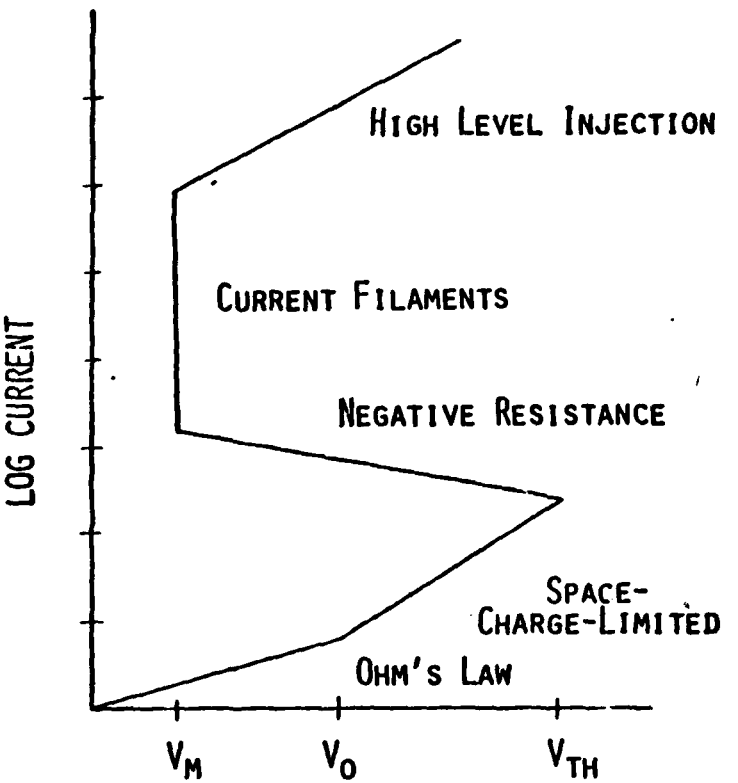

LOG-LOG PLOT OF CURRENT-VOLTAGE

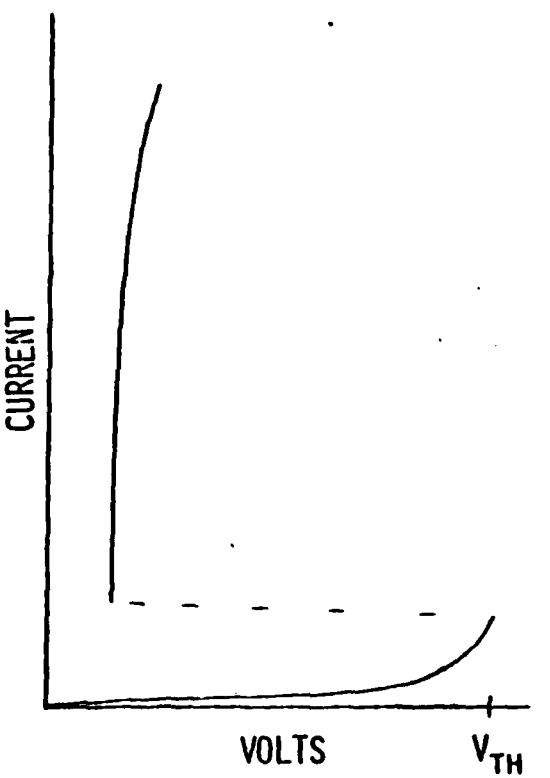

LINEAR CURRENT-VOLTAGE CURVE

IN THE UPPER PORTION OF THIS FIGURE IS SHOWN A DOUBLE INJECTION, GOLD DOPED, n-TYPE SILICON DIODE WITH TWO GATES ADDED. WE REFER TO THEM AS MOS (METAL OXIDE SEMICONDUCTOR) VOLTAGE GATES. APPLYING A POSITIVE VOLTAGE TO THE CATHODE GATE (OR NEGATIVE TO THE ANODE GATE) DECREASES THE THRESHOLD VOLTAGE FROM V_{TH} TO V_{TH}" OR IT MAY TURN THE DIODE OFF FROM A CONDUCTING STATE. WE HAVE DEMONSTRATED THAT THE CATHODE GATE IS MORE EFFECTIVE IN CONTROLLING THE SWITCHING BEHAVIOR. THEREFORE, IN PRACTICE, BOTH GATES HAVE BEEN REPLACED BY ONE GATE LOCATED NEAR THE CENTER OF THE CHANNEL, BUT CLOSER TO THE CATHODE. AS THE GATE VOLTAGE IS INCREASED POSITIVELY, V_{TH} DECREASES AND VICE VERSA. THE HOLDING VOLTAGE IS NOT MUCH AFFECTED BY THE GATE VOLTAGES.

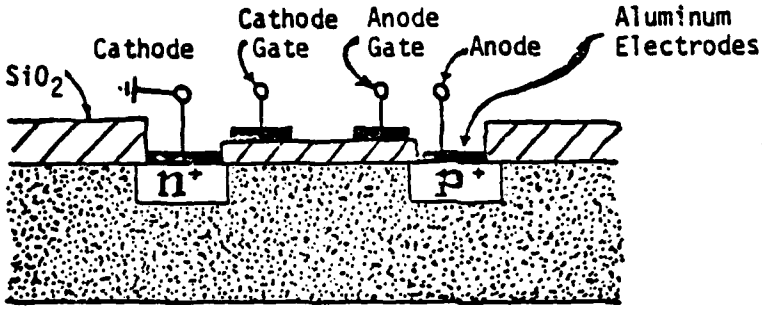

N -TYPE, GOLD-DOPED SILICON SUBSTRATE

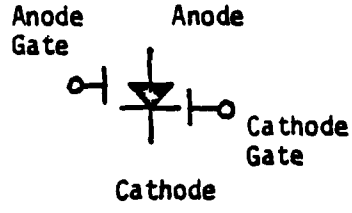

PROPOSED DEVICE SYMBOL

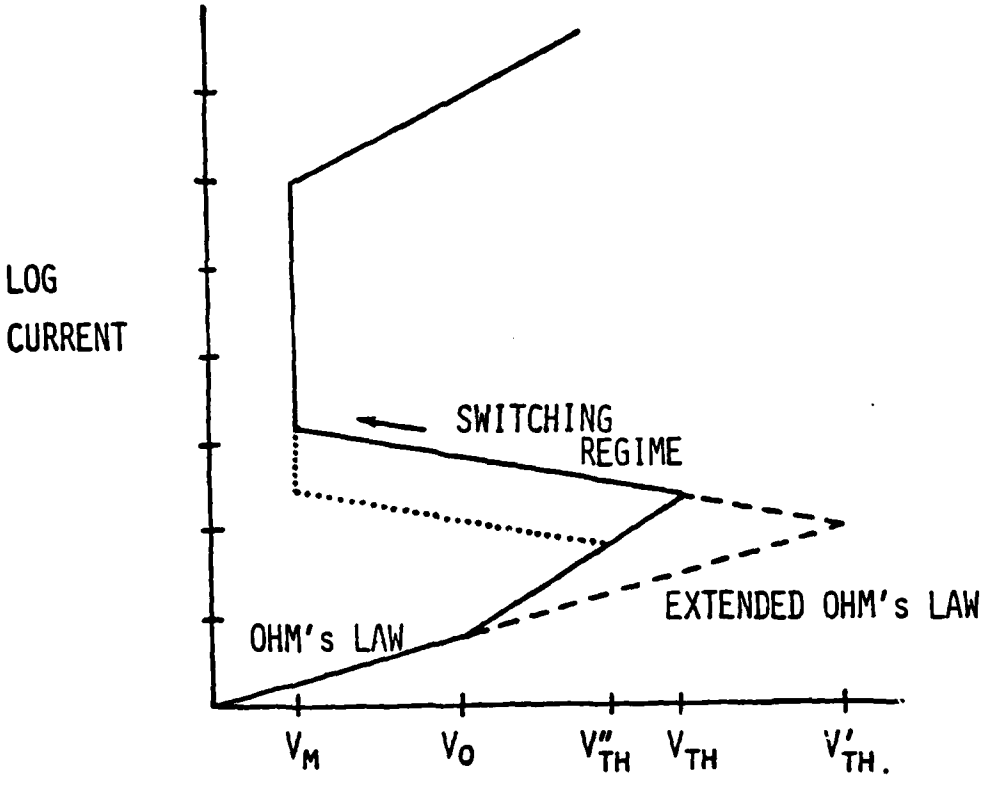

VOLT-AMPERE CHARACTERISTIC SHOWING VOLTAGE GATING

THIS FIGURE SHOWS A TOP VIEW AND A CROSS-SECTION OF A GOLD DOPED, COMPENSATED SILICON DEVICE WITH AN INJECTION GATE LOCATED IN THE CHANNEL BETWEEN ANODE AND CATHODE. THIS DRAWING SHOWS A p+ INJECTION GATE WHICH HAS BEEN USED FOR MOST OF THE EXPERIMENTAL WORK TO DATE. HOWEVER, SOME SIMILAR EFFECTS HAVE BEEN SHOWN RECENTLY WITH AN n+ INJECTION GATE. WITH THE p+ GATE, A POSITIVE GATE TO CATHODE VOLTAGE USUALLY GIVES AN N-TYPE CURVE OF BREAKDOWN LEADING TO OSCILLATORY BEHAVIOR. BUT, A NEGATIVE GATE TO CATHODE VOLTAGE ACTS TO DECREASE THE HOLDING VOLTAGE.

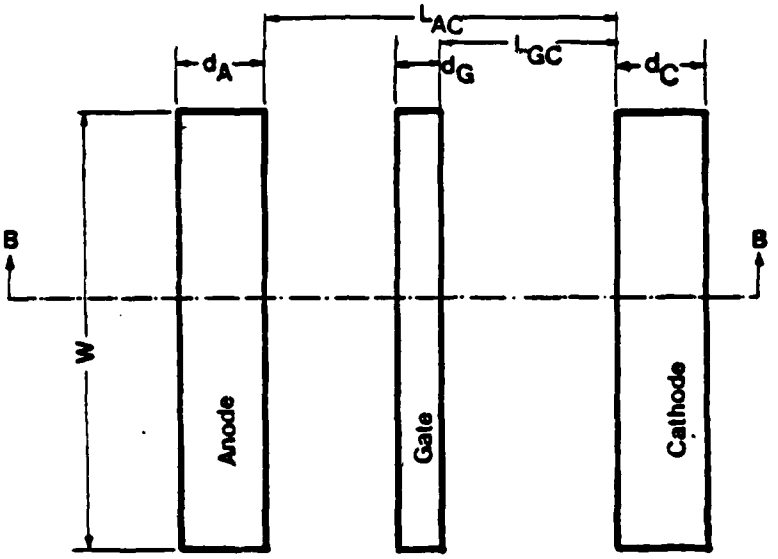
L_{AC}
L_{GC}
d_A
d_G
d_C
B
B
W
Anode
Gate
Cathode

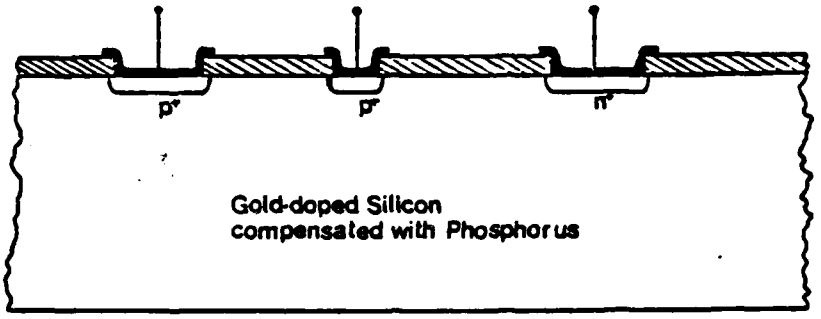
p+
p+
n+
Gold-doped Silicon
compensated with Phosphorus

Section B-B

HERE ARE SHOWN TWO OSCILLOSCOPE PICTURES OF THE SWITCHING CHARACTERISTICS OF THE INJECTION GATED DEVICE. BOTH PICTURES SHOW CURRENT ON A SCALE OF 10 mA PER DIVISION VS. VOLTAGE AT 20V PER DIVISION. THE TOP PICTURE SHOWS A THRESHOLD VOLTAGE OF ABOUT 155 VOLTS AND A HOLDING VOLTAGE OF 16 TO 20 VOLTS DEPENDING ON THE CURRENT LEVEL. THE GATE VOLTAGE IS ZERO FOR THIS PICTURE. THE REMARKABLE RESULT OF AN INJECTION GATE IS SHOWN IN THE SUPERPOSITION OF SEVERAL TRACES IN THE LOWER PICTURE. AS THE GATE TO CATHODE VOLTAGE IS MADE MORE NEGATIVE IN -4 VOLT INCREMENTS, THE HOLDING VOLTAGE IS DECREASED. IN FACT, WITH V_{GC} = -16 VOLTS, THE HOLDING VOLTAGE IS AT OR NEAR ZERO. THIS PRESENTS THE VERY EXCITING POSSIBILITY OF A DEVICE WITH ZERO FORWARD VOLTAGE DROP LEADING TO A VERY ENERGY EFFICIENT SWITCH. OBVIOUSLY, THERE IS SOME POWER LOSS IN THE GATE, BUT EXPERIMENTAL DATA HAS SHOWN THESE LOSSES TO BE LESS THAN 10% OF THE PRIMARY CONDUCTION LOSSES. ADDITIONAL EFFORTS IN PROCESSING OF THE BULK SILICON HAVE REDUCED V_H BY A FACTOR OF 4 OR 5 ALSO.

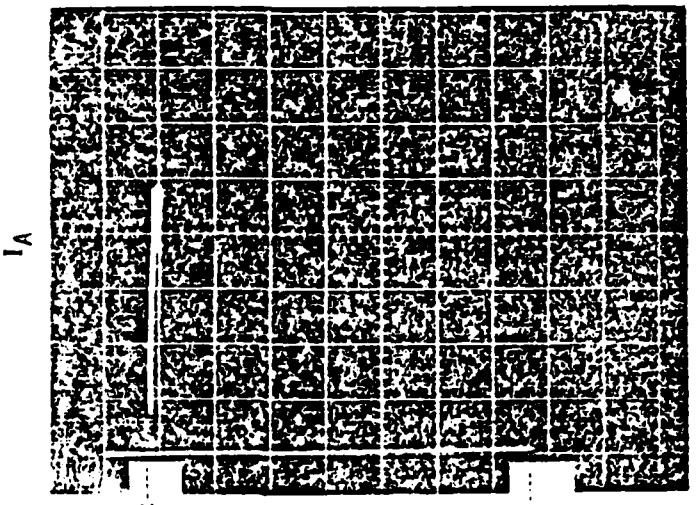

(a)

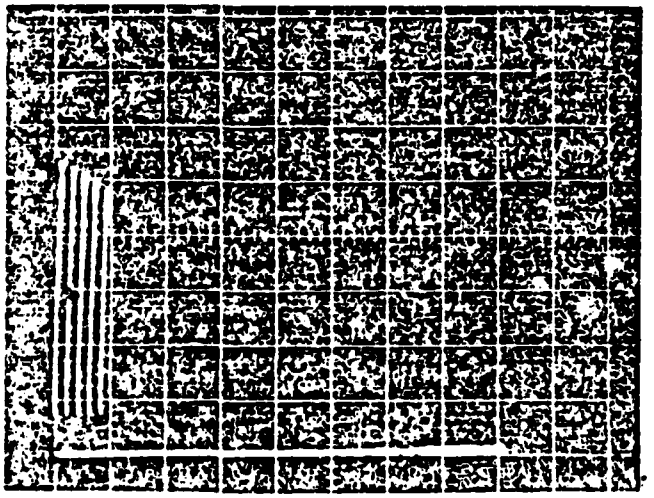

(b)

NOW KEEPING IN MIND THE BASIC PHYSICS OF THE DEEP IMPURITY DEVICE AND ITS SWITCHING CAPABILITIES WITH THE ABILITY TO VARY BOTH THE THRESHOLD AND HOLDING VOLTAGES, WE WANT TO LOOK AT THE VOLTAGE LIMITATIONS IN SILICON. ON THIS GRAPH, I HAVE PLOTTED THRESHOLD VOLTAGE AS A FUNCTION OF LENGTH IN OR ACROSS A SLAB OF SILICON. THE BREAKDOWN LIMIT IS SHOWN AS A LINEAR FUNCTION OF LENGTH IN BULK SILICON. THE CALCULATED CURVE FOR p-n JUNCTION DEVICES IS QUITE CONSERVATIVE IN THAT IT CALCULATES THE BREAKDOWN LIMIT ACROSS THE DEPLETION REGION ASSUMING ONE SIDE OF THE JUNCTION TO BE VERY LIGHTLY DOPED. THIS GIVES AN UPPER LIMIT IN THE REGION AROUND 10,000 VOLTS. DEEP IMPURITY DEVICES ALSO HAVE A SQUARE LAW BREAKDOWN THRESHOLD, BUT A SMALLER COEFFICIENT. THE CALCULATED CURVE FOR THE DEEP IMPURITY MATERIAL LIES TO THE RIGHT OF THE p-n JUNCTION CURVE AND SHOWS A FACTOR OF 10 OR MORE HIGHER BREAKDOWN LIMIT. NEGLECTING SURFACE EFFECTS AND MATERIAL DEFECTS, THERE APPEARS TO BE A VERY REAL POSSIBILITY OF DEVICES WITH THRESHOLD VOLTAGES IN THE 10 TO 100 KILOVOLT REGION. RECENT EXPERIMENTAL DATA CONFIRMS THE CURVE UP TO 800 VOLTS.

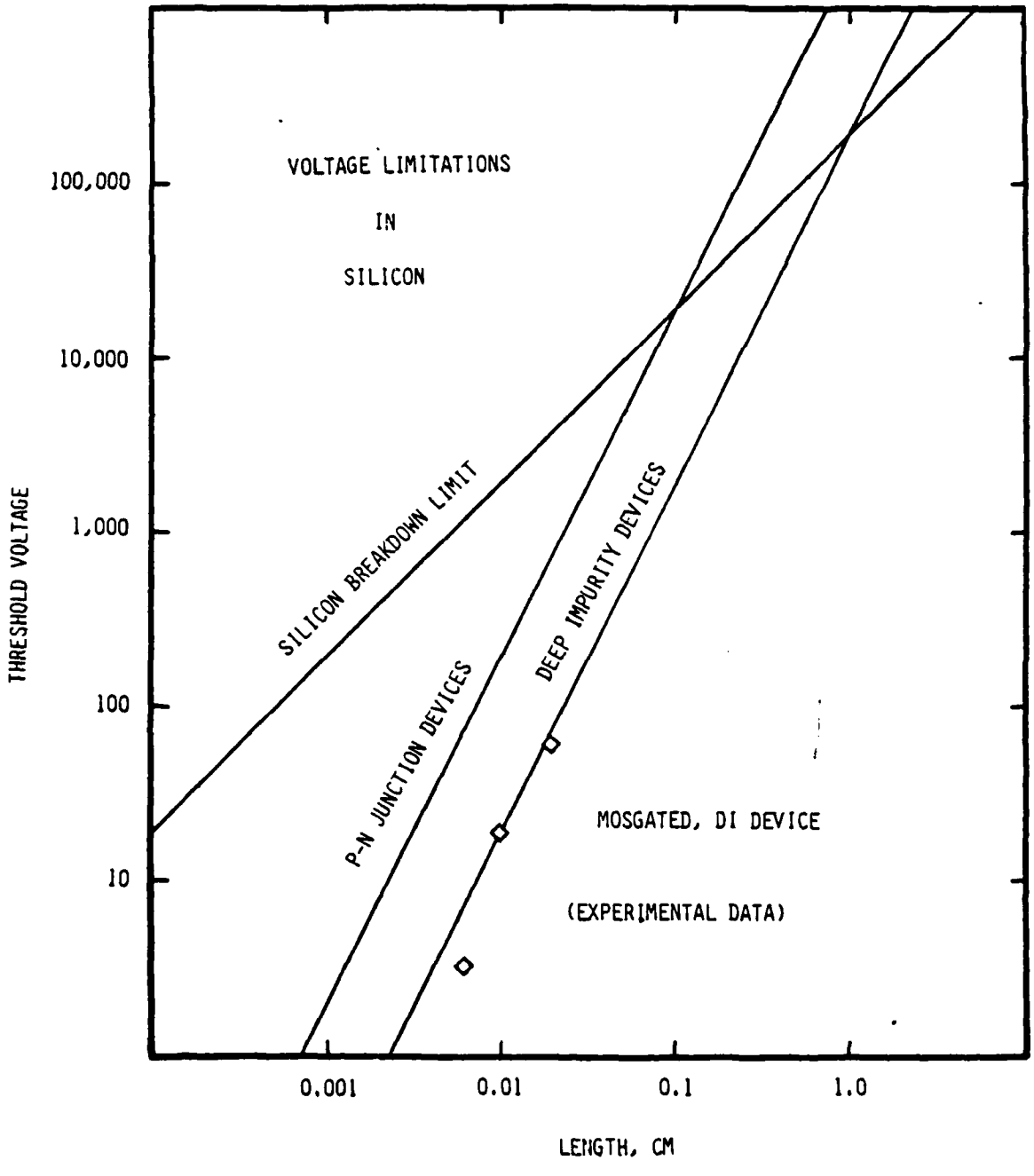
VOLTAGE LIMITATIONS
IN
SILICON
100,000
10,000
1,000
100
10
THRESHOLD VOLTAGE
SILICON BREAKDOWN LIMIT
P-N JUNCTION DEVICES
DEEP IMPURITY DEVICES
MOSGATED, DI DEVICE
(EXPERIMENTAL DATA)
0.001
0.01
0.1
1.0
LENGTH, CM

WITH THE POSSIBILITY OF THRESHOLD VOLTAGES EXTENDING BEYOND 10 KILOVOLTS AND CURRENT CAPABILITY DIRECTLY PROPORTIONAL TO ELECTRODE AREA, A MULTITUDE OF NEW APPLICATIONS ARE POSSIBLE FOR SEMICONDUCTOR DEVICES. WITH CONTROLLABLE THRESHOLD VOLTAGES, ZERO FORWARD VOLTAGE DROP, AND LOW STANDBY POWER, DEEP IMPURITY DEVICES BECOME VERY ATTRACTIVE SWITCHING CANDIDATES FOR FUTURE HIGH ENERGY SPACE AND AERONAUTICAL POWER SYSTEMS. CIRCUIT BREAKERS, SWITCHING AND PROTECTION DEVICES AND INVERTERS FOR THE PRIME POWER SYSTEM ARE SOME POTENTIAL APPLICATIONS. POWER SWITCHING AND CIRCUIT PROTECTION SWITCHES FOR HIGH POWER TRAVELING WAVE TUBES, BEAM WEAPONS AND RADARS ALSO APPEAR FEASIBLE.

SWITCHING APPLICATIONS OF DEEP IMPURITY DEVICES

SPACE

- REMOTE POWER CONTROLLERS AND CIRCUIT BREAKERS
- TRAVELING WAVE TUBES
- HIGH INTENSITY LASERS, BEAM WEAPONS
- HIGH VOLTAGE INVERTERS

AERONAUTICS

- REMOTE POWER CONTROLLERS AND CIRCUIT BREAKERS
- CROSS-STRAPPING OF GENERATORS
- RADAR

IN THE APPLICATION AS A POWER CONTROLLER OR CIRCUIT BREAKER, A DEEP IMPURITY SWITCH COULD COMBINE THE ADVANTAGES OF ALL SOLID STATE SWITCHING WITH ZERO VOLTAGE DROP, LOW STANDBY POWER, SMALL SIZE AND HIGH VOLTAGE LIMITS. THE BASIC DISADVANTAGES OF ONE TO TWO KILOVOLT VOLTAGE LIMITS AND HIGH FORWARD VOLTAGE OF CONVENTIONAL SOLID STATE DEVICES AND THE ONE TO TWO KILOVOLT VOLTAGE LIMITATION--SLOW RESPONSE, LARGE SIZE AND WEIGHT OF AN ELECTRO-MECHANICAL/SOLID STATE CIRCUIT BREAKER--CAN BE ELIMINATED. THE ONLY BASIC LIMITATION AT THIS POINT IN TIME IS THE LACK OF TECHNOLOGY DEVELOPMENT.

DEEP IMPURITY POWER CONTROLLER

ADVANTAGES

- ALL SOLID STATE, CONTACT-LESS SWITCHING
- HIGH VOLTAGE
- ZERO FORWARD VOLTAGE
- LATCHING TYPE, LOW STANDBY POWER
- LIGHTWEIGHT
- SMALL IN SIZE

LIMITATIONS

- TECHNOLOGY NEEDS TO BE DEVELOPED

UP TO THIS POINT, I HAVE FOCUSED MAINLY ON SWITCHING APPLICATIONS FOR DEEP IMPURITY DEVICES. HOWEVER, AS NOTED AT THE BEGINNING OF THIS PRESENTATION, THEY HAVE MANY OTHER POSSIBLE APPLICATIONS. ON THIS FIGURE ARE SHOWN OTHER TRANSDUCERS AND DETECTORS THAT HAVE OR CAN BE DEVELOPED USING DEEP IMPURITY EFFECTS. THESE DEVICES ARE ALL USING SILICON OR SILICON/GERMANIUM ALLOY IN THE IR DETECTORS. WE ARE STARTING TO EXPLORE GaAs AS A BULK MATERIAL SINCE IT HAS PROPERTIES THAT COULD LEAD TO BOTH INCREASED THRESHOLD VOLTAGES AND FASTER SWITCHING SPEEDS.

THE IR DETECTOR HAS SEVERAL INTERESTING PROPERTIES AS SHOWN WITH A DETECTIVITY CURVE THAT IS FLAT OUT BEYOND 160^{o}K. WE BELIEVE THIS CAN BE PUSHED EVEN NEARER TO ROOM TEMPERATURE. THE GAS FLOW TRANSDUCER HAS MANY MEDICAL APPLICATIONS. OTHER APPLICATIONS CONSIDERED ARE: MAPPING AIR FLOW AROUND A HIGH ENERGY LASER, AIR FLOW THROUGH A RADIATOR OF LARGE EARTH MOVING EQUIPMENT, AND WITH MODIFICATIONS GAS FLOW IN A CARBURETOR.

SPINOFFS OF DEEP IMPURITY RESEARCH

- MULTIPLE INTERNAL REFLECTION IR DETECTOR
  - -- OPERATION NEAR ROOM TEMPERATURE
  - -- MULTIPLE FREQUENCY RANGES/MATRIX ARRAY
  - -- SMALL AREA (0.004 cm^2)
  - -- INCREASED SENSITIVITY QUANTUM EFFICIENCIES TO 34%
- INTEGRATED SILICON GAS FLOW TRANSDUCER
  - -- EXTREMELY SMALL (LESS THAN 0.2 mm)
  - -- FAST RESPONSE (ORDER OF 1 SECOND)
  - -- MEASURES VELOCITY
  - -- SENSITIVITY (1000 TIMES BETTER THAN p-n JUNCTION)
- POST BREAKDOWN OSCILLATORS
  - -- VOLTAGE CONTROLLED OSCILLATOR
  - -- THERMOMETER/TEMPERATURE TO FREQUENCY TRANSDUCER
  - -- PULSE WIDTH MODULATOR
  - -- VOLTAGE CONTROLLED DELAY OR PHASE SHIFTER
- OTHER UNIQUE DEVICES
  - -- MAGNETIC FIELD MEASUREMENT/HALL EFFECT
  - -- MEMORY IMMUNE TO RADIATION EFFECTS

IN SUMMARY, A NEW FAMILY OF DEEP IMPURITY SEMICONDUCTORS HAS BEEN DESCRIBED THAT HAS OUTSTANDING POTENTIAL FOR FUTURE NASA AND MILITARY APPLICATIONS IN HIGH ENERGY SPACE AND AERONAUTICAL ELECTRICAL SYSTEMS WHERE SMALL SIZE, HIGH VOLTAGE AND LOW FORWARD VOLTAGE DROPS WOULD BE PRIMARY ADVANTAGES. WITH THESE NEW SEMICONDUCTORS, SWITCHING APPLICATIONS APPEAR POSSIBLE AT VOLTAGE AND POWER LEVELS IMPOSSIBLE WITH CONVENTIONAL SEMICONDUCTORS. IN ADDITION, THESE DEVICES HAVE A MULTITUDE OF OTHER APPLICATIONS AS DETECTORS, TRANSDUCERS, AND OSCILLATORS THAT APPEAR TO GIVE SIGNIFICANT IMPROVEMENTS OVER CONVENTIONAL DEVICES AVAILABLE TODAY.

A NEW FAMILY
OF
DEEP IMPURITY SEMICONDUCTORS

MAJOR TECHNOLOGY PROGRAM THRUSTS

- HIGH VOLTAGE DEVICES
  - -- SPACE AND AERONAUTICAL
  - -- NASA AND MILITARY
  - -- CANNOT BE DONE WITH CONVENTIONAL SEMICONDUCTORS
- ZERO VOLTAGE DROP DEVICES
  - -- SPACE AND AERONAUTICAL
  - -- NASA AND MILITARY
  - -- CANNOT BE DONE WITH CONVENTIONAL SEMICONDUCTORS
- OTHER SPINOFF APPLICATIONS
  - -- SPACE AND AERONAUTICAL
  - -- NASA AND MILITARY
  - -- IMPROVEMENTS OVER CONVENTIONAL TRANSDUCERS
  - -- NOT POWER RELATED

Q & A - G. Sundberg

From: P. J. Turchi, R & D Associates

Could deep-impurity trapping concepts be used to modify performance of photovoltaic cells, thermoelectrics, etc.?

A.

The answer is ,"yes". The addition of deep impurities will definitely modify performance. Whether for good or bad, however, would need some study. Gold and/or radiation are often used to speed up p-n junction devices such as thyristors by enhancing electron-hole recombination. This gives fast recovery times but at the expense of increased forward voltage drop. Usually designers of p-n junction devices shy away from addition of materials giving deep energy levels. Addition of relatively large amounts of gold 10^{10} to $10^{14}/cm^3$ will increase resistivities of the starting material from 10-100-Ω-cm to the orders of 10 to 20 kΩ-cm. This may be desireable in the case of an edge illuminated stacked solar cell where higher resistivity appears to be helpful. We've not yet pushed our study in the direction of deep impurities with p-n junction materials - this would open up a whole new arena of research. Thank you.

BIBLIOGRAPHY

SELECTED PAPERS PUBLISHED BASED UPON RESEARCH OF UNIVERSITY OF CINCINNATI GROUP

1. Henderson & Ashley, "Space-Charge-Limited Current in Neutron-Irradiated Silicon, with Evidence of the Complete Lampert Triangle," Phys. Rev., 186, 811 (1969).

2. Henderson et al., "Third Side of the Lampert Triangle: Eivdence of Traps-Filled-Limit Single-Carrier Injection," Phys. Rev. B, 6, 4079 (1972).

3. Henderson & Ashley, "A Negative Resistance Diode Based Upon Double Injection in Thallium-Doped Silicon," Proc. IEEE, 57, 1677 (1969).

4. Vanvari & Henderson, "Double-Injection Negative Differential Resistance in Compensated Gold-Doped Germanium," Phys. Stat. Sol, (a), 12, K81 (1972).

5. Nevin & Henderson, "Thallium-Doped Silicon Ionization and Excitation Levels by Infrared Absorption," J. Appl. Phys., 46, 2130 (1975).

6. Henderson & Asbrock, "A New (SCR-Like) DI Switching Device Based Upon Deep Impurity Trapping and Relaxation Effects," Digest, IEEE International Electron Devices Meeting, Washington, D.C., p. 680 (1978).

7. Mantha & Henderson, "Post-Breakdown Bulk Oscillations in Gold-Doped Silicon p^+-i-n^+ Double-Injection Diodes," Solid-St. Electron, 23, 275 (1980).

8. Ko & Henderson, "The Use of Multiple Internal Reflection on Extrinsic Silicon Infrared Detection," IEEE Trans. Electron Devices, ED-27, 62 (1980).

9. Kapoor & Henderson, "A New Planar Injection-Gated Bulk Switching Device Based Upon Deep Impurity Trapping," IEEE Trans. Electron Devices, ED-27, 1268 (1980).

10. Kapoor & Henderson, "Variable N-Type Negative Resistance in an Injection-Gated Double-Injection Diode," IEEE Trans. Electron Devices, (to be published March, 1981).

11. Kapoor & Henderson, "Injection-Gated DI Diode with Gate-Controlled Holding Voltage," IEEE Trans. Electron Devices (submitted for publication).

12. Kapoor & Henderson, "Double-Injection Diode as a Pulse Width Modulation Element," Electron Devices Lett. (submitted for publication).

RELEVANT UNIVERSITY OF CINCINNATI
THESES AND DISSERTATIONS

1. Infrared

   (a) Chih-Sieh Teng, "Infrared Extrinsic MOSFET Detectors with and without Memory, Based Upon Epitaxial Silicon/Germanium Alloy," Ph.D. Dissertation (1979).

   (b) Prateep Tuntasood, "Use of Activated Gold Donor in Silicon for Fabrication of MOS and Photoconductive Infrared Detectors," M.S. Thesis (1979).

   (c) Shang-Bin Ko, "Exploration of New Schemes of Extrinsic IR Photodetection Using Deep Impurities in Silicon Planar Configurations," Ph.D. Dissertation (1978).

   (d) Joseph H. Nevin, "Analytical and Experimental Contributions to the Characterization of Deep Impurities in IV-IV Semiconductors," Ph.D. Dissertation (1974).

2. Injection Characteristics (Single and Double) in Polysilicon and Neutron-Irradiated Silicon

   (a) Anant D. Dixit, "Electronic Injection Studies of Silane-Deposited Polycrystalline Silicon Films," Ph.D. Dissertation (1974).

   (b) Jerry E. Sergent, "An Investigation of Double Injection---Using Neuron-Irradiated Silicon as a Case in Point," Ph.D. Dissertation (1971).

3. Deep Impurities

   (a) Mana Rungseanuvatgul, "Characterization of an Indirect Source Open-Tube Method of Gold-Doping in Silicon, Using Transient Capacitance Measurements," M.S. Thesis (1980).

   (b) Bhaskar Mantha, "Electrical Properties of Zinc-Doped Silicon," M.S. Thesis (1976).

   (c) N. Jayaram, "Optical Studies in Semiconductor Technology Using Multiple Internal Reflections," M.S. Thesis (1975).

   (d) Thallium in Silicon, see J.H. Nevin dissertation in 1(d) above.

   (e) Narayan L. Vanvari, "Czochralski Growth of Compensated Gold-Doped Germanium for Double-Injection Switching Diodes," M.S. Thesis (1972).

   (f) Sushil K. Kapoor, "Annealing of Neutron Irradiated Silicon with Implications in Device Technology," M.S. Thesis (1969).

4. MOS-Gated Double-Injection

   (a) Ramaswamy Narasimhan, "Terminal Characterization and Transient Analysis of MOS-Gated Double-Injection Devices," M.S. Thesis (1980).

   (b) James F. Asbrock, "Control of Breakdown Voltages in Double Injection Devices Using a MOS Gate," M.S. Thesis (1972).

5. Bulk Oscillations

   (a) Bhaskar L. Mantha, "Analysis and Modeling of Post-Breakdown Low Frequency Bulk Instabilities in Planar Gold-Doped Silicon," Ph.D. Dissertation (1979).

   (b) Vivek R. Kulkarni, "New Planar Device Development Based Upon Bulk Space-Charge Interactions in Zinc-Doped Silicon," M.S. Thesis (1977).

   (c) Harish H. Hoshi, "Two and Three-Terminal Switching Characteristics of Zinc-Doped Silicon," M.S. Thesis (1977).

6. Injection-Gated Double-Injection Devices

   (a) Ashok K. Kapoor, "Injection Gating of Planar Double-Injection Devices, Based Upon Charge Trapping in Gold Doped Silicon," M.S. Thesis (1979).

   (b) Harish J. Joshi. (See Item 5(c) above.)

7. Light-Gating of Double-Injection Devices

   (a) Vivek R. Kulkarni. (See Item 5(b) above.)

8. Single Injection TFL Behavior

   (a) Harish J. Joshi. (See Item 5(c) above.)

   (b) Michale K.L. Shen, "Surface Band-Bending Implications for Charge Injection into Neutron-Irradiated Silicon," M.S. Thesis (1972).

9. Time Delay

   Virtually all recent theses and dissertations deal with voltage-controlled switching delay, particularly that of R. Narasimhan (Item 4(a) above).

10. Transducers

   (a) Richard L. Stanton, "Development of a High-Sensitivity Gas Flow Transducer Based Upon Gold Doped Silicon," M.S. Thesis (1979).

   (b) Jason Wang, "Microelectronic Deep Impurity Gas Flow Transducer Fabricated by V-Groove Techniques," (Tentative title of M.S. Thesis to be completed about December, 1980).

APPLICATIONS OF MATERIALS SURFACE MODIFICATION TO PRIME POWER SYSTEMS

F. L. Milder
Spire Corporation, Bedford, MA 01730

ABSTRACT

Perhaps the single most pervasive design consideration in engineering for space applications, including prime power, is weight. Not only is the question of weight dealt with directly, but it is also couched in such terms as cost effectiveness or efficiency. Often basic component functions can be thought of as twofold. Bulk material requirements are usually items like lightweight strength, structural integrity, dimensional stability or high temperature strength. Surface requirements more often deal with wear, erosion and corrosion resistance, electrochemical activity or electrical properties such as conductivity or emissivity. For these reasons, the new technologies of surface modification are ideally suited for space applications. Surface modification offers the ability of custom creating materials with one set of surface properties conjoined to a dissimilar or even mutually exclusive set of bulk properties. The benefit of such specifically engineered materials is an efficiency in component design which translates to weight minimization.

Modern surface modification techniques, including ion implantation, sputter deposition, and plasma/ion deposition, deal with thin film layers in the range from a few nanometers to a few micrometers. Ion implantation is unique in that it forcibly injects an element of choice into the near surface region of a material. Thus, alloys or solid solutions are formed unaccompanied by dimensional changes. The numerous and varied deposition techniques, on the other hand, grow coating layers, often with unique properties.

The developmental areas related to space prime power which will be amenable to surface modification include wearing components such as turbine blades, bearings and MHD walls, fuel cell and battery electrodes, superconductors, spark gap switches, transformer cores for magnetic switching, storage capacitors, and thin film solar cells.

THE ADVANTAGES OF SURFACE MODIFICATION TECHNOLOGY FOR SPACE PRIME POWER

Many components would benefit from the separate optimization of bulk and surface properties.

Surface Modification techniques make available that ability of dual optimization.

The benefits will be predominantly in weight reduction and increased efficiency.

Part	Desired bulk structure property	Desired surface function
bearing	strength	corrosion and wear resistance, low friction
turbine blade	high temp. structural integrity	oxidation and erosion resistance
MHD electrode wall	high temp. structural integrity	alternating high and low electrical resistance; oxidation and erosion resistance
superconducting energy storage coil	low temp. strength, rigidity	superconductivity, flexibility
fuel cell or battery electrode	strength, corrosion resistance, high electrical conductivity	good electrochemical/catalytic activity, long lifetime, large surface area
spark gap electrode	high electrical conductivity, structural rigidity	erosion, sputtering, and vaporization resistance

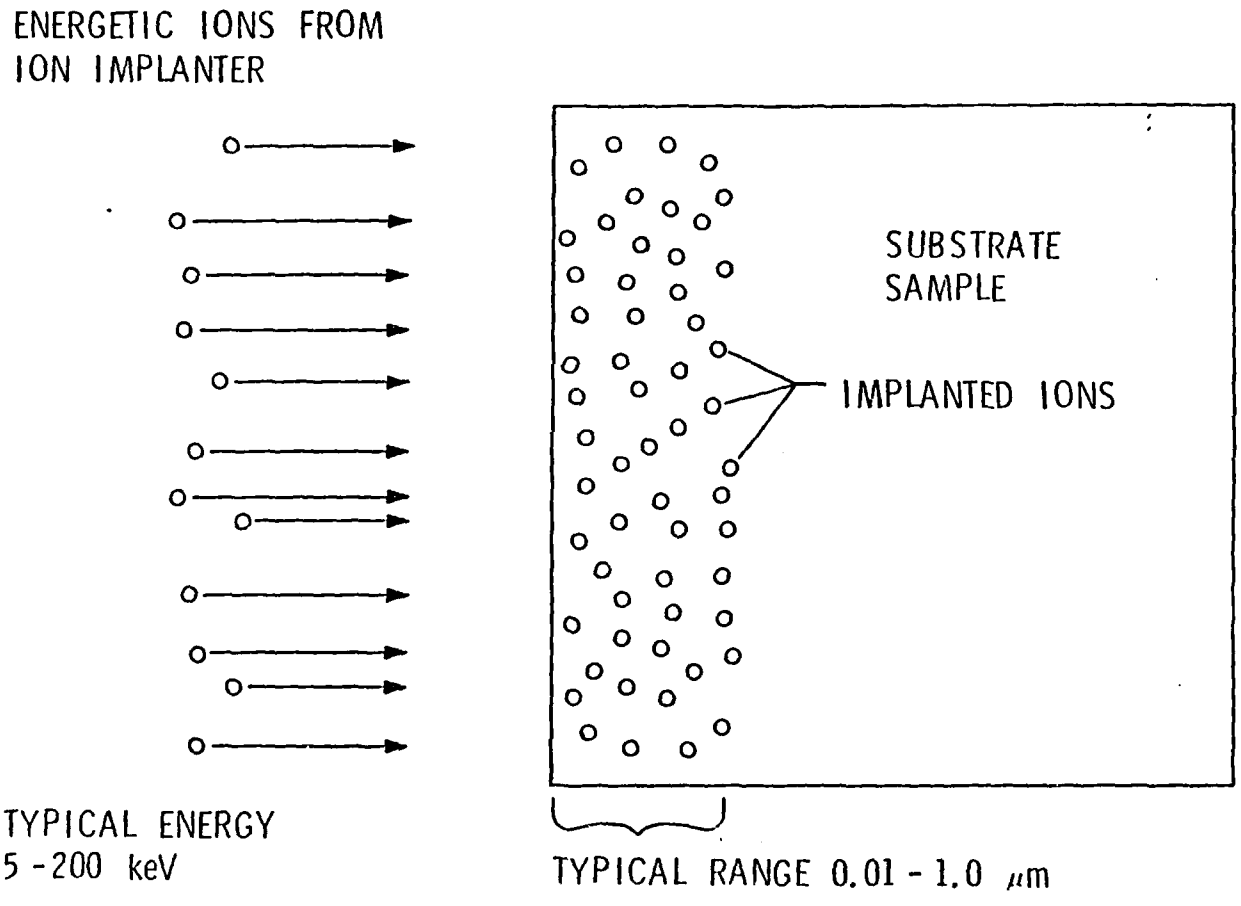

VII-10-2

FIGURE 1. ION IMPLANTATION INTRODUCES ISOTOPICALLY PURE IONS INTO THE NEAR SURFACE REGION OF MATERIALS. Alloys are formed in the surface without altering the bulk properties.

POTENTIAL APPLICATIONS OF ION IMPLANTATION IN S.P.P.

battery/fuel cell electrodes	- choice of catalyst independent of support system. Large specific activity. (Li → electrodes, Pt → Fe, etc.)
superconductors	- novel alloys, controlled compositions, basic research. (Nb_3Sn on NbTi?)
spark gap electrodes	- custom surfaces not subject to delamination
bearings	- bearing designed for performance optimization or strength; implanted surface improves lifetime (implanted foil bearings subject to abrasion)
turbine blades	- high temp. alloys need improved oxidation resistance (Y → Ti alloy)
MHD electrodes	- specific control of conductivity of ceramic components; alter emissivity of electrodes for higher efficiency.

In fig. 4 the activity values measured at −50 mV overpotential are plotted against values calculated under the assumption of additive behaviour of the constituents of the implanted catalyst. We assumed that a sample with 10% surface coverage behaves like a hypothetical sample consisting of 90% original target material and 10% of the implanted element as smooth metal. Every deviation from the 45° line illustrates an additional effect caused by the implantation process itself. The figure shows that only the pure metals are situated on the 45° line. All implanted samples show orders of magnitude deviations: the lead implantation in the direction of low activity, gold and platinum high activity, even higher than smooth gold or platinum metal. It can also be seen that the effect is a chemical rather than a physical one, because samples in which only defects were produced (Pt^+ implanted in Pt, or Ar^+ implanted in iron) display only a moderate increase in activity.

The highest positive effect arises from platinum in iron. Fig. 5 shows the actual measurement, cathodic current density–potential curves, under different implantation conditions compared with smooth iron, smooth platinum and platinum sputtered onto the surface of iron (≈1 monolayer). The current density values as a function of the applied potential are a direct measure of the amount of hydrogen formed at the specific potential. There is no doubt that implanted samples are much more active than smooth platinum or a platinum layer sputtered onto iron. Also, a change in slope with increasing implantation dose takes place. This indicates that the high dose samples approach in their performance that of supported platinum catalysts, even though the current densities achievable with the latter are still higher. Grouped by the activity at $\eta = 50$ mV we find the following order of catalysts:

$$Pb < Fe + Pb^+ < Fe < Au < Pt < Fe + Au^+ < Fe + Pt^+ < \text{supported Pt catalyst}.$$

The benefit of the ion implantation technique in this field appears to be even more promising when

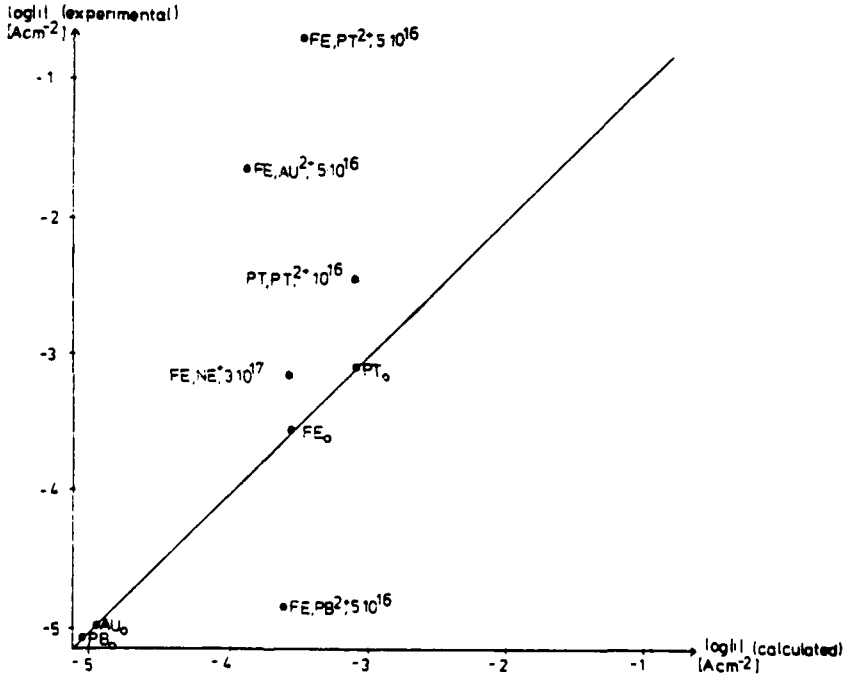

Fig. 4. Experimental current-densities of implanted iron electrodes at −50 mV overpotential for the hydrogen redox reaction in 1 N H_2SO_4 as compared with calculated ones. The values are computed under the assumption that the surface of an implanted electrode acts as a smooth metal surface consisting of both components as a ratio of their surface coverage. The distance from the 45° line illustrates the magnitude of the additional implantation effect (beyond this assumption).

WITHOUT BOR
IMPLANTATIO
(160x)

WITH BORON
IMPLANTATIO
(160x)

FIGURE 3. REDUCTION OF BERYLLIUM GAS BEARING MATERIAL WEAR BY SPIRE ION IMPLANTATION OF $5x10^{17}$ BORON AT 50 keV.

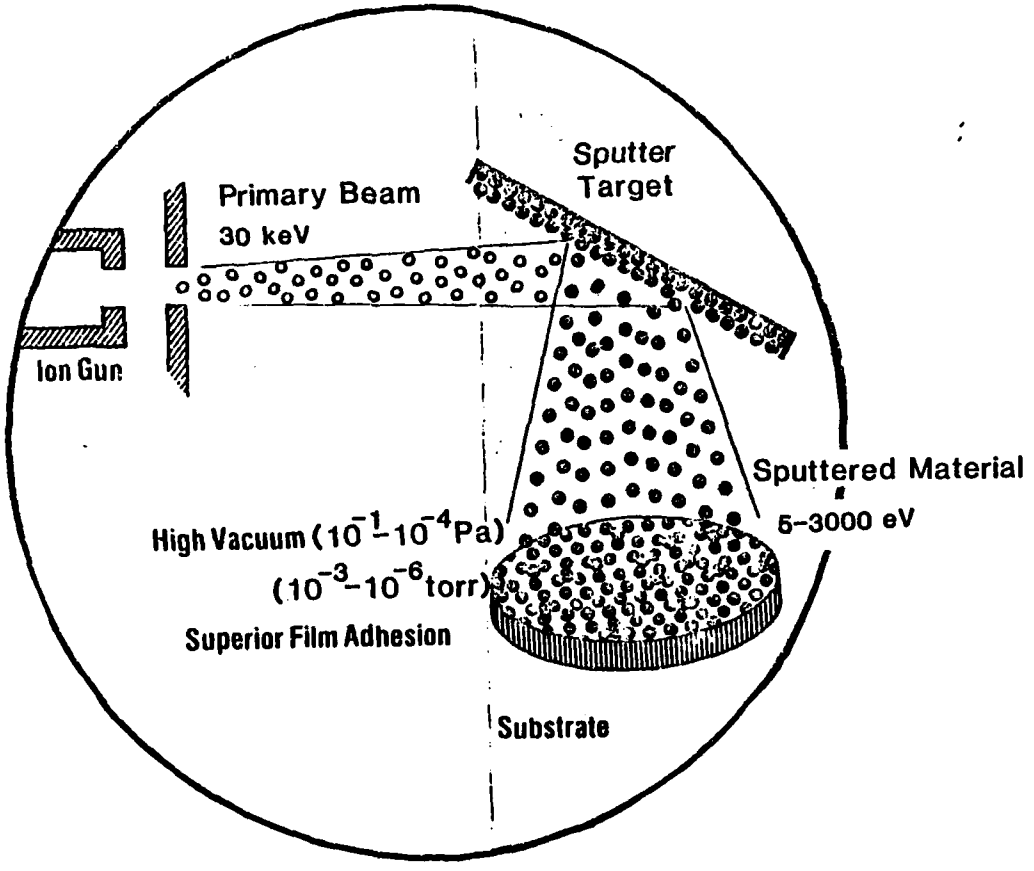

FIGURE 6. IN ION BEAM SPUTTERING A HIGH-ENERGY BEAM OF IONS SPUTTERS MATERIAL FROM THE TARGET AT ENERGIES BETWEEN 5 AND 3000 eV (50 eV TYPICAL). The target material coats the substrate.

POTENTIAL APPLICATIONS OF SPUTTER COATINGS IN S.P.P.

battery electrodes	- active electrode material on support of choice
MHD electrode walls	- ceramics mated to metals? amorphous metal electrodes for erosion resistance
superconductors	- sputter deposited thin films or fiber coatings
transformer cores for switching	- ultra-thin metallic glasses for higher efficiency cores. Monolithic structure with insulators possible.
bearings	- sputter coating of solid lubricants (e.g., MoS_2) on many materials possible.
turbine blades	- sputter coated fibers for Ti composite structures; non-metallic (ceramic) composites.
capacitor storage	- controllable composition dielectrics; amorphous dielectrics

FIGURE 7. LEFT SIDE: END-ON VIEW OF TANTALUM COATING ON CARBON FILAMENTS (2160X).
RIGHT SIDE: SAME VIEW, TANTALUM X-RAY FLUORESCENCE MAP.

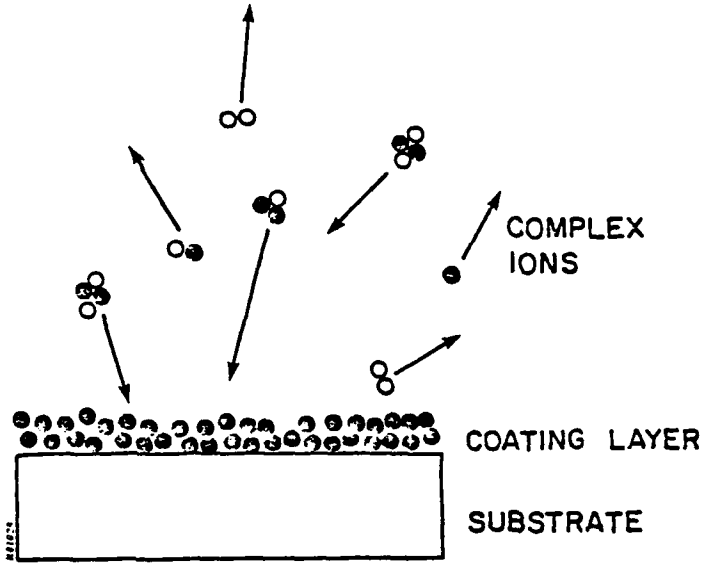

FIGURE 16. SCHEMATIC OF PLASMA ION DEPOSITION. Complex ions at energies up to 2 keV react on the substrate surface to grow coatings.

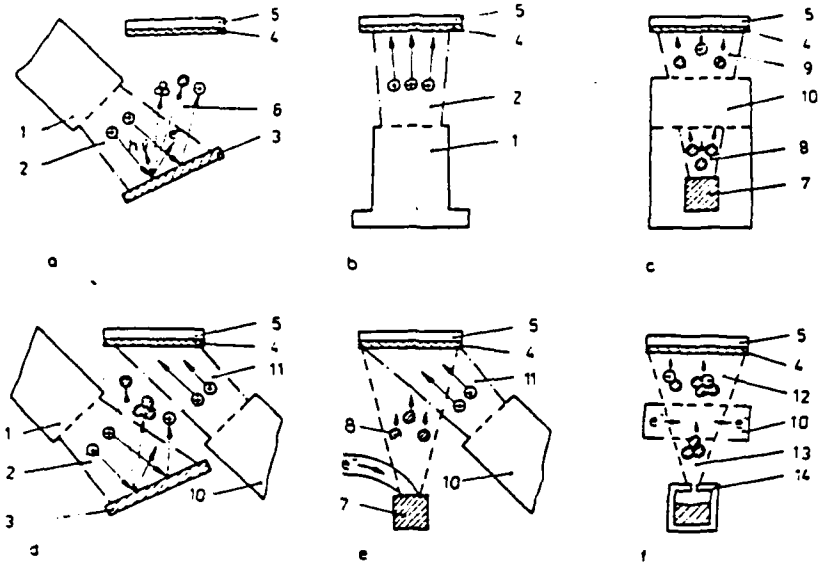

Figure 1. Setups for ion-activated film preparation
a - ion beam sputter deposition; b - ion beam deposition; c - ion beam plating; d - dual beam sputter deposition; e - ion beam activated evaporation; f - cluster resp. molecule ion deposition
1 - ion source; 2 - ion beam; 3 - target; 4 - film; 5 - substrate; 6 - sputtered species; 7 - evaporation source; 8 - molecular beam; 9 - partly ionised molecular beam; 10 - ionisation device; 11 - second ion beam; 12 - partly ionised cluster beam; 13 - cluster beam; 14 - cluster source

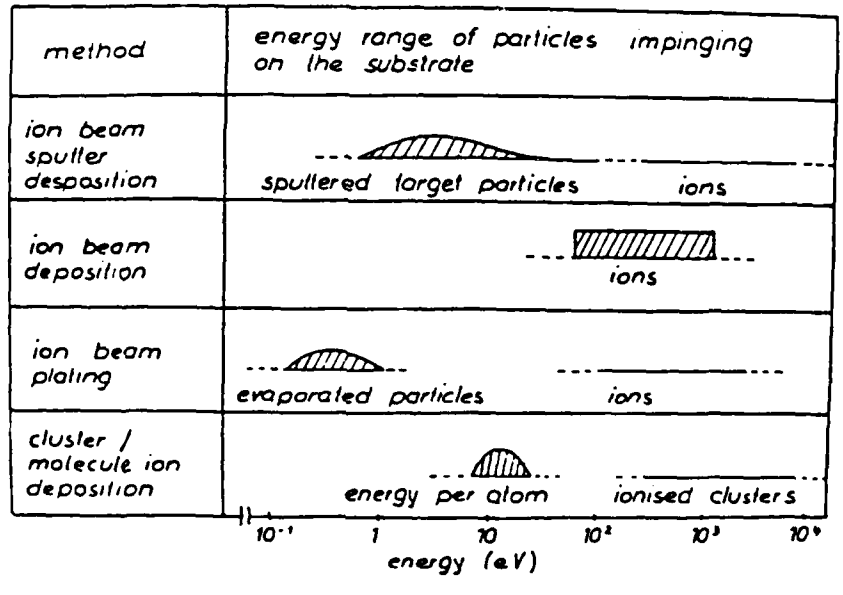

Figure 2. Energy spectra of the particles impinging on the substrates for different modes of ion-activated film preparation

POTENTIAL APPLICATIONS OF PLASMA/ION DEPOSITION FOR S.P.P.

critical wearing components of rotating generators and turbines	- hard coatings (e.g., TiN, cubic BN) can be put on high strength steels, etc.
photovoltaic	- plasma grown thin film solar cells

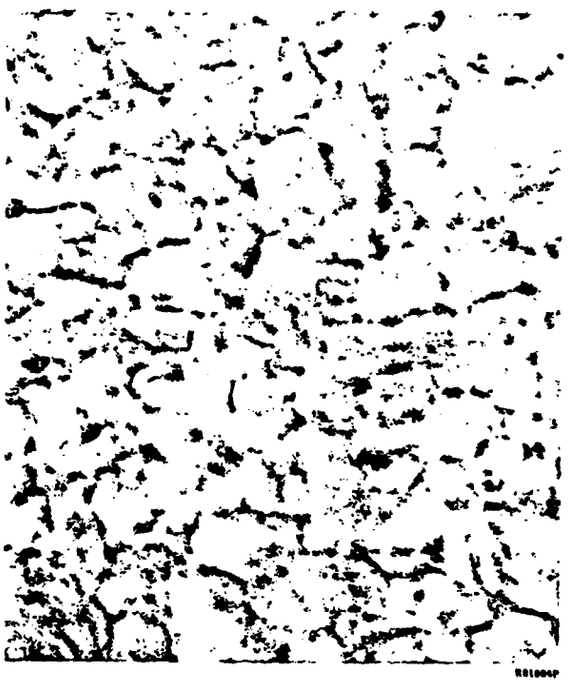

FIGURE 18. SEM (40,000X) VIEW OF SILICON FILM GROWN IN THE PLASMA ION DEPOSITION APPARATUS The grain size is approximately 0.3 μm.

SUMMARY

Surface Modification technologies are ideal for space applications:

1. They offer dual optimization of component design
2. Surface layers are truly thin, guaranteeing weight minimization
3. The technologies are varied enough to meet many different specialized needs

BIBLIOGRAPHY

R. E. Benenson, E. N. Kaufmann, G. L. Miller, and W. W. Scholz (eds.), Proc. Second Int. Conf. on Ion Beam Modification of Materials, Albany, NY, 1980.

C. Weissmantel, G. Reisse, H. J. Erler, K. Benilogua, U. Ebersbach, and C. Schurer, "Preparation of Hard Coatings by Ion Beam Methods," Thin Solid Films, 63(1979)315.

W. Fleischer, D. Schulze, R. Wilberg, A. Lunk, and F. Schrade, "Reactive Ion Plating (RIP) with Auxiliary Discharge and the Influence of the Deposition Condition on the Formation and Properties of TiN Films," Thin Solid Films, 63(1979)347.

T. Spalvins, "Coatings for Wear and Lubrication," NASA TM-78841, 1978.

S. J. Solomon, "Silicon from Silane Through Plasma Deposition," 15th IEEE Photovoltaic Specialists Conf., Orlando, Fla., 1981 (Spire Report TR81-11B).

IN SITU MONITORING OF CRITICAL SYSTEM COMPONENT EROSION BY NUCLEAR ACTIVATION TECHNIQUES

F. L. Milder
Spire Corporation, Bedford, MA 01730

ABSTRACT

Surface layer activation is a nuclear material loss measurement technique capable of measuring minute amounts of wear, erosion, or corrosion in situ. Possible applications in the area of prime power would concern parts subject to erosion in MHD and plasma sources, corrosion studies of electrodes, wearing parts in rotating generators and pitting studies of spark gap switches. The technique could be utilized in development stage experiments or in order to monitor component health in space.

The technique concept is straightforward. The wear point of interest is first bombarded with a high energy beam of nuclei from an accelerator. Some of the atoms in the bombarded material become radioactive as a result and continuously emit low level radiation. The depth distribution of the radioactivity is approximately uniform; a typical depth might be 50 μm. The irradiated part is placed back in the system where it is normally used. A nuclear scintillation detector is placed nearby the wear point but totally external to the system, and the radioactivity is measured by the detector. This can be done through any intervening material, since the nuclear gamma-radiation is highly penetrating. As the point of interest is worn away, the radioactivity, as measured by the detector, decreases and indicates the depth of material removed. The depth sensitivity is approximately a fixed percentage (1-2%) of the total activated depth. Thus, with the 50 μm total activation depth noted, one would be able to measure reliably 1 μm of wear.

In actual usage, the radioactivity profile as a function of depth is not assumed linear. Instead, the profile is obtained on a calibration part identical to the one being tested by the controlled removal of material and simultaneous measurements on the remaining radioactivity. This calibration curve is then used, in reverse, to obtain the total wear depth from an observation of the remaining activity in the test part. As an example of its application, an ongoing program measuring erosion in an MPD thruster engine will be briefly discussed.

The original application of SLA was in missile nosetip erosion measurements. This work began almost a decade ago and continued through to 1981.

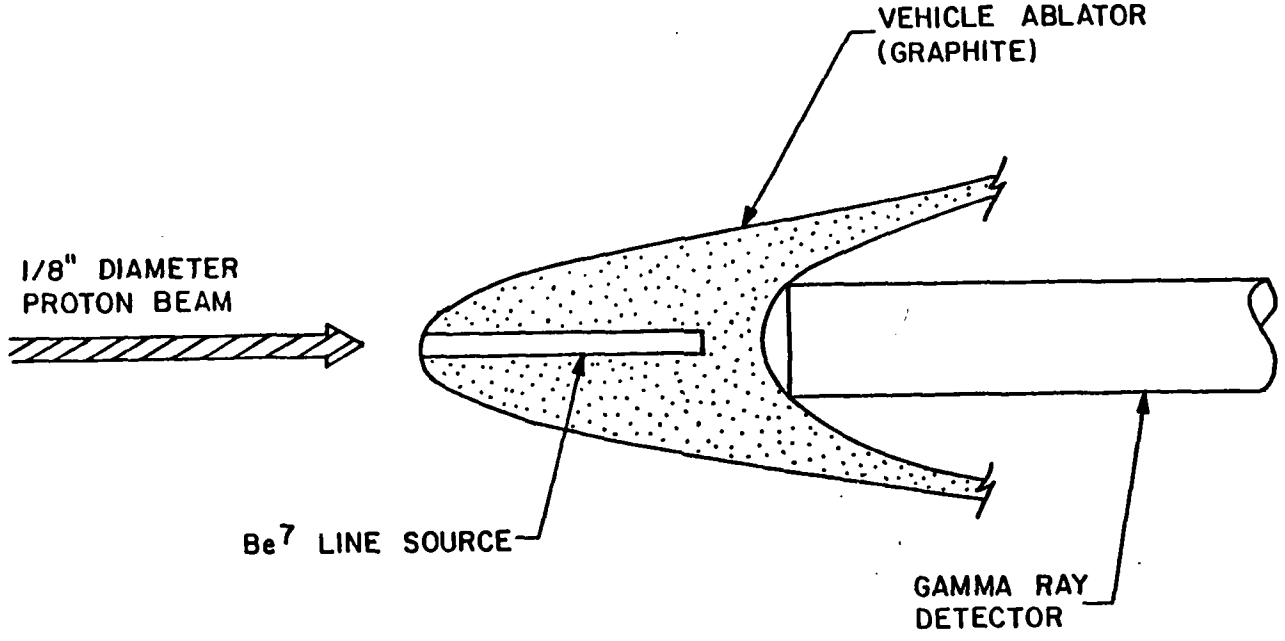

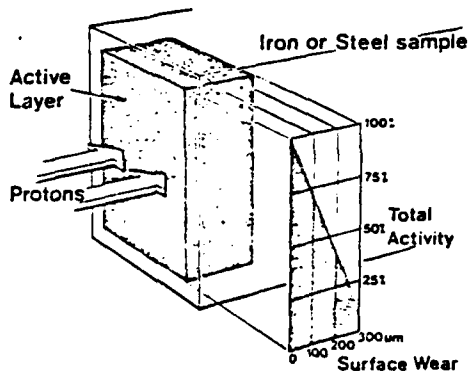

Fig. 1. Thin layer activation of iron or steel by a proton beam.

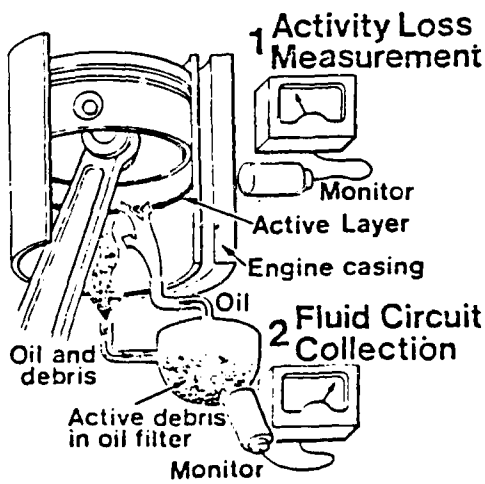

Fig. 2. Loss of activity is measured directly (1) or indirectly via a fluid circuit (2). No dismantling is required.

Accelerator Beam Line and Scattering Chamber for Alignment and Activation of Parts to be Measured

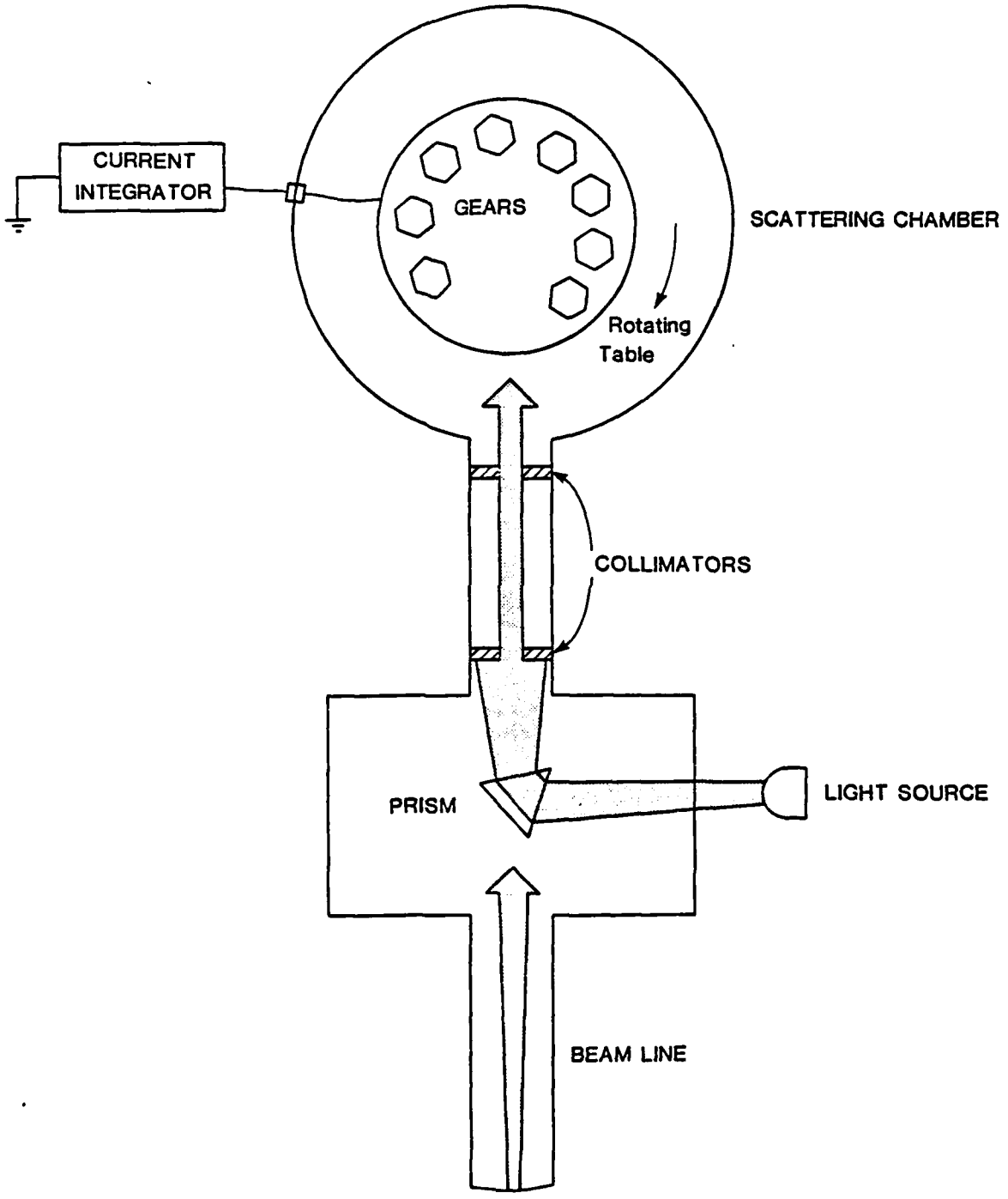

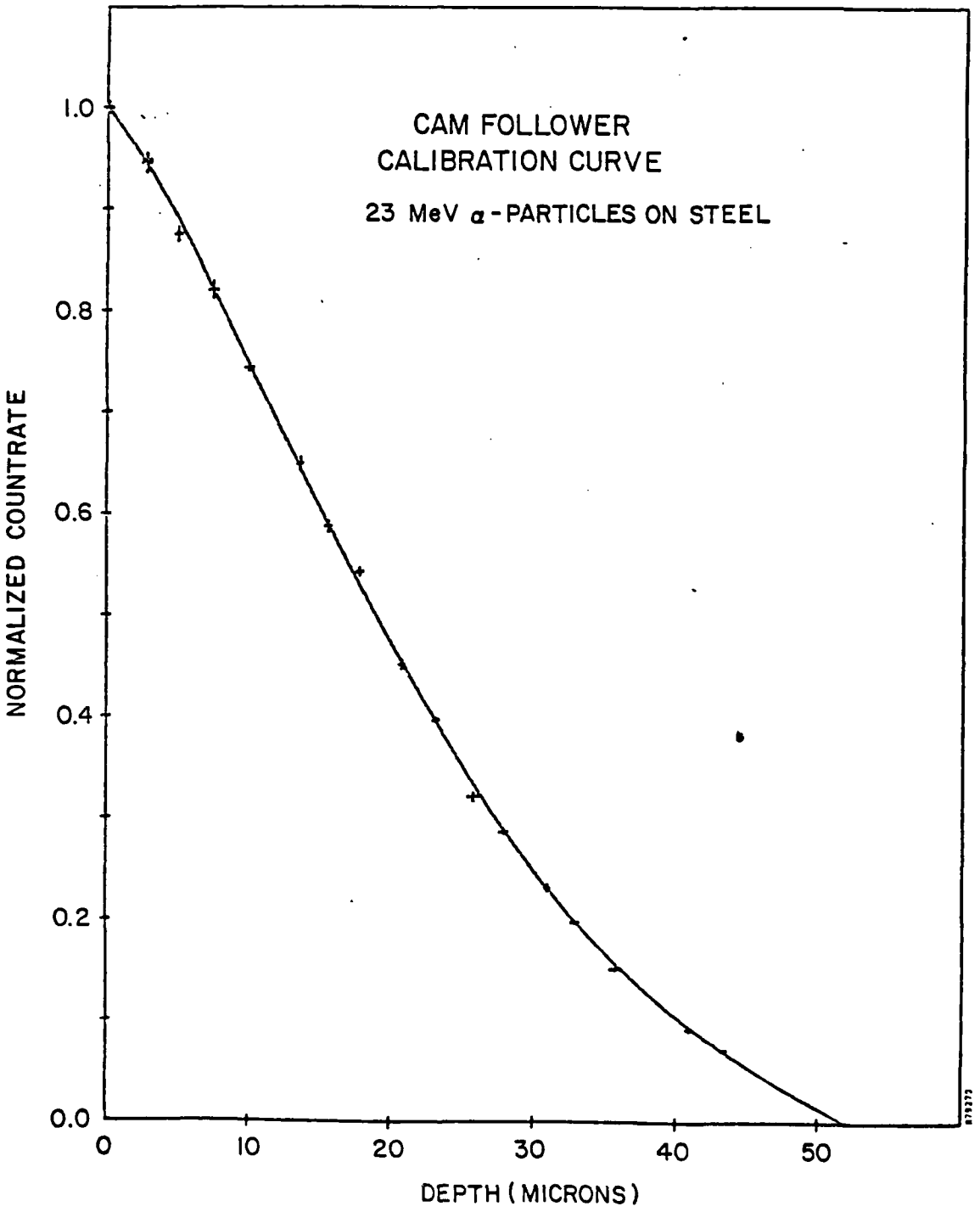
CAM FOLLOWER
CALIBRATION CURVE
23 MeV α-PARTICLES ON STEEL
NORMALIZED COUNTRATE
1.0
0.8
0.6
0.4
0.2
0.0
0
10
20
30
40
50
DEPTH (MICRONS)

V-79-061
FLM

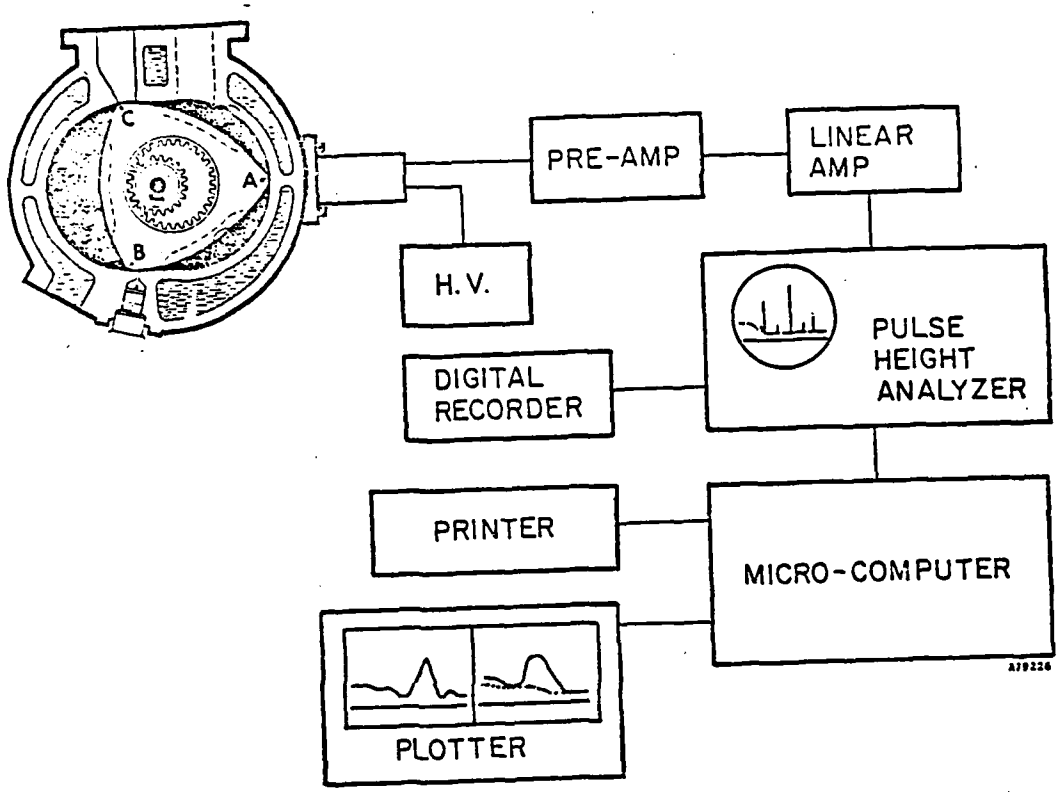

Equipment Used in a Surface Layer Activation Measurement (Wankel engine)

V-79-061
FLM 8/30/79

The most accurate measurement of the radioactivity on a part of interest is the area under the fitted gaussian photopeak

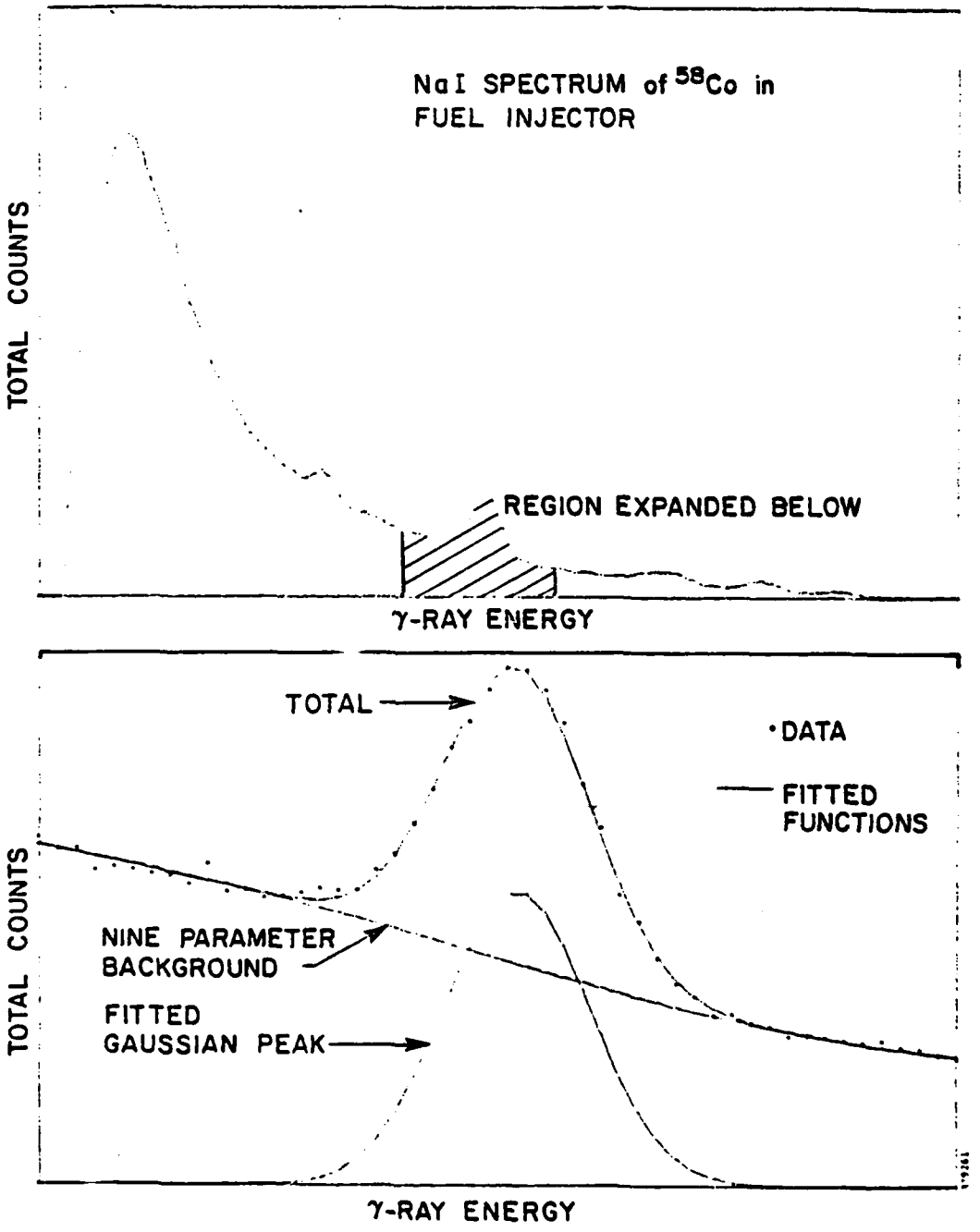

SURFACE LAYER ACTIVATION

Advantages:

1. In situ measurement
2. Direct measurement possible
3. High sensitivity to wear ($<1\ \mu m$ or $<10^{-7}$ cc)
4. Only wear point of interest is measured--shape is controlled
5. Most common engineering materials can be activated
6. Long time scale for health monitoring or short time scale for developmental efforts
7. Custom activation profiles possible

Disadvantages:

1. Relatively expensive
2. Some materials are difficult to activate
3. Some knowledge of radioactive handling necessary
4. Needs access to a particle accelerator

Materials which have had successful application of the SLA technique:

C, N, O, Al, Si, Ti, U, Cr, Fe, Co, Ni, Cu, W, Pb, Sn

Depths which have been used:

15μm (0.3μm sensitivity) to 10 cm

Time scale measurements:

data every three days down to data every 50 ms

Adaptability of technique:

Internal combustion engines - much intervening material

Missile reentry nosetips - extreme vibration and heat environment, telemetry necessary

MPD thruster - many simultaneous, closely-space measurement points

POSSIBLE DEVELOPMENT APPLICATIONS

erosion measurements for MHD walls and electrodes

in situ pitting measurements for spark gap switches

corrosion measurements on battery/fuel cell electrodes

wear measurements on bearings, turbine blade tips, seals, etc.

POSSIBLE HEALTH MONITORING APPLICATIONS

bearings and wearing components upon assembly

failure onset prediction of critical components

useful lifetime/replacement real-time monitoring

The Princeton MPD Satellite Thruster (full scale cross section), showing 11 measurement points on BN, W, and Cu components

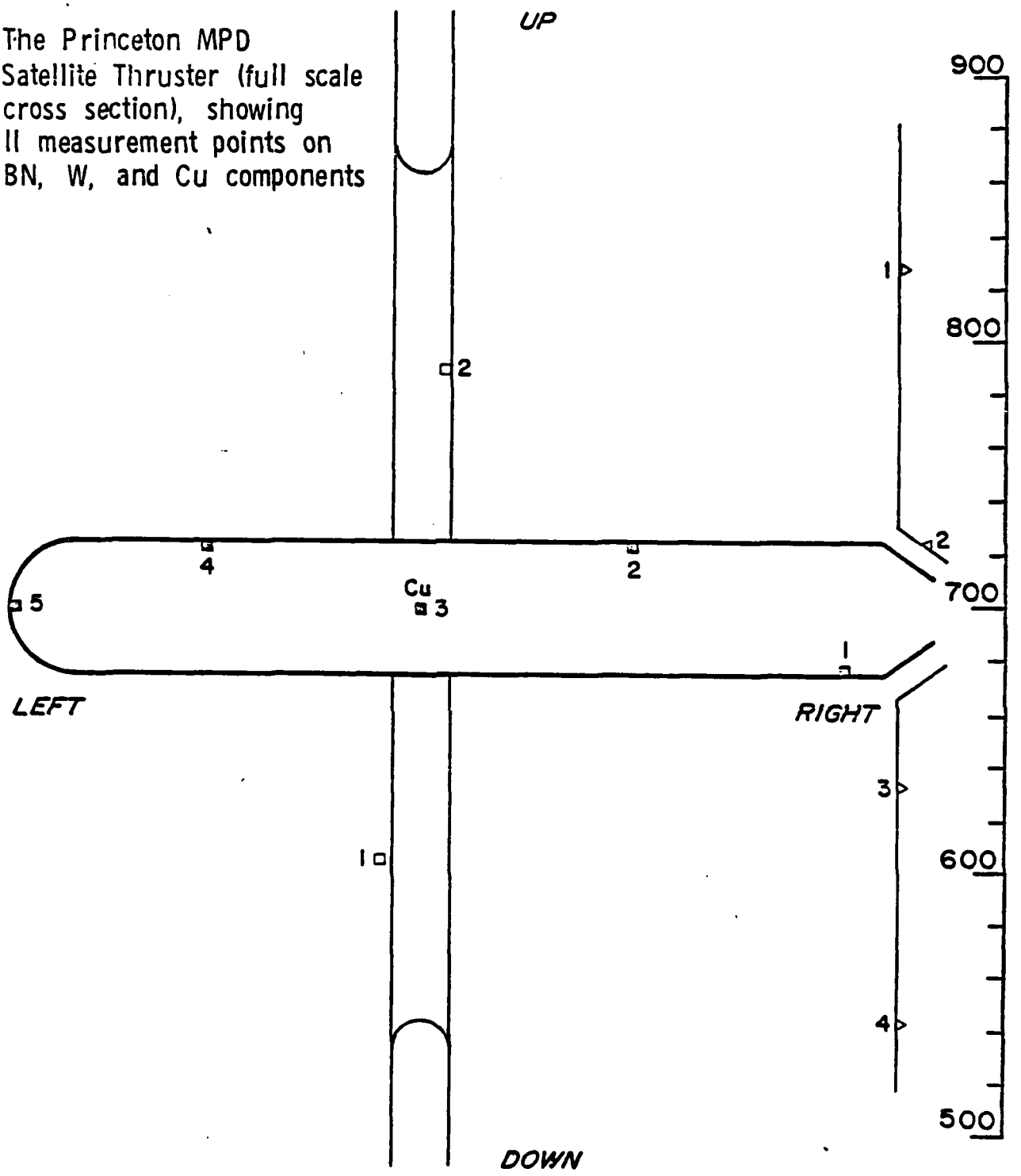

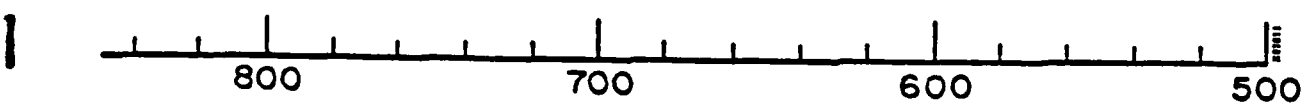

COLLIMATOR HORIZONTAL POSITION

Gamma-ray Spectrum of W Activated by α's Showing the Unique Thumbprint of ^{185}Os

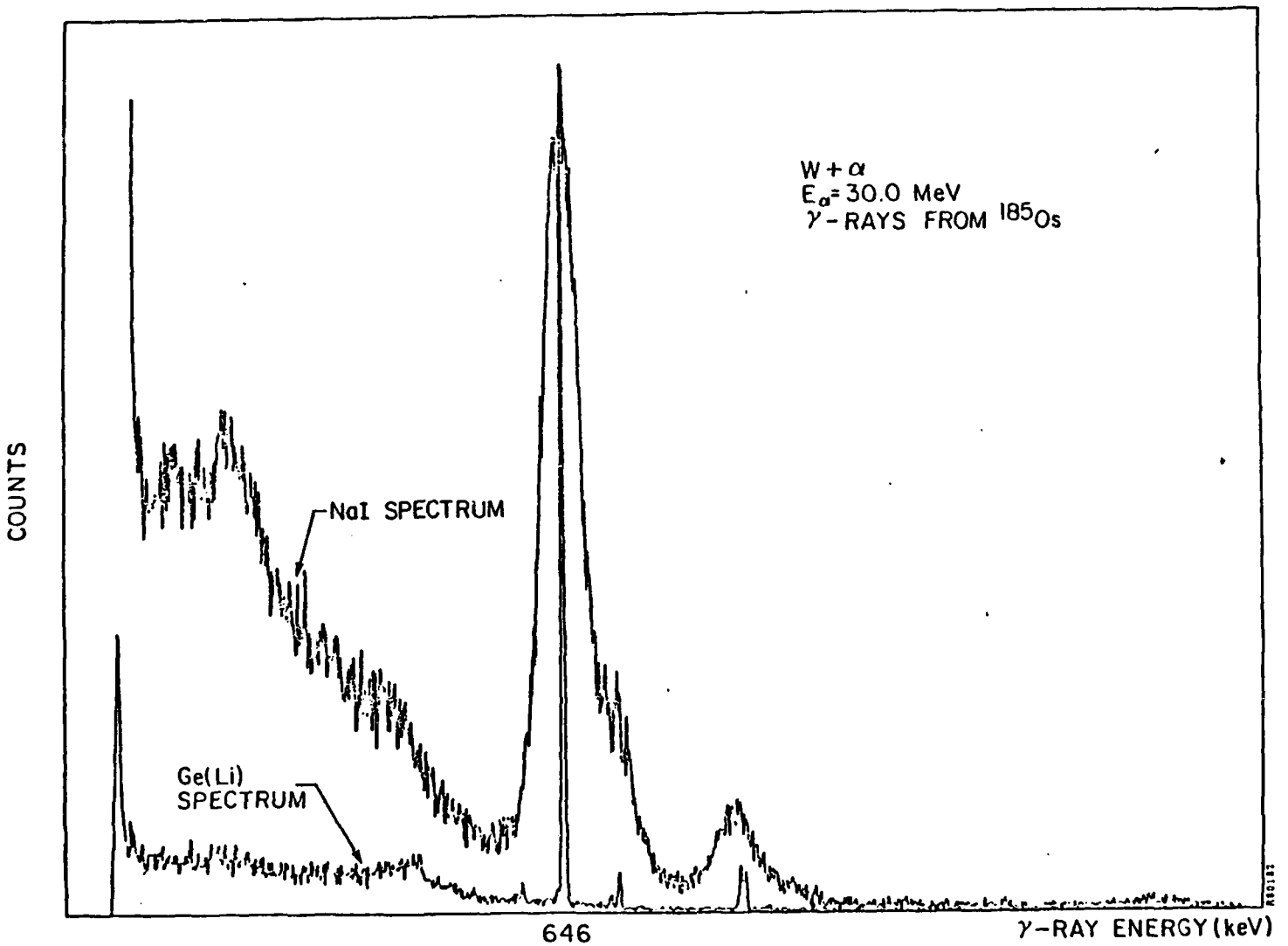

Gamma-ray Spectrum of BN Activated by Protons Showing the Unique Thumbprint of ^{7}Be

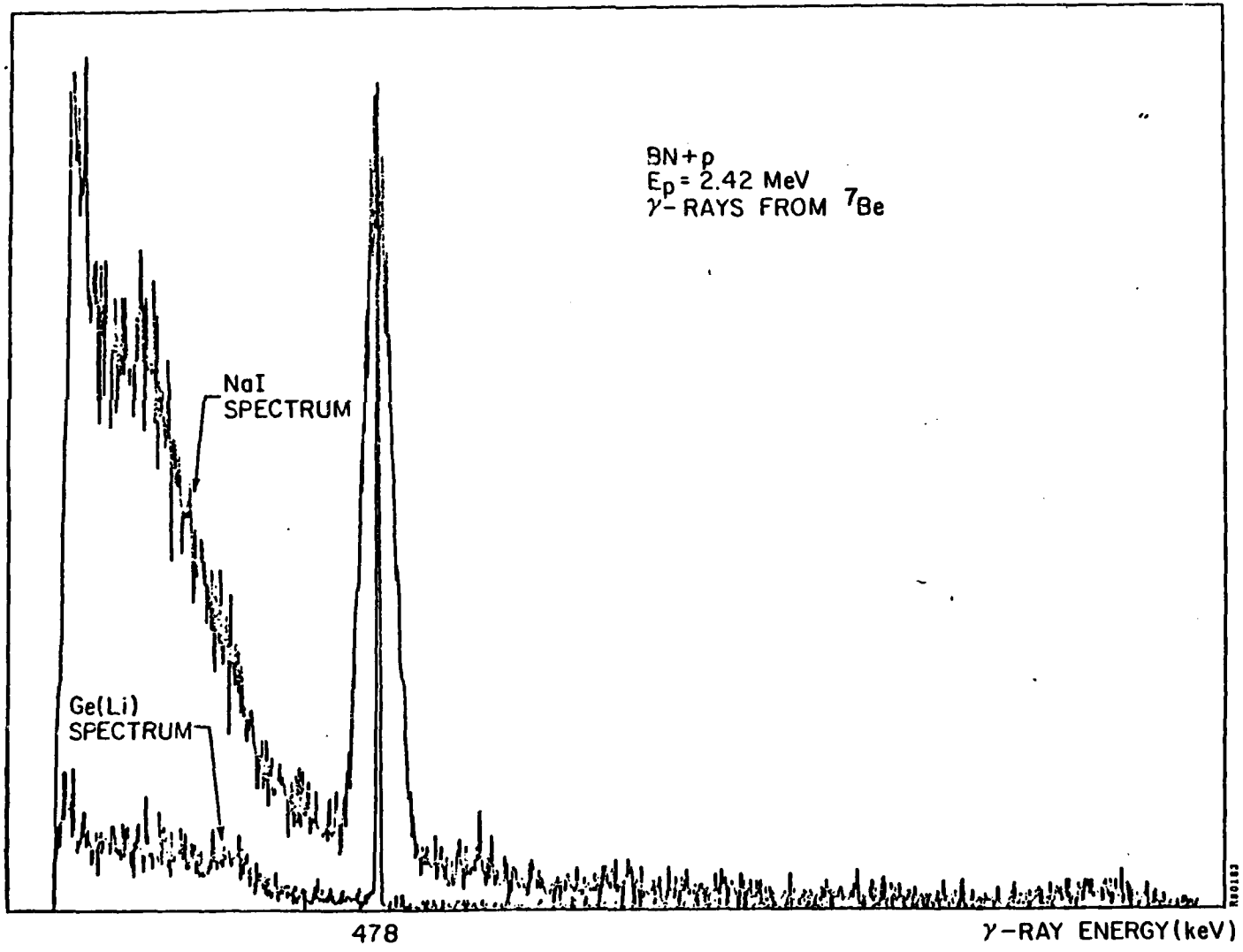

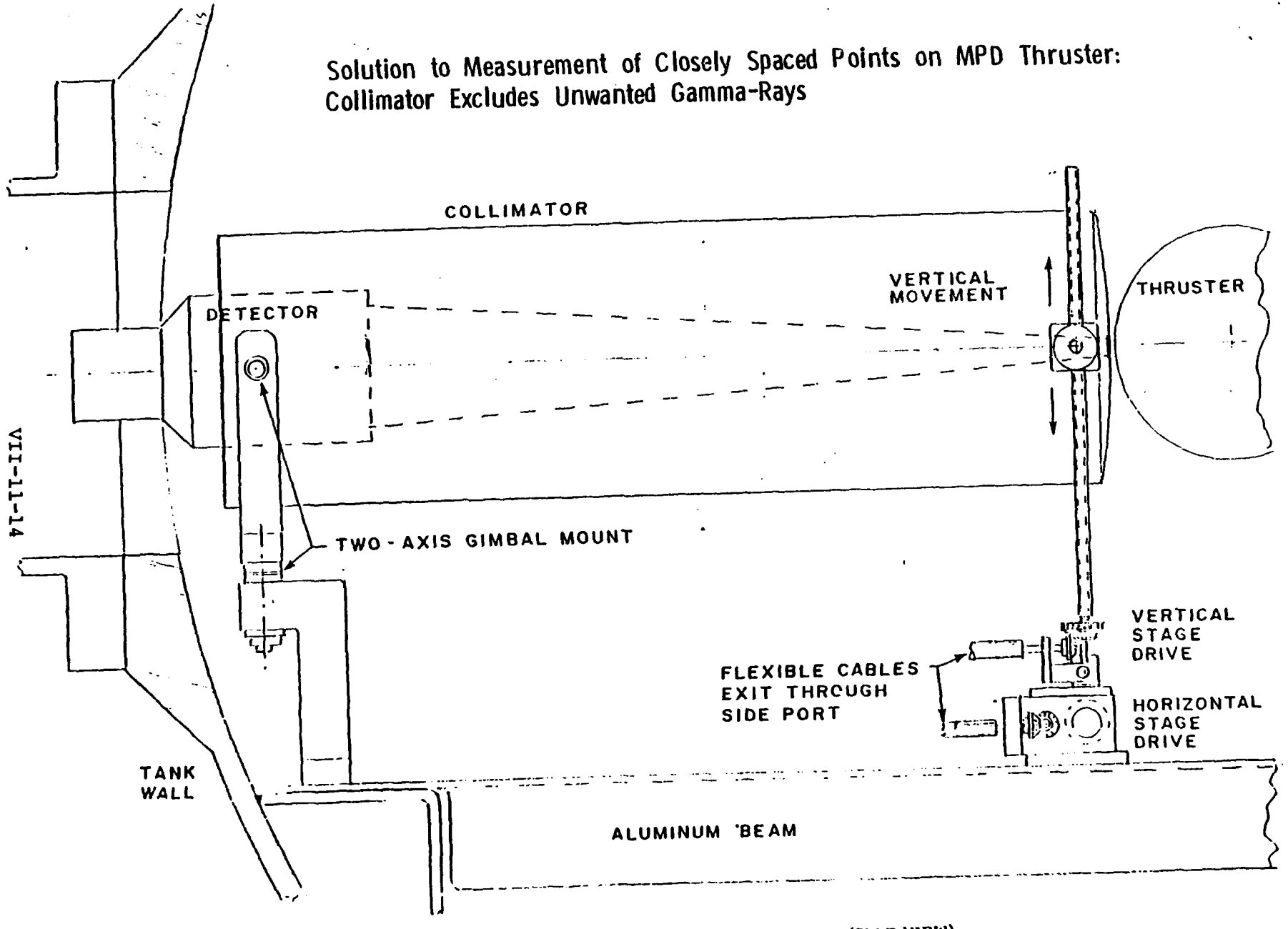

FIGURE 12. COLLIMATOR ALIGNMENT MECHANISM (SIDE VIEW)

NASA

LEWIS RESEARCH CENTER

GROWTH OF DIAMONDLIKE FILMS FOR POWER APPLICATIONS

B. BANKS

ABSTRACT

Diamond has a high thermal conductivity (approximately 5 times that of copper) and is an ideal heat sink material for high power semiconductor devices as well as being of interest as a semiconductor material. Numerous vacuum deposition processes are being evaluated by NASA-LeRC which have demonstrated the capability to deposit carbon films having some of the properties of diamond. Current activities include investigation of high deposition rate vacuum processes suitable for synthesis of diamondlike carbon films. The results of recent film characterization tests are reported.

THERE ARE TWO PROPERTIES OF DIAMOND
THAT MAKE IT OF INTEREST FOR SPACE
POWER APPLICATIONS. THEY ARE:
HIGH THERMAL CONDUCTIVITY AND
WIDE BAND GAP.

	NASA LEWIS RESEARCH CENTER	NAME BANKS DATE OCT. 1981

PROPERTIES OF DIAMOND
OF INTEREST FOR ELECTRONICS APPLICATION

- HIGH THERMAL CONDUCTIVITY ELECTRICAL INSULATOR
- WIDE BAND GAP

THE THERMAL CONDUCTIVITY OF DIAMOND

AT ROOM TEMPERATURE IS APPROXIMATELY

FIVE TIMES THAT OF COPPER.

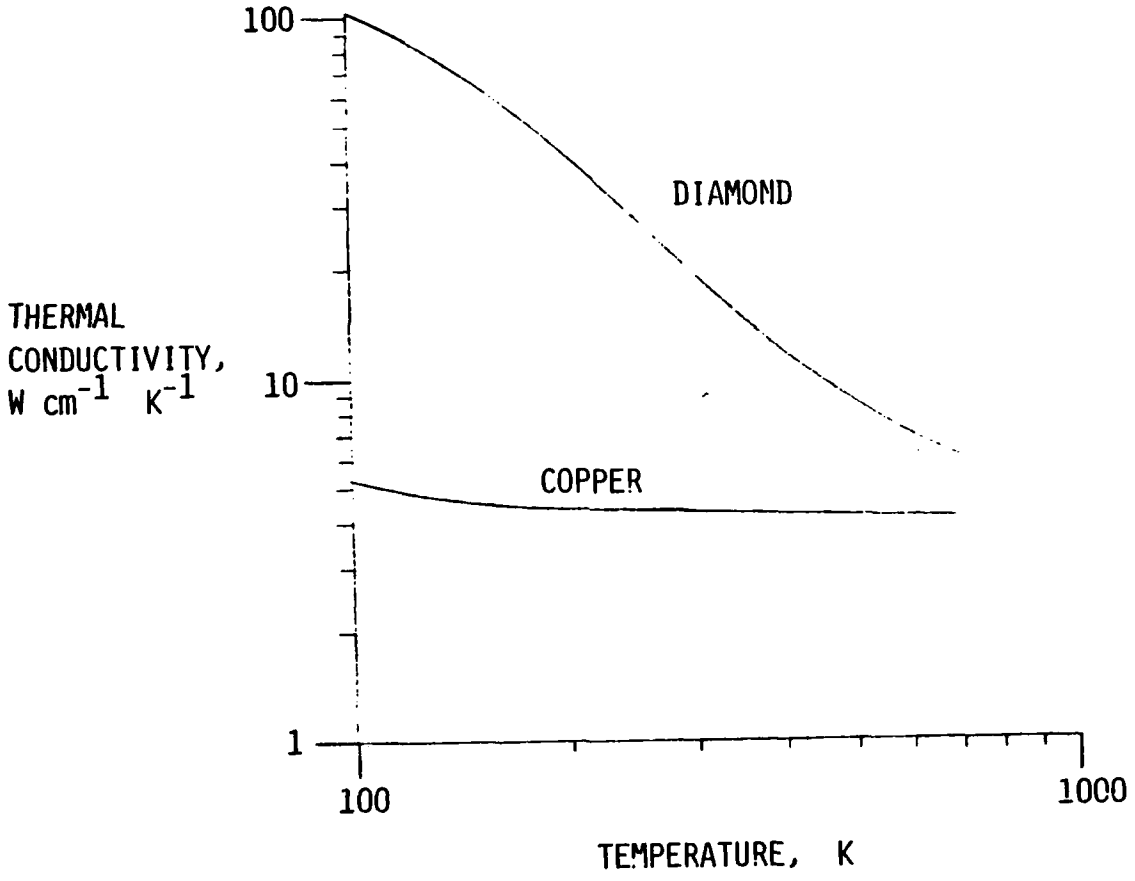
100
10
1
DIAMOND
COPPER
THERMAL
CONDUCTIVITY,
W cm^{-1} K^{-1}
100
1000
TEMPERATURE, K

DIAMOND HEAT SINKS ARE USED TO TRANSFER HEAT FROM AVALANCHE DIODES SUCH AS IMPATT AND TRAPATT DIODES FOR MICROWAVE OSCILLATORS.

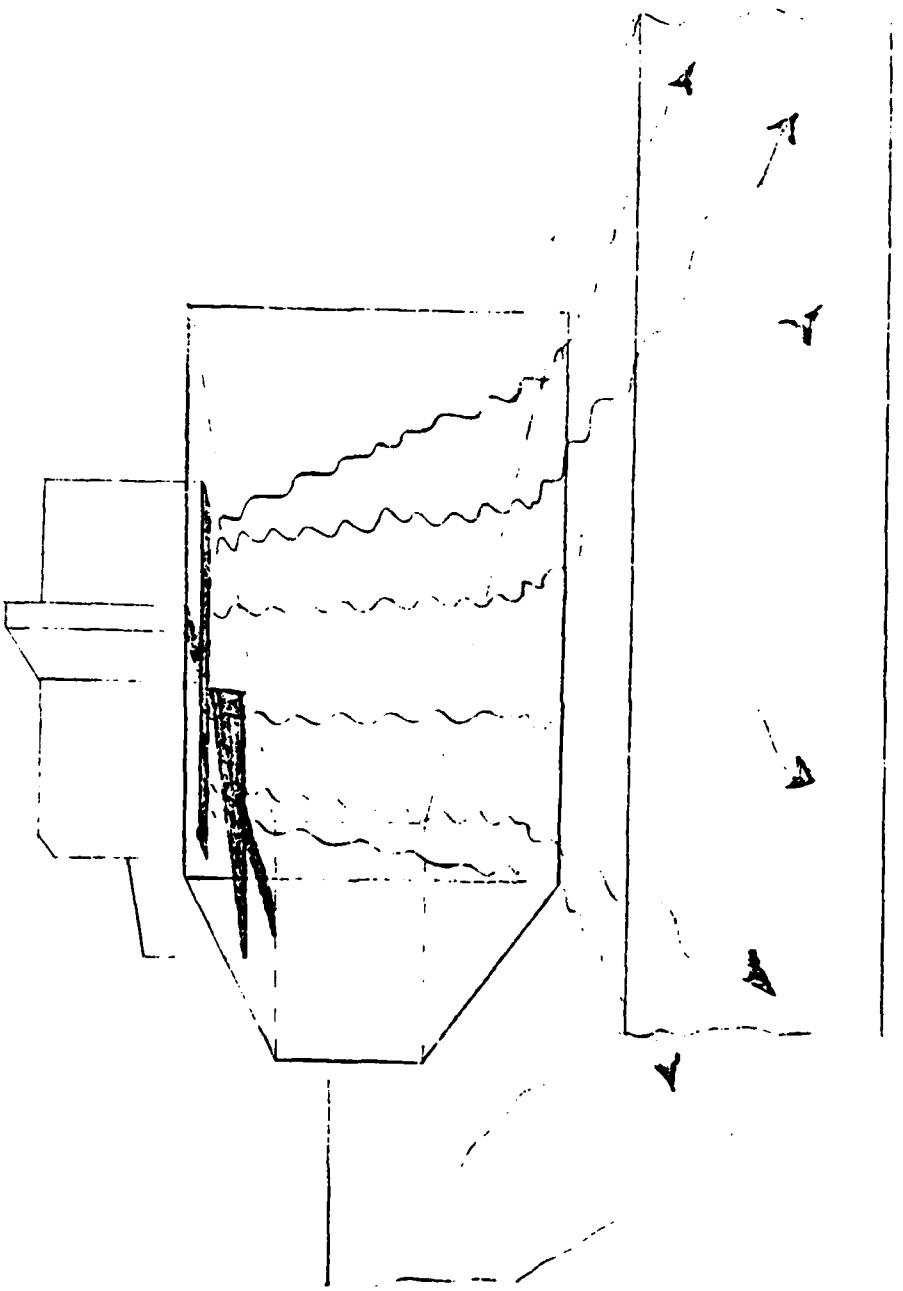

IF THICK DIAMONDLIKE FILMS COULD BE PRODUCED WITH HIGH THERMAL CONDUCTIVITIES, EXTENSIVE APPLICATION AS INTERMEDIARY HEAT TRANSFER DEVICES TO BULK THERMAL HEAT SINKS WOULD RESULT.

GUNN DIODE

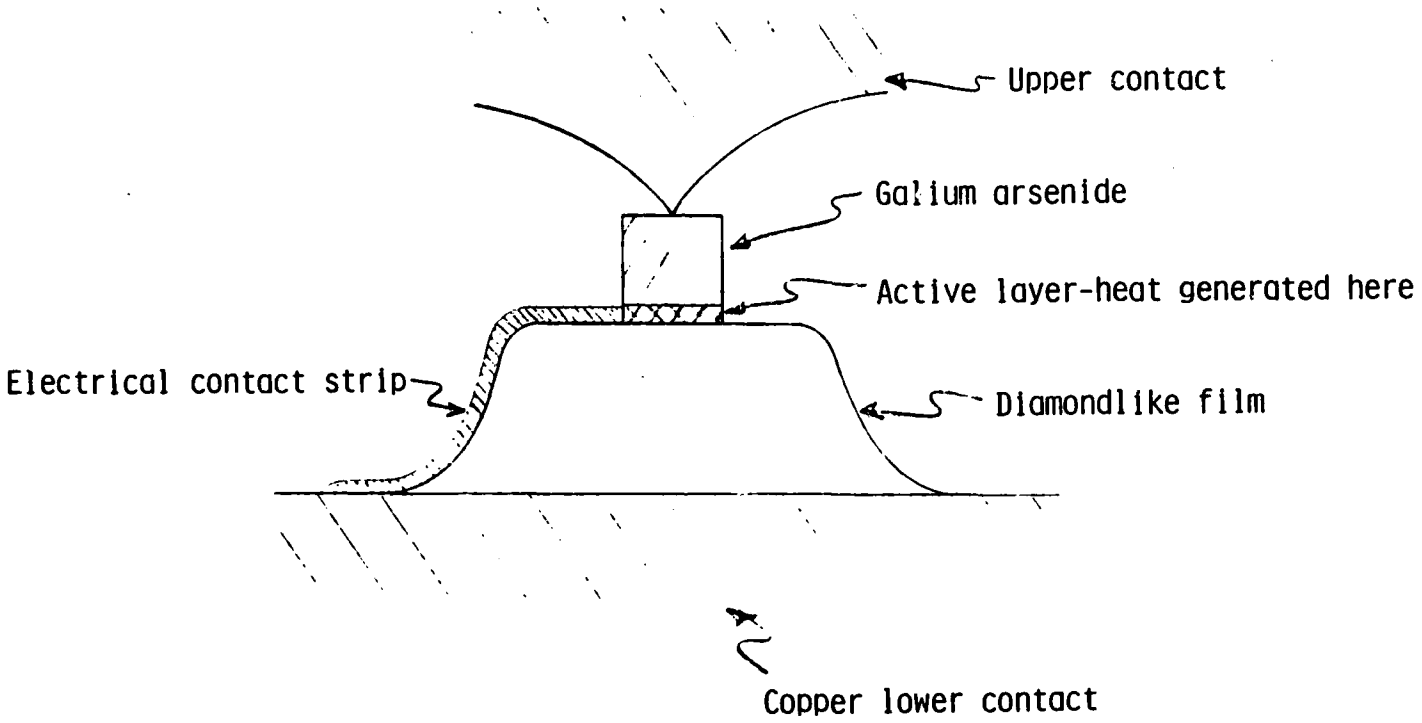
Upper contact
Galium arsenide
Active layer-heat generated here
Electrical contact strip
Diamondlike film
Copper lower contact

DIAMOND'S WIDE BAND GAP MAY ENABLE THE FABRICATION OF NEW TYPES OF HIGH TEMPERATURE SEMICONDUCTORS.

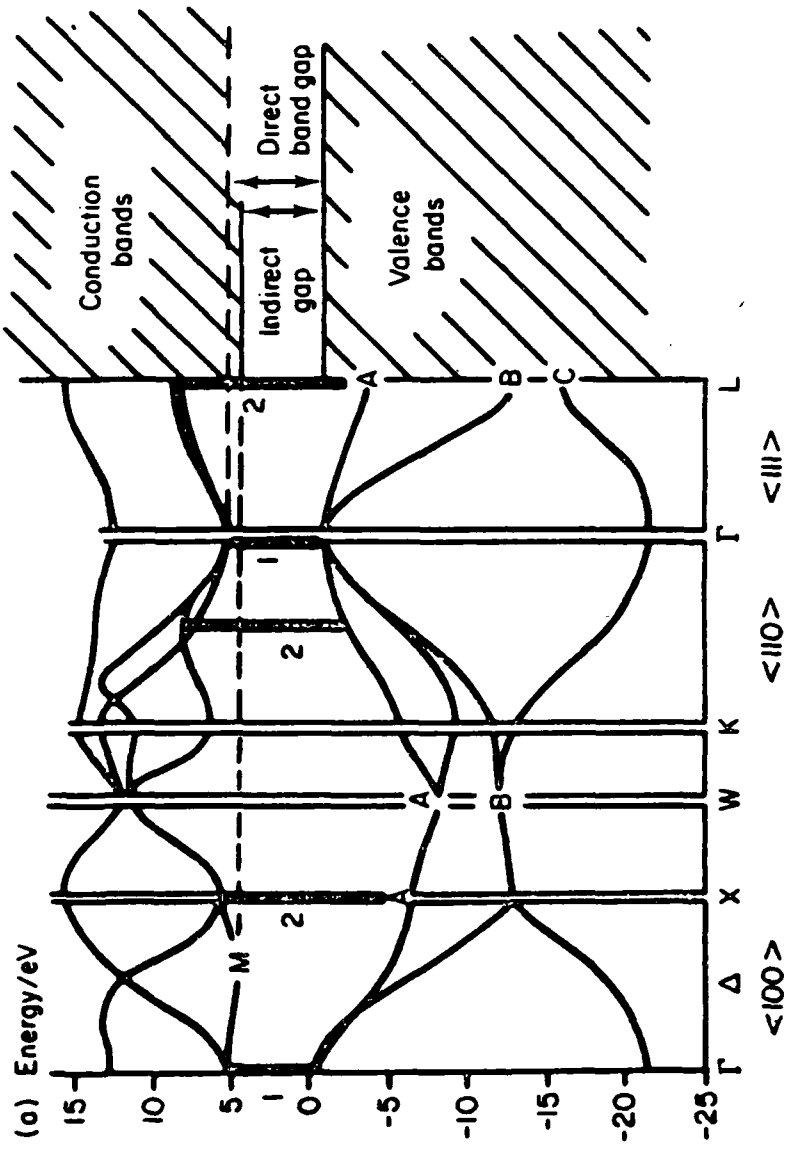
Conduction bands
Direct band gap
Indirect gap
Valence bands
(a) Energy/eV
15
10
5
0
-5
-10
-15
-20
-25
Γ
Δ
X
W
K
Γ
L
<100>
<110>
<111>
M
A
B
C
1
2

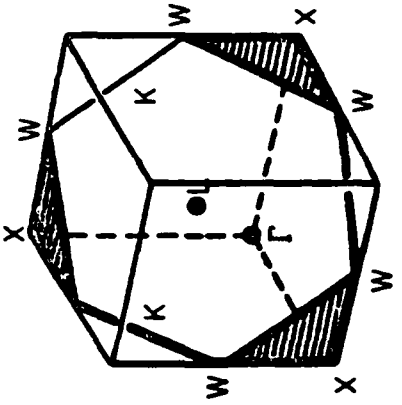
W
X
K
W
X
Γ
K
W
W
X

(b)

DIAMOND SEMICONDUCTORS MAY POTENTIALLY HAVE THE COMBINED ADVANTAGES OF UNIQUE SEMICONDUCTOR CHARACTERISTICS AND GOOD HEAT DISSIPATION.

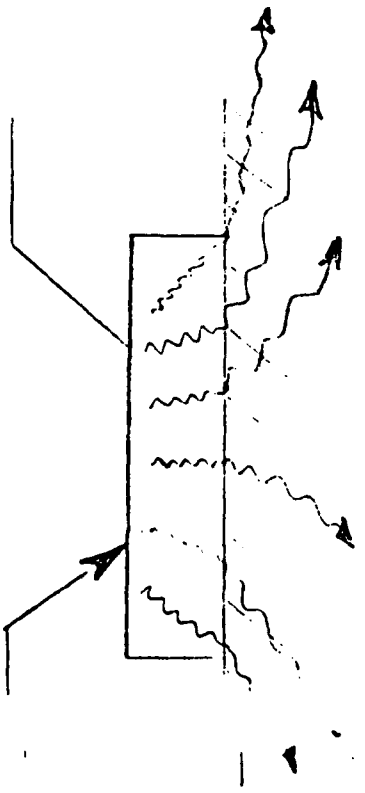

THE CARBON PHASE DIAGRAM SHOWS THAT DIAMOND IS NOT IN A STATE OF STABLE EQUILIBRIUM AT ROOM TEMPERATURE AND PRESSURE. MOST PROCESSES USED TO PRODUCE SYNTHETIC DIAMOND INVOLVE GOING FROM A HIGH PRESSURE AND HIGH TEMPERATUE STABLE DIAMOND STATE TO A HIGH PRESSURE AND LOW TEMPERATURE STABLE STATE THEN TO THE FINAL UNSTABLE LOW PRESSURE AND LOW TEMPERATURE STATE WHERE THE REVERSAL PROCESS TO GRAPHITE TAKES PLACE AT A NEGLIGIBLY SLOW RATE BECAUSE OF THE LOW TEMPERATURE. IT IS THOUGHT THAT MOST OF THE ENERGETIC CARBON ATOM OR ION VACUUM DEPOSITION PROCESSES INVOLVE THIS SAME SEQUENCE OF ENVIRONMENTS BUT IN A QUICK SUCCESSION AND ON AN ATOMIC SCALE.

CARBON PHASE DIAGRAM

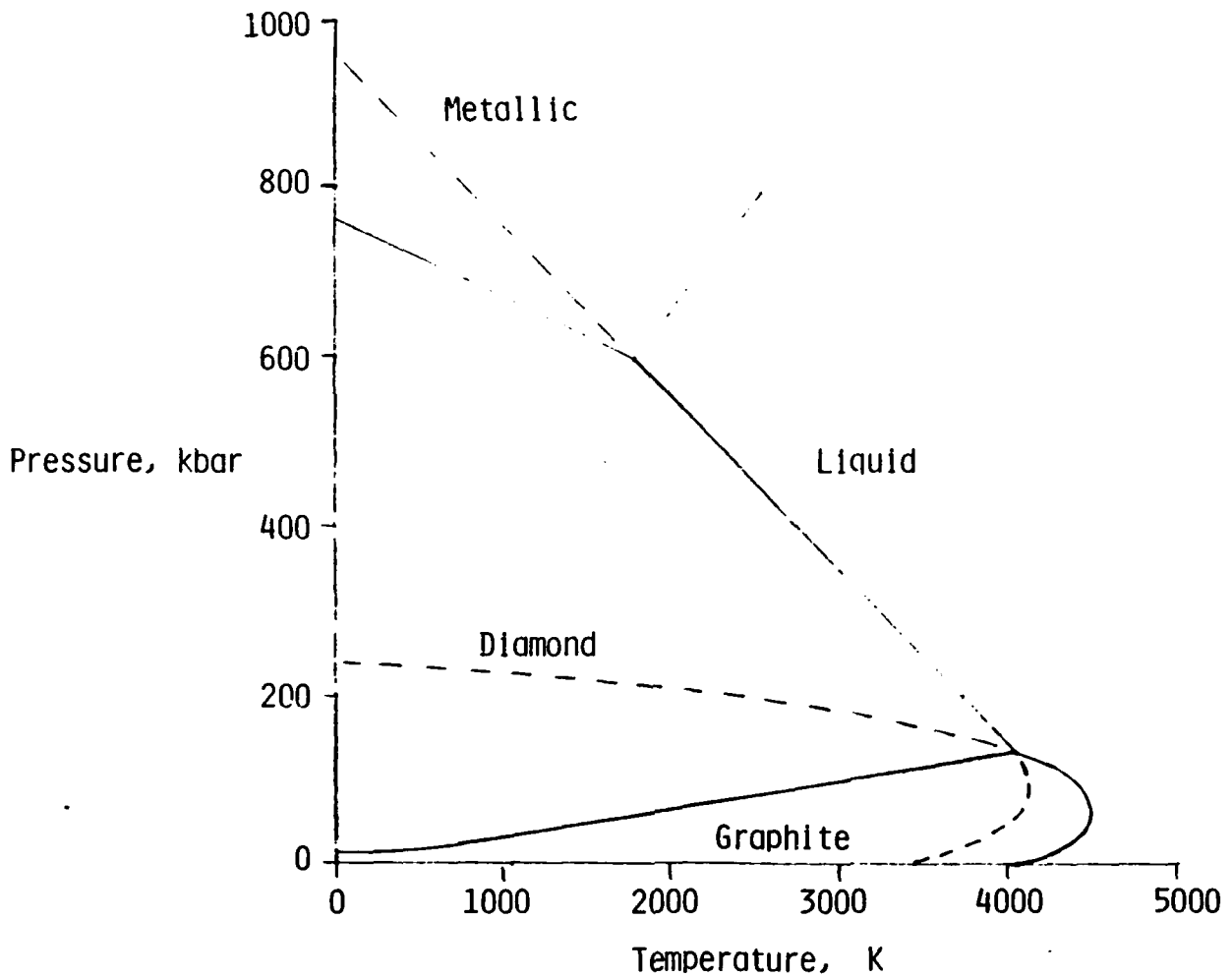

The high pressure high pressure (>60 k bars), high temperature (>1600 k), solvent-catalyst (N_i, C_o, or F_e) technique was first used to produce synthetic diamond by an ASEA laboratory in Sweden in 1953 and later by G.E. in 1955 in U.S.A. It has been the standard technique used to produce commercial industrial diamonds. Shock wave techniques involve dynamic pressures of ~ 1400 K bars and temperatures from 1800 to 3300 K. High temperature (~ 1300 K), low pressure (~ 0.15 torr), and high pressure (~ 2500 K bar) organic gas decomposition onto diamond seed crystals has been used to epitaxially grow diamond. The last general process, energetic carbon deposition in vacuum, allows low temperature fabrication of diamondlike films and is subject of processess currently under investigation by NASA LeRC.

	NASA LEWIS RESEARCH CENTER	NAME BANKS DATE OCT. 1981

DIAMOND SYNTHESIS

- HIGH PRESSURE, HIGH TEMPERATURE, SOLVENT-CATALYST
- SHOCK WAVE
- HIGH TEMPERATURE, LOW PRESSURE AND HIGH PRESSURE ORGANIC GAS DECOMPOSITION ONTO DIAMOND SEED CRYSTALS
- ENERGETIC CARBON DEPOSITION IN VACUUM

Of the nine listed approachs for synthesis of diamondlike films, the top six have been tested to date at LeRC. The last four techniques will be evaluated as soon as construction of the individual experimental apparatus is completed. The top four techniques are relatively low rate ($\sim 10^2 A^o$/min) film deposition processes while the last six are much higher rate ($\sim 10^4 A^o$/min) processes.

	NASA LEWIS RESEARCH CENTER	NAME BANKS DATE

LeRC APPROACH FOR SYNTHESIS OF DIAMONDLIKE FILMS

- CARBON-ARGON ION BEAM SOURCE
- DC HYDROCARBON PLASMA SOURCE
- RF SPUTTERING WITH HYDROCARBONS
- DUAL BEAM METHANE AND ARGON ION SOURCES
- ARGON ION SOURCE WITH CARBON TARGET
- VACUUM ARC CARBON SOURCE
- VACUUM ARC CARBON SOURCE WITH ARGON ION BOMBARDMENT
- COAXIAL CARBON PLASMA GUN SOURCE
- CARBON ION BEAM SOURCE

Use of two ion beam sources has produced our most transparent (with brown to grey color) diamondlike films. The larger ion source is used to deposit the carbon atoms while the small ion source more energetically bombards the surface of the target.

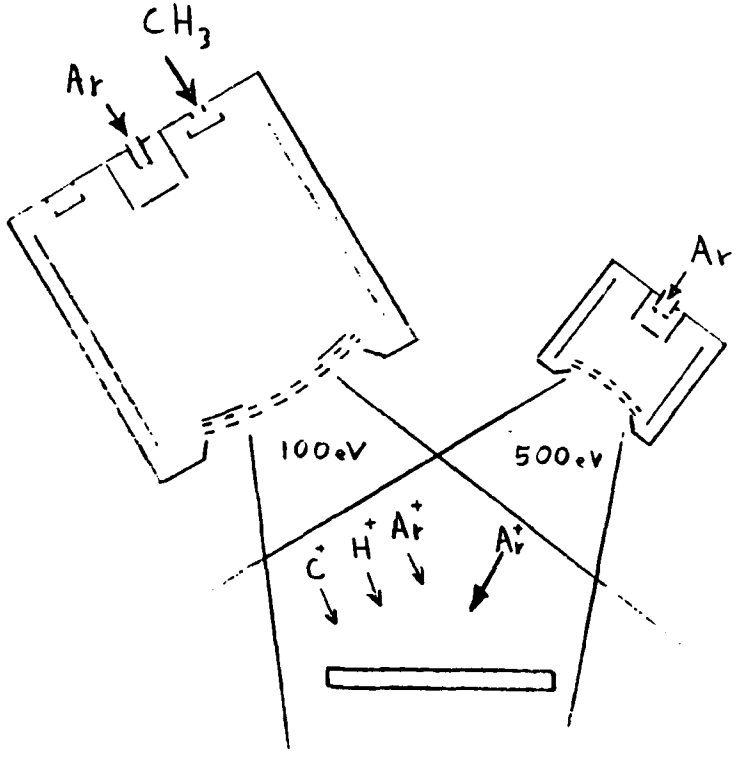

DUAL BEAM METHANE AND ARGON ION SOURCES

A single ion beam can also be used to produce a diamondlike film by sputter deposition simultaneous with lower current density fringe ion beam bombardment of the deposited carbon.

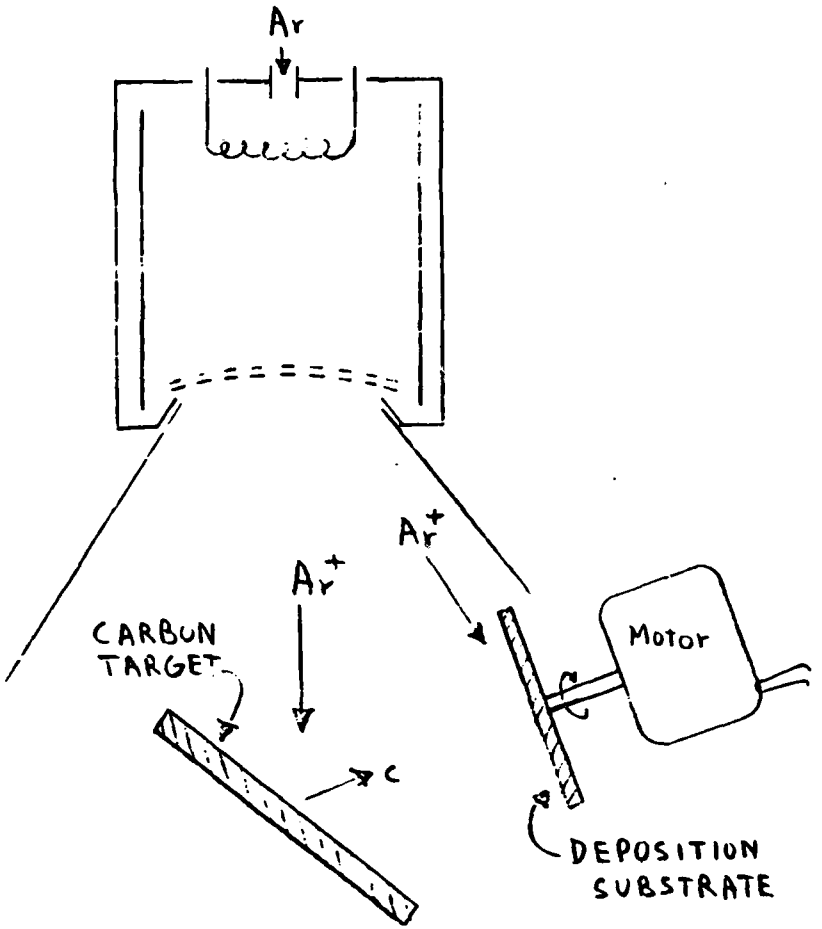

ARGON ION SOURCE WITH CARBON TARGET

A vacuum arc of ~ 30 volts and 100 - 150 amperes can produce a cathode jet along with thermal evaporation of carbon to form high density (2.8 gm/cm^3) diamondlike films.

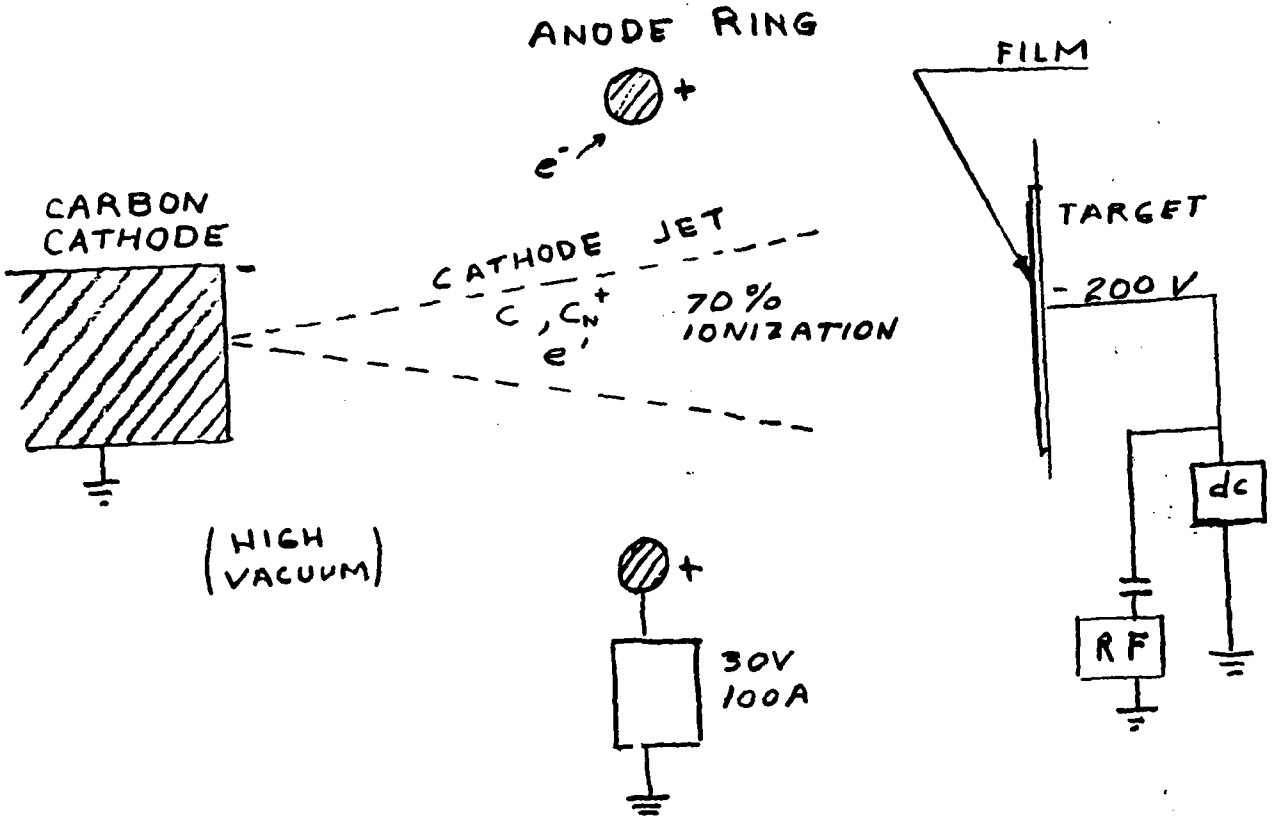

VACUUM ARC CARBON SOURCE

BY ..... DATE .....
CHKD. BY ..... DATE .....
SUBJECT .....
SHEET NO. ..... OF .....
JOB NO. .....

A coaxial carbon rail gun can also produce an intense carbon plasma and accelerate it into a target. Such a device is currently under construction at LeRC.

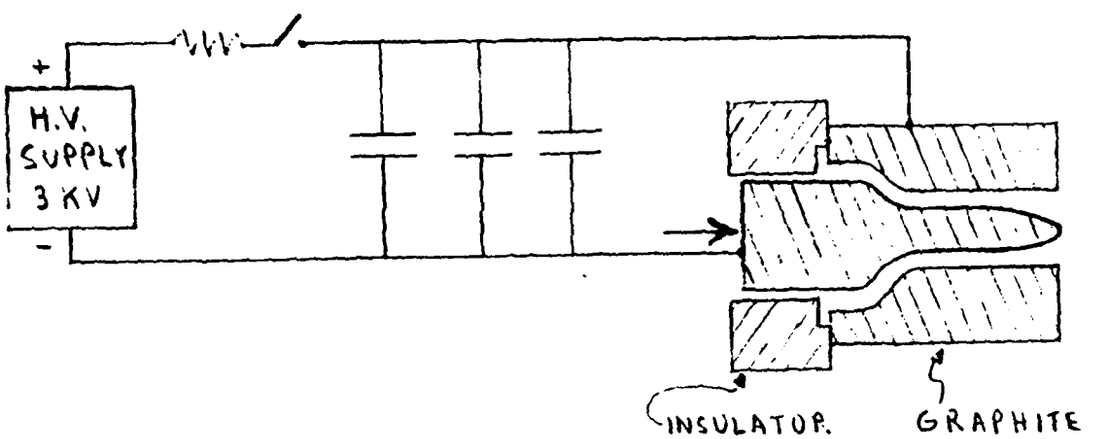

COAXIAL CARBON PLASMA GUN SOURCE

Characterization of the diamondlike films shown in this list is being performed to evaluate film properties, synthesis techniques and potential for applications.

	NASA LEWIS RESEARCH CENTER	NAME BANKS DATE OCT. 1981

CHARACTERIZATION OF DIAMONDLIKE FILMS

- o RHEED
- o AUGER
- o ESCA
- o DENSITY
- o INDEX OF REFRACTION
- o RESISTIVITY
- o RESISTANCE TO $3H_2SO_4$-HNO_3
- o TRANSMISSION ELECTRON DIFFRACTION
- o THERMAL CONDUCTIVITY
- o ELECTRICAL BREAKDOWN STRENGTH

Film characterics known to date indicate strong evidence that they indeed have some but not all of the characteristics of diamond. The films appear to be amorphous yet possess a high population of the sp^3 tetrahedral bonding of diamond.

	NASA LEWIS RESEARCH CENTER	NAME BANKS DATE OCT., 1981

DIAMONDLIKE FILM CHARACTERISTICS

PROPERTY	DIAMONDLIKE FILM	DIAMOND	GRAPHITE
INDEX OF REFRACTION	1.3 - 1.7	2.4	---
RESISTIVITY, CM	10^{10}	10^{4} TO 10^{16}	10^{-5}
RESISTANCE TO $3H_2SO_4$-HNO_3	YES	YES	NO
DENSITY, gm/cm^3	1.9 - 2.8	3.5	2.3

Q & A - B. A. Banks

From: A. H. Guenther, AFWL/CA

Are you aware of anyone using diamond-like films routinely for optical coatings particularly in adverse or advanced technology applications? (Besides Minn-Honeywell Gulf Western Applied Research Lab.)

References

1. Banks, B. A., "Ion Beam Applications Research--a 1981 Summary of Lewis Research Center Programs", NASA TM 81721, 1981.

2. Angus, J. C., Mirtich, M. J. and Wintucky, E. G., "Ion Beam Deposition of Amorphous Carbon Films with Diamond Like Properties", Materials Research Society Conference, November 1981, Boston, Mass.

3. Angus, J. C., "Characterization of Diamond Like Films", NASA Contract Report NASA CR 165493, December 22, 1981.

Ceramics for High Power Sources in Space

Roy W. Rice
Naval Research Laboratory
Washington, D. C. 20375

Abstract

The general potential issues, and forms, of using ceramics in high power sources in space are first briefly reviewed; then some specific examples of using ceramics in energy systems are outlined. Next general ceramic research needs are discussed followed by a discussion of the research opportunities that are seen for ceramics; namely ceramic composites, fiber/whisker processing (especially by polymer pyrolysis), ternary and higher order compounds, and mimicing certain natural fiber-or bio-structures.

GENERAL POTENTIAL AND ISSUES FOR CERAMICS IN HIGH POWER SOURCES IN SPACE

POTENTIAL

- MEDIUM-HIGH STIFFNESS
- LOW-MEDIUM DENSITY
- MEDIUM-HIGH STABILITY (RADIATION AND CHEMICAL)
- HIGH TEMPERATURE CAPABILITY
- WIDE RANGE OF MATERIALS AND HENCE PROPERTIES TO SELECT COMPROMISE FROM
- AVAILABILITY
- COST

ISSUES

- SHAPE, SIZE } (PROCESSING, JOINING)
- PROCESSING, QA; TOUGHNESS, STRENGTH } RELIABILITY
- COST

Fig. 1 lists the major potential advantages of using ceramics and the key issues in their application. The advantages of ceramics mean that they will often be a major factor in the KW/KG effectives of power systems. Note under the issues that processing appears both as a factor in the size and shape as well as a factor in the reliability. Note also that the cost is listed as both an issue and a potential advantage. This results from the fact that potential costs of many ceramics can be quite low when fully developed, but may in fact by an issue in low volume, high technology applications through much of their earlier stages of development.

CERAMIC FORMS AND COMPETITORS

FORMS	COMPETITORS
FIBERS — INSULATION / REINFORCEMENT	REFRACTORY METALS
COATINGS	INTERMETALLICS
BULK	(CARBON)

Fig. 2 lists the ceramic forms and competitors for use in high power sources in space. Ceramic fibers are almost assurredly going to be used in any application, most likely as reinforcement and possibly as insulation. Some important aspects of ceramic fiber opportunities will be addressed later. Ceramic coatings have potential for corrosion, abrasion, and wear resistance. However, since these are likely to be more specialized applications, they are not treated further. The primary focus will be on the possible utility of ceramics in bulk form. The primary competitors for many ceramic applications will be refractory metals and intermetallics; however, the refractory metals suffer the significant disadvantage of high weight and very poor stiffness to weight ratios, as well as cost and often corrosion problems. Intermetallics may have some specialized applications, but in general have many of the same problems of ceramics without some of the important advantages of ceramics. Carbon is listed in parenthesis as a competitor. Carbon materials are really a subset of the ceramic family, but are often considered as a separate class of materials. Carbon both as fibers as well as carbon-carbon composites appear to provide a fairly broad and significant potential for application in high power sources in space, but will not be further directly addressed here.

EXAMPLES OF CERAMIC USES IN HIGH POWER SOURCES

- MHD - INSULATION, ELECTRODES
- HEAT ENGINE COMPONENTS
  - TURBINES - COMBUSTORS, VANES, BLADES, ETC.*
  - PISTON ENGINES - PISTON CAPS, CYLINDER LINERS, ETC.
- HEAT EXCHANGERS*
  - CONTAINERS FOR H. T. SOLAR, E.G. THERMAL/PHOTOVOLTAIC
- NUCLEAR-REACTOR FUEL, CONTROL, MODERATOR (STRUCTURAL?)

*SEE "PROCEEDINGS OF THE WORKSHOP ON HIGH-TEMPERATURE MATERIALS FOR ADVANCED MILITARY ENGINES, VOL. I", ED. BY D. M. DIX, J. E. HOVE, F. R. RIDDELL, IDA LOG #HQ79-2144/1, MAY 1979.

Fig. 3 simply lists some possible examples of high power sources in which ceramics might be used in space based application.

EXAMPLES OF POSSIBLE CERAMIC MATERIALS IN PARTICULAR ENERGY SYSTEMS

TURBINES: CARBON-CARBON (MAINLY CLOSED CYCLE), Si_3N_4, SiC, CERAMIC COMPOSITES, PSZ, COATINGS

PISTON ENGINES: PSZ, CERAMIC COMPOSITES, COATINGS

HEAT EXCHANGERS: SiC, CARBON-CARBON (SEALED, E.G. WITH SiC), Si_3N_4

THERMAL-PHOTOVOLTAIC (HEAT STORAGE BOTTLE): Si_3N_4, $3Al_2O_3 \cdot 2SiO_2$

MHD
- ELECTRODES: ZrO_2, CHROMITES? SPINELS, SiC, ZrB_2-SiC
- INSULATOR: MgO, Al_2O_3, BeO

Fig. 4 lists some of the specific ceramic materials that might be used in some of the possible space power sources. Note that while new candidates might be added at any time for any of these applications the candidates listed for the last two items, thermal photo voltaic and MHD, and are probably the most uncertain at this time. Also the MHD materials listed are those for long term application, since short term MHD power sources may not require ceramics.

Fig. 5 lists some of the general ceramic research needs that will have to be addressed for many if not all applications of ceramics in space power sources. In general the needs are listed in order of decreasing overall importance as one proceeds both down the page and to the right of the page. While this list may appear as motherhood and mundane items, it covers the central issues that typically pace ceramic development. Those seriously wanting or needing the significant advantages of ceramics must "bite the bullet" and do some of the necessary R & D, glamorous or not.

GENERAL CERAMIC RESEARCH NEEDS

- PROCESSING - METHODS, CONTROLS
  POWDER PROCESSING
  OTHER PROCESSING, E.G. MELT, CVD
- QA - NDE, PROOF TESTING
- JOINTS - MECHANICAL, SOLDERED, BRAZED, BONDED, WELDED
- COMPATIBILITY - PHASE DATA
- STABILITY (RADIATION, COMPOSITION, VAPORIZATION)

Fig. 6 lists some ceramic research opportunities which could have quite significant impact on not only ceramic utilization in high power sources in space, but a variety of other important applications. Note that the first three of these can all have significant impact on fibers and whiskers for reinforcement in a variety of matrices, and that the first three and also possibly the fourth one, can have significant impact on the development of ceramic composites, which probably represents one of the most significant new opportunities for use of bulk ceramics in this, as well as many other, applications.

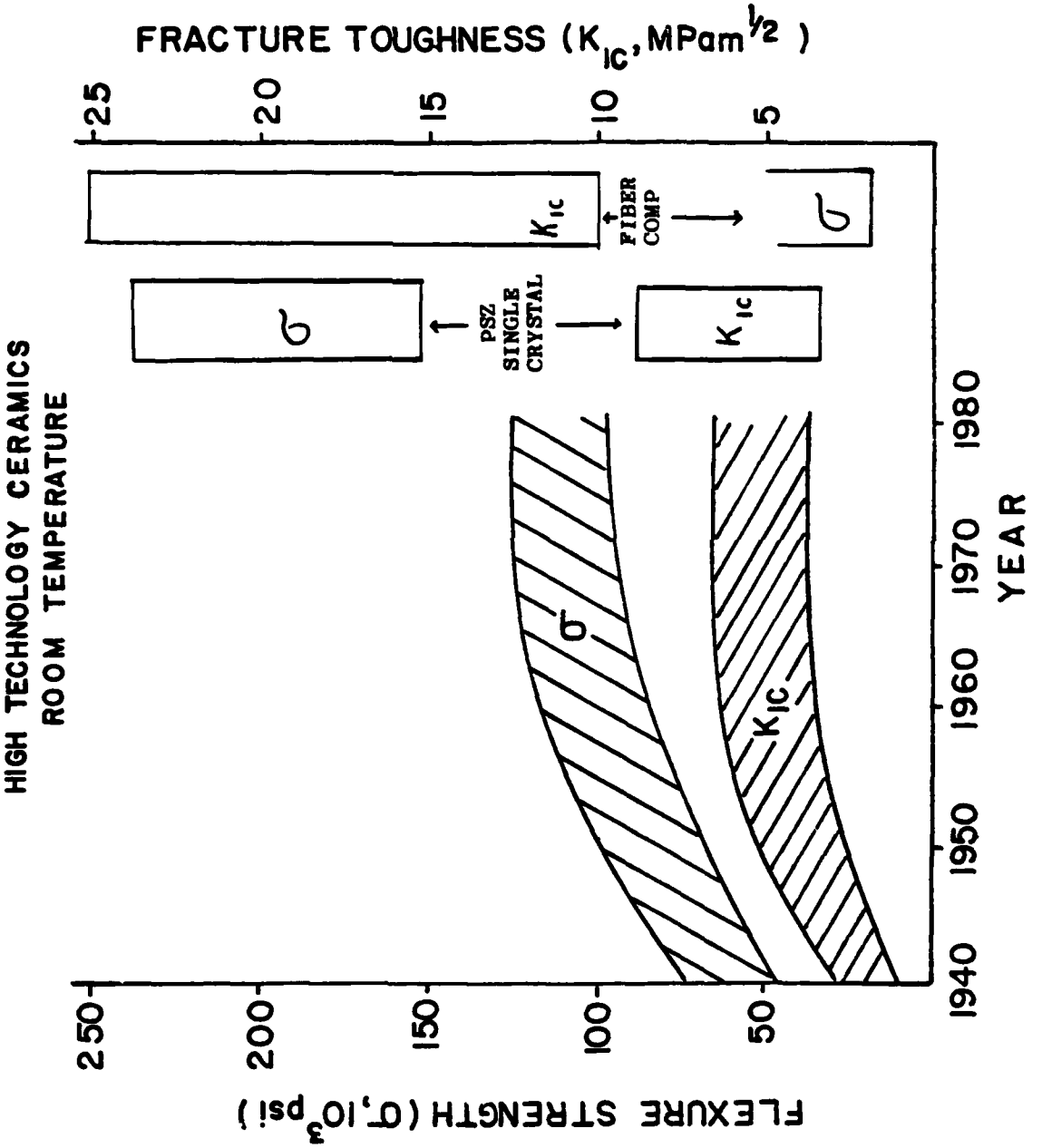
FRACTURE TOUGHNESS (K_{IC}, MPam$^{1/2}$)
25
20
15
10
5
K_{IC}
FIBER COMP
σ
σ
PSZ SINGLE CRYSTAL
K_{IC}
HIGH TECHNOLOGY CERAMICS
ROOM TEMPERATURE
σ
K_{IC}
1940
1950
1960
1970
1980
YEAR
250
200
150
100
50
FLEXURE STRENGTH (σ, 10^3 psi)

CERAMIC RESEARCH OPPORTUNITIES

- POLYMER PYROLYSIS
- OTHER FIBER AND WHISKER PROCESSES
- TERNARY AND HIGHER ORDER COMPOUNDS
- UNIQUE STRUCTURES (E.G. MIMICING BIOSTRUCTURES)
- CERAMIC COMPOSITES

Fig. 7 illustrates some of the significant potential that ceramic composites have already demonstrated. The crossed hatched regions illustrate the history of fracture toughness and strength at room temperature of essentially the best high technology ceramics. Note that we have been approximately on a plateau for about twenty years, until the recent composite developments illustrated here by the two most significant examples; namely, partially stabilized zirconia (PSZ) single crystals and ceramic fiber composites. Note the very high PSZ range of average strengths for different compositions are due to significant improvement in fracture toughness (K_{IC}) in these single crystals. These single crystals are sufficiently large in size and potentially low enough in cost that they could be used for some important components, such as small nozzles, possibly even turbine blades. The mechanisms involved also imply significant opportunity for further toughening and strengthening ceramics by precipitation or other techniques such as dispersing fine ceramic particles of the right character in appropriate matrices. The second item shown is fiber composites where refractory ceramic fibers are in refractory ceramic, nonglass based, matrices. The ranges shown are based on initial work in the author's laboratory showing fracture toughnesses approaching, if not in fact overlapping those of metals. While the present strengths are not particularly high, it should be noted that the same range, if not a higher range, of fracture toughnesses with strengths in the 50,000 to 100,000 PSI range, have been fairly extensively demonstrated in excellent work at United Technology Research Center, using either graphite or fine silicon carbide fibers in glass based matrices. This later material system might be a particulary interesting and potentially very important for some space applications.

CERAMIC OPPORTUNITIES

TERNARY AND HIGHER ORDER COMPOUNDS

- MOST CERAMIC WORK ON BINARY COMPOUNDS, E.G. Al_2O_3, MgO, AlN, Si_3N_4, B_4C, SiC
- TERNARY AND HIGHER ORDER COMPOUNDS OFFER WIDER RANGE OF PROPERTIES:

  E.G. MULLITE ($3Al_2O_3.2SiO_2$) - LOWER DENSITY,

  10-FOLD GREATER CREEP RESISTANCE THAN Al_2O_3

  AT 1400°C

- MANY MORE KNOWN AND FEASIBLE, E.G.

$9Al_2O_3 \cdot 2B_2O_3$	Al_4SiC_4
$AlNbO_4$	$BeSiN_2$
$ZrO_2 \cdot SiO_2$	Al_5NC_3

Fig. 8 briefly outlines the opportunities of developing ternary and higher order ceramic compounds. Most ceramic development, especially for structural or high temperature applications, has focused almost exclusively on binary compounds, that is compounds consisting of only two different types of atoms, as indicated by the examples shown. However, ternary and higher order compounds consisting of three, four, etc., different types of atoms are known to exist in a far wider range of properties. This is widely illustrated in the area of electronic and magnetic materials and also in some of our low expansion ceramic materials, where we have already gone to many of these more complex compounds, because of the better properties that can often be obtained in them. That this opportunity also exists for mechanical and thermal behavior is illustrated by only one example here, mullite which has lower density and yet ten fold greater creep resistance than Al_2O_3 at 1400°C. Many more compounds are known and still many, many more are feasible. Only a few limited examples are cited here. There are a number of examples that are known or about which sufficient information exists, to suggest that they could be quite beneficial, if they were developed. In the longer range, what is needed is to take advantage of the developing capability in solid state physics and chemistry, to estimate, project, or even predict, properties or ranges of properies with new structures, in order to identify promising classes of compounds for advanced applications.

Fig. 9 outlines the opportunity of making ceramics by polymer pyrolysis. This is probably one of the most significant opportunities of ceramics, especially with reference to space applications. Basically, the concept here is in direct analogy with the forming of many carbon products, such as graphite fibers, wherein a polymer consisting of many of the necessary carbon-carbon bonds, is utilized often with shaping of the final product in the original polymer state, followed by heating to remove the hydrogens leaving only the carbon skeleton. It is now known that several important ceramics such as BN, B_4C, SiC and Si_3N_4 can be made via this route. There may be potentially important opportunities of making bulk materials, especially as composities and coatings by using this technique. However, for space applications forming of foams and especially fibers may be of particular importance. There are important opportunities for single compositions made by polymer pyrolysis of which one of the most important is probably BN-BN composites in direct analogy with carbon-carbon composites. However, there are also a number of important opportunities for mixed compositions as illustrated on the next slide.

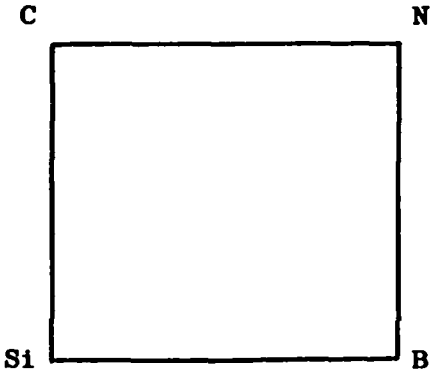
C
N
Si
B

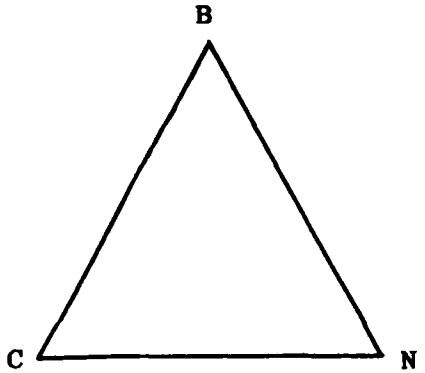
B
C
N

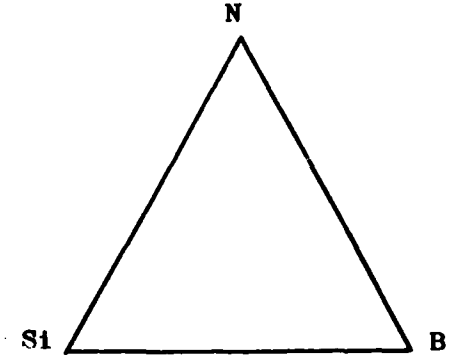
N
Si
B

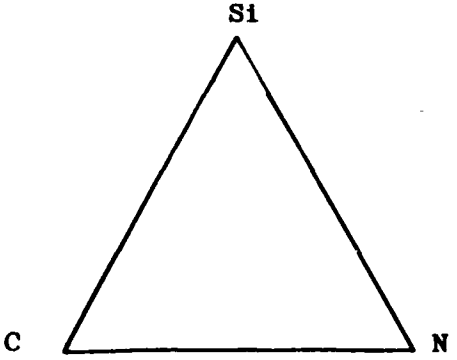
Si
C
N

CERAMIC OPPORTUNITIES

POLYMER PYROLYSIS

FORMS: BULK (ESP. COMPOSITES), COATINGS,
FOAMS, FIBERS

COMPOSITIONS: SINGLE (E.G. BN-BN IN ANALOGY
(WITH CARBON-CARBON), MIXED

Fig. 10 illustrates the "quaternary" system over which polymer pyrolysis is probably of greatest interest, and the three "ternary" systems are illustrated to suggest three of the potentially most important combinations out of that "quaternary" system. Whether such pyrolysis was used for fibers, bulk or other forms, it is important to note two potentially significant advantages that might be obtained from bodies from these ternary mixtures. Thus note that BN is a very good dielectric, while B_4C is an intrinsic electrical conductor and Si_3N_4 is a fairly good dielectric and SiC ranges from a fairly good dielectric to a semiconductor. Thus, a wide range of electrical behavior which may be important in some applications should be achievable from these different combinations. Similarly note that BN has extremely anisotropic expansion, ranging from $\leq 1 \times 10^6$ in the "a" direction, to probably of the order of 30×10^6 ^oC in the "c" direction. On the other hand, B_4C and SiC are reasonably isotropic in their expansion and average about 5×10^6 $^oC^{-1}$, Si_3N_4 is relatively isotropic and has an even lower expansion about 3×10^6 $^oC^{-1}$. Thus, there also may be significant opportunities for varying thermal expansion of either fibers or matrices made from these different systems. Developing fibers of good strength and high modulus with a significantly wider range of thermal expansions to better match to either ceramic or other matrices for further improved composite development could be very significant.

CERAMIC OPPORTUNITIES

UNIQUE STRUCTURES

FIBER STRUCTURES

	YOUNGS MODULUS, E, (10^6 PSI)	FRACTURE TOUGHNESS K_{IC} (MPA $M^{1/2}$)
JADITE	20	7
NEPHRITE	30	5-10

BIOSTRUCTURES - SOME BIOSTRUCTURES, SUCH AS SOME ANIMAL SHELLS, HAVE EXTREMELY HIGH STRENGTH TO DENSITY RATIOS, OFTEN DUE TO GEOMETRY OF OPEN STRUCTURES FORMED BY GEOMETRY OF CRYSTAL (E.G. $CaCO_3$) PLATELETS, OR RODS (WHISKERS).

Fig. 11 outlines ceramic opportunities from unique structures Basically two classes of materials are seen here. First are fiber structures of which jadite and nephrite are two of the most important natural examples. They have reasonable Young's moduli and substantially higher than normal toughness in comparison to other ceramic (for reference toughnesses of 4 to 6 $MPa/m^{1/2}$ are normally considered high for ceramic materials). Synthetically duplicating these Jade type structures in appropriate ceramic materials could have very significant impact on ceramic applications because of the toughness potential this offers. Note that this might be done in very similar compositions to those of the natural materials, but may also be an important product of research from ternary and higher order compounds wherein one might be able to achieve these same fibrous structures which are associated with high toughness in much more refractory syscems, e.g. possibly some nitro-silicide or carbo-boride etc., systems. The second area of unique structures is the possibility of mimicing bio-structures, such as some animal shells which have extremely high strength to density ratios. Duplicating these structures, which often consist of partially open structures of crystal platelets or whiskers, also could have extremely important long range impact on the ability of ceramic materials.

BIBLIOGRAPHY

1. R. W. Rice, "Ceramic Composites-Processing Challenges," Cer. Eng. and Sci. Proc. 2 (7-8) 493-508, July/Aug 1981.

2. R. W. Rice, "Mechanisms of Toughening in Ceramic Matrix Composites," Ibid, pp 661-701.

3. R. W. Rice, "C. E. Matt, W. J. McDonough, K. R. McKinney, and C. Cm. Wu, "Refractory Ceramic Fiber Composites, Progress, Needs, and Opportunities," to be published in Cer. Eng. and Sci. Proc.

4. R. W. Rice and K. J. Wynne, "Ceramics Made by Polymer Pyrolysis," to be published in Annual Rev. of Mat. Sci., Vol. 12.

5. Karl M. Prewo, John J. Brennan, "High-Strength Silicon Carbide Fibre-Reinforced Glass-Matrix Composites", J. Mat. Sci., 15 (1980), 463-468.

6. R. A. J. Sambell, A. Briggs, D. C. Phillips, D. H. Bowen, "Carbon Fibre Composites with Ceramic and Glass Matrices", J. Mat. Sci., 7 (1972) 676-681.

MATERIALS TECHNOLOGY FOR LARGE SPACE STRUCTURES

CHARLES P. BLANKENSHIP and DARREL R. TENNEY
LANGLEY RESEARCH CENTER

SPECIAL CONFERENCE ON
PRIME POWER FOR HIGH-ENERGY SPACE SYSTEMS
AIR FORCE OFFICE OF SCIENTIFIC RESEARCH
NORFOLK, VIRGINIA
FEBRUARY 22-25, 1982

INTRODUCTION

Large space structures systems technology is a continuing research activity within NASA. This research relates to several spacecraft concepts for future space missions such as communications antennae, solar reflectors, science and applications platforms, satellite power systems, and a space operations center. Figures 1-3 illustrate three concepts for large space structures. The wrapped-rib and hoop-column antenna concepts represent deployable structures. Both are designed to be packaged in a compact manner for launch using a space shuttle type mission. An erectable structure can be of compact design also and meet the volume limitations of a shuttle mission. The truss structure shown has several unique design features to make erection in space fairly simple and expedient. Several of the system definition studies related to these advanced concepts have progressed to the conceptual design stage. Thus, adequate guidelines are available to assess some of the key material technology needs. Research related to several of the identified needs has been initiated.

This paper will outline several of the key material technology needs that have been identified for large space structures. They include lightweight structural materials, materials durability in the space environment, and some special aspects of materials fabrication technology. Examples of current materials research directed toward large space structures are described. Additional research needs and opportunities are noted. A short bibliography is included of selected references that describe large space structural concepts and related technology needs in detail.

NASA
L-82-1,658

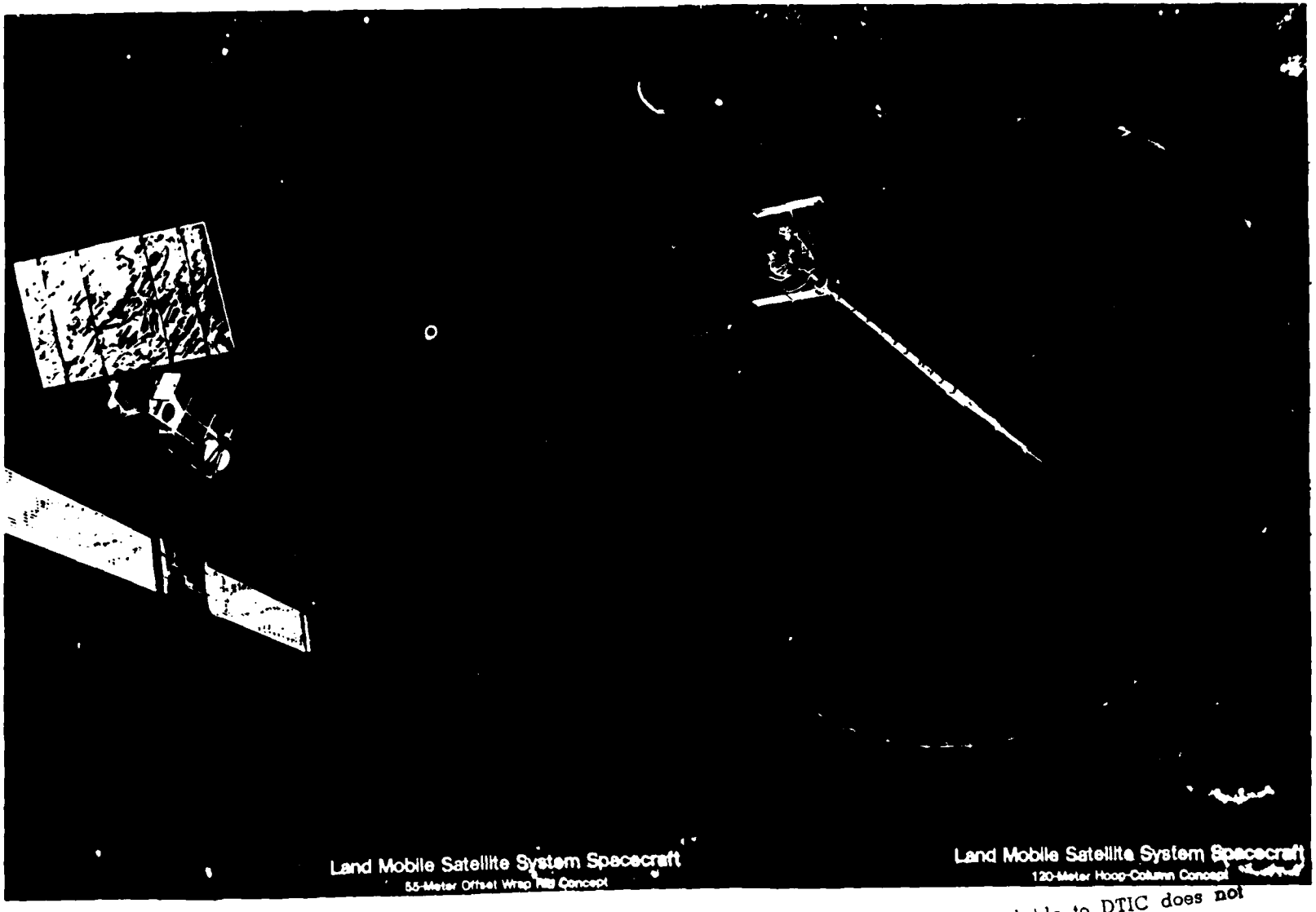

Figure 1.

Copy available to DTIC does not permit fully legible reproduction

NASA
L-82-1,168

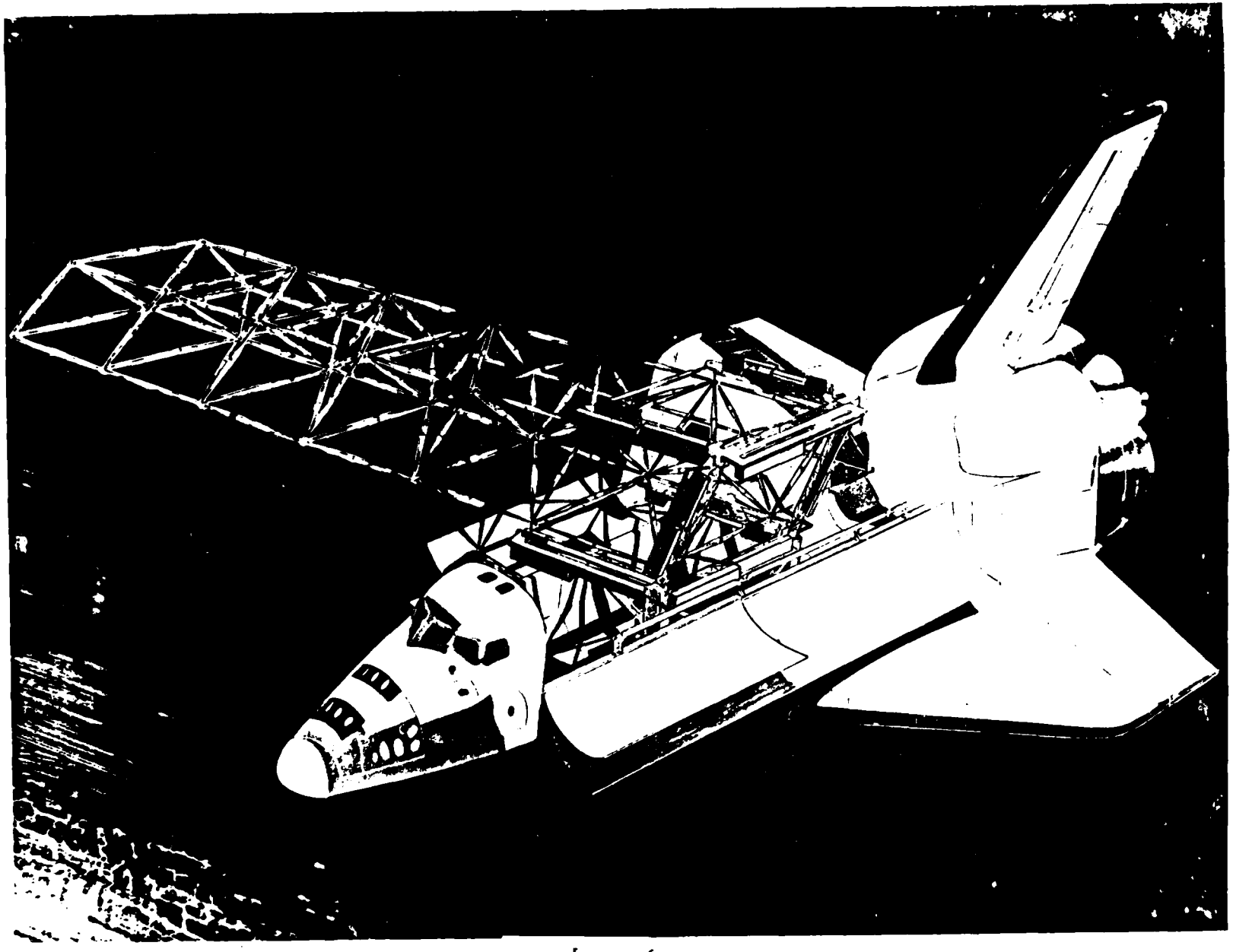

VII-14-3

Figure 2

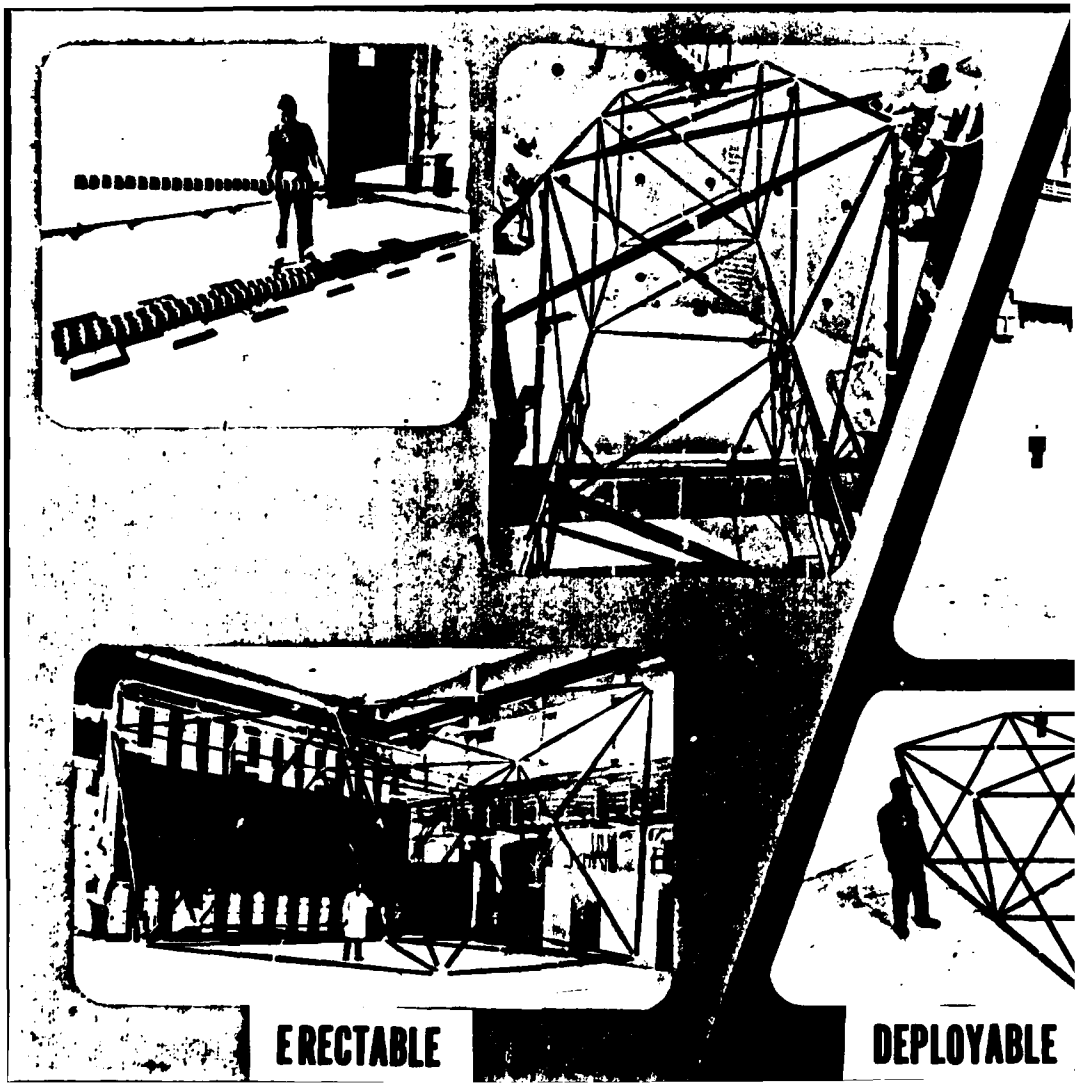
ERECTABLE
DEPLOYABLE

MATERIALS TECHNOLOGY NEEDS

Materials technology needs for large space structures are summarized in figure 4. Structural requirements generally focus on lightweight and high stiffness. Minimizing structural weight is a driver from the aspects of payload capability of launch vehicles and costs associated with a space mission. Stiffness is a key requirement from the aspects of structural stability, particularly in structural configurations exceeding 10-15 meters in diameter. For applications demanding high precision, such as antennae, both stiffness and dimensional stability become significant design factors. Composite materials, both of the metal and polymer matrix class, generally offer the best potential of meeting the requirements of high stiffness combined with low weight. Providing composite materials with the optimum characteristics for large space structures presents a long term, research challenge.

Materials durability in the space environment becomes a dominant issue for long-life space missions, e.g., 10 to 20 years. This is of particular importance for spacecraft operating in geo-synchronous orbit where space radiation (e^-, p^+, UV) intensities are sufficient to degrade the performance of materials. Spacecraft temperature changes can range as much as $\pm 200^{o}F$. Minimizing this temperature change becomes critical for those applications requiring precision structural stability. Thermal control coatings offer the potential to significantly reduce changes in structural temperatures. However, their long-term durability in the space environment is uncertain.

Construction of large, precision structures that can be packaged for a space launch and subsequently erected in space offers many opportunities for innovative material fabrication concepts. Structural members require close dimensional tolerances as well as reliable and highly efficient joints. Some structural concepts have unique requirements such as high stiffness tension cables and thin, polymeric membranes to provide durable reflective surfaces.

MATERIALS TECHNOLOGY NEEDS FOR LARGE SPACE STRUCTURES

STRUCTURAL EFFICIENCY

- o LIGHTWEIGHT
- o HIGH STIFFNESS
- o DIMENSIONAL STABILITY

ENVIRONMENTAL STABILITY

- o RADIATION
- o THERMAL

FABRICATION CONCEPTS

- o PRECISION MEMBERS
- o STRUCTURAL JOINTS
- o THIN MEMBRANES
- o TENSION CABLES

Figure 4.

HIGH STIFFNESS LOW THERMAL EXPANSION SPACE MATERIALS

Materials suitable for large space structures, where dimensional stability is critical, must possess both a high specific stiffness (E/P) and a low thermal expansion (CTE). Conventional aerospace materials such as aluminum and titanium do not provide these characteristics whereas advanced graphite fiber reinforced composites do. The CTE values and specific stiffnesses of graphite composites and selected other low expansion materials are compared in figure 5. Quartz and ULE (titanium silicate glass) fall within the preferred range of CTE but do not provide the needed stiffness. A range of values are shown for both the graphite/resin and graphite/metal composites indicating the flexibility that these composites offer for tailoring properties by varying the fiber type and ply orientation. Graphite/resin and graphite/metal composites both provide the needed CTE values and can be selected for a particular application depending on the stiffness requirements. Graphite/glass (GY70/Gl) has a very low CTE and high stiffness but its low thermal conductivity may make it undesirable in applications where large thermal gradients could cause warping of the structure.

Metal matrix composites (graphite/aluminum and graphite magnesium) research for space structures is being conducted in several Department of Defense programs. Resin matrix composites (graphite/epoxy, graphite/polyimide, and graphite/advanced resins) research is the primary focus of the NASA program. Each of the composite materials has potential advantages for large space structures. Continued research on both classes of composite materials is warranted to assure their technology readiness and to provide the designer with material options for optimum structural design.

HIGH STIFFNESS LOW THERMAL EXPANSION SPACE MATERIALS

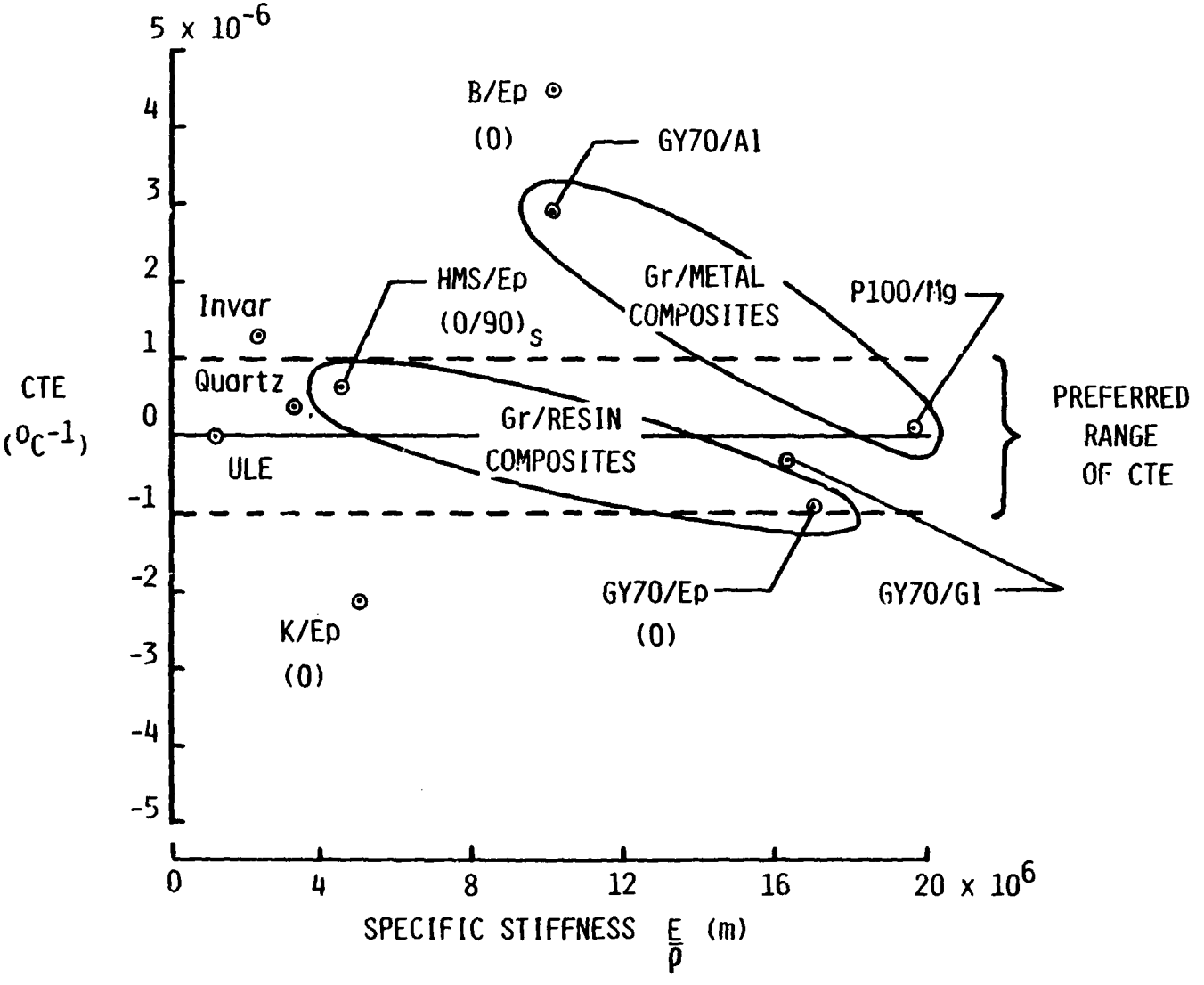

Figure 5.

ADVANCED POLYMERIC MATERIALS

Research opportunities to enhance the potential of polymeric materials for large space structures include the development of tougher matrix resins and high performance films, figures 6, 7, and 8. Current graphite/epoxy composites appear to meet stiffness and weight requirements. But the brittle nature of epoxies makes this class of material suspect for long life missions. Resistance to microcracking from thermal strains and radiation induced embrittlement is of primary concern. Other resin systems such as thermoplastics would appear to have excellent potential to improve composite toughness. However, space radiation induced property changes are not well understood in any of the polymeric materials of interest for advanced matrix resins. Current research in understanding the performance of polymers in the space radiation environment is described in another section of this paper. This research should provide guidance in the synthesis of polymer resins having the potential of long-time structural stability in the space environment.

High performance polymer films covers that class of material with properties tailored to enhance the performance of space structure systems. For example, the addition of metallic ions to polymer films can increase the electrical conductivity several orders of magnitude. This type of material can be useful in controlling spacecraft charging. Also, the metallic ions might provide some unique features to the polymers in resisting space radiation degradation. Tailoring the chemical structure of polymer films to achieve transparency or a specific color for applications such as thermal control coatings illustrates another example of a materials research opportunity for large space structures.

NASA
L-81-2568

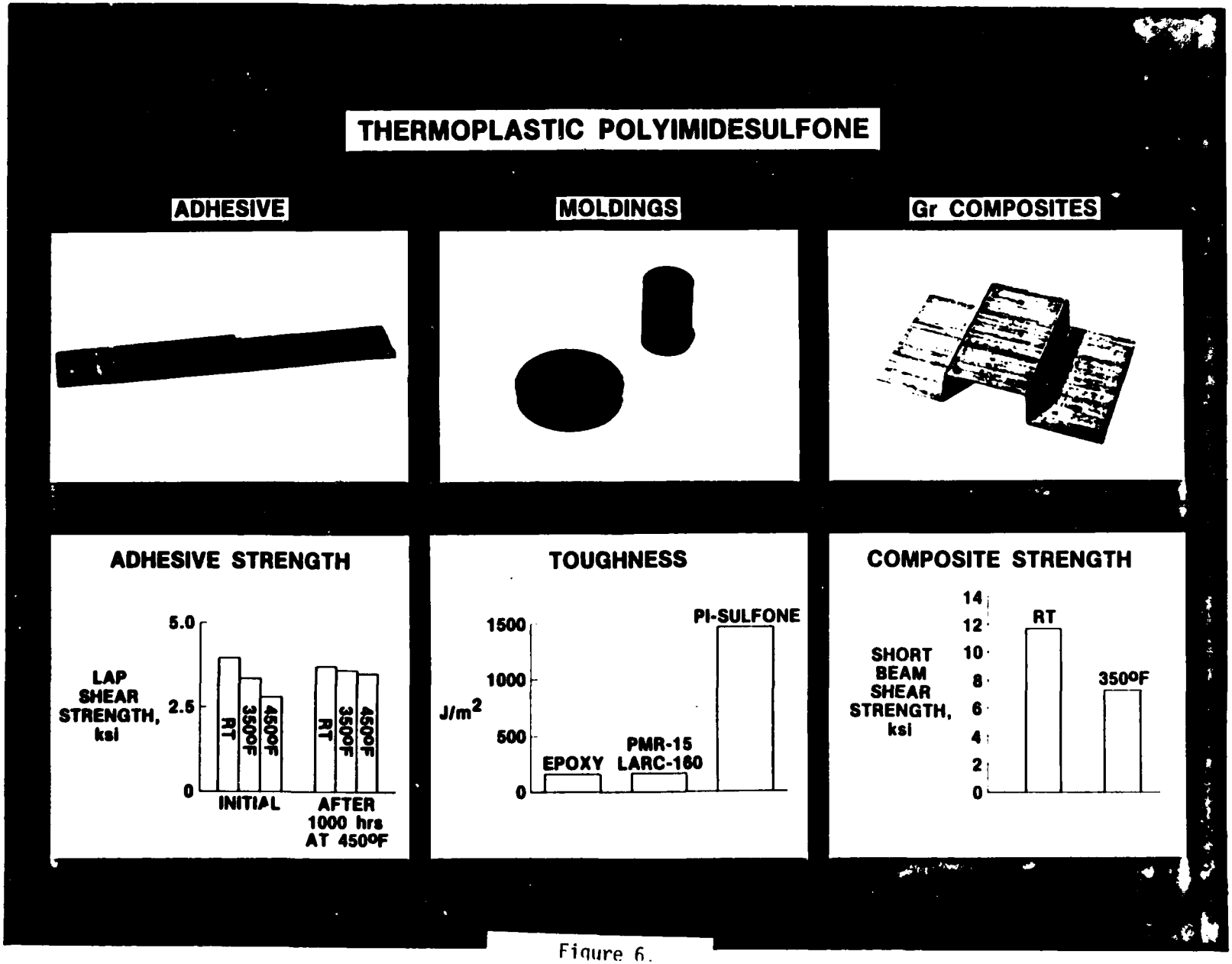

Figure 6.

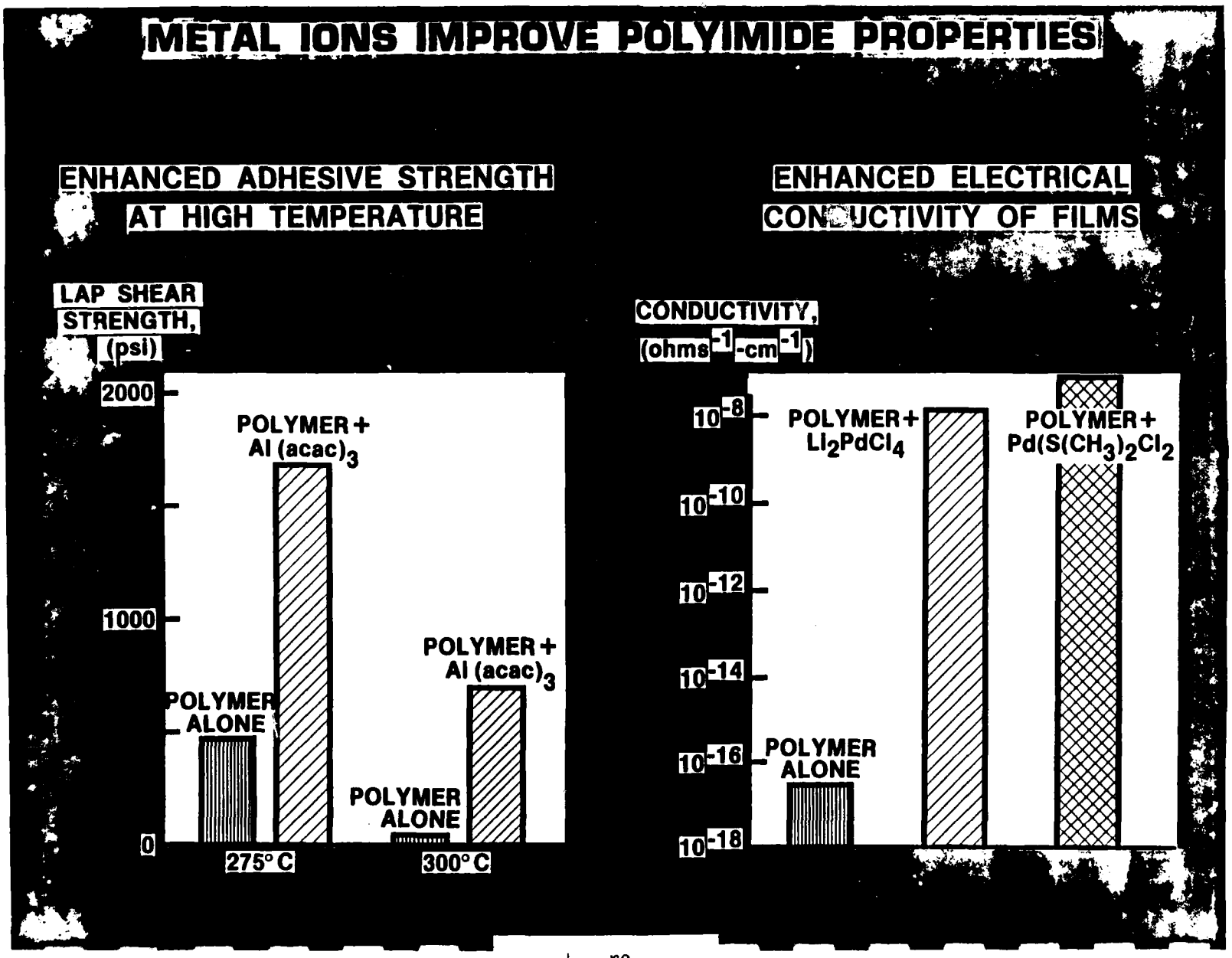
METAL IONS IMPROVE POLYIMIDE PROPERTIES
ENHANCED ADHESIVE STRENGTH AT HIGH TEMPERATURE
LAP SHEAR STRENGTH, (psi)
2000
1000
0
POLYMER + Al (acac)3
POLYMER ALONE
POLYMER + Al (acac)3
POLYMER ALONE
275° C
300° C
ENHANCED ELECTRICAL CONDUCTIVITY OF FILMS
CONDUCTIVITY, (ohms-1-cm-1)
10-8
10-10
10-12
10-14
10-16
10-18
POLYMER + Li2PdCl4
POLYMER + Pd(S(CH3)2Cl2
POLYMER ALONE

Figure ..

NASA
L-81-10,398

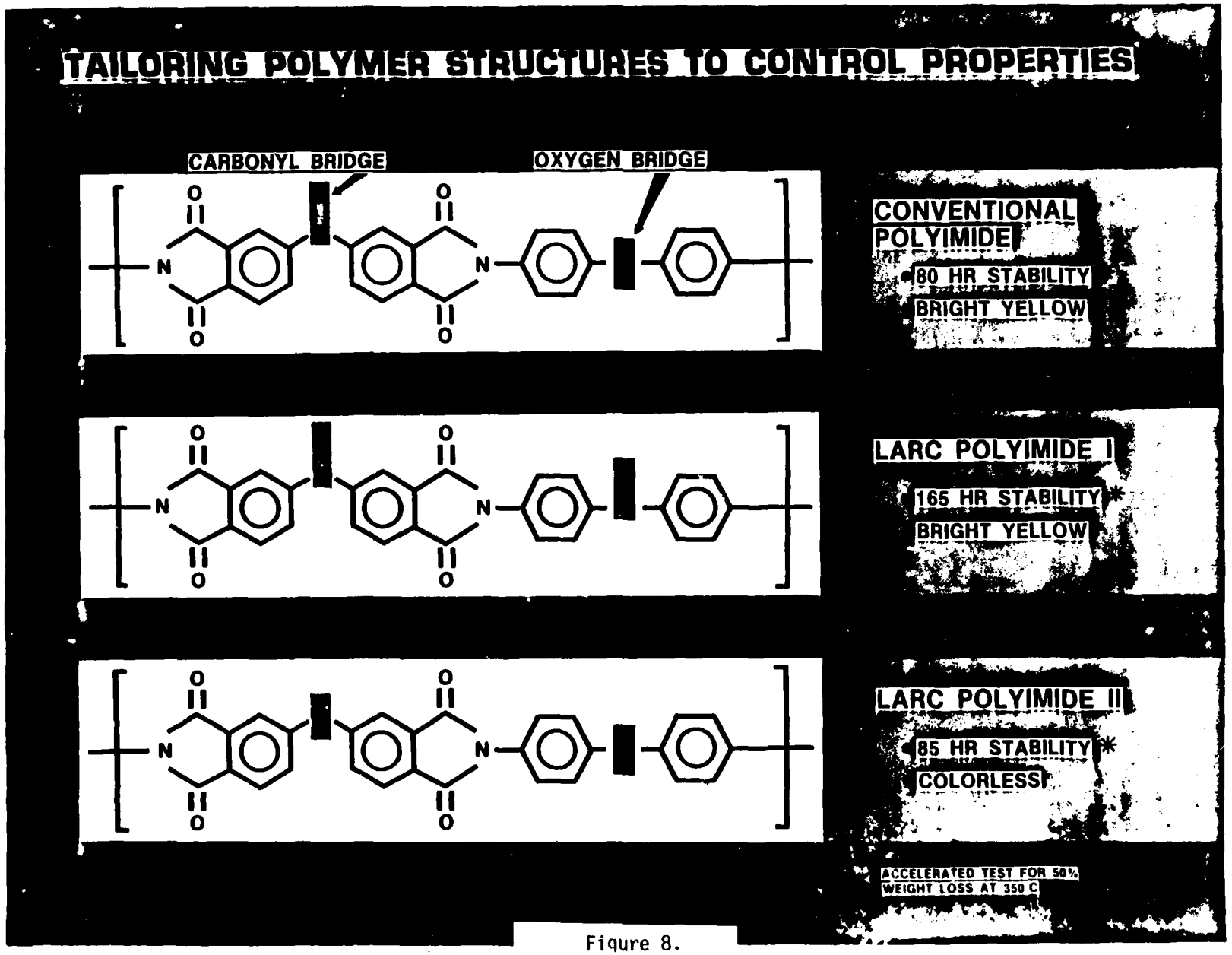

Figure 8.

DURABLE SPACE MATERIALS

Space durable materials are a necessary requirement to achieving long-life space structures, figure 9. As previously noted, materials of construction will include advanced metal and polymer matrix composites, coatings for thermal control, polymer films, and adhesives. In low earth orbit (LEO) materials will be subjected to repeated thermal cycles from approximately +200°F to -200°F, UV radiation, and ultra-high vacuum. Micrometeroids and space debris are also considered hazards in LEO. For higher orbits, such as geo-synchronous earth orbit (GEO), the materials will be subjected also to large doses of high energy electrons and protons. The primary concerns for resin matrix composites are radiation induced changes in mechanical and physical properties and dimensional stability as well as microcracking due to residual stresses produced during thermal cycling. Similarly, the residual strains produced by the thermal expansion mismatch between the fibers and the matrix in metal matrix composites are likely to affect the dimensional stability of these materials.

Long-life coatings are required to keep the spacecraft system within design temperature limits. Degradation of the optical properties of these coatings by UV and particulate radiation and by contamination appears to be a significant problem that must be solved to achieve long-life (10 to 20 years) systems.

The ability to predict the long-term performance of all classes of materials in space must be a central part of any durability program and may require flight experiments, such as LDEF, for verification of ground exposure data and analytical predictions.

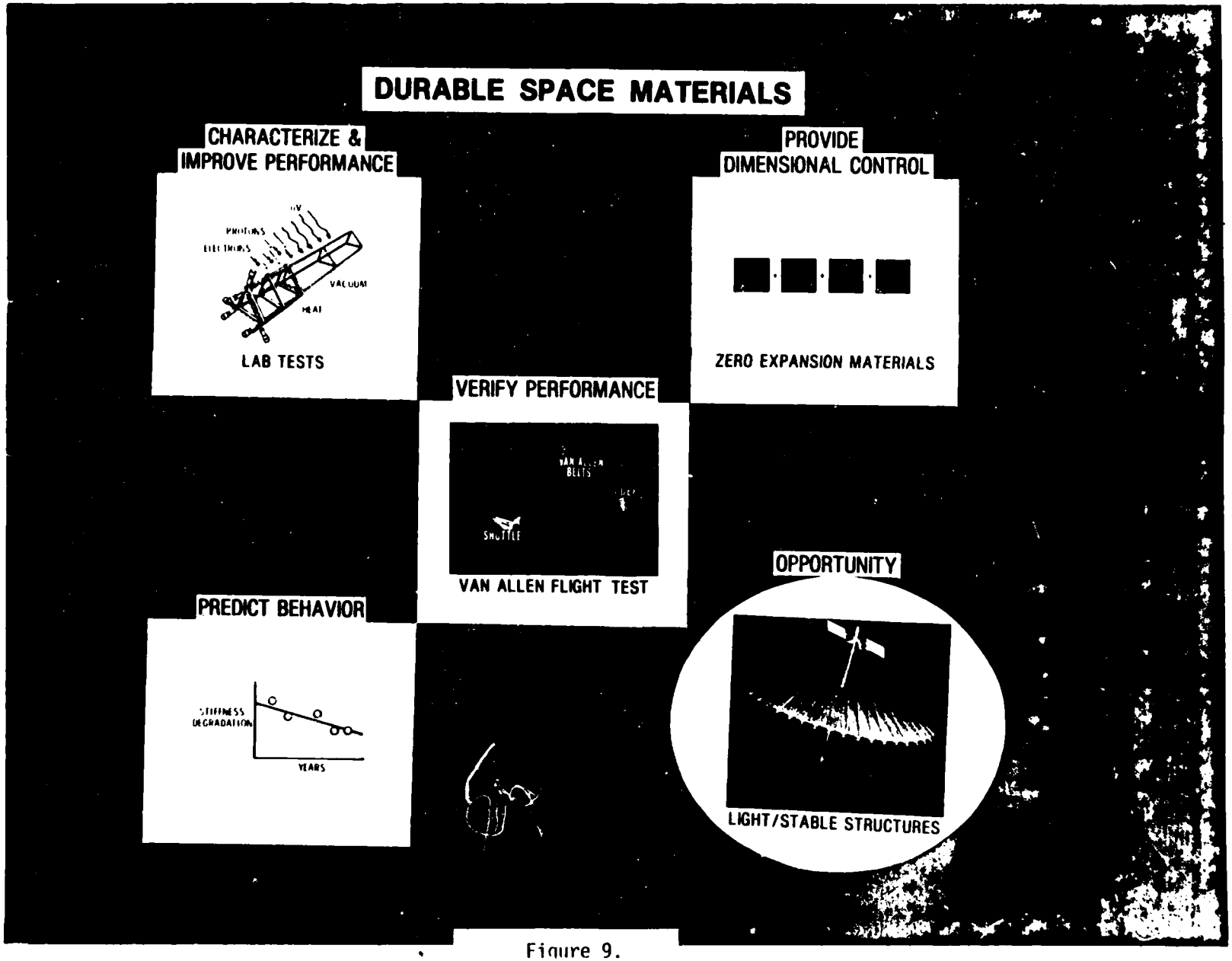
DURABLE SPACE MATERIALS
CHARACTERIZE & IMPROVE PERFORMANCE
LAB TESTS
PROVIDE DIMENSIONAL CONTROL
ZERO EXPANSION MATERIALS
VERIFY PERFORMANCE
VAN ALLEN FLIGHT TEST
PREDICT BEHAVIOR
STIFFNESS DEGRADATION
YEARS
OPPORTUNITY
LIGHT/STABLE STRUCTURES

Figure 9.

SPACE MATERIALS DURABILITY LABORATORY

Figure 10 shows the Space Materials Durability Laboratory under construction at NASA Langley for evaluation of the effects of space radiation on composite materials. This laboratory has a 2.5 MeV proton accelerator, a 1 MeV electron accelerator, and a solar simulator all focused on a 12-inch diameter target in a clean ultra-high vacuum chamber. The accelerators were selected to cover the most prevalent energy range found in space for generation of bulk damage to composite materials.

NASA
L-81-11,256

SPACE MATERIALS DURABILITY LABORATORY

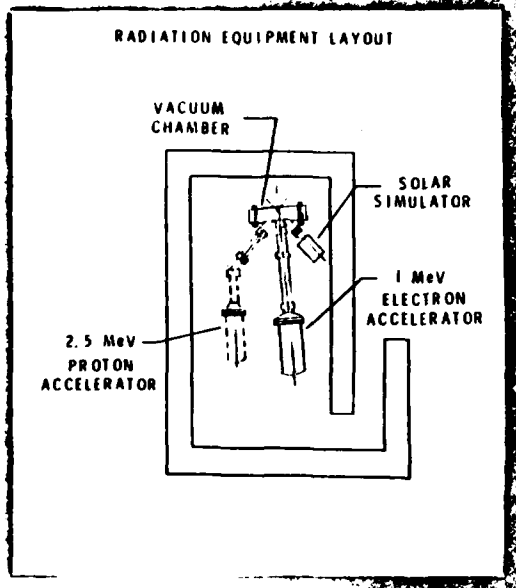

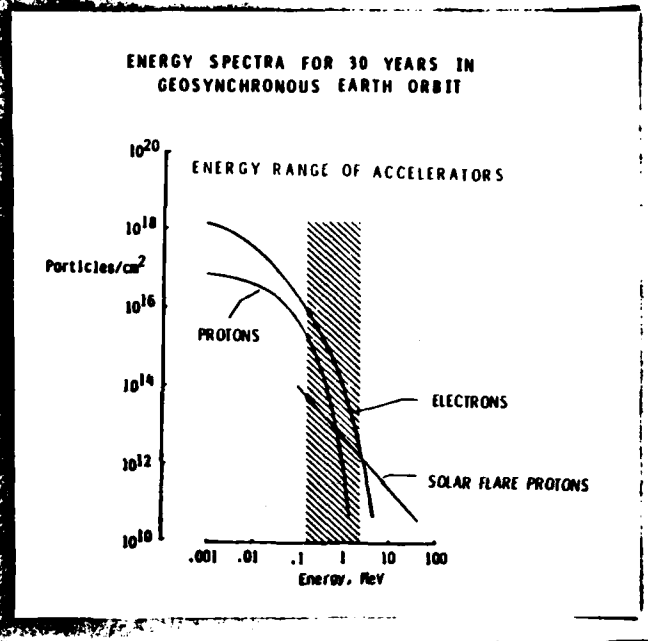

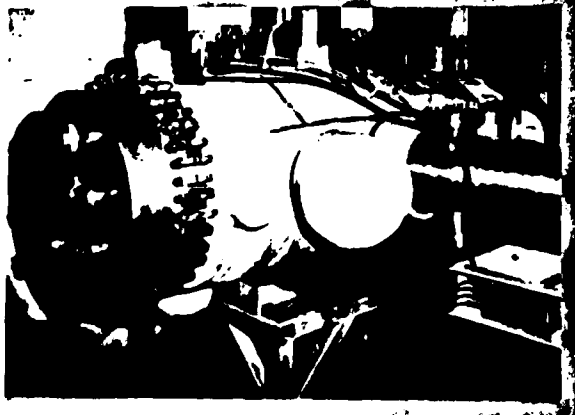

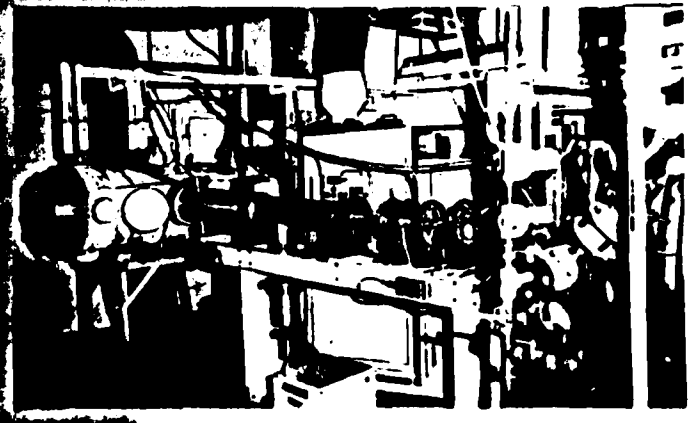

Figure 10

EFFECT OF ELECTRON RADIATION ON THE MODULUS OF POLYSULFONES

The effect of total electron dose on the observed modulus of polysulfone films following irradiation between 10^8 and 10^{10} rad at $2(10)^8$ rad/hr is shown in figure 11. The modulus of the unirradiated film is given on the y-axis. Modulus values were obtained using an automated Rheovibron, with all data obtained at a frequency of 3.5 Hz.

When determining a modulus value, the film was inserted in the Rheovibron, several readings were taken, and the film was removed completely from the clamps and remounted. Several readings were again taken. This was done to attempt to eliminate sample mounting effects. All modulus values obtained for that particular film were then averaged.

For all materials, the modulus increased as dose level increased, and the threshold value for a major change in modulus appears to be near 10^9 rad. The percent increase ranges from about 24% for P-1700, to 58% for Radel 5000. This increase with higher dose suggests that crosslinking is occurring in all materials, particularly after 10^9 rad.

THE EFFECT OF ELECTRON RADIATION ON MODULUS

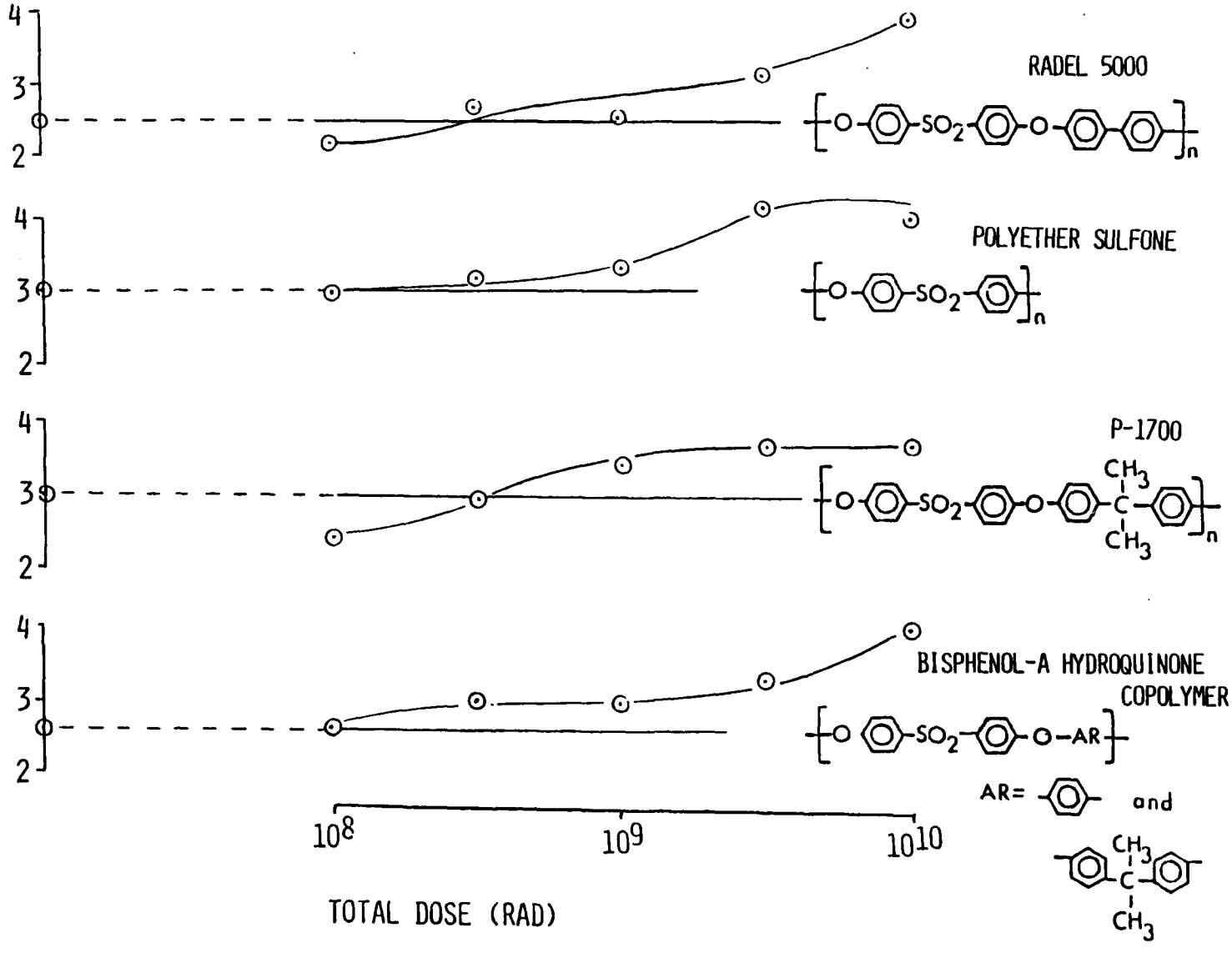

SPACE MATERIALS DURABILITY PROGRAM FLOW DIAGRAM

A data base which would allow confident design of long-life large space systems with polymer matrix composites does not exist. Furthermore, the relationship between radiation damage and mechanical and physical property changes are not understood well enough to be predicted analytically. The effects of variables such as type of radiation, dose rate, total dose, specimen temperature, load and vacuum on polymers of current interest for advanced composites have yet to be determined.

A program designed to consider each aspect of space environmental exposure on polymeric matrix composite materials and thus identify and/or develop materials with enhanced durability to this environment, is shown schematically in figure 12. The program begins with an assessment of the space durability of current composites and culminates with development of a new class of materials optimized for space. Between these end points are major milestones involving development of an accelerated test methodology, radiation damage models, and identification of radiation damage mechanisms. The overall program shown will meet the technology needs in a logical and orderly fashion by focusing on specific research goals that are achievable and will build toward improved materials for use in space.

SPACE MATERIALS DURABILITY PROGRAM FLOW DIAGRAM

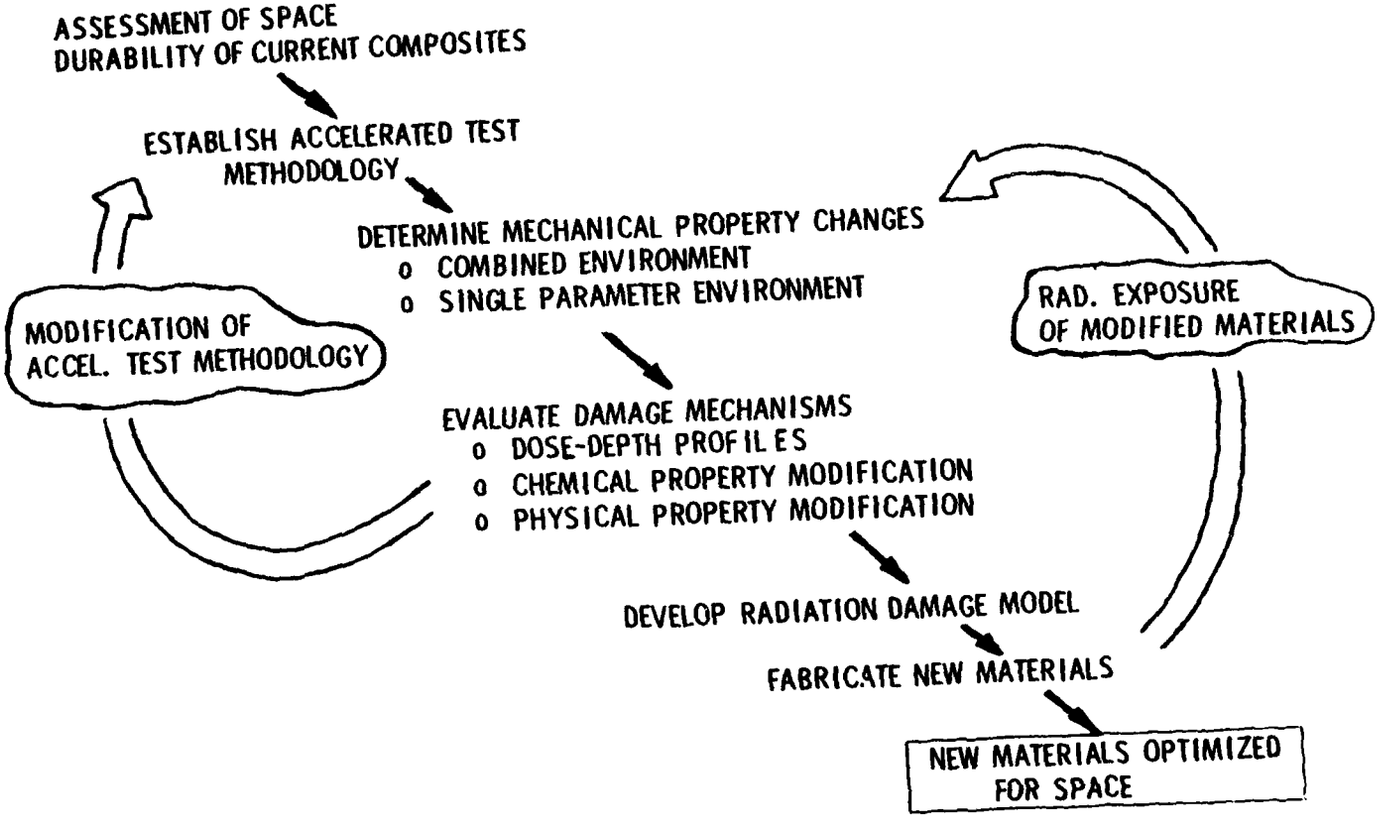

Figure 12.

THERMAL CONTROL COATING REQUIREMENTS

The basic requirement for thermal control coatings is to keep spacecraft components within allowable temperature limits. Thermal designers have two major types of problems: one where the temperature limit is dictated by the structural materials with only the solar heat input to be considered, as composite structures, and the second where both solar and internal heat are thermal inputs, like a manned habitat. In these cases different ratios of solar absorptance to thermal emittance are required. In figure 13 the coating requirements for a composite structure in GEO are compared to the requirements for a manned habitat in LEO. The major differences are, (1) low emittance coatings are required for the composite structure to reduce the extent of cool-down during a solar occult, (2) coating to be used in GEO must be able to withstand high energy electrons and protons in addition to UV, and (3) a higher electrical conductivity is required in GEO to eliminate spacecraft charging. Because a manned habitat would be visited by the shuttle, the major contamination source would be the STS. However, repair or refurbishment of coatings can be considered for LEO applications but not for GEO.

Some of the best available long-time data on coating performance in space flight are shown in figure 14. These data are from an Air Force flight experiment ML-101 conducted in a polar orbit. The interesting part of this figure is that the 3 white paints exhibit a substantial increase (130%) in solar absorptance in 5 years and all three have about the same degradation rate. The second-surface mirror type coatings, which do not have pigments, also are grouped together in degradation but exhibit a much lower degradation of only 40%. Since most of this degradation occurred in the first 2 or 3 months of flight, contamination is suspected as a primary source of degradation for these nonpigmented coatings.

In light of these and other similar studies, NASA Langley has developed a program for development and evaluation of new coatings using metallic and metallic-oxide pigments. The major thrusts and expected results of this program are summarized in figure 15. New coating concepts requiring additional work include high conductivity organometallic complexes in polymers, vacuum deposition of metallic oxides and incorporation of pigments in the outer layer of laminated-composites. The major goal of this effort is to provide coatings with long-term radiation stable optical properties.

THERMAL CONTROL COATING REQUIREMENTS

	COMPOSITE STRUCTURE GEO	MANNED HABITAT LEO
OPTICAL PROPERTIES	α/ϵ - SELECTIBLE WITH $\epsilon \leq 0.3$	α/ϵ - SELECTIBLE WITH $\epsilon \geq 0.8$
TEMPERATURE	-100^0 TO $+80^0$C	-100^0 TO $+40^0$C
ENVIRONMENT	UV, e^-, p^+, VAC, ΔT	UV, VAC, ΔT
ELECT. CONDUCTIVITY	$\leq 10^{-8}$ $(OHM^{-1}\text{-}CM^{-1})$	$10^{-8} - 10^{-17}$ $(OHM^{-1}\text{-}CM^{-1})$
LIFETIME	10 TO 20 YEARS	10 YEARS
PRIMARY CONTAMINATION SOURCE	MATERIALS	STS
REPAIR OR REFURBISHMENT	NO	YES

Figure 13.

DEGRADATION OF THERMAL CONTROL COATINGS

(FLIGHT EXPERIMENT ML-101)

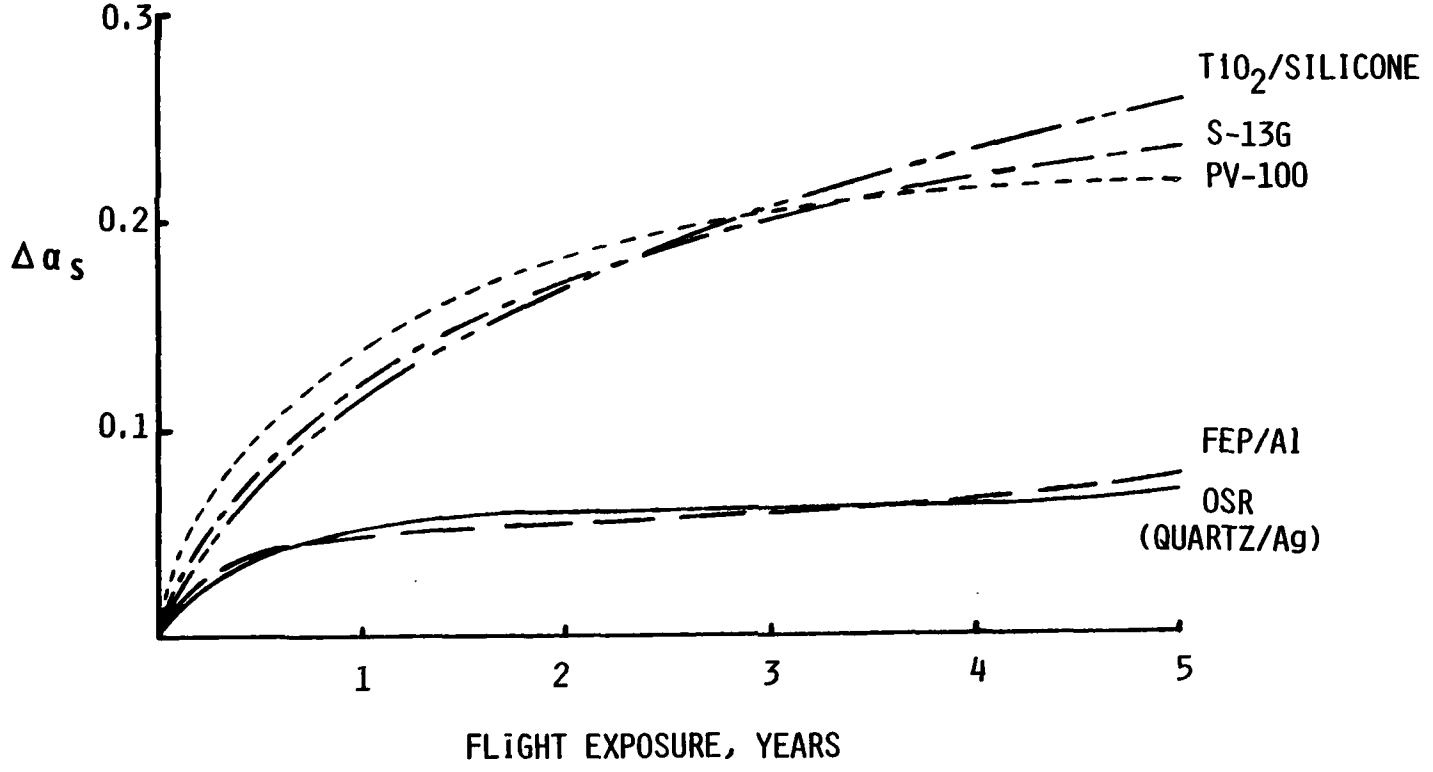

ure

LONG-LIFE THERMAL CONTROL COATINGS

MAJOR THRUSTS	EXPECTED RESULTS
NEW COATING CONCEPTS o METALLIC/OXIDE COATINGS o IMPREGNATED POLYMER FILMS o ORGANO-METALLIC POLYMERS	NEW COATINGS WITH REQUIRED OPTICAL PROPERTIES AND CONDUCTIVITY
SPACE RADIATION STABILITY o LABORATORY EXPOSURE TO RADIATION AND THERMAL CYCLING o LDEF FLIGHT EXPERIMENT	ESTABLISH LONG-TERM STABILITY OF OPTICAL PROPERTIES
SPACECRAFT CONTAMINATION EFFECTS o EFFECTS OF COMMON S/C AND STS CONTAMINANTS ON OPTICAL PROPERTIES	NEW COATINGS LESS SUSCEPTIBLE TO DEGRADATION BY CONTAMINATION

Figure 15.

THERMAL EXPANSION OF UNIDIRECTIONAL AND ISOTROPIC T300/5208 Gr/Ep LAMINATES

The performance characteristics of space communication antennae are sensitive to small dimensional changes in the antenna structure which cause a defocusing of the antenna or an increase in the surface roughness of the reflector surface. Dimensional changes in resin matrix composites can be caused by thermal expansion, loss of moisture, microcracking of the resin, applied stress, and radiation damage to the resin matrix. To make precision measurement of these changes in anisotropic materials, such as composites, several laser interferometry techniques have been developed. Thermal expansion data collected from one such technique for unidirectional and quasi-isotropic T300/5208 Gr/Ep over a temperature range from 116K to 366K are shown in figure 16. The expansion behavior of these laminates is expected to bound the behavior of the laminates chosen for space structures. This type of data for different graphite fibers and resins is essential for verification of analyses used for tailoring laminates to achieve required stiffness and low CTE.

THERMAL EXPANSION OF UNIDIRECTIONAL AND ISOTROPIC T300/5208 Gr/Ep LAMINATES

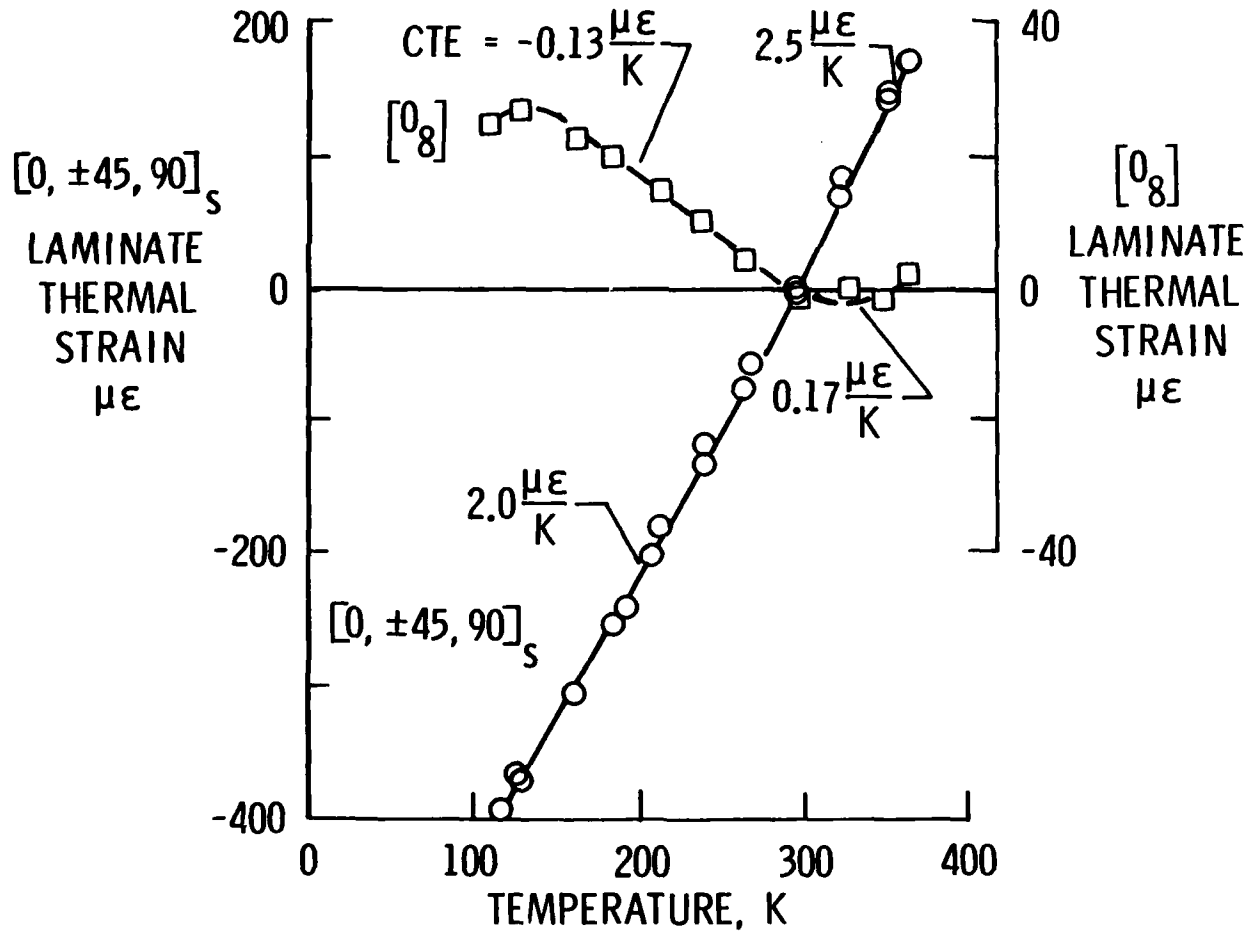

Figure 16.

ANALYSIS OF THE EFFECTS OF MICROCRACKING ON THERMAL EXPANSION

Microcracks in organic matrix composites are small cracks in the matrix which extend parallel to the fiber direction. They occur when the internal stresses exceed the transverse strength of an individual lamina. The two primary causes of microcracking are thermal stresses set up on repeated thermal cycles and mechanical loading. Typical microcracking due to these two causes are shown in figure 17. The effect of this type of microcracking on the thermal expansion behavior of a $(0,\pm45,90)_S$ Gr/Ep laminate is shown in the lower left of figure 17. Microcracking produces a decrease in the CTE of the laminate and an extensional elongation of the sample on the order of 20 με (data not shown in this figure).

The lower right hand figure shows the results of an experimental and analytical investigation conducted to correlate the change in CTE with microcrack density. Microcracks were induced in the laminates by mechanical load because the amount of damage could be easily controlled and characterized. Specimens from two quasi-isotropic T300/5208 laminate configurations were loaded to produce varying amounts of microcracking in plies perpendicular to the load direction. The amount of microcracking was characterized by computing an average crack density in the damaged plies. The average CTE over the temperature range 300 to 420K for the various specimens was measured using a moire interferometry technique.

The measured CTE values were plotted as a function of crack density in the 90^0 plies (i.e., perpendicular to the load direction). Reductions in CTE of 21 and 25% occurred in specimens that were loaded to 73 and 82% of ultimate, respectively, with the amount of reduction appearing to approach some stabilized value. Also shown are predictions using simple linear laminate analysis. These predictions agree well with measured values for specimens with zero crack density. Two different schemes were used to account for microcracks. The first consisted of reducing only the transverse stiffness (E_2) of the cracked plies as a function of the crack density, shown as the upper bound in the figure. In the second lower bound, both E_2 and the CTE ($\alpha 2$) of the cracked plies were reduced. The correlation between the crack density and the reduction in E_2 was based on finite element calculations. These preliminary results indicate that linear laminate analysis can be used to predict the reduction in CTE as a function of crack density when reduced values of E_2 and α_2 of the damaged plies are used.

Future work will include characterizing the amount of microcracking due to thermal loads (i.e., thermal cycling) and measuring the effect on CTE. Also work will continue to improve the modeling capability to predict CTE degradation due to damage formation.

ANALYSIS OF THE EFFECTS OF MICROCRACKS ON THERMAL EXPANSION

MICROCRACKING DUE TO THERMAL CYCLING IN GRAPHITE-EPOXY

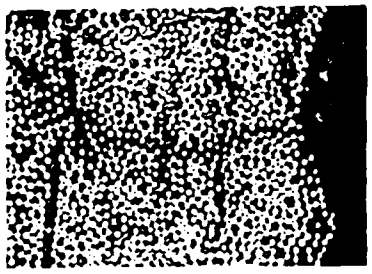

TYPICAL MICROCRACKING DUE TO MECHANICAL LOADING

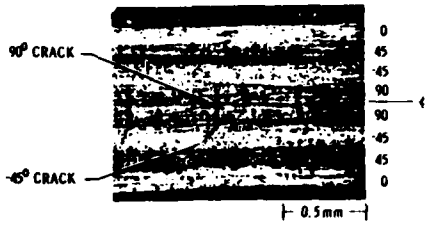

APPLIED STRESS = 73% ULT.

EFFECT OF MICROCRACKING ON THE THERMAL EXPANSION OF $[0/\pm45/90]_S$ Gr/Ep

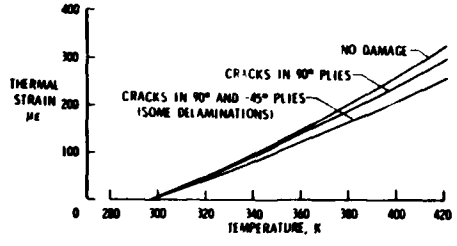

COMPARISON OF EXPERIMENTAL DATA WITH ANALYTICAL PREDICTIONS

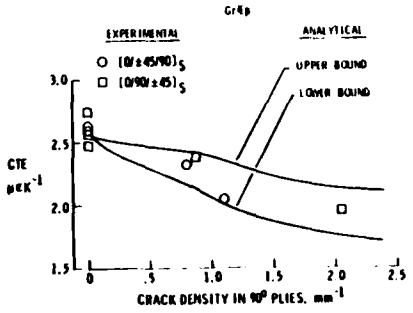

Figure 17.

MANUFACTURING FACILITY FOR OCTETRUSS ELEMENTS

As part of efforts to reduce costs of nestable column truss members, a manufacturing facility is being developed by Lockheed. The photo in figure 18 shows a tube-stand facility suitable for making half columns up to 5 meters in length. The heart of the facility is a movable platform on which is mounted spools (near top of photo) for circumferential winding and a gathering ring and tension plate for laying 0 degree filaments. The tension plate is perforated with small guide holes containing ceramic rollers which can be tensioned against the filament.

To initiate the tube manufacturing of a 90-0-90 configuration, a tapered mandrel is first placed in the stand. Then a single upward winding pass from bottom to top of the mandrel is made to form the inner surface circumferential ply. The tube is then completed with a single downward pass of the movable platform in which the tensioned 0 degree filaments are fed through the tension plate and gathering ring, then overwound with the external 90^{0} ply. Either film or painted resin can be used in the process and tubes may be bagged and cured in place.

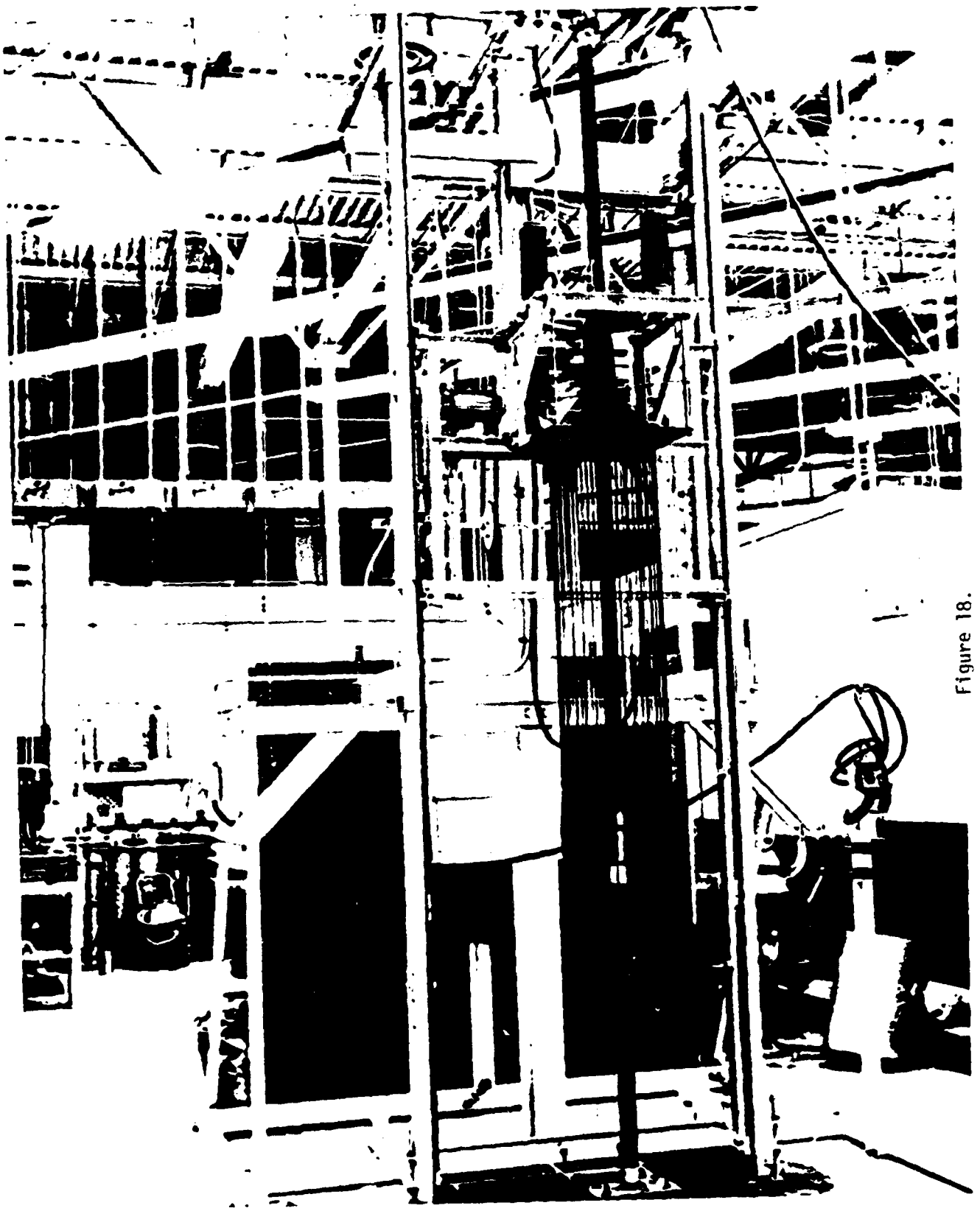

Figure 18.

JOINT CONCEPTS

Along with the development of basic elements, ways to join erectable components are being studied. Several joint concepts which have been fabricated are shown in figure 19. All models exhibit side entry and can be manually removed from, or inserted into, existing structure. However, disassembly of two joint models requires special tools. Also, all models are designed to be compatible with automated assembly of erectable structures. The joints were designed to represent actual flight quality components so that meaningful evaluations of each model's operational, structural and dynamic characteristics may be made.

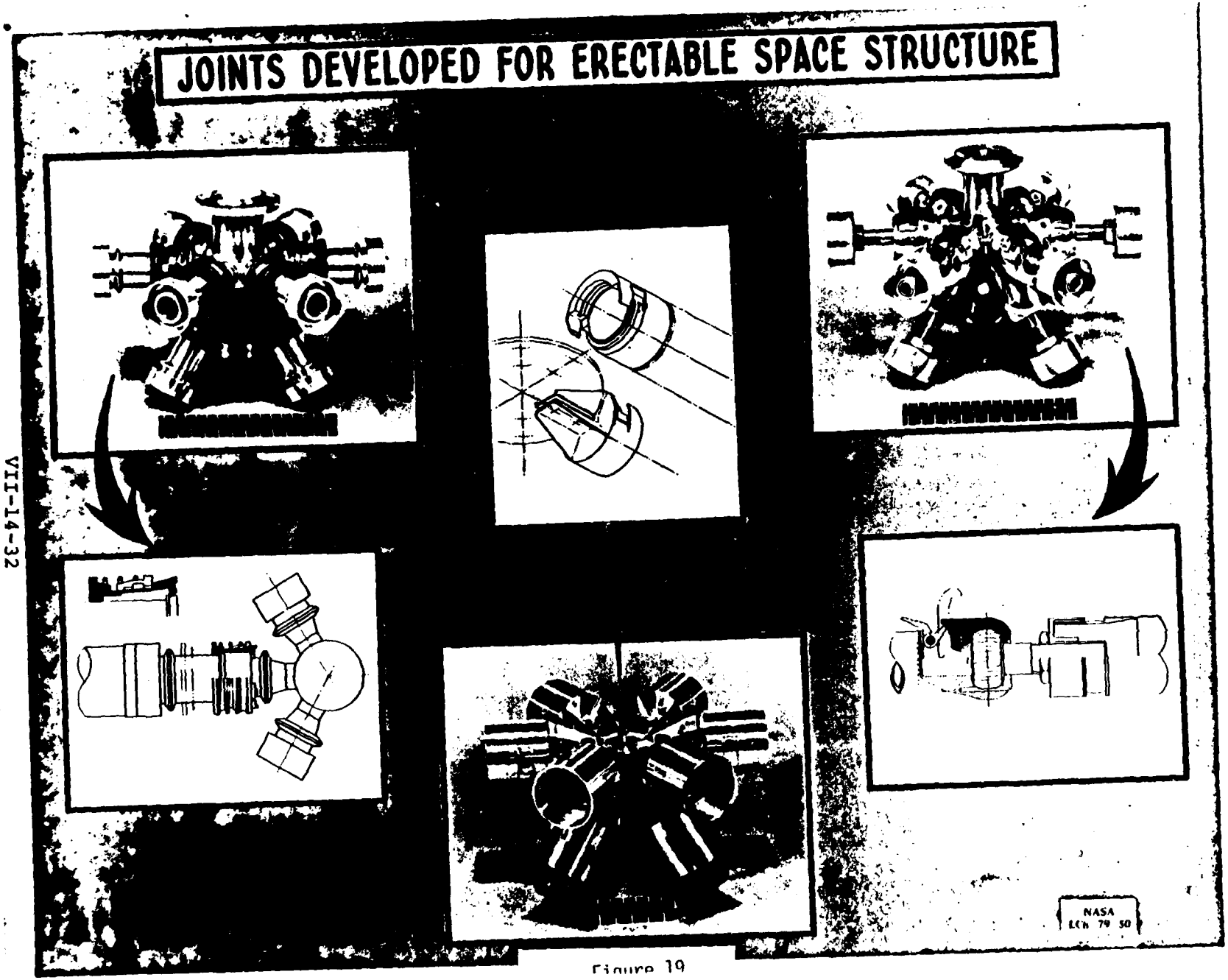
JOINTS DEVELOPED FOR ERECTABLE SPACE STRUCTURE
NASA
LCh 79 50

Figure 19

JOINING TECHNOLOGY

Adhesives technology for large space structures ranges from joining structural members to large area bonding of polymeric films. In addition to the concerns noted for environmental durability, adhesive resins with special features are required. For example, bonding large areas of polymer films for membrane or thermal control coatings presents some unique adhesive requirements. Void-free bonds are desirable to maintain joint strength and stability. Most adhesive resins process via a cure cycle to remove solvents which normally preclude obtaining void-free bonds. One approach to circumvent this problem is provided by a new resin LARC-TPI (figure 20). This linear, thermoplastic resin is formulated to be used in the imidized form, free of volatiles. Thus, large area bonding of films can be achieved to obtain optimum joint properties.

NASA
L-81-2569

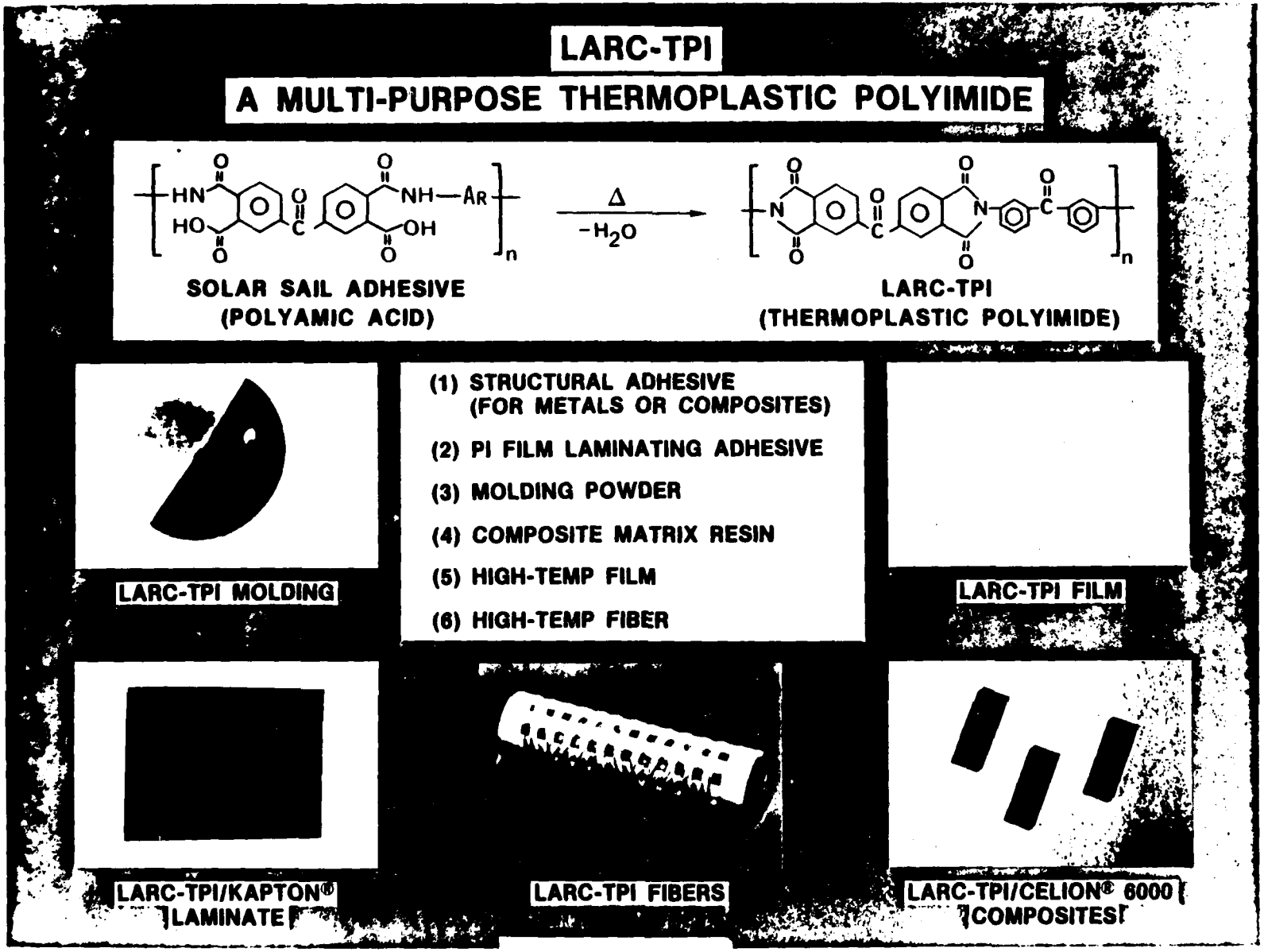

Figure 20.

IMPROVED ANTENNA TENSION CABLE MATERIALS

Lightweight deployable cables are currently being used to shape the mesh reflector surface on the TDRSS antenna and are being considered for the same purpose on the hoop-column antenna concept under study by NASA. The cables used on TDRSS are made of quartz fibers because quartz has a low thermal expansion, is inherently stable in the space environment, and can be made in small diameter fibers. A typical size cord would be approximately 450 μm in diameter and would be composed of approximately 2000 individual quartz fibers, 9 μm in diameter, held together by a Teflon cross wrap. One of the problems with this type of construction is that it is very difficult to get all of the fibers aligned and keep them aligned during handling and storage of the cables with the result that a small (60 μm) but significant residual strain is produced in the cable when subjected to repeated load or thermal cycles with a small tensile preload applied to the cable. Also, considerable variability is observed in this residual strain making it difficult to accurately bias this out during fabrication when the precise length of each cord is determined.

The results of a recent program conducted to develop an improved cable are summarized in figure 21. Two major improvements were made which significantly advanced space cable technology. To achieve a better alignment of fibers and minimize the amount of twist in the fiber along the cord, unidirectional composites were made by impregnating the bare fibers with Teflon while holding the fibers straight under tension. This resulted in a substantial increase in the relative stiffness of the cable and reduction in residual strain after repeated thermal/mechanical cycling. Further improvements were achieved by using graphite fibers in place of the quartz fibers.

IMPROVED ANTENNA TENSION CABLE MATERIALS

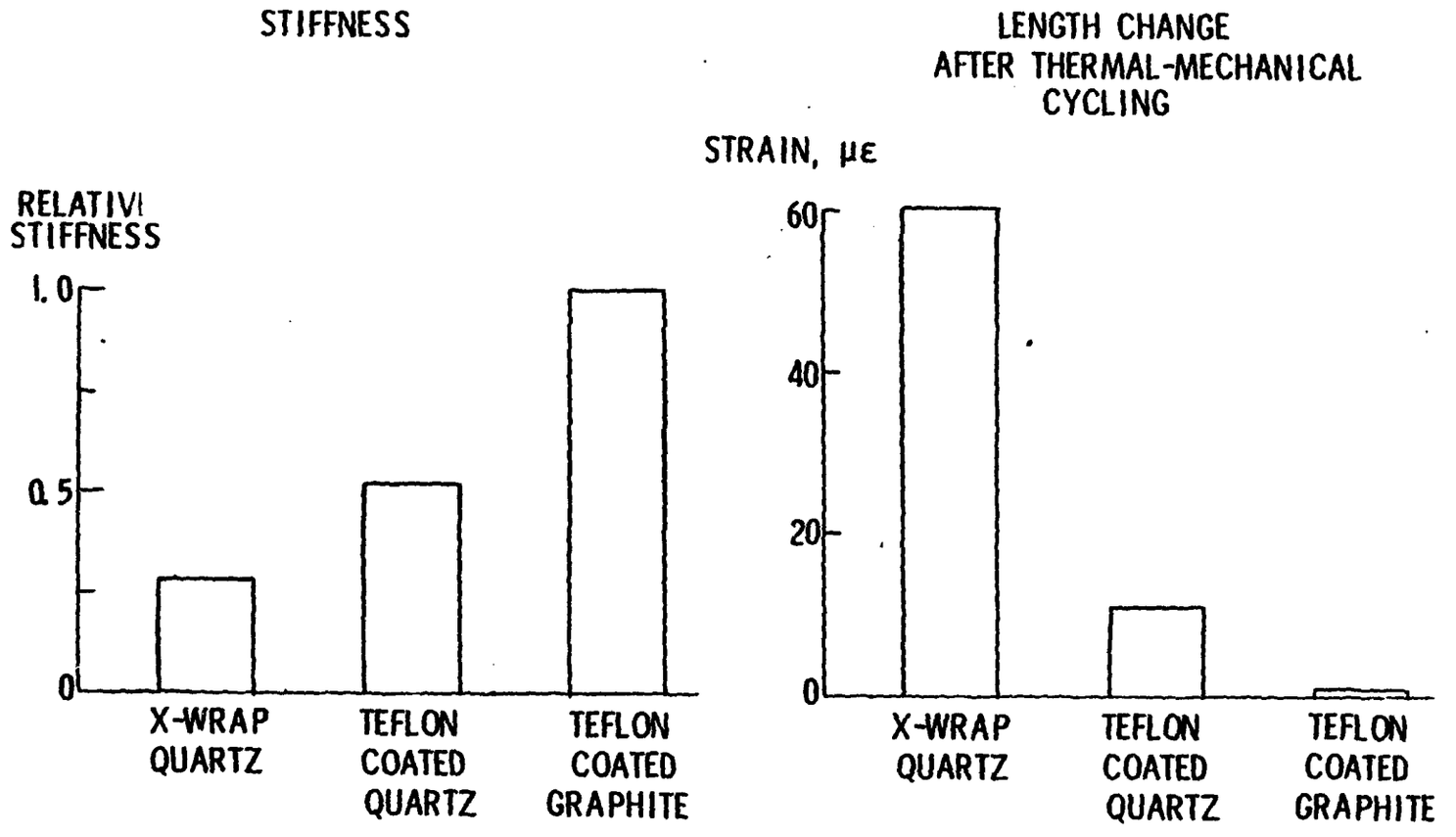

VII-14-36.

Figure 21.

SUMMARY

- o LIGHTWEIGHT COMPOSITE MATERIALS
  - TOUGH POLYMER MATRIX RESINS
  - DIMENSIONAL STABILITY
- o LONG-LIFE THERMAL CONTROL COATINGS AND FILMS
  - TAILORED OPTICAL PROPERTIES
  - RADIATION, UV RESISTANT
  - MINIMUM SENSITIVITY TO CONTAMINATION
- o PRECISION MANUFACTURING TECHNOLOGY
  - STRUCTURAL SUBELEMENTS
  - JOINTS

BIBLIOGRAPHY

1. Large Space Systems Technology - 1980, Vols. I and II, NASA CP-2168, 1980.

2. Large Space Structures Technology - 1981, Vols. I and II, NASA CP-2215, 1981.

3. Bush, H. G. and Heard, W. L.: Recent Advances in Structural Technology for Large Deployable and Erectable Spacecraft. NASA TM-81905, Oct. 1980.

4. Wright, R. L. (Editor): The Microwave Radiometer Spacecraft - A Design Study. NASA RP 1079, Dec. 1981.

5. Russell, R. A.; Campbell, T. G.; and Freeland, R. E.: A Technology Development Program for Large Space Antennas. NASA TM-81902, 1980.

6. St. Clair, A. K. and St. Clair, T. L.: A Review of High Temperature Adhesives. NASA TMX 83141, July 1981.

7. St. Clair, A. K. and St. Clair. T. L.: A Multi-Purpose Thermoplastic Polyimide. *Proceedings of the 26th National SAMPE Symposium*, April 1981.

8. Rubin, L. A.: Applications of Metal-Matrix Composites, The Emerging Structural Materials. SAMPE Journal, July/August 1979.

9. Kwan, J. W. and Chow, D. T.: Thermal Control Film Bonding for Space Applications. Proceedings of the 25th National SAMPE Symposium, May 1980.

10. Campbell, W. A., Jr.; Marriott, R. S.; and Park, J. J.: Outgassing Data for Spacecraft Materials. NASA RP 1061, Aug. 1980.

11. Santos B. and Sykes, G. F.: Radiation Effects on Four Polysulfone Films. Proceedings of the 13th National SAMPE Technical Conference, Oct. 1981.

12. Schwinghmaer, R. J.: Space Environmental Effects on Materials. NASA TM 78306, Aug. 1980.

13. Tennyson, R. C.: Composite Materials in a Simulated Space Environment. Structures, Structural Dynamics, and Materials Conference, Seattle, Washington, May 12-14, 1980 Technical Papers, Part 2, AIAA, 1980, pp 1009-1018.

14. Shepic, J. A.: Evaluation and Prediction of Long Term Space Environmental Effects on Nonmetallic Materials. NASA CR-161585, Oct. 1980.

Structural Characterization of Materials for High Energy Space Systems

Richard Gilardi
Laboratory for the Structure of Matter
Naval Research Laboratory, Washington, D.C. 20375

A review will be presented describing the use of diffraction techniques for the characterization of the atomic arrangements of materials in the amorphous, crystalline and fibrous forms. This research relates structure to function or to physical and chemical properties.

The techniques of x-ray, neutron and electron diffraction are employed. The resulting diffraction patterns are transformed into detailed structural information. An additional special technique involves the use of synchrotron radiation. It is of particular significance to studies of small samples, surfaces and anomalous dispersion applications.

Examples that illustrate the broad applicability of structural analysis are battery electrodes, photon energy conversion devices, metallic glasses, active carbons, explosives and propellants and biologically active substances.

MODUS OPERANDI

STRUCTURAL CHARACTERIZATIONS ARE PERFORMED IN COLLABORATION WITH INVESTIGATORS WHO ARE DEVELOPING NEW OR IMPROVED MATERIALS OR HAVE PROBLEMS WITH EXISTING ONES.

EXPERIMENTAL AND ANALYTICAL TECHNIQUES

X-RAY, NEUTRON AND ELECTRON DIFFRACTION TECHNIQUES ARE EMPLOYED

DIFFRACTION PATTERNS ARE TRANSFORMED INTO DETAILED STRUCTURAL INFORMATION

A SPECIAL TECHNIQUE INVOLVES SYNCHROTRON RADIATION OF SIGNIFICANCE TO SMALL SAMPLES, SURFACES AND ANOMALOUS DISPERSION APPLICATIONS

PRODUCT

CHARACTERIZATION OF THE ATOMIC ARRANGEMENTS OF MATERIALS IN THE AMORPHOUS, CRYSTALLINE AND FIBROUS FORMS.

RELATIONSHIP OF STRUCTURE TO FUNCTION OR PHYSICAL AND CHEMICAL PROPERTIES.

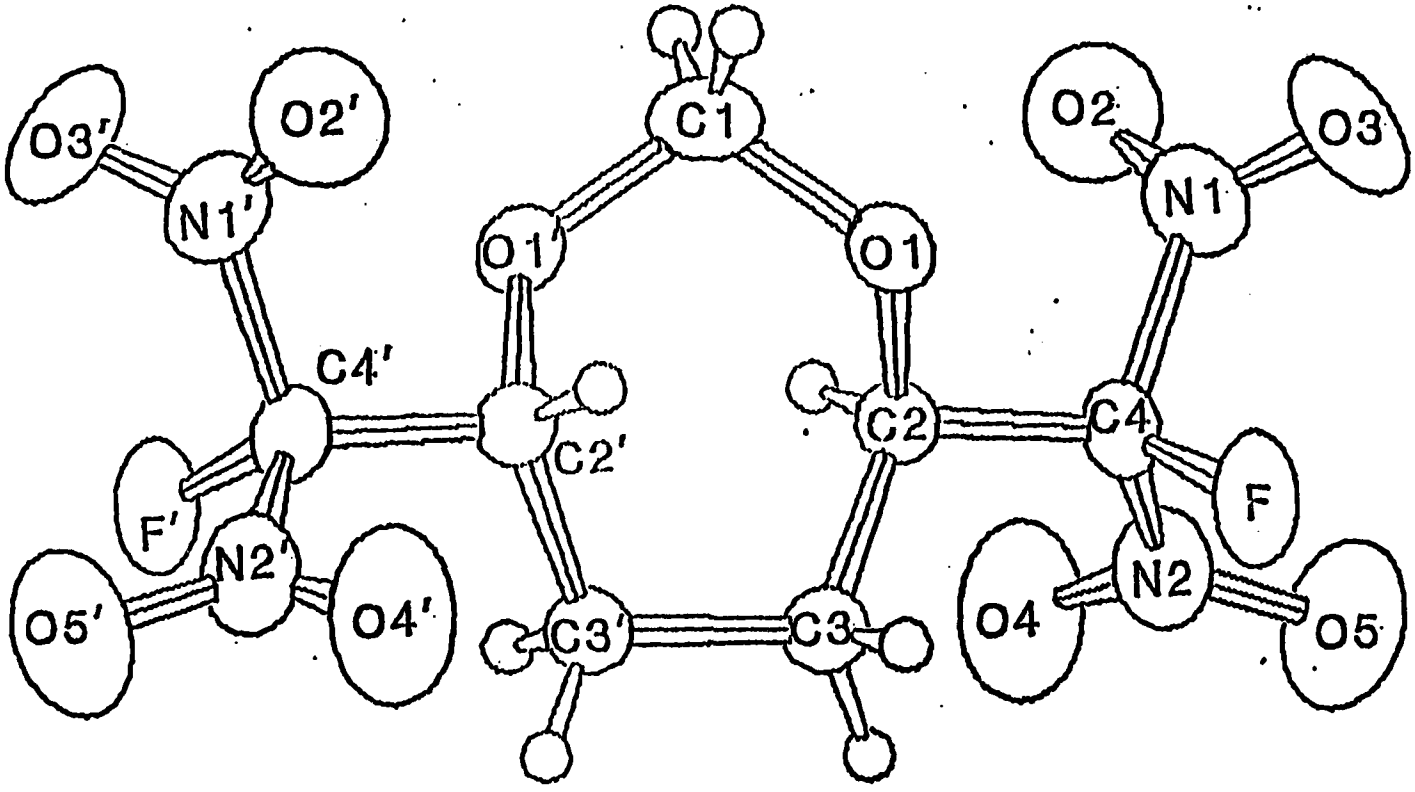

THE MOLECULAR STRUCTURE OF 4,7 - BIS(DINITROFLUOROMETHYL) - 1,3 - DIOXEPANE. THIS MOLECULE IS A NEWLY SYNTHESIZED MONOMER DEVELOPED AT NSWC (WHITE OAK) DURING RESEARCH ON THE SYNTHESIS OF DENSE NITRO-POLYMERS.

BAMO

3-3-Bis-AzidoMethylOxetane

$C_5 H_8 N_6 O$

COLORLESS LIQUID (B.P.67C. AT 0.25mmHg)

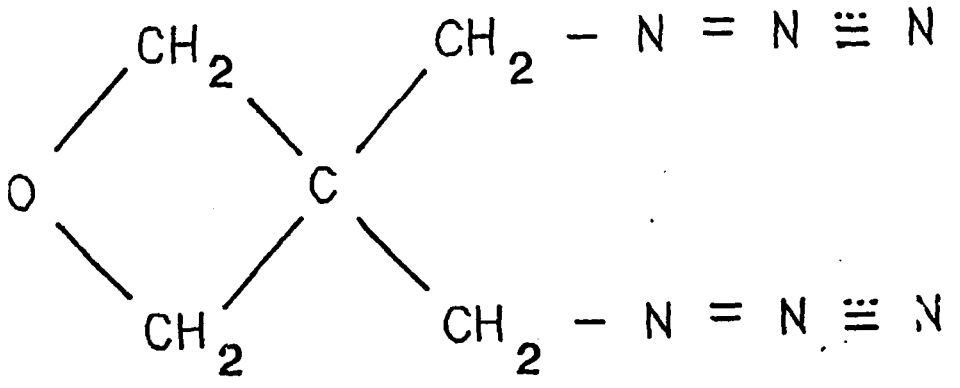

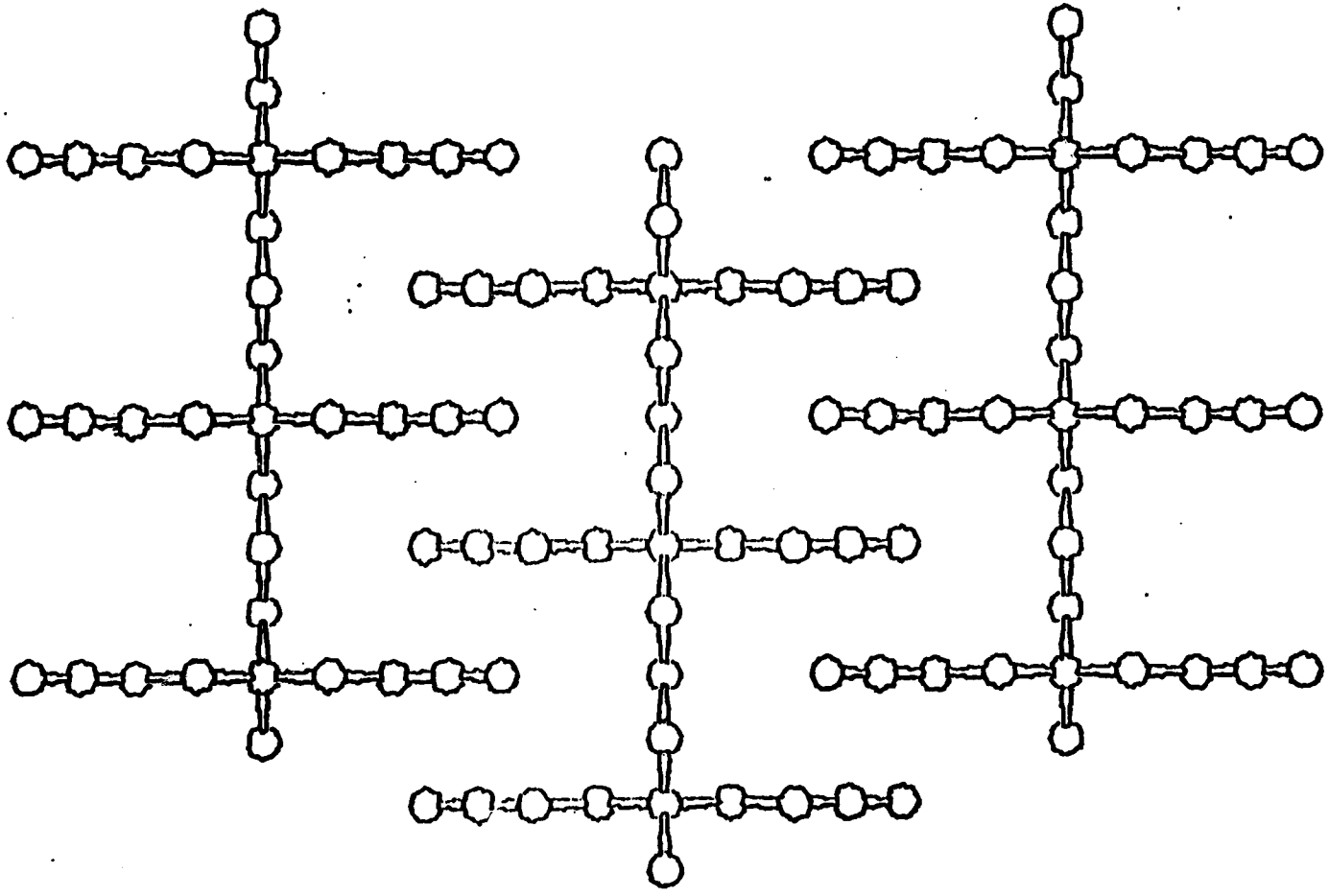

A CRYSTAL STRUCTURE MODEL FOR THE ENERGETIC ELASTOMER, $(BAMO)_N$. THIS MODEL EXPLAINS ALL FEATURES OF THE FIBER DIFFRACTION PATTERN QUITE WELL, BUT EXHIBITS UNUSUALLY CLOSE AZIDO-AZIDO CONTACTS. REFINEMENT ON THIS MODEL, AND OTHERS WHICH DIFFER ONLY IN SIDE-CHAIN PACKING, IS CONTINUING.

The following Figure shows the intensity of scattering of Cu Kα X-rays by hydrogenated Silicon solar cell device material which was prepared by deposition on substrates at 130°C. (low T) and at 250°C. (high T). At scattering angles less than 10°, the scattered intensity rises rapidly for the low-T material, but not the high-T material. Empirically, it is found that the low-T material is an inefficient solar energy converter, although chemically it differs little from the effective high-T material. The analysis of the small angle scattering provides a measure of the volume distribution of voids in the solid. The results for the low-T solid are shown in the succeeding figure. As much as 10% of the volume of this solid is occupied by very small voids. These voids may be empty or filled with some form of Hydrogen, which is essentially transparent to the X-rays used in this experiment.

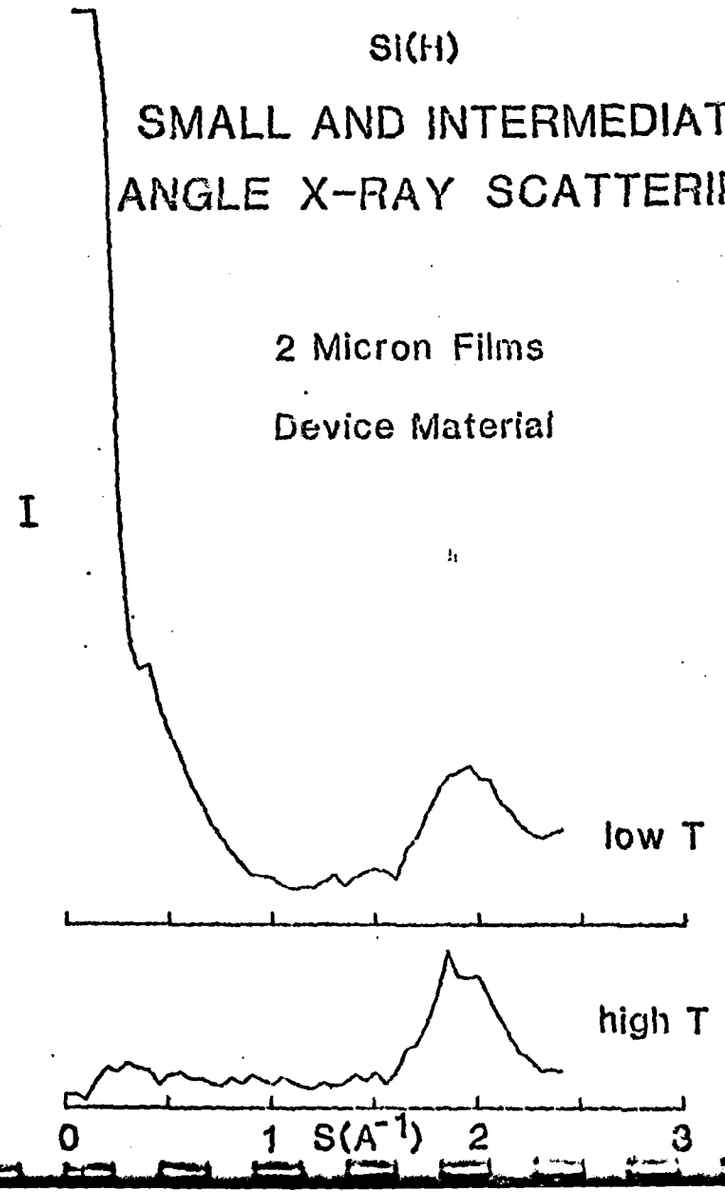
SI(H)
SMALL AND INTERMEDIATE
ANGLE X-RAY SCATTERING
2 Micron Films
Device Material
I
low T
high T
0
1
S(A⁻¹)
2
3

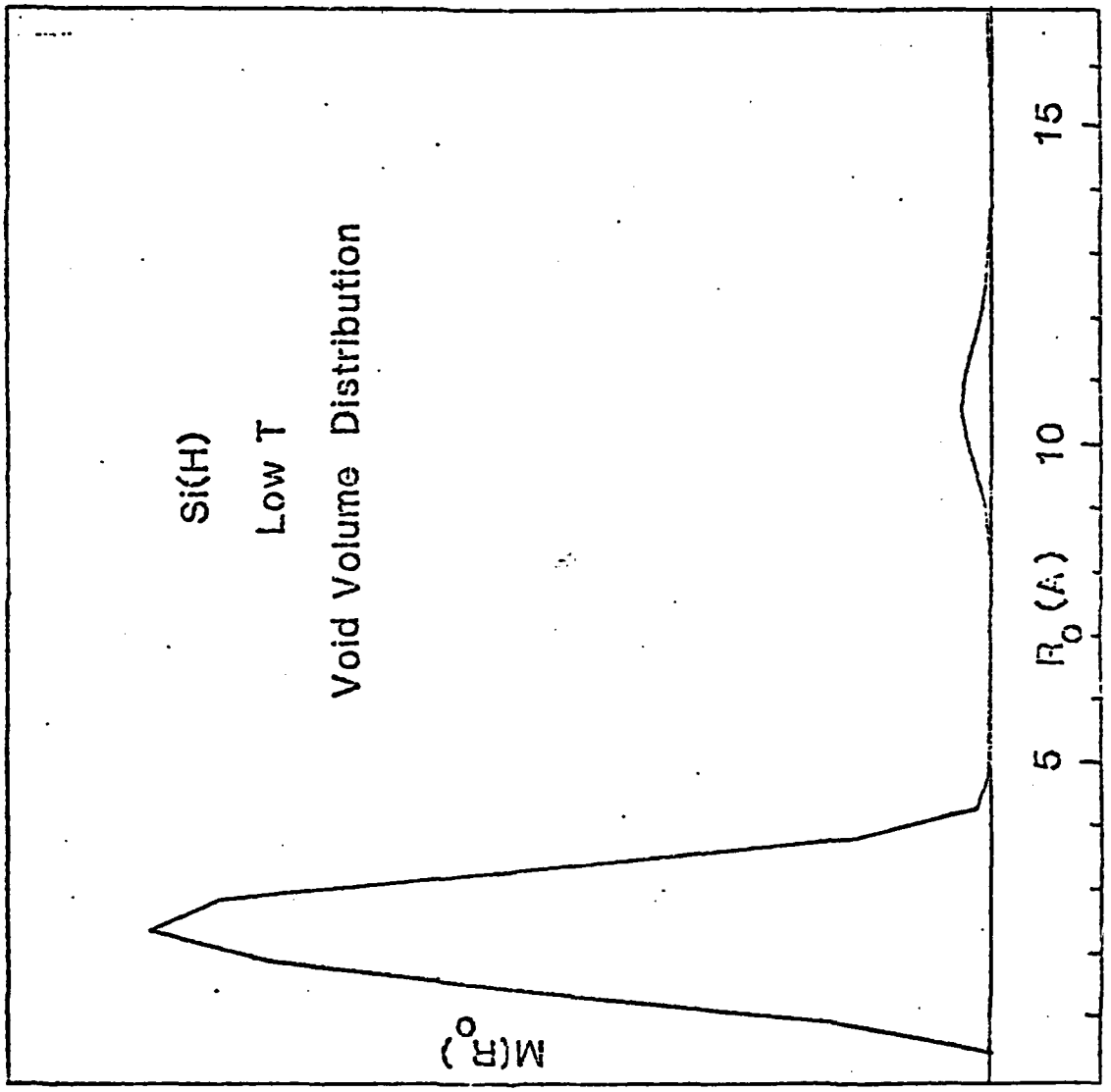
Si(H)
Low T
Void Volume Distribution
M(R$_o$)
5
10
15
R$_o$ (Å)

A carbon prepared from petroleum coke possesses an extremely large adsorbent surface area (3500 m^2/g); X-ray diffraction techniques were used to examine its microstructure. The predominant bonding topology exhibited by the diffraction-derived radial distribution function corresponds to distorted, intertwined ribbons of graphite-like layers which are extended preferentially along the "b" direction defined in the next figure.

GRAPHITE LAYER

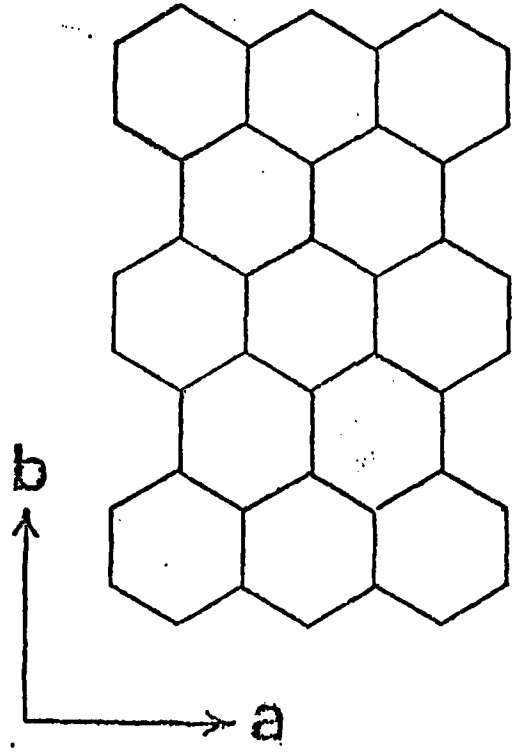

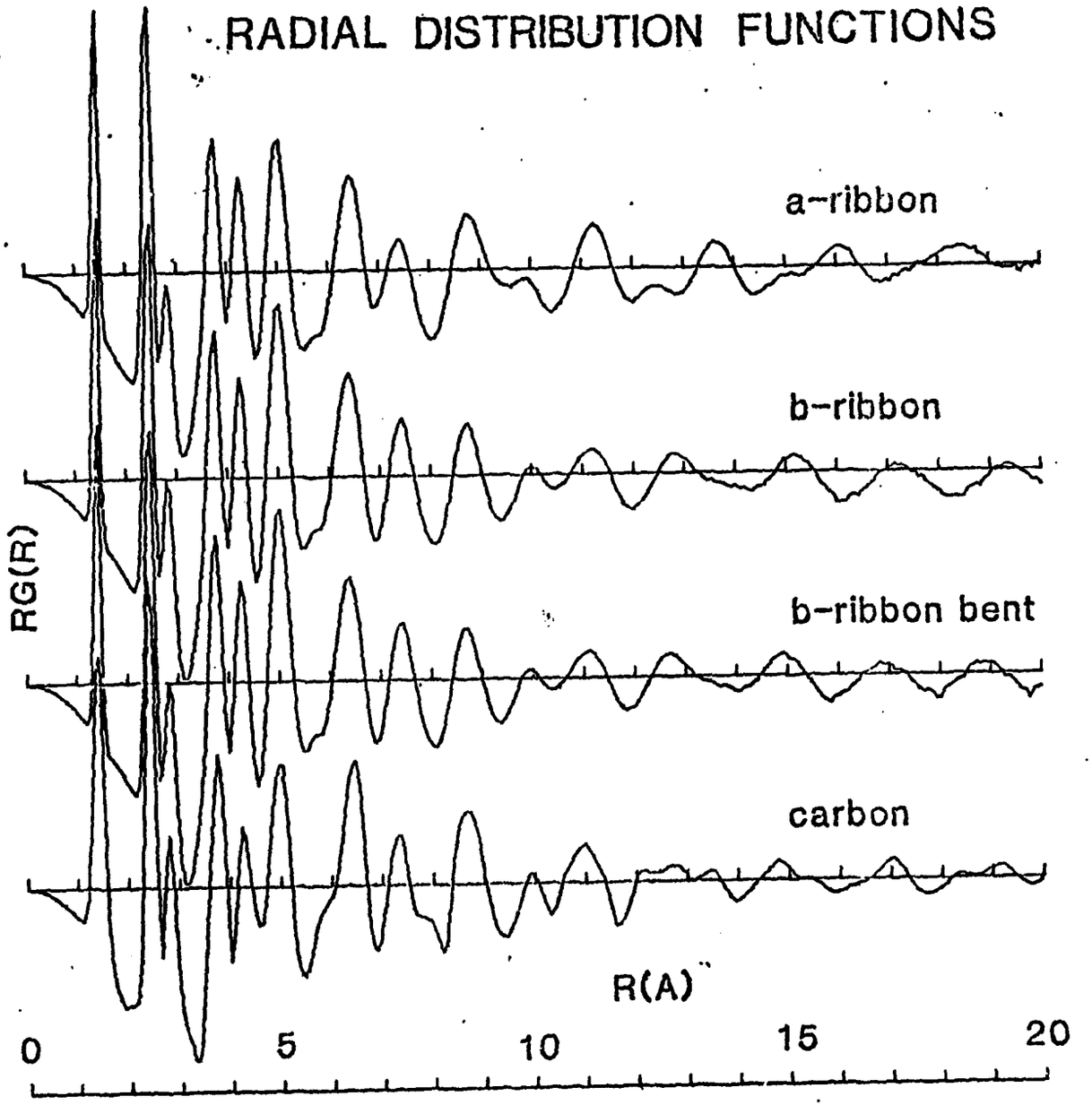
RADIAL DISTRIBUTION FUNCTIONS
a-ribbon
b-ribbon
b-ribbon bent
carbon
RG(R)
R(A)
0
5
10
15
20

CORRELATION OF EXPERIMENTAL CARBON RDF WITH CALCULATED RDF'S

	0A - 10A	10A - 20A
B-RIBBON BENT	0.92	0.73
B-RIBBON	0.92	0.43
A-RIBBON	0.93	0.04

$$CORR = \frac{\int (RDF)_{EXP} \cdot (RDF)_{CALC} \, dR}{\left[\int (RDF)^2_{EXP} \, dR \int (RDF)^2_{CALC} \, dR \right]^{\frac{1}{2}}}$$

Amorphous metals (also called metallic glasses) have unique and often useful magnetic, electrical and mechanical properties. The X-ray and neutron diffraction analysis of two amorphous alloys, Yttrium-Iron and Terbium-Iron, showed that short-range order persists in the amorphous state. Much of the order can be related to the extended order which is present in crystalline phases of the same alloys. In YFe_2 and $TbFe_2$, the Fe-Fe coordination framework persists in the amorphous state (at least out to second neighbors) while the rare-earth component changes its near-neighbor bonding substantially, showing a tendency to form self-clusters which are not seen in the crystal.

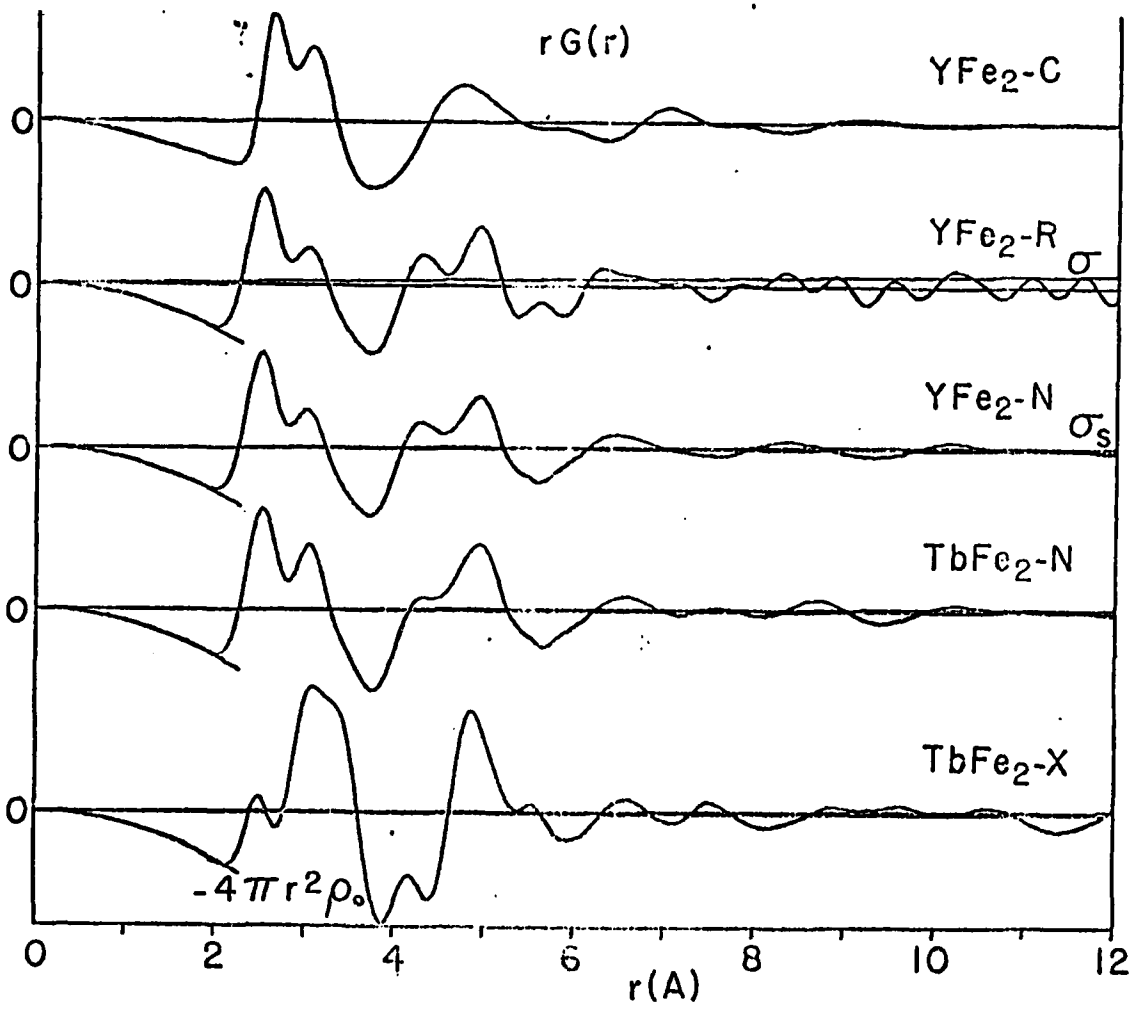

THE RADIAL DISTRIBUTION FUNCTIONS, rG(r), FOR THE LAVES CRYSTALLINE TOPOLOGY, YFe_2-C; THE UNSMOOTH RAW INTENSITY DATA, YFe_2-R; THE SMOOTH INTENSITY DATA FOR YFe_2-N, $TbFe_2$-N AND $TbFe_2$-X. THE BULK DENSITIES, ρ_o, AND ERROR ESTIMATES BASED ON RANDUM ERRORS IN THE UNSMOOTH, σ, AND SMOOTH, σ_s, INTENSITIES ARE ALSO SHOWN.

SYNCHROTRON RADIATION

PROPERTIES:
- HIGH INTENSITY (>50 TIMES CONVENTIONAL SOURCES)
- HIGHLY COLLIMATED (MILLIRADIAN DIVERGANCE)
- TUNEABLE WAVELENGTH (CONTINUOUS RADIATION EMITTED)

SPECIAL USES:
- RAPID DATA COLLECTION (LARGE DATA SETS, SHORT-LIVED SPECIES)
- SURFACE STUDIES (INTENSITY AND COLLIMATION HELP)
- ENHANCEMENT OF LOCAL STRUCTURE THROUGH WAVELENGTH TUNING

RORIDAN A

A MEMBER OF THE TRICHOTHECENE COMPLEX OF ANTIBIOTICS WHICH HAVE ATTRACTED A GREAT DEAL OF INTEREST DUE TO THEIR POTENT BIOLOGICAL ACTIVITY.

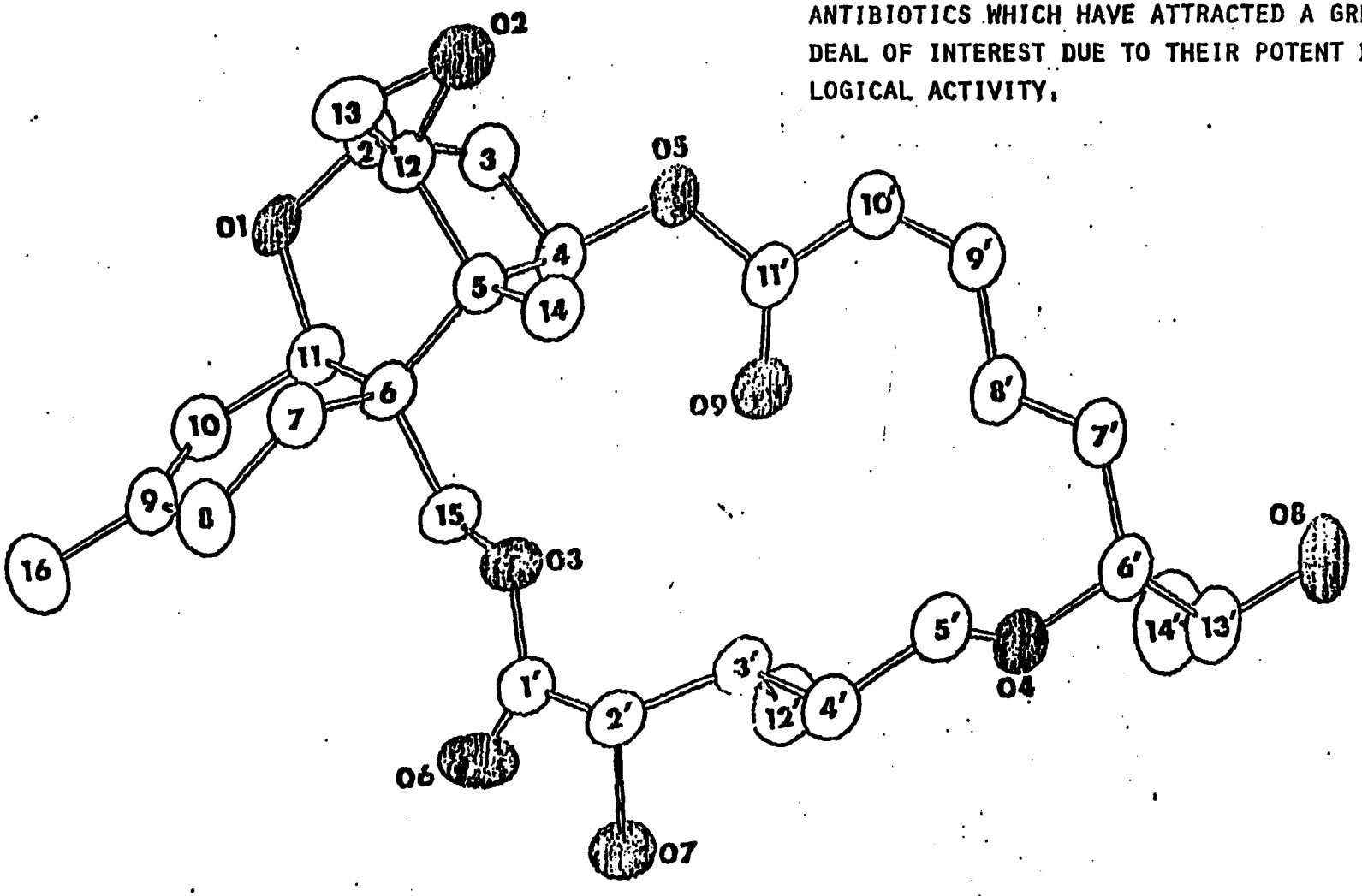

VII-15-18

HEMOGLOBIN

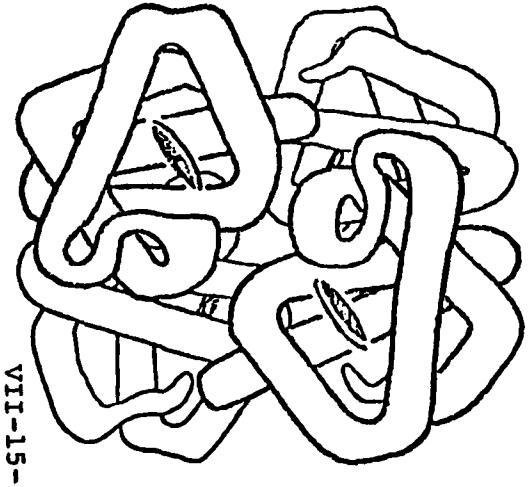

VII-15-19

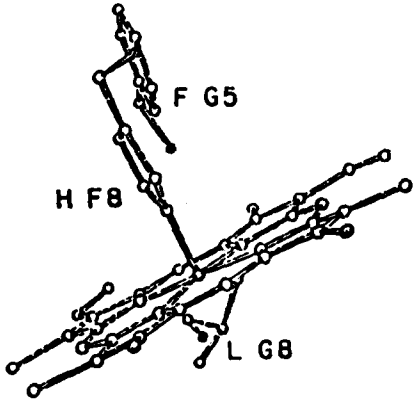

HEMERYTHRIN

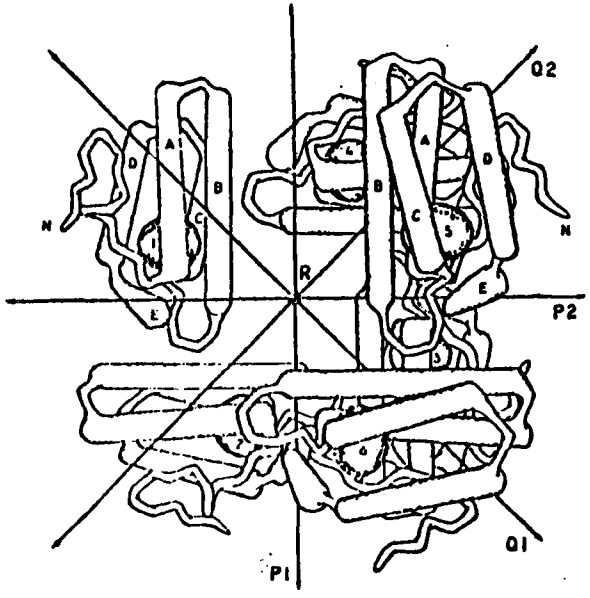

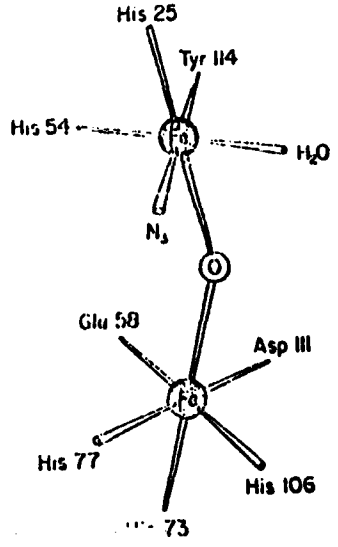

HEMOCYANIN

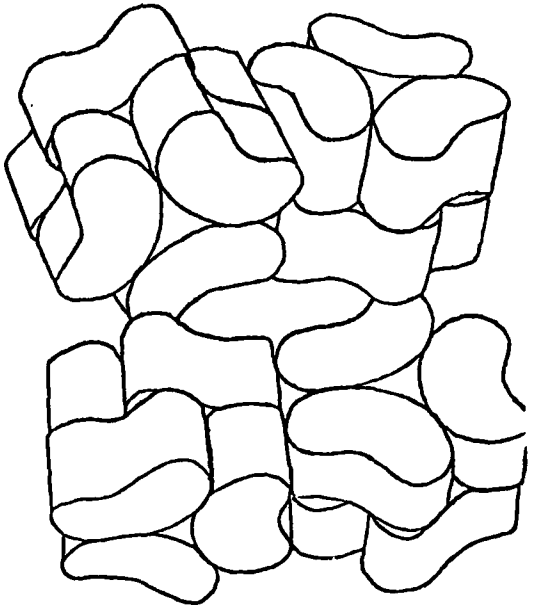

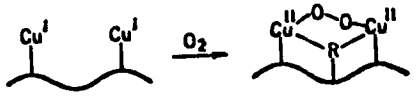

Structural Characterization of Materials

for High Energy Space Systems

Richard Gilardi

Laboratory for the Structure of Matter

Naval Research Laboratory, Washington,D. C. 20375

Bibliography (preprints/reprints available from above address)

A. Amorphous Materials Diffraction Analysis

1. Structural Ordering in Amorphous $TbFe_2$ and YFe_2, P. D'Antonio and J. H. Konnert, Acta Cryst. (1982), to be published.

2. Diffraction Evidence for Distorted Graphite-Like Layers in an Activated Carbon of Very Large Surface Area, J. H. Konnert and P. D'Antonio, Carbon, to be published.

3. Comparison of Radial Distribution Function for Silica Glass with those for Various Bonding Topologies: Use of Correlation Function", J. H. Konnert, P. D'Antonio and J. Karle, J. Non-Cryst. Solids, to be published.

B. Small Angle Scattering Analysis

1. Small Angle Scattering Study of Solar Cell Device Materials prepared at Substrate Temperatures of 130°C and 250°C, P. D'Antonio and J. H. Konnert, AIP Conf. Proceedings No. 73, pp. 117-119(1981).

C. Battery Materials

1. Powder Neutron Diffraction Study of Chemically Prepared β-Lead Dioxide, P. D'Antonio and A. Santoro, Acta Cryst. (1980), B36, 2394.

D. Propellants

1. New Energetic Materials: Structural Characterization, R. Gilardi, C. F. George and J. Karle, NRL Report LSM 81-1 (1981).

SESSION VIII. CHEMICAL PHYSICS

Recent Advances in Molecular Dynamics

Presented by

Herschel Rabitz

Princeton University

at the

Space Prime-Power Conference 1982

The efficient generation of prime-power in space will ultimately be achieved by drawing on fundamental and practical achievements. Regardless of whether nuclear, magnetohydrodynamic, gas turbine or other power sources are ultimately utilized, many common areas of chemistry and physics will be drawn on to achieve the desired result. For example, materials science, particularly in the high temperature regime, and various aspects of molecular physics will enter into all of these solutions to the prime-power problem. The purpose of this presentation is to give a summary of current basic research directions in the field of molecular dynamics and illustrate the present capabilities in the field. The words molecular dynamics refer to atoms, molecules or ions which are undergoing changes due to interactions with their environment typically by collisions or radiative processes. The subject encompasses a wide variety of experimental and theoretical endeavors and the presentation aims to summarize some key activities in the field. Much of the basic research carried out in molecular dynamics during the past several years has been motivated by various practical needs; space prime-power requirements could play a similar role in the future. The capabilities and present directions of the molecular dynamics field will be summarized in the presentation.

Recent Advances in Molecular Dynamics

Descriptive Material for the Viewgraph Presentation*

1. Molecular dynamics research has been carried out with two broad motivations in mind. In the context of the present conference, the practical need for space prime-power is of central importance. Fundamental concerns will also continue to play a role and their spin-off to practical applications can also be expected.

2. The subject of chemical change lies at the heart of the field of molecular dynamics and a number of specific areas of applied concern are continuing to motivate research in the field. The chemical dynamics community has responded very strongly to research needs from the areas listed in the viewgraph and some of these have direct impact on space prime-power. The following portion of the talk will be divided into two sections: Experimental studies followed by a summary of theoretical methodology.

3. The subject of chemical kinetics as a macroscopic phenomena concerns the spatial and time-dependent evolution of reacting systems. Such problems inherently involve a mix of traditional chemical reaction processes as well as transport effects. All too often one or the other of these items is ignored largely for the sake of simplicity. In fact, most real problems will involve an interactive mix between transport and reaction dynamics and this point must always be kept in mind especially when attempting to theoretically understand laboratory kinetic phenomena.

*The numbered paragraphs correspond to the viewgraphs on the preceeding pages.

4. The chemical rate constants $k_{i \to j}(T)$ can be expressed in terms of a velocity average over the more fundamental collision cross sections $\sigma_{i \to j}(\underline{v})$. The indices i and j refer to molecular states or species undergoing change. Recognizing this connection between rate constants and cross section has led to efforts to invert the rate constants back to the more fundamental cross sections. An important point regarding this subject is the fact that the distribution function $F(\underline{v},T)$ can in many cases not be a Boltzmann distribution. In fact, an important goal in many problems is to establish this distribution function when the system is in a highly non-equilibrium circumstance. Problems of this sort can occur in thermionic converters and magnetohydrodynamic devices.

5. The transport of energy, momentum, angular momentum or other properties is most easily expressed in terms of transport coefficients entering into the kinetics of motion. There is continuing effort at measuring these coefficients especially in the presence of unusual stresses. For example, transport in the presence of external thermal and magnetic field gradients have been studied. These measurements are often very delicate but they can yield valuable information for practical circumstances as well as fundamental insights into the underlying molecular processes.

6. There is an entire family of measurements which can be categorized in the field of relaxation phenomena. These measurements can either be done in the time or frequency domain which are related to each other by a Fourier transform. In essence, an experiment of this type is performed by perturbing an otherwise equilibrium system and monitoring its relaxation back to equilibrium. Since there are many different ways of performing

such a perturbation, it is always desirable to do as many (linearly the independent) experiments as possible and therefore extract out a family of relaxation times τ_1, τ_2,... . Measurements of this type are also attractive since they often can be carried out under conditions closely simulating those actually of concern in practical engineering applications. From a fundamental point of view difficulties can arise since the measurements are in the bulk phase and unique characterization of the perturbed state can be a problem.

7. Spectral line shape measurements represent a relaxation experiment carried out in the frequency domain. The measurements are relatively easy since they just involve the recording of spectral intensity as a function of frequency for the substance of concern. The width $\Delta\nu$ of such spectral features is inversely related to the characteristic relaxation time for the system. Measurements of this type are often referred to as half-state selected since the optical radiation can many times be tuned to unique initial and final states from which the bulk relaxation is connected. A rich body of data can be generated when many independent spectral transitions can be observed. With this in mind and the availability of current high resolution spectrometers there has been much recent activity in the area of inverting such spectral information into more fundamental underlying collisional rate constants. These fundamental constants could then be used to describe entirely different physical phenomena of interest relying on the same underlying dynamical processes.

8. A variety of time domain relaxation experiments can be performed using several system preparation and observational tools. Perhaps the most far-reaching of these methods is the laser pump/probe technique

whereby the system is prepared in a non-equilibrium state by an intense laser pulse and subsequently probed after a time delay by a weaker radiative source. These type of experiments have generated a wealth of information and may be expected to continue to do so.

9. The ultimate tool for probing individual atomic and molecular encounter is the molecular beam technique. In this procedure, two beams of species A and B in particular molecular states and relative velocity can be crossed in a high vacuum chamber and the resultant products examined for their own energy content and molecular arrangement. Both ions and neutrals can be studied. These experiments are very difficult to perform particularly at high resolution and with complete state selection, however the technique is available and can be applied when necessary. There has been recent emphasis on its applications to very large complex polyatomic systems.

10. The subject of interfacial phenomena is receiving much attention in chemical physics and the most basic process in this regard concerns gas surface scattering. In many respects, this research is a spin-off of molecular studies and the field has blossomed recently with the availability of high vacuum technology and various surface characterization techniques. Both reactive and non-reactive processes may be studied including those where the surface may actually be damaged in a controlled fashion. The parallel area of research on spectral studies of surface absorbed molecules is receiving much attention.

11. The theoretical treatment of molecular dynamics has followed along two lines: an ab-initio route which aims to start with the hamiltonian

H and proceed through to the calculation of observables and the second approach of using theory to provide a theoretical framework for the analysis of experiments. This latter category of work has largely been a recent activity and its motivation derives from the increasing availability of high quality laboratory data particularly in the area of relaxation experiments. Both avenues of work will be illustrated in the following viewgraphs.

12. From an ab-initio point of view the microscopic realm of molecular dynamics becomes a problem in solving Schrodinger's equation. This equation becomes a multi-dimensional partial differential equation for problems of realistic concern. The conventional approach is through eigenfunction expansions yielding large sets of coupled ordinary differential equations. More recently there has been an increased interest in directly approaching the partial differential equations by discretization methods such as finite differences or finite elements. The boundary integral method appears to be a useful way of dealing with the problem.

13. Although quantum mechanics provides the proper description of microscopic phenomenon, classical mechanics still has a wide realm of applicability, when the wavelength associated with molecular motion is much smaller than the actual particle sizes. In practice, this condition is often satisfied and Hamilton's equationsof motion provide a very physical picture for molecular processes. The resultant initial value differential equations are relatively easy to solve and classical mechanics has become a very popular approach in the field.

14. The classical approach is most useful for treating large multi-particle

systems particularly involving polyatomic motion. Intramolecular energy transfer from this classical perspective is a subject which has received considerable attention. Along the same lines the classical study of an ensemble of atoms such as constituting a solid surface is quite feasible to treat. Atom-surface scattering including reactive sputtering processes have been examined in this fashion and considerable insight has been gained. The structure of liquids can also be examined from this approach.

15. The second realm of active development in theoretical methodology is for the inversion of laboratory data. Inverse problems come up in all types of molecular dynamics considerations and they represent a particularly interesting and challenging field for study. Fundamental questions of uniqueness of the inversion given a body of limited experimental data are always a matter of concern. The goal here is to invert a certain class of data back to more fundamental information such as cross sections or even the hamiltonian and thereby use this information to predict other new observables. The role of theory here is provide the framework for this analysis without actually having to solve Schrodinger's equation.

16. The goal of inverting experimental data has naturally led to the subject of scaling between different observations. The goal is to see if a subset of the system observables can be found whereby the remainder may be expressed (particularly a simple linear form) in terms of the critical subset. Under certain dynamical approximations, one can show that scaling naturally follows and there is a mounting list of experimental data that exhibits scaling behavior to a high degree of approximation. The linearized scaling relations can be viewed as just the first term in

a Taylor series whose coefficients are a special type of sensitivity gradient.

17. There is a certain common structure to all mathematical modelling in science and engineering and recognition of this commonality naturally leads to the development of powerful sensitivity analysis tools. All mathematically defined physical problems can be viewed from an input/output perspective where the input information is often parametrically represented by the parameters α_1, α_2, ... and the observables O_1, O_2, ... are functions of the input information. The equations (usually differential or integral) connecting the input and output provide a scrambler or filter in this connection. Sensitivity analysis aims to probe the relation between the input and output information and the subject has already found use in engineering and other applied disciplines.

18. The elementary sensitivity coefficients are defined as gradients of the observables with respect to the input parameters and functional analogs of the same gradients can be generated for systems having distributed parameters. In addition, an entire family of derived sensitivities may be easily calculated by interchanging the systems dependent and independent variables. In this fashion the interrelationship between system parameters and observables themselves as well as a host of other questions may be explored. At a further level of sophistication, a feature sensitivity analysis can be performed whereby any mathematically or physically meaningful feature in the observables may be probed where there is dependence on the underlying parameters in the system.

19. An example of the general mathematical modelling logic occurs in

chemical kinetics and this is schematically depicted in the viewgraph. The input parameters consist of rate constants, fluid mechanical transport coefficients and any other physical conditions such as initial species concentrations or boundary conditions on the differential equations. The observables are typically the actual species themselves but other bulk properties may also be considered. In recent years considerable effort has gone into the numerical solution of the generally non-linear differential equations describing such processes. In addition, efficient sensitivity codes are also being developed with particular emphasis on the use of Green's function techniques.

20. This figure illustrates two derived sensitivity densities for a one-dimensional reaction-diffusion system. For example, the bottom figure is a density profile for how chemical species c_1 at position x and time t is influenced by a variation in chemical species concentration c_2 at position x' and prior t'. Clear evidence for a time delay on the species perturbation is evident in the picture where the heavy dark line represents the locus of sensitivity time delay maxima. When species 1 is probed at larger values of x the time delay correspondingly increases. Densities such as this may be used as a guide for how to judiciously introduce perturbing species or physical effects in order to control the overall spatial and time history of the evolving system. A similar analysis can be carried out in quantum mechanical systems where the input parameters now reside in the hamiltonian and the output consists of all possible observables in the system.

21. The relationship between modelling laboratory experiments and sensitivity analysis is shown in the accompanying viewgraphs. Often laboratory

measurements are performed for the purpose of deducing structural information about the underlying mathematical model such as a kinetic mechanism or a force field. Sensitivity analysis can provide a very powerful quantitative aid for the design and analysis of models and experiments in such circumstances. A variety of questions can be addressed which would be very difficult to treat by any other means.

22. The present capabilities of molecular dynamics for handling various chemical systems is summarized in the accompanying viewgraph. Very detailed questions of about energy transfer and molecular properties can be addressed for small diatomic systems and more coarse grained treatments are available for larger polyatomic systems. Intense research activity is continuing in all of these areas and the frontier of the field is directed toward treating larger systems. These problems are raising new questions and new experimental and theoretical tools are being developed to address these matters. On the one hand, molecular dynamics provides a readily available ongoing resource for relevant problems in the space prime-power area. In the addition, the latter applied topic will undoubtedly raise its own unique molecular questions which could be addressable by presently available or specifically designed techniques of molecular dynamics.

Molecular Dynamics:

An Experimental and Theoretical Overview.

Motivation:

1. Practical phenomena and devices.

2. Fundamental concerns.

Chemical Reaction Dynamics and Chemical Kinetics

The primary motivation behind the field.

Combustion

Atmospheric Chemistry

Chemical reaction control (design)

Catalytic activity

Surface Chemistry

Laser development

Materials science

Chemical Kinetics

$t = 0$, prepare the system

$$A_1(0),\ A_2(0),\ A_s(0),\ldots$$

Let it react and sample at $t > 0$.

Set up coupled kinetic and fluid mechanical equations

$$\frac{\partial A_i}{\partial t} = \begin{matrix}\text{transport}\\ \text{terms}\end{matrix} + \begin{matrix}\text{reaction}\\ \text{terms}\end{matrix}$$

A mixed Initial/Boundary value problem.

Modelling is <u>necessary</u> to analyze the measurements.

Advantage/disadvantage - <u>real, complex</u> systems can be studied.

Temperature Dependence

Measurements at a given T.

Calculations at a given E.

$$k_{i \to j}(T) = \rho \int d\underline{v} F(\underline{v},T) \sigma_{i \to j}(\underline{v})$$

Need $\sigma_{i \to j}$ at "all" energies

A Laplace transform of σ:

invert $k_{i \to j}$ to yield $\sigma(E)$.

Transport Coefficients

Mass diffusion, thermal diffusion, viscosity, etc.

E and H field free: Little sensitivity to anisotropic or target structure.

In an E or H field:

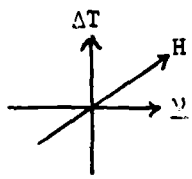

Slip effects, etc.

Transport effects on reaction rates

A bulk question of concern.

General Relaxation Experiments

In the time or frequency domain.

Disturb a system in equilibrium and observe its rate of return.

Ideal case: do N independent experiments $\tau_1, \tau_2, \cdots \tau_N$

T jump, NMR, ESR, acoustic, shock tubes, etc.

Advantage: often easy to perform

Disadvantage: often difficult to know what "state" has been prepared and what τ_i means.

Spectral Line Shapes

Half-state selected observations

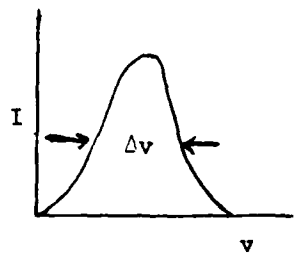

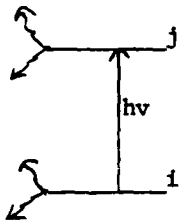

Δ_ν versus pressure is measured.

$\Delta\nu$ is a relaxation rate - a known (but complicated) function of S-matrix elements.

Advantages: relatively easy to do (with some care).

Disadvantages: the bulk phase. More unknown rates than possible experiments. Theory is needed to analyze the data.

Laser Pump/Probe Measurements

$h\nu + m \rightarrow m^*$ (pump)

$m^* + n \rightarrow$ new products (probed)

probe

pump

Careful time control is needed.

Yields collision rates k(T)

Advantages: a bulk medium, polarization effects present.

Disadvantage: a bulk medium, kinetic modelling is needed to interpret the data.

Molecular Beams

Ideal: Crossed beams with full state and energy selection.

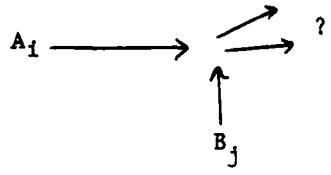

$$E = \varepsilon_i + \varepsilon_j + \frac{\hbar^2 k^2}{2\mu}$$

yields $\frac{d\sigma}{dr}$ versus all dynamical variables

Advantage: A maximum of information can be gained.

Disadvantage: Very difficult to perform; preparation and detection problems.

Gas-Surface Scattering

reactive and non-reactive

goal: understand surface chemistry

Experimental problems: characterization of the surface and detection

Theoretical problems: (a) phonon coupling (many states)
(b) surface defects (an ensemble *of Hamiltonians*)

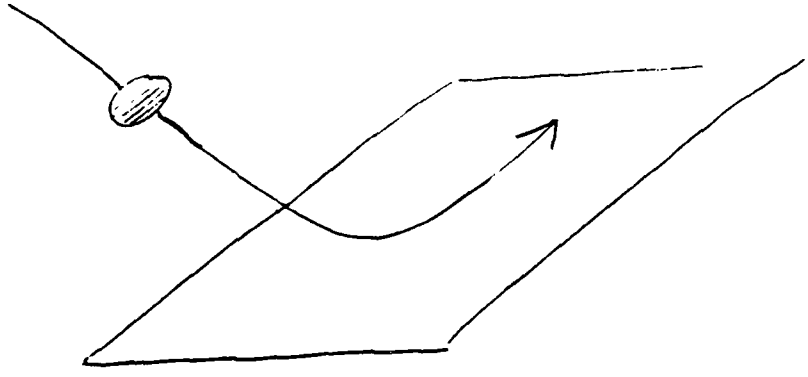

Theoretical Molecular Dynamics

Realm of operation:

1. *ab initio*

$$H \rightarrow \psi \rightarrow \text{observables}$$

2. Framework for the analysis of experimental data.

   a) H is unknown.

   b) do not want to solve $H\psi = E\psi$

Partial Differential Equation Methods

Conventional approach:

$H(r)\psi(\underline{r}) = E\psi(\underline{r})$, a single partial differential equations (PDE)

Break into many sets of coupled ordinary differential equations

$$\psi = \sum_{nJ} a_n^J(r_1)\phi_n^J(r_2, r_3, \ldots)$$

$$\underline{\underline{H}}^J(r_1)\underline{a}(r_1) = E\underline{a}^J(r_1)$$

Alternative Approach:

Solve P.D.E. directly by full (or partial) discretization

Finite differences, boundary integral, etc.

Advantage: No problem with strong coupling, and break-up can be easily handled.

Disadvantage: Must handle (efficiently) large sets of sparse matrices.

Classical Mechanics

Decision: $\lambda = \frac{h}{p}$ { < target size classical; > target size quantum mechanical

$$\dot{q}_i = \frac{\partial H}{\partial p_i} \qquad \dot{p}_i = -\frac{\partial H}{\partial q_i}$$

$\underline{q}(0), \underline{p}(0) \Rightarrow \underline{q}(t), \underline{p}(t)$

Initial value problem

Calculate the distribution of final (energy) momenta averaged over initial conditions.

Advantage: Very physical and each trajectory is easy.

Disadvantage: No quantum structure and good statistics is expensive.

Classical Applications

Large multiparticle systems

Polyatomic motion

Surface studies

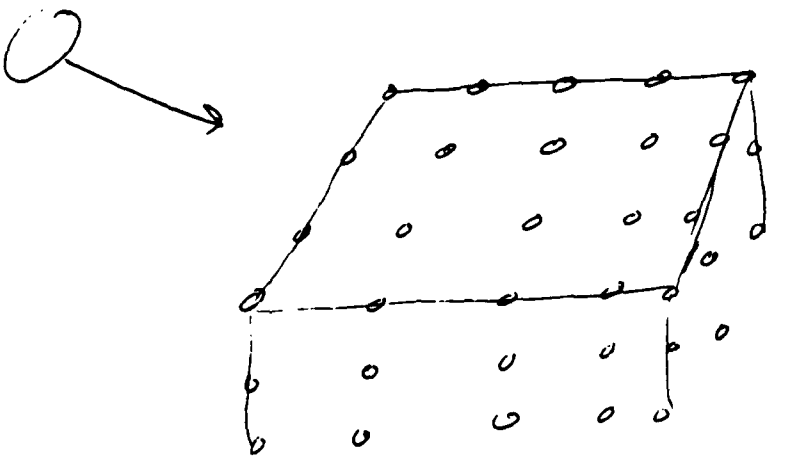

Inversion of Data

Assume a body of (good) data $\frac{\partial\sigma}{\partial r}$ is available for "all" states and

seek: $V(\underline{r})$ intermolecular potential

Present method: parameterize V and fit to the data.

Uniqueness questions

Goal: Understand the mapping:

$$\underline{\underline{H}} \Leftrightarrow \underline{\underline{S}}$$

Sensitivity Questions $\frac{\delta S}{\delta H}$

Scaling of Observables?

Scaling

Observations: $O_1, O_2, \ldots$

Goal: Seek a subset $\{O_i'\}$ such that

$$O_j = O_j(\{O_i'\}) \approx \sum_i{}' c_{ij} O_i'$$

a) Use theory to find c_{ij}

b) Use experiment to find O_i'

$$c_{ij} = \frac{\partial O_j}{\partial O_i}$$

Modelling in Science

Input Information

$\alpha_1, \alpha_2, \alpha_3 \ldots$

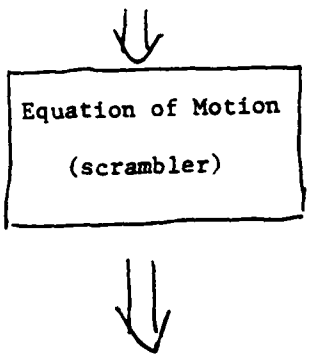

Output Observables

$O_1(\alpha_1, \alpha_2 \ldots)$

$O_2(\alpha_1, \alpha_2 \ldots)$

etc.

Sensitivity Analysis

elementary $\frac{\partial O_i}{\partial \alpha_j}$, $\frac{\partial^2 O_i}{\partial \alpha_j \partial \alpha_\ell}$, etc.

Functional analog: $O_i = O_i(x)$

$\alpha_j = \alpha_j(x')$

$\Rightarrow \frac{\delta O_i(x)}{\delta O_j(x')}$

Derived: interchange variables

$\alpha_1, \alpha_2, \alpha_3 \rightarrow O_1, O_2, O_3 \ldots$

$\left(\frac{\partial \alpha_j}{\partial O_i}\right)$, $\left(\frac{\partial \alpha_i}{\partial \alpha_j}\right)_{obs.}$, $\left(\frac{\partial O_i}{\partial O_j}\right)$

Feature analysis:

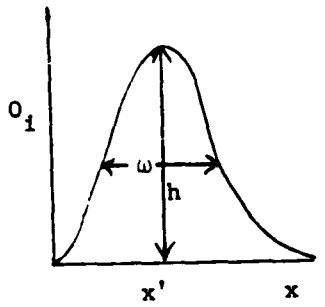

$\left(\frac{\partial \omega}{\partial \alpha_i}\right)$, $\left(\frac{\partial h}{\partial \alpha_i}\right)$

$\left(\frac{\partial x'}{\partial \alpha_i}\right)$, etc.

Modelling of Complex Kinetic Systems

Fluid Mechanics + $A + B \underset{k_2}{\overset{k_1}{\rightleftharpoons}} C + D$

$C + E \xrightarrow{k_3}$ ...

etc.

Procedure

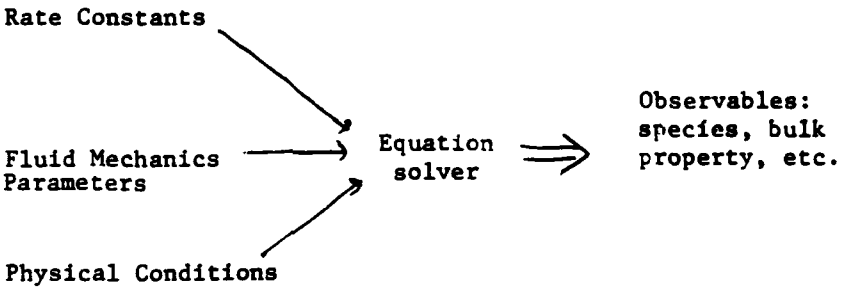

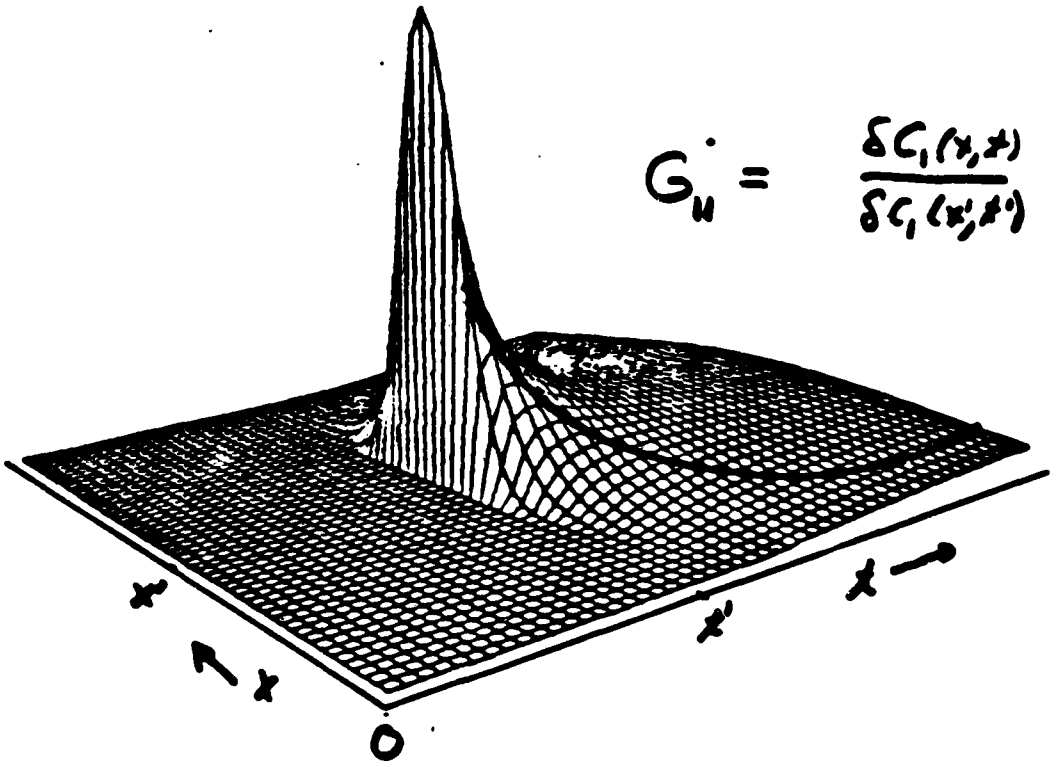
$G_{11} = \frac{\delta C_1(x,t)}{\delta C_1(x',t')}$
x''
x
0
x'
x

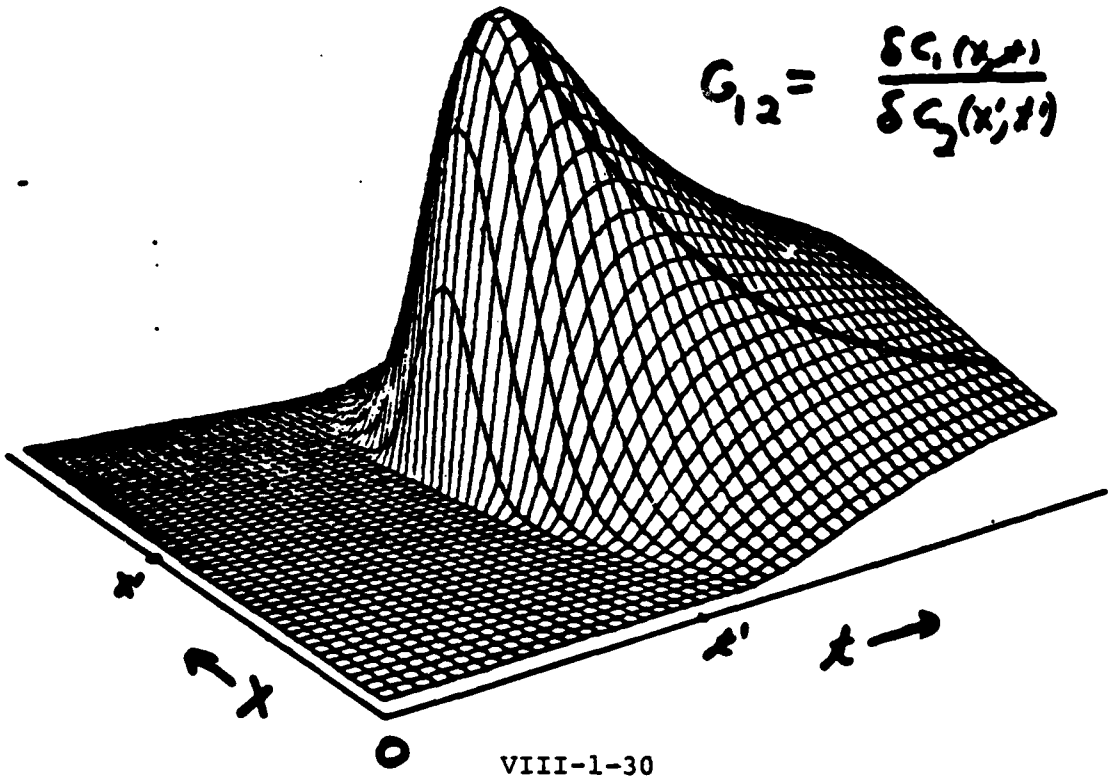
$G_{12} = \frac{\delta C_1(x,t)}{\delta C_2(x',t')}$
x''
x
0
x'
t

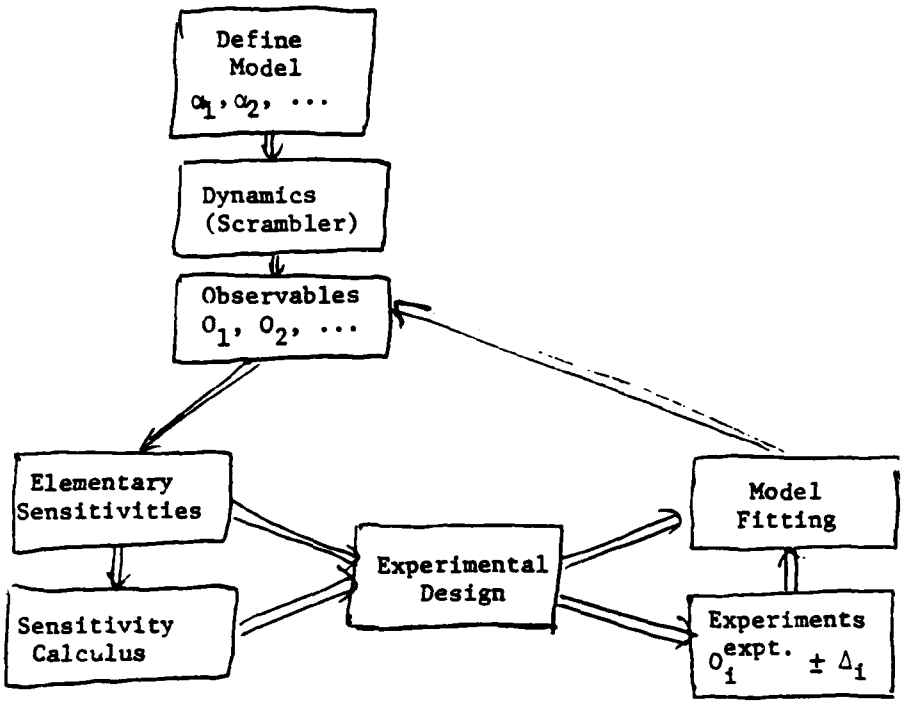
Define Model
$\alpha_1, \alpha_2, \ldots$
Dynamics (Scrambler)
Observables
$O_1, O_2, \ldots$
Elementary Sensitivities
Sensitivity Calculus
Experimental Design
Model Fitting
Experiments
$O_i^{expt.} \pm \Delta_i$

Present Capabilities

a) detailed electronic, vibrational, rotational questions on small systems (diatomics).

b) coarse analysis on polyatomic systems.

Frontier

Large systems!

a) new questions

b) new tools

Q & A - H. Rabitz

From: P. J. Turchi, R & D Associates

Do sensitivity techniques provide a new method of deriving scale laws (predictions)?

A.

Sensitivity techniques do provide two perspectives on scaling:

I. The gradients ($\partial 0i/\partial 0j$) measure the relationship between observables. The information can be used to (1) scale one observable with respect to another and (2) allow rank ordering of the observables with respect to their system significance.

II. The gradients with respect to system parameter, α, can be used in non-linear Pade approximants to scale the observations to new regions of parameter space.

$$Q_i\ (\alpha\ \Delta\alpha)\ P_N\ (\Delta\alpha)/Q_M\ (\Delta\alpha),$$

where Q and P are polynomials.

Recent Advances in Molecular Dynamics

Herschel Rabitz

BIBLIOGRAPHY

Listed below are general references which give background and further access to current literature on research in the area of molecular dynamics.

1. R. B. Bernstein, Editor, Atom-Molecule Collision Theory: A Guide for the Experimentalist (Plenum Press, New York, 1979).

2. J. Nicholas, Chemical Kinetics: Modern Survey of Gas Reactions (John Wiley and Sons, New York, 1976).

3. W. H. Miller, Editor, Dynamics of Molecular Collisions (Plenum Press, New York, 1976). This volume contains review articles on both quantum and classical collision dynamics.

4. R. G. Breene, Theories of Spectral Line Shapes (John Wiley and Sons, New York, 1981).

5. A. DePristo, S. Augustin, R. Ramaswamy and H. Rabitz, " Quantum Number and Energy Scaling for Non-Reactive Collisions", J. Chem. Phys. 70, 850 (1979).

6. H. Rabitz, " Chemical Sensitivity Analysis Theory of Applications to Molecular Dynamics and Kinetics", Computers and Chemistry, 5, 167 (1981).

Abstract for Special Conference
on Prime Power for High-Energy
Space Systems

Chemical Physics of Vaporization, Condensation and Gas-Surface Energy Exchange

Gerd M. Rosenblatt
Chemistry-Materials Science Division
Los Alamos National Laboratory

Current understanding of the rates and atomistic mechanisms of vaporization and condensation will be described. Recent results on the dynamics of gas-surface interactions will be reviewed, with an emphasis upon the degree of energy accommodation, both translational and internal, which occurs when molecular gases interact with solid surfaces. The discussion will center upon work from the author's laboratory.

SPACE PRIME POWER

Some generic research issues

High temperature materials
Vaporization of fuel and components
High temperature corrosion, chemical corrosion
Heat transfer — radiative, interfacial
Thermoelectric and thermionic materials and properties
Heat pipe fundamentals
O_2 diffusion and solubility

CHEMICAL PHYSICS OF VAPORIZATION, CONDENSATION, AND GAS-SURFACE ENERGY TRANSFER

Chemical physics approach

Understand phenomena and their dynamics on an atomistic basis (particularly phenomena involving molecules)

Rapidly advancing areas

Probe molecular quantum states with lasers

Surface structure and dynamics

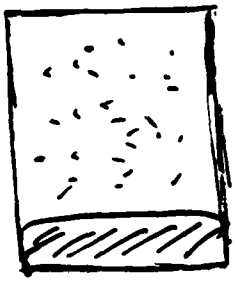

Equilibrium

$$J_E = P_E / \sqrt{2\pi m k T}$$

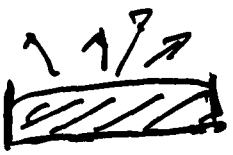

Vacuum

$$J_v^\circ = \alpha_v^\circ P_E / \sqrt{2\pi m k T}$$

Net vaporization

$$J_v = \alpha_v (P_E - P) / \sqrt{2\pi m k T}$$

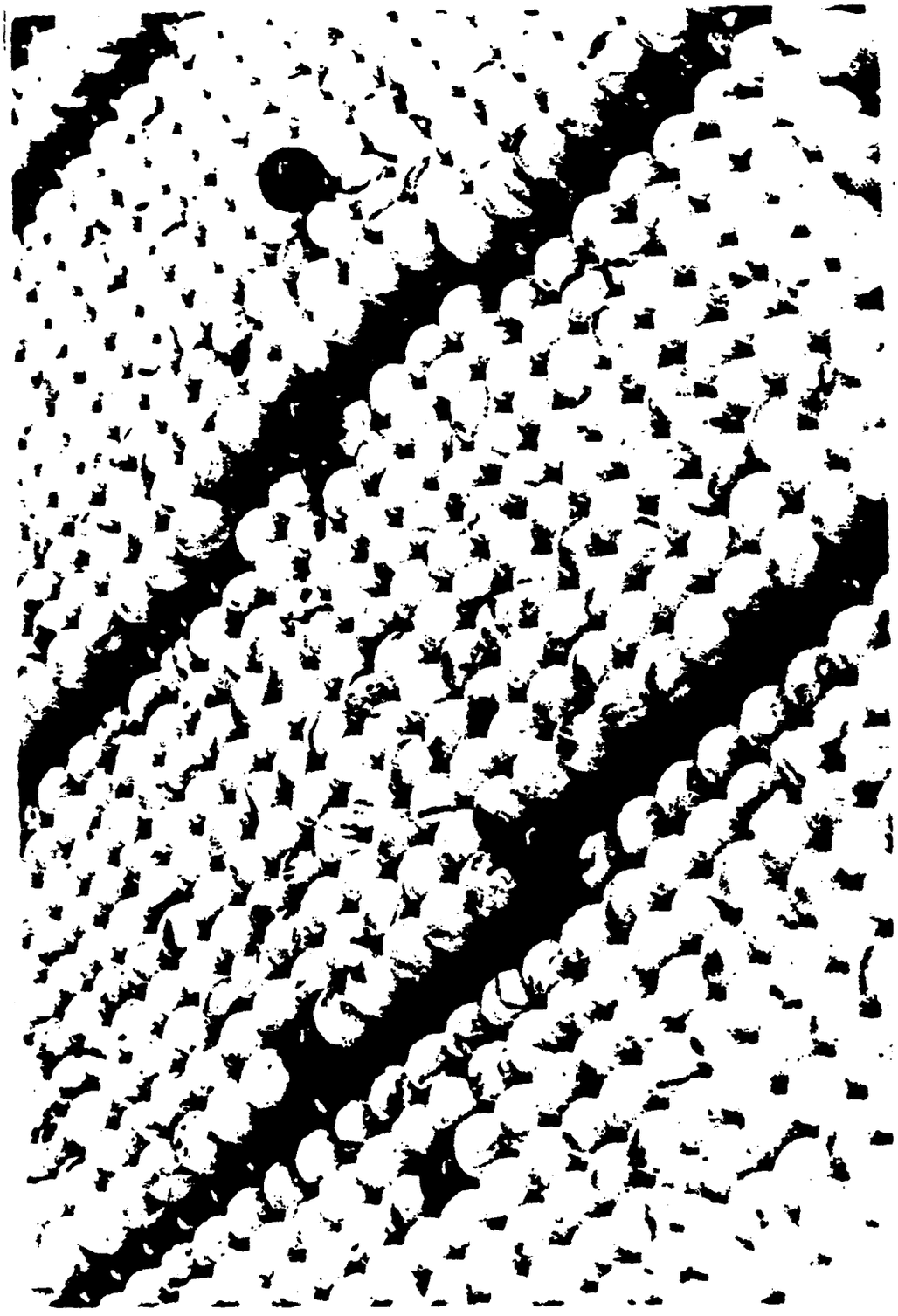

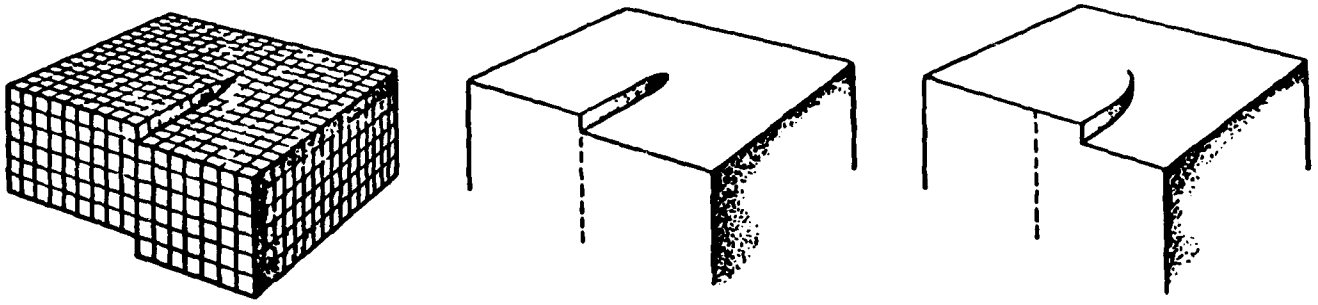

Fig. 18.20. (a) SCREW DISLOCATION, illustrated at left, produces its spiral growth steps in the manner indicated by the succeeding diagrams. A screw dislocation is the type of imperfection that would result if a cut were made part way through a crystal and the two sides slipped over one another. The result is a permanent step extending across a portion of the crystal face and anchored at the boundary of the cut.

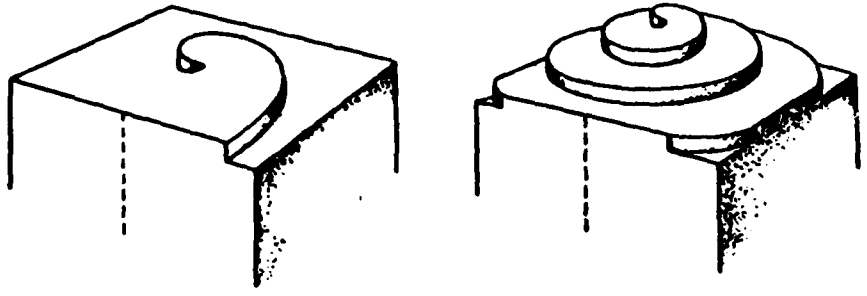

Molecules depositing on the surface from a vapor would lodge against the step, causing it to advance. Since one end is fixed, the step would pivot around that point, with the outer points falling behind the inner, producing a never-ending spiral layer on the surface.

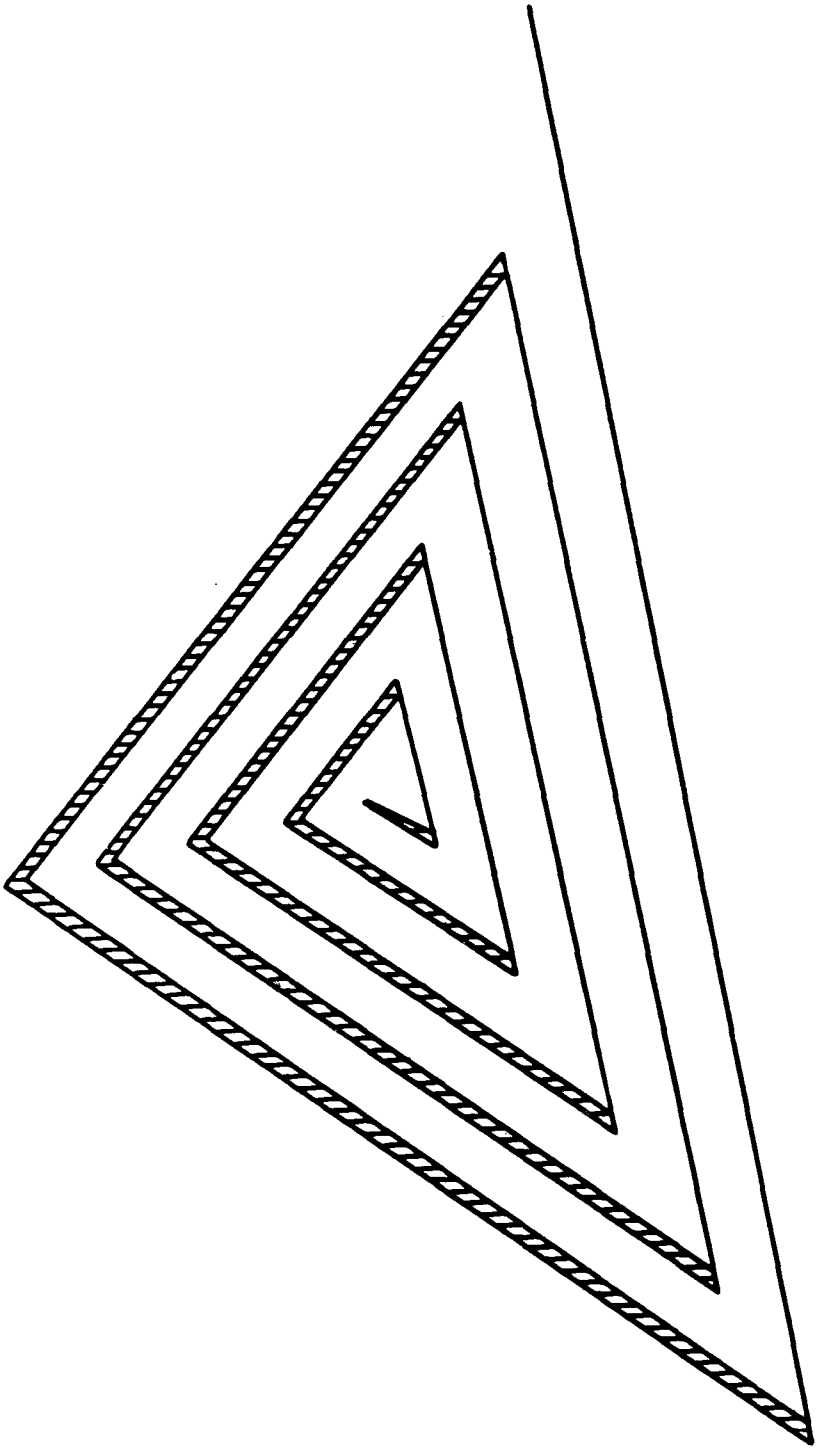

r_L = vacuum vaporization rate

$$P_L = r_L \sqrt{2\pi RT/M}$$

$$\alpha_v^\circ = P_L / P_E$$

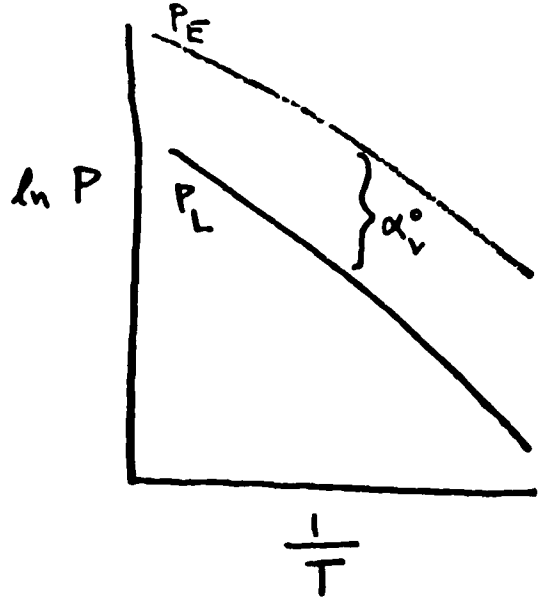

$$R \ln P_E(atm) = -\frac{\Delta H^\circ}{T} + \Delta S^\circ$$

$$R \ln P_L(atm) = -\frac{\Delta H^*}{T} + \Delta S^*$$

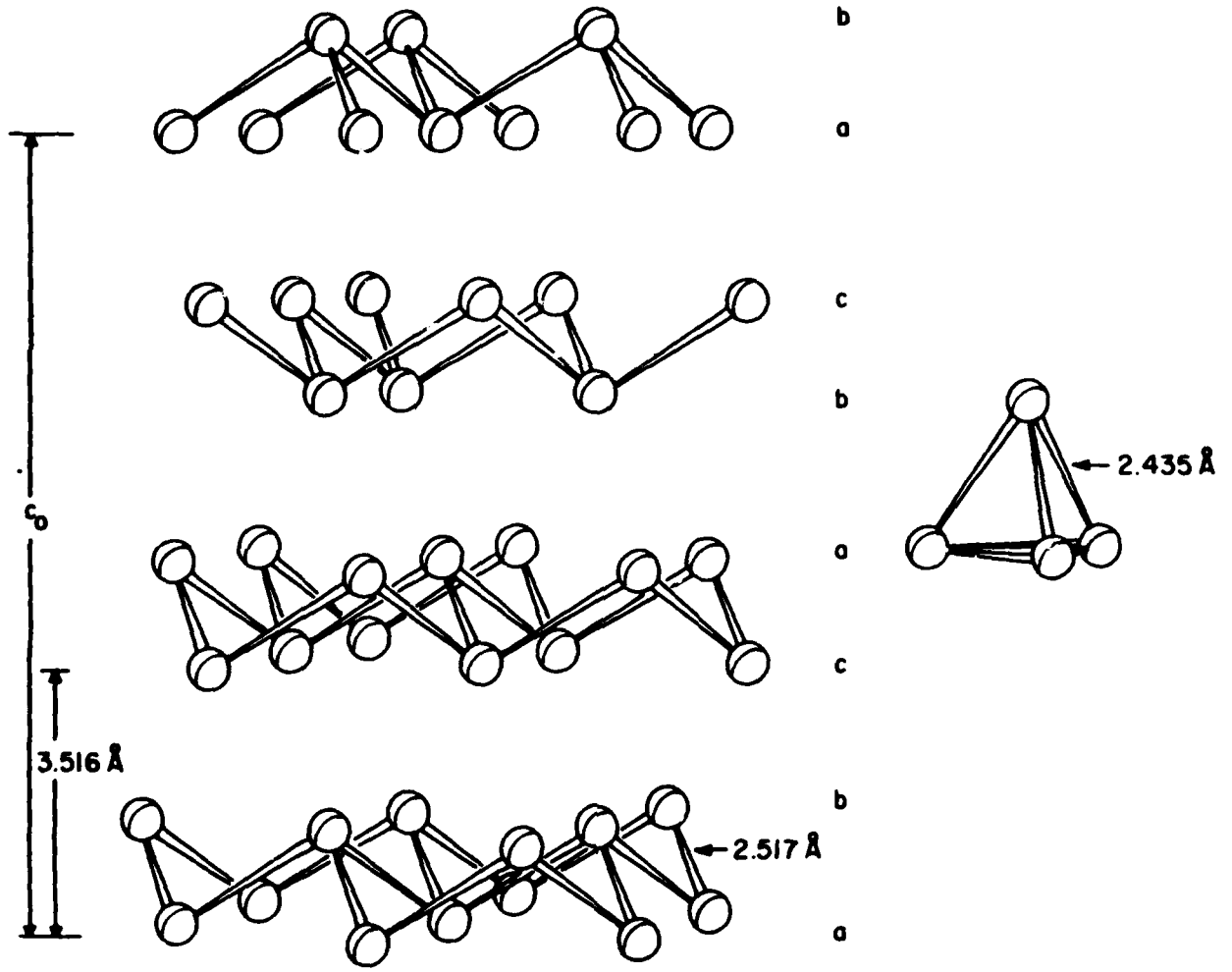
b
a
c
b
a
c
b
a
c_o
3.516 Å
2.517 Å
2.435 Å

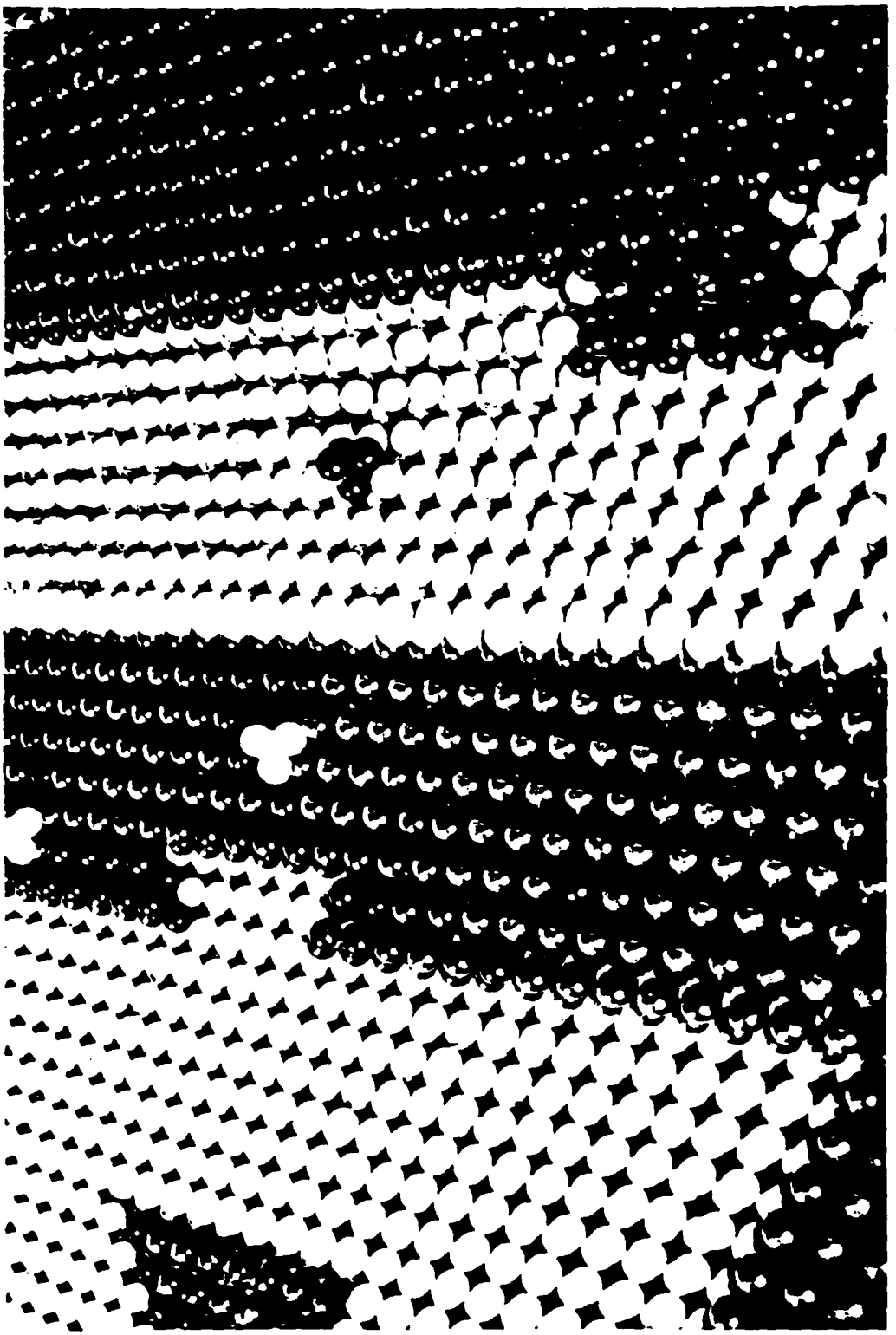

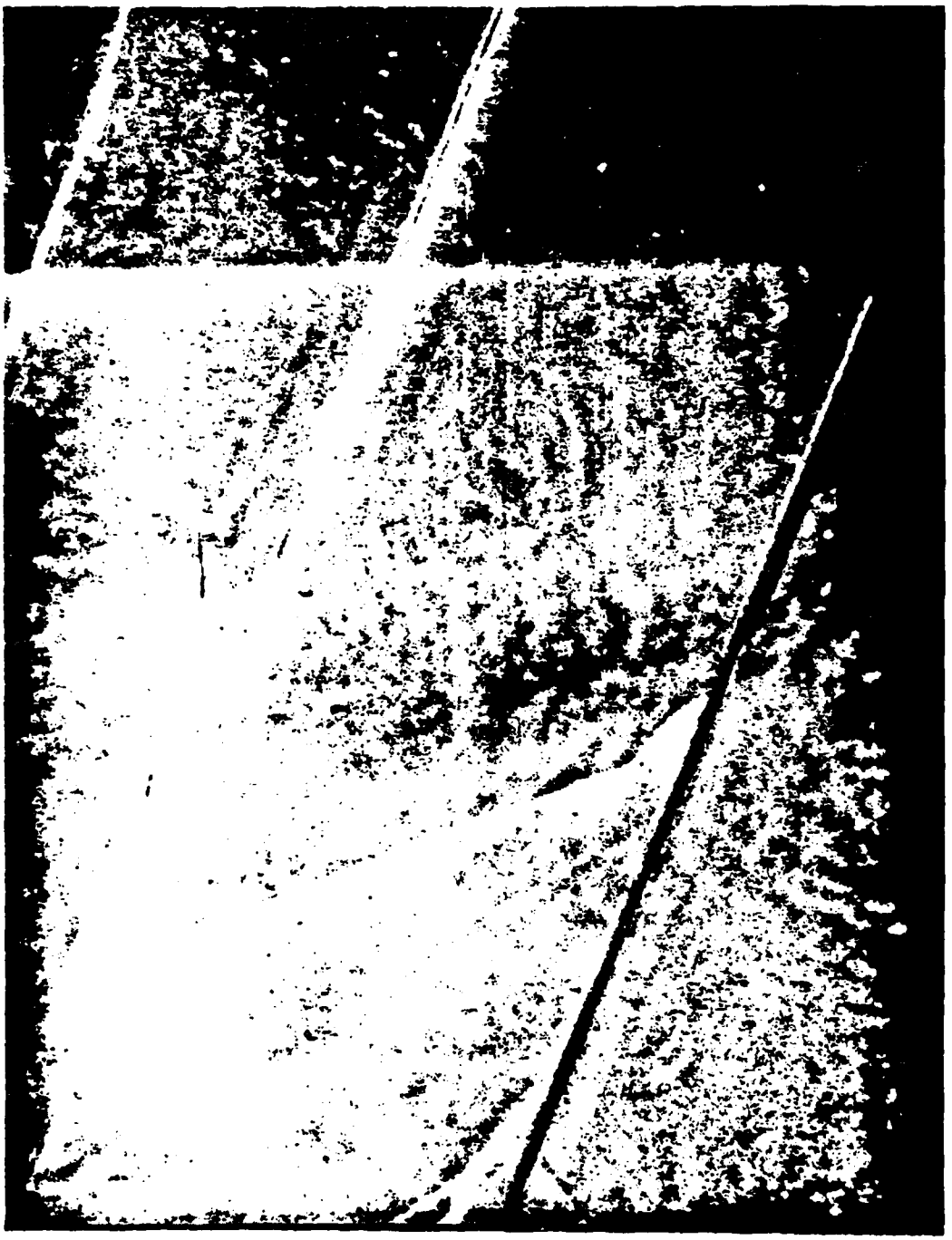

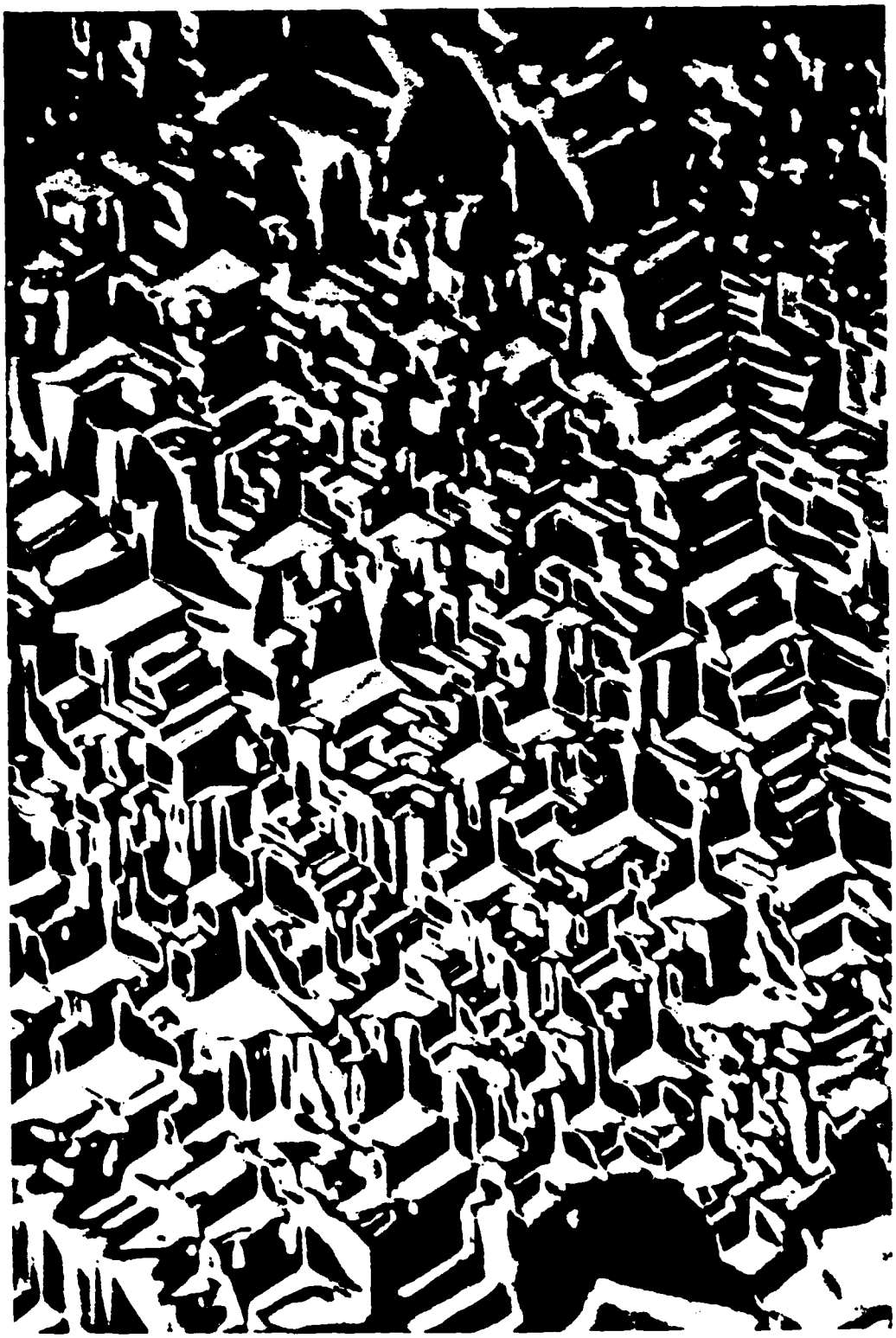

VAPORIZATION PIT PROFILE

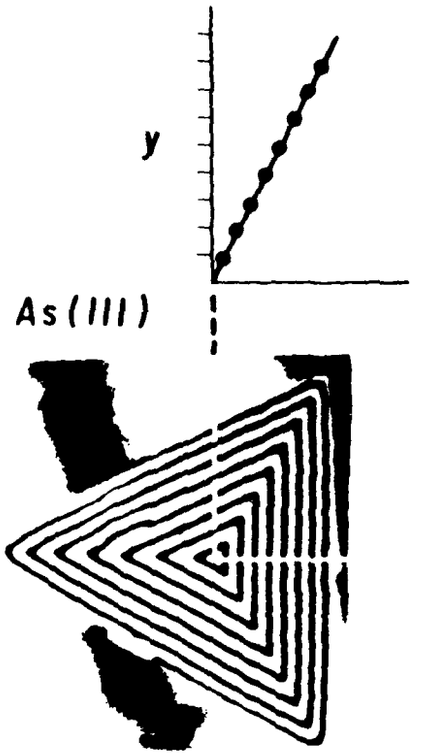

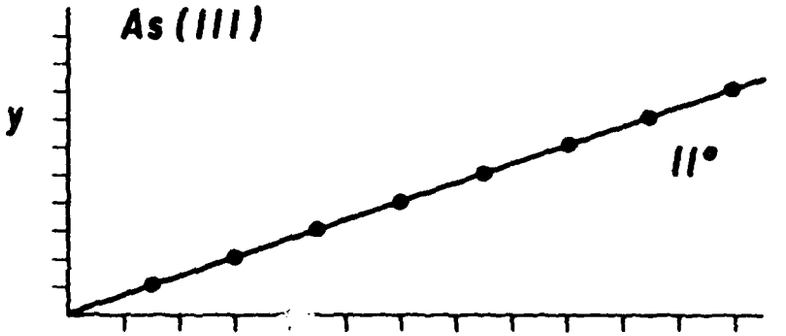

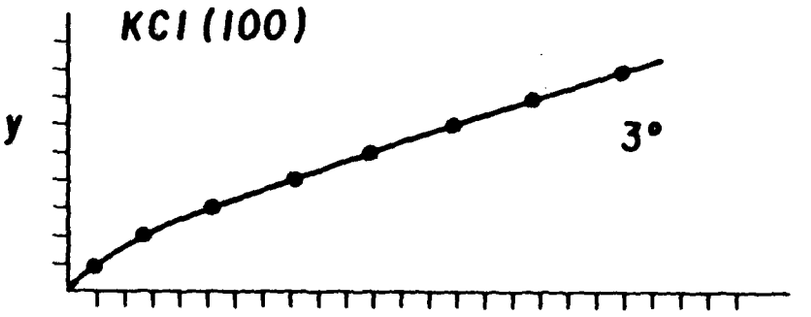

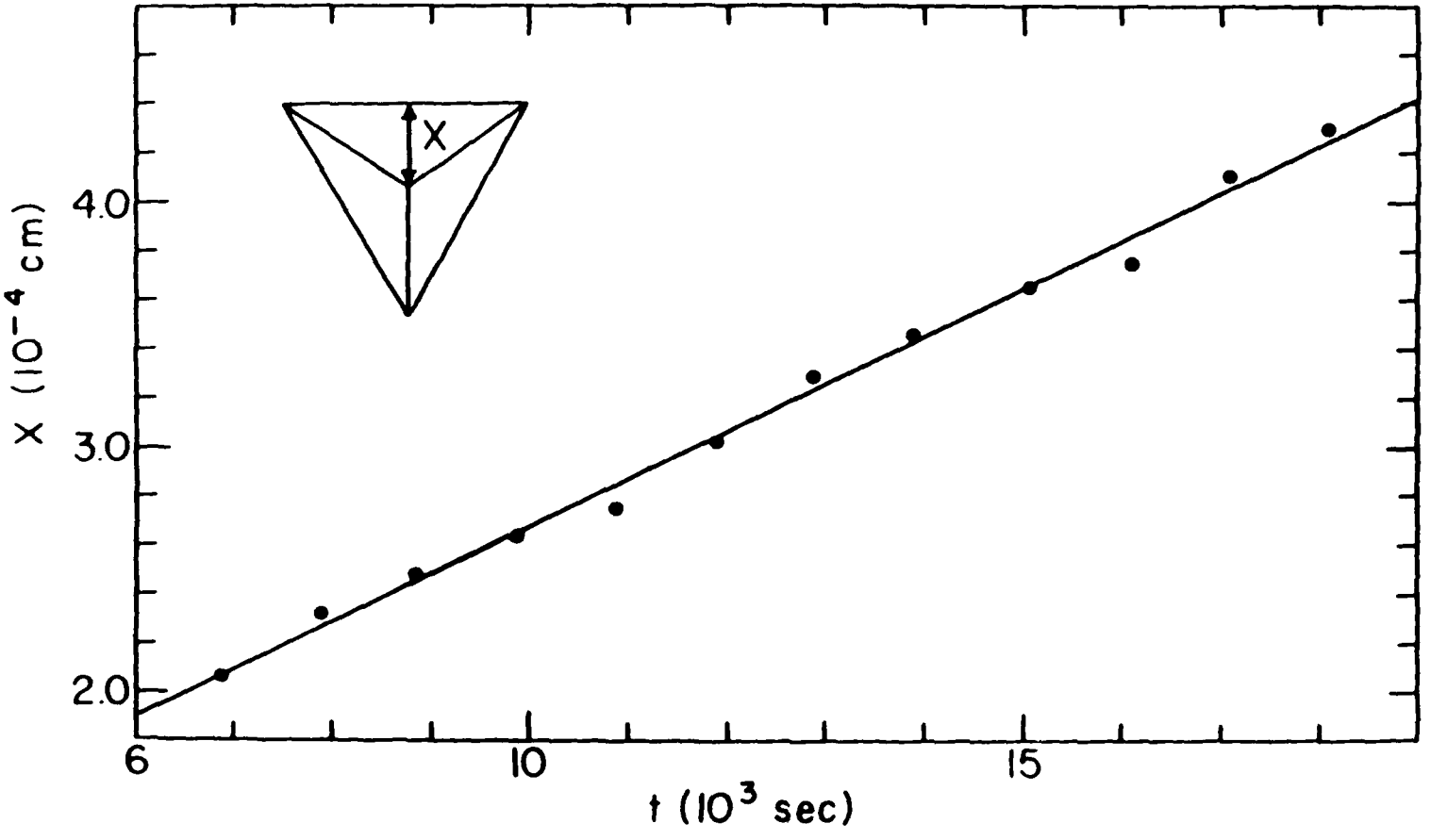
X
4.0
3.0
2.0
X (10^{-4} cm)
6
10
15
t (10^3 sec)

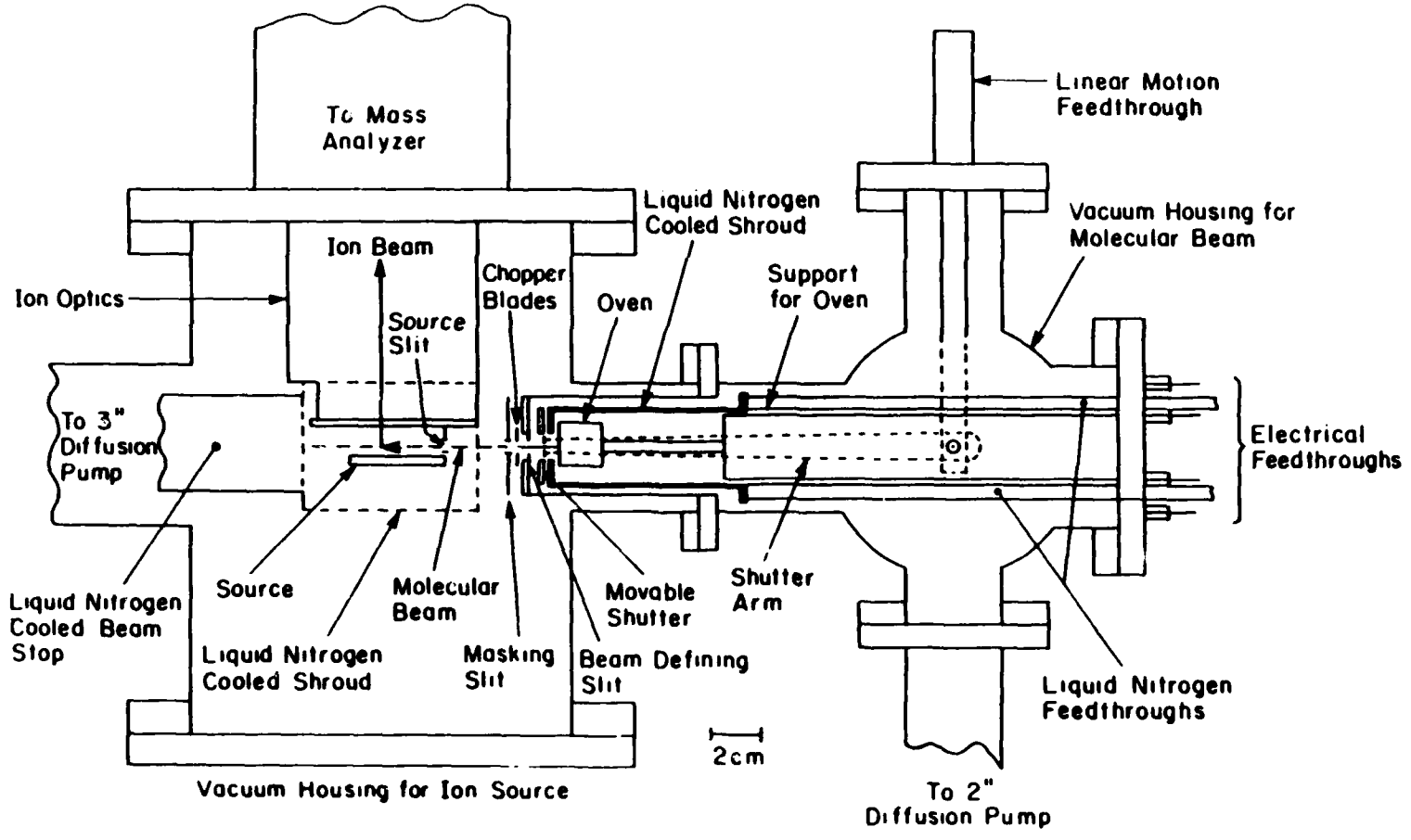
To Mass Analyzer
Linear Motion Feedthrough
Liquid Nitrogen Cooled Shroud
Vacuum Housing for Molecular Beam
Ion Beam
Ion Optics
Chopper Blades
Oven
Support for Oven
Source Slit
To 3" Diffusion Pump
Electrical Feedthroughs
Liquid Nitrogen Cooled Beam Stop
Source
Molecular Beam
Movable Shutter
Shutter Arm
Liquid Nitrogen Cooled Shroud
Masking Slit
Beam Defining Slit
Liquid Nitrogen Feedthroughs
2cm
Vacuum Housing for Ion Source
To 2" Diffusion Pump

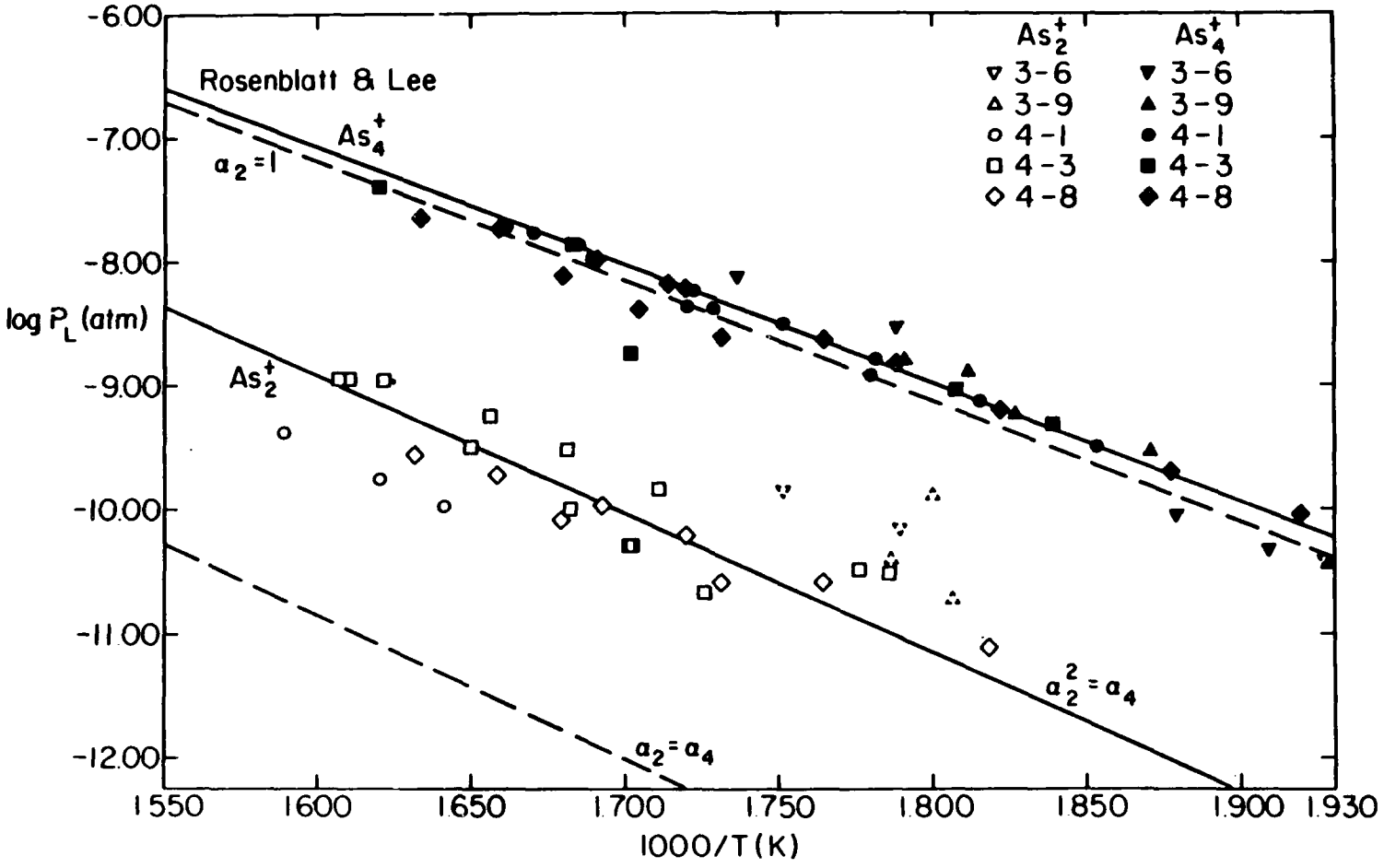
Rosenblatt & Lee
As_4^+
$\alpha_2 = 1$
As_2^+
$\alpha_2^2 = \alpha_4$
$\alpha_2 = \alpha_4$
As_2^+ As_4^+
3-6 3-6
3-9 3-9
4-1 4-1
4-3 4-3
4-8 4-8
log P_L (atm)
-6.00
-7.00
-8.00
-9.00
-10.00
-11.00
-12.00
1550 1600 1650 1700 1750 1800 1850 1900 1930
1000/T (K)

Surface Equilibrium Model

$$A_{s_4}(\text{surface}) = 2\, A_{s_2}(\text{surface})$$

$$K_s = \frac{C_{e2}^2}{C_{e4}} = \frac{C_{s2}^2}{C_{s4}}$$

equilibrium — vacuum vaporization

$$\alpha_4 = \frac{C_{s4}}{C_{e4}} \qquad \alpha_2 = \frac{C_{s2}}{C_{e2}}$$

$$\boxed{\alpha_4 = \alpha_2^2}$$

VIII-2-19

Table 1
Determinations of the translational energy accommodation coefficient, relative to the surface emissivity, for As_4 on As(111)

P (10^{-3} Torr)	T_G (K)	ΔT	γ/ϵ	ϵ	γ
4.2	544.02	0.378	5.72		
4.2	544.02	0.406	6.15		
5.7	549.00	0.473	5.47		
5.7	549.00	0.475	5.49		
5.7	549.00	0.482	5.58		
Mean			5.68 ± .28	0.17 ± .04	0.98 ± .28

Energy accommodation

$$\gamma = \frac{E_I - E_R}{E_I - E_S} = 1.0$$

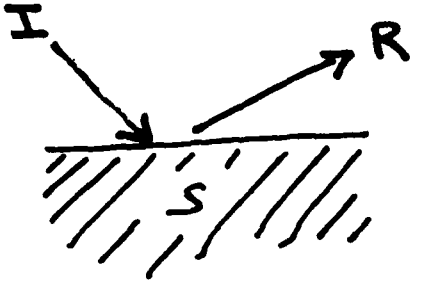

Mass accommodation

$$\alpha = \frac{J_I - J_R}{J_I - J_S}$$

Vaporization

$J_I < J_S$

$\alpha_v^\circ = 8 \times 10^{-5}$

Condensation

$J_I > J_S$

$\alpha_c \simeq 3 \times 10^{-5}$

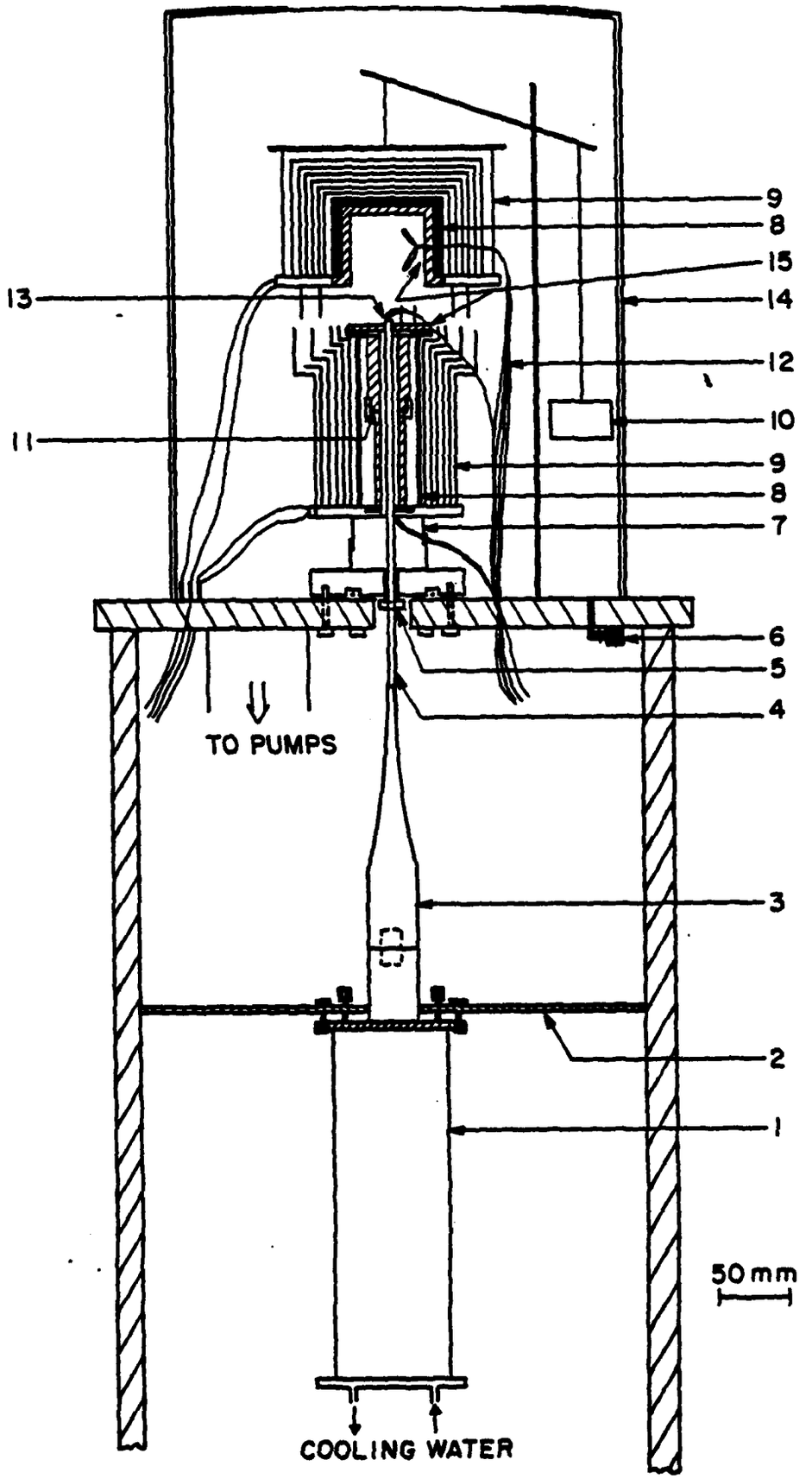
9
8
15
13
14
12
10
11
9
8
7
6
5
4
TO PUMPS
3
2
1
50 mm
COOLING WATER

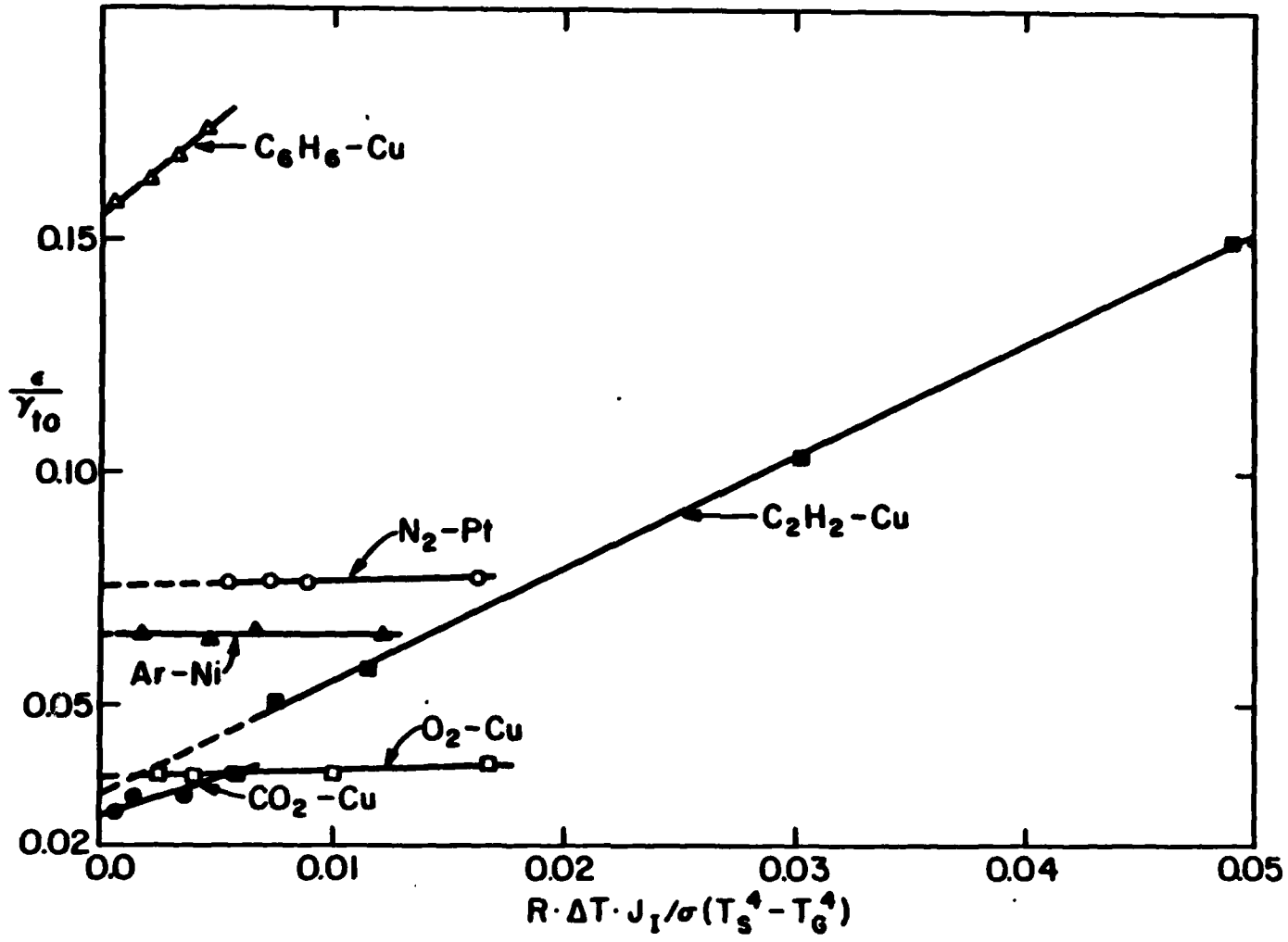
C_6H_6-Cu
0.15
$\frac{\epsilon}{\gamma_{to}}$
0.10
N_2-Pt
C_2H_2-Cu
Ar-Ni
0.05
O_2-Cu
CO_2-Cu
0.02
0.0
0.01
0.02
0.03
0.04
0.05
$R \cdot \Delta T \cdot J_I / \sigma (T_S^4 - T_G^4)$

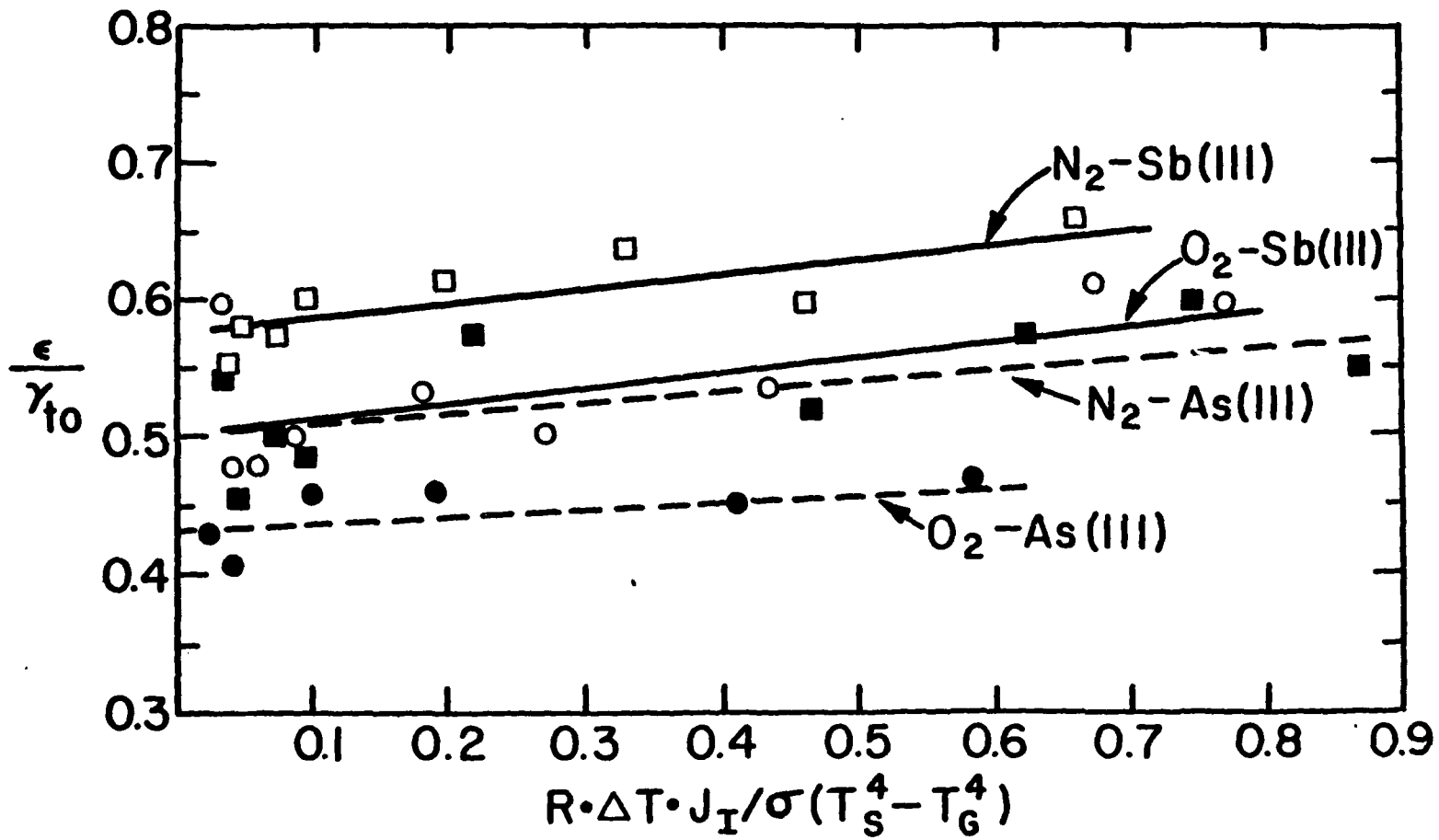
0.8
0.7
0.6
0.5
0.4
0.3
$\frac{\epsilon}{\gamma_{to}}$
0.1
0.2
0.3
0.4
0.5
0.6
0.7
0.8
0.9
$R \cdot \Delta T \cdot J_I / \sigma (T_S^4 - T_G^4)$
N_2-Sb(III)
O_2-Sb(III)
N_2-As(III)
O_2-As(III)

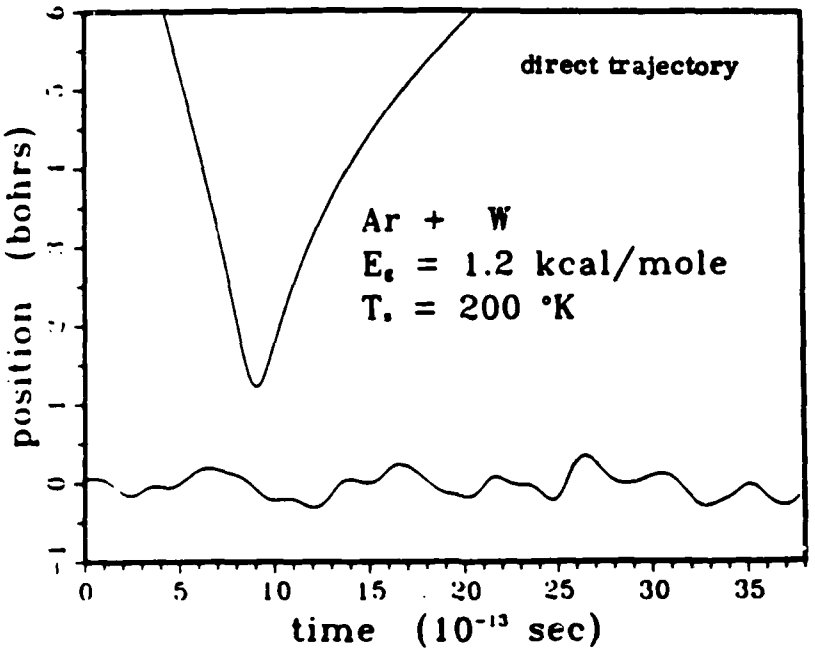

M. Shugard
J.C. Tully
A. Nitzan

J. Chem. Phys.
66, 2534 (1977).

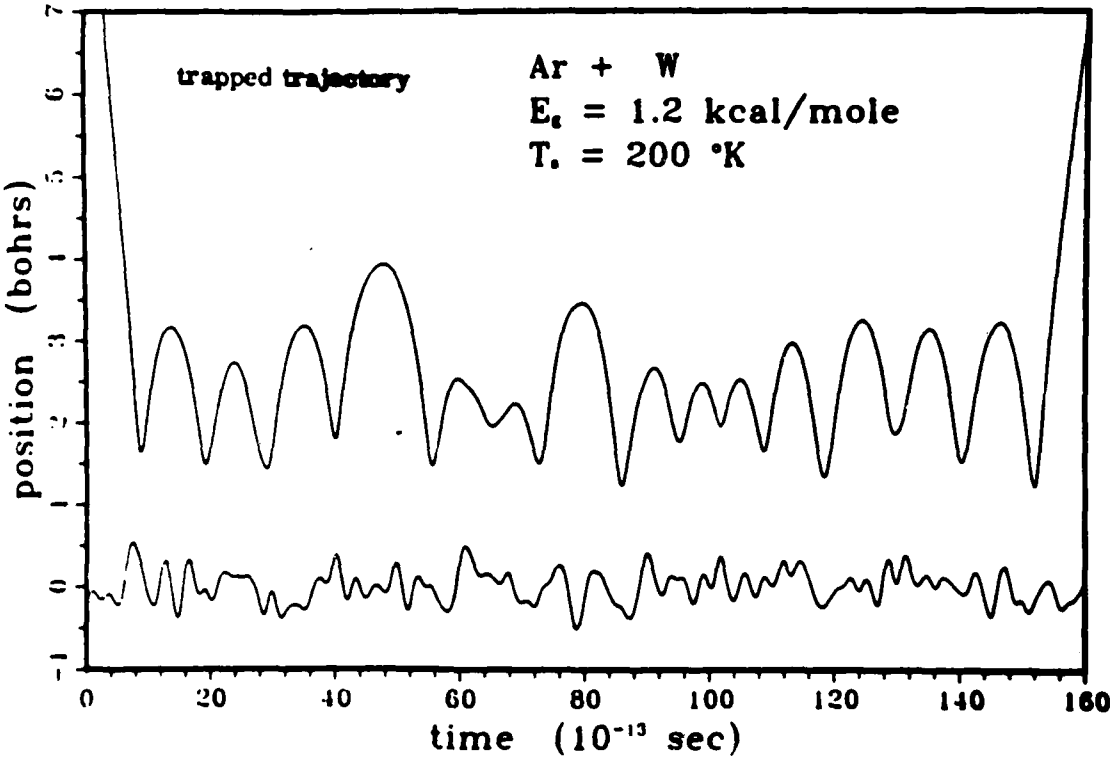

M. Shugard, J.C. Tully, A. Nitzan
J. Chem. Phys. 66, 2534 (1977).

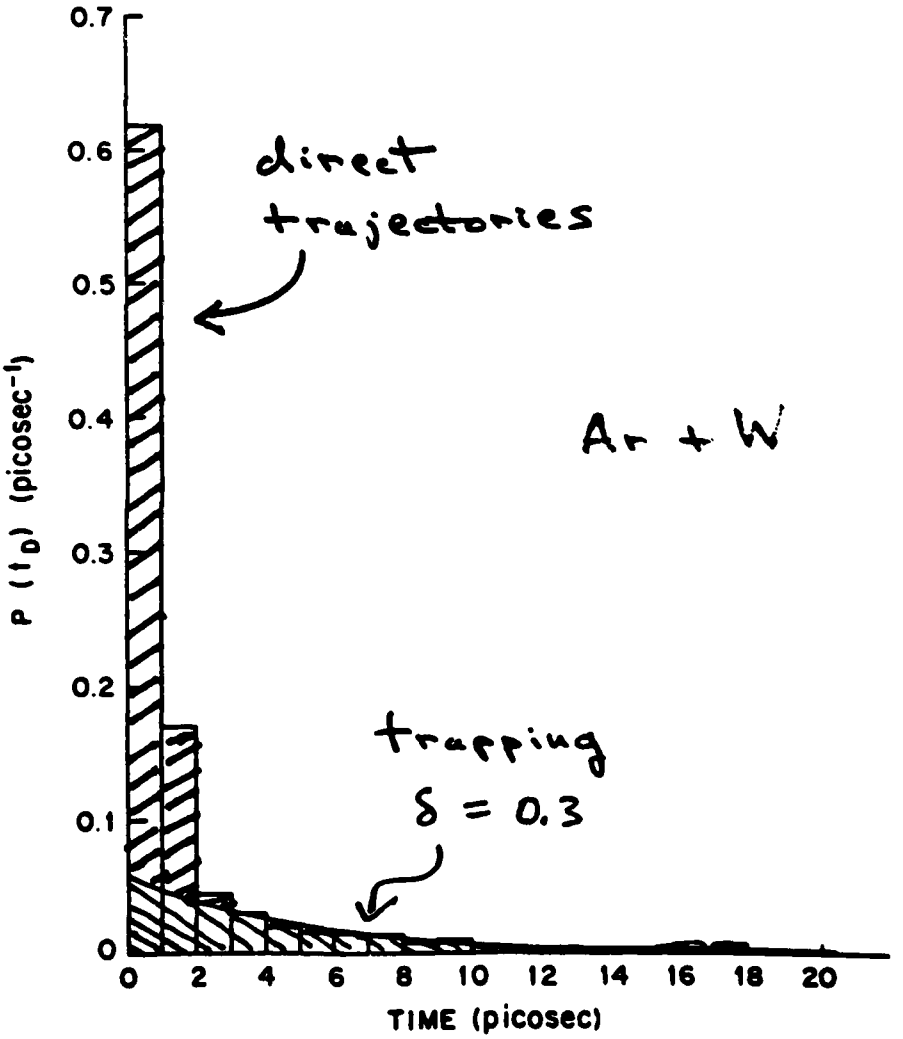

Histogram plot of $P(t_D)$ obtained from stochastic trajectories for incident energy of 2.4 kcal/mole and $T_s = 300\,°K$. The smooth curve is an exponential fit of the long time tail.

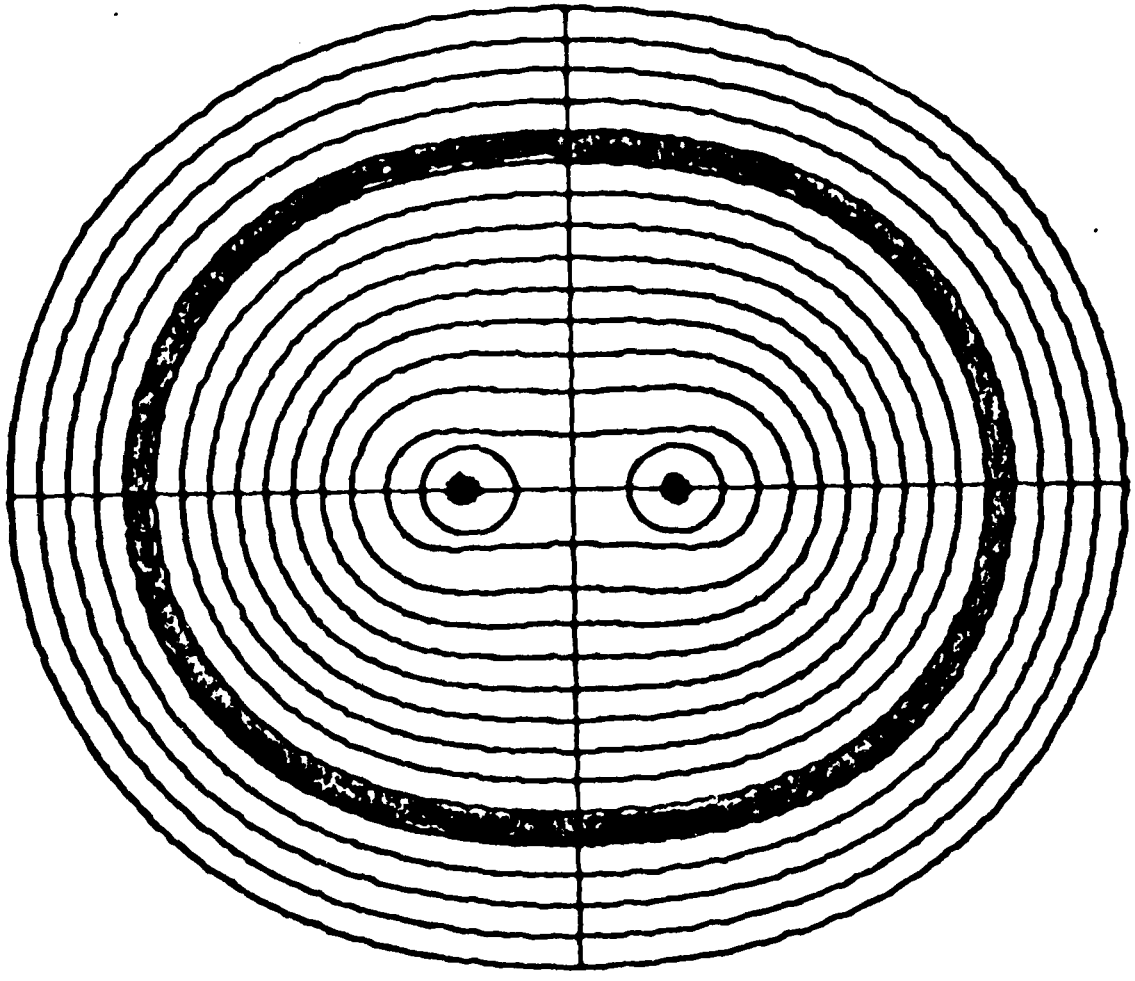

N_2 Total electron density

A. C. Wahl, Science **151**, 961 (1966).

TRANSLATIONAL AND INTERNAL ENERGY ACCOMMODATION COEFFICIENTS

	$\frac{\Delta H_{vap}}{R}$	$\langle n_L \rangle$	γ_{trans}	γ_{rot}	γ_{vib}
Weakly physisorbed molecules					
N_2	670	10	0.5	0.07	5×10^{-4} [a]
O_2	810	15	0.6	0.06	—
Moderately physisorbed molecules					
C_2H_6	1800	400	0.7	0.6	0.5
CO_2	2000	900	0.7	0.7	0.5
Strongly physisorbed molecules					
C_8H_{18}	>3000	$>10^4$	1.0	1.0	0.9
Cl_2			1.0	1.0	1.0

a. Spectroscopic. Black et al (1974)

Uncertainties in γ are 0.05 - 0.10 with exception of CO_2 for which γ_{rot} and γ_{vib} are ± 0.25.

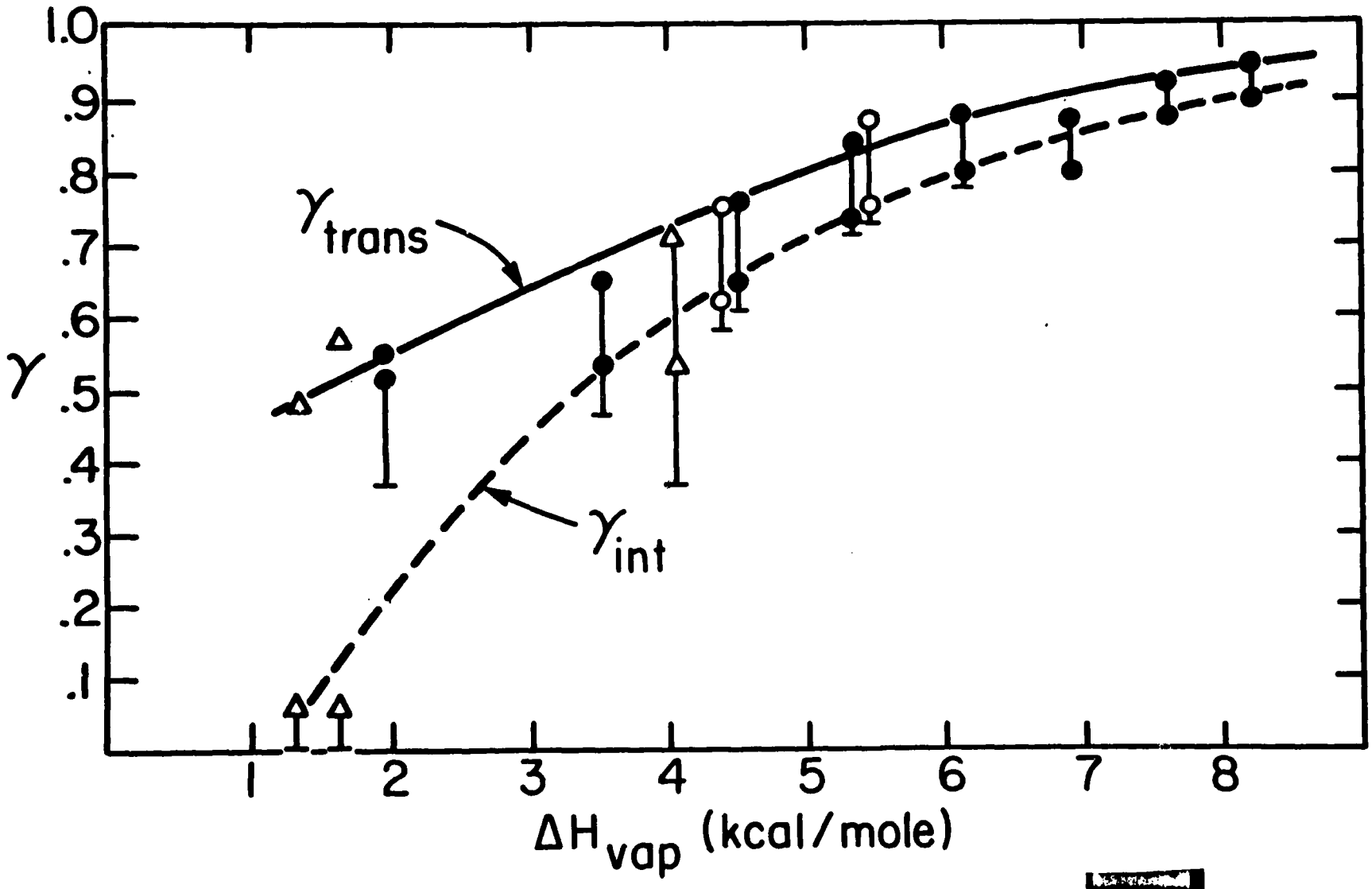
1.0
.9
.8
.7
.6
.5
.4
.3
.2
.1
γ
γ_{trans}
γ_{int}
1
2
3
4
5
6
7
8
ΔH_{vap} (kcal/mole)

VIII-2-28

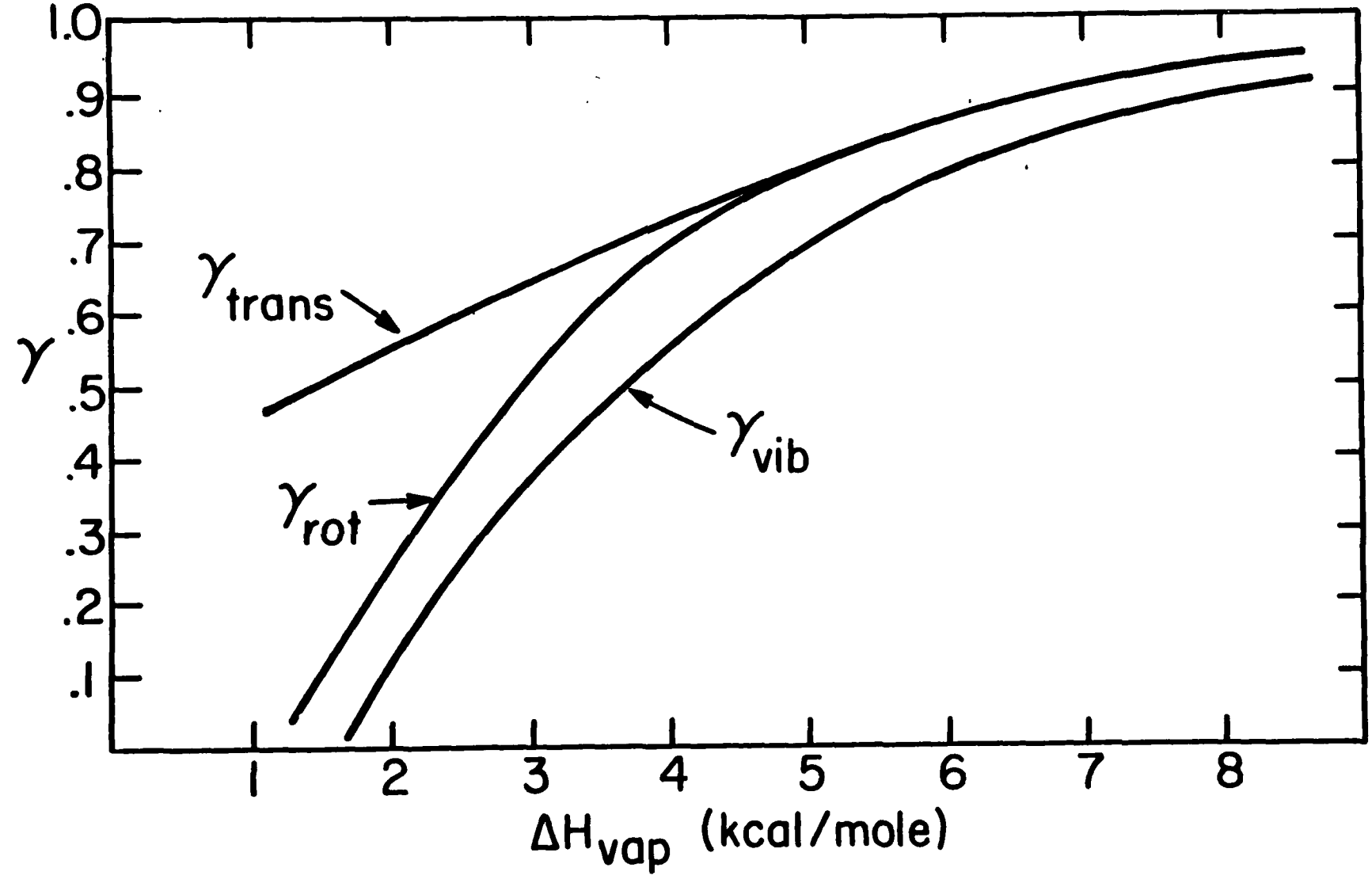
1.0
.9
.8
.7
.6
.5
.4
.3
.2
.1
γ
γtrans
γrot
γvib
1
2
3
4
5
6
7
8
ΔHvap (kcal/mole)

DATE PREPARED _____ SPEAKER _____

MEETING _____

DATE _____

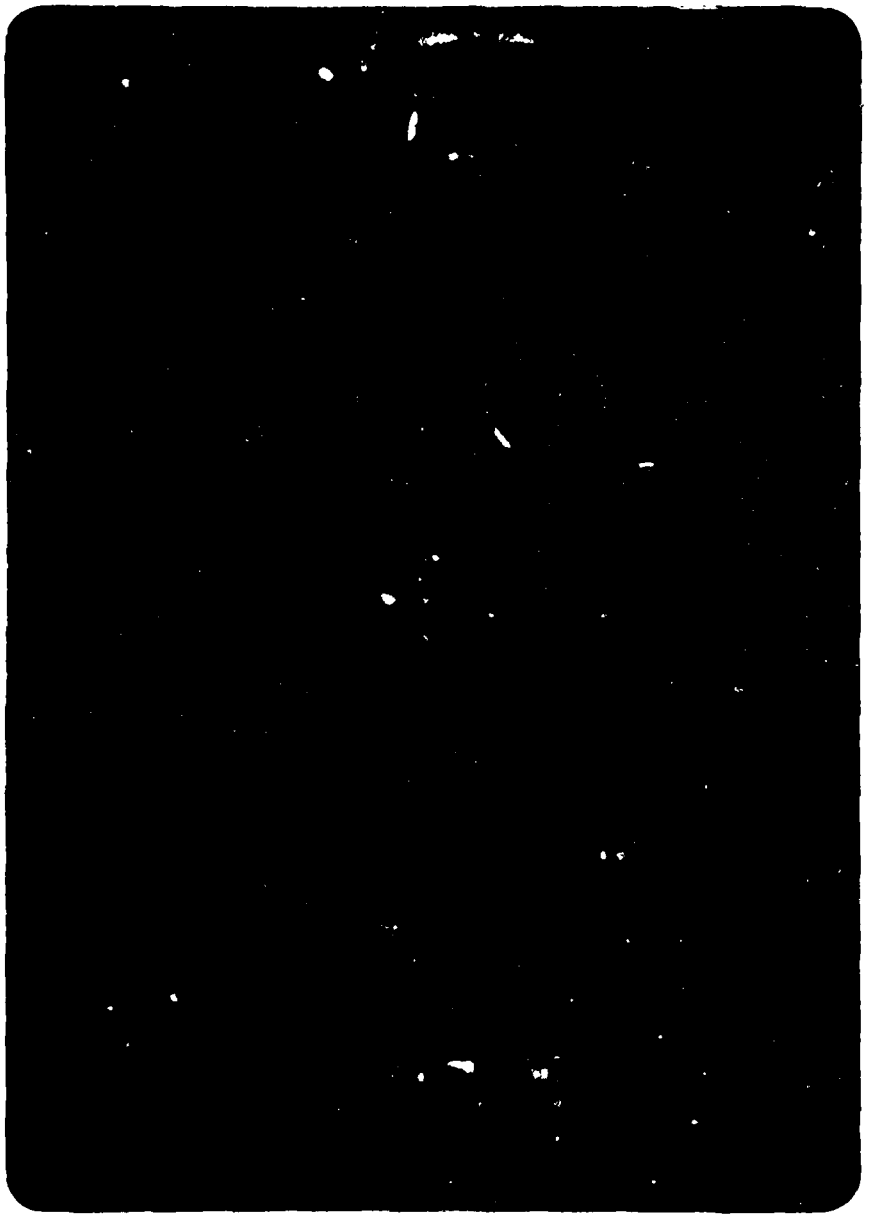

MEETING _____

DATE _____

THE BLIND MEN AND THE ELEPHANT

IT was six men of Indostan
To learning much inclined,
Who went to see the Elephant
(Though all of them were blind),
That each by observation
Might satisfy his mind.

The *First*, approaching the Elephant,
And happening to fall
Against his broad and sturdy side,
At once began to bawl:
"God bless me! but the Elephant
Is very like a wall!"

The *Second*, feeling of the tusk,
Cried, "Ho! what have we here
So very round and smooth and sharp?
To me 'tis mighty clear
This wonder of an Elephant
Is very like a spear!"

The *Third* approached the animal,
And happening to take
The squirming trunk within his hands,
Thus boldly up and spake:
"I see," quoth he, "the Elephant
Is very like a snake!"

The *Fourth* reached out an eager hand,
And felt about the knee.
"What most this wondrous beast is like
Is mighty plain," quoth he;
"'Tis clear enough the Elephant
Is very like a tree!"

The *Fifth*, who chanced to touch the ear,
Said: "E'en the blindest man
Can tell what this resembles most;
Deny the fact who can,
This marvel of an Elephant
Is very like a fan!"

The *Sixth* no sooner had begun
About the beast to grope,
Than, seizing on the swinging tail
That fell within his scope,
"I see," quoth he, "the Elephant
Is very like a rope!"

And so these men of Indostan
Disputed loud and long,
Each in his own opinion
Exceeding stiff and strong,
Though each was partly in the right
And all were in the wrong!

JOHN GODFREY SAXE

G. M. Rosenblatt, "Evaporation from Solids," Treatise on Solid State Chemistry, Vol. 6A, Surfaces I, edited by N. B. Hannay (Plenum Press, New York, 1976), pp. 165-240.

G. M. Rosenblatt, "Vaporization Rates, Surface Topography, and Vaporization Mechanisms of Single Crystals: A Case Study," Accounts Chem. Res. 9, 169 (1976).

G. M. Rosenblatt, "The Role of Defects in Vaporization: Arsenic and Antimony," Surface and Defect Properties of Solids, Vol. V, edited by M. W. Roberts and J. M. Thomas (Specialist Periodical Reports, The Chemical Society, London, 1976), pp. 36-64.

G. M. Rosenblatt, "Translational and Internal Energy Accommodation of Molecular Gases with Solid Surfaces," Accounts Chem. Res. 14, 42 (1981).

"Thin Films"
by
Donovan, T./Guenther, A.

(Paper not available)

Q & A - A. Guenther

From: P. J. Turchi, R & D Associates

Will local shuttle environment be significantly different from true operating one?

A.

Assuming you mean LDEF environment - probably so. But it is very mission character specific (e.g., CW or pulsed).

SESSION IX. THERMIONICS

THERMIONIC CONVERSION FOR SPACE POWER APPLICATION

L. Yang and G. Fitzpatrick

ABSTRACT

Extensive efforts were made during 1960 to 1980 to develop thermionic conversion for space power application. Between 1960 and 1972, the efforts were devoted to the development of in-core thermionics. Tungsten, niobium and Al_2O_3 were selected as the emitter, collector, and insulator materials for the converter. Uranium carbides and uranium oxide were selected as candidates for the nuclear fuel. A total of 36 fueled thermionic converters and fuel elements were life-tested during 1965 to 1972. These tests, supported by a dozen of out-of-pile converter tests and several material irradiation tests, provided the base of the in-core thermionic technology. Unfueled converter has demonstrated a life of five years or more, while fueled converters and fuel elements have been operated for one to one and one-half years. The major limiting factors for converter life and performance were fuel component diffusion through cladding and emitter cracking for the carbide-fueled converters, and emitter swelling for the oxide-fueled converters. Various means for mitigating the fuel effects on converter life and performance were proposed but they were not thoroughly evaluated before the in-core thermionic program was terminated at the beginning of 1973.

Between 1973 and 1980, some limited efforts were made to replace the in-core thermionic with out-of-core thermionics in order to eliminate the undesirable fuel effects on converter life and performance. Various approaches for improving converter performance were investigated in order to either improve overall system performance or lessen the burden on the nuclear heat source and the heat pipes used for transferring the heat from the nuclear heat source to the converters. The use of inert gas plasma and structured emitter and collector surfaces were found to be promising means for lowering the voltage drop between the emitter and the collector and thus improving the converter performance.

The test results available indicate that the base technology exists for the development of an in-core thermionic nuclear system of a life of about one year, and for out-of-core thermionic conversion system with a life exceeding five years. In the latter case, the life-limiting factors rest with the reactor heat source, not the converters. Further work on converter performance improvement and fuel and insulator material development will lead to thermionic systems of longer life and better performance.

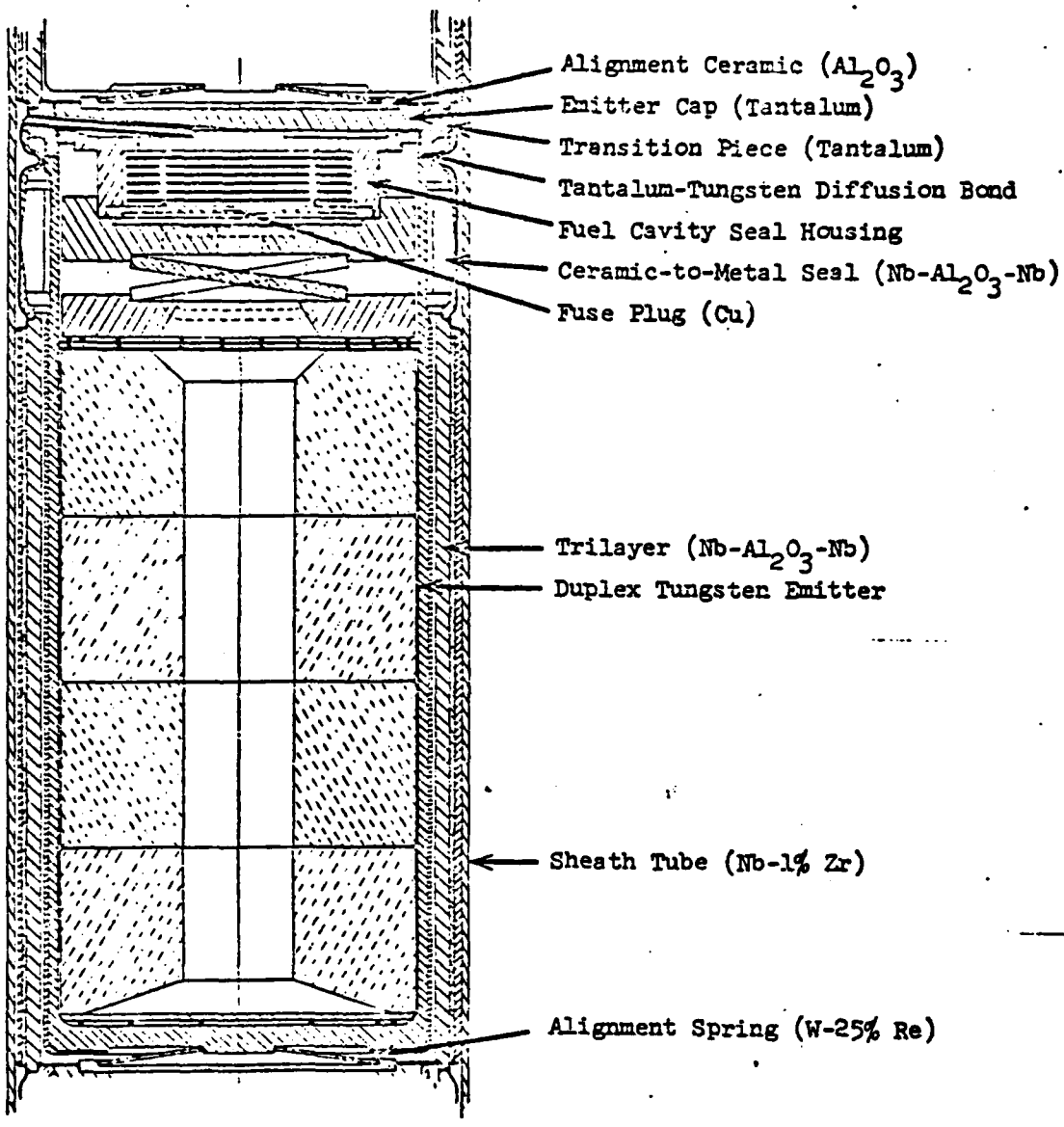

COMPONENT	OPERATING TEMPERATURE, °K	
Duplex Emitter	1881	(Average)
Trilayer	983	(Collector Average) 710°C
Tantalum-Tungsten Diffusion Bond	1262	
Ceramic-to-Metal Seal	1078	(Ceramic Maximum)
Emitter Cap	1213	(Center)
Transition Piece	1153	(Average)
Sheath Tube	973	
Alignment Spring	1773	(Maximum)

Arrangement of Components and Operating Temperatures for F Series Cells

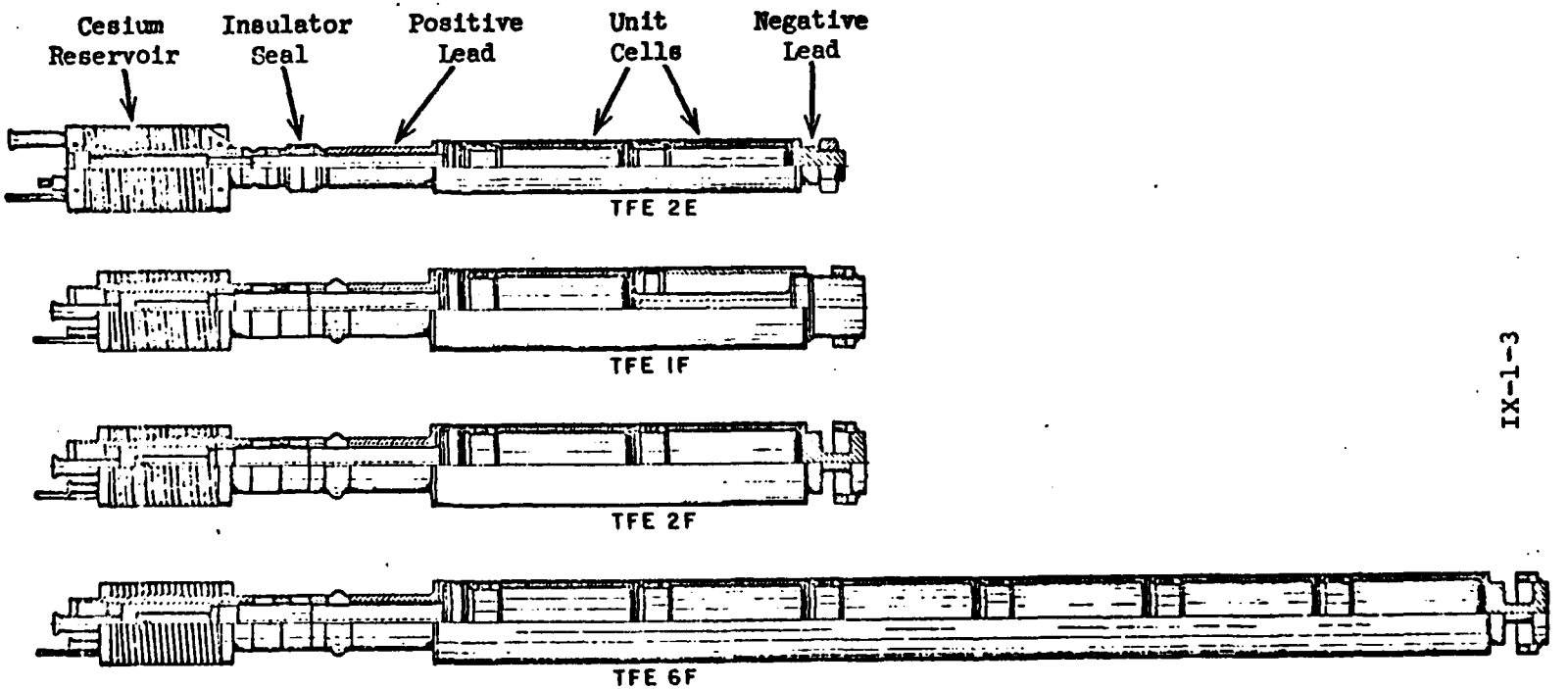
Cesium Reservoir
Insulator Seal
Positive Lead
Unit Cells
Negative Lead
TFE 2E
TFE 1F
TFE 2F
TFE 6F

TFE Designs

THERMIONIC DEVICES
TEST SUMMARY
(1965 - 1972)

* IN-PILE TESTS
  - 15 MK6 EXPERIMENTAL CONVERTERS (EMITTER 5/8 INCH DIAMETER AND 1 INCH LENGTH)
  - 3 MK7A PROTOTYPICAL CONVERTERS (EMITTER 5/8 INCH DIAMETER AND 2 INCH LENGTH)
  - 3 MK7B PROTOTYPICAL CONVERTERS (EMITTER 1 INCH DIAMETER AND 2 INCH LENGTH)
  - 3 PARTIAL LENGTH THERMIONIC FUEL ELEMENTS CONTAINING MK7B CONVERTERS
  - 5 FULL LENGTH THERMIONIC FUEL ELEMENTS CONTAINING MK7B CONVERTERS

* OUT-OF-PILE TESTS
  - 12 FUELED AND UNFUELED MK6 EXPERIMENTAL CONVERTERS
  - 4 CARBIDE FUELED CAPSULES
  - 3 OXIDE FUELED CAPSULES

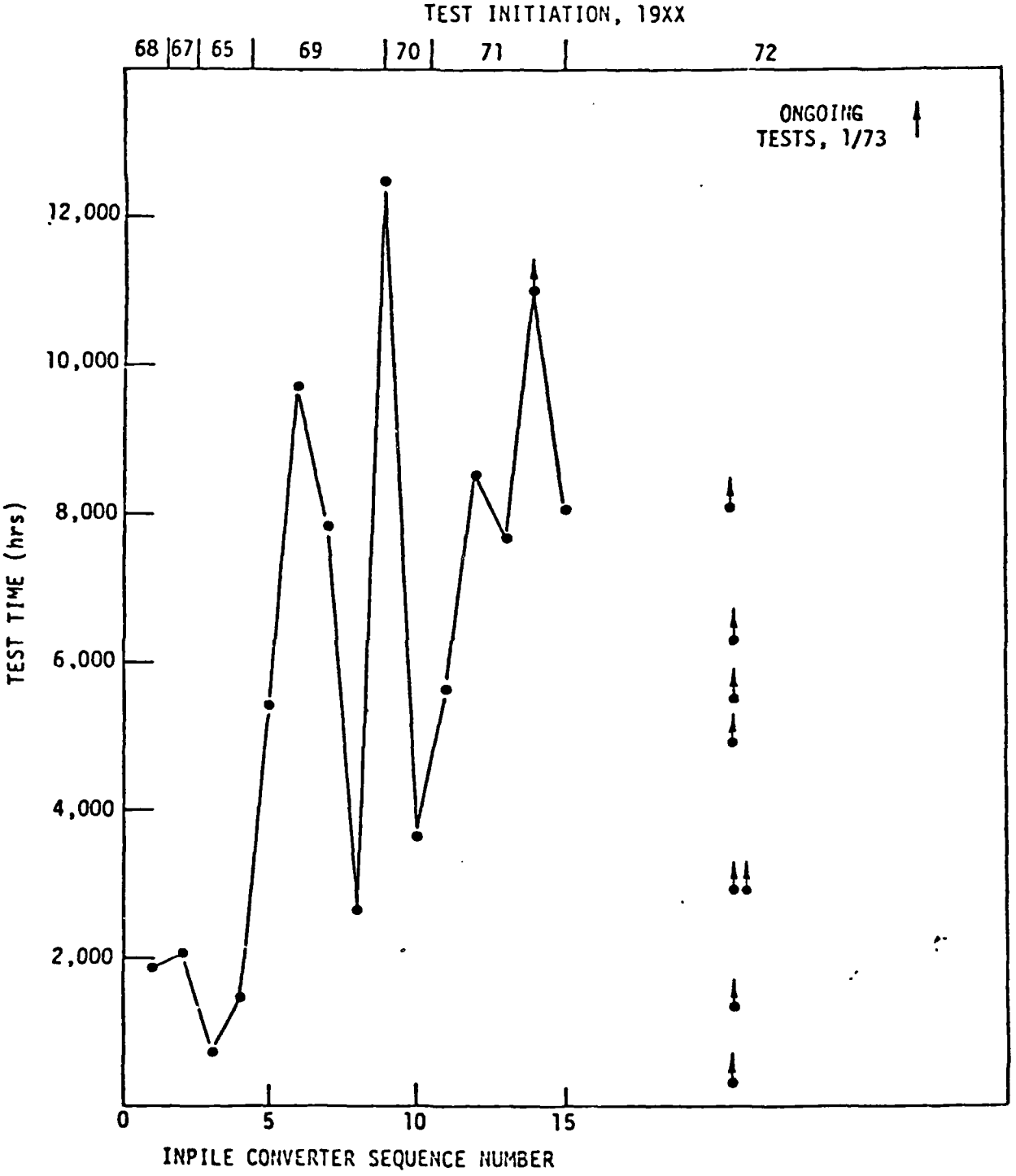

IN-CORE THERMIONIC CONVERTER TESTS

SUMMARY OF THERMIONIC TESTS

Type of Test	Device Designation	Fuel	Emitter Temp. (°K)	Average Electrode Power (W/cm^2)	Testing Time (hours)	Burnup (10^{19} fission/cc)	Fast Neutron Fluence (10^{20} nvt) (>0.1 MeV)	Failure Model of Converter
1. Out-of-pile unfueled	LC-9	--	1970	8.0	46647	--	-	Still Operable
2. Out-of-pile fueled	LC-11	90UC-10ZrC -4W	1870	6.5	18569	--	-	Still Operable
	LC-3	W-UO_2 cermet	2000	8.9	10406	--	-	Electrode short by Ti getter ring
3. Capsule Irradiation	V-2C	90UC-10ZrC -4W	1873	-	11000	30	-	---
	FC-3	UO_2	1910	-	10244	12	9	---
4. In-pile MK6 experimental converter	I-4	UO_2	1840	6.0	8754	31	4	Envelope Leak
5. In-pile MK7B prototype converter	C11	90UC-10ZrC	1840	3.4	7881	6.8	3	Emitter crack
6. In-pile MK7A partial fuel element	2E-1	UO_2	1820	4.0	12534	24	9	Emitter swelling
	2E-2	UO_2	1820	5.6	11084	22	8	Still operable
7. In-pile MK7B Partial Length Fuel Element	1F-1	UO_2	1780	4.0	8560	6.6	4	Emitter Swelling
8. In-pile MK7B Full Length Fuel Element	6F-2	90UC-10ZrC -4W	1780 - 1950	2.3	7685	6.6	4 - 8	Emitter Cracking
	6F-3	UO_2	1740 - 1820	3.0	8062	7.3	2.7 - 5.9	Still Operable

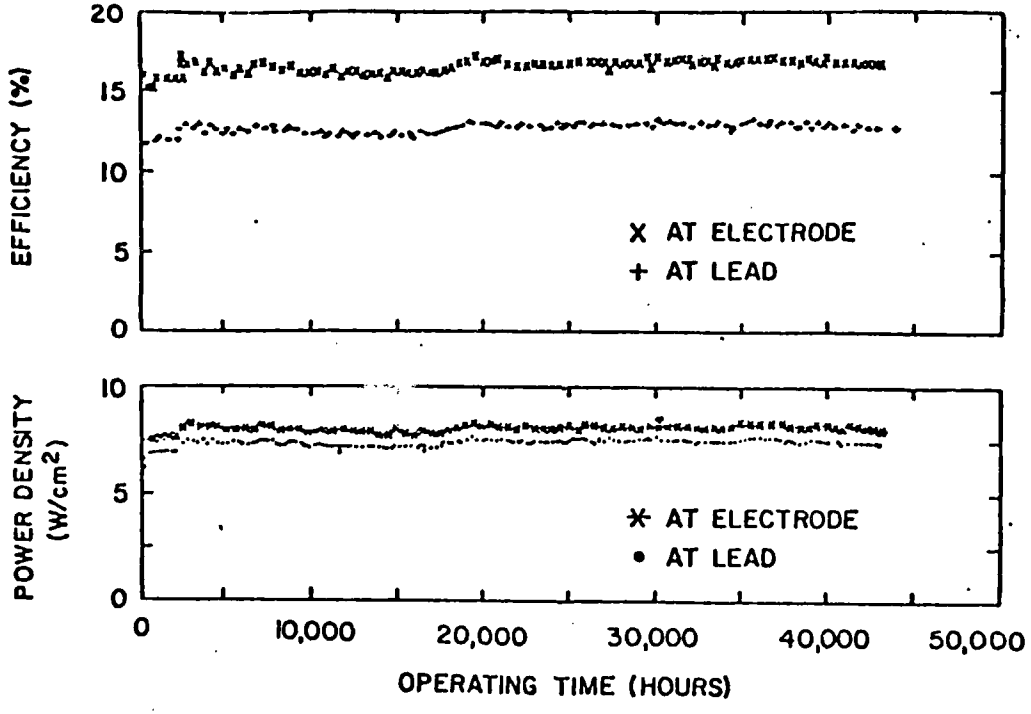

LC-9 OUT-OF-PILE THERMIONIC CONVERTER TEST HISTORY.
EMITTER TEMPERATURE: 1970K

THERMIONIC CONVERTER PERFORMANCE

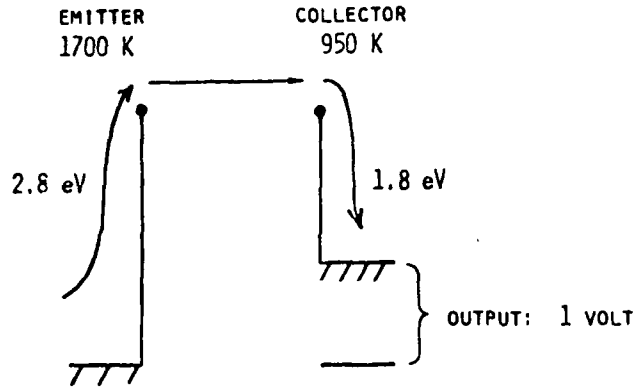

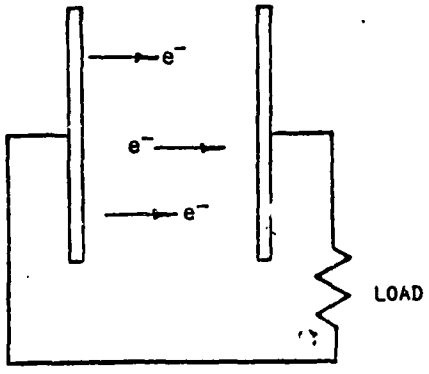

- IDEAL CONVERTER PERFORMANCE IS DETERMINED BY THE PHYSICS OF ELECTRON EMISSION FROM SURFACES:
- EXAMPLE:

  ELECTRON EFFICIENCY: $\frac{1}{2.8} = \underline{\underline{36\%}}$

  RADIATION AND CONDUCTION LOSSES REDUCE THIS TO A

  LEAD EFFICIENCY = $\underline{\underline{23\%}}$

- LOW WORK FUNCTION SURFACES ARE REQUIRED

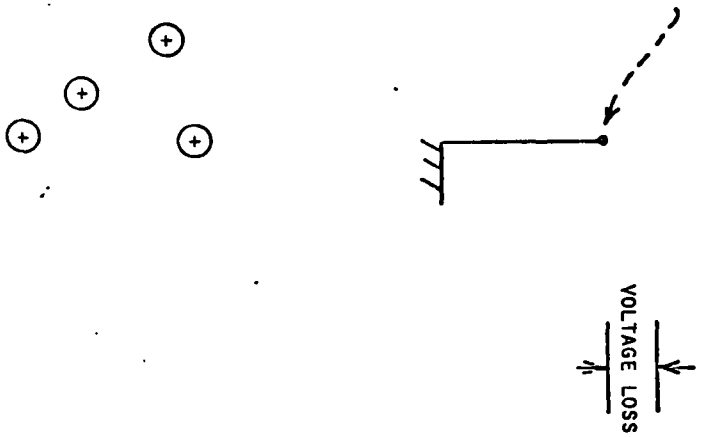
VOLTAGE LOSS

ELECTRON TRANSPORT LOSSES REDUCE PERFORMANCE

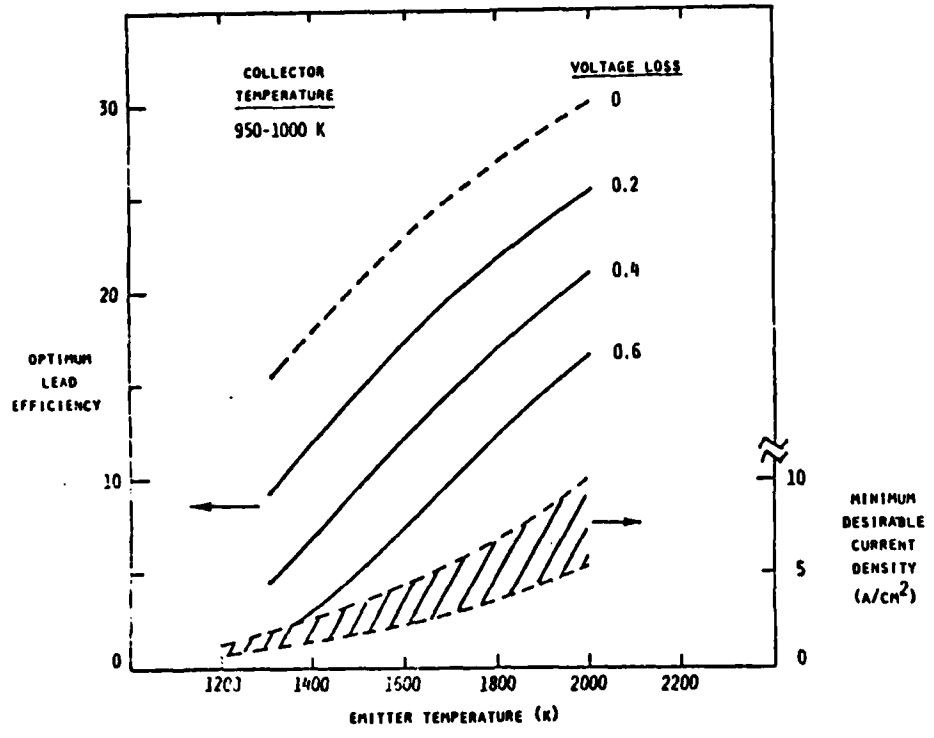

CONSTRAINTS:

- EFFICIENCY IS REDUCED TWO PERCENTAGE POINTS FOR EACH 0.1 VOLT DROP ACROSS THE INTERELECTRODE SPACE.
- SEVERAL AMPERES PER SQUARE CENTIMETER OF ELECTRODE ARE REQUIRED TO DOMINATE RADIATION AND CONDUCTION LOSSES.

KEY PROBLEM:

OVERCOMING ELECTRON SPACE CHARGE LIMITS TO CURRENT DENSITY WITHOUT A LARGE INTERELECTRODE VOLTAGE DROP.

APPROACHES:

CLOSE ELECTRODE SPACING OR SPACE CHARGE NEUTRALIZATION WITH POSITIVE IONS.

Solution Number One: Close Spacing

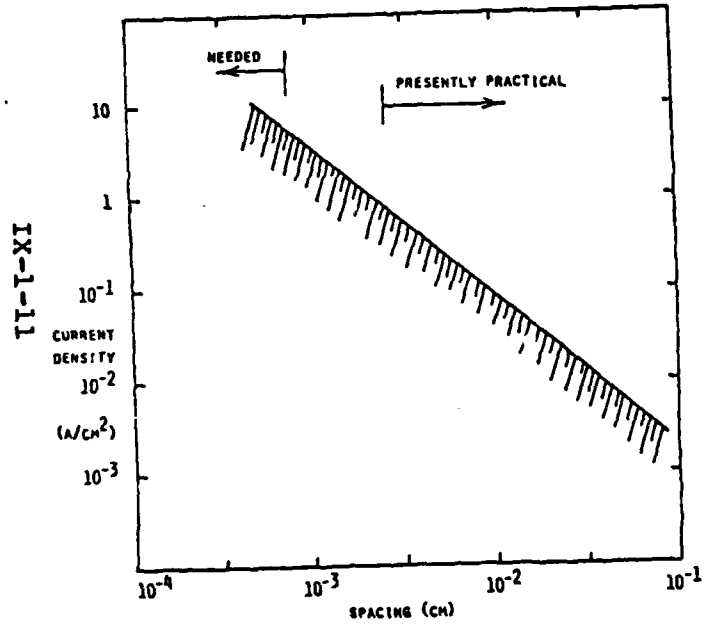

IX-1-11

Requirement:

- Spacing less than 5×10^{-4} cm (a few tenths of a mil)

Status:

- A very difficult problem practically.
- Spacing below 2×10^{-3} is unreliable.
- Compatible with cesiated electrodes.

Recent Progress:

- New techniques under evaluation (micro-fabrication, etc.)
- No demonstrated success

Key Problem:

- Inter-electrode short circuits.

Solution Number Two: Spontaneous Cesium Discharge

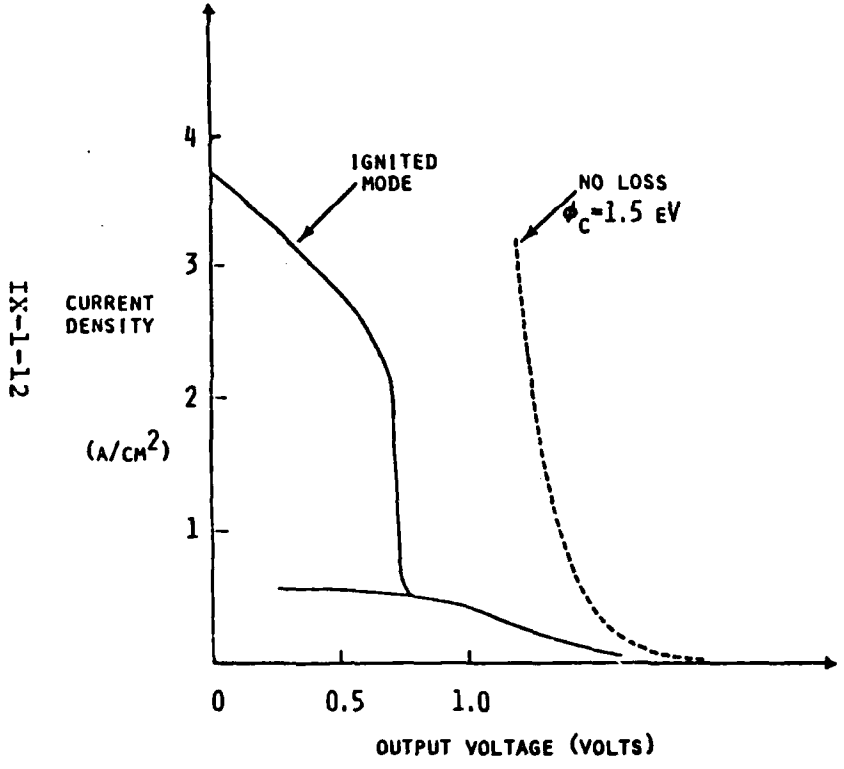

IX-1-12

Requirement:

- High cesium pressure (> 0.1 Torr)

Status:

- Very well demonstrated, competitive
- Compatible with cesiated electrodes
- Produces ions very inefficiently (< 1%) with 0.5 volt arc drop.

Recent Progress:

- Structured Electrodes

  Theory and experiment show a 0.05 to 0.1 volt gain.

- Divergent Geometry

  Theory projects a 0.1 to 0.2 volt gain; early experiments encouraging.

- Multiple Species Discharge

  Alkali mixtures under evaluation.

Solution Number Three: Auxiliary Ion Source

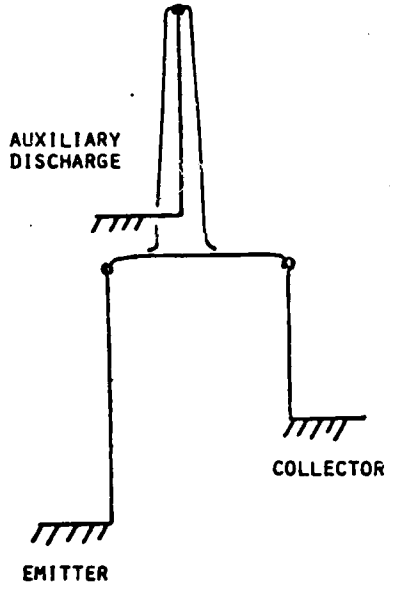

Requirements:

- Inert gas (Xe) plasma (Ramsauer effect)
- Low cesium pressure ($< 10^{-2}$ Torr)

Status:

- Plasma well understood
- Several auxiliary ion generation techniques are possible

Key Problem:

Finding stable low work function surfaces at low cesium pressures.

Recent Progress:

Two attractive collector surfaces identified; 2D-W110-O, "thick" Cs_XO_Y.

Outstanding Need:

Suitable emitter, and sound theory of surface-plasma interface.

SOLUTION NUMBER FOUR: UNIGNITED CESIUM DISCHARGE

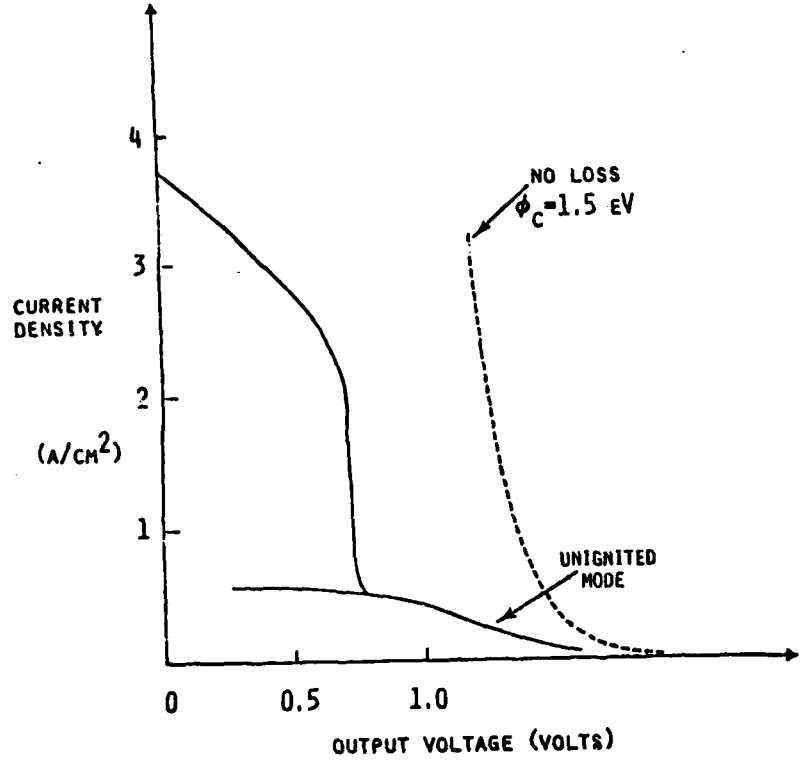

STATUS

1. WELL DEMONSTRATED
2. REQUIRES T_E > 2000 K

RECENT PROGRESS

NO U.S. EFFORT

USSR

- DATA SHOWS FEASIBILITY AT 1850 K WITH STRUCTURED EMITTER
- DATA SHOWS EFFICIENCY OF 30-40% AT 2400 K

SUMMARY

* ACCOMPLISHMENTS
  - DEVELOPMENT OF CONVERTER COMPONENT MATERIALS AND FABRICATION TECHNOLOGY
  - DEMONSTRATION OF FIVE YEAR LIFE FOR UNFUELED CONVERTERS
  - DEMONSTRATION OF ONE TO ONE AND ONE HALF YEAR LIFE FOR FUELED CONVERTER AND FUEL ELEMENTS

* RECOMMENDED FUTURE WORK
  - INVESTIGATION OF MEANS FOR IMPROVING THERMIONIC CONVERTER PERFORMANCE
  - INVESTIGATION OF MEANS FOR REDUCING FUEL SWELLING AND FUEL COMPONENT DIFFUSION THROUGH CLADDING
  - DEVELOPMENT OF INSULATORS RESISTANT TO FAST NEUTRON DAMAGE

Bibliography for Session IX: Thermionics

"Thermionic Conversion for Space Power Application", Ling Yang and Gary Fitzpatrick.

1. "Material Development for Thermionic Fuel-Cladding Systems", L. Yang, R. G. Hudson, H. Johnson, H. Horner, and D. Allen, Proceedings of the 3rd International Conference on Thermionic Electrical Power Generation, p 873 - 893, Julich, Federal Republic of Germany, June 5 - 9, 1972.

2. "Development Status of Thermionic Materials", L. Yang and J. Chin, Proceedings of the 7th Intersociety Energy Conversion Engineering Conference, p 1041 - 1049, San Diego, California 1972.

3. "Thermionic Fuel Element Testing at General Atomic", M. K. Yates, G. O. Fitzpatrick, and d. E. Schwarzer, Proceedings of the 3rd International Conference on Thermionic Electric Power Generation, p 479 - 489, Julich, Federal Republic of Germany, June 5 - 9, 1972.

4. "Multicell Thermionic Fuel Element Fabrication Technology", M. H. Horner, J. C. Grebetz, and J. Kay, Jr., Proceedings of the 3rd International Conference on Thermionic Electrical Power Generation, p 491 - 500, Julich, Federal Republic of Germany, June 5 - 9, 1972.

5. "Development of a Thermionic Reactor Space Power System, Final Summary Report", Contract AT(04-3)-840, Gulf-GA-A12608, June 30, 1973.

6. "Experimental and Analytical Study of Advanced Mode Thermionic Converter", G. L. Hatch et. al., NASA-CR-159638, June 1979.

7. "Advanced Thermionic Conversion, Joint Highlights and Status Report", Rasor Associates, COO-2263-16, July - September 1979.

8. "Investigation of Cesium Diode with ZrC Cathode", T. L. Matskevich and T. V. Krachino; Ioffe Physical Technical Institute Conference on Phenomena in Ionized Gases, Bucharest, Romania, 1969.

9. "Increase in Specific Power of a Thermionic Converter in Region with Surface Ionizaation by Use of a Developed Cathode", V. I. Babanin et. al., Proceedings of the Thermionic Conversion Specialist Conference, Eindhoven, Netherlands, September 1975.

10. "Thermionic Converters and Low Temperature Plasma", F. G. Bakshit et. al., USSR Academy of Science, English Edition by L. Hansen; DOE-TR-1, 1978.

11. "Thermionic Energy Conversion", G. N. Hatsopoulos and E. P. Gyftopoulos, MIT Press, 1973.

Thermo Electron CORPORATION

Special Conference on Prime Power
for High Energy Space Systems
22-25 February 1982
Norfolk, VA

THERMIONIC TECHNOLOGY FOR SPACECRAFT POWER: PROGRESS AND PROBLEMS

Fred Huffman, David Lieb, Peter Reagan and Gabor Miskolczy

THERMO ELECTRON CORPORATION
85 First Avenue
Waltham, Massachusetts 02254

INTRODUCTION

Thermionic conversion is one of the most attractive options for use with space reactors. It has a combination of characteristics, shown on the FIRST SLIDE (1), favorable for space application. The mechanical simplicity associated with no moving parts implies reliability. The high temperature of heat rejection minimizes the mass of the radiator - which is usually the heaviest component of large space power systems. The high heat rejection temperature also limits the size of the radiator, which is an important consideration, since all space reactor systems in the foreseeable future must fit inside the space shuttle bay. Modularity maximizes reliability by eliminating single point system failures. Although thermionic efficiencies up to 15 percent have been demonstrated, much higher efficiencies are theoretically possible with reduced electrode and plasma losses. In addition, thermionics is a demonstrated conversion technology coupled to nuclear reactors. Unfortunately, the most impressive demonstrations have been in the Soviet Union.

The apparent choice of thermionics by the Soviets for their high-power space missions should be given careful consideration. This choice

822-39

THERMIONIC CONVERSION

- NO MOVING PARTS
- REJECTS HEAT AT A HIGH TEMPERATURE
- MODULAR
- EFFICIENCY
  - 12 TO 15 PERCENT WITH PRESENT TECHNOLOGY
  - 20 TO 25 PERCENT THEORETICALLY POSSIBLE
- SYSTEMS ESPECIALLY ATTRACTIVE AT POWER OUTPUTS $\geq$ 100 kWe
- DEMONSTRATED CONVERSION TECHNOLOGY

was made by the same people who brought you Sputnik, the first hydrogen weapon, the first nuclear powerplant, the first nuclear-powered surface ship, the world's largest breeder reactor and reactors for submarines that outrun U.S. submarines.

NEXT SLIDE (2), PLEASE.

As is evident from this table of direct conversion reactors that have been built and operated, the decision makers in the USSR were fully aware of the potential and the limitations of thermoelectric reactors, having built and operated Romashka using a silicon-germanium thermopile. SNAP-10A, built by the United States, also used silicon-germanium thermoelectrics. Although the design concepts of the Romashka and SNAP-10A thermoelectric reactors were quite different, it is remarkable that both power systems yielded almost identical performances - namely, power outputs of about 0.5 kWe at efficiencies of around 1.5 percent. The Soviets were also well aware of the potential and problems of TOPAZ thermionic reactors, having reported on four generations in the open literature. The United States has yet to build a single thermionic reactor. With the TOPAZ thermionic reactors, the Soviets obtained over four times the efficiency of the Romashka and SNAP-10A thermoelectric reactors as well as almost twenty times their power output. It is quite likely that the USSR COSMOS reconnaissance satellites are powered with thermionic reactors.

One does not have to have the strategic genius of von Clausewitz to appreciate the military significance of the reactor power sources on the Soviet satellites which are far less vulnerable to countermeasures than the higher-drag solar arrays on our reconnaissance satellites. It is a sobering thought that the USSR is now a decade ahead of this country in space reactors.

8012-91A

DIRECT CONVERSION REACTOR SUMMARY

REACTOR	SNAP-10A[1]	ROMASHKA[1]	TOPAZ[2,3]	COSMOS 954[4,5,6]
COUNTRY	UNITED STATES	USSR	USSR	USSR
CONVERSION SYSTEM	THERMOELECTRIC (SiGe)	THERMOELECTRIC (SiGe)	THERMIONIC (W & Mo EMITTERS, Nb COLLECTORS)	THERMIONIC?
POWER OUTPUT, kWe	0.5	0.5 - 0.8	9	--
OVERALL EFFICIENCY	1.6	1.5	7	--

1. S.D. Strauss, "Romashka in Perspective," Nucleonics, p. 68 (December 1968).
2. F.N. Huffman and R. Rufeh, "Trip Report: Visit to USSR Thermionic Facilities," (July 1977).
3. Kuznetsov, et al., "Development and Construction of the Thermionic Nuclear Power Installation TOPAZ," Trans. from Atomnaya Energiya, 36, p. 450 (June 1974).
4. E. Galloway, "United Nations Consideration of Nuclear Power for Satellites," IAF-79-IISL-19 Preprint, XXX Congress, Int'l Astronautical Federation, Munich (September 1979).
5. V.V. Bel'giy, "The On-Board Computer for Diagnosis of Satellite Power Unit," IAF-79-F-168 Preprint, XXX Congress, Int'l Astronautical Federation, Munich (September 1979).
6. J. Grey and M. Gerard, "A Critical Review of the State of Foreign Space Technology," AIAA Report to NASA, Contract NASW-3093 (February 1978).

SYSTEMS APPROACH

Two basic system approaches have been pursued for thermionic reactors, in-core and out-of-core.

NEXT SLIDE (3), PLEASE.

The former approach, which incorporates the converters inside the core and is illustrated in this slide, represents the design concept that has been utilized in the TOPAZ reactor and in-pile tests conducted in the United States in the sixties and early seventies.

NEXT SLIDE (4), PLEASE.

The out-of-core system shown on this slide transfers the thermal energy outside the reactor to a bank of thermionic converters. For a given power level, the reactor and shield have a lower mass and the conversion system is decoupled, to a large extent, from the reactor. In addition, mechanical coolant pumping is eliminated and heat pipes lend themselves to redundant systems.

It is not the purpose of this paper to contest the merits of these two system concepts. Suffice it to say that out-of-core systems presently are the more favored approach in this country.

In order to realize the system advantages of thermionic conversion, it is necessary to operate the emitters of the converters at temperatures of at least 1750 K. The emitter operating temperature is a compromise between system performance, mission life and materials selection. The temperature constraints imposed by using molybdenum in previous JPL-LANL studies limited the thermionic system performance. It would appear that tungsten, or tungsten-based alloys, will be necessary for a high-performance thermionic reactor system using lithium as the heat pipe working fluid.

822-40

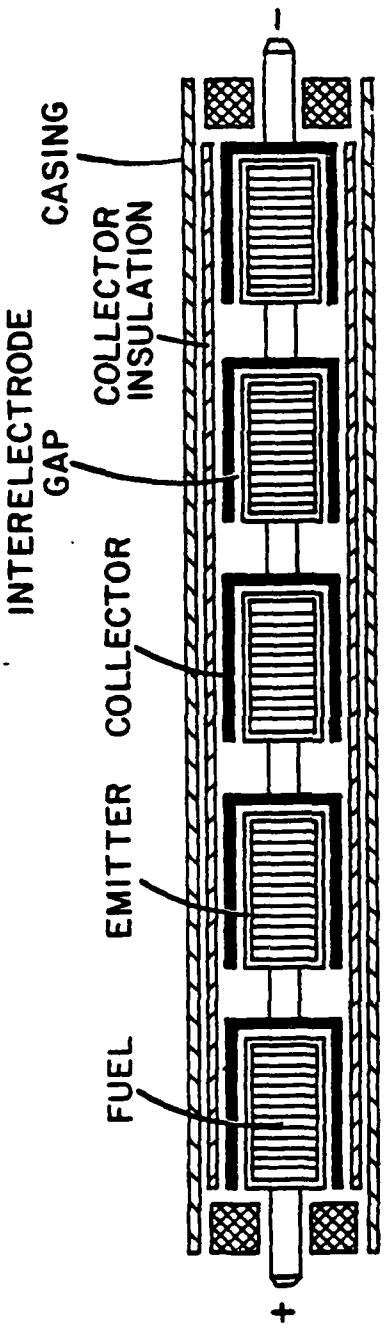

Slide No. 3

NEP POWER SYSTEMS

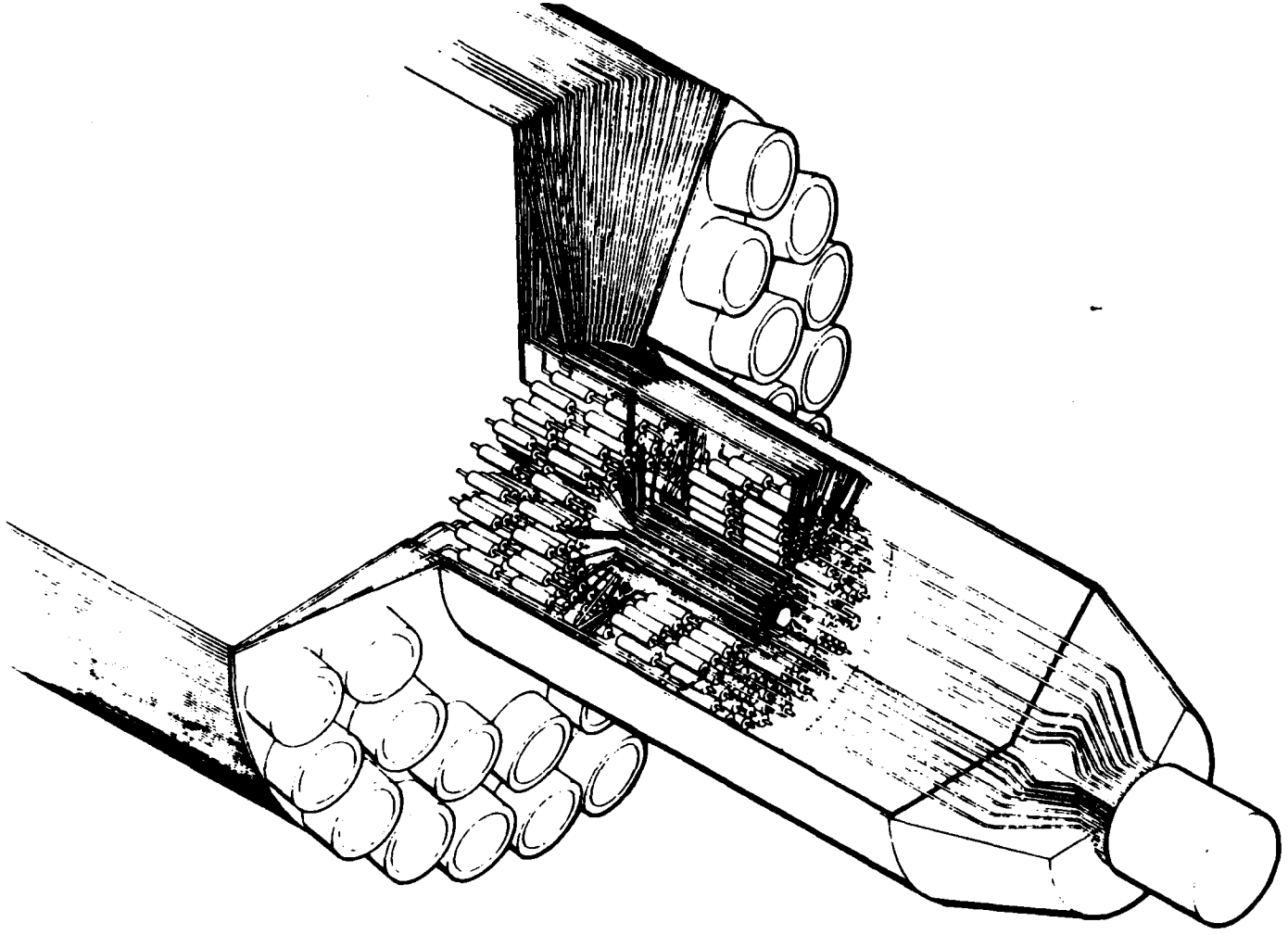

MARCH 28, 1979

TECHNICAL PROBLEMS

Based on the foregoing discussion, it appears reasonable to assume that a thermionic reactor would be a high-temperature out-of-core system.

NEXT SLIDE (5), PLEASE.

Such a design concept presents the set of well-defined problems shown on this slide. Nucleonics is outside the scope of this paper and will not be considered further. High-temperature lithium heat pipes must be developed with the required configuration. For out-of-core systems the emitters of the converters must be electrically insulated from the reactor heat pipe through a thermally conductive interface so that they can be connected in series to obtain a more convenient and practical output voltage for the power conditioning unit. A similar problem must be resolved between the collector electrodes and the associated radiator heat pipes. The radiator heat pipes will probably use sodium as the fluid.

Although available thermionic converter performance yields systems with attractive specific masses of around 20 kG/kWe, higher efficiency and power density are certainly desirable. For space systems, this improvement must accrue from reduced potential losses in the interelectrode plasma since the radiator temperature will be too high to take advantage of collector work functions lower than those already available.

HARDWARE PROGRESS

Fortunately, we are not starting from ground zero on these problems. I will next summarize some developments which impact on these technical problems.

NEXT SLIDE (6), PLEASE.

As you recall, the out-of-core concept requires that the thermionic converter be coupled to both an emitter heat pipe and a collector heat pipe. This photograph shows a module of three thermionic converters, each with an emitter and a collector heat pipe. This module effort was sponsored by NASA through the Lewis Research Center.

822-41

THERMIONIC CONVERSION PROBLEM AREAS

- HEAT PIPE DEVELOPMENT
  - *REACTOR HEAT PIPE*
  - COLLECTOR HEAT PIPE
- ELECTRICAL INSULATION
  - EMITTER TO REACTOR HEAT PIPE
  - COLLECTOR TO RADIATOR HEAT PIPE
- REDUCED POTENTIAL LOSSES IN THE INTERELECTRODE SPACE

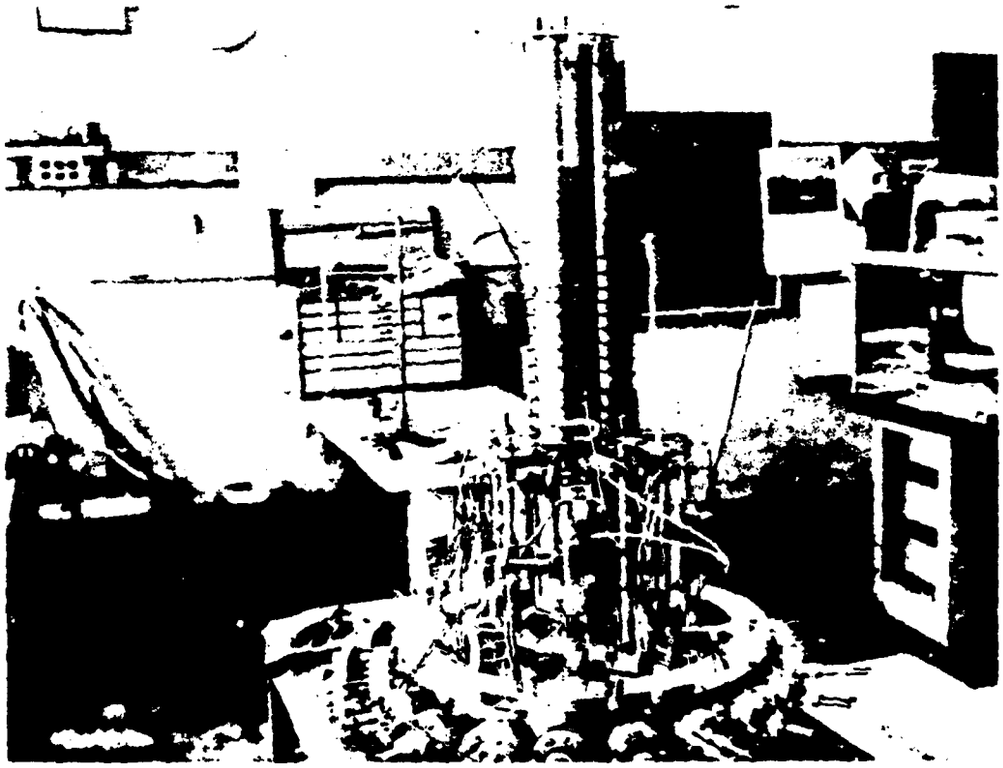

Slide No. 6

NEXT SLIDE (7), PLEASE.

This drawing shows a cutaway view of the cylindrical converter. The tungsten emitter is heated by a tungsten-lithium heat pipe. The heat pipes are immersed in a furnace insulated by MULTI-FOIL thermal insulation and heated by radiation from tungsten filaments. The collector consists of a layer of tungsten oxide vapor deposited on a niobium-1% zirconium alloy. The collector heat is rejected by radiation from a niobium, 1% zirconium heat pipe utilizing a potassium working fluid. This module was tested over an emitter temperature range from 1300 to 1850 K and a collector temperature from 700 to 850 K.

This effort was significant in demonstrating the design and fabrication of a prototypic out-of-core thermionic converter module for the first time.

NEXT SLIDE (8), PLEASE.

This drawing shows a combustion-heated thermionic converter typical of those built under the DOE program. The relevance of this terrestrial converter to space applications will become evident in a few minutes. The hemispherical end is the active area of the converter. The tungsten emitter is protected from the flame atmosphere by a silicon carbide coating, via an intermediate graphite layer. This structure is fabricated by depositing tungsten onto the inside of a graphite mandrel to form the emitter and emitter lead from tungsten hexafluoride by chemical vapor deposition, or CVD. Next, silicon carbide is chemically vapor deposited onto the outside of the graphite of the trialyer structure. A converter of this type has recently operated stably for over 10,000 hours at an emitter temperature of 1730 K. In addition, such structures have demonstrated excellent thermal shock and thermal cycle characteristics.

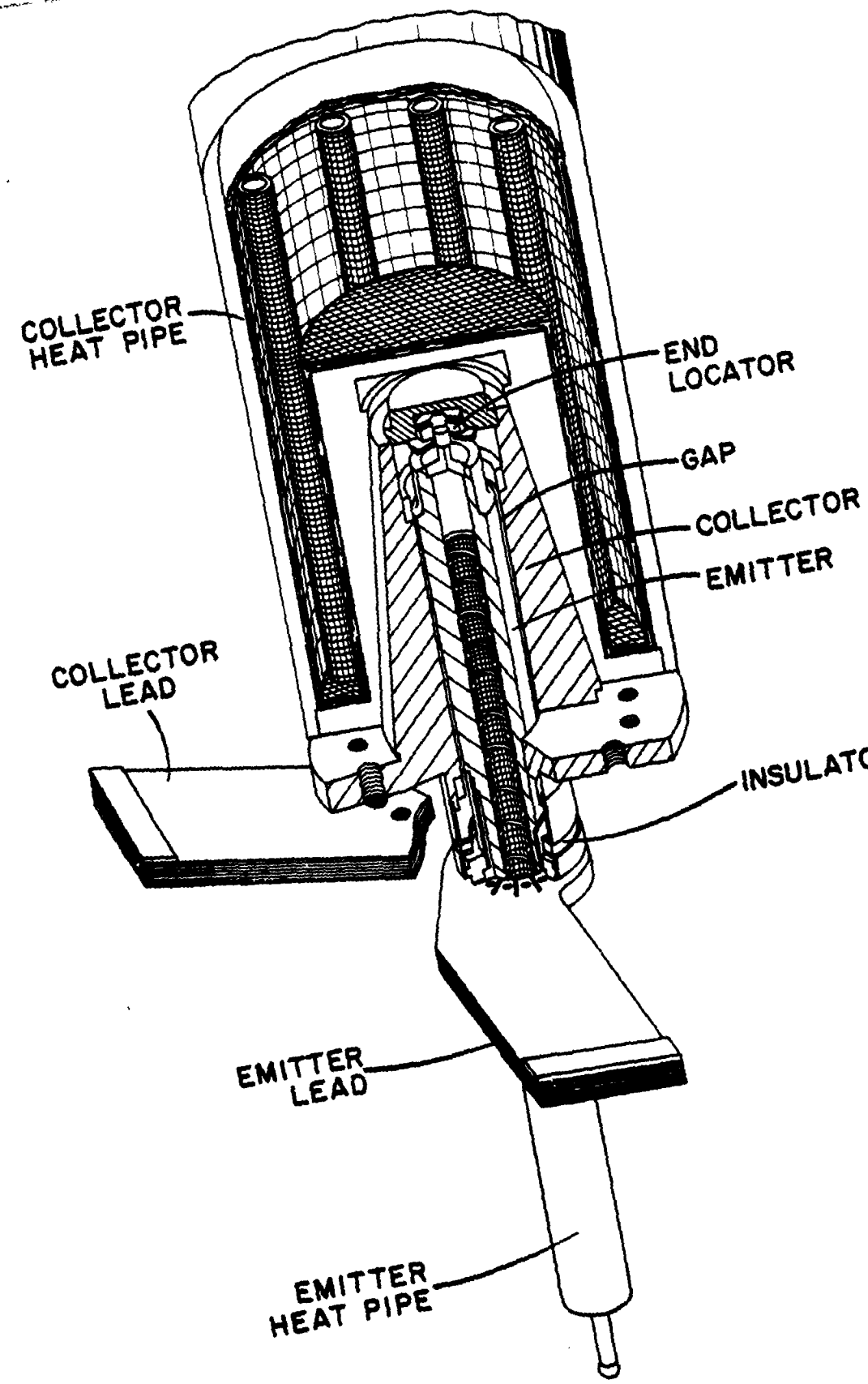
COLLECTOR HEAT PIPE
END LOCATOR
GAP
COLLECTOR
EMITTER
COLLECTOR LEAD
INSULATOR
EMITTER LEAD
EMITTER HEAT PIPE

Slide No. 7

7912-43

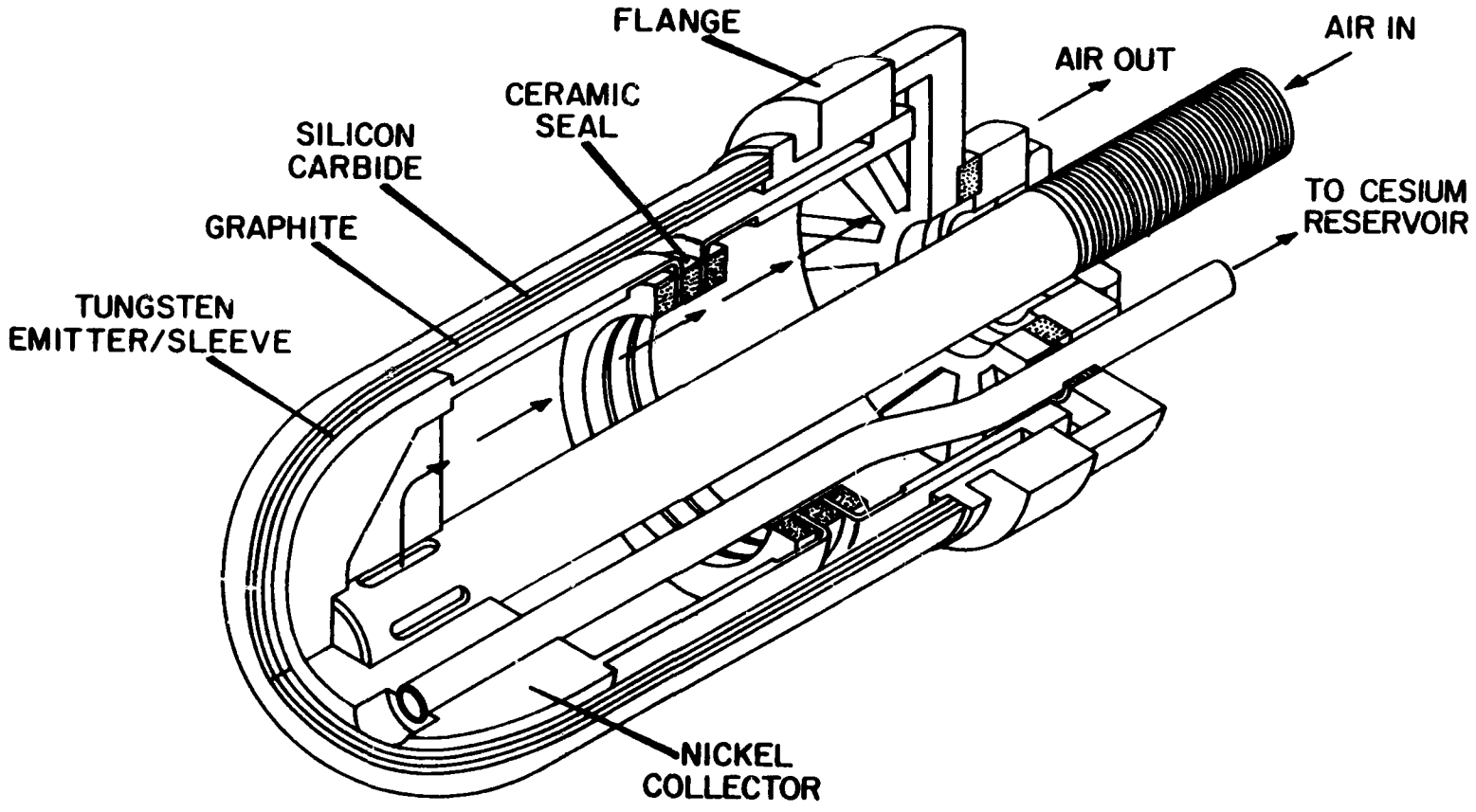

IX-2-13

Slide No. 8

NEXT SLIDE (9), PLEASE.

This drawing shows the application of the CVD trilayer technology to heat pipes which can operate at high temperature in air. This heat pipe is charged with lithium.

NEXT SLIDE (10), PLEASE.

This photograph shows a short heat pipe of this type operating at a temperature of about 1600 K. Clearly, the tungsten chemical vapor deposition technology can also be applied to space converter and heat pipe fabrication. In addition, CVD silicon carbide is a candidate material for electrically insulating the converter from the heat pipe at emitter temperature. Since silicon carbide has a band gap of 2.4 eV, the pure material should be an electrical insulator at projected operating temperatures. Although the present CVD silicon carbide has a room temperature resistivity of around 80 ohm-cm, no effort has yet been made to formulate higher resistivity material by using better grade reagents, additives or by modifying the deposition parameters. Therefore, the tungsten and silicon carbide CVD technology represents a valuable resource for space technology.

NEXT SLIDE (11), PLEASE.

This photomicrograph shows a niobium-alumina cermet that has been used quite successfully to electrically insulate the collector while providing a low thermal resistance path to the coolant. Unfortunately, the technology of making these cermets must be resurrected and refined. One problem is that the starting materials are no longer commercially available. However, the lab books for formulating the cermet are available and should greatly reduce the development time for the collector insulator.

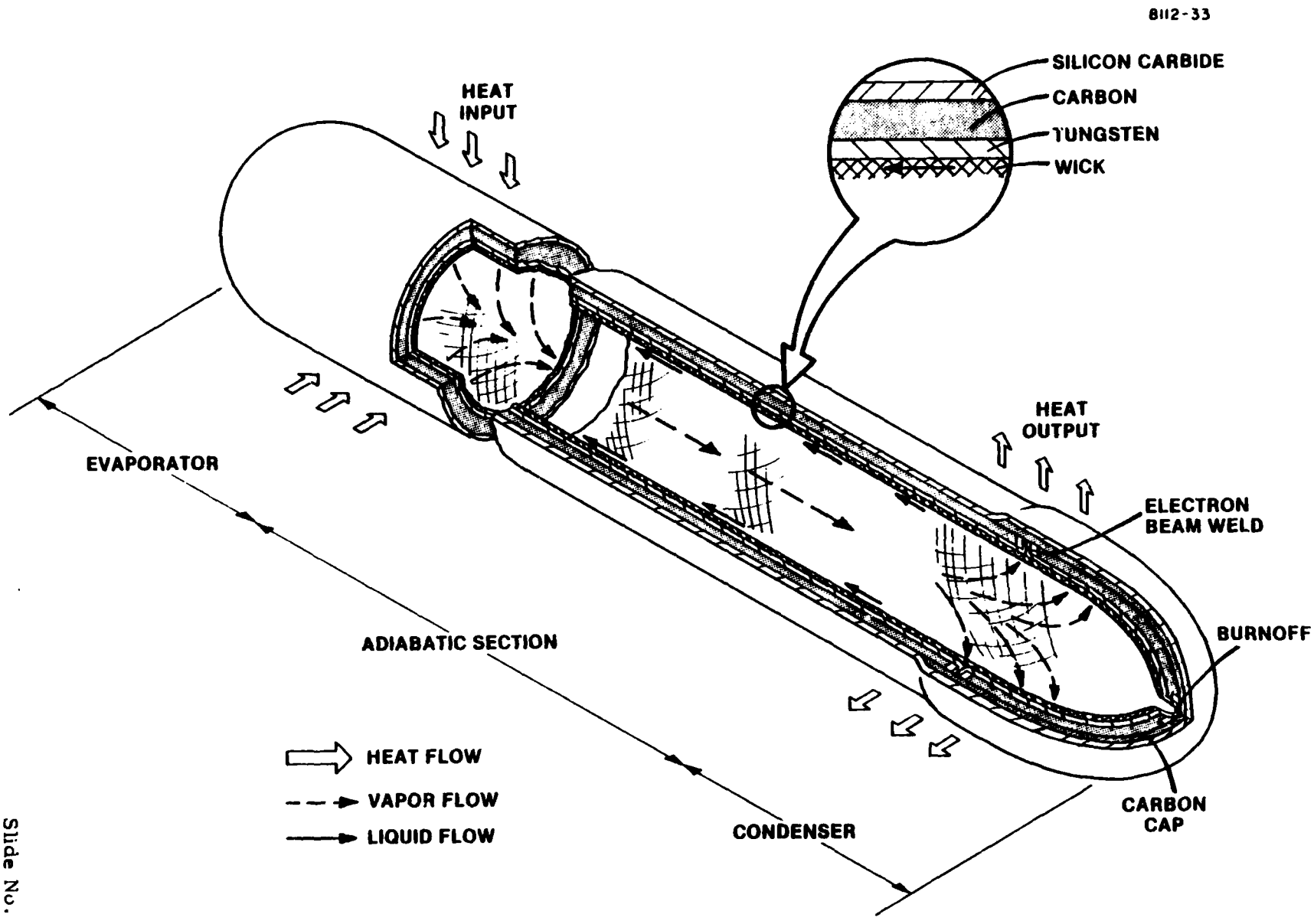
8112-33
SILICON CARBIDE
CARBON
TUNGSTEN
WICK
HEAT INPUT
HEAT OUTPUT
EVAPORATOR
ELECTRON BEAM WELD
ADIABATIC SECTION
BURNOFF
CARBON CAP
CONDENSER
HEAT FLOW
VAPOR FLOW
LIQUID FLOW

822-42

Slide No. 11

SUMMARY OF REQUIRED RESEARCH AND DEVELOPMENT

NEXT SLIDE (12), PLEASE.

This table summarizes the areas of research and development required for thermionic conversion. It is convenient to group these activities under the headings of reduced voltage loss in the plasma, heat pipe development, converter technology, systems analyses and fuel development. These groups span both 6.1 and 6.2 funding categories.

NEXT SLIDE (13), PLEASE.

This chart illustrates a technology tree relative to reducing the arc drop in the interelectrode plasma. Presently, the arc drop - or potential loss in the plasma - is about 0.5 to 0.6 volts. Theoretically, it should be possible to reduce this loss to about 0.1 volt. If only half of the theoretically possible arc drop reduction can be achieved, it would mean a large increase in thermionic efficiency and power density. In no other candidate conversion system for space is the potential for improvement so large and the technical approaches for achieving the improvement as well defined.

Almost two dozen techniques for reducing the arc drop have been proposed. It is evident that the electrode and plasma problems are coupled so that arc drop reduction may well require electrode development. Because of priorities established in the DOE fossil energy thermionic program, there has been only a superficial effort in this area. Clearly, there is an immediate need for research in arc drop reduction.

NEXT SLIDE (14), PLEASE.

Heat pipe development areas are identified on this slide. Although there is no question that reactor heat pipes made with tungsten walls and lithium working fluid operate reliably with excellent heat transport, questions of alloy composition, configuration and fabrication remain, along with the development of charging procedures to reduce oxygen concentration to an acceptable level. A similar statement applies to the collector heat pipes. Note that these activities span both 6.1 and 6.2 areas.

822-43

REQUIRED R&D FOR THERMIONIC CONVERSION

- REDUCED VOLTAGE LOSS IN INTERELECTRODE PLASMA
- HEAT PIPE DEVELOPMENT
- CONVERTER TECHNOLOGY
- SYSTEM ANALYSES
- FUEL DEVELOPMENT

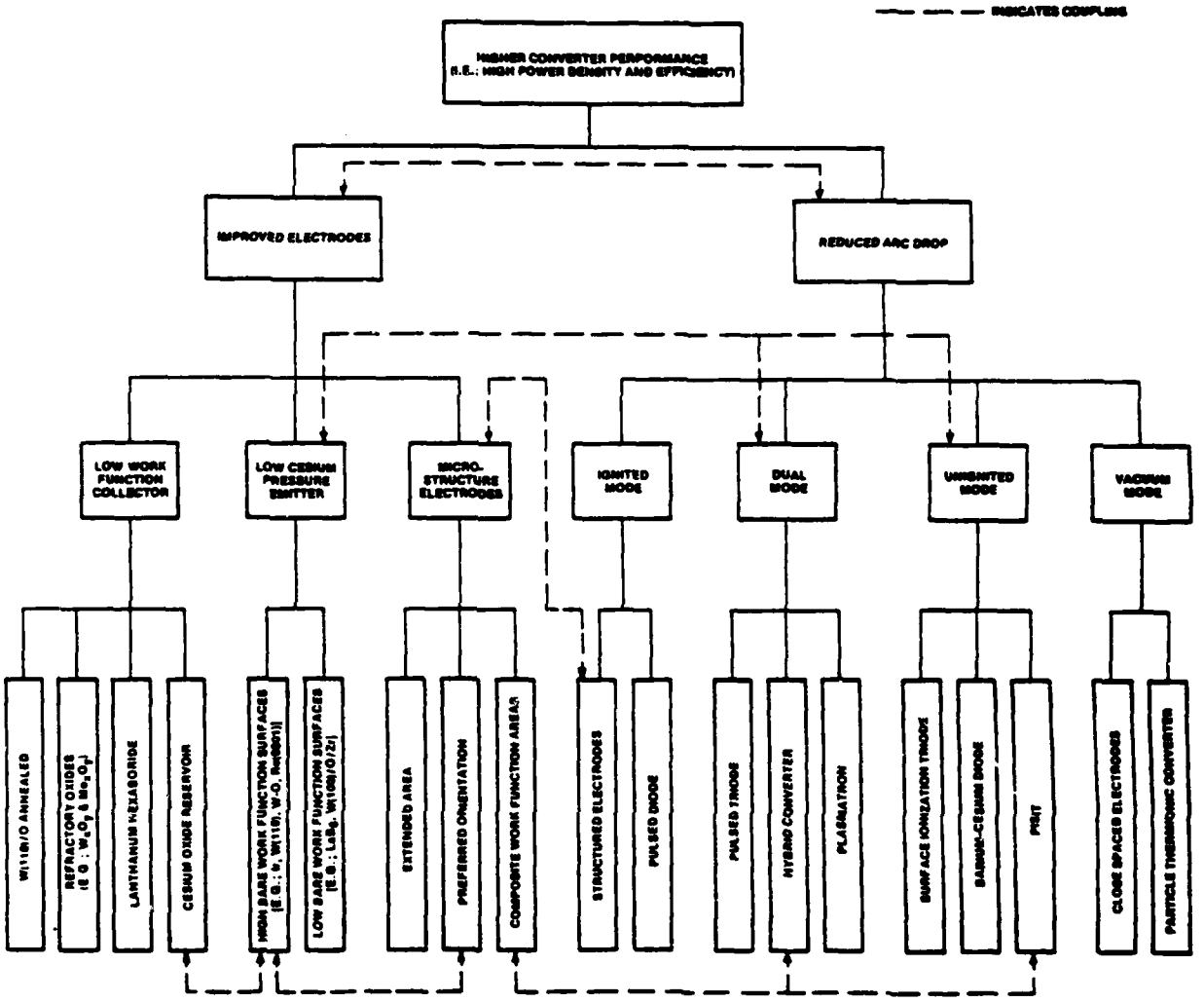
INDICATES COUPLING
HIGHER CONVERTER PERFORMANCE (I.E.; HIGH POWER DENSITY AND EFFICIENCY)
IMPROVED ELECTRODES
REDUCED ARC DROP
LOW WORK FUNCTION COLLECTOR
LOW CESIUM PRESSURE EMITTER
MICRO-STRUCTURE ELECTRODES
IONITED MODE
DUAL MODE
UNIONITED MODE
VACUUM MODE
W(110)/O ANNEALED
REFRACTORY OXIDES (E.G.: W_xO_y & Ba_xO_y)
LANTHANUM HEXABORIDE
CESIUM OXIDE RESERVOR
HIGH BARE WORK FUNCTION SURFACES (E.G.: Ir, W(110), W-O, Re(001))
LOW BARE WORK FUNCTION SURFACES (E.G.: LaB_6, W(100)/O/Zr)
EXTENDED AREA
PREFERRED ORIENTATION
COMPOSITE WORK FUNCTION AREAS
STRUCTURED ELECTRODES
PULSED DIODE
PULSED TRIODE
HYBRID CONVERTER
PLASMATRON
SURFACE IONIZATION TRIODE
BARIUM-CESIUM DIODE
PNIT
CLOSE SPACED ELECTRODES
PARTICLE THERMIONIC CONVERTER

Slide No. 13

822-44

HEAT PIPE DEVELOPMENT

- REACTOR HEAT PIPE
- RADIATOR HEAT PIPE

} WALL MATERIAL
CONFIGURATION
FABRICATION
CHARGING
QUALIFICATION

NEXT SLIDE (15), PLEASE.

Converter technology areas are tabulated on this slide. The problems of electrically insulating the emitter from the reactor heat pipe and the collector from the radiator heat pipe have been discussed previously. Oxygen addition can significantly increase the optimum interelectrode spacing to alleviate construction problems. Cesium-graphite reservoir development also requires refinement.

NEXT SLIDE (16), PLEASE.

Some of the major system analyses that are needed are indicated on this slide. The viability of the in-core approach needs to be resolved, factoring in the existing technology base and schedule considerations.

NEXT SLIDE (17), PLEASE.

Fuel development is an area needing immediate attention. In this country, this area has much in common with the weather - since everyone talks about it, but no one does anything about it. Much of the systems analysis is hampered by the lack of adequate fuel swelling data for the fuel compositions, claddings, temperatures and geometries of most interest.

FINAL SLIDE (18), PLEASE.

This slide is an attempt to summarize this presentation. Thermionic conversion is a primary option for space reactors, as evidenced by its choice by the USSR. Although R&D problems exist, the technology infrastructure built up over the past quarter century provides a sound basis for resolving these technical problems. However, the only funding source for thermionics is about to be zeroed and, unless some agency assumes responsibility for this technology in the immediate future, an important national option for future space reactor systems and fuel conservation will go down the drain. It will be cold comfort that thermionic technology is alive and well in the Soviet Union.

822-45

THERMIONIC CONVERTER TECHNOLOGY

- ELECTRICAL INSULATION
  - EMITTER FROM REACTOR HEAT PIPE
    - SILICON CARBIDE
    - BERYLLIUM OXIDE
    - RADIATION COUPLING
    - INERT GAS GAP CONDUCTION
  - COLLECTOR TO RADIATOR HEAT PIPE
    - NIOBIUM-ALUMINA CERMET
    - (TECHNOLOGY MUST BE RESURRECTED)
- EMITTER DEVELOPMENT
  - W(110)FROM CVD OF WCl_6
  - W(110) FROM CVD OF WFl_6 AND ELECTROETCHING
- COLLECTOR DEVELOPMENT
  - MICROSTRUCTURED SURFACE
  - OXIDE-COATED SUBSTRATE
- CESIUM-GRAPHITE RESERVOIR

822-46

SYSTEM ANALYSES
(IN-CORE AND OUT-OF-CORE)

- MATERIAL SELECTIONS
- EMITTER TEMPERATURE
- COLLECTOR TEMPERATURE
- CONVERTER CURRENT DENSITY
- FUEL CAPSULE DESIGN
- THERMAL COUPLING OPTIONS BETWEEN REACTOR HEAT PIPE AND CONVERTER

822-47

FUEL CAPSULE SWELLING DATA

- COMPOSITION
  - Mo-UO_2 CERMETS
  - W-UO_2 CERMETS
  - UC-ZrC
  - ETC.
- BURNUP
- TEMPERATURE
- VOID FRACTION
- GEOMETRY

SUMMARY

- THERMIONIC CONVERSION IS A PRIMARY OPTION FOR SPACE REACTORS
- TECHNICAL PROBLEMS EXIST
- THERE EXISTS A FIRM TECHNOLOGY BASE FOR RESOLVING THE TECHNICAL PROBLEMS
- THERMIONIC FUNDING IS ABOUT TO BE ZEROED
- IF SO, AN IMPORTANT NATIONAL OPTION WILL GO DOWN THE DRAIN
  - SPACE POWER SYSTEMS
  - FUEL CONSERVATION

Q & A - F. Huffman

From: Dave Bartine, ORNL

Does your out-of-core concept have the thermionic converters between the reactor core and the shielding? If so, do you envision any problem with radiation damage or heating effects?

A.

The converters can be either between the reactor core and the shielding or on the far side of the shielding. In neither case are radiation damage or heating effects expected to be a severe problem in view of: 1) in-pile converter experiments in the US during the sixties and early seventies and 2) the in-core thermionic reactors built in the USSR. In neither case were radiation damage or heating effects significant. If the converters are located between the reactor core and the shield, radiation effects may become a problem for long missions. If the converters are located on the far side of the shield, radiation effects should be negligible.

From: A. P. Fraas

What was the efficiency of the combustion heated thermionic cell that ran 12,000 hr @ 1730° K?

A.

$\sim$ 11%

What was the current density?

A.

7 A/cm^2

How many power cycles occurred in the 12000 hr test?

A.

14

From: LTC J. Lee, AFWL

On what factual basis did you (or AIAA) conclude that COSMOS 954 used thermionic conversion? Many folks disagree with that conclusion.

A.

Apparently, the AIAA based its conclusion that the power system for COSMOS 954 was probably a thermionic reactor on the publications given at the 28th International Astronautical Congress. Their conclusion was given in an AIAA report to NASA, "A Critical Review of the State of Foreign Space Technology" (February 1978).

Personally, I feel that the AIAA is probably correct based on:

1. The visual evidence of a large thermionic reactor program which I observed as a member of the U.S. Thermionic Delegation which visited the USSR thermionic facilities (Leningrad, Moscow, Obninsk, Kiev and Sukhumi). In particular, the Soviets showed us a large facility dedicated to testing thermionic reactors at the Power Reactor Laboratory in Obninsk.

2. The publication of test results on four generations of TOPAZ thermionic reactors. The latest data are from 1977.

3. The latest results on the ROMASHKA thermoelectric reactor of which I am aware date back to 1965. The U.S. Thermionic Delegation was shown spare components of ROMASHKA at the Kurchatov Laboratory outside Moscow. At that time, the Soviets stated that they had stopped development of thermoelectric reactors.

4. The Soviets have consistently identified thermionic reactors for space applications requiring more than a few kWe at:

   a. 1975 Thermionic Specialists Conference at Eindhoven
   b. Visit of the USSR Thermionic Delegation to the U.S. in 1976
   c. Visit of the U.S. Thermionic Delegation to the USSR in 1977
   d. Knorre, Elena, "Nuclear Energy for Space Exploration", New Times (Translation) No. 7, Moscow (Feb. 10, 1978).

5. The hundreds of USSR publications on thermionics.

6. The continued publication of thermionic papers in "Technical Physics".

7. The active thermionic program at the Ioffe Institute outside Leningrad (Ioffe was the "Father" of modern thermoelectrics).

8. The high level support of thermionics in the USSR:

   a. Kuznetsov, head of the USSR thermionics program, is a Deputy Director of the Power Reactor Laboratory at Obninsk.
   b. Morozoff, former head of the USSR thermionics program is a member of the USSR State Committee on Atomic Energy.

9. The national pride of using an energy converter invented in the USSR (Morgulis, 1956).

10. The continuity of organization and large resources (Kuznetsov said that their thermionic program was planned on a five year basis). It was the consensus of the U.S. Thermionic Delegation that visited the USSR in 1977 that their space power oriented thermionic program was over 10 times larger than the U.S. terrestrial thermionic program. Subsequently, the U.S. program has been cut to less than half its size at that time.

11. The clear superiority of the TOPAZ thermionic reactor performance relative to the ROMASHKA thermoelectric reactor (> 4 X efficiency and > 15 X output power).

12. The identification of the TOPAZ thermionic reactor in the paper by V. V. Bel'giy , "The On-Board Computer for Diagnosis of a Satellite Power Unit", IAF-79-F-168 Preprint, XXX Congress, Int'l Astronautical Federation, Munich (Sept., 1979).

The foregoing reasons are factual, but circumstantial. I know of no conclusive evidence that the COSMOS 954 reactor was thermionic or thermoelectric. However, I have no doubt (based on my interaction with the Soviets and monitoring of their literature) that the USSR has the capability of operating a thermionic reactor in space. Clearly, thermionics has significantly higher performance and development potential

than thermoelectrics which have been chosen for the only space reactor system now under development in this country.

I am absolutely astounded that this conference has been conducted with so little consciousness of the present USSR capability in space power. Even if the SP-100* can be available in 6-8 years, it will be a second rate system with little growth potential which will very probably be inferior to what the Soviets can now do. In my opinion, this is the important question for this country and this conference to address. Whether COSMOS 954 used thermoelectric or thermionic conversion is a peripheral issue.

*As stated by J. Mullin in Session I

A SURVEY OF RECENT ADVANCES IN AND FUTURE PROSPECTS FOR THERMIONIC ENERGY CONVERSION

JOHN LAWLESS
CARNEGIE-MELLON UNIVERSITY

A Survey of Recent Advances in and Future Prospects for Thermionic Energy Conversion

ABSTRACT

J.L. Lawless
Carnegie-Mellon University

Some powerful advances in the fundamental understanding of Thermionic Conversion have occurred recently. These include numerical computer simulations and simple analytical models. As a consequence of these advances, many new ideas are being developed with the potential for major improvements in thermionic converter performance. In particular, structured electrodes and oscillation effects now show strong possibilities for important improvements. Further, modeling techniques now exist to consider pore converters and third electrode converters in detail whereas past studies have been mainly empirical. In summary, greatly superior performance can be expected from future thermionic converters.

THERMIONIC ENERGY CONVERSION

MOTIVATION:

- LONG RANGE MISSIONS
- MODULAR CONSTRUCTION
- HIGH TEMPERATURE HEAT REJECTION

RECENT THEORETICAL ADVANCES:

- QUANTITATIVE COMPUTER SIMULATIONS
- SIMPLE ANALYTICAL MODELS

PROSPECTS FOR NEAR-TERM MAJOR IMPROVEMENTS:

- GEOMETRY
- IONIZATION KINETICS
- FLOW/OSCILLATIONS

CONCLUSION:

BECAUSE OF NEW THEORETICAL UNDERSTANDINGS, MANY NEW IDEAS ARE BEING DEVELOPED WITH THE POTENTIAL FOR MAJOR IMPROVEMENTS IN THE PERFORMANCE OF THERMIONIC ENERGY CONVERTERS.

RECENT THEORETICAL ADVANCES

QUANTITATIVE COMPUTER SIMULATION:

STEADY (RASOR, TECO)

UNSTEADY (PRINCETON/CARNEGIE-MELLON)

SIMPLE ANALYTICAL MODELS:

ISOTHERMAL

NON-ISOTHERMAL

PERFORMANCE IMPLICATIONS (LOW PD REGION)

1). ARC-DROP IS GOVERNED BY:

A) ELECTRON TEMPERATURE NEAR ELECTRODES

B) ELECTRODE/SHEATH BEHAVIOR

2). THE ELECTRON TEMPERATURE IS GOVERNED MAINLY BY A PLASMA IGNITION CONDITION WHICH IN TURN IS GOVERNED BY:

A) IONIZATION KINETICS

B) AMBIPOLAR DIFFUSION

3). ELECTRODE/SHEATH BEHAVIOR IS GOVERNED BY:

A) GEOMETRIC SHAPE (STRUCTURE)

B) SIZE OF STRUCTURE

C) ELECTRODE ELECTRON REFLECTION/TRANSMISSION

D) SPACE CHARGE BEHAVIOR, E.G., TRAPPED IONS

THERMIONIC ENERGY BALANCE

PLASMA POWER LOSS = THERMAL LOSS AT COLLECTOR
+ THERMAL LOSS AT EMITTER
+ INELASTIC COLLISION LOSS

FOR CONVENTIONAL PLANAR DESIGNS:

$$I V_D = 2 I_E(\kappa T_e - \kappa T_E)/e + S^{(E)}$$

I=CURRENT
V_D=SHEATH PEAK TO PEAK VOLTAGE DROP
I_E=EMITTED CURRENT
K =BOLTZMANN'S CONSTANT
T_e=ELECTRON TEMPERATURE
T_E=EMITTER TEMPERATURE
$S^{(E)}$=INELASTIC COLLISION LOSS
e =ELECTRON CHARGE

STRUCTURED ELECTRODES

COMPARISON OF THERMAL ENERGY LOSSES FROM THE CONVENTIONAL PLANAR ELECTRODE DESIGNS AND IDEAL COLLISIONLESS STRUCTURED ELECTRODES:

CONVENTIONAL PLANAR ELECTRODE:	2kT
TWO-DIMENSIONAL STRUCTURES:	(3/2)kT
THREE-DIMENSIONAL STRUCTURES:	1kT

THIS REDUCED THERMAL ENERGY LOSS DIRECTLY REDUCES THE PLASMA ARC-DROP.

POTENTIAL REDUCTION IN ARC-DROP:	OVER 200mV

PRESENT EXPERIMENTS INDICATE THAT STRUCTURED ELECTRODES DO WORK BUT THE DESIGN OF OPTIMAL STRUCTURES REQUIRES FURTHER THEORETICAL WORK.

STRUCTURED ELECTRODES

COMPARISON OF THERMAL ENERGY LOSSES FROM THE CONVENTIONAL PLANAR ELECTRODE DESIGNS AND IDEAL COLLISIONLESS STRUCTURED ELECTRODES:

CONVENTIONAL PLANAR ELECTRODE:	2kT
TWO-DIMENSIONAL STRUCTURES:	(3/2)kT
THREE-DIMENSIONAL STRUCTURES:	1kT

THIS REDUCED THERMAL ENERGY LOSS DIRECTLY REDUCES THE PLASMA ARC-DROP.

POTENTIAL REDUCTION IN ARC-DROP: OVER 200mV

PRESENT EXPERIMENTS INDICATE THAT STRUCTURED ELECTRODES DO WORK BUT THE DESIGN OF OPTIMAL STRUCTURES REQUIRES FURTHER THEORETICAL WORK.

MORE POSSIBILITIES FOR POTENTIALLY MAJOR IMPROVEMENTS

GEOMETRY:

- -THE CONVENTIONAL PLANAR DESIGN IS NOT OPTIMAL.
- -THERE ARE THREE INHERENT LENGTH SCALES:
  - A. THE GAP SIZE
  - B. THE MEAN FREE PATH
  - C. THE DEBYE LENGTH
- -THEORY AND EXPERIMENT FOR STRUCTURED ELECTRODES HAS CONCENTRATED ON STRUCTURE SIZES BETWEEN B AND C.
- -MICROFABRICATION
- -PORE CONVERTERS
- -THIRD ELECTRODES

IONIZATION KINETICS

- -ELECTRON-ATOM IONIZATION KINETICS ARE NOW FAIRLY WELL UNDERSTOOD
- -MOLECULAR PROCESSES ARE NOT AT ALL UNDERSTOOD AND HOLD MANY POSSIBILITIES

FLOW/OSCILLATIONS

- -PRELIMINARY EVIDENCE FROM BOTH THEORY AND EXPERIMENT HOLDS THAT THIS AREA HAS MUCH POTENTIAL.

SUMMARY

1). RECENT THEORETICAL ADVANCES HAVE OCCURRED IN THE FOLLOWING:

- STRUCTURED ELECTRODES AND OTHER GEOMETRIC EFFECTS,
- OSCILLATIONS

THESE NOW SHOW STRONG POSSIBILITIES FOR MAJOR IMPROVEMENTS IN THERMIONIC PERFORMANCE

2). MODELING TECHNIQUES NOW EXIST TO CONSIDER THE FOLLOWING IN MORE DETAIL:

- PORE CONVERTERS
- THIRD ELECTRODES

3). MOLECULAR IONIZATION PROCESSES NEED MORE STUDY BOTH THEORETICALLY AND EXPERIMENTALLY BUT MAY POTENTIALLY BE VERY IMPORTANT

SESSION X. HEAT/SYSTEMS

THERMAL MANAGEMENT
OF
LARGE PULSED POWER SYSTEMS

presented at the

Air Force Office of Scientific Research
Special Conference on Prime Power for High-Energy Space Systems

22-25 February 1982
Omni International Hotel, Norfolk, Virginia

by
Bob Haslett
(516) 575-3924

Grumman Aerospace Corporation
Bethpage, New York 11714

T-X

GRUMMAN

Abstract

Air Force space power trends indicate requirements for systems with 10 to 200 KW average power with pulse/average power ratios of 10/1 to 1000/1. Thermal system definition is complicated by the variety of possible power systems although solar and nuclear (Brayton and Thermionic) appear to be the leading candidates.

Current thermal control technology is reviewed and limitations assessed compared to a typical high pulse power application. Thermal management is a significant weight factor (~50%) of even medium power systems which points to a large potential payback from innovative techniques. Thermal research is recommended in the areas of concentrating and thermovoltaic solar arrays, two phase heat transport loops, direct contact heat exchangers and advanced radiator systems.

Air Force space average power requirements are expected to increase tenfold to meet expanded mission requirements. In addition, directed energy devices being studied will require multi-megawatt pulse power levels. The trends shown are based on recent A.F. projections (Ref. 1).

AIR FORCE POWER SYSTEM TRENDS

TIME FRAME	POWER REQUIRED	MISSIONS
CURRENT	1-2 Kw	COMMUNICATION, NAVIGATION, WEATHER, SURVEILLANCE
1980's	2-10 Kw	– MISSION GROWTH – INCREASED ON-BOARD DATA PROCESSING – SATELLITE DATA RELAY
1990 AND BEYOND	10-100 Kw	– LARGE MULTIPURPOSE PLATFORMS – LARGE CRYOCOOLERS FOR IR SURVEILLANCE – SPACE BASED RADAR – MANNED MISSIONS
	>100 Kw	– ELECTRIC PROPULSION
	100-200 Kw AVG 1-100 Mw PULSE PULSE/AVG 10/1 TO 1000/1	DIRECTED ENERGY DEVICES (LASERS, NEUTRAL BEAMS)

X-1-3

GRUMMAN

Although many power generation and storage systems are feasible for Air Force missions, parametric studies (Ref. 1) indicate that nuclear reactor systems have a weight advantage for large systems (> 30-50 KW). Solar array/battery systems upgraded with new technology are expected to remain in favor for near term applications.

SOME POWER SYSTEM OPTIONS

GENERATION	STORAGE
SOLAR ARRAYS – HIGH EFFICIENCY CELLS – CASCADE CELLS – CONCENTRATING – THERMOVOLTAIC	BATTERIES – NICKEL HYDROGEN – LITHIUM/METAL SULFIDE – SODIUM SULFUR
	REGENERATIVE FUEL CELLS
FUEL CELLS	CAPACITORS – ELECTROLYTIC
NUCLEAR REACTOR/THERMIONIC	INDUCTIVE – SUPERCONDUCTING MAGNETS
NUCLEAR REACTOR/BRAYTON – OPEN LOOP OR CLOSED LOOP – VARIOUS REACTOR TYPES	MECHANICAL – COMPOSITE FLY WHEELS
	THERMAL – PHASE CHANGE MATERIAL

X-1-5

GRUMMAN

Space power presents the thermal control engineer with the full spectrum of design extremes, from cryo cooling systems for inductive storage to liquid metal heat pipes for nuclear reactors. As power levels increase, thermal control components become a very significant part of the power system weight, especially if, a low heat rejection temperature is required.

X-1-6

THERMAL CONTROL IMPLICATION

SYSTEM	THERMAL CONTROL
SOLAR ARRAYS	CONCENTRATOR OR THERMOVOLTAIC SYSTEMS MINIMIZE VULNERABILITY BUT ACCEPTABLE CELL TEMPERATURES MAY BE DIFFICULT TO ACHIEVE.
FUEL CELLS	RADIATOR WEIGHT AND RELIABILITY/ VULNERABILITY PENALTY FOR LARGE SYSTEMS MUST BE MINIMIZED.
BATTERIES AND CAPACITORS	RELATIVELY LOW AND STABLE TEMPERATURE REQUIRED FOR HIGH RELIABILITY AND GOOD DISCHARGE CHARACTERISTICS.
INDUCTIVE STORAGE	CRYO COOLING SYSTEM REQUIRED.
NUCLEAR REACTOR – THERMIONIC	REQUIRES HOT AND COLD JUNCTION LIQUID METAL HEAT PIPE SYSTEMS.
– BRAYTON (CLOSED LOOP)	REJECTION AT ≈ 200° C REQUIRES VERY LARGE RADIATOR FOR HIGH POWER APPLICATIONS.

X-1-7

BRUMMAN

0311-004(T)

The pulsed power systems being considered for directed energy devices will be so large and expensive that every subsystem must be selected to minimize transportation costs and to provide the maximum on-orbit capability, reliability and growth potential.

X-1-8

THERMAL MANAGEMENT SYSTEM SELECTION CRITERIA

COMPATABILITY

- MEETS SPECIFIC POWER SYSTEM REQUIREMENTS, E.G. STABLE TEMP, LOW GRADIENTS, PULSED HEAT REJECTION, CRYO COOLING, ETC.

TRANSPORTABILITY

- MINIMUM VOLUME AND WEIGHT FOR COST EFFECTIVE DELIVERY TO ORBIT.
- DEPLOYMENT OR ON-ORBIT ASSEMBLY FOR VERY LARGE SYSTEMS.

SURVIVABILITY

- MINIMUM VULNERABILITY TO NATURAL ENVIRONMENTS AND TO HOSTILE ATTACK.

RELIABILITY

- COMPONENTS AND SYSTEM CONFIGURATION TO SATISFY LONG LIFE MISSIONS (10 YEARS OR MORE)

GROWTH

- ON-ORBIT GROWTH COMPATIBLE WITH MISSION/POWER SYSTEM EVOLUTION.

X-1-9

GRUMMAN

Passive and fluid loop thermal control systems have been the mainstays for satellites and manned vehicles respectively. Recent research (Ref. 2 & 3) however, is directed at developing more efficient two phase heat transfer systems. These include heat pipes, phase change thermal storage systems and liquid-vapor heat transport loops.

X-1-10

THERMAL CONTROL STATE OF THE ART

EXISTING	APPLICATION
PASSIVE	ALL SATELLITES
LOUVERS AND THERMAL SWITCHES	MANY SATELLITES
PHASE CHANGE CANISTERS	A NUMBER OF SATELLITES
FLUID LOOPS WITH EVAPORATORS OR RADIATORS	GEMINI, SKYLAB, APOLLO, SHUTTLE
HEAT PIPES INCLUDING DIODES AND VCHP's	OAO, ATS, CTS AND OTHERS

NEAR TERM DEVELOPMENT PROGRAMS AT GRUMMAN	
EQUIPMENT TEMP CONTROL PLATE (NASA MSFC)	SHUTTLE/LDEF
BATTERY TEMP CONTROL SYSTEM (INTELSAT)	COMMUNICATIONS SATELLITES
DEPLOYABLE HEAT PIPE RADIATOR (NASA MSFC)	SHUTTLE PAYLOADS
THERMAL CANISTER (NASA GSFC)	SHUTTLE PAYLOADS
DIRECT CONTACT THERMAL STORAGE (DOE SERI)	GROUND OR SPACE POWER SYSTEMS
SPACE CONSTRUCTABLE RADIATOR (NASA JSC)	SPACE OPERATIONS CENTER
TWO PHASE HEAT TRANSPORT LOOP (NASA GSFC)	SCIENCE PLATFORM

X-1-11

GRUMMAN

The Transverse Plate (Ref. 4) is a flat variable conductance heat pipe with an integral honeycomb structure. Heat dissipating equipment is mounted to one side and the other side is the radiator. The radiator area is automatically modulated by a non-condensible gas to control equipment temperature. A flight test of this device will be conducted in 1984 on the Shuttle Long Duration Exposure Facility.

X-1-12

TRANSVERSE VARIABLE CONDUCTANCE FLAT PLATE

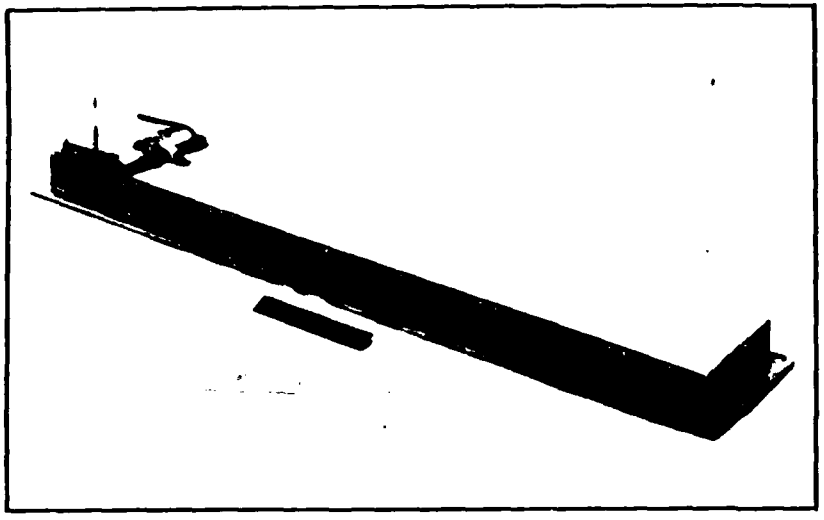

X-1-13

STATUS

- DEVELOPED FOR MSFC (GRUMMAN PATENT)
- IN FINAL ASSEMBLY
- WILL FLY ON SHUTTLE LDEF

FEATURES

- HONEYCOMB STRUCTURE/VCHP
- COMPLETELY PASSIVE SYSTEM
- MAINTAINS EQUIPMENT ±5°F

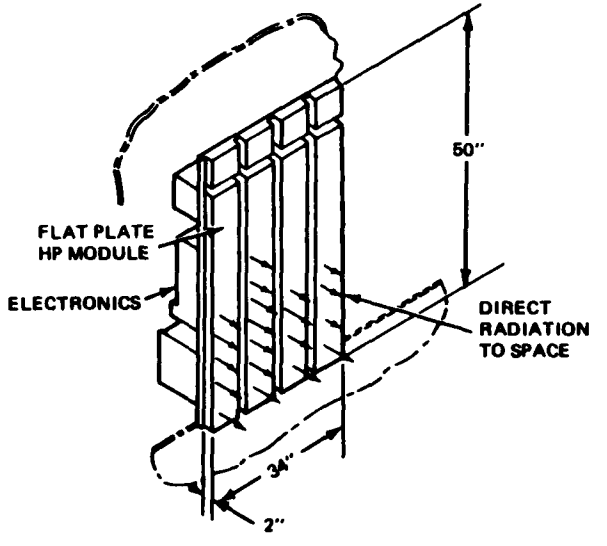

GRUMMAN

0474-143

This variable conductance heat pipe system provides stable temperature level and minimizes temperature gradients across the NiCd cells to achieve very high battery reliability. A prototype (Ref. 5) has been subjected to flight qualification and life testing.

X-1-14

BATTERY/RADIATOR HEAT REJECTION SYSTEM

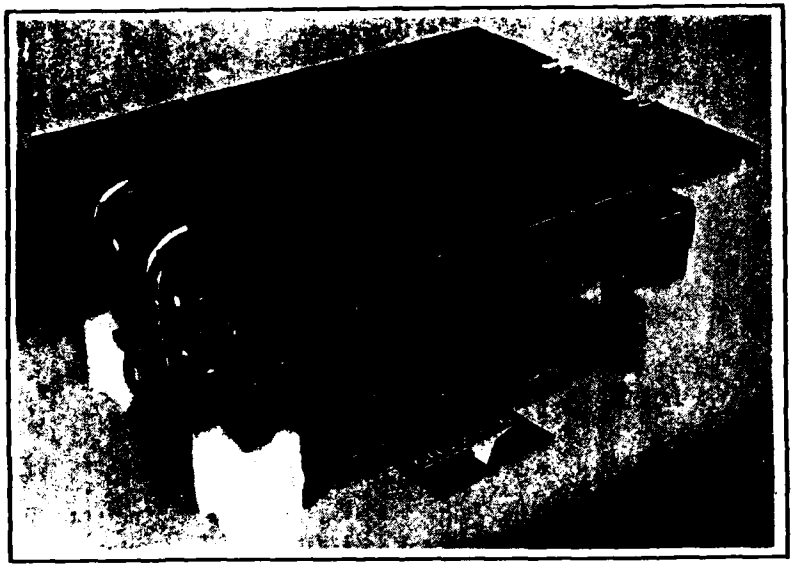

STATUS

- DEVELOPED FOR COMSAT
- SPACE QUALIFIED
  - VIBRATION
  - INTELSAT V MISSION SIMULATION (TV)
- CANDIDATE SYSTEM FOR INTELSAT VI

X-1-15

FEATURES

- INTEGRAL STRUCTURE/RADIATOR
- EMPLOYS FEEDBACK VCHP'S
- BATTERY TEMP MAINTAINED 5±1°C

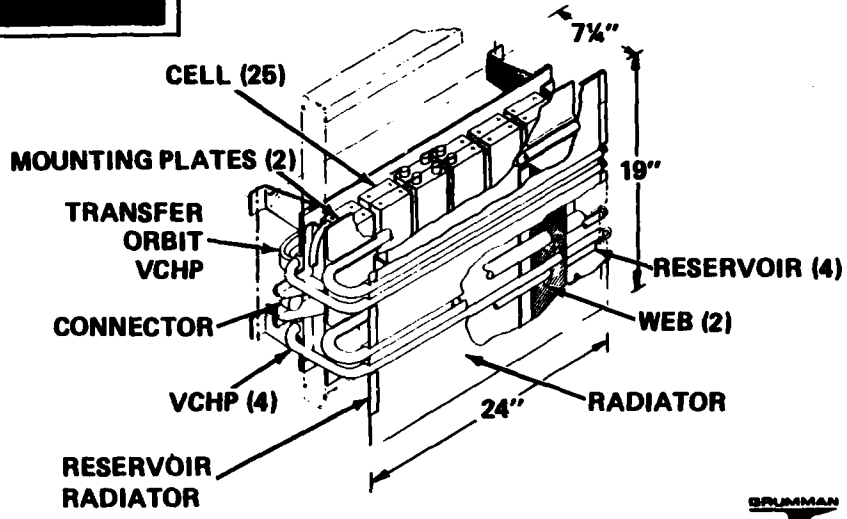

GRUMMAN

1097—020D

This variable conductance radiator (Ref. 6) is connected to the spacecraft heat source via a flexible heat pipe which allows the radiator to deploy on-orbit.

X-1-16

DEPLOYABLE RADIATOR WITH FLEXIBLE HEADER HEAT PIPE

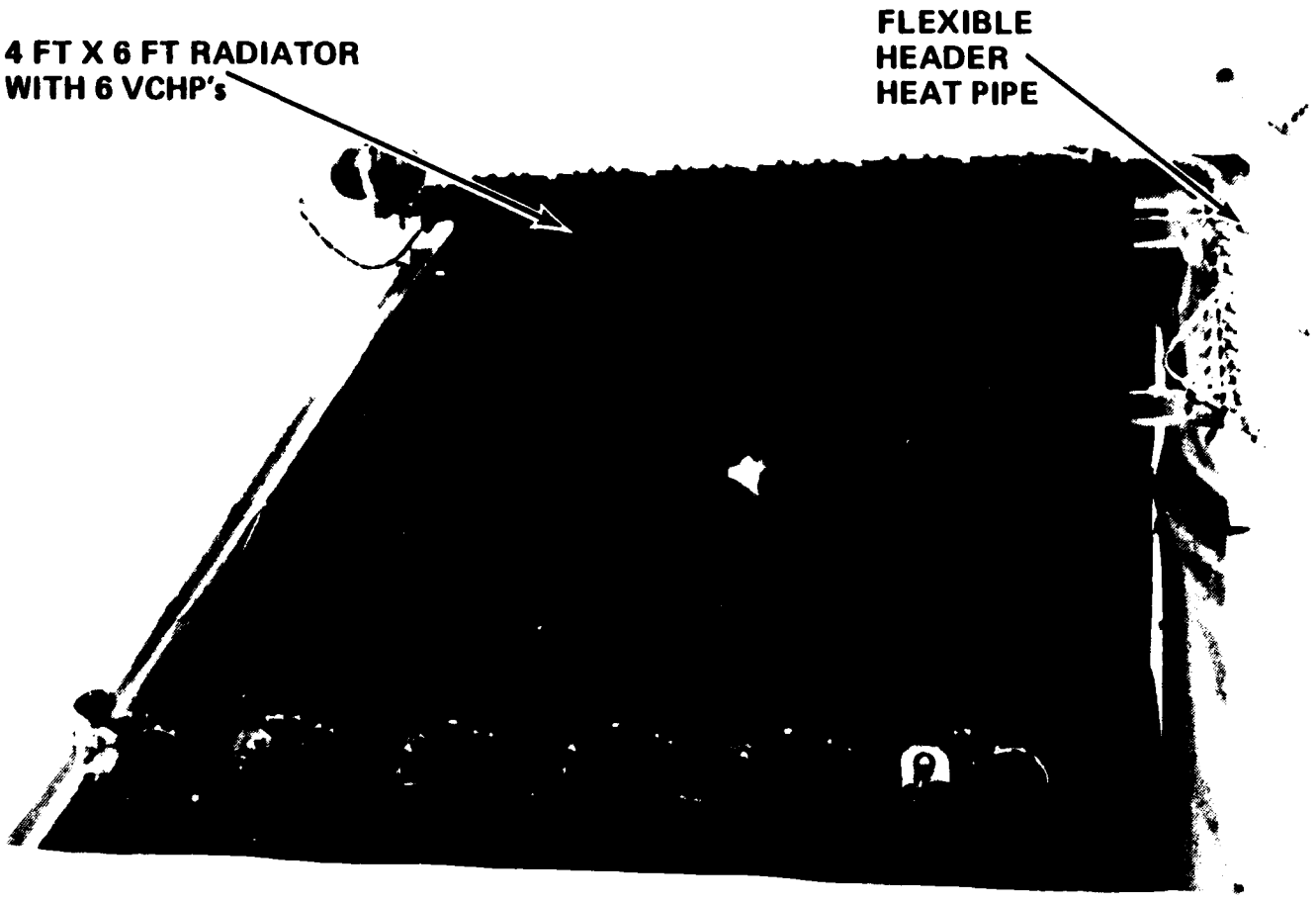

X-1-17

The Thermal Canister (Ref. 7, 8 & 9) is an integrated heat pipe system providing very fine temperature control (± 1°C) of Shuttle payloads by a system of microprocessor controlled feedback variable conductance heat pipe radiators. The 1m x 1m x 3m prototype will fly on the next Shuttle (March '82) and much larger operational versions are planned.

X-1-18

[redacted]

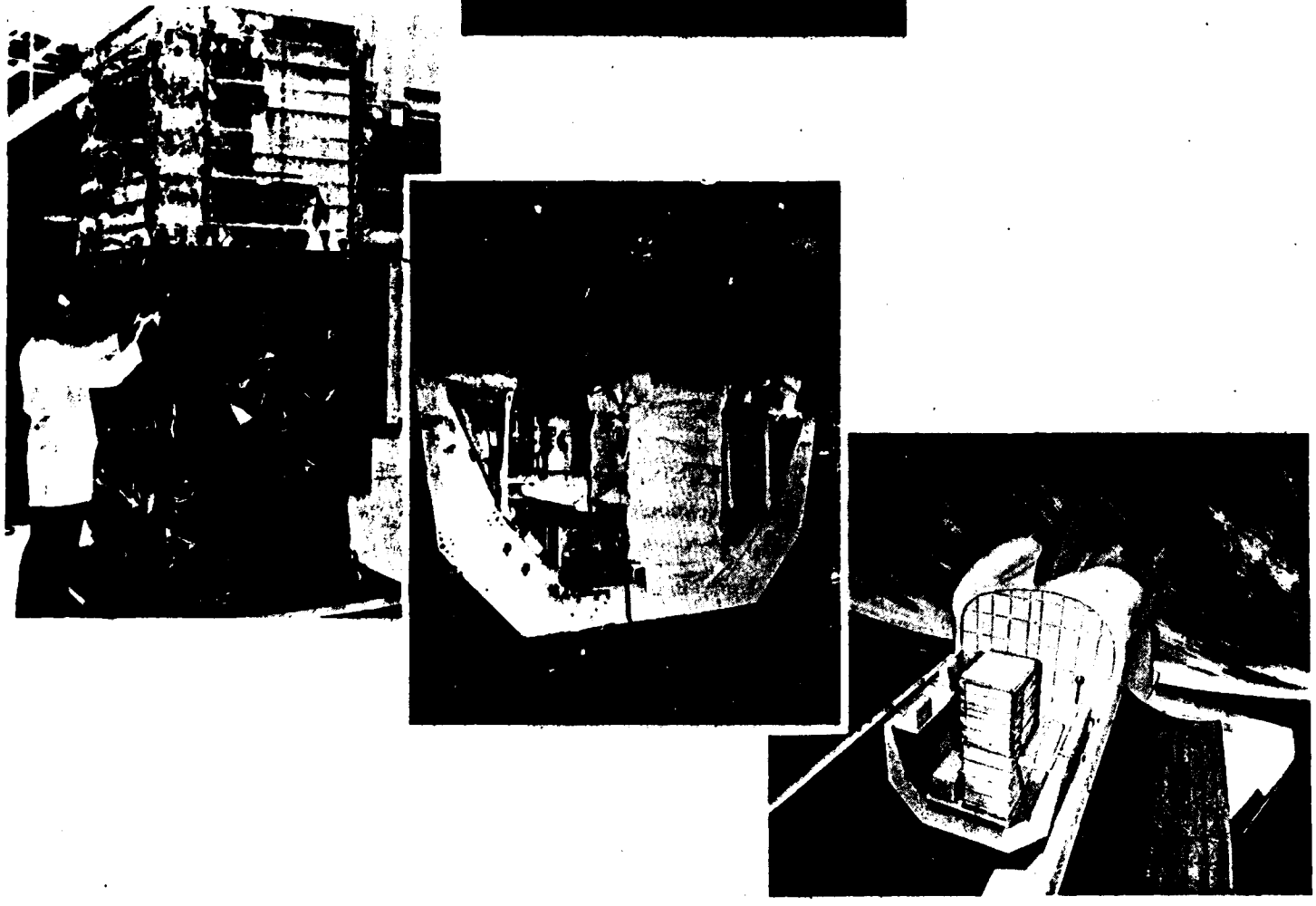

X-1-19

The low thermal conductivities of most phase change materials used in thermal storage systems prevents high charge/discharge rates unless the heat source (heat pipes or conducting fins) are very closely spaced which is heavy and expensive. Under DOE sponsorship a direct contact heat exchanger (Ref. 10) is being tested. The heat transfer fluid (Lead Bismuth eutectic) is heated by direct contact with solidifying droplets of the phase change material (a chloride salt eutectic) which melts at 725°F.

X-1-20

THERMAL STORAGE UNIT WITH DIRECT CONTACT HEAT EXCHANGER

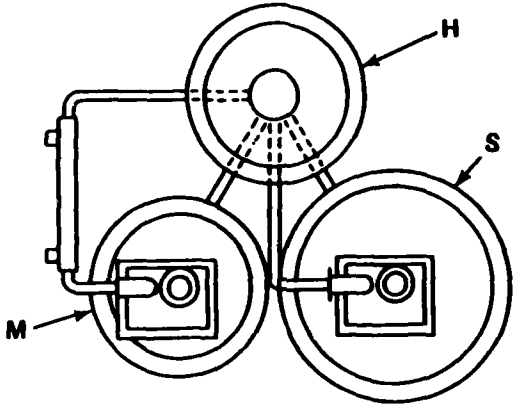

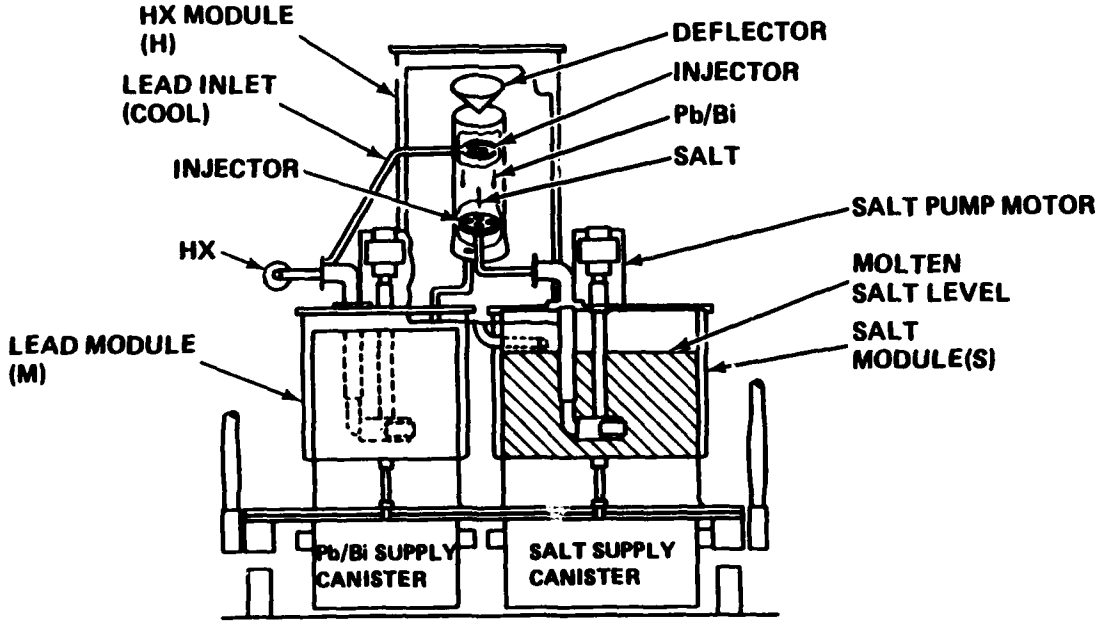

X-1-21

0311-013(T)

Very large heat rejection systems must be assembled in orbit. Individual elements can not exceed 60ft in order to be Shuttle transportable. Currently under test is a 54 ft long heat pipe radiator element (Ref. 11) being developed under NASA JSC sponsorship for a nominal 200 KW heat rejection system. A dry interface with the Space Operation's Center (SOC) coolant loop permits on-orbit growth or replacement of heat pipe radiator elements without affecting SOC operation.

X-1-22

SPACE CONSTRUCTABLE RADIATOR

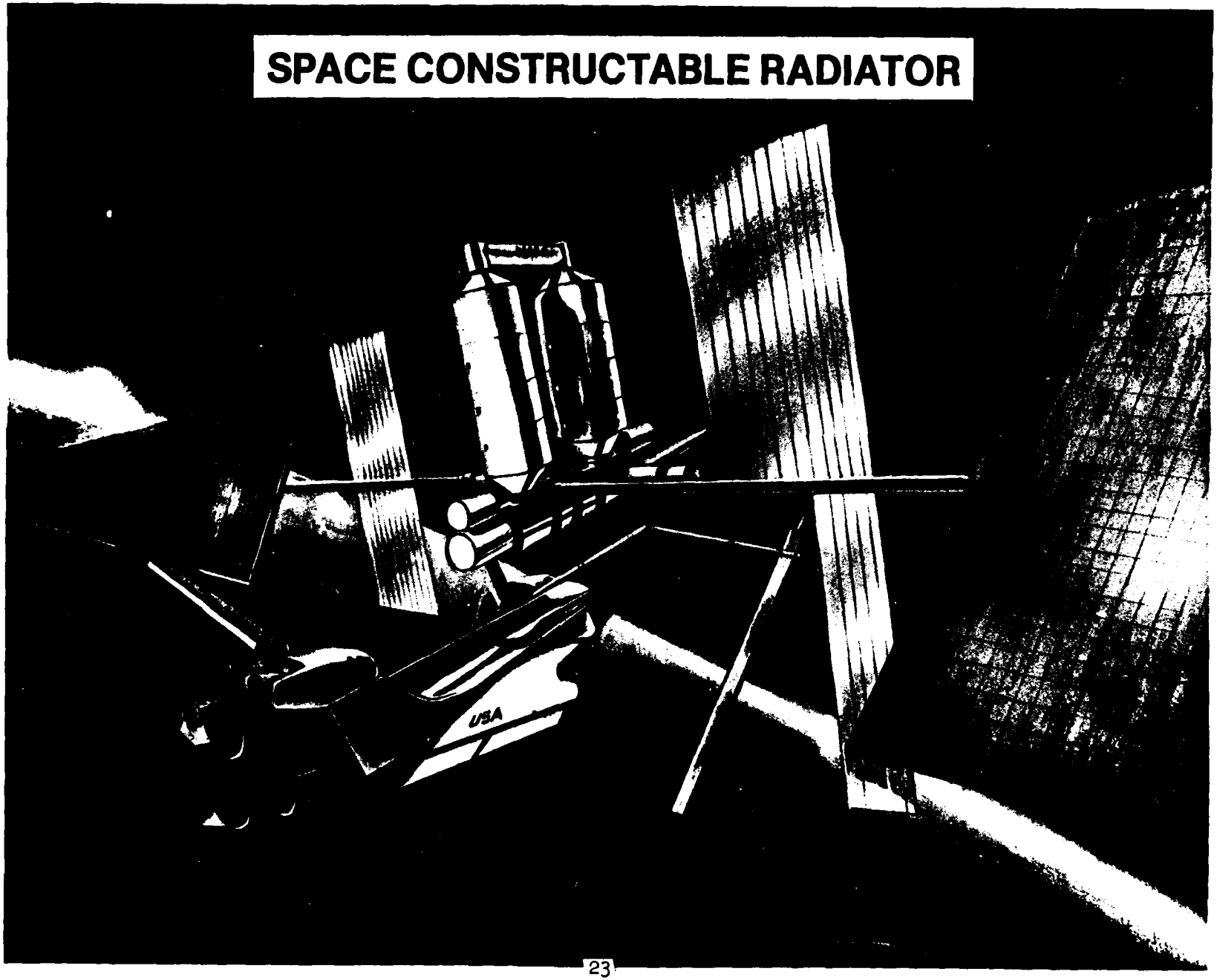

X-1-23

All existing thermal management techniques have limitations that become critical when applied to future power systems requiring at least an order of magnitude greater heat rejection. The need for research to develop innovative new thermal systems is clearly indicated.

X-1-24

LIMITATIONS OF CURRENT THERMAL SYSTEMS

SYSTEM	CONSTRAINT
PASSIVE, LOUVERS, SWITCHES	PROVIDES LOCAL HEAT REJECTION; HIGH POWER APPLICATIONS REQUIRE HEAT TRANSPORT TO EXTENDED AREA RADIATOR.
PHASE CHANGE CANISTERS	TEMPERATURE GRADIENTS IN LOW CONDUCTIVITY PCM PREVENT HIGH CHARGE/DISCHARGE RATES.
FLUID LOOPS	LINE SIZES, FLUID WEIGHT AND PUMP POWER BECOME EXCESSIVE FOR HIGH POWER APPLICATIONS.
EXPENDABLES	WEIGHT EXCESSIVE FOR LONG MISSIONS OR HIGH POWER.
FLUID RADIATORS	SIZE ~ 2 m^2/kw (22 ft^2/kw) AT 50°C (NO SUN) WEIGHT ~ 5.4 kg/m^2 (1.1 lb/ft^2) VULNERABLE TO MICROMETEROIDS AND HOSTILE ACTION.
HEAT PIPES	TRANSPORT CAPACITY LIMITED – CURRENT ~ 10^3w-m (40,000 w-in) – NEAR TERM ~ 10^4w-m (400,000 w-in)
HEAT PIPE RADIATOR	SIZE AND WEIGHT SIMILAR TO FLUID LOOP RADIATOR

X-1-25

GRUMMAN

A sample problem was selected to illustrate the thermal design trades that are presented by megawatt power levels. The system shown might be a relatively near term test of a directed energy device using available technology (SEPS solar array, NiH_2 batteries and conventional thermal storage and heat pipe radiator systems). To achieve high battery reliability and good discharge characteristics it is assumed that the battery temperature will be held constant.

X-1-26

ILLUSTRATIVE THERMAL DESIGN PROBLEM – SOLAR POWER

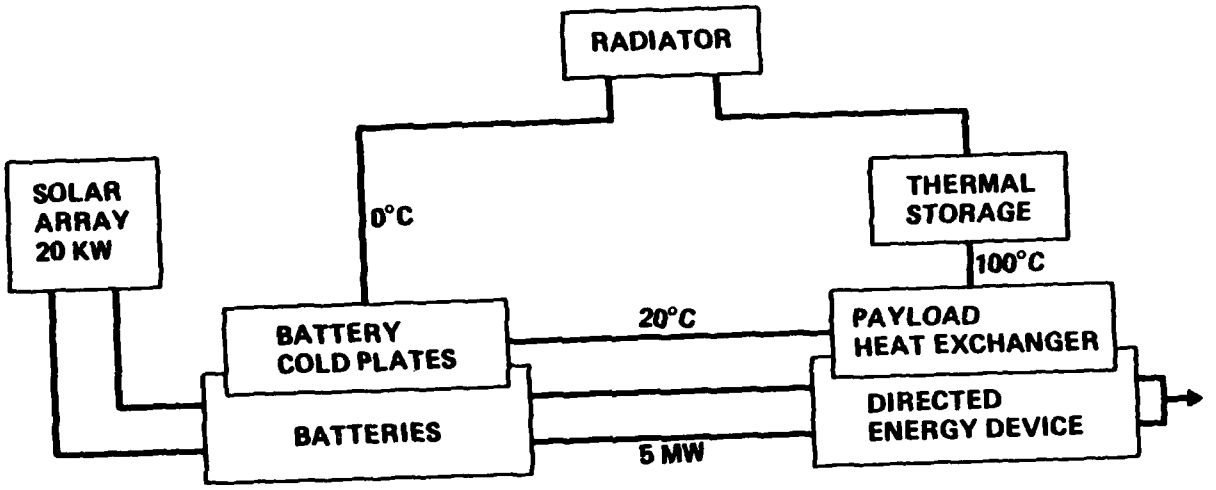

MISSION: 5 MW TO DEVICE AT 20% DUTY CYCLE FOR 15 MINUTES
REUSE AFTER 24 HOURS (20 TIMES)

CONFIGURATION: SOLAR ARRAY (SEPS), 55 W/KG
BATTERIES (NiH_2) 35 W-HRS/KG
RADIATOR (HEAT PIPE), .5 KW/m^2 AT T_{AVG} = 50°C
THERMAL STORAGE (GLAUBERS SALT), 58 W-HRS/KG
AT T_{MELT} = 50°C

ASSUMPTIONS: BATTERY TEMP HELD CONSTANT (NOT A HEAT SINK)
THERMAL MASS OF DEVICE IS NEGLIGIBLE
CONVERSION EFFICIENCY – BATTERIES 80%
– DEVICE 20%

X-1-27

The radiator/thermal storage system is the lightest for the assumed mission. As expected, a radiator without storage is large and heavy since the rejection rate is then 1 MW. An expendable is somewhat heavier than the preferred system, but would be lighter if the total energy requirement was reduced, for example, 10 system reuses instead of 20. The advantages of a two phase coolant loop are also apparent with a reduction in fluid flow rate of ~75%. It is important to note the significance of the thermal control system (TCS) even for this relatively modest power application. The TCS weight is over 40% of the total weight.

THERMAL DESIGN TRADES

SIZING

BATTERY – 5 MW X .2 X 15 MIN/60 = 250 KW-HRS

DEVICE – 5 MW X .2 = 1 MW (AVG. POWER DURING USE)
5 MW X .2 X 15/60 X 24 = 10.4 KW (MISSION AVG.) } ≈ 100/1 PEAK/AVG

LOOP FLOW RATES

- CIRCULATING WATER GLYCOL, 11,000 Kg/HR
- TWO PHASE AMMONIA 2,920 Kg/HR

SYSTEM WEIGHT (Kg)

	EXPENDABLE COOLANT (WATER)	RADIATOR (NO THERMAL STORAGE)	RADIATOR WITH THERMAL STORAGE
SOLAR ARRAY	360	360	360
BATTERIES	7150	7150	7150
EXPENDABLE (+ 10% TANKAGE)	8500	0	0
THERMAL STORAGE (PCM + 20%)	0	0	5160
RADIATOR	0	10,800	110
TOTAL SYSTEM WT	16,010	18,310	12,780

X-1-29

GRUMMAN

The sample problem illustrates that there is no "one best" thermal system that should be developed for high power applications; the selection is dependent on the mission. Expendables will be feasible for some applications and certainly advanced thermal storage systems will be used to satisfy high pulse/average power requirements. Probably the most important thermal parameter for any system is the heat rejection temperature. For example, a low rejection temperature to optimize Brayton cycle efficiency might be an illusionary advantage because of the very large radiator required. This application motivates research in very light radiator concepts to offset this penalty.

X-1-30

OBSERVATIONS

THERMAL MANAGEMENT SYSTEM SELECTION IS TOTALLY DEPENDENT ON MISSION SCENARIO

- PULSE/AVERAGE POWER
- TOTAL ENERGY
- *HEAT REJECTION TEMPERATURE*

GENERAL TRENDS

- EXPENDABLES FEASIBLE FOR LOW TOTAL ENERGY REGARDLESS OF PEAK POWER
- HIGH PULSE/AVG POWER FAVORS THERMAL STORAGE
- HIGH REJECTION TEMPERATURE GREATLY REDUCES RADIATOR SIZE
  - NUCLEAR/THERMIONIC AT T_{rad} = 500°C AREA = 580 ft^2/Mw
  - NUCLEAR/BRAYTON AT T_{rad} = 200°C AREA = 4170 ft^2/Mw

X-1-31

Thermal management system improvements are definitely indicated to meet the requirements of large pulsed power systems. Research can be directed in four generic technology areas to support various mission scenarios. A common theme is two phase heat transfer to reduce flow rates and improve heat transfer coefficients. Because of the problems associated with collecting condensate or solidified pellets in zero-g it is expected that many new concepts will require flight testing. Low cost Shuttle cargo-bay experiments are assumed to be a first step.

THERMAL DESIGN ISSUES IDENTIFIED

SOLAR ARRAYS

- CONCENTRATORS OR THERMOVOLTAICS REDUCE VULNERABILITY TO DIRECT ENERGY WEAPONS BUT REQUIRE INNOVATIVE THERMAL DESIGN.

POWER SYSTEM TEMPERATURE CONTROL

- TWO PHASE LOOP REDUCES WEIGHT AND PUMP POWER AND IMPROVES TEMPERATURE CONTROL OF POWER SYSTEM COMPONENTS BY DIRECT EVAPORATION AND CONDENSATION AT COMPONENT SURFACE. ADVANCED FLUID COLLECTION SYSTEMS WILL BE REQUIRED. ZERO-g FLIGHT TESTS ARE INDICATED

THERMAL STORAGE

- COULD BECOME A PACING ITEM FOR LARGE PULSED SYSTEMS. CURRENT TECHNOLOGY (CONDUCTION INTO SOLID BLOCK) NOT ADEQUATE. DIRECT CONTACT HEAT EXCHANGE STORAGE SYSTEMS (PARTICLES OR DROPLETS) SHOULD BE DEVELOPED.

HEAT REJECTION

- ADVANCED HEAT PIPE RADIATORS ARE SURVIVABLE. WEIGHT AND SIZE ACCEPTABLE FOR NEAR AND INTERMEDIATE TERM REQUIREMENTS. OTHER CONCEPTS SUCH AS LIQUID DROPLET RADIATORS NEED CONTINUING R&D TO DETERMINE FEASIBILITY FOR FUTURE VERY HIGH POWER APPLICATIONS.

X-1-33

GRUMMAN

SUGGESTED THERMAL MANAGEMENT R & D PROGRAMS

SOLAR ARRAYS

- THERMAL OPTIMIZATION OF CONCENTRATING ARRAYS
- THERMAL DESIGN OF THERMOVOLTAIC SYSTEM

POWER SYSTEM COOLING/HEAT TRANSPORT

- INTEGRATION OF POWER SYSTEM (s) WITH TWO-PHASE LOOP

THERMAL STORAGE

- DEFINITION OF THERMAL STORAGE MATERIALS, DIRECT CONTACT HEAT EXCHANGER CONFIGURATION AND INTEGRATION WITH TWO-PHASE LOOP

HEAT REJECTION

- ADVANCED HEAT PIPE RADIATORS
- ADVANCED CONCEPTS (FLUID DROPLET, MOVING BELTS, ETC)

Q & A - R. Haslett

From: M. Cooper, Westinghouse

What is the maximum operating temperature of the flat plate, variable conductance heat pipes? What is the working fluid and heat capacity per unit?

A.

Fluid is methanol. Nominal operation is for electronics i.e. around room temperature (0 to 50° C). Capacity is not limited by heat pipe performance but by surface area (radiator)

From: G. Parker, Westinghouse

Do not agree with your statement that Brayton systems "always optimize at low heat rejection" (200° C). Optimize with respect to what? Certainly not system size and probably not on system weight. For MW(e) level systems, Brayton systems in space will give up some efficiency-yes-by rejecting heat at higher temp's. But this will be an acceptable price to pay to get a reasonably sized radiator.

A.

I was referring to Thermal Cycle efficiency which requires rejecting at lowest possible temp. I certainly agree with your comment that a "real" optimization (either size or weight) will not necessarily result in a 200° C Brayton or 300° C or any other specific temp. My only point was that the radiator (or whatever heat-ejection system) is such a large part of the total weight that it must be accounted for in even very preliminary system trades.

From: P. J. Turchi, R & D Associates

Please comment on low temperature heat removal from circuit components and system costs of refrigerators.

A.

Refrigerators can be applicable to boost reject temp. providing the cost of power is cheap enough. Systems trades are necessary but large nuclear power systems might make for effective use of refrigerators.

References

1) Cohen, M., Fornoles, E. and Mahefkey, T., "Requirements and Technology Trends for Future Military Space Power Systems", presented at the 1981 Intersociety Energy Conversion Engineering Conference, Atlanta, GA., August 9-14, 1981.

2) Alario, J., Edelstein, F. and Haslett, R., "Radiator Concepts For Future Space Systems", presented at the AIAA Conference on Large Space Platforms: Future Needs and Capabilities (AIAA Paper 78-1677), Los Angeles, California, 27-29 September 1978.

3) Alario, J., and Haslett, R., "Modular Heat Pipe Radiators for Enhanced Shuttle Mission Capabilities", presented at the 9th Intersociety Conference on Environmental Systems, San Francisco, California, July 16-19, 1979 (ASME Paper No. 79-ENAs-17)

4) Edelstein, F., "Transverse Flat Plate Heat Pipe Experiment," presented at the 3rd International Heat Pipe Conference (Paper No. 78-429), Palo Alto, California, 22-24 May 1978.

5) Edelstein, F. and Flieger, H., "Satellite Battery Temperature Control", presented at the 3rd International Heat Pipe Conference (Paper No. 78-448) Palo Alto, California, 22-24 May 1978.

6) Edelstein, F., "A 2.2 Sq. M. (24 Sq. Ft.) Self-Controlled Deployable Heat Pipe Radiator - Design and Test", ASME Paper No. 75-ENAs-43, presented at the Intersociety Conference on Environmental Systems, San Francisco, California, 21-24 July 1975.

7) Harwell, W., Haslett, R., and Ollendorf, S., "Instrument Canister Thermal Control", AIAA Paper 77-761, presented at the AIAA 12th Thermophysics Conference, Albuquerque, New Mexico, 27-29 June 1977.

8) Harwell, W. and Ollendorf, S., "The Heat Pipe Thermal Canister", presented at the 15th Thermophysics Conference, July 14-16, 1980, Snowmass, Colorado (AIAA 80-1461)

9) Harwell, W., Haslett, R., and Ollendorf, S., "Thermal Canisters for the Instrument Pointing System (IPS)", presented at the IV International Heat Pipe Conference, Sept. 7-9, 1981, London, England.

10) Alario, J. and Haslett, R., "Active Heat Exchange - System Development for Latent Heat Thermal Energy Storage", presented at the DOE Thermal and Chemical Storage Annual Contractor's Review Meeting, McLean, Virginia, 14-16 October 1980.

11) Alario, J., Haslett, R., and Kosson, R., "The Monogroove High Performance Heat Pipe", presented at the AIAA 16th Thermophysics Conference, June 23-25, 1981, Palo Alto, California (AIAA 81-1156)

THE LIQUID DROPLET RADIATOR

A.T. Mattick, A. Hertzberg,

University of Washington, Seattle, WA

and R. Taussig,

Mathematical Sciences Northwest, Inc., Bellevue, WA

Abstract

A new type of radiator will be discussed which uses a recirculating stream of liquid droplets as a radiating element in place of the solid surfaces used in conventional tube and fin radiators for space. By virtue of the large surface to volume ratio of small droplets the liquid droplet radiator (LDR) has the potential of being many times lighter than the lightest solid surface radiators yet developed (heat pipes). In addition the LDR may be much more simply and economically deployed since the radiating element is transported as a liquid. Preliminary studies of the physics and engineering of the LDR have not revealed any exceptional obstacles to development of a practical LDR based on existing technology. Generation of droplets ($\lesssim$100μm diameter) may utilize the methods developed for ink-jet printing, and collection devices using rotation to simulate gravity appear workable. Liquids have been identified which have low enough vapor pressures that evaporation losses over durations of tens of years are tolerable. Liquid tin is best for heat rejection between 500°K and 1000°K, tin eutectics between 370°K and 600°K, and silicone oils between 260°K and 400°K. These span a temperature range for virtually any heat rejection requirement in space. Moreover, the LDR is scalable over a wide thermal power range (10^3-10^9W, depending on the liquid) and is virtually immune from permanent damage due to micrometeoroids. Several applications, including thermal engines, active cooling of photovoltaic cells, and refrigeration have been investigated. Emphasized in this paper is the need for lightweight structures and fluid-handling components for an LDR system, to take best advantage of the low mass of the droplet sheet itself.

FIGURE EXPLANATIONS

Figure 1 illustrates how the liquid droplet radiator (LDR) could be deployed on a solar power satellite. Waste heat from the power cycle on one module is transferred to the radiator liquid which is then projected toward the second module. After radiating energy the cooled droplets are collected, reheated, and sent back to the first module to complete the loop. The droplets form a thin sheet, edge-on to the sun, to minimize solar absorption.

Figure 2 shows a LDR deployment scheme for a nuclear thermoelectric power cycle in space. The heated liquid is fed to the droplet generator along a pipe which also serves as a support boom for the power conditioning and transmitting equipment.

Figure 3 indicates the method of droplet generation. Jets of liquid emerge from a pressurized plenum through small ($\lesssim$100μm) orifices. These jets break up into droplets via surface tension instability. A vibrator can be used to perturb the emerging streams at a desired frequency to assure uniformly sized and spaced droplets. This technique has been successfully used for ink jet printing, which requires very accurately directed streams of droplets in the 30-100μm diameter range.

Figure 4 shows photographs of mercury droplet streams generated at the University of Washington. Conditions are identical for streams A and B, except stream B is driven acoustically at 9 kHz by a piezoelectric element. This dramatically improves droplet uniformity. Studies of droplet generation, collection, splashing, and collisions are underway at the authors laboratory to identify suitable technologies and potential problems of manipulating droplets in a droplet radiator.

Figure 5 illustrates a means of collecting the droplet streams in space. The collector is essentially a rotating drum to produce an artificial g-field. The collected liquid migrates to the periphery where it is effectively pressurized by centrifugal accelleration, and collected by scoops for transfer to a heat exchanger.

Figure 6 shows the operating temperature ranges and figures of merit (proportional to power/mass) of candidate liquids for the LDR. The lower temperature corresponds to either the freezing point or high viscosity limit, and the upper temperature to an evaporation rate that would yield a mass loss of 0.03 kg/m^2-year. (By comparison the lightest heat pipe radiators weigh 5-10 kg/m^2.) The oils KEL-F and Dow 705 are excellent because of their light weight and high potential emissivity, but have excessive vapor pressures above 300-400°K. Gallium and indium would also be excellent materials, except they are probably too expensive to be practical.

Figure 7 compares the masses of the radiating surfaces (neglecting fluid-handling components) of the LDR and heat pipe radiators for a radiated power of 7.7 MW. The LDR uses liquid tin droplets having emissivity ε_o=0.1. As indicated, the LDR droplet sheet mass is proportional to droplet radius and can be made arbitrarily small, subject only to the difficulty of producing small droplets.

Figure 8 illustrates the mass breakdown for a liquid tin LDR system, and for a heat pipe radiator system, both performing the same heat rejection function for a potassium Rankine cycle. The LDR components are: droplet sheet (DS), droplet generator(G), collector(C), heat exchanger (HX), and pump (P). The heat pipe radiator includes: heat pipes (HP), manifolds (M), through-pipes (TP), and potassium inventory for the radiator section (K). This heat pipe radiator was designed by Boeing to reject heat at 930°K from the Rankine cycle. The mass of tin is accounted for in each LDR component and, in fact, dominates the mass of each component. Although this breakdown for the LDR is speculative, it indicates that to realize the low mass potential, structures and fluid-handling components must be designed to emphasize the low mass of the radiating element (droplet sheet) itself.

Figure 9 shows a rotating-boom LDR configuration which creates a very large radiating surface compared to the linear configuration for equal sized generation and collection components. The droplets are ejected on radial trajectories which by virtue of the rotation of the system as a whole, results in a spiral sheet pattern. This configuration is especially suitable for compact energy sources such as nuclear reactors.

Figure 10 depicts a lightweight structure that would be appropriate for deploying the droplet generator or collector for an LDR. The liquid could be fed to a generator in a pipe along the structure, with the droplet stream passing down the axis to a collector at the power-generation end. This structure can be made very light and can have a stowed length 1/20-1/50 of the deployed length, and is thus ideal for transport by the space shuttle, for example.

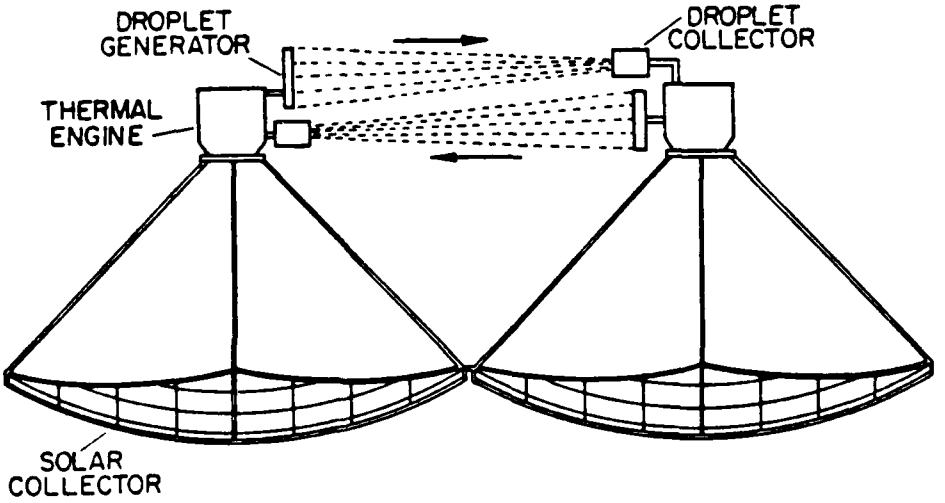

Solar thermal power satellite using the liquid droplet radiator.

FIGURE 1

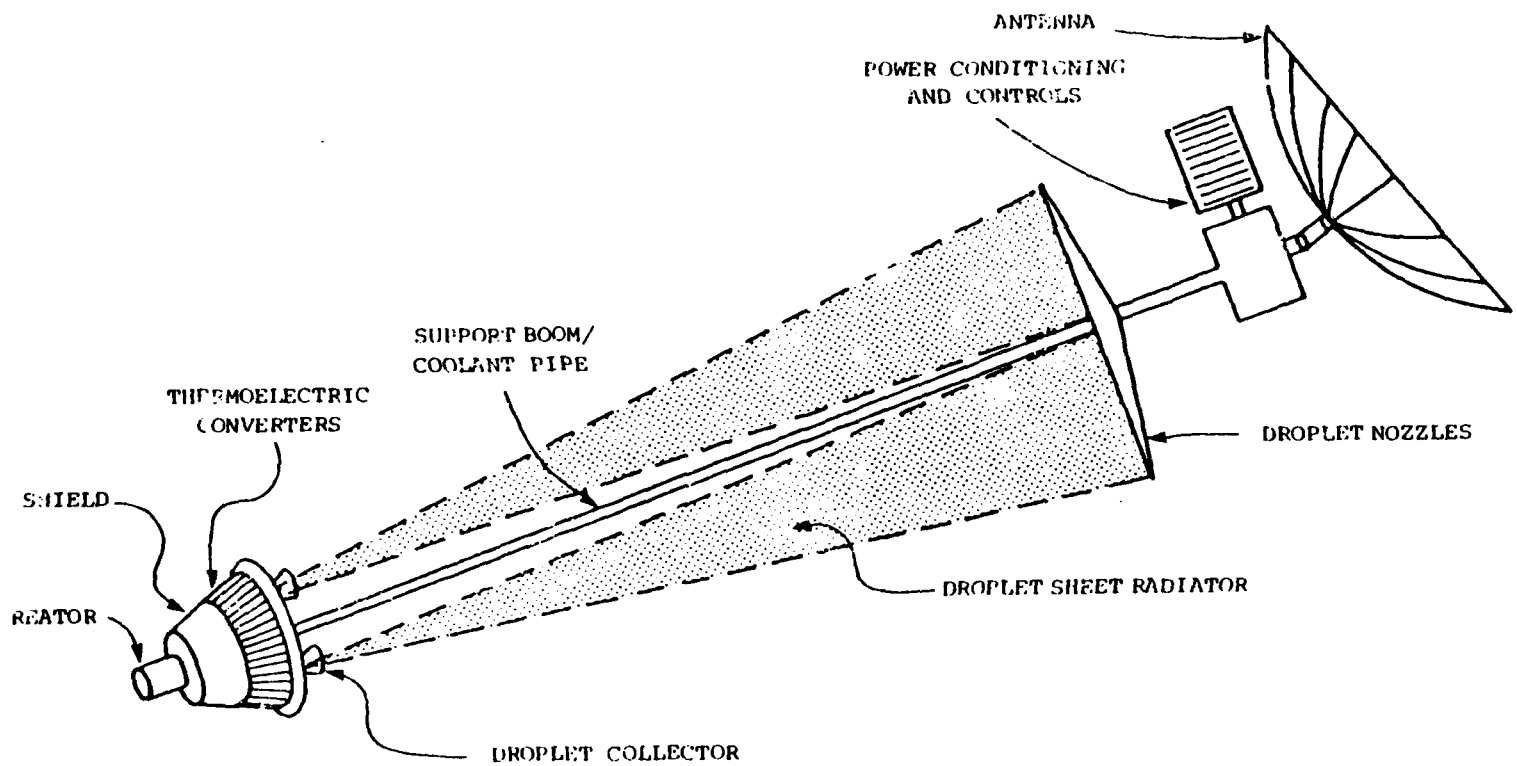
ANTENNA
POWER CONDITIONING
AND CONTROLS
SUPPORT BOOM/
COOLANT PIPE
THERMOELECTRIC
CONVERTERS
SHIELD
REATOR
DROPLET NOZZLES
DROPLET SHEET RADIATOR
DROPLET COLLECTOR
81 05717

X-2-5

FIGURE 2

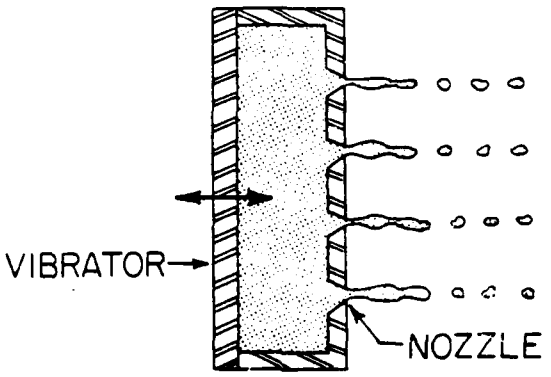

DROPLET GENERATOR

FIGURE 3

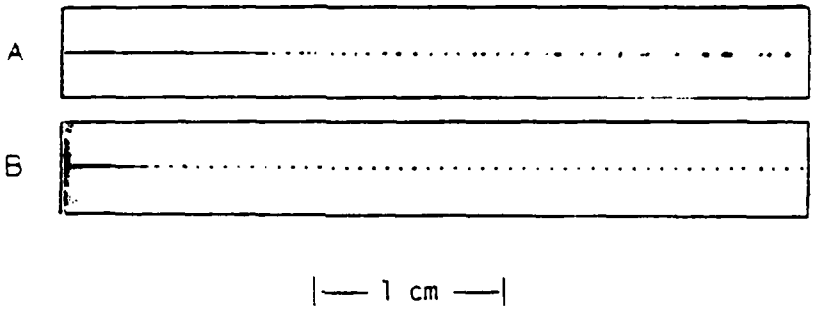

Mercury droplet streams produced a) without vibration, and b) with acoustic drive of 9 kHz. Droplet diameter ≈ 200μm.

FIGURE 4

(a) Collector Cross-Section

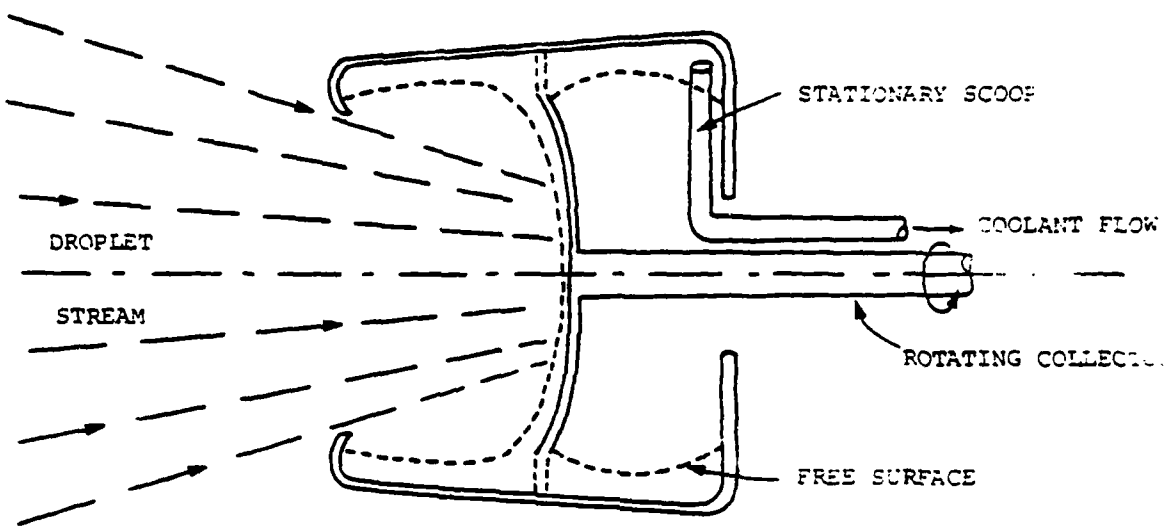

(b) Side View of Scoop

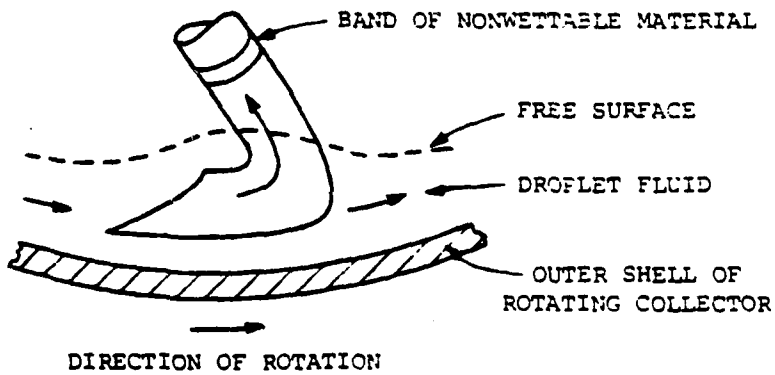

81 05827

Rotating Droplet Collector with Shell Mass Characteristics and Nonrotating Seal.

FIGURE 5

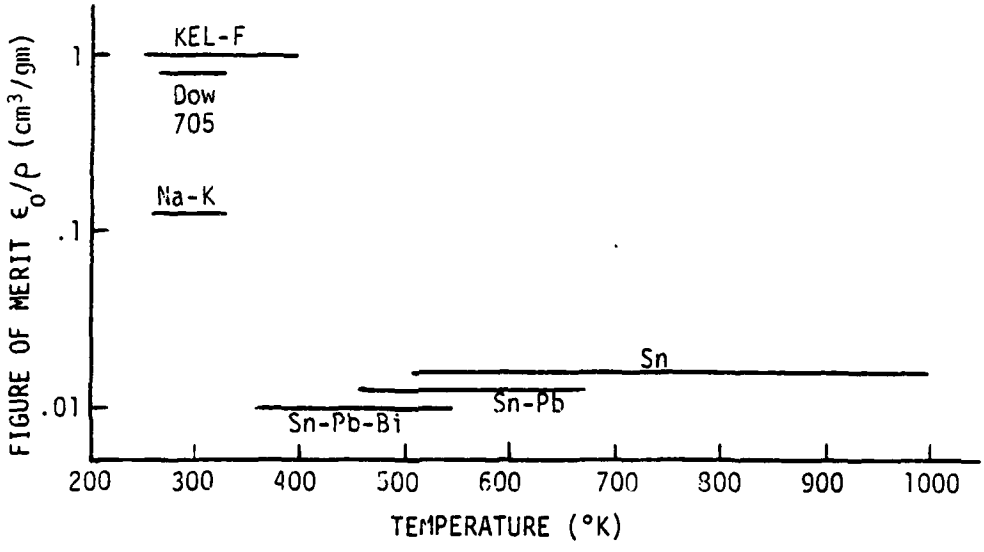

Temperature ranges of candidate radiator fluids. Figure of merit ~ power/mass. [KEL-F is chlorotrifluoroethylene; Dow 705 is pentaphenyltrimethyltrisiloxane]

FIGURE 6

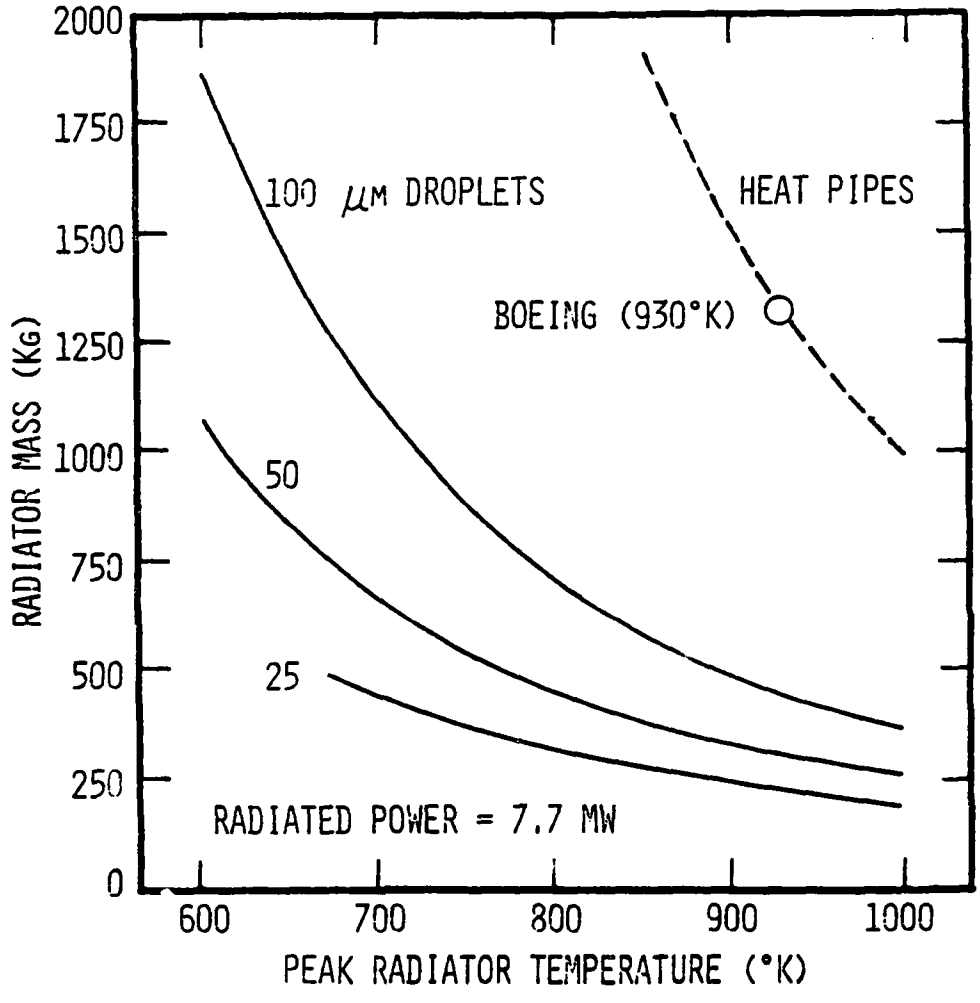
2000
1750
1500
1250
1000
750
500
250
0
RADIATOR MASS (KG)
100 μM DROPLETS
HEAT PIPES
BOEING (930°K)
50
25
RADIATED POWER = 7.7 MW
600
700
800
900
1000
PEAK RADIATOR TEMPERATURE (°K)

FIGURE 7

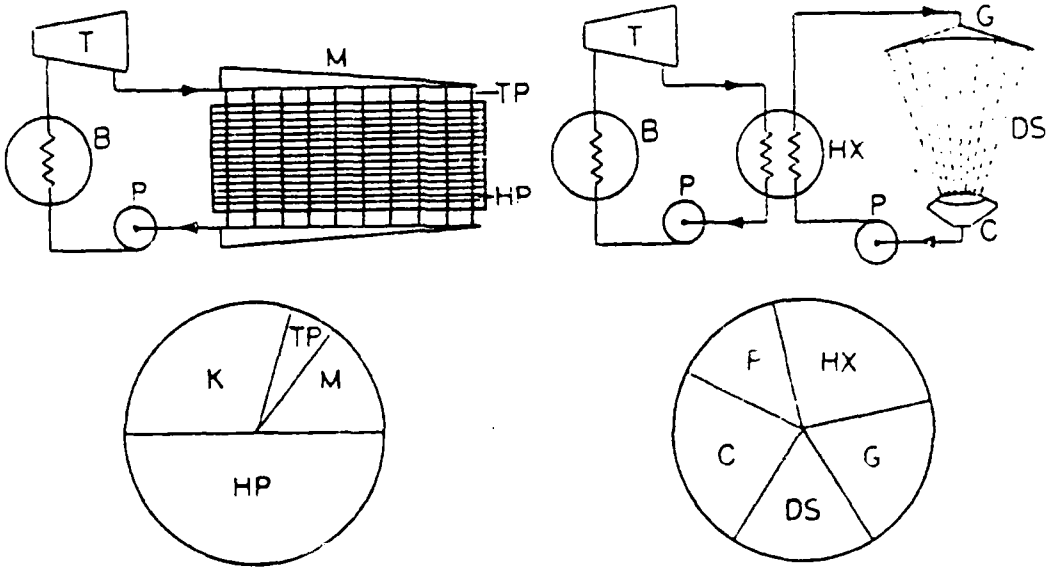

Comparison of heat pipe and droplet radiators for a Rankine cycle.

FIGURE 8

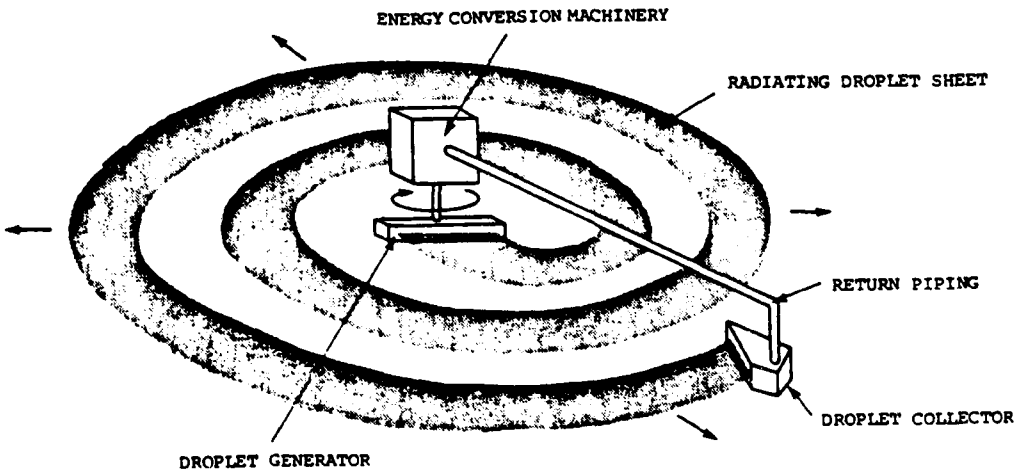

Rotating boom droplet radiator.

FIGURE 9

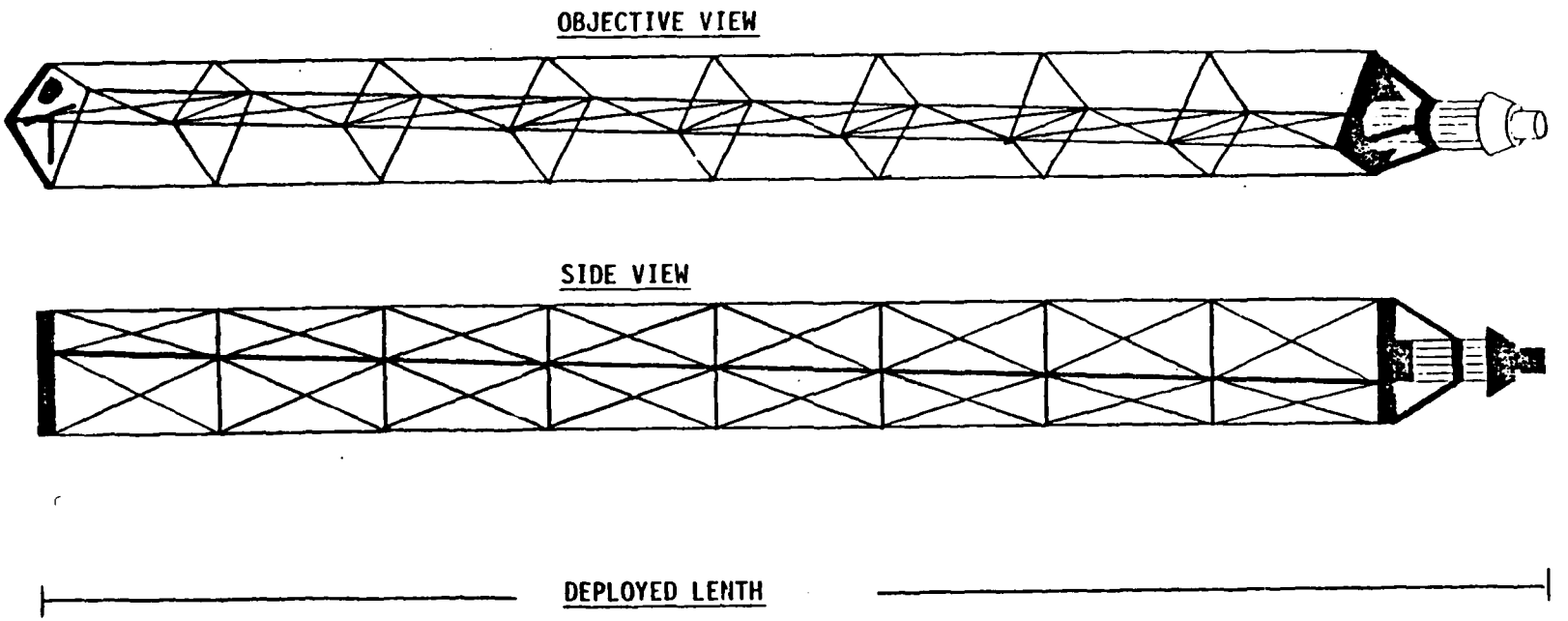

X-2-13

SPACE POWER SATELLITE DEPLOYED CONFIGURATION

FIGURE 10

Q & A - A. T. Mattick

From: H. Brandhorst, NASA Lewis Research Center

Droplet charging and collisions appear to be magnetic loss mechanisms in the liquid drop radiator. Would you comment on magnitude of the problem and solutions. What's the effect of the earth's magnetic field @ tin?

From: P. J. Turchi, R & D Associates

Please comment on interactions of droplet flow/cloud with space plasma, magnetic field, EM fluctuations and induced currents.

A.

We have begun to study the problem of droplet charge accumulation and the effect on droplet trajectories. Assuming an electric field at the surface of a droplet sheet $E \sim \phi/\lambda_D$ ($\phi \sim kT_{elec}$, λ_D = shielding length), and that this field is due to uniform distribution of charge on droplets within the cloud, the accumulated charge would lead to tolerable deflections ($\lesssim$ 10 mrad) for both dense, cool plasmas (up to 1 R_E) and also for tenuous hot plasmas (near geosync. $T_e \sim$ 500ev). Work remains to be done on charge transfer between drops and spacecraft and among drops.

From: Martin Cooper, Westinghouse

How do you handle self-shielding in the liquid droplet radiator as the diameter of the cloud of droplets increases?

From: Steve Wax, AFOSR

Are the system efficiencies you calculated based on the effective radiation from a cloud of drops which is, of course, less than the radiation from the same number of isolated drops?

From: P. J. Turchi, R & D Associates

To what extent do the droplets obscure each other in attempting to radiate. Does the cloud essentially radiate from the total surface or the summation of the droplet areas?

A.

We have analyzed the radiative properties of the droplet sheet taking into account the low emissivity of liquid

metals and the finite view factor of drops. The result for liquid metals is that the mass/power is 10-15 times as great as for isolated "black" droplets. The LDR can still be for lighter than a heat pipe radiator ($\varepsilon \sim .7$ typically) for droplets $\gtrsim$ 100μm diameter.

From: E. Walbridge, Argonne National Laboratory

1) Is it not the case that a missile-penetrating laser pulse scoring a direct "hit" on the liquid droplet stream would "kill" the entire system?

2) As a % of rejected (heat) energy, how much energy is needed to create the droplet surfaces?

A.

1) It might evaporate the liquid in space during the hit. But the system could easily be restored with new fluid. We are currently exploring the use of a droplet sheath to protect satellites against such beams.

2) Surface tension energy (even for liquid metals with $\alpha \sim 500$ d(cm) is not important unless droplets on the order of 1μm diameter are used.

From: M. Cooper, Westinghouse

What is the projected life of a liquid tin liquid drop radiator at 1400° K considering losses because of evaporation?

A.

$\simeq$ 1 day for liquid tin (30 years at 1000° K)

From: C. Badcock, Aerospace

Do all droplets remain in the system? Any loss would pose severe contamination problems.

From: Robert Barthelemy, USAF

What are the estimated losses of your "liquid" to space in a practical system? (say for 10 Kw system over 1 year) not just vapor pressure losses)

A.

No estimates of droplet loss due to droplet collisions or misdirection of jets have yet been made. Only solutions to contamination due to these loss mechanisms appear to be the use of bottles or the enclosure of the droplet cloud by a very thick transparent sheet.

THE LIQUID DROPLET HEAT EXCHANGER

A.P. Bruckner
University of Washington
Seattle, WA 98195

Direct contact heat exchange between a gas and a molten metal dispersed into droplets offers an attractive new approach to increasing the efficiency and decreasing the specific weight of thermal power cycles for space applications. The ability of a droplet heat exchanger to transfer heat directly from a liquid metal to a working gas over a wide temperature range circumvents many of the material limitations of conventional tube-type heat exchangers and does away with complicated plumbing systems and their tendency toward single point failure. Droplet heat exchangers offer large surface to volume ratios in a compact geometry, very low pressure drop, and high effectiveness.

In the simplest configuration the molten material is sprayed axially through a counterflowing, high pressure inert working gas in an insulated cylindrical chamber. The droplets transfer heat directly to the gas by convection as they traverse the heat exchanger and are subsequently collected for recycling through the heat source. A number of suitable liquid metals and eutectic alloys having negligibly low vapor pressures in the temperature range of 350-1300°K have been identified. Experimental studies of droplet formation with mercury have demonstrated that near perfect control of droplet size can be easily achieved.

While studies of the droplet heat exchanger have shown it to be very promising for a variety of Earth-based applications, the zero "g" environment of space can lead to entrainment of the droplets in the gas flow. This problem can be circumvented by the application of artificial "g" fields and/or by using the principle of the cyclone dust separator. By configuring the heat exchanger to produce a vortex flow, the droplets can be driven through the swirling gas by the induced centrifugal forces. Since excellent uniformity of droplet size is possible, the separation efficiency of such a cyclonic heat exchanger can in principle be made nearly perfect.

Heat transfer in a droplet heat exchanger can occur in either direction--i.e., gas can be heated by hot droplets or cold droplets can be used to extract waste heat from a working gas. In the latter case the droplet heat exchanger can be integrated with a droplet space radiator to make a complete heat rejection loop based entirely on the droplet concept.

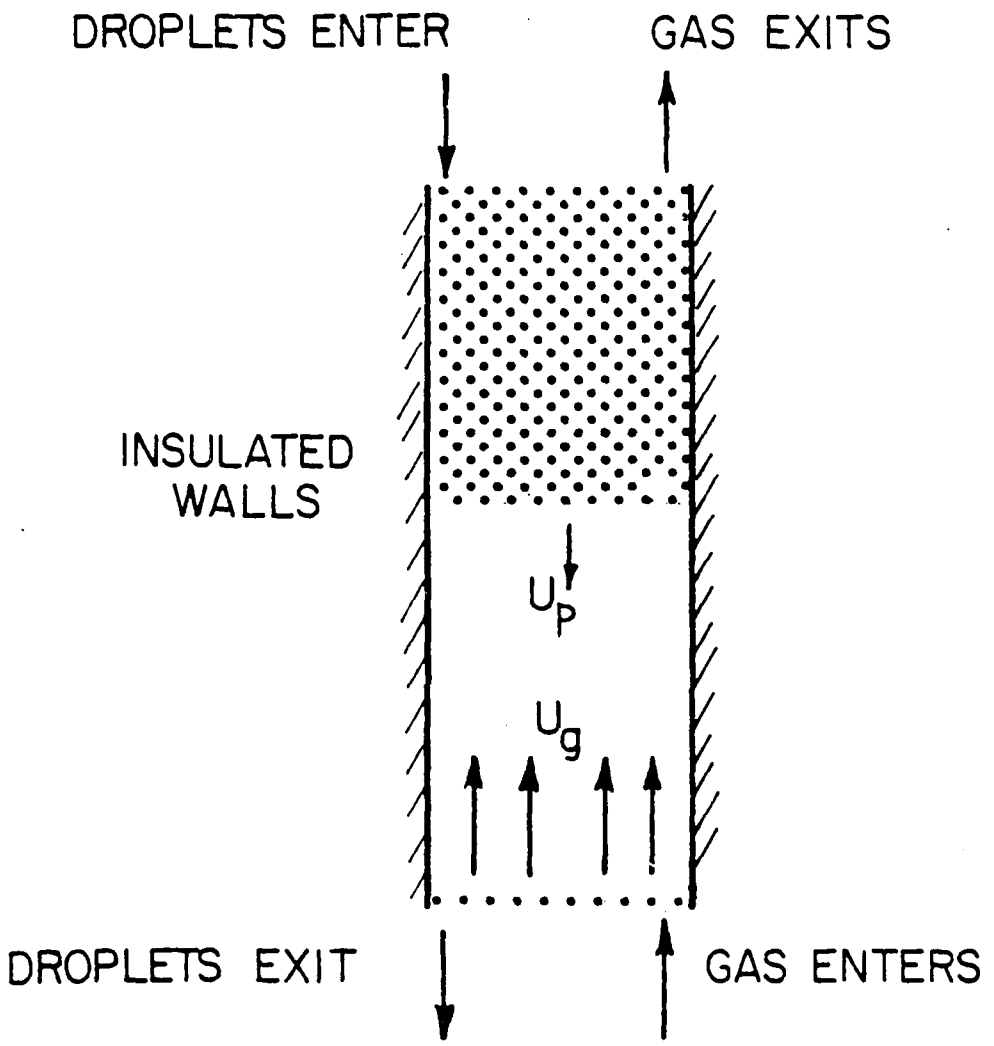

SCHEMATIC OF DROPLET HEAT EXCHANGER CONCEPT

FIG. 2

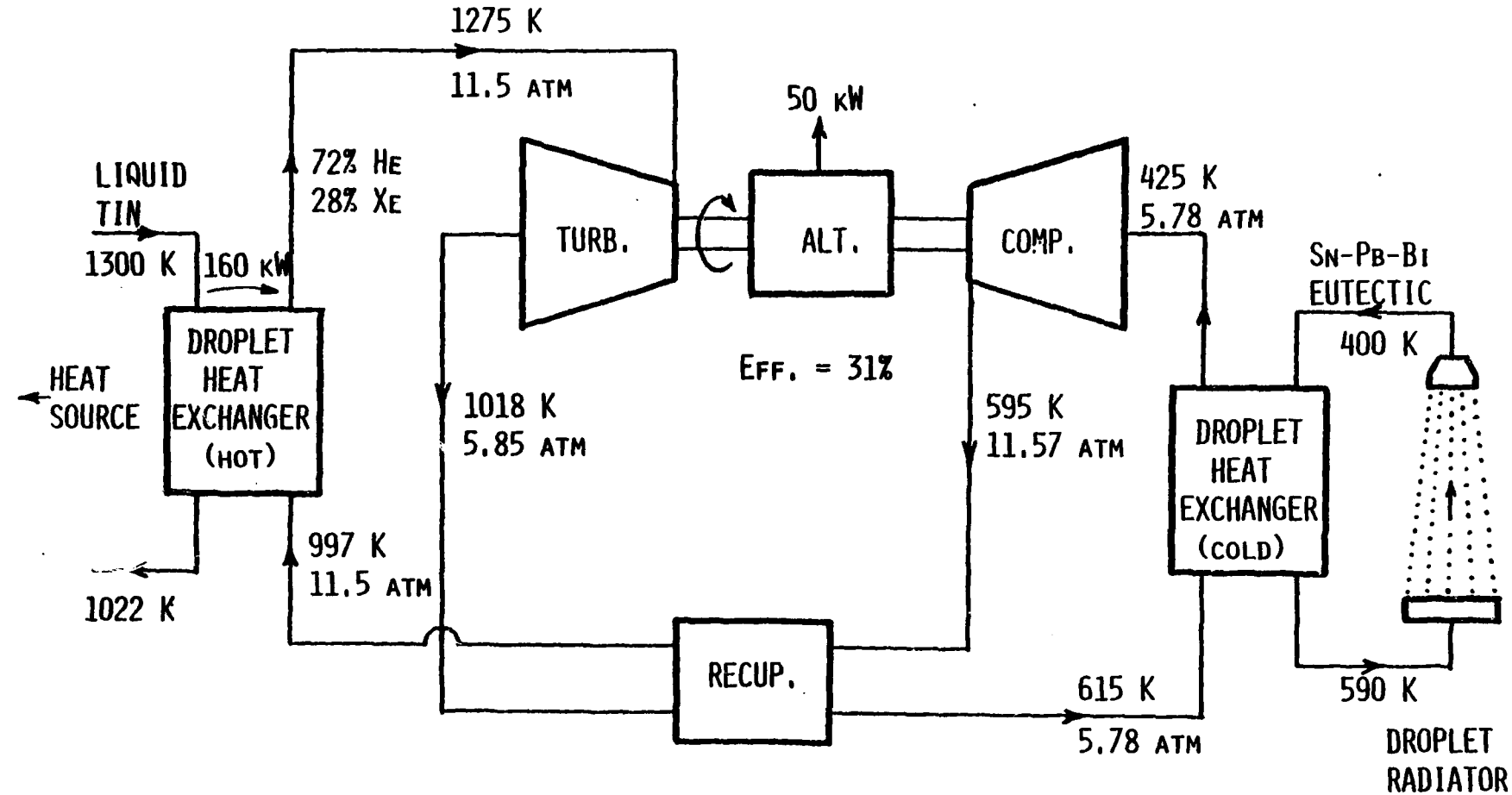

DROPLET HEAT EXCHANGERS IN BRAYTON CYCLE

FIG. 3

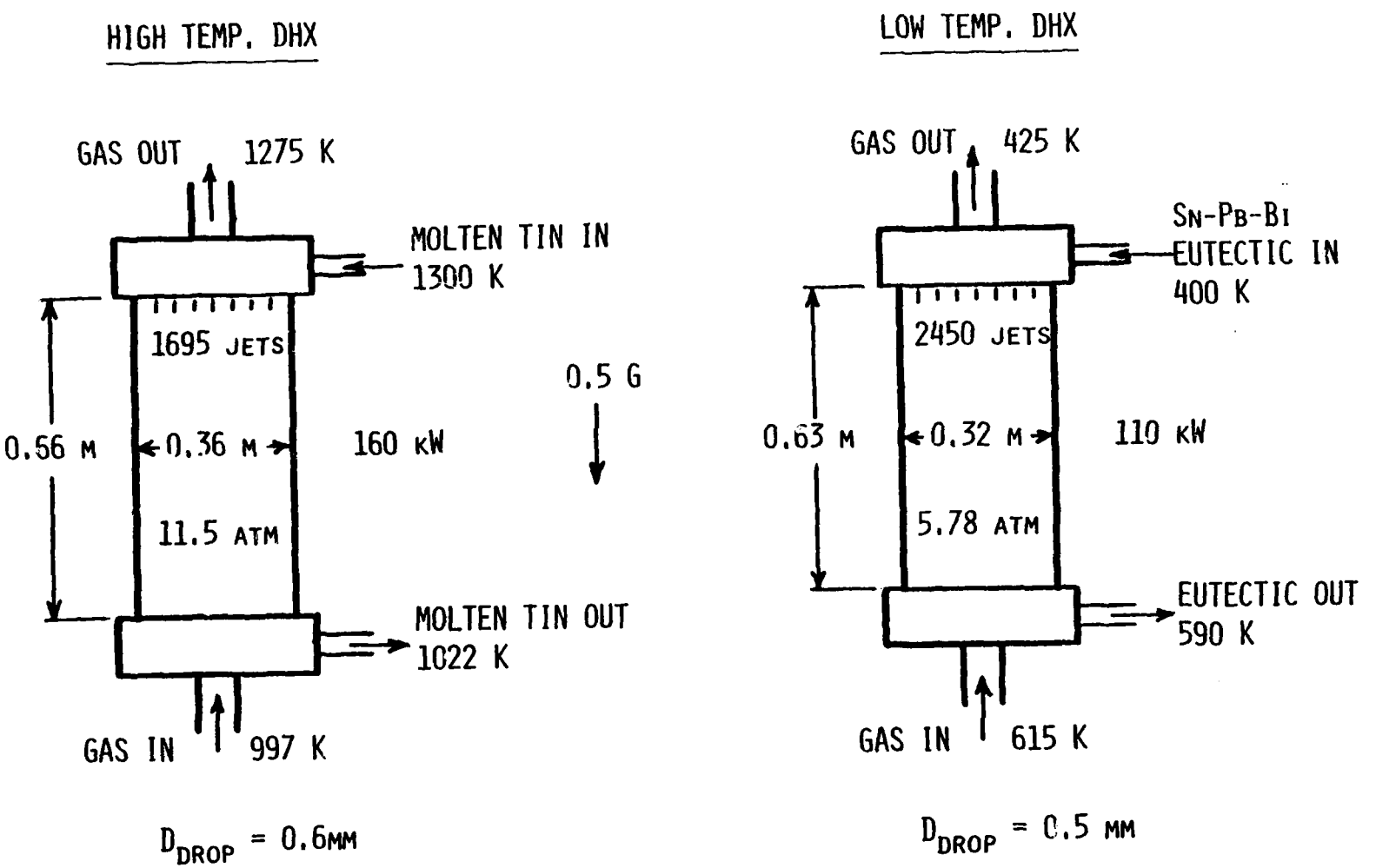

DROPLET HEAT EXCHANGER CONFIGURATIONS
FOR 50 kW BRAYTON CYCLE

FIG. 4

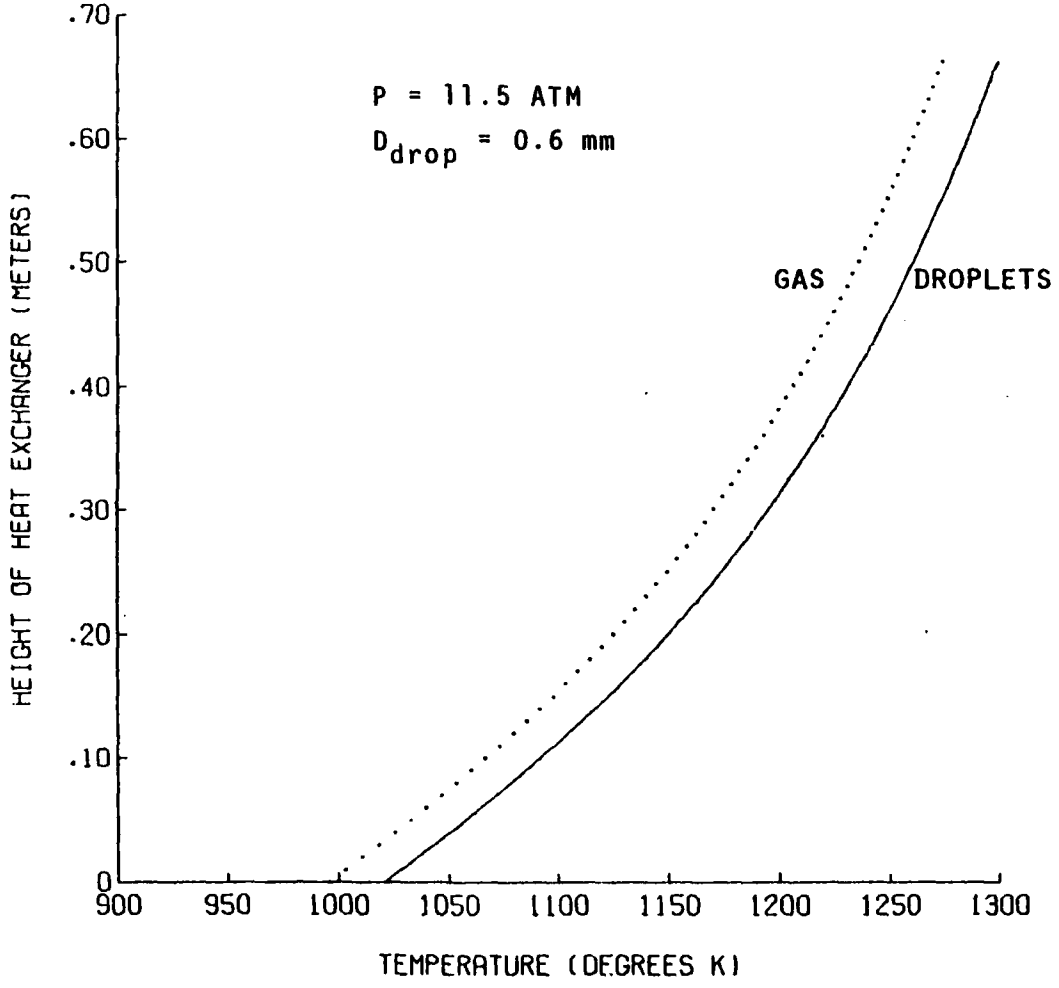

DROPLET HEAT EXCHANGER TEMPERATURE PROFILE
(HIGH TEMP. HEAT EXCHANGER)

FIG. 5

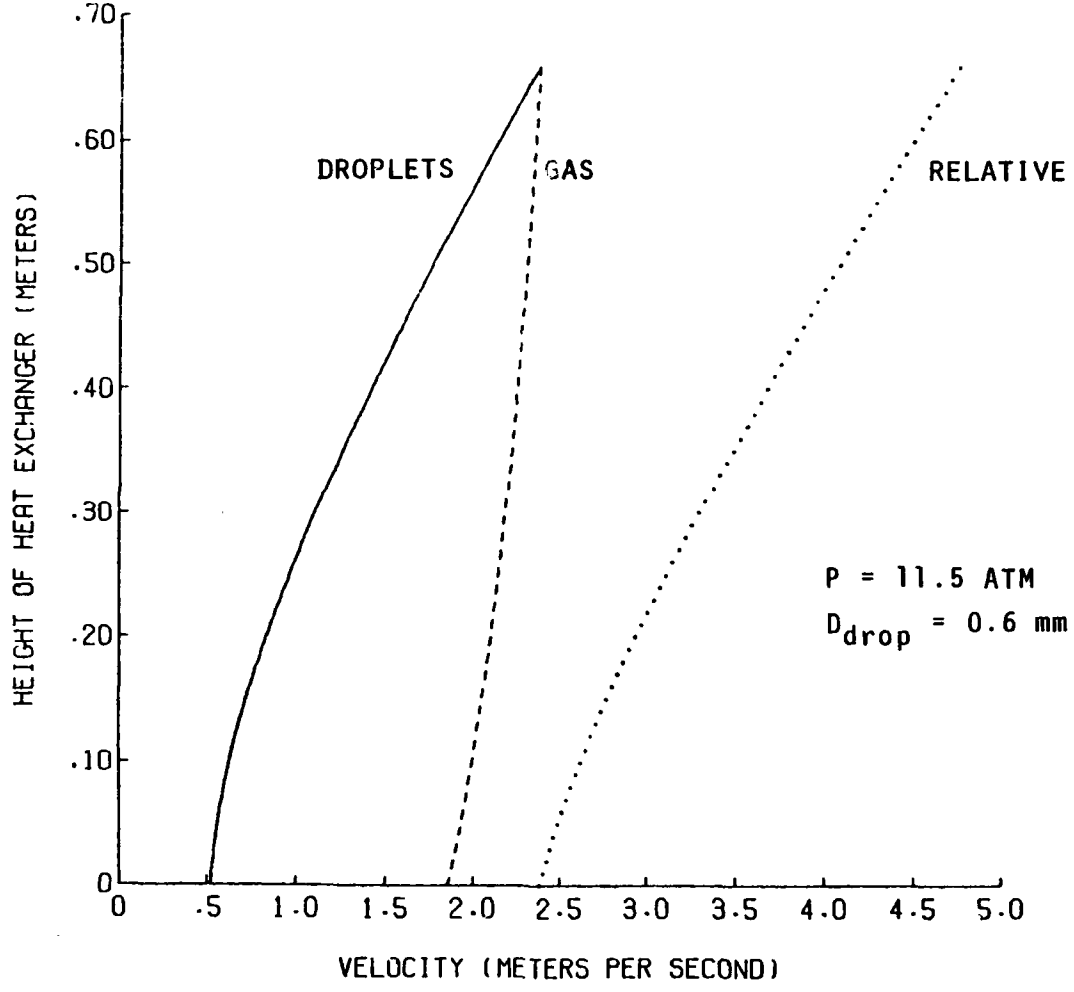

FIG. 6 DROPLET HEAT EXCHANGER VELOCITY PROFILE (HIGH TEMP. HEAT EXCHANGER)

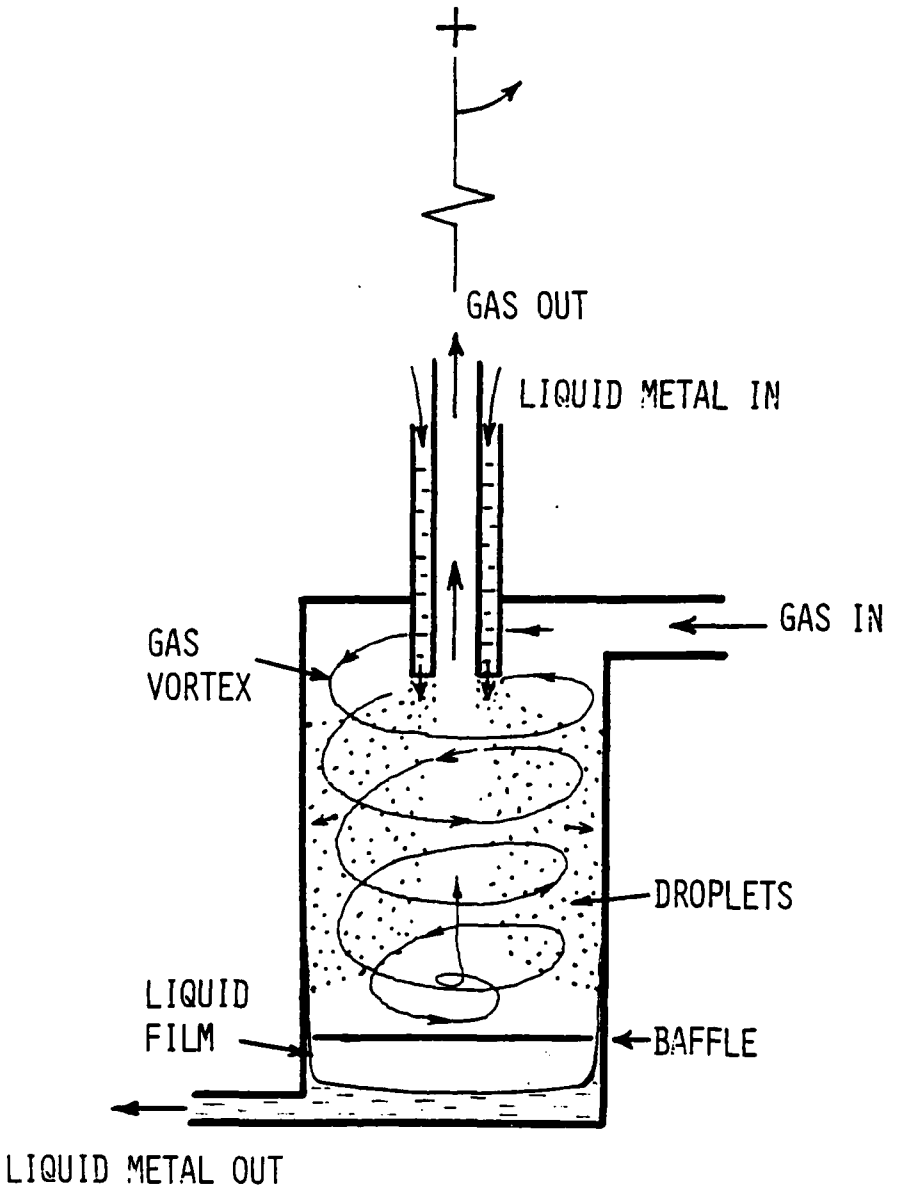

SCHEMATIC OF CYCLONE DROPLET HEAT EXCHANGER

FIG. 7
X-3-6

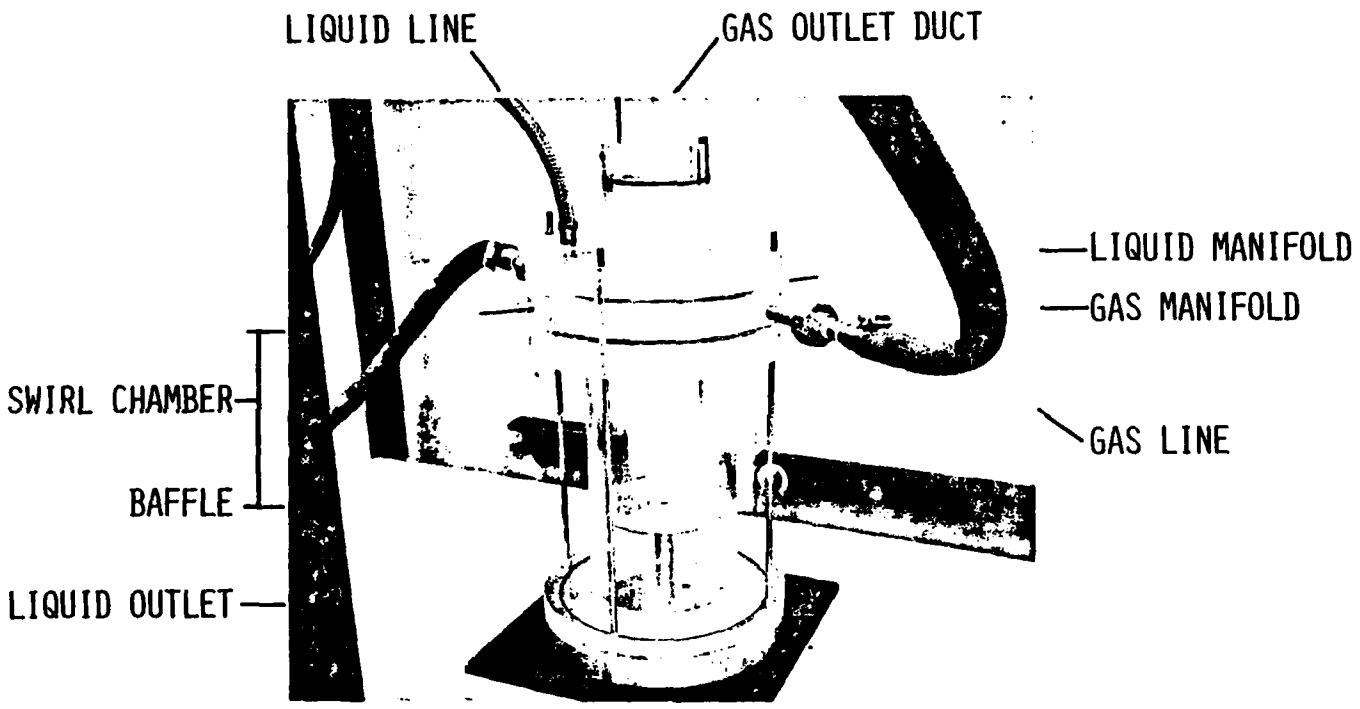

X-3-7

PHOTOGRAPH OF EXPERIMENTAL CYCLONE FACILITY

FIG. 8

DROPLET HEAT EXCHANGERS

- o DIRECT CONTACT HEAT TRANSFER
- o VERY HIGH TEMPERATURE CAPABILITY
- o VERY LARGE SURFACE TO VOLUME RATIO
- o HIGH EFFECTIVENESS
- o VERY LOW PRESSURE DROP
- o SIMPLE CONFIGURATION
- o NON-EXOTIC CERAMICS AND ALLOYS
- o IMMUNE TO SINGLE-POINT FAILURE AND FOULING

FIG. 9

DROPLET HEAT EXCHANGERS
A.P. Bruckner

Fig. 1. (Self explanatory)

Fig. 2. Schematic of Droplet Heat Exchanger Concept

In its simplest form a droplet heat exchanger consists of a column through which two fluids of different phase and temperature simultaneously flow in direct contact and exchange energy by convective, conductive and radiative processes. Heat transfer can occur from either the gas or liquid phase to the other, depending on the heat exchange requirements. Injecting the liquid as a multitude of droplets into the counterflowing gas provides a large heat transfer area. A heat exchanger effectiveness of 0.9-0.95 is attainable in a compact geometry through proper choice of operating parameters. Gas pressure drop through the heat exchanger is very small. For closed cycle inert gas systems operating over the range of 350-1300°K tin and various eutectic alloys of tin are suitable as the droplet materials because of their very low vapor pressures and other desirable properties. Although it is possible to operate the droplet heat exchanger in a zero-"g" environment, droplet entrainment in the gas can occur and thus artificial "g" fields or other means to ensure phase separation are desirable.

Fig. 3. Droplet Heat Exchanger in Brayton Cycle

This figure shows how droplet heat exchangers and a droplet radiator might be integrated into a typical 50 kW space Brayton cycle power plant. The cycle parameters were obtained from a LASL study of power plant elements for future reactor space electric power systems (Ref. 6 in bibliography). They are based on a design developed by AiResearch for DOE (Brayton Isotope Power System). In applying droplet heat exchangers to this particular reference cycle the pressure drops in the heat exchangers were neglected because they are so small. The conventional recuperator was retained, although the possible use of droplet heat exchangers for this purpose is currently under study. Due to the lower pressure drops the cycle efficiency increases from 25% to 31%.

Fig. 4. Droplet Heat Exchanger Configurations for 50 kW Brayton Cycle

This figure shows the geometry of the two droplet heat exchangers in Fig. 3. No attempt at optimization was made. The only criterion was to develop configurations of approximately equal size and compact geometry. Considerable reductions in size appear possible through judicious choice of operating parameters. Gas flow rate is 1.1 kg/sec for both heat exchangers. The liquid metal flow rates are 2.2 kg/sec and 3.7 kg/sec for the hot and cold heat exchangers, respectively.

Fig. 5. Droplet Heat Exchanger Temperature Profile

Fig. 6. Droplet Heat Exchanger Velocity Profile

These two figures show the temperature and velocity profiles in the high temperature heat exchange· based on a one-dimensional flow model (see Refs. 1 and 2 in bibliography). An artificial "g" field of 0.5g is assumed to be set up through rotation of the heat exchanger around a perpendicular axis. The droplet injection velocity and gas exit velocity were chosen to be numerically equal to the droplet terminal velocity in the 0.5g field. The initial velocity of the droplets with respect to the gas is thus twice terminal. Droplets of 0.6 mm dia. result in a compact geometry with a length to diameter ratio of 2.

Fig. 7. Schematic of Cyclone Droplet Heat Exchanger

Cyclone dust separators are commonly used in earth-based industrial plants and power stations to efficiently and inexpensively separate particulates from dust laden gases. The principle of the cyclone can be used in droplet heat exchangers to effect complete separation of the droplets from the gas. The working gas enters the cylindrical chamber tangentially, setting up an inwardly spiralling vortex flow which exits through the central outlet. The liquid metal droplets are injected axially in an annular pattern and are entrained in the swirling flow, acquiring a radially outward velocity component from the resulting centrifugal acceleration. The droplets form a liquid film when they reach the wall. This film can be driven towards the "bottom" of the heat exchanger by, again, rotating the device about a perpendicular axis. In this case very small artificial "g" fields suffice. Other methods of collecting the spent droplet medium which do not require artificial gravity, such as porous sidewalls, are being investigated.

Fig. 8. Photograph of Experimental Cyclone Facility

A small scale transparent (Plexiglas) cyclone has been constructed for experimental studies of gas and droplet dynamics in this type of device. Single or multiple jet injection is possible. Ethylene glycol doped with Rhodamine 6-G, a strongly fluorescent dye, is used as the droplet medium and the swirling two-phase flow field is illuminated with a temporally chopped and spatially expanded argon-ion laser beam. A camera records the flourescing droplet streaks from which droplet velocities and trajectories can be obtained. Gas flow parameters are measured using static pressure taps and pitot tubes.

Fig. 9. (Self explanatory)

Q & A - A. P. Bruckner

From: H. Brandhorst, NASA Lewis Research Center

In countercurrent droplet heat exchanger, will there be a problem with the gas flow causing coalescence of droplets and also causing wall collisions?

A.

Droplet coalescence is not likely to be a problem due to the low volume fraction of droplets ($\sim 10^{-3}$) and low flow velocities. Furthermore, liquid metals have very high surface tension, - thus small droplets would require a greater collision energy than is likely to occur.

Wall collisions are a more likely problem, currently under investigation.

Bibliography

1. D.J. Shaw, A.P. Bruckner and A. Hertzberg, "A New Method of Efficient Heat Transfer and Storage at Very High Temperatures," Proc. 15th Intersociety Energy Conversion Engineering Conference, 1980, pp. 125-132.

2. A.P. Bruckner and A. Hertzberg, "A New Method for High Temperature Solar Thermal Energy Conversion and Storage," Proc. Solar Thermal Test Facilities Users Association Annual Meeting, 1981, pp. 186-198.

3. A.T. Mattick and A. Hertzberg, "Liquid Droplet Radiators for Heat Rejection in Space," J. Energy 5, 387, 1981.

4. J.N. Anno, The Mechanics of Liquid Jets, D.C. Heath & Co., Lexington, MA, 1977.

5. G. Rudinger, "Relaxation in Gas-Particle Flow," in Nonequilibrium Flows, Part I, P.P. Wegener, ed., Marcel Dekker, New York, 1969, pp. 119-161.

6. D. Buden, et al., "Selection of Power Plant Elements for Future Reactor Space Electric Power Systems," Los Alamos Scientific Laboratory Report No. LA-7858, 1979.

7. K. Rietma and C.G. Verver, Cyclones in Industry, Elsevier Publishing Co., Amsterdam, 1961.

THERMACORE

SPACE POWER

THE NEED FOR IMPROVED HEAT PIPE FLUIDS

D. M. ERNST AND G. Y. EASTMAN

THERMACORE, INC.

LANCASTER, PA.

X-4-1

SPECIAL CONFERENCE ON

PRIME POWER FOR HIGH ENERGY SPACE SYSTEMS

FEBRUARY, 1982

Extemporaneous Remarks

Preceding D. M. Ernst's Papers 4 and 5

Session X

Heat pipes are deceptively simple devices. This is borne out by the fact that almost all of the future space systems presented at the Space Prime Power Conference have the heat pipe as an integral part of the design. However, only the organizations involved in actual heat pipe development and testing spoke of the need for improved theoretical understanding and fabricational techniques for enhanced heat pipe performance.

To some the age of the heat pipe has come and gone, to others it is in the future. Paraphrasing Gerry Mullin and the famous Canadian football owner, the future is now. Thanks to Will Ranken and other speakers the ground work for the need for heat pipe research has been laid. The important thing to remember about heat pipes is their applicability to almost all systems discussed at this conference.

Heat pipes are horizontially disposed components in a vertically orientated technology. They can be useful from several degrees Kelvin to 3000 K. Heat pipes can be used for:

- o Cooling semiconductors-power conditioners-transformers and other on board electronic components.
- o Heat removal from nuclear reactors or other heat sources.
- o Heat rejection from energy conversion devices.
- o Thermal management within the spacecraft.

From the rebirth of the heat pipe in 1963, to the shutdown of the U.S. Space Reactor Program in 1972 the heat pipe was an object of curosity and not taken seriously by many. The R&D effort was sporadic and funding sparse. When DOE/NASA initiated work in 1979 on what is now known as SP-100, the heat pipe was an accepted key technology compcnent and development began. What has been missed is some fundamental research on the basic understanding of the heat pipe which is now coming into focus as a result of technology development.

Heat pipe research for advanced space systems should include:

- o Innovative designs including:
  - Unfurlable thin film plastic and/or metal heat pipes for low mass radiators.
  - Space fabricated heat pipes to remove earth constraints on design.
  - New wick concepts for low mass designs.
- o Materials technology including:
  - Carbon/carbon and graphite envelopes for low mass heat pipes.
  - New fluids.
  - New and refined metals and alloys for long life envelopes.
- o Heat transfer problems
  - Evaporation, vapor transport, and condensation in a self pumped closed system in thermal equilibrium.
  - Impurity levels and their effects on heat pipe life performance, erosion/corrosion and mass transfer.
- o Fabrication technology
  - High performance wick structures.

- Integral wick and envelope structures.

- Improved fluid loading and processing.

An example of the capability of thin film evaporation is a test recently carried out at Thermacore in which an excess of 2 kW/cm^2 was dissipated by the evaporation of water in an unpressurized system as compared to the hundreds or thousands of pounds water pressure normally required for forced convective cooling of high heat flux devices.

Today, I want to specifically address the need for new low temperature heat pipe fluid/vessel combinations and improving the understanding of thin film evaporation from a self pumping wick structure.

Before proceeding I would like to address Will Ranken's comment on the need for radiators with a mass less than 0.05 kg/kWt. In the late 1960's, RCA built and tested a 50 kWt radiator for a potassium Rankine system. The individual heat pipes radiated 500 watts @ 1000 K and had a mass of 50 grams, which is 0.1 kg/kWt. Maybe part of the answer to low mass radiators is higher heat rejection temperatures achieved by more efficient energy conversion devices.

THE NEED FOR
IMPROVED HEAT PIPE FLUIDS

D. M. Ernst* - G. Y. Eastman**
Thermacore, Inc.
Lancaster, PA

Abstract

Low mass high performance radiators and thermal management systems need to be developed for advanced space systems. The key to these new/improved thermal systems are high performance heat pipes. One aspect in achieving low mass/high performance heat pipes requires working fluids compatible with low mass materials of construction, such as aluminum, magnesium, beryllium and titanium. The application of heat pipe systems in manned spacecraft also requires the use of low or non-toxic working fluids.

The development of new or improved heat pipe fluid/vessel combinations for advanced space systems should be carried out. Two approaches worthy of investigation are: the synthesis of new high performance fluids compatible with appropriate envelope materials and the development of integral impervious coatings and/or passivation to prevent the reaction of currently acceptable working fluids with the envelope.

Background

Heat pipes have successfully been used on board space systems and are currently being designed as key components in advanced systems. Applications range from the heating (heat removal from the reactor) and cooling of thermoelectric modules (large high temperature radiators) for the SP-100 and cryocoolers for surveillance satellites, to thermal buses and space constructable radiators for large scale thermal utility systems and the cooling of instruments and power components.

These and other heat pipes for space systems applications are in various stages of development. However, since the heat pipe is generally looked upon as a thermal super conductor, the required performance pushes the state-of-the-art of most heat pipe systems. This trend will continue as the system size increases from the current 100 kW_e to 1-10 MW_e continuously operating systems. Accordingly, new ideas need to be continuously generated to improve heat pipe performance.

---

* Vice President and Chief Technical Officer, Thermacore, Inc.
** President, Thermacore, Inc.

There are several factors which control the performance of heat pipes in gravity free space. The most commonly acknowledged one is the liquid transport factor or figure of merit which relates the working fluid's ability to transfer thermal power through a frictionless unit area duct. Closely aligned to the figure of merit is the wick's permeability, which is the unit area friction factor, and capillary radius which generates the liquid pumping pressure.

Need

The ability to fabricate wicks with low permeability and small capillary radii is a strong function of the choice of heat pipe envelope and wick materials and their formability. Likewise the working fluid for a given heat pipe must be compatible with the wick and envelope. Thus there are fluid/envelope combinations which are not currently used, which if implemented could increase the applicability of the heat pipe as would developing new high performance fluids in the 500-800 K range. Several low temperature fluid/envelope combinations not currently useable include water/aluminum, methanol/aluminum, and ethanol/aluminum, Magnesium for low temperature and beryllium and titanium for high temperature are also candidates for low mass envelopes and need to be tested with appropriate known and new working fluids.

Improvements in heat pipe systems could be achieved by the development of new fluids and compatible fluid/envelope systems. This objective could be reached by several methods including the passivation or application of a coating to the envelope and wick to prevent reaction with the working fluid and the synthesis of new fluids.

Methods

Methods of passivation and/or application of a fluid compatible coating worthy of investigation include diffusion of metals into the surface, the physical or chemical vaporization of metal on to the surface with or withut a subsequent diffusion and the addition of minute chemical impurities to the working fluid to reduce, alter or regenerate the reaction process.

Examples of the use of thin protective coatings for heat pipes are the water compatible steels which have operated as heat pipe envelopes at temperatures up to 200 C with undegraded life times in excess of 35,000 hours. These steels utilize an integrally formed, continuous thin film

of a complex aluminum/titanium/silicon oxide to form the protective barrier.

The key to a protective layer is one which is non-reactive with the working fluid, is flexible and does not spall off the base material upon thermal cycling. Aluminum oxide is non-reactive with most fluids, but it is not flexible and its thermal expansion does not match that of aluminum thus promoting cracking of the protective oxide layer. Coatings of protect aluminum from reacting with heat pipe working fluids could use metals and alloys containing one or more of the reactive elements including titanium, silicon, yttrium, and possibly hafnium, tantalum and niobium, thus forming a protective metal/oxide layer which has flexibility and/or a good thermal expansion match.

Higher temperature heat pipes could use low mass envelope materials of beryllium, titanium and their alloys, with or without coatings, with known working fluids or newly developed ones.

An alternative to coating the envelope to protect it from reacting with the working fluid is to have a non-reactive working fluid. Preliminary tests at Thermacore indicate that impurities in methanol, ethanol and acetone may be the reasons these fluids generally are not considered compatible with aluminum. These tests also indicate that impurities in the aluminum left as a result of heat pipe fabrication may also cause fluid/envelope incompatibility. Accordingly, a better understanding of the chemistry of the real system may provide the way to a compatible system.

A second alternative to protective coatings for envelopes is the synthesis of new fluids specifically designed for heat pipes. Thermacore under contract to DOE uncovered several previously unknown heat pipe fluids for use in heat pipe solar collectors. The fluids, trimethlborate and tetramethylsilane led Dr. Alan G. MacDiarmid, Thermacore's consultant in chemistry, to believe that a family of heat pipe fluids could be synthesized by the controlled hydrolysis of the organosilicon monomer $(CH_3O)_4Si$, to form short chain polymer and cyclic species. These fluids would be for the use in the 475-775 K range and have unknown compatibility with low mass envelope materials. However, a fundamental study and synthesis of new and/or previously known compounds should be considered for the development of new high performance heat pipe working fluids.

THERMACORE

ADVANCED SPACE SYSTEM HEAT PIPES

SPACE POWER

- LOW MASS - ALUMINUM/MAGNESIUM/BERYLLIUM/TITANIUM
- HIGH PERFORMANCE - GOOD WORKING FLUID-HIGH FIGURE OF MERIT
- LONG LIFE - FLUID/VESSEL COMPATIBILITY
- MANNED SYSTEM - NON TOXIC

THERMACORE

HEAT PIPE FLUIDS FOR SPACE APPLICATIONS

SPACE POWER

System *	System **	Fluid	Aluminum Compatible	Performance	Temperature - °K (250 300 350 400 450 500)
?	Yes	Refrigerants	Yes	Low	==========
No	Yes	Ammonia	Yes	High	----------
?	Yes	Methanol	No?	Moderate	==========
?	Yes	Ethanol	No?	Low	==========
?	Yes	Acetone	Yes?	Moderate	==========
Yes	Yes	Water	No	High	==========
?	Yes	Trimethylborate	?	Low	----------

* Manned

** Unmanned

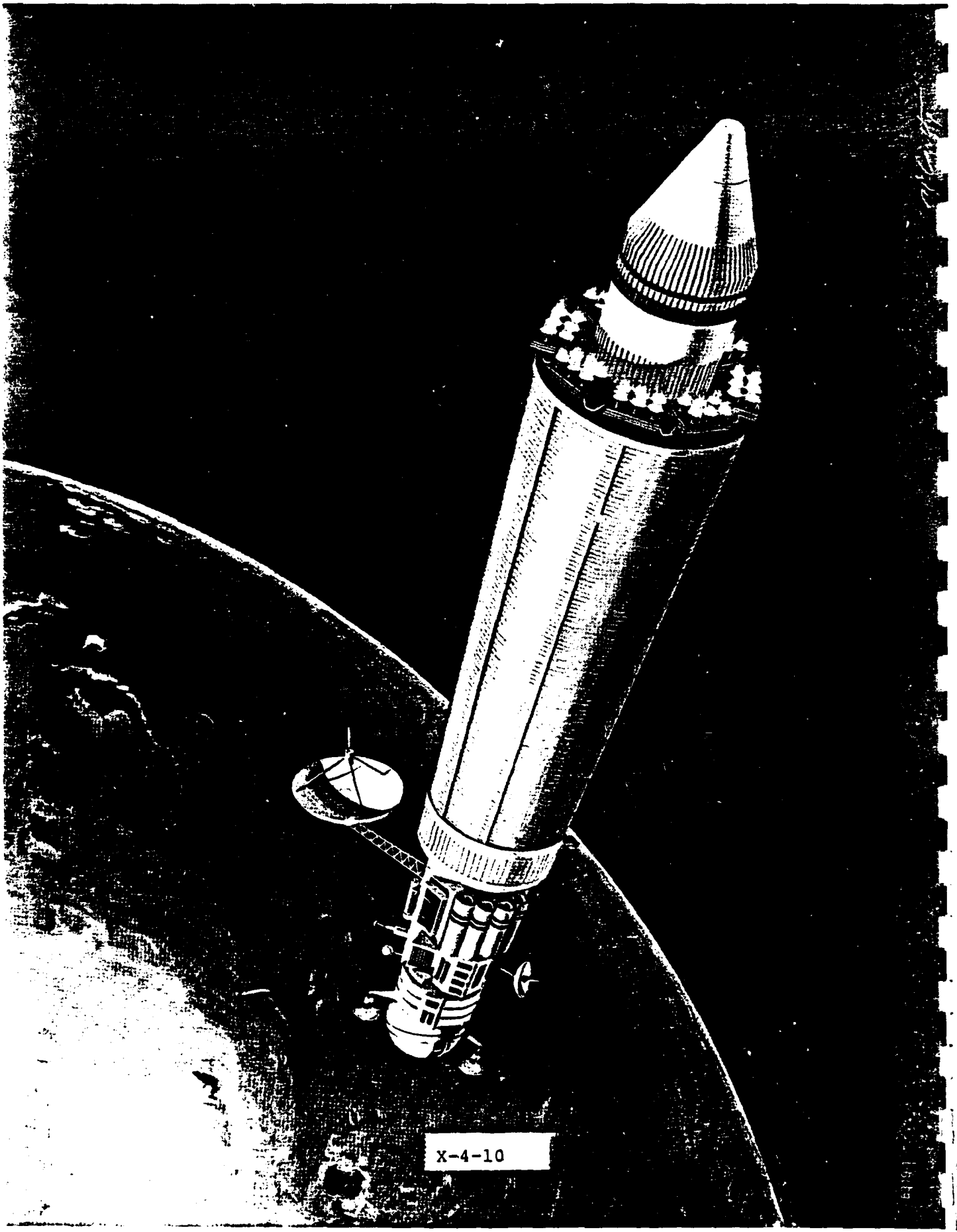

X-4-10

THERMACORE

LARGE DEPLOYABLE RADIATOR CONCEPTS FOR BRAYTON SYSTEMS

SPACE POWER

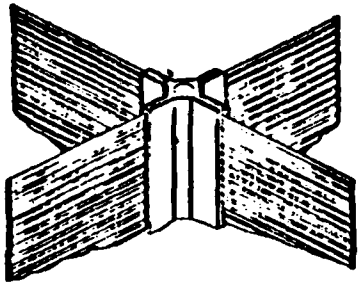

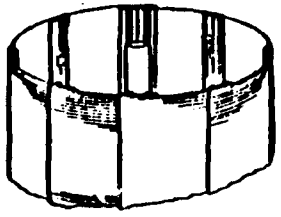

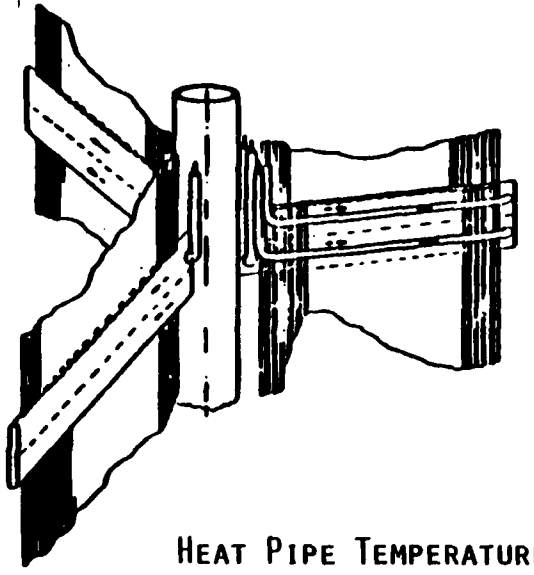

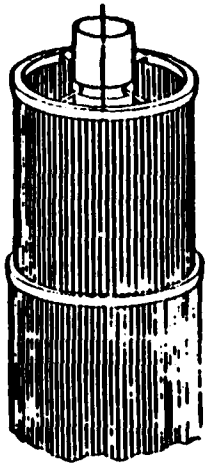

HEAT PIPE TEMPERATURES RANGE FROM 500 TO 700 K

THERMACORE

HIGHER TEMPERATURE HEAT PIPE SYSTEMS

SPACE POWER

FLUID	ENVELOPE	PERFORMANCE	TEMPERATURE - ^{O}K 500 600 700 800 900 1000
NA	Mo/SS	HIGH	═══════
K	Mo/SS/Ti	HIGH	═══════
CS	Ti	MODERATE	═══════
HG	?	MODERATE	═══════
NEW FLUIDS	?	?	═══════

THERMACORE

DEMONSTRATED APPROACHES

SPACE POWER

- Water Compatible Steels Using Thin Layers of Al/Ti/Si Oxides.
  35,000 Hours @ 200 C

- Improved Life With Pure Methanol/Aluminum
  1000 Hours and 500 Thermal Cycles @ 100 C

- New Fluid Investigation - Thrimethylborate/CRS
  31,000 Hours @ 165 C

SUMMARY

NEED

- IMPROVED HEAT PIPE WORKING FLUID/VESSEL COMBINATIONS FOR USE ON ADVANCED SPACE SYSTEMS.

APPROACHES

- COATING/PASSIVATION OF WICK AND ENVELOPE.
- PURIFICATION OF WORKING FLUIDS.
- PURIFICATION OF VESSEL/WICK MATERIAL.
- SYNTHESIS OF NEWLY DESIGNED FLUIDS.
- INVESTIGATION OF MAGNESIUM, BERYLLIUM, TITANIUM AND THEIR ALLOYS.

Summary

There exists a need for improved working fluids for use with low mass heat pipes for advanced space systems. The approaches to achieving improved working fluids include:

- o The coating or passivation of the envelope and wick to permit the use of fluids which normally react with the envelope and wick.
- o The purification of fluids and/or the purification of the envelope to remove unwanted elements on or embedded in the surface.
- o The synthesis and study of newly designed fluids.
- o Investigation of alternate materials such as magnesium, beryllium and titanium with and without passivation or coatings.

Bibliography

Advances in Space Power Research and Technology at the National Aeronautics and Space Administration, J. P. Mullin, L. P. Randolph, W. R. Hudson and J. H. Ambrus, NASA Headquarters, Paper No. 819180, 16th Annual IECEC, Atlanta, Georgia, August, 1981.

"Articulated Heat Pipe Feasibility Demonstration", AFWAL/WPAFB Contract No. F33615-81-C-3413, Thermacore, Inc., Lancaster, PA.

Experimental Results for Space Nuclear Power Plant Design, W. A. Ranken, LANL, Paper No. 809142, 15th Annual IECEC, Seattle, Washington, August, 1980.

Future Space Power - The DOD Perspective, Dr. Tom Mahefkey, AFWAL, Paper No. 809016, 15th Annual IECEC, Seattle, Washington, August, 1980.

"Space Constructable Long Life Radiator-Prototype Development", NASA Johnson Space Center Contract No. NAS-9-15965, Grumman Aerospace Corporation, Bethpage, L.I. N.Y.

"Systems Evaluation of Thermal Bus Concepts", NASA Johnson Space Center Contract No. NAS-9-16321, Vought Corporation, Dallas, Texas.

ENHANCED HEAT PIPE

THEORY AND OPERATION

D. M. Ernst* - G. Y. Eastman**
Thermacore, Inc.

Abstract

Heat pipes to extract heat from the cores of compact fast reactors require unusually high power densities. This performance appears to be feasible, but necessitates more detailed exploration of theoretical and operational limits than has then carried out to date. Closely aligned to heat pipes for heat removal from the core are the low mass high performance, high temperature radiator heat pipes.

Much of the work concerning the theory and operational limits of high performance heat pipes has been hit or miss, distorted by funding limits or specific mission requirements. To reach the levels of performance required by large space power systems, the work must be unified, a fully descriptive analytical model developed and the analyses experimentally verified. The areas requiring the greatest attention are the startup and shutdown characteristics of long heat pipes, the limits on wick-augmented thin film evaporation (burn out heat flux) and the prediction of the true temperature profile along the heat pipe. It will also almost certainly require exploration and analysis of higher capacity capillary wicks than have been demonstrated to date.

Background

During the decade of the 70's the heat pipe became an integral part of most prime power space system concepts. Some of these concepts, the 120 and 400 kW_e nuclear electric propulsion (NEP) and the SP-100 systems have entered into technology development programs. These programs have

*Vice President and Chief Technical Officer, Thermacore, Inc., Lancaster, PA
**President, Thermacore, Inc., Lancaster, PA

scratched the surface and shown the need for improved heat pipe theory and operation.

The attached figures show: the only full scale (50 kW_t), high temperature (1000 K) space radiator built using heat pipes (RCA - AF), the 400 kW_e thermionic and 120 kW_e thermoelectric NEP systems (Thermacore-JPL) and the SP-100 system (LANL-DOE). Heat pipes which have been built and tested for these systems include: a transition and radiator heat pipe for the NEP system (Thermacore) and the radiator heat pipe for the SP-100 system (LANL-Thermacore). A core heat pipe for the SP-100 is currently being put together at LANL. Thermacore under contract to DOE demonstrated a sintered powder metal wick in a non-limited lithium heat pipe which transported 21 kW/cm^2 through the vapor space at 2100 K.

These isolated demonstrations, while being successful in their own right also pointed out the need for a deeper understanding of the fundamental processes of self pumped two phase flow in a closed container.

These processes include the intricate balance in achieving thin film evaporation in the wick without dry out. To prevent dry out or boiling, the wick must be thin, however, as the wick becomes thin the crossectional area for liquid flow is reduced. These two phenomena, liquid flow in a capillary wick and thin film evaporation are in direct opposition to one another.

Evaporation from a wick has the advantage that as the power density increases the level of liquid is reduced. However, it is this reduced liquid level which ultimately causes dry out. Also the fact that the liquid and vapor in a heat pipe are in quasiequilibrium introduces a factor which generally is not the case for other boiling/evaporating systems.

The fundamental understanding of the evaporation of working fluid from high performance wick structures needs to be carefully studied. Some of the higher performance wick structures, some demonstrated, some untried are seen in the enclosed figures.

In addition to the thin film/wick evaporation process in heat pipes but closely aligned to it is the performance of long heat pipes under varying conditions. i.e. what are the consequences of short and long term startup and shut-down sequences on the operation of the heat pipe. Also of great importance is the actual temperature profile of the heat pipe under these varying conditions.

Thermacore has taken the first step in looking at this problem by writing a computer program which forces the internal two phase flow calculations to be influenced by the external conditions into which the heat pipe operates. However, this program does not take transients into consideration. It does take thin film evaporation into account but does not allow this to be a limiting factor, since the process is not fully characterized.

Summary

High performance, high temperature heat pipes are a key element for use in future high power space systems.

Fundamental understanding of several inter-related processes need to be investigated and include:

- Thin film evaporation
  - Self pumping wick structures.
  - Quasiequilibrium of liquid and vapor.
  - Heat fluxes and temperatures compatible with space power systems.
- Temperature profiles and stability during
  - Short and long transients during startup and shutdown.
  - Steady state.

THERMACORE

SPACE POWER SYSTEMS
TECHNOLOGY DEMONSTRATIONS

SPACE POWER

CONCEPTS

- o 120 kW_E NEP
- o 400 kW_E NEP
- o SP - 100

HEAT PIPE DEMONSTRATIONS

- o HEAT PIPE-TO-HEAT PIPE TRANSITION 925 K - 2.6 kW_{TH}
- o 4.4 METER LONG SODIUM/SS RADIATOR HEAT PIPE 925 K - 2.6 kW_{TH}
- o 5.5 METER LONG POTASSIUM/TITANIUM RADIATOR HEAT PIPE 775 K - 1.8 kW_{TH}
- o 0.3 METER LONG LITHIUM/MOLYBDENUM CORE TYPE 2100 K - 21 kW/cm^2 (VAPOR SPACE)

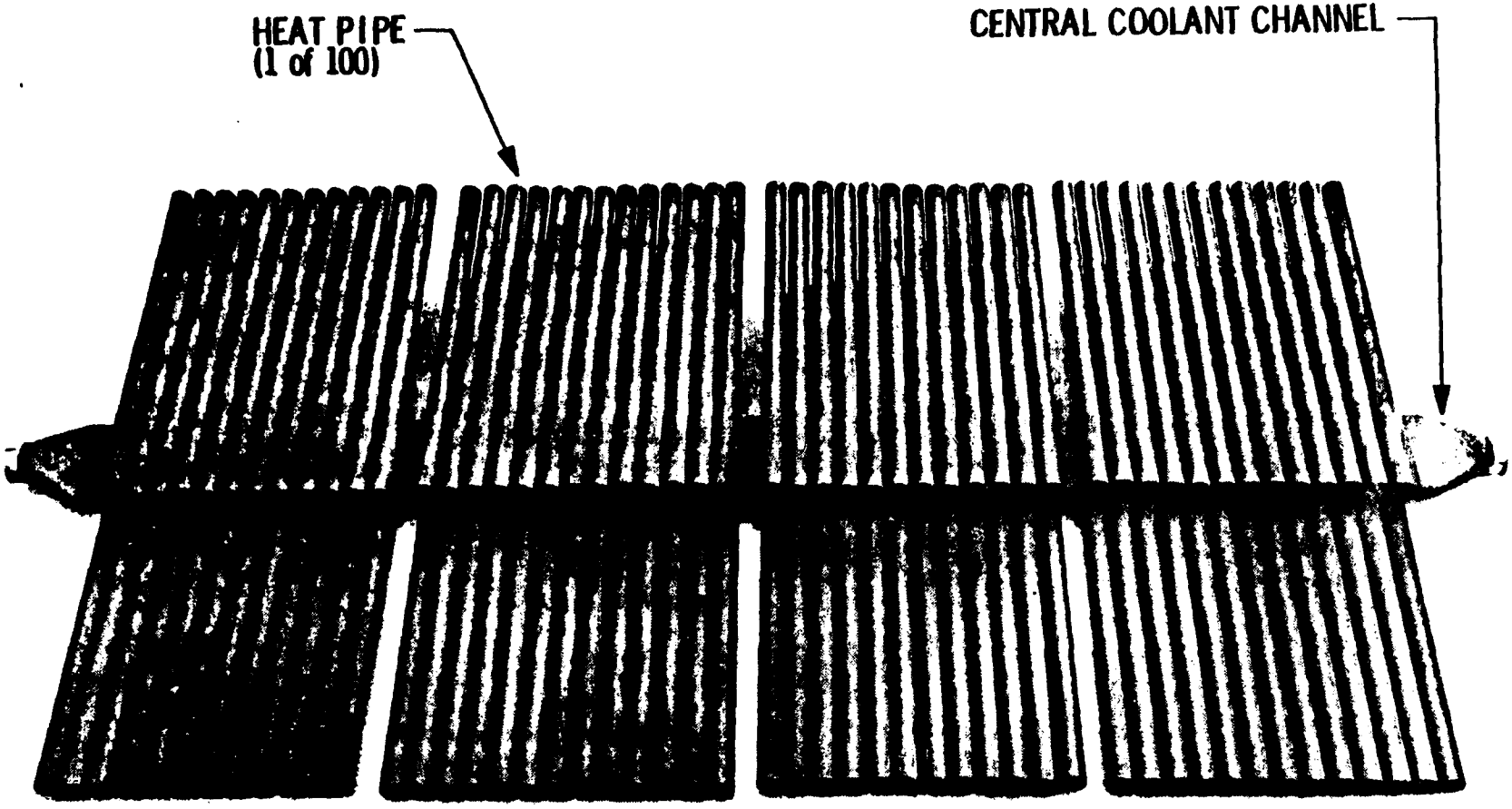

Fig. 1. Heat pipe radiator

THERMACORE

THERMIONIC NEP HEAT REJECTION SYSTEM - EARLY '79

SPACE POWER SYSTEMS

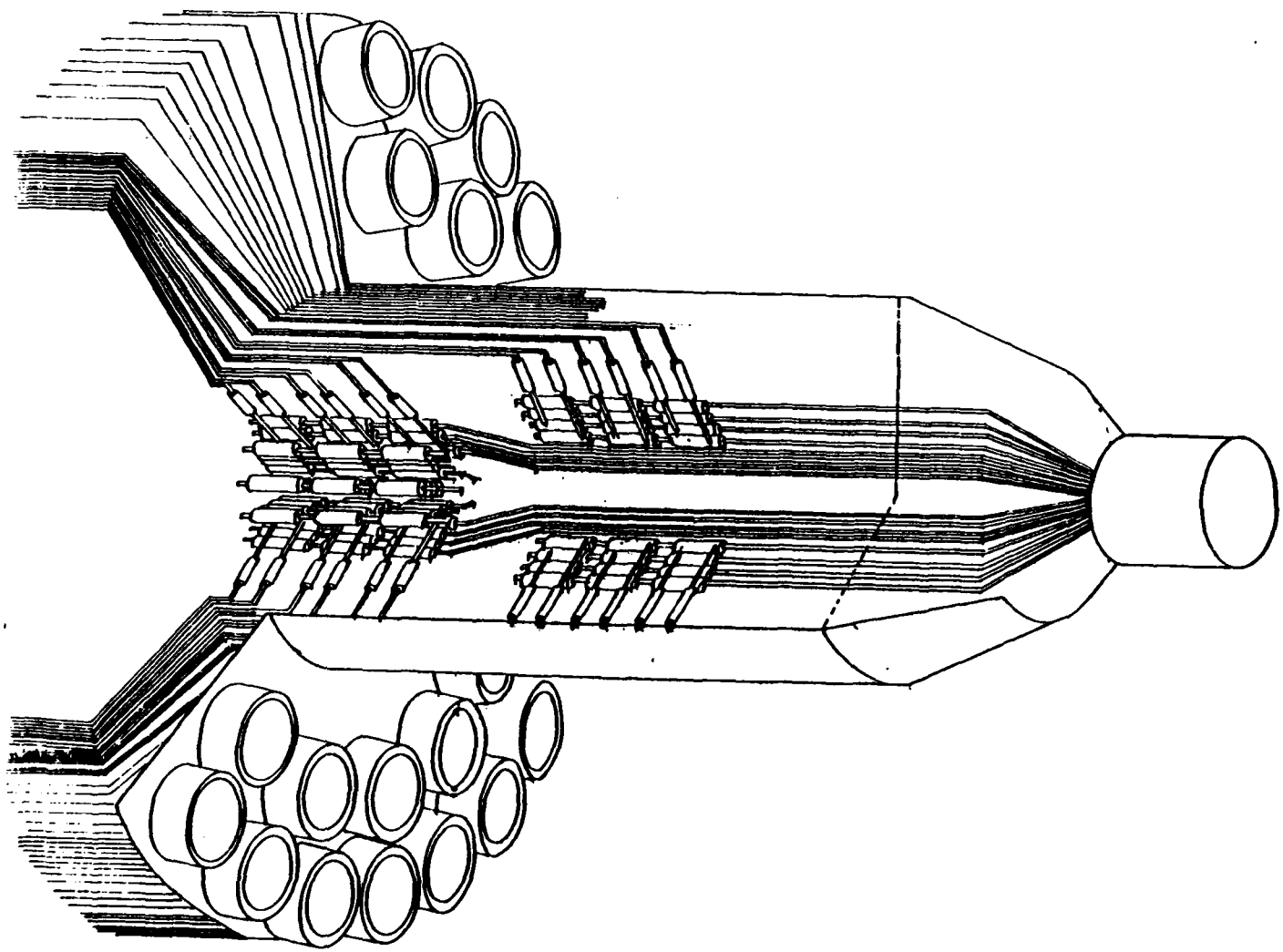

THERMACORE

SPACE POWER SYSTEMS

THERMIONIC NEP HEAT REJECTION CONCEPT - EARLY '79

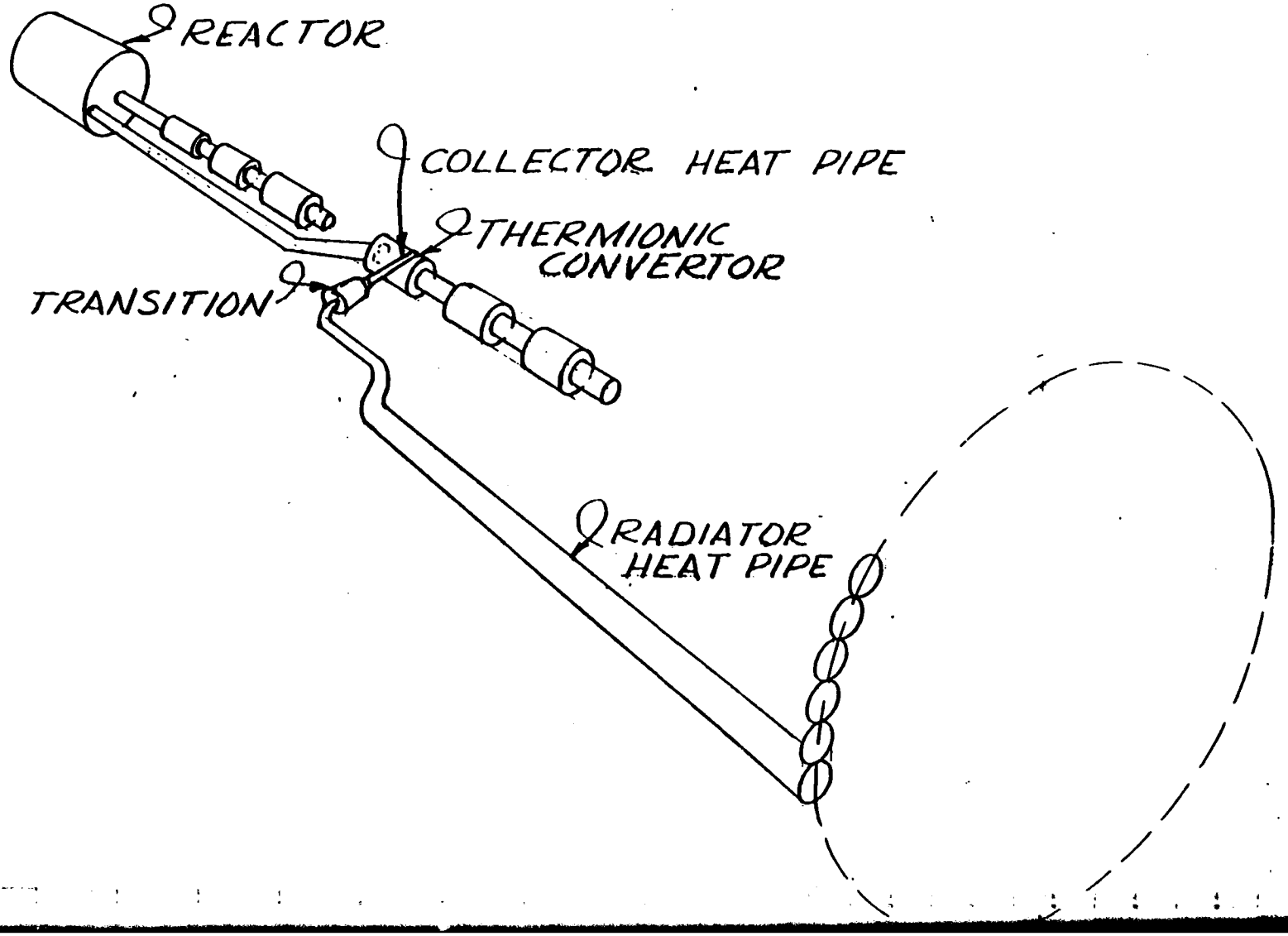

THERMACORE

Space Power

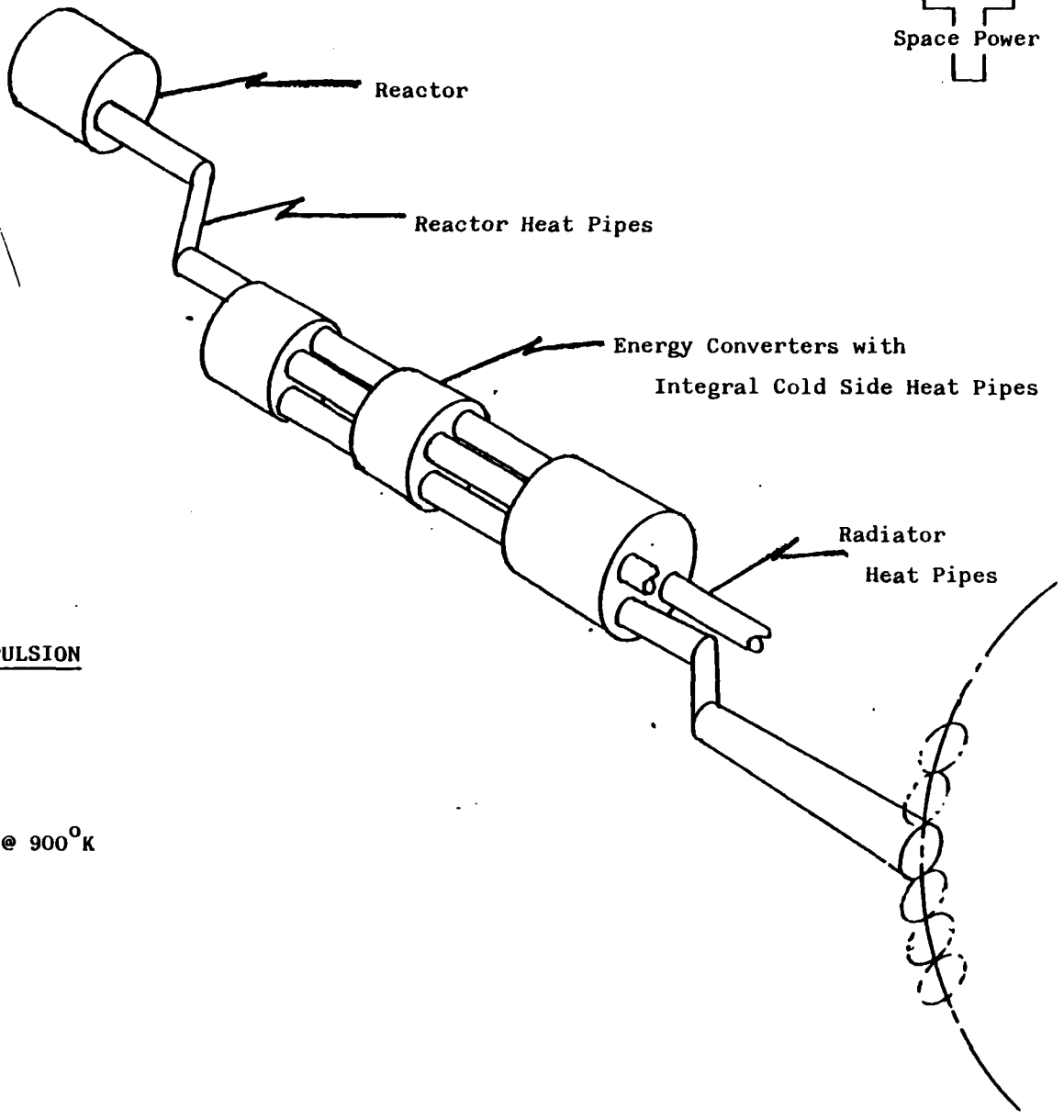

X-5-7

NUCLEAR ELECTRIC PROPULSION

POWER SUB SYSTEM

120 kW_e - 1 MW_T Radiator @ 900^{o}K

THERMACORE

SPACE POWER

FLUID FILLED HEAT PIPE-TO-HEAT PIPE JOINT

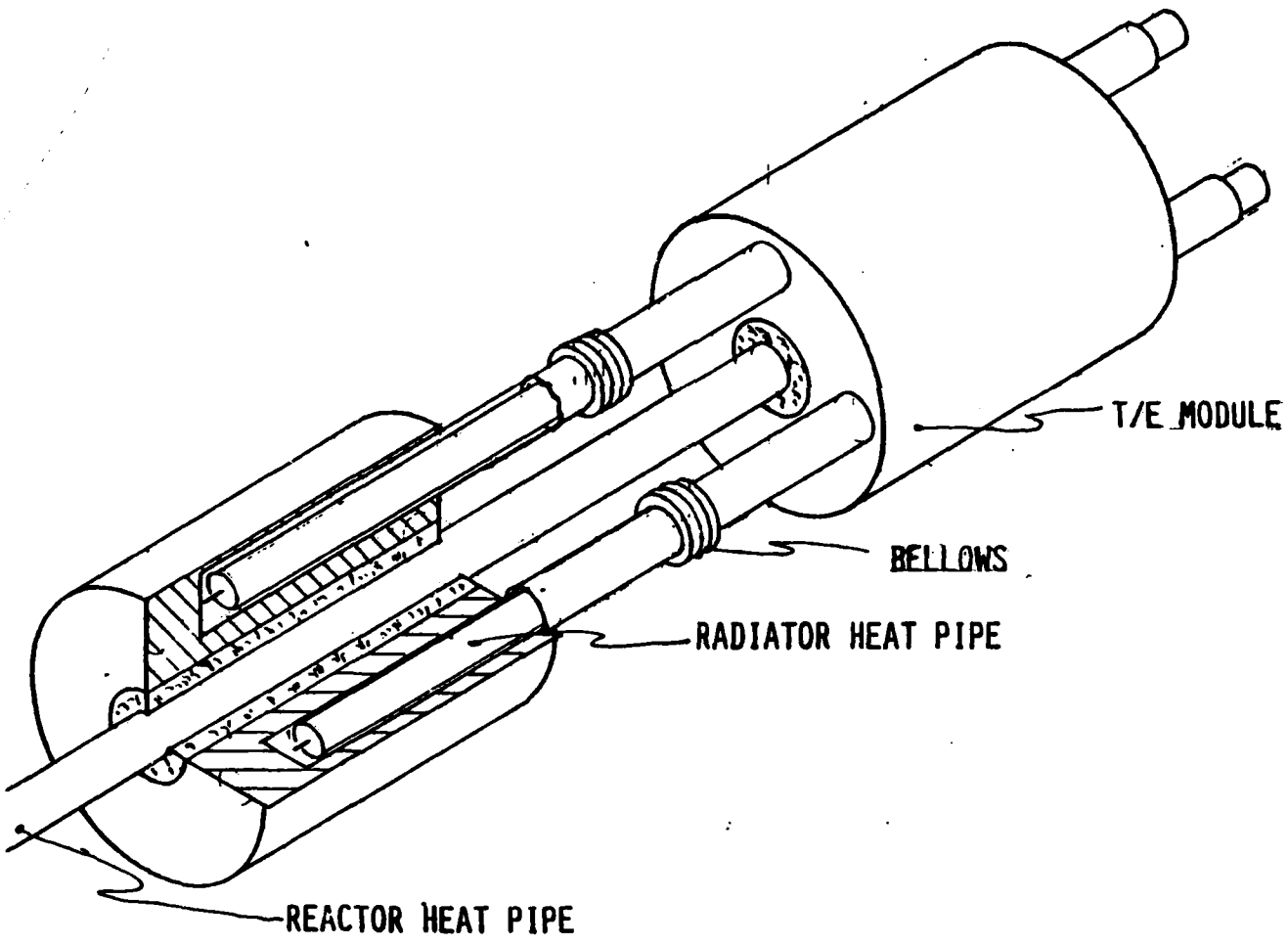

THERMACORE

SP-100

SPACE POWER

RADIATOR CONCEPT

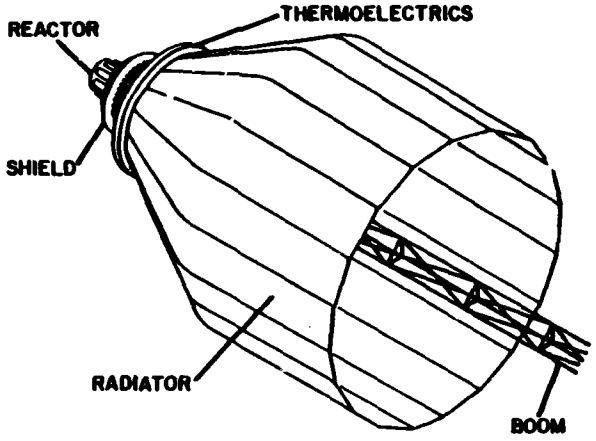

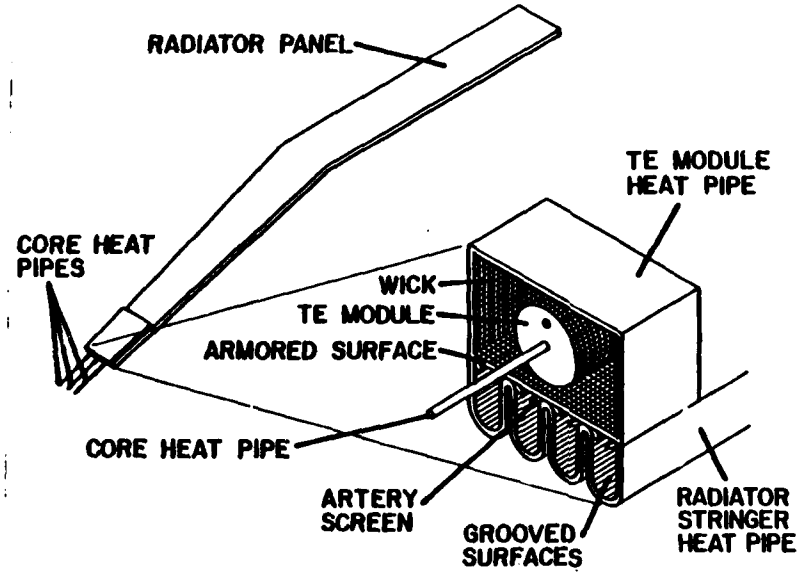

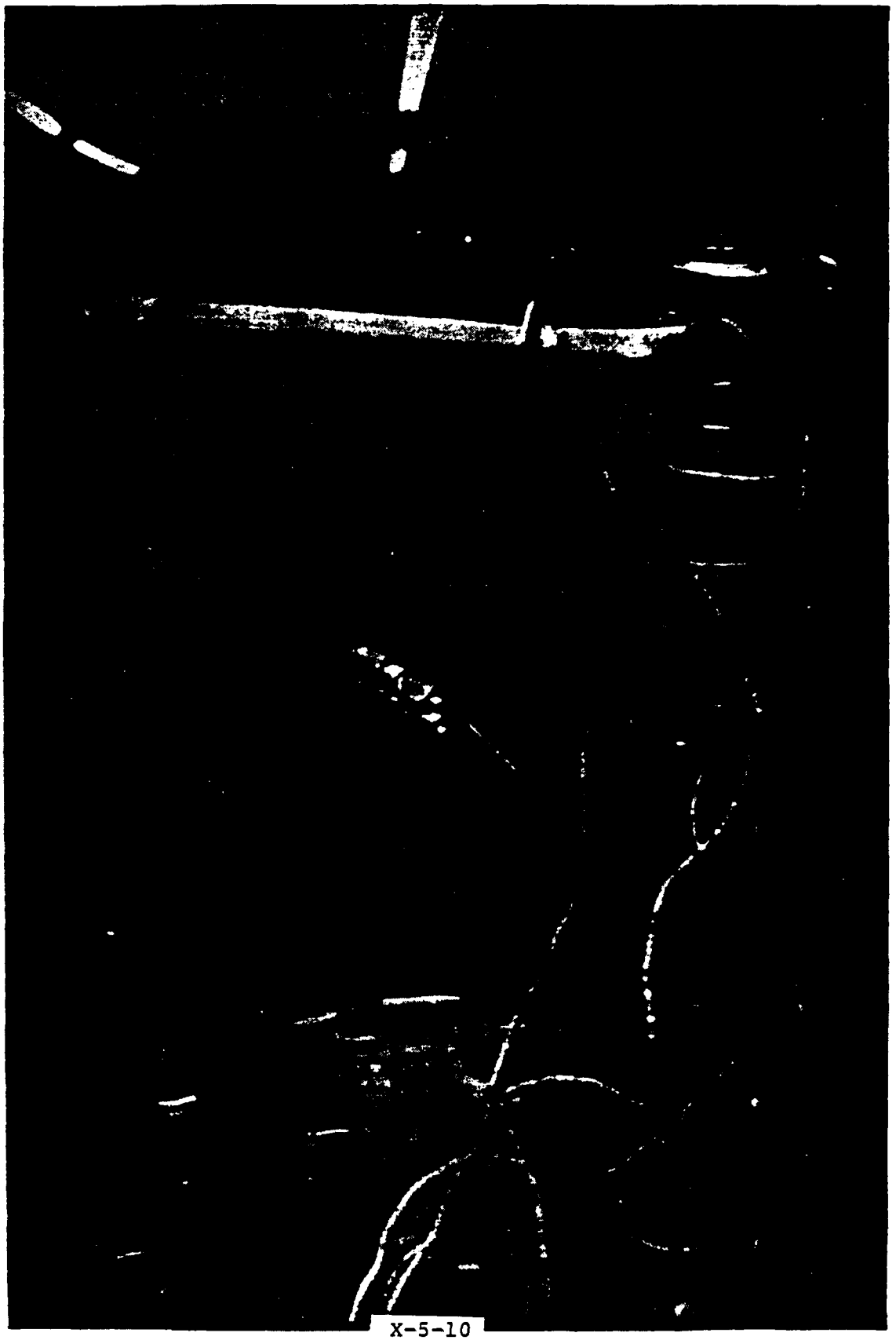

X-5-10

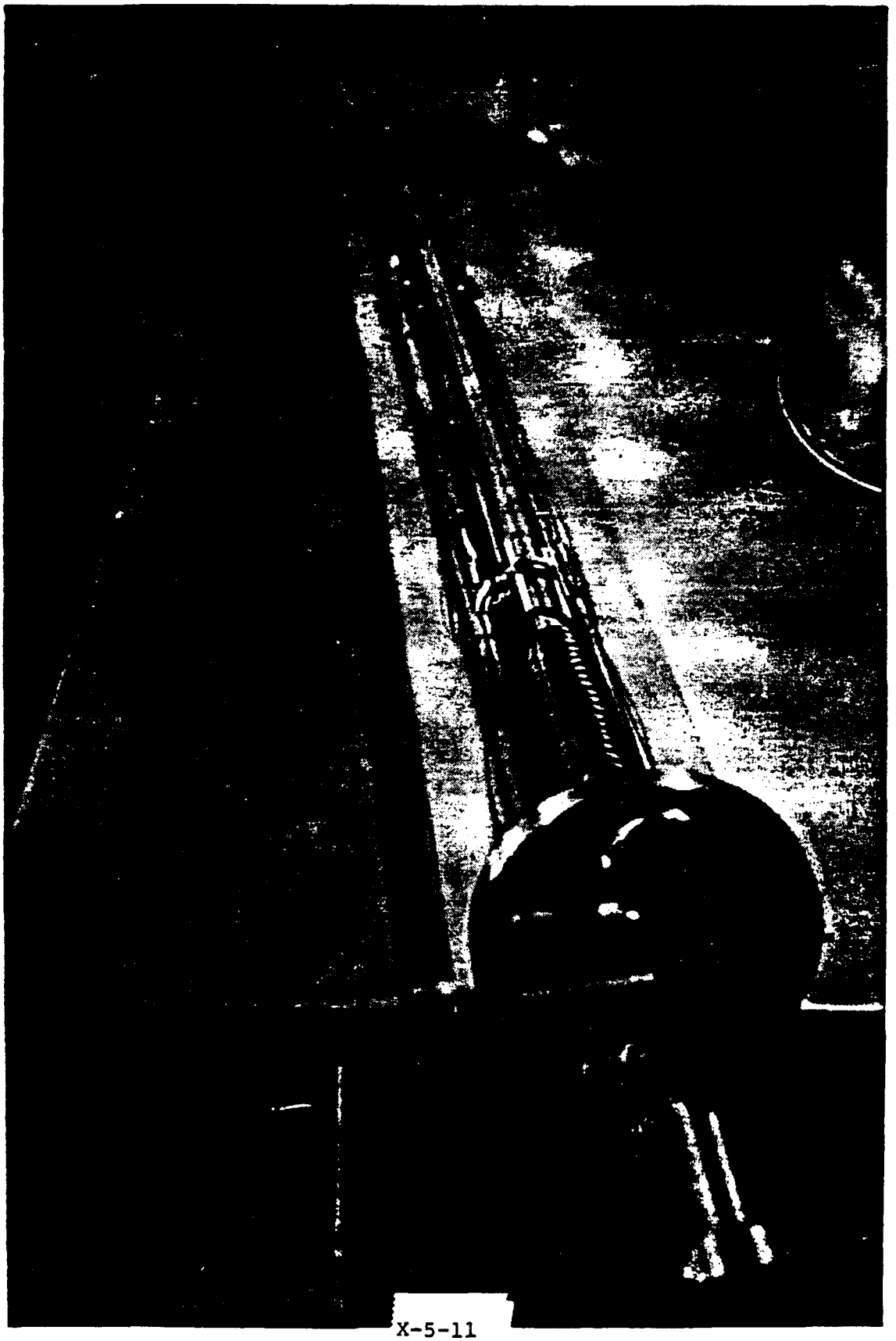

X-5-11

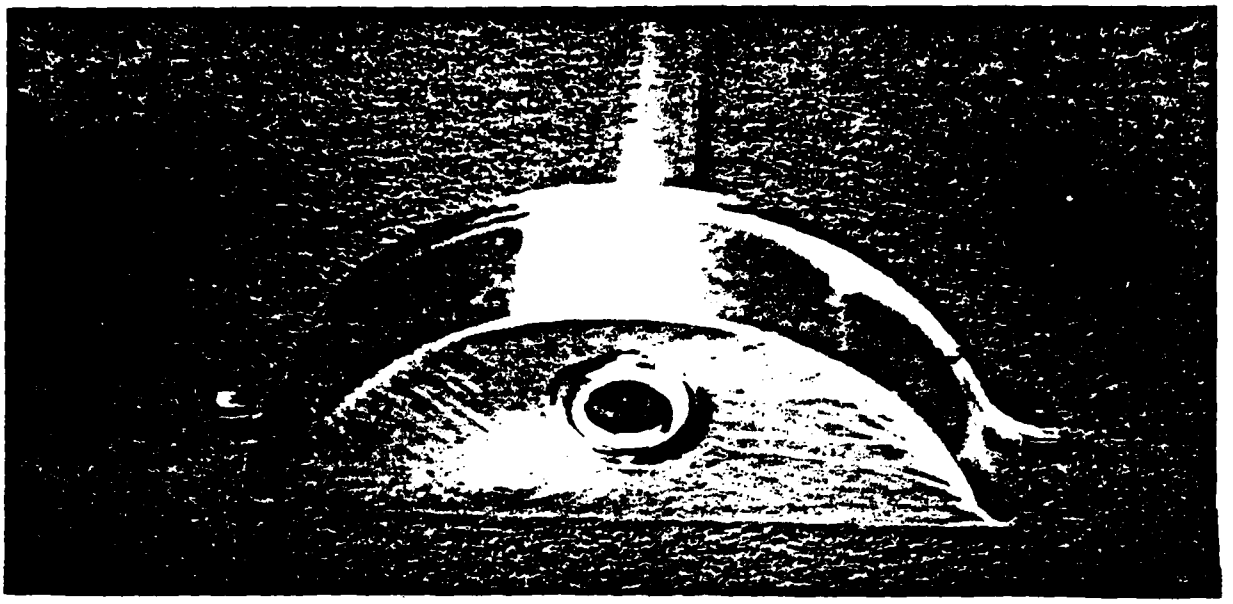

Fig. End cap with EB welded fill tube.

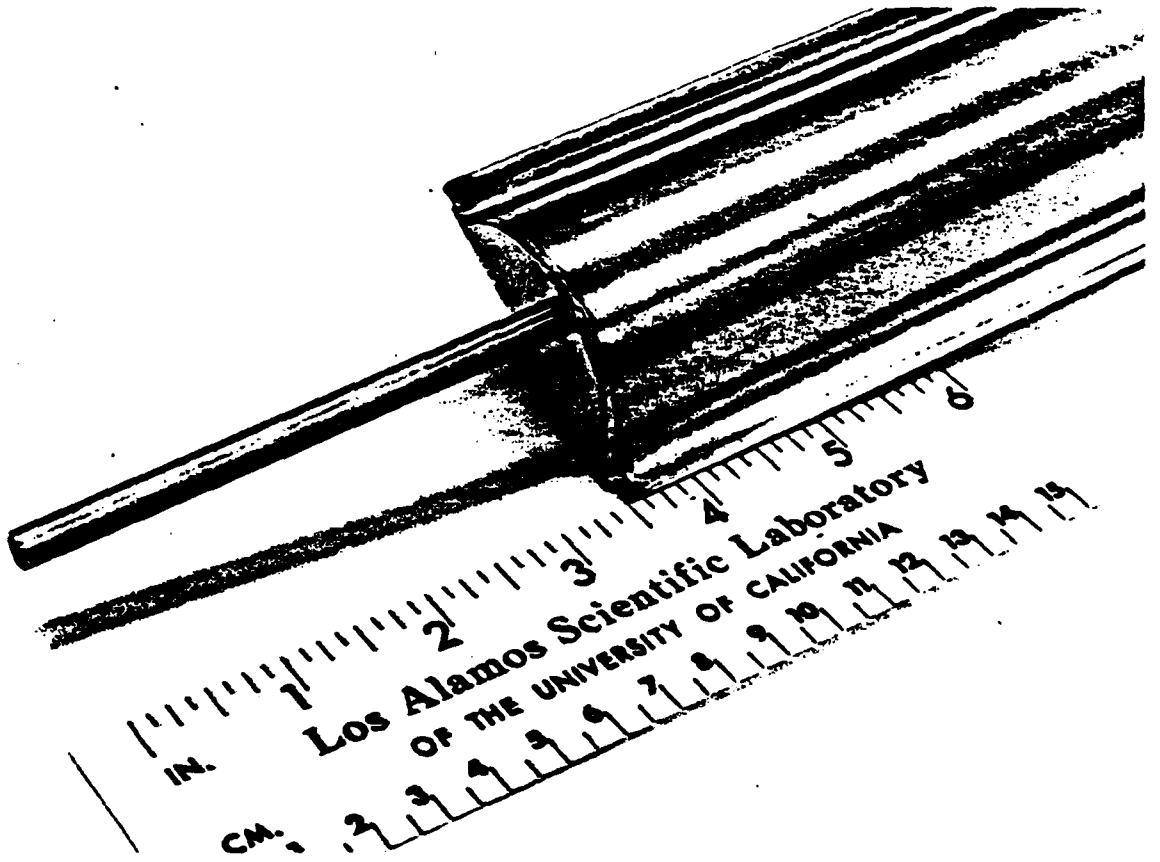

Fig. End view of a titanium heat pipe showing a laser end cap to tube weld.

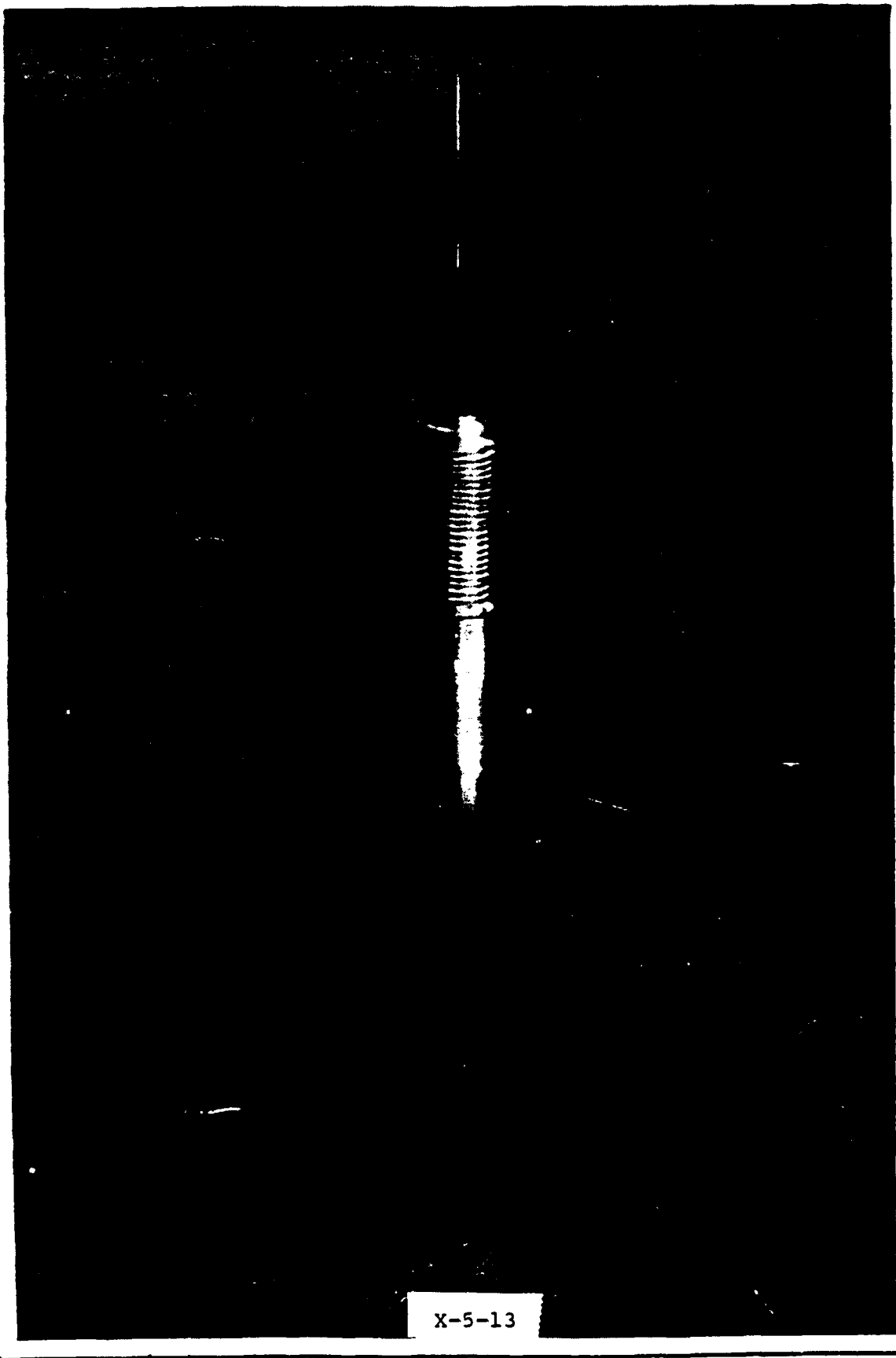

X-5-13

LIMITS

- Viscous
- Sonic
- Entrainment
- Capillary
- Boiling

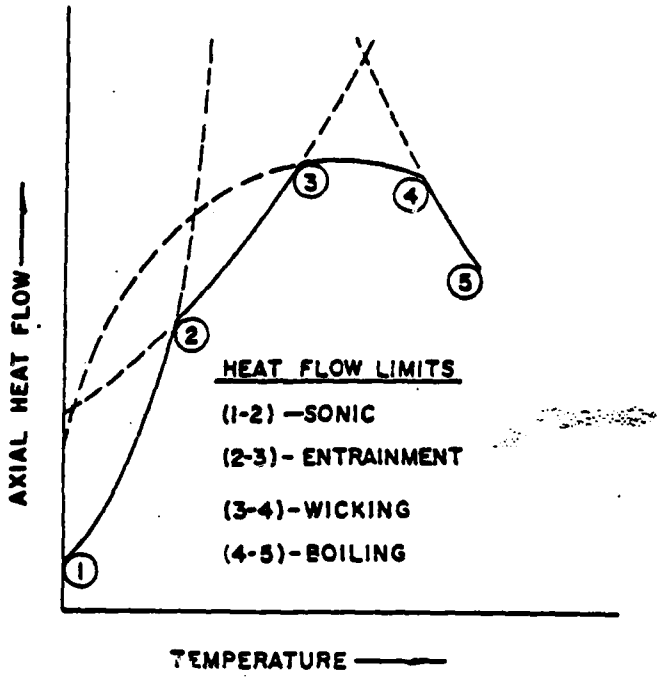

Heat Pipe Limitations.

WICKS

- WIRE MESH
- AXIAL GROOVES
- CIRCUMFERENTIAL GROOVES
- ARTERIES
- SINTERED POWDER
- GEOMETRIC CONFIGURATION IN WALL

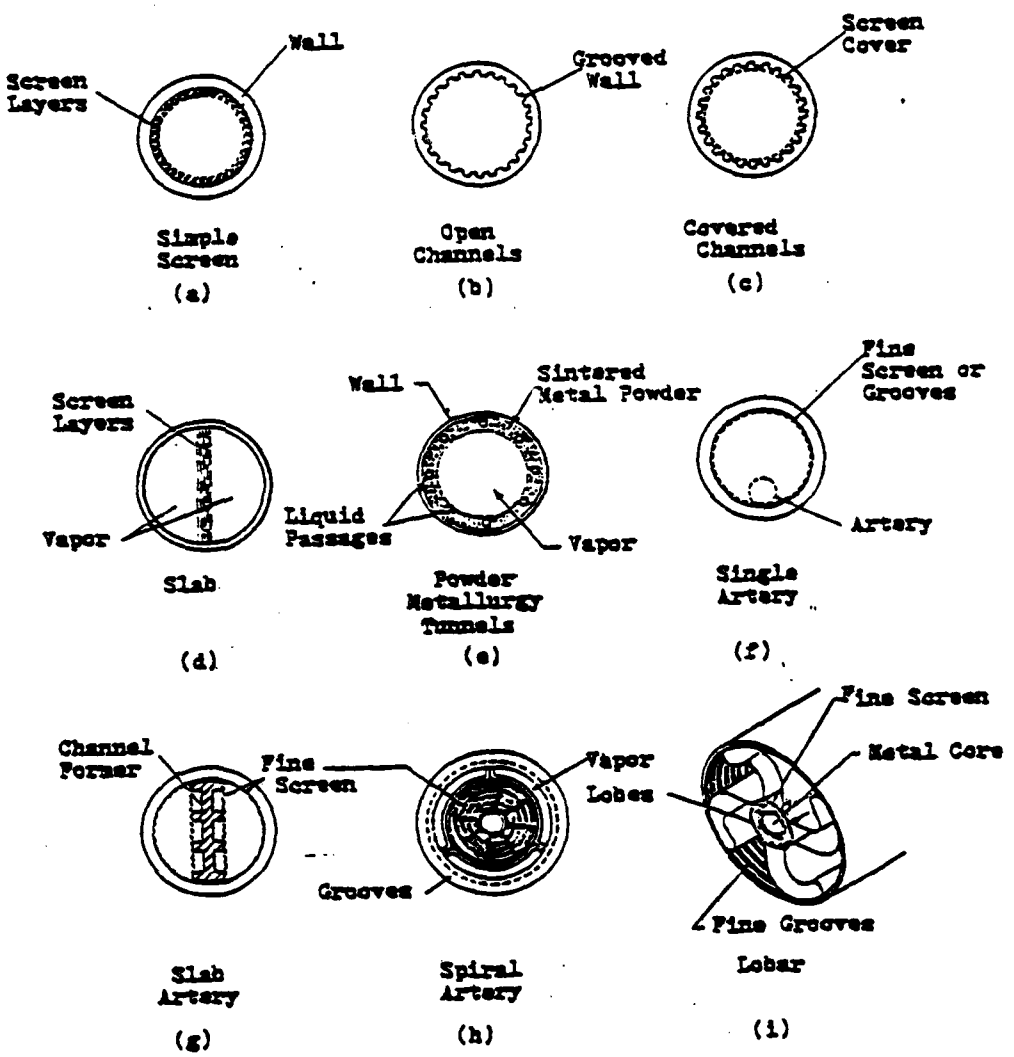

Representative Wick Geometries

DWG. NO.

FLEXIBLE WICK OF
BIAS-ROLLED SCREEN

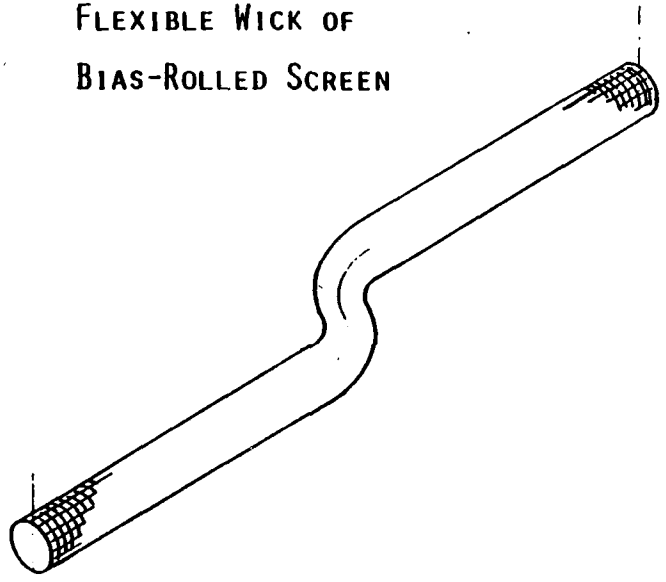

X-5-18

TITLE			
NAME			ST'D. TOLERANCES
DRAWN		DATE	DECIMAL .xx = +.015 .xxx = +.005
APPROVED			FRACTION + 1/64
SCALE	MATL.		ANGULAR + .003 PER. INCH OF LENGTH
ASS'Y or BILL			
THERMACORE, INC. HEAT TRANSFER SPECIALISTS			DWG. NO.

-8

Powder Metal Tunnel Wick Geometries
With High Capillary Capability

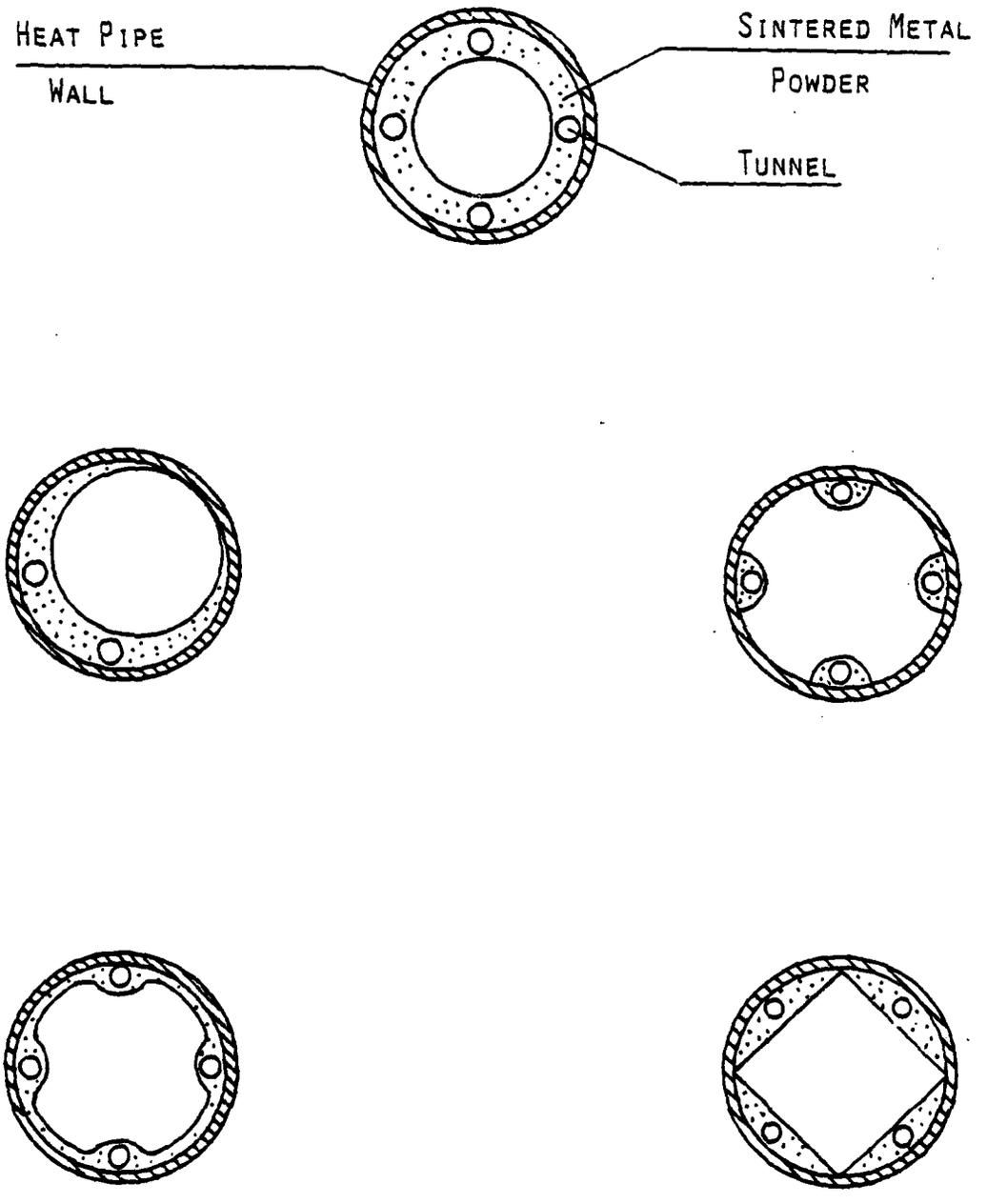

WG. NO.

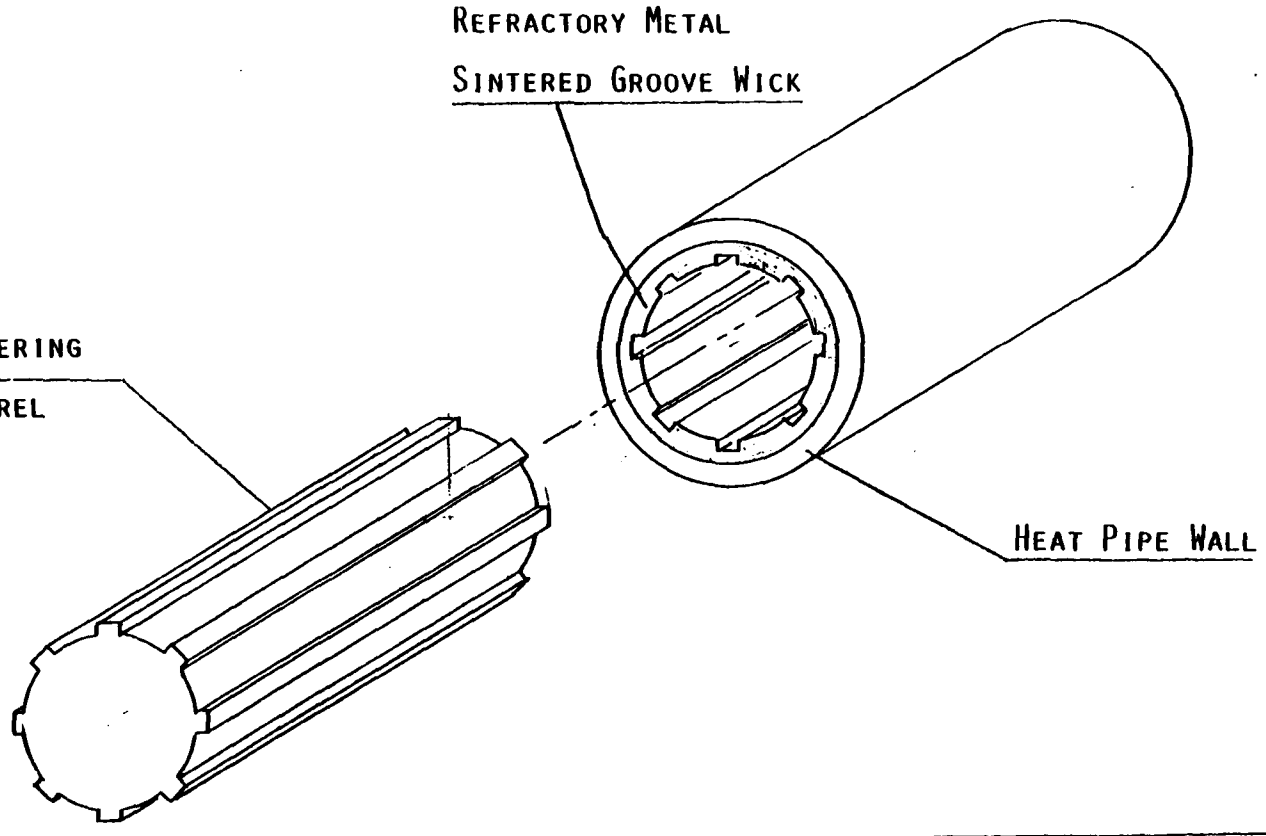

X-5-20

TITLE			
NAME			ST'D. TOLERANCES
DRAWN	DATE		DECIMAL .xx = ±.015 .xxx = ±.005
APPROVED	DATE		FRACTION ± 1/64
SCALE	MATL.		ANGULAR ± .003 PER. INCH OF LENGTH
ASS'Y or BILL			
THERMACORE, INC. HEAT TRANSFER SPECIALISTS			DWG. NO.

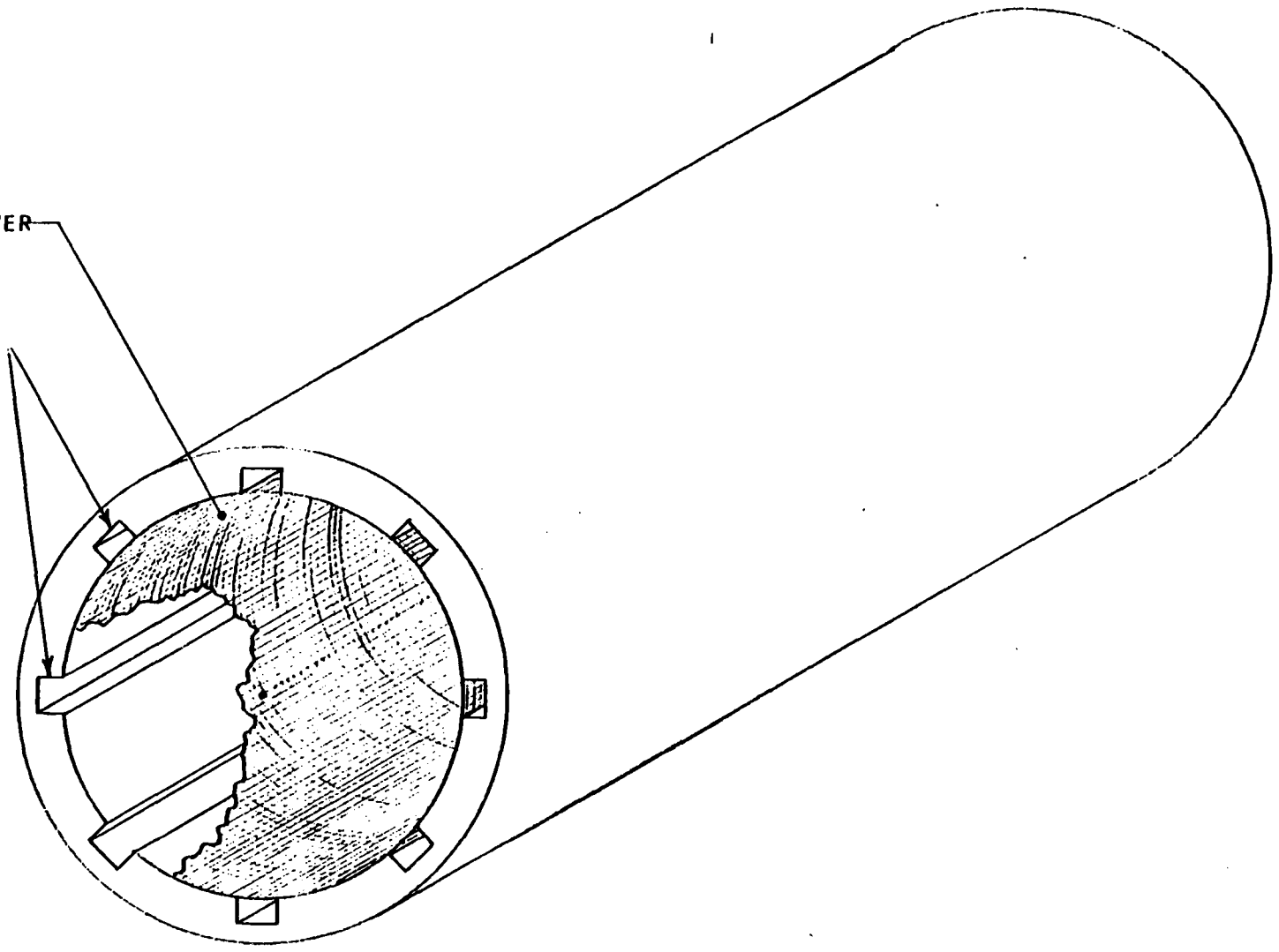

X-5-21

SCREEN WITH GROOVES

13-79

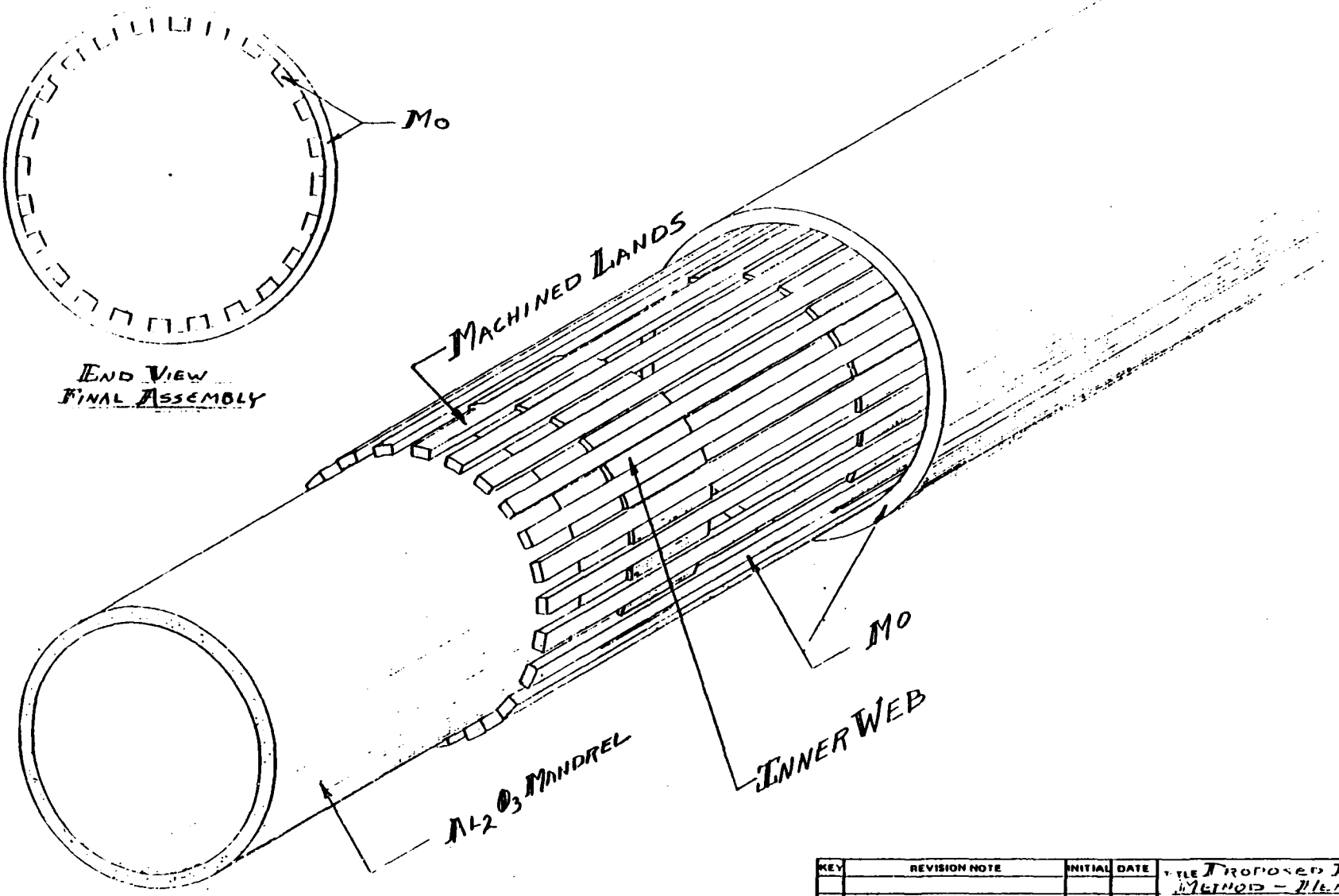

X-5-22

KEY	REVISION NOTE	INITIAL	DATE

TITLE Proposed Fabr
Method - Heat
NAME Grooved Heat
DRAWN CJD DATE 11-2
APPROVED
SCALE — MATL
ASS'Y or BILL

THERMACORE, INC.
HEAT TRANSFER SPECIALISTS

DWG. NO.

Low Mass, Configuration Pumped Heat Pipe Geometries

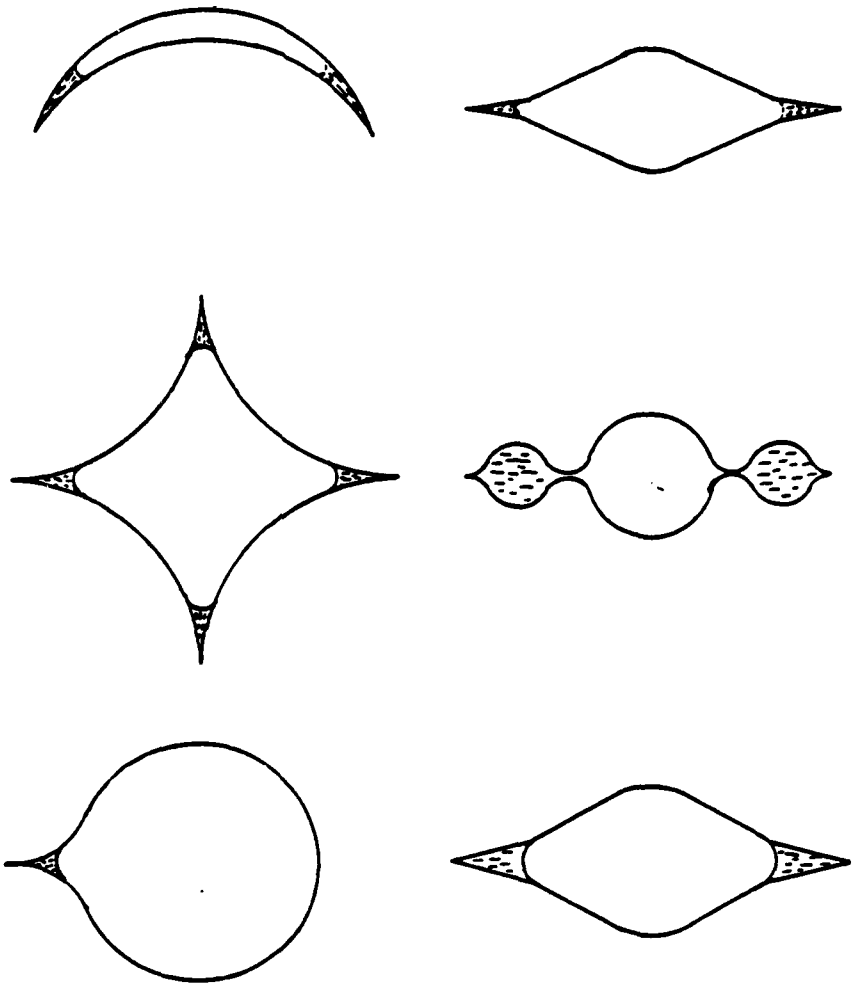

NAS936

THERMACORE

SUMMARY

SPACE POWER

ANALYZE AND EXPERIMENTALLY VERIFY THE FUNDAMENTAL PROCESS IN HEAT PIPES

- THIN FILM EVAPORATION
  - SELF PUMPING WICK STRUCTURES
  - QUASIEQUILIBRIUM OF LIQUID AND VAPOR
  - HEAT FLUXES AND TEMPERATURE COMPATIBLE WITH SPACE POWER SYSTEMS.
- TEMPERATURE PROFILES AND STABILITY DURING
  - SHORT AND LONG TERM TRANSIENTS DURING STARTUP AND SHUTDOWN.
  - STEADY STATE

TWO-PHASE HEAT TRANSPORT FOR THERMAL CONTROL

Prepared for

AIR FORCE OFFICE OF SCIENTIFIC RESEARCH

Special Conference On

Prime Power for High-Energy Space Systems

February 22-25, 1982

by

ARTHUR D. LITTLE, INC.
Cambridge, Mass. 02140

ABSTRACT

The thermal control of future orbiting payloads will require the transfer of tens of kilowatts of thermal power over tens of meters with small driving temperature differences.

To help meet these needs, a pumped, two-phase thermal transport system has been conceived and subjected to preliminary evaluation. These evaluations show the concept has potential advantages compared to heat pipes and liquid flow loops in many applications sufficient to warrant its further development.

A brief outline of this concept and its performance characteristics is presented, together with the principal and basic area for further R&D needed to validate and optimize system design.

BACKGROUND

It is anticipated that orbiting space platforms planned for the future will have greatly extended geometries, much higher levels of heat dissipation, and/or a multiplicity of systems and instruments requiring more exacting temperature level control than is represented by current space systems. New technologies for thermal control should be developed to service these future needs because the continued use of existing ones lead to systems that will not serve or will be burdened with a complexity, lack of reliability, weight and power that cannot – or need not – be accepted.

To help meet these needs, a pumped, two-phase thermal transport system has been conceived, built, and tested with funding support from NASA-GSFC under contract NAS5-26350 and with an equivalent IR&D investment by Arthur D. Little, Inc. These preliminary evaluations show the concept has potential advantages sufficient to warrant its further development. The principal and basic scientific areas for further R&D required to validate and optimize system design are near zero-g evaporative and condensing heat transfer and fluid flow regimes.

X-6-3

PUMPED, TWO-PHASE HEAT TRANSPORT SYSTEM CONCEPT

The concept of the pumped, two-phase flow heat transport system is illustrated in its elementary form in the opposite figure. The system consists of a closed fluid-loop maintained in circulation by a pump. The fluid is preconditioned in a supply reservoir to be near saturation at a temperature level best suited to provide the heat source or sink necessary to the temperature control of the subsystems on the loop. A liquid-vapor, two-phase, saturated mixture of the working liquid is made to flow through heat stations (instrument modules in the case shown) arranged in series along the flow loop. Heat exchange at the heat stations involves change of phase, either condensation or evaporation, depending on whether cooling or heat addition is required.

The net heat added by all instrument modules is rejected by a space radiator. The radiator functions as a condenser and is sized to handle the largest net heat addition to the fluid loop occurring during operation of the system. A temperature-controlled fluid bypass and mixing valve (or other control means) establishes the set point temperature of the fluid in the reservoir slightly below the saturation temperature corresponding to its pressure. The pump inlet is, therefore, supplied with slightly subcooled liquid from the reservoir to minimize the power required to circulate the fluid in the loop and to avoid cavitation-induced difficulties.

PUMPED, TWO-PHASE FLOW HEAT TRANSPORT SYSTEM CONCEPT

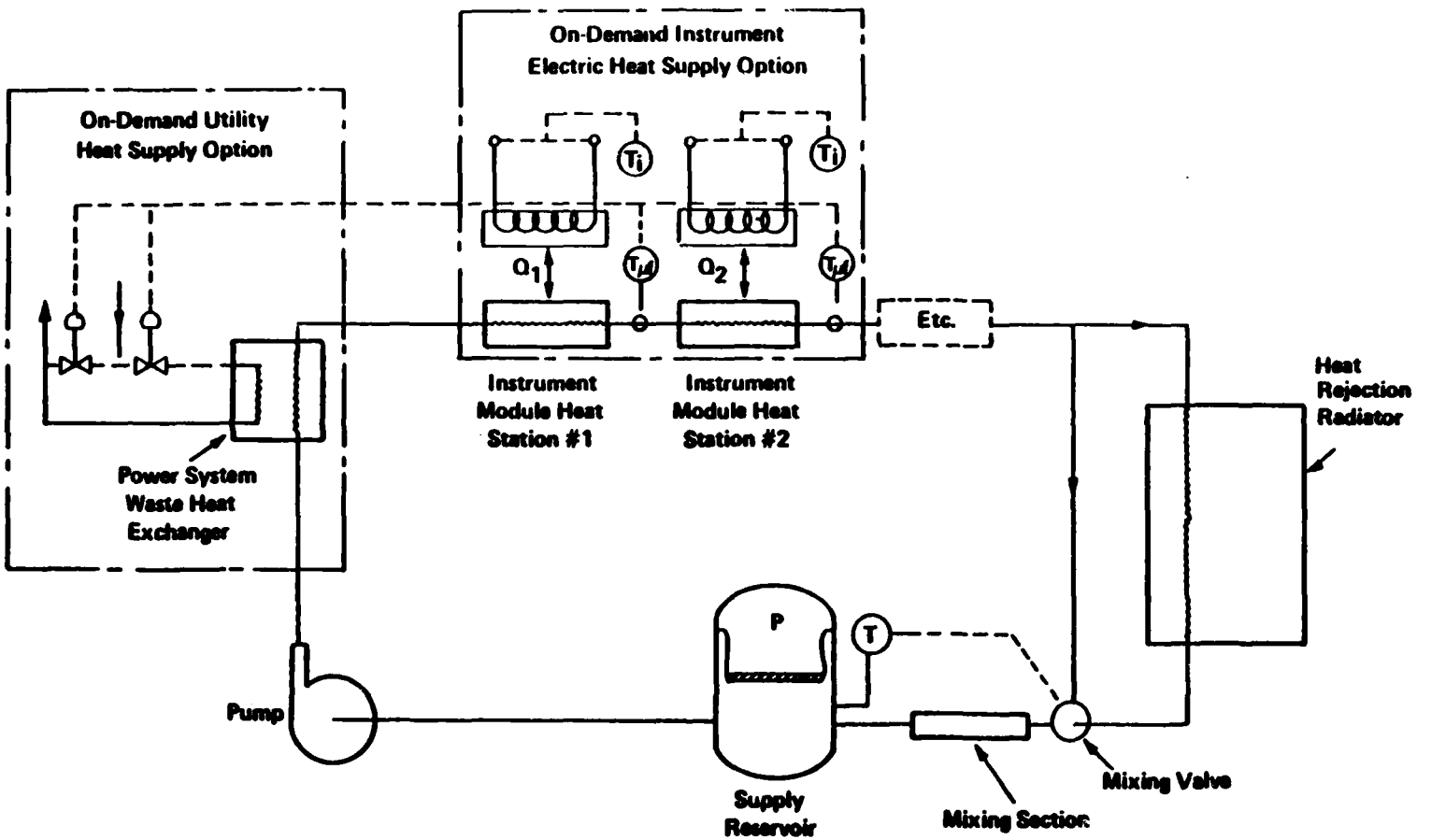

X-6-5

HEAT TRANSPORT CHARACTERISTICS

The opposite figure shows the calculated heat transport limits (W-m) for an ammonia, pumped, two-phase fluid loop. The transport limits are presented as a function of mass flow rate and tube size for a specified end-to-end temperature span of 5°C. The allowable end-to-end pressure drop is set by the allowable end-to-end drop in saturation temperature. Pressure changes in the fluid loop arising from any cause, e.g., elevation change in a 1-g field or altered flow regimes will be accommodated by the positive displacement liquid pump.

9-9-X

HEAT TRANSPORT CHARACTERISTICS

- Ammonia (R717) is the working fluid at 20°C
- End-to-end temperature span of 5°C
- End-to-end pressure drop of 19.4 psi

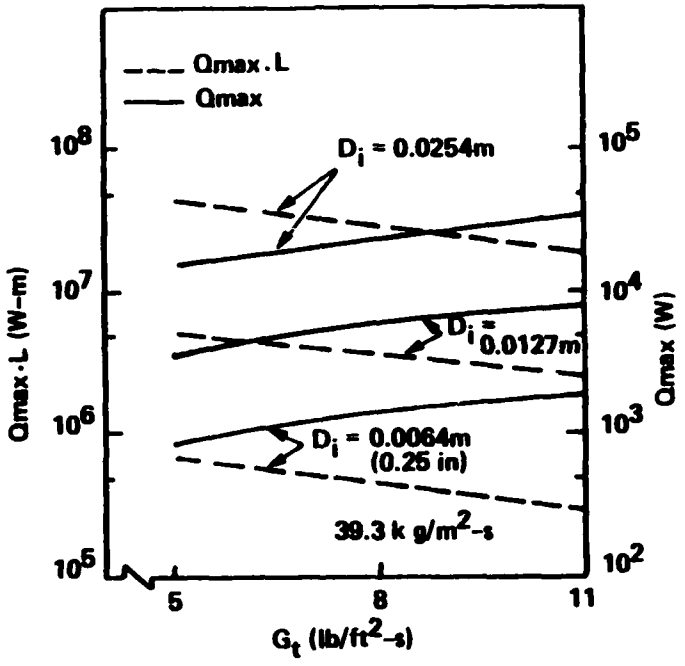

Transport length conservatively evaluated with assumption that two-phase mixture flows as saturated vapor; that is, the pressure drop per unit length is everywhere at its maximum value.

X-6-7

SUMMARY OF CHARACTERISTICS

The list opposite summarizes the characteristics of a pumped, two-phase heat transport system. Noteworthy features are:

- About 100 times less pumping power than equivalent single-phase systems;
- About 1000 times greater Q x L product than most advanced heat pipe concepts;
- Behavior of two-phase heat transfer and fluid flow is less well understood than single-phase behavior, particularly in a near-zero gravity environment;
- R&D required to validate and optimize design.

8-9-X

CHARACTERISTICS OF PUMPED, TWO-PHASE HEAT TRANSPORT SYSTEM

- Capillary pressure, boiling, priming, and entrainment limits of the heat pipe do not apply.
- The end-to-end pressure drop in the fluid stream is set by the end-to-end drop in saturation temperature of the bulk fluid.
- No fundamental restrictions on pipe routings or elevation changes as influenced by gravity.
- Pressure changes in the fluid loop arising from any cause (elevation change, altered flow regime, etc.) will be accommodated by a positive displacement liquid pump supplying fluid at constant mass flow rate.
- Very large heat capacity – transport length products are possible.
- Only a few watts of electric pumping power is required to transfer kilowatts of thermal power over tens of meters.
- The heat transfer taking place at heat stations and space radiators involves change of phase with coefficients which are large but are influenced by gravity.
- Has readily controllable set-point temperature for system working fluid.

SYSTEM APPLICATION

By way of example, the figure opposite shows a concept for a pumped, two-phase thermal utility loop applied to a multiplicity of instruments mounted on representative pallets. The system dissipates about 8 kW maximum at 20°C, weighs about 350 kg (50% being the radiators), uses ammonia as the working fluid, and requires about 1 W of electric power for the pump.

X-6-10

CONFIGURATION FOR A TWO-PHASE HEAT TRANSPORT LOOP USING RADIATORS WITH HEAT PIPE DISTRIBUTION

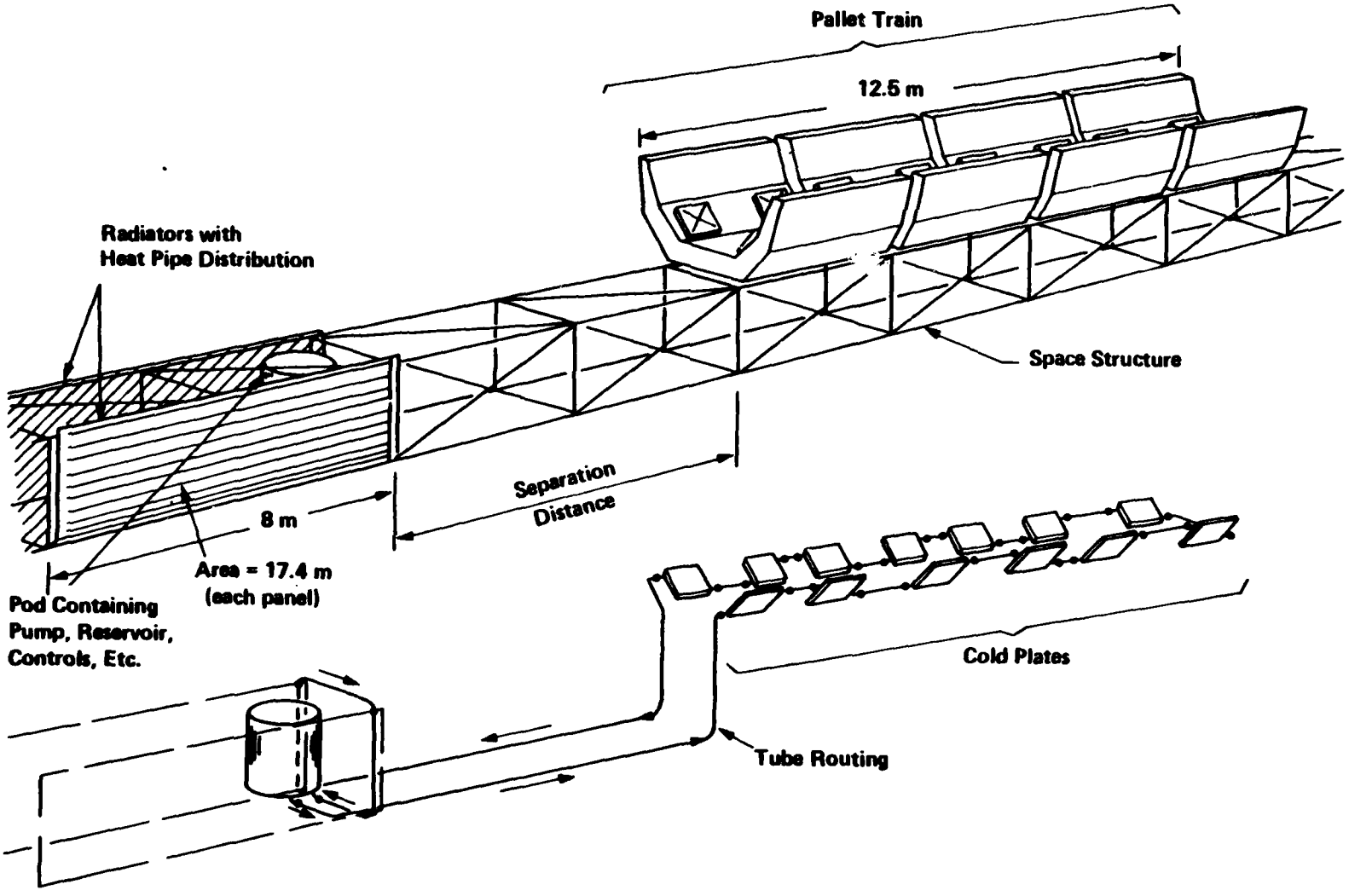

X-6-11

BASIC SCIENTIFIC RESEARCH GOALS AND RESEARCH APPROACH

The first step toward realizing the goals expressed opposite is to create a flow system in an earth-based laboratory model system that has flow and change of phase heat-transfer characteristics that can be interpreted unambiguously for the space-based application. The basic approach to this objective is to create the same steady flow regimes and have scaled-force polygons at homologous points in the earth-model and space-prototype system. This is the conventional approach of dimensional analysis but, as always, when considering a system whose behavior is determined by a multiplicity of dimensions (properties of the system), a good deal of physical insight and ingenuity is required in its application.

The limitation of producing scaled-force polygons at homologous points in model and prototype is sufficient to give unambiguous predictions for the behavior of the prototype flow if it is adiabatic. Adherence to this scaling method should also give accurate data on condensing heat-transfer characteristics, because the controlling aspect of these characteristics is the dominant thermal resistance of the liquid film. If the configurations of this film is identically similar in model and prototype flows, test data on the model should suffice for accurate extrapolation to the prototype.

On the other hand, gravity has an important small-scale (bubble dimensions) influence on boiling heat transfer due to induced circulation and mixing effects. Similitude in these respects will not be preserved in the proposed approach and results relating to boiling heat transfer would have accurate quantitative significance only in cases where forced convective effects across relatively thin liquid films are dominant.

In any event, the first-order effect of forcing the fluid into the same configuration within the tube would appear to be an appropriate first step in approaching similarity as regards evaporative heat transfer and, moreover, forced convection across relatively thin films is expected to be a dominant effect for many flows of interest at flow qualities in excess of 10 or 20 percent.

The justification of the work outlined has been based primarily on its application to the optimum design of a two-phase heat transport system. However, research and development of such a fundamental nature in an area of fluid mechanics and heat transfer which is incompletely understood will have a payoff in yet unanticipated applications.

BASIC SCIENTIFIC RESEARCH GOALS
AND RESEARCH APPROACH

Basic Scientific Research Goals:

- Develop the knowledge sufficient to predict unambiguously the flow-pressure drop characteristics of a two-phase flow (under flow conditions of interest) in a near-zero gravity environment.
- Develop the knowledge sufficient to predict evaporative and condensing heat transfer (under flow conditions of interest) in a near-zero gravity environment.

Research Approach:

- Utilize analysis and dimensionally scaled, earth-based model studies to establish the same steady flow regimes that would exist in the space prototype system.
- Make predictions of pressure drop vs flow-rate based on established models and compare with measurements.
- Make predictions of evaporative and connective heat transfer, based on established models.
- Conduct zero-g verification tests on CX-135 (possibly) or Shuttle/Spacelab.

X-6-13

MODELLING OF ZERO-G, TWO-PHASE FLOWS: AN EXAMPLE

The figure opposite depicts possible flow circumstances within the constraints of an adiabatic, incompressible, steady flow in a pipe with system characteristics as defined and within the assumption that either annular or axi-symmetric slug/bubble flow regimes will occur. The prediction results from the application of momentum and continuity laws. An evaluation of pressure drop is inherent to and results from the analysis.

Application of dimensional analysis to the system shows that, in general, six independent dimensionless moduli are the determinants of possible flow regimes. Further, by the arguments and tests set forth by Suo and Griffith, for small Bond number (low-gravity) and large ratios of liquid-to-gas density and viscosity, the dimensionless moduli which determine the flow regimes are reduced to three. In the range of values that the three moduli had in their tests, three flow regimes appeared: slug/bubble, annular, and bubbly or frothy. The transitions from slug/bubble to annular and from slug/bubble to bubbly were correlated empirically as functions of the dimensionless parameters.

The analyses and tests of Suo and Griffith were carried out with laminar gas and liquid two-phase flows. As suggested by them, they have applications in the case of low-gravity environments. The figure opposite extends the analysis to a more useful flow circumstance where the gas is turbulent and the liquid is laminar. The actual flow regimes which will occur under these circumstances would have to be determined by model tests of the kind performed by Suo using capillary tubes to achieve small Bond numbers.

X-6-14

PREDICTED TWO-PHASE FLOW CHARACTERISTICS OF R-11 AT LOW-GRAVITY
GAS-TURBULENT; LIQUID-LAMINAR

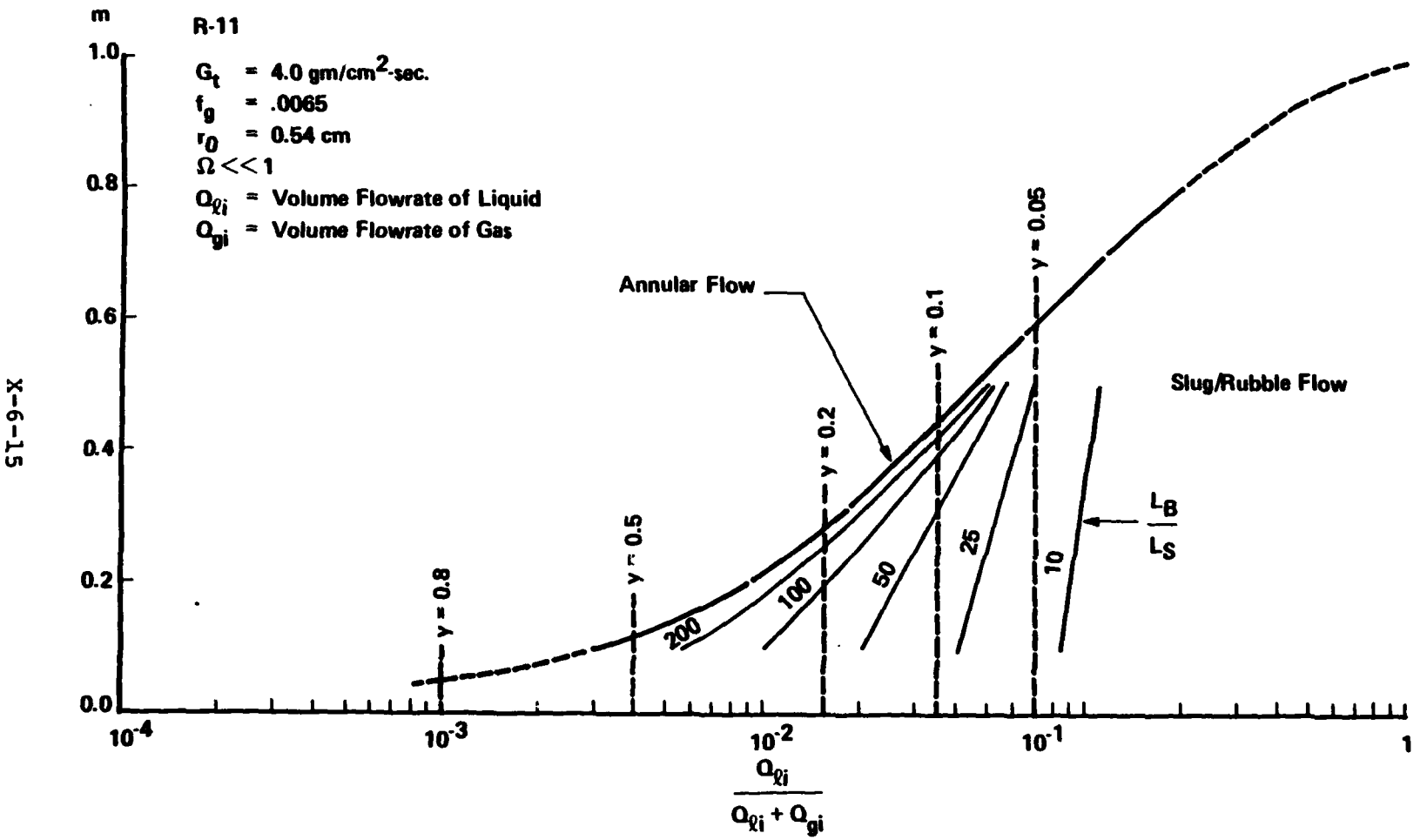

X-6-15

Q & A - A. A. Fowle

From: P. J. Turchi, R & D Associates

Question re: Interaction of space environment (magnetic fields, etc.) with liquid metal ribbon radiator

Answer:

I'll submit to author. I presume your concern is with electro-magnetic effect on moving conductor. I'd venture effects too small to threaten integrity of ribbon system. They are in common with droplet spray radiator.

SELECTED BIBLIOGRAPHY

Anderson, S.W., Rich, D.C., and Geary, D.F., "Evaporation of Refrigerant 22 in a Horizontal 3/4 in. o.d. Tube," ASHRAE J, Vol. 6, Sept. 1964, pp. 58-65, and Vol. 6, Oct. 1964, pp. 73-77.

Baker, O., "Simultaneous Flow of Oil and Gas," Oil Gas J., 53, 185 July 26, 1954.

Chawla, J.M., "Local Heat Transfer and Pressure Drop for Refrigerants Evaporating in Horizontal Tubes," (translated from German) Kältetecknik-Klimatisierung, 19. Jahrgang-Heft 3, 1967.

Chisholm, D., "Pressure Gradients Due to Friction During the Flow of Evaporating Two-Phase Mixtures in Smooth Tubes and Channels," Int. J. Heat Mass Transfer, Vol. 16, 1973, pp. 347-358.

Feldmanis, C.J., "Performance of Boiling and Condensing Equipment Under Simulated Outer Space Conditions," ASD-TR-63-862, Nov. 1963.

Fowle, A.A., "A Pumped, Two-Phase Flow Heat Transfer System for Orbiting Instrument Payloads," AIAA 16th Thermophysics Conference, June 1981.

Furse, F.G., "Heat Transfer to Refrigerants 11 and 12 Boiling Over a Horizontal Copper Surface," paper presented to ASHRAE, Jan. 1965.

Homman, G.H., "Boiling Heat Transfer from Freons on Horizontal Smooth and Firmed Tubes," Heat Transfer-Soviet Research, Vol. 4, No. 3, May-June 1972.

Gouse, S.W., Jr., and Dickson, A.J., "Heat Transfer and Fluid Flow Inside a Horizontal Tube Evaporator," paper presented to ASHRAE, Jan. 1966.

Kamotani, Yasuhiro, "Evaporator Film Coefficients of Grooved Heat Pipes," American Institute of Aeronautics and Astronautics, 1978.

Keshock, E.G. and Sadeghipour, M.S., "Analytical Comparison of Condensing Flows Inside Tubes Under Earth-Gravity and Space Environments," Paper IAF-81-130, 32nd International Aeronautical Congress, Rome Italy, Sept. 1981.

SELECTED BIBLIOGRAPHY (Continued)

Kubanek, G.R. and Miletti, D.L., "Evaporative Heat Transfer and Pressure Drop Performance of Internally-Finned Tubes with Refrigerant 22," ASME Paper No. 77-WA/HT-25, Dec. 1977.

Lockhart, R.W. and Martinelli, R.C., "Proposed Correlation of Data for Isothermal Two-Phase, Two-Component Flow in Pipes," Chem. Eng. Prog., Vol. 45, No. 1, 1949, pp. 39-48.

Luu, Minh and Bergles, A.E., "Experimental Study of the Augmentation of In-tube Condensation of R-133," prepared for ASHRAE Transactions, May 1979.

Marner, W.J. and Bergles, A.E., "Augmentation of Tubeside Laminar Flow Heat Transfer by Means of Twisted-Tape Inserts, Static-Mixer Inserts, and Internally Finned Tubes," International Heat Transfer Conference, Aug. 1978.

Palen, J.W., Breber, G., and Taborek, J., "Prediction of Flow Regimes in Horizontal Tube-Side Condensation," Heat Transfer Engineering, Vol. 1, No. 2, Oct.-Dec. 1979, pp. 47-57.

Pierre, B., Kylteknisk Tidskrift, No. 3, May 1957, p. 129, "Flow Resistance with Boiling Refrigerants," ASHRAE J., Vol. 6, Sept. 1964, pp. 58-64, Vol. 6, Oct. 1964, pp. 73-77.

Robertson, J.M. and Lovegrove, P.C., "Boiling Heat Transfer with Freon 11 in Brazed-Aluminum Plate-Fin Heat Exchangers," ASME Paper No. 80-HT-58, July 1980.

Rohsenow, W.M., Ed., Developments in Heat Transfer, the M.I.T. Press, 1969.

Siegel, R. and Usiskin, C., "Photographic Study of Boiling in the Absence of Gravity," Trans. ASME, J. Heat Trans., Vol. 81, No. 3, Aug. 1959.

Suo, M. and Griffith, P., "Two-Phase Flow in Capillary Tubes," Transactions ASME, Sept. 1964.

Suo, M., "Two-Phase Flow in Capillary Tubes," S&D Thesis, Mechanical Engineering Department, Massachusetts Institute of Technology, March 1963.

LIQUID RIBBON RADIATOR FOR LIGHTWEIGHT SPACE RADIATOR SYSTEMS

Prepared for

AIR FORCE OFFICE OF SCIENTIFIC RESEARCH

Special Conference On

Prime Power for High-Energy Space Systems

Norfolk, Virginia

by

ARTHUR D. LITTLE, INC.
Cambridge, Mass. 02140

February 29, 1982

ABSTRACT

THE LIQUID METAL RIBBON (CMR) RADIATOR CONCEPT DESCRIBED OPERATES BY FORMING A THIN (10-100 μm) LIQUID METAL MENISCUS ON A WIDE MESH SCREEN STRUCTURE WHICH IS DRAWN THROUGH SPACE BY A RETRACTABLE PULLEY SYSTEM. THE LIQUID METAL BATH FROM WHICH THE LIQUID METAL RIBBON IS FORMED CAN BE A HEAT DISSIPATION SINK FOR A SPACE BORN POWER SYSTEM OR SPACE THERMAL CONTROL SYSTEM.

PRELIMINARY ANALYSIS INDICATES THAT RADIATORS FORMED IN THIS WAY SHOW PROMISE OF ACHIEVING WEIGHTS ONE TENTH TO ONE FOURTH THOSE OF CONVENTIONAL SPACE RADIATORS UTILIZING HEAT PIPE CONFIGURATIONS. FILM MATERIALS WHICH HAVE BEEN COMBINED INCLUDE GALLIUM, TIN, AND LITHIUM. THESE MATERIALS COVER A WIDE RANGE OF POTENTIAL HEAT REJECTION TEMPERATURE NEEDS.

IMPORTANT TECHNICAL ISSUES TO BE ADDRESSED IN EVALUATING THE POTENTIAL FOR THE CMR CONCEPT INCLUDE DETERMINING APPROACHES FOR INCREASING SURFACE EMISSIVITIES OF THE FILMS AND MAINTAINING STABLE, THIN, FILM STRUCTURES WITH THE PULL SPEEDS AND MATERIALS OF INTEREST.

SYSTEM COMPONENT

- A BATH OF LIQUID METAL. THIS BATH IS SHOWN AS THE HEAT REJECTION SINK OF A THERMAL POWER PLANT. IT COULD ALTERNATIVELY BE A HEAT REJECTION SINK OF A SPACECRAFT EQUIPMENT COOLING SYSTEM.

- AN EXTENDABLE PULLEY SYSTEM OVER WHICH IS STRETCHED A WIDE MESH, LIGHTWEIGHT, SCREEN MATERIAL.

CONCEPT RATIONALE

- ONE OF THE MAJOR PROBLEMS IN GENERATING LARGE AMOUNTS OF POWER IN SPACE IS THE LARGE WEIGHT OF THE RADIATORS REQUIRED TO REJECT HEAT.
- IN MANY CASES, THE RADIATOR WEIGHT REPRESENTS OVER 50 PERCENT OF TOTAL POWER PLANT WEIGHT USING PRESENTLY AVAILABLE CONFIGURATIONS (PRIMARILY VARIOUS FORMS OF HEAT PIPE SYSTEMS).
- PRESENT RADIATOR SYSTEMS DO NOT LEND THEMSELVES PARTICULARLY WELL TO COMPACT STORAGE DURING SPACE VEHICLE LAUNCH OR EASE OF DEPLOYMENT ONCE IN SPACE.
- THE LMR CONCEPT PROMISES MARKEDLY IMPROVED CHARACTERISTICS COMPARED TO THOSE OF CONVENTIONAL DESIGN. I.E., LIGHTER WEIGHT AND COMPACT STORAGE.

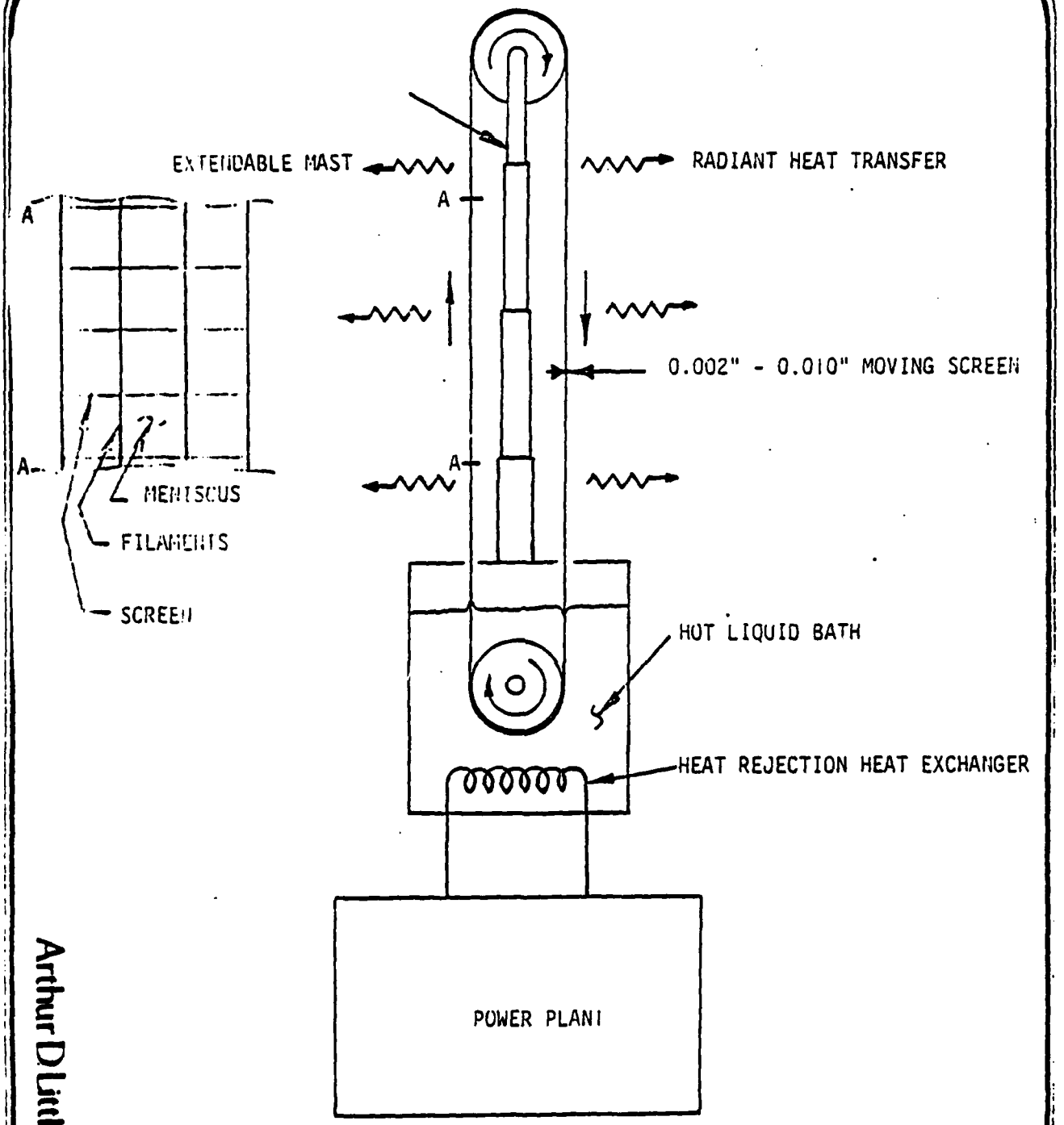

FIGURE 1 SCHEMATIC OF LIQUID SPACE RADIATOR SYSTEM

Arthur D Little Inc

2-12

SYSTEM OPERATION

- DURING OPERATION THE SCREEN MATERIAL IS DRAWN THROUGH THE HOT LIQUID BATH. A THIN MENISCUS (<5 MILS) OF THE BATH MATERIAL IS FORMED WITH THE BOUNDARIES DEFINED BY THE THREADS OF THE SCREEN (SIMILARLY AS A SOAPY WATER MENISCUS IS FORMED IN A BUBBLE BLOWING FORM).

- AS THE THIN MENISCUS/SCREEN RIBBON IS DRAWN THROUGH SPACE, THE MENISCUS RADIATES TO THE ENVIRONMENT AND THEREBY DISSIPATES ENERGY. THE COLDER MATERIAL IS RETURNED TO THE BATH FOR REHEATING, AND A NEW MENISCUS WITH HEATED MATERIAL IS FORMED THEREBY REPEATING THE PROCESS.

OPERATING MODES

(A) NON-PHASE CHANGE MODE

THE COMBINATION OF PULLEY SPEED ON BOTH MATERIAL AND OPERATING TEMPERATURES CAN BE ADJUSTED SO THAT THE MENISCUS WILL STAY LIQUID THROUGHOUT THE PROCESS. IN THIS ARRANGEMENT THE HEAT DISSIPATION TAKES PLACE IN THE FORM OF A SENSIBLE HEAT LOSS (AND CORRESPONDING TEMPERATURE REDUCTION) IN THE MENISCUS MATERIAL DURING ITS TRAVERSE THROUGH SPACE.

(B) PHASE CHANGE MODE

PULLEY SPEED, TEMPERATURES, AND MATERIAL COMBINATIONS CAN ALSO BE SELECTED WHEREBY THE MENISCUS ACTUALLY SOLIDIFIES DURING THE COURSE OF RADIANT HEAT REJECTION. IN THIS CASE, THE HEAT REJECTION MECHANISM IS PRIMARILY DUE TO THE HEAT OF FUSION OF THE MENISCUS MATERIAL AND CAN TAKE PLACE OVER A VERY NARROW TEMPERATURE RANGE.

BATH WORKING FLUID REQUIREMENTS

- A LOW VAPOR PRESSURE IN THE LIQUID STATE SO THAT ONLY TOLERABLE AMOUNTS OF MATERIAL WILL NOT BE LOST TO SPACE BY EVAPORATION.
- A HIGH SURFACE TENSION SO THAT A STABLE MENISCUS CAN BE FORMED IN THE WIDE SPACED MESHES OF THE SCREEN MATERIAL.
- EXIST AS A LIQUID IN A SUITABLE RANGE OF OPERATING TEMPERATURES.

TABLE 1

PROPERTIES OF CANDIDATE MATERIALS

MAT'L	M.W.	SP.GR.	M.P. (°)	B.P. (°)	C_p (CAL/GM-°C)	HEAT OF FUSION J/GM	SURFACE TENSION (GM/SEC^2)	APPROX. VAPOR PRESS. @ M.P., P_V (TORR.)	P_V^*(1) (TORR.)
Ga	69.7	6.1	29.8	2071	0.082	82.1	720	$<10^{-30}$	6.9×10^{-10}
Hg	200.6	13.6	-38.6	357	0.033	11.3	480	2×10^{-6}	7.9×10^{-10}
In	114.8	7.31	156.4	>1450	0.057	28.5	590	1×10^{-16}	7.7×10^{-10}
Li	6.94	0.53	180.0	1347	0.83	663	394	1×10^{-10}	2.3×10^{-10}
Na	22.99	0.87	97.8	883	0.30	114	202	1×10^{-7}	1.9×10^{-10}
Sn	118.7	7.30	231.9	2270	0.054	60.3	530	1×10^{-18}	8.2×10^{-10}

(1) P^* IS VAPOR PRESSURE OVER THE LIQUID RESULTING IN EVAPORATED LOSS OF 1 μM/YR. ACTUAL MATERIAL LOSS IS $\frac{P_V}{P_V^*}$ MICROMETERS PER YEAR.

Arthur D Little, Inc

ESTIMATED PERFORMANCE

FIGURE 2 COMPARES THE MASS OF A RIBBON RADIATOR WITH THAT OF A CONVENTIONAL TYPE RADIATOR AS DEPENDENT ON THE PROPERTIES OF THE LIQUID FILM. WITH AN EMISSIVITY OF 0.1 A $\rho\delta$ VALVE OF 0.1 CORRESPONDS ROUGHLY TO A LIQUID FILM THICKNESS OF 10 μm AND 100 μm WHEN GALLIUM AND LITHIUM ARE USED RESPECTIVELY. THE CORRESPONDING RADIATOR WEIGHT RATIO IS ABOUT 0.5. INCREASING FILM EMISSIVITIES WOULD MARKEDLY IMPROVE THE WEIGHT SAVINGS.

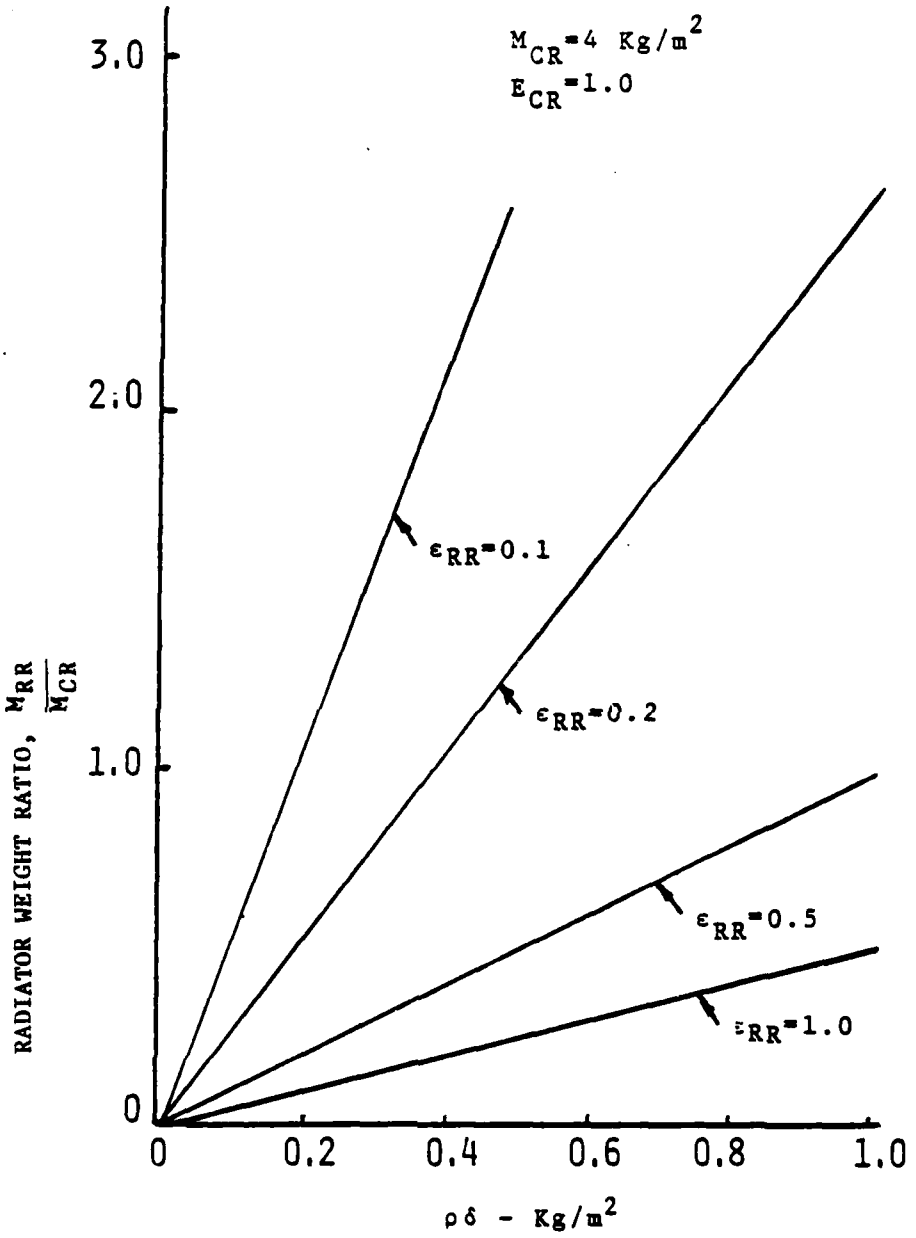

FIGURE 2 MASS OF LIQUID RIBBON RADIATOR COMPARED TO CONVENTIONAL DESIGN

Arthur D Little Inc.

4.0 COMPARISON WITH PRESENT PRACTICE

- THE CONCEPT OF THE LIQUID RIBBON RADIATOR HAS THE POTENTIAL OF REALIZING A REDUCED MASS AS MUCH AS ONE TENTH THAT OF CONVENTIONAL RADIATORS.

- THE CONCEPT HAS THE CHARACTERISTIC OF RELATIVELY EASY AND COMPACT STORAGE FOR LAUNCH AND EASY ERECTION FOR OPERATION.

- THE CONCEPT IS INVULNERABLE TO METEORITE IMPACT. A HIT WOULD ONLY KNOCK OUT A PORTION OF THE RADIATING SURFACE-- THE REST WOULD FUNCTION WITHOUT CHANGE.

- THE CONCEPT IS READILY ADAPTABLE TO SERVE AS A THERMAL CONTROL ELEMENT BY SIMPLY CHANGING THE LENGTH OF THE BELT AND, THEREBY, MATCHING THE HEAT REJECTION REQUIREMENTS AND THE TEMPERATURE AT WHICH THE HEAT IS REJECTED.

TECHNICAL ISSUES

- INCREASING THE SURFACE EMITTANCE OF LIQUID METAL FILMS BY MEANS OF CONTAMINENTS.

- DETERMINING PRACTICAL LIMITS OF MINIMUM FILM THICKNESS AS INFLUENCED BY:

  - BATH MATERIAL
  - MESH DIMENSIONS AND MATERIAL
  - MESH/FILM PULL SPEEDS
  - OPERATING MODE (PHASE CHANGE VS. NON-PHASE CHANGE)

SOFTWARE FOR COMPARISON AND OPTIMIZATION OF POWER SYSTEMS

BY

GREG BERRY

ARGONNE NATIONAL LABORATORY
ARGONNE, ILLINOIS

SOFTWARE FOR COMPARISON AND OPTIMIZATION OF POWER SYSTEMS

by

Greg Berry

Argonne National Laboratory
Argonne, Illinois

Interest in examining alternative power system concepts have increased recently. Such analysis have become very involved, regardless of the degree of sophistication employed in modeling the individual component models of the system or the extent of the property data base used. Specification of the models, interconnecting flow streams, property data, constraints independent variables and objective function (for optimization problems) can quickly become a formidable task, especially in attempting to conform to the format of any particular systems code.

The systems code presented herein has been designed for the non-expert user by the development of a sophisticated language translator and executive code preprocessor. These two modules also permit great flexibility in allowing the user to specify the system in his own style rather than conforming to a rigid structure determined by a precompiled computer code. The user may also choose his only naming convention and can use free format input.

This paper will also be concerned with the solution procedures available. The systems code uses Powell's hybrid method for solving N-dimensional non-linear equations and Brent's method for a 1-dimensional equation. Powell's variable metric constrained method is used for N-dimensional non-linear optimization and Brent's method for the optimization of one variable.

This systems code (SALT) has been written to be used as an evolving analysis tool rather than a definitive encompassing code. It is easy to modify the code (which is completely modularized) to meet particular needs, especially to include the users component models which may be of interest to him.

EVALUATION REQUIREMENTS FOR ALTERNATIVE CONCEPTS

I FLEXIBLE SYSTEM CODE

II OPTIMIZATION

III TECHNICAL ASSESSMENT

IV RISK/BENEFIT ANALYSIS

V COST AND TIME

EVALUATION REQUIREMENTS FOR ALTERNATIVE CONCEPTS

This viewgraph describes the requirements for performing the necessary evaluations of different system concepts. As the system becomes more complicated, and as some of the alternatives become seemingly less comparable, a systems code is needed to handle the complexity and assure a common basis of comparison. Optimization capability is important because it allows the evaluator to examine a full range of parameters and select the best parameters for each concept for the various scenarios the evaluator is interested in. Not only must the evaluator be concerned with the system comparison, but he must also make sure the system performs as stated in the system performance specifications; therefore, he needs a means to check system performance. Risk/Benefit analysis is performed because the bottom line is usually economics and thus cost models, economic models and forecasting models should be included in the evaluation. Finally, the evaluation itself will cost time and money, thus the evaluator will prefer inexpensive and fast methods of comparison.

SYSTEMS CODE

LANGUAGE TRANSLATOR

PREPROCESSOR

DRIVER (EXECUTIVE CODE)

INTERFACE

COMPONENT MODELS

PROPERTY LIBRARY

UTILITY SUBROUTINES

SOLUTION PROCEDURES

OUTPUT PROCESSING

SYSTEMS CODE

The systems code (SALT) is in actuality a combination of many modules. These modules and their function are: (1) a language translator to allow the user maximum flexibility in specifying the system configuration with a minimum amount of syntax; (2) a preprocessor which uses the data generated by the language translator to assemble a meaningful system, correctly formatting each statement, and then writing a driver using the computer language compiler; (3) a driver whose function is to control and monitor the solution of the system analysis problem; (4) an interface to couple the code hierarchy to the elements representing the actual system to be analyzed; (5) component models which simulate the performance of the actual system components; (6) a property library (or libraries) to provide state point information; (7) utility subroutines which perform the actual computations and are also common to the higher level portions of the systems code; (8) solution procedures, the numerical essence of the code (e.g., equation solvers and optimizers) which should be the state-of-the-art in numerical software; and (9) output processing to present the results in a form understandable by the user (including pertinent error messages and graphics packages).

EXECUTIVE CODE

CONNECTS COMPONENT MODELS

FLOW OF INFORMATION

CONSTRAINTS

OPTIMIZATION

SOLUTION TECHNIQUES

EXECUTIVE CODE

The executive code has several functions. First, it must connect the component models in the correct manner to simulate the system under study. Secondly, it must process the flow of information (e.g., thermodynamic properties, power, cost) between the component models. Thirdly, it must make sure all of the constraints on system performance are met. Fourthly, it must select the type of problem to be solved (e.g., optimization, parameter sweep, operation simulation or design analysis). Finally, it must select and monitor the solution procedure to assure progress is being made.

SOLUTION TECHNIQUES

EQUATION SOLVERS

- INVERSE CALLING
- NESTING
- SUBROUTINE FUNCTION
- BUILT-IN SELF-SCALING
- RETENTION OF JACOBIANS
- SPECIFIC TECHNIQUES
  - POWELL'S HYBRID METHOD
  - BROYDEN UPDATE
  - 1-D BRENT'S METHOD

OPTIMIZERS

- INVERSE CALLING
- NESTING
- SPECIFIC TECHNIQUES
  - POWELL'S VARIABLE METRIC CONSTRAINED METHOD
  - BRENT'S METHOD FOR 1-D
- POLYALGORITHMIC OPTIMIZATION

SOLUTION TECHNIQUES

A modification to Powell's hybrid method is the equation solver used because it is the fastest and most reliable for the general non-linear problem. Other methods are also available if the user wishes. The methods have been coded so that they are in an inverse calling sequence; hence, they can be recursive and be used by the component models and/or the property library routines simultaneously with the executive code. To make a problem more manageable, it is also possible to nest the sub-systems. A built-in self scaling capability has eliminated errors eminating from a set of poorly scaled equations. By retaining the Jacobians, automatic restart is possible. This greatly reduces the computational time for many problems (e.g., parameter sweeps).

Powell's variable metric constrained method is used to solve the generalized non-linear optimization problem. Again, it has inverse calling sequence (for subsystem optimization) and nesting. A polyagorithmic optimization routine is also available for highly non-linear problems. In this routine optimization is automatically switched between several optimizers depending the apparent smoothness of the objective function iterative evaluations.

PROCESS MODELING

COMBUSTION

GAS-PARTICLE RADIATION

PARTICLE FORMATION

PARTICLE GROWTH

NO KINETICS

SECONDARY COMBUSTION

PARTICLE DEPOSITION

FAST CHEMICAL EQUILIBRIUM

PARTICLE REMOVAL

SLAG/SEED INTERACTION

ZONE METHOD OF HEAT TRANSFER

OPTICAL PROPERTIES OF SLAG

PROCESS MODELS

Most of the models currently available were developed to model coal-fired power plants (including MHD, fuel cells and combined cycle gasification). These models are used to calculate accurate process information which is then used in the component models. All models needed to simulate certain types of coal-fired power plant performance are available. The user can also supply his own models and connect it to the system through the interface module.

LONG RANGE ACTIVITIES

I. CONFIGURATION OPTIMIZATION

II. RISK ASSESSMENT

III. DYNAMIC ANALYSIS

IV. LIFE CYCLE ANALYSIS

LONG RANGE ACTIVITIES

There are specific areas where we project a systems analysis need and are processing the state-of-the-art to meet those needs.

A heat exchanger configuration optimization code has been developed (not fully tested) that can automatically reconfigurate a heat exchanger network to select the minimum cost design subject to thermodynamic and process limitations. Hopefully, this technique can be extended to the entire power system.

Risk assessment implies probability analysis. Using chance constrained programming techniques, the existing system code can be used to solve generalized system stochastic programming problems.

Work is underway to determine if the existing system methodology can be extended to the power system control problem.

Daily cycle analysis have been performed for very simple systems with time dependent capacitance. It is planned to extend this method to life cycle analyses of power systems.

BIBLIOGRAPHY

1. Dennis, C., and Berry, G., "User's Guide for the GSMP/OCMHD System Code," ANL/MHD-80-7, 1980.

2. Cook, J., "User's Guide for GSMP, A General System Modeling Program," ANL/MHD-79-11, 1979

3. Berry, G., and Cook, J., "Application of a General System Modeling Program," Advances in Computer Technology, Emerging Technology Conference, 1980.

4. Berry, G., and Cook, J., "Application of Polyalgorithmic Optimization to MHD Power Plant Design," International Energy Symposia, SFE-81-85, 1981.

5. Berry, G., and Dennis, C., "Performance Analysis of the MHD Steam Combined Cycle, Including the Influence of Cost," ANL/MHD-80-3, 1980.

6. Berry, G., and Dennis, C., "Performance Analysis of the MHD Steam Combined Cycle, Including the Influence of Cost," Proc. Symposium on Instrumentation and Control for Fossil Energy Processes, A059, 1981.

7. Powell, M. J. D., "A Hybrid Method for Nonlinear Equations," in Numerical Methods for Nonlinear Algebraic Equations, Gordon and Breach Science Publishers, 1970.

8. Powell, M. J. D., "A Fortran Subroutine for Solving Systems of Nonlinear Equations," ibid.

9. Geyer, H., "GPSAP/V2 with Applications to Open-Cycle MHD Systems," ANL/MHD-80-15, 1980.

10. Geyer, H., "A Simple Code for Chemical Equilibrium and Thermodynamic Properties for Use with GPSAP," ANL/MHD-81-11, 1981.

11. Doe, N., Graph Theory with Applications to Engineering and Computer Science, Prentice-Hall Inc., 1974.

12. Himmelblau, D., ed., Decomposition of Large-Scale Problems, North-Holland Publishing Co., 1973.

13. Powell, M. J. D., "The Convergence of Variable Metric Methods for Nonlinearly Constrained Optimization Calculations," ANL/AMD-TM-315, 1977.

14. Technical Assessment Guide, EPRI-PS-1201 SR, July 1979.

15. Powell, M. J. D., "A Fast Algorithm for Nonlinearly Constrained Optimization Calculations," presented at the 1977 Dundee Conference on Numerical Analysis.

UNCERTAINTIES IN THERMAL-STRUCTURAL ANALYSIS OF LARGE SPACE STRUCTURES

Earl A. Thornton, Associate Professor
Mechanical Engineering and Mechanics Department
Old Dominion University
Norfolk, Virginia 23508

ABSTRACT

Uncertainties in the thermal-structural analysis of large space structures are briefly described. Thermal-structural design challenges faced by structural engineers are highlighted. Some basic questions arising in predictive analyses are identified and illustrated with recent research. Areas for further research are discussed, and the need for fundamental thermal-structural experiments is cited.

INTRODUCTION

The flights of Columbia have given added impetus to large space structures research. The United States is developing large space structures to be placed in earth orbit during the last two decades of this century and the early part of the next century. These structures of precedented size and complexity present significant challenges to structural engineers. Their large size but stringent requirements for small deformations have focused attention on the role of thermal effects on the structural response. Utilization of multimegawatt power systems may have a significant effect upon the structural design. This paper briefly describes challenges faced by structural engineers and identifies some uncertainties in the thermal-structural analysis (T-S-A) of large space structures.

INTRODUCTION

- NEW CHALLENGES OF LARGE SPACE STRUCTURES
  - –IMPORTANCE OF THERMAL–STRUCTURAL ANALYSIS (T–S–A)
  - –SIZE OF STRUCTURES
  - –CONTROL OF DEFORMATION
- PURPOSE OF TALK
  - –DESCRIBE UNCERTAINTIES IN T–S–A OF LARGE SPACE STRUCTURES
- SCOPE
  - –CHARACTERISTICS OF TYPICAL STRUCTURES
  - –MOTIVATION FOR HIGHLY EFFECTIVE ANALYSIS
  - –HEATING, THERMAL AND STRUCTURAL RESPONSE
  - –SOME UNCERTAINTIES
  - –RECENT STUDIES

A TETRAHEDRAL TRUSS SPACE STRUCTURE

To illustrate some aspects of the challenges arising in the design of large space structures consider a parabolic tetrahedral truss designed to support a microwave radiometer. The truss has a diameter of 725 m (2380 ft.) yet operational requirements limit surface deformations to within approximately 6 mm (0.020 ft.). The role of thermal deformations in the structural response thus has basic importance. A fundamental impediment to the analysis and optimized design of such structures is the size of required analytical models; the structure shown consists of 900 nodes and 2700 members. The structural analysis alone involves solving 2700 time-dependent simultaneous equations. Because of their light weight, high stiffness and low coefficient of thermal expansion (CTE), advanced composites are the structural materials under consideration. Although advanced composite materials have been extensively studied for low speed aircraft, there is a lack of understanding of: (1) their properties over the wide temperature range experienced in space, and (2) their performance in the long-term cyclical thermal environment of earth orbit.

24 BAY PARABOLIC TETRAHEDRAL TRUSS

- 900 NODES, 2700 MEMBERS
- LOW WEIGHT, HIGH STIFFNESS DESIGN
- "ZERO" CTE

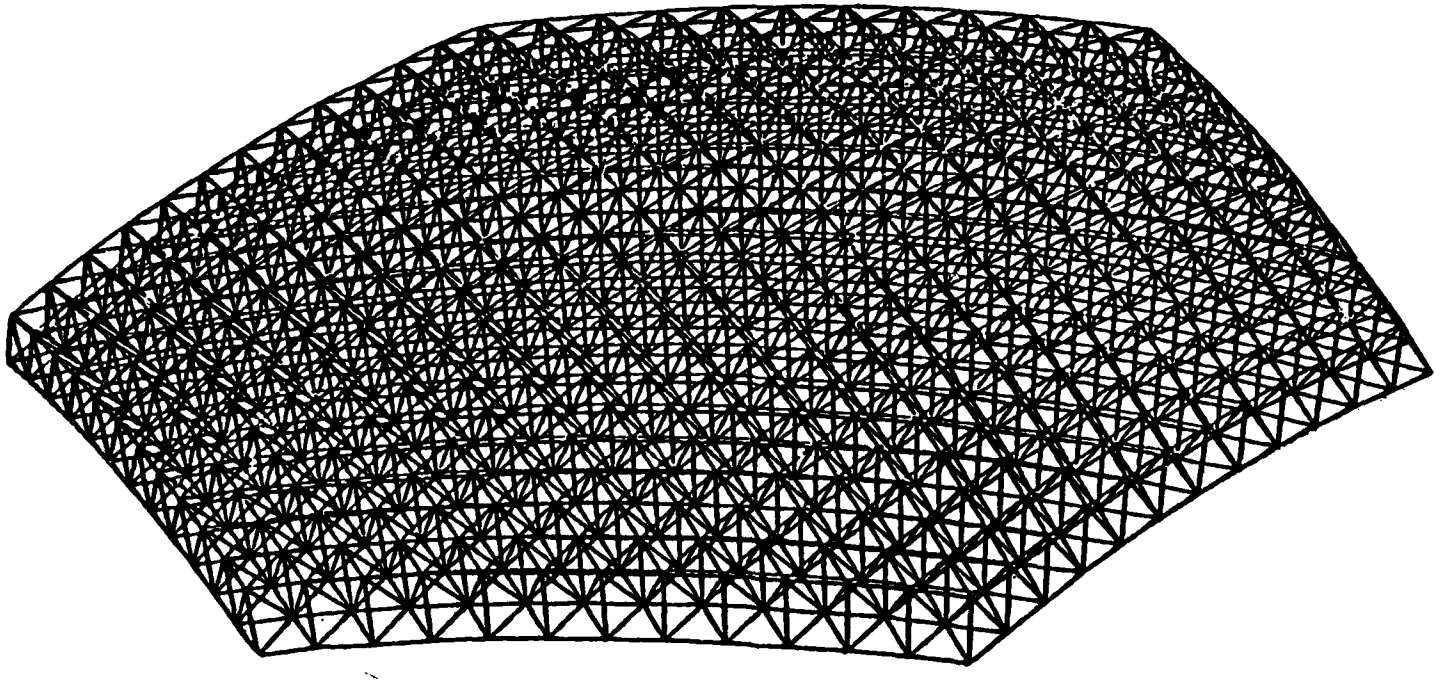

MOTIVATION FOR HIGHLY EFFECTIVE T-S-A

Although the thermal-structural response of earth satellites has been considered for over two decades, the necessity to predict and control thermal deformations of large space structures within very small tolerances has caused a re-examination of existing analytical capabilities. Important factors underlying the need for effective analysis methods include: (1) the size of the proposed structures will limit ground testing, (2) the design of active and passive structural control systems depend on a knowledge of distortions, (3) new structural designs and materials introduce novel problems, and (4) the complex thermal environment of space requires solution of very large nonlinear, transient thermal-structural problems.

MOTIVATION FOR HIGHLY EFFECTIVE T-S-A

- SMALL TOLERANCES ON DISTORTIONS
- LACK OF GROUND TESTING
- ACTIVE AND PASSIVE DISTORTION CONTROL SYSTEM DESIGNS
- NEW STRUCTURAL DESIGNS AND MATERIALS
- COMPLEX THERMAL ENVIRONMENT

SOME UNCERTAINTIES

The basic uncertainties concern the capability and reliability of the analysis methods required to predict heat loads, temperature distributions and structural response. The interaction between these analyses is significant, and important questions remain unanswered. Examples include: (1) What is the required accuracy of temperatures needed to predict deformations (sensitivity effects)?, (2) How are such large structures best modeled?, (3) Are our computer programs efficient enough to do such large analyses?, and (4) How significant are structural nonlinearities? There is a clear need for additional data to define structural material properties and material performance in space. The required precision of this data is not clear, however, because of the interaction between thermal-structural analysis. In other words, how sensitive are predicted thermal distortions to thermal-structural material properties? Additionally, there is a general lack of understanding of the dynamic performance of large space structures including thermal effects. Are thermally induced structural dynamic distortions important? Are structural dynamic instabilities possible? To illustrate some of the uncertainties previously mentioned, results from current research are presented in the next three figures. In each example, a number of uncertainties arise indicating the need for additional study.

SOME UNCERTAINTIES

- INTERACTION BETWEEN HEATING, THERMAL AND QUASI-STATIC STRUCTURAL ANALYSIS
  - -SENSITIVITY EFFECTS
  - -EFFECTIVE MODELS
  - -EFFICIENCY
  - -STRUCTURAL NONLINEARITIES SIGNIFICANCE
- MATERIAL PROPERTIES
  - -AVAILABILITY ?
  - -RELIABILITY IN SPACE ENVIRONMENT
  - -ANALYSIS SENSITIVITIES
- STRUCTURAL DYNAMICS PROBLEMS
  - -LACK OF COMPUTATIONAL EXPERIENCE
  - -NONLINEARITIES
  - -INSTABILITIES ?

SHADOW EFFECTS OF SPACE TRUSSES

The effect of slender member shadowing effects at a typical point on a truss member are illustrated by the temperature history shown. The numerous short-duration drops in temperature indicate the passage of shadows of adjacent truss members. The large, longer-duration temperature drop near the center of the history denotes passage through the earth's shadow.

The prediction of the details of slender member shadowing effects is quite complex and therefore is very expensive for a truss with thousands of members. A basic question exists: Is the consideration of slender member shadowing effects required for accurate prediction of structural deformations?

SHADOW EFFECTS ON SPACE TRUSSES

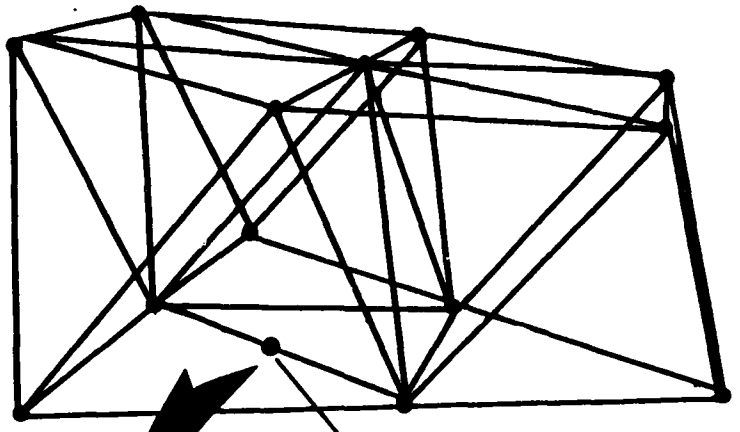

TYPICAL POINT

TYPICAL SLENDER MEMBER SHADOWING EFFECTS

X-9-10

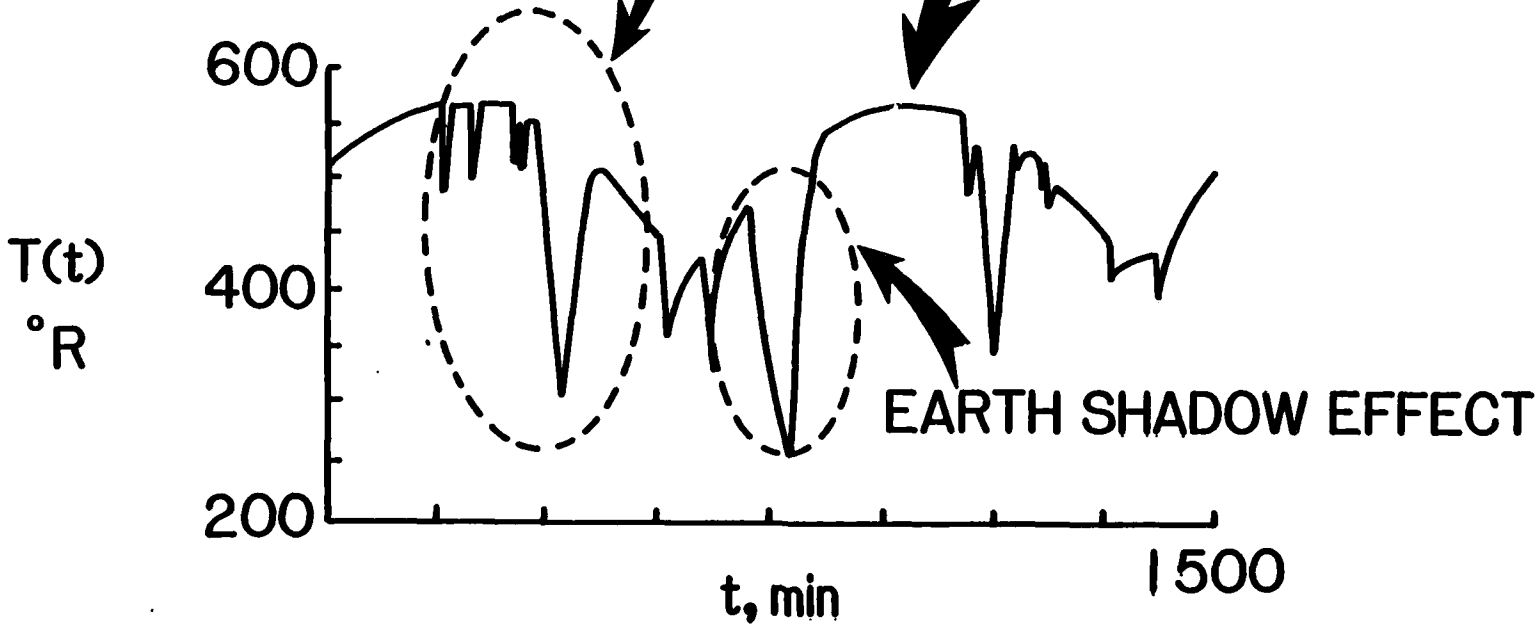

source: AIAA-81-1179, O'Neill, et.al.

THERMAL EXPANSION OF GRAPHITE/EPOXY

The thermal expansion of eight layers of a unidirectional graphite epoxy specimen, $[0_8]$, is shown for a representative temperature range encountered in earth orbit. The slope of the curve, the coefficient of thermal expansion (CTE), is the most important structural material property needed to predict thermal distortions. The data from this test shows the CTE varies significantly with temperature. (In contrast, the CTE of aluminum varies less and is always positiv over the same temperature range.) The CTE data shown, however, is only part of the information required since structural members are designed as laminates with layers oriented at different angles. Additional data is needed to define the CTE of actual laminates and ascertain how these properties will vary in space.

THERMAL EXPANSION OF GRAPHITE/EPOXY

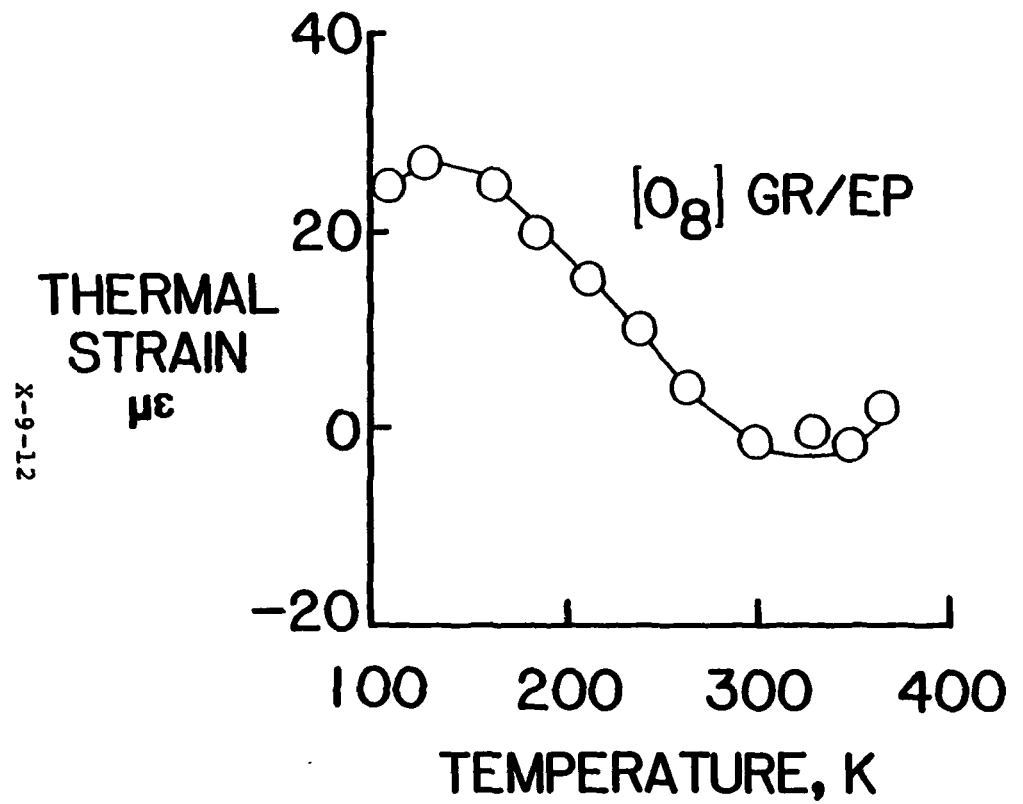

CTE = $d\varepsilon/dT$

T(K)	CTE (με/K)
200	-0.13
350	2.0

source: Short, Hyer et.al., VPISU, LSS TECH. REVIEW, NASA LRC, Nov.81

ISOTHERMAL VIBRATION AND BUCKLING OF PRETENSIONED STRUCTURES

Effects of stay (cable) pretension on the vibration and buckling behavior of a stayed column are shown. Cables are basic structural components in several current space structures, but they are difficult for structural engineers to analyze because they support only tensile loads. The results show the importance of cable pretension and cable slackening on two measures of the structural performance in an isothermal environment. How do the thermal effects encountered in a typical earth orbit affect the performance of pretensioned structures?

ISOTHERMAL VIBRATION AND BUCKLING OF PRETENSIONED STRUCTURES

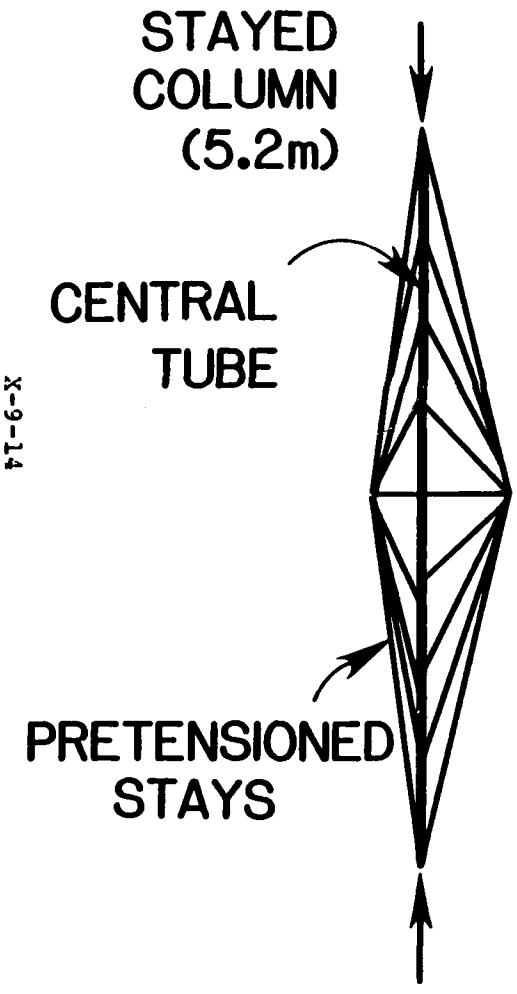

X-9-14

EFFECTS OF PRESTRESS

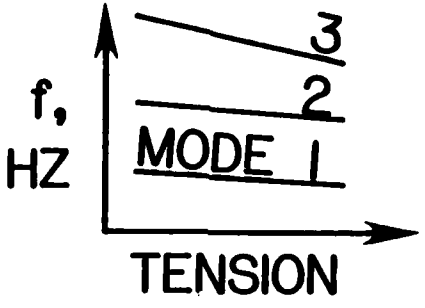

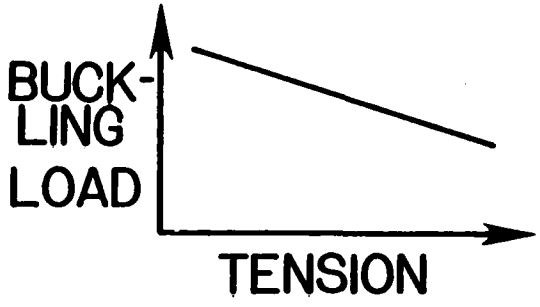

CONCLUSIONS

- EXP. VERIFICATION DIFFICULT
- IMPERFECTIONS IMPORTANT
- DYNAMIC LOADING AFFECTS REQUIRED PRETENSION
- STAY SLACKENING SIGNIFICANT

source: Belvin, LSS Tech. Review, NASA LRC, Nov.81

CONCLUDING REMARKS

Some representative uncertainties in thermal structural analysis (T-S-A) of large space structures are described. The figure lists important areas for further study. Additional computational experience is needed to further delineate problem areas. These computations should be performed on well-defined structures including realistic material properties and heat loads. Computations with preliminary structural designs have only partially identified some of the problem areas in analysis capabilities. Improvements in capabilities and efficiency of computer programs will undoubtably be required. Finally, many of the uncertainties will be finally resolved only through the interplay of analysis and experiment. There is definite need for fundamental thermal-structural experiments to validate the analysis of large space structures.

CONCLUDING REMARKS

- UNCERTAINTIES IN T–S–A OF LARGE SPACE STRUCTURES DESCRIBED
- IMPORTANT AREAS FOR FURTHER STUDY INCLUDE:
  - –SHADOWING EFFECTS
  - –MATERIAL PROPERTIES
  - –ANALYTICAL MODELING
  - –NONLINEAR STRUCTURAL COMPONENTS
  - –THERMAL EFFECTS ON DYNAMICS
  - –SENSITIVITY STUDIES
- COMPUTATIONAL EXPERIENCE WITH WELL–DEFINED STRUCTURES NECESSARY
- IMPROVEMENTS IN COMPUTER PROGRAMS CAPABILITIES REQUIRED
- THERMAL–STRUCTURAL EXPERIMENTS NEEDED TO VALIDATE ANALYSIS

BIBLIOGRAPHY

1. Technology for Large Space Systems, a Special Bibliography, NASA SP-7046, Supplements 01-05, July 1979 - January 1981.

2. Card, M. F., Bush, H. G., Heard, W. L., Jr., and Mikulus, M. M., Jr.: "Efficient Concepts for Large Erectable Space Structures," Large Space Systems Technology, An Industry/Government Seminar held at NASA Langley Research Center, Hampton, VA, January 17-19, 1978. NASA CP 2035, pp. 627-656.

3. Chambers, B. C., Jensen, C. L. and Coyner, J. V.: "An Accurate and Efficient Method for Thermal-Thermo-elastic Performance Analysis of Large Space Structures," AIAA 16th Thermophysics Conference, June 23-25, 1982, Palo Alto, CA, AIAA Paper No. 81-1178.

4. Mahaney, J., Thornton, E. A. and Dechaumphai, P., "Integrated Thermal-Structural Analysis of Large Space Structures," Symposium on Computational Aspects of Heat Transfer in Structures held at NASA Langley Research Center, November 3-6, 1981, NASA CP to be published.

5. Thornton, E. A., Mahaney, J. and Dechaumphai, P., "Finite Element Modeling of Orbiting Truss Structures," Large Space Systems Technology - 1981. Third Annual Technical Review, NASA Langley Research Center, November 16-19, 1981, NASA CP to be published.

6. O'Neill, R. F. and Zich, J. L., "Space Structure Heating (SSQ), A Numerical Procedure for Analysis of Shadowed Space Heating of Sparse Structures," AIAA 16th Thermophysics Conference, June 23-25, 1981, Palo Alto, CA, AIAA Paper No.-81-1179.

7. Short, J. S., Hyer, M. W., Bowles, D. E. and Tompkins, S. S., "Thermal Expansion of Gr/Ep Between 116K and 366K," Large Space Systems Technology - 1981, Third Annual Technical Review, NASA Langley Research Center, November 16-19, 1981, NASA CP to be published.

8. Belvin, W. K., "Vibration and Buckling Studies of Pretensioned Structures," Large Space Systems Technology - 1981, Third Annual Technical Review, NASA Langley Research Center, November 16-19, 1981, NASA CP to be published.

SESSION XI. SUMMARY

POWER AND ELECTRIC PROPULSION

ROBERT J. VONDRA
AIR FORCE ROCKET PROPULSION LABORATORY
EDWARDS AFB CA

The Air Force Rocket Propulsion Laboratory considers prime space power and primary electric propulsion to be enabling technologies for future Air Force missions. However, primary thrust requires power not yet available. Therefore, not only must the propulsion systems be developed but so too must the power sources to energize them.

Until now electric thruster power requirements for auxiliary propulsion applications have been modest and not a deciding factor in the selection of electric propulsion. Modest payoffs and the reluctance of mission planners to try something new have been the major reasons for the paucity of U.S. electric flights. But, as the enclosed figure shows, other countries, particularly the U.S.S.R. and Japan, have been actively pursuing the development and use of electric propulsion. This foresight will reap significant benefits as mission Δ Vs (velocity increments) increase.

Recent studies have shown that there is a trend towards large space system (LSS) missions requiring high Δ V. High Δ V requires high specific impulse as shown in the following rocket equation:

$$\frac{m_f}{m_o} = 1 - e^{-\frac{\Delta V}{Ve}}$$

where: $m_f \equiv$ fuel mass
$m_o \equiv$ initial spacecraft mass (including fuel)
$\Delta V \equiv$ mission velocity increment
$Ve \equiv$ rocket exhaust velocity
$= g\, I_{sp}$ (g = GRAVITATIONAL CONST., I_{sp} = SPECIFIC IMPULSE)

The rocket exhaust velocity (or equivalently specific impulse) must be comparable to Δ V if the fuel to spacecraft mass fraction (m_f/m_o) is to be reasonable. Future mission Δ Vs, expected to be on the order of 1,000's m/s (up from 100's m/s today), will require specific impulses of thousands of seconds for reasonable mass fractions. For example, the Δ V for a low earth orbit to geosynchronous earth orbit (LEO-GEO) transfer is approximately 5,000 m/s. Thus, the mass fraction for a chemical propulsion system with a 300s specific impulse is 80%. The mass fraction for an electrical system (3,000s specific impulse) is 15%. This means that 32,000 lbs of fuel are required to chemically propel a 40,000 lb spacecraft (8,000 lbs payload, 32,000 lbs fuel) from LEO-GEO, but only 6,000 lbs are required if electric propulsion is used.

The rocket equation and the preceding example point out the weight savings available when electric propulsion is used and Δ V is high. However, thrust

levels are usually high too (for electric) and resulting in the demand for larger amounts of power. Generally, 1 pound of electric thrust requires 250 KW of electric power. The following is representative of anticipated power needs:

MISSION	POWER	TIME
ORBIT CONTROL LSS	FEW KW	10 YR.S
MANEUVERING FOR SURVIVABILITY	10's KW	10 YR.S
LEO-GEO TRANSFER	100's KW-MW	1000 HR.S

Solar power is probably suitable for the first two ranges and nuclear for the last. The last is representative of missions that require a pound of thrust at several thousand seconds specific impulse.

To reiterate, primary electric propulsion and prime space power are enabling technologies for big and ambitious space missions. Unless the U.S. gets serious about developing these technologies it will be second to the Russians in the peaceful and military uses of space. The U.S.S.R. has already space tested nuclear-electric propulsion and, as shown in the figure, is expected to make these systems operational during this decade.

SPACE FLIGHTS of ELECTRIC PROPULSION....

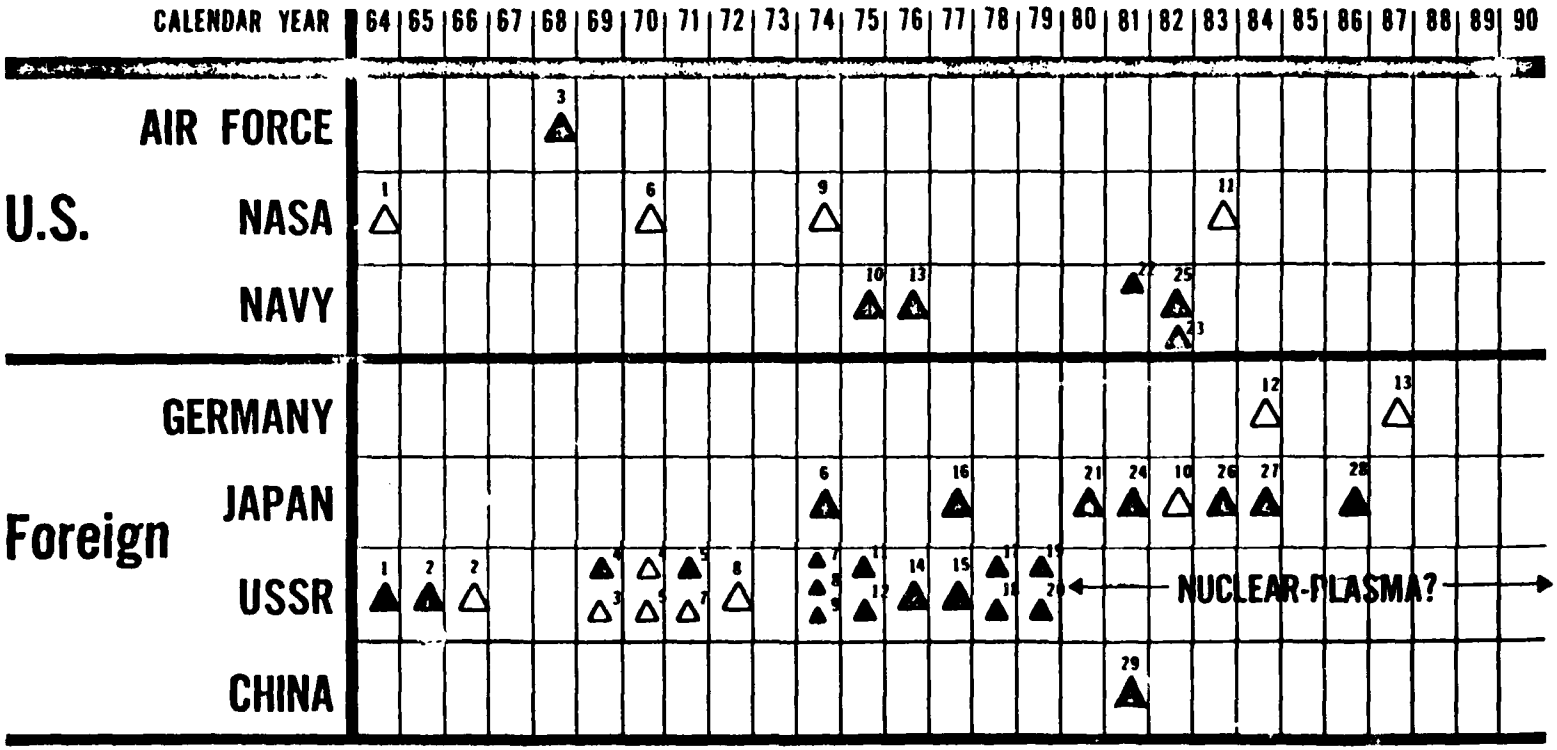

XI-2-3

▲ PLASMA

1 ZOND 1
2 ZOND 2
3 LES 6
4 YANTAR 1
5 METEOR 18
6 ISAS ROCKET
7 METEOR 18
8 ISL/VZA
9 ISL/VZA
10 TIP 1
11 COSMOS 728
12 COSMOS 780
13 TIP 2
14 METEOR
15 MR
16 K-9M-58
17 KUST
18 GEOPHYSICAL ROCKET
19 METEOR
20 MR
21 MTS-4
22 NOVA 1
23 NOVA 2
24 ETS-4
25 NOVA 3
26 SPACELAB 1
27 SPACELAB 6
28 SPACELAB 11
29 MDT-2A

△ ION

1 SERT 1
2 YANTAR 2
3 GEOPHYSICAL ROCKET
4 YANTAR 3
5 GEOPHYSICAL ROCKET
6 SERT 2
7 METEOR 18
8 YANTAR 4
9 ATS-F
10 ETS-3
11 PEO 1
12 TV SAT B3
13 TV SAT B5

POWER CONVERSION: OVERVIEW*

J. Preston Layton**
Consultant

ABSTRACT

The central position of power conversion systems in relation to other elements of space power systems is identified and the recognized types of power conversion are shown to be: photovoltaic, thermoelectric, Brayton cycle, Rankine cycle, Stirling cycle, thermionic and electromagnetic.

The requirement for space electric power levels versus calendar years are presented historically and projected beyond the turn of the century.

A number of space power systems that may employ thermoelectric, Brayton, Rankine and magnetohydrodynamic power conversion are illustrated and discussed.

The need for mission and systems analyses to support the identification of applied research in power conversion is argued and the approach for conducting these analyses is presented.

---

*Prepared for presentation at AFOSR Special Conference on Prime Power for High Energy Space Systems, Norfolk, Virginia, 22-25 February 1982.

**60 Penn-Lyle Road, Princeton Junction, NJ 08550, USA, (609) 799-3094.

"THERE IS NOTHING MORE DIFFICULT TO TAKE IN HAND, MORE PERILOUS TO CONDUCT, OR MORE UNCERTAIN IN ITS SUCCESS, THAN TO TAKE THE LEAD IN THE INTRODUCTION OF A NEW ORDER OF THINGS"

MACHIAVELLI'S "THE PRINCE"

"TO DITHER AND DELAY ANY LONGER IS DAFT"

LORD ORR-EWING
CHAIRMAN,
BRITISH METRICATION BOARD

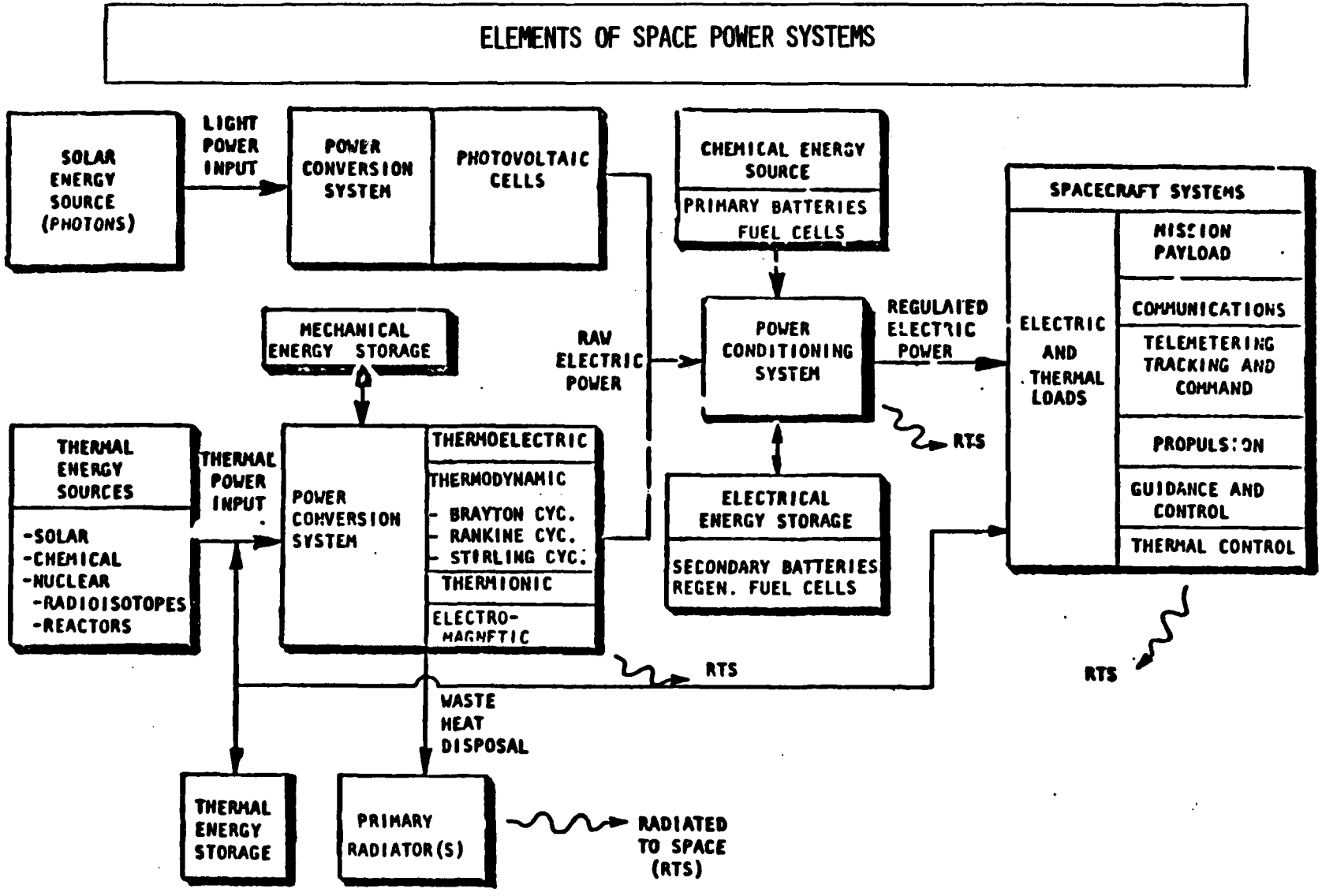
ELEMENTS OF SPACE POWER SYSTEMS
SOLAR ENERGY SOURCE (PHOTONS)
LIGHT POWER INPUT
POWER CONVERSION SYSTEM
PHOTOVOLTAIC CELLS
CHEMICAL ENERGY SOURCE
PRIMARY BATTERIES
FUEL CELLS
SPACECRAFT SYSTEMS
MISSION PAYLOAD
COMMUNICATIONS
TELEMETERING TRACKING AND COMMAND
PROPULSION
GUIDANCE AND CONTROL
THERMAL CONTROL
ELECTRIC AND THERMAL LOADS
MECHANICAL ENERGY STORAGE
RAW ELECTRIC POWER
POWER CONDITIONING SYSTEM
REGULATED ELECTRIC POWER
RTS
THERMAL ENERGY SOURCES
-SOLAR
-CHEMICAL
-NUCLEAR
-RADIOISOTOPES
-REACTORS
THERMAL POWER INPUT
POWER CONVERSION SYSTEM
THERMOELECTRIC
THERMODYNAMIC
- BRAYTON CYC.
- RANKINE CYC.
- STIRLING CYC.
THERMIONIC
ELECTRO-MAGNETIC
ELECTRICAL ENERGY STORAGE
SECONDARY BATTERIES
REGEN. FUEL CELLS
RTS
RTS
WASTE HEAT DISPOSAL
THERMAL ENERGY STORAGE
PRIMARY RADIATOR(S)
RADIATED TO SPACE (RTS)

SPACE ELECTRIC POWER LEVEL VS CALENDAR YEARS

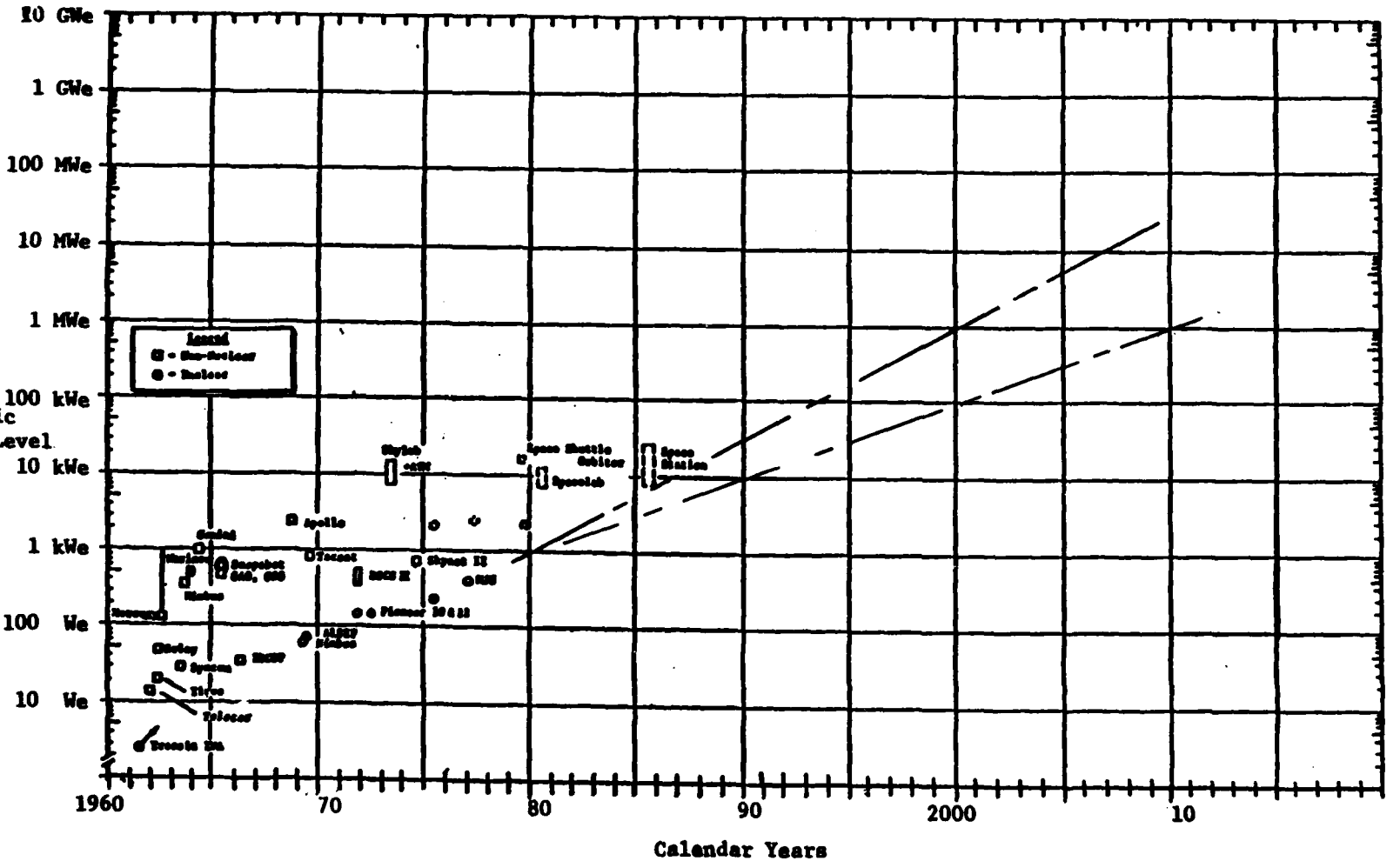

PROGRAM TERMINOLOGY

PROGRAM & BUDGET CATEGORY	INITIAL OPERATING CAPABILITY	PROGRAM STATUS
BASIC RESEARCH	-	UNCERTAIN FUTURE
APPLIED RESEARCH (6.1)	1995	REASONABLE PROSPECT
EXPLORATORY TECHNOLOGY (6.2)	1990	CREDIBLE POTENTIAL
ADVANCED TECHNOLOGY (6.3)	1987	PLANNED
ENGINEERING DEVELOPMENT (6.4)	1985	AUTHORIZED

CONFIGURATION OF 100 kWe SPAR NUCLEAR THERMOELECTRIC POWER SYSTEM

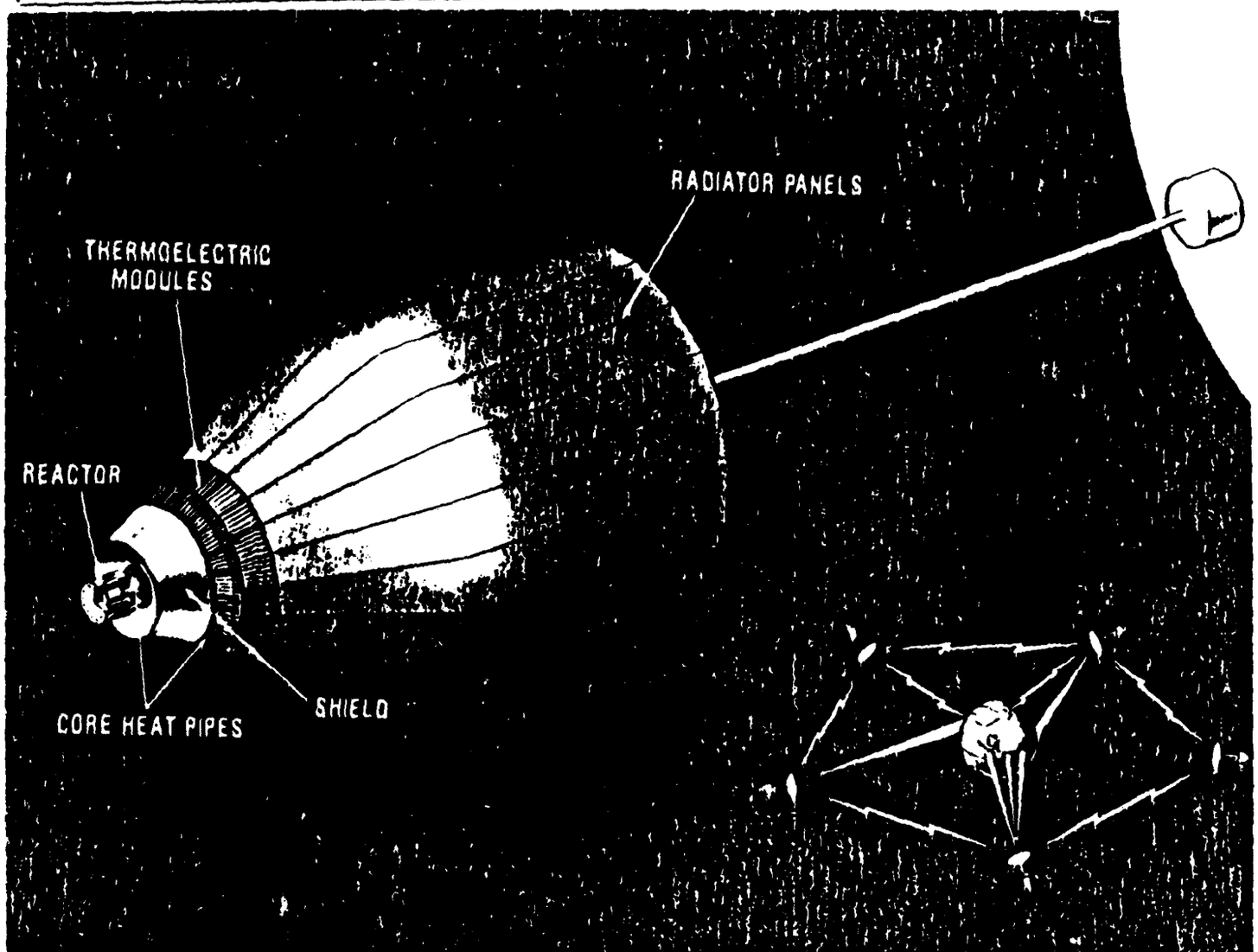

NUCLEAR ELECTRIC SPACECRAFT DESIGN WITH A 400 kWe BRAYTON POWER SYSTEM

MASS SUMMARY	kg
REACTOR	950
REACTOR SHIELD	900
HEAT SOURCE HEAT EXCHANGERS (2)	420
CRU (2)	430
ALTERNATOR RADIATOR	150
RECUPERATORS (2)	730
RADIATOR	4040
DUCTING & MISCELLANEOUS	400
POWER CONDITIONING	160
STRUCTURE	300
	8270

SPECIFIC MASS = 20.7 kg/kW$_e$

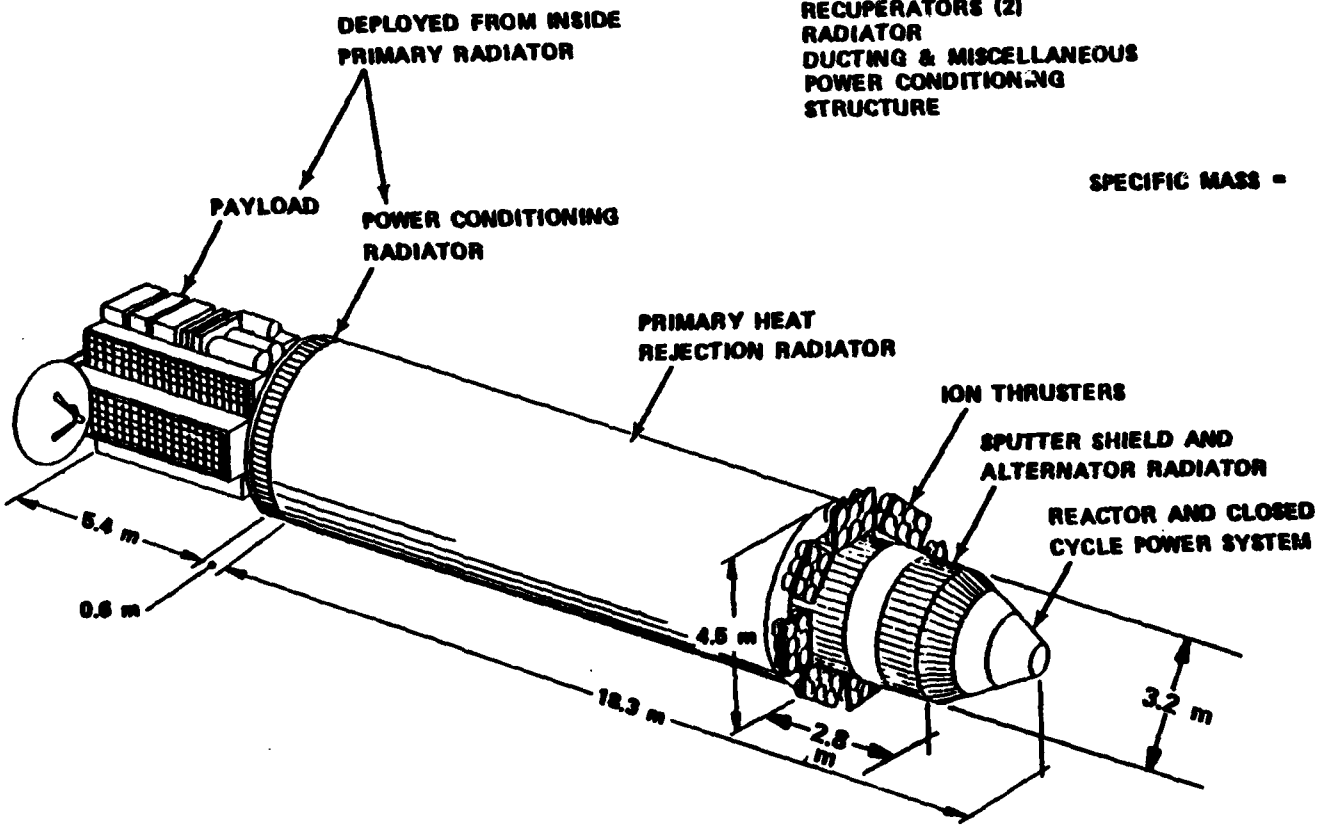

DUAL BRAYTON POWER SYSTEMS SCHEMATIC FOR NUCLEAR ELECTRIC SPACECRAFT

NOTE: DUAL FULL POWER CONVERSION SYSTEMS ARE COMPLETELY INDEPENDENT

LEGEND

R - REACTOR

HSHX - HEAT SOURCE HEAT EXCHANGER

T - TURBINE

RECUP - RECUPERATOR

ACC - WORKING FLUID SUPPLY

C - COMPRESSOR

ALT - ALTERNATOR

CRU - COMBINED ROTATING UNIT

HX - PRIMARY RADIATOR HEAT EXCHANGER (MANIFOLD)

RAD - PRIMARY RADIATOR

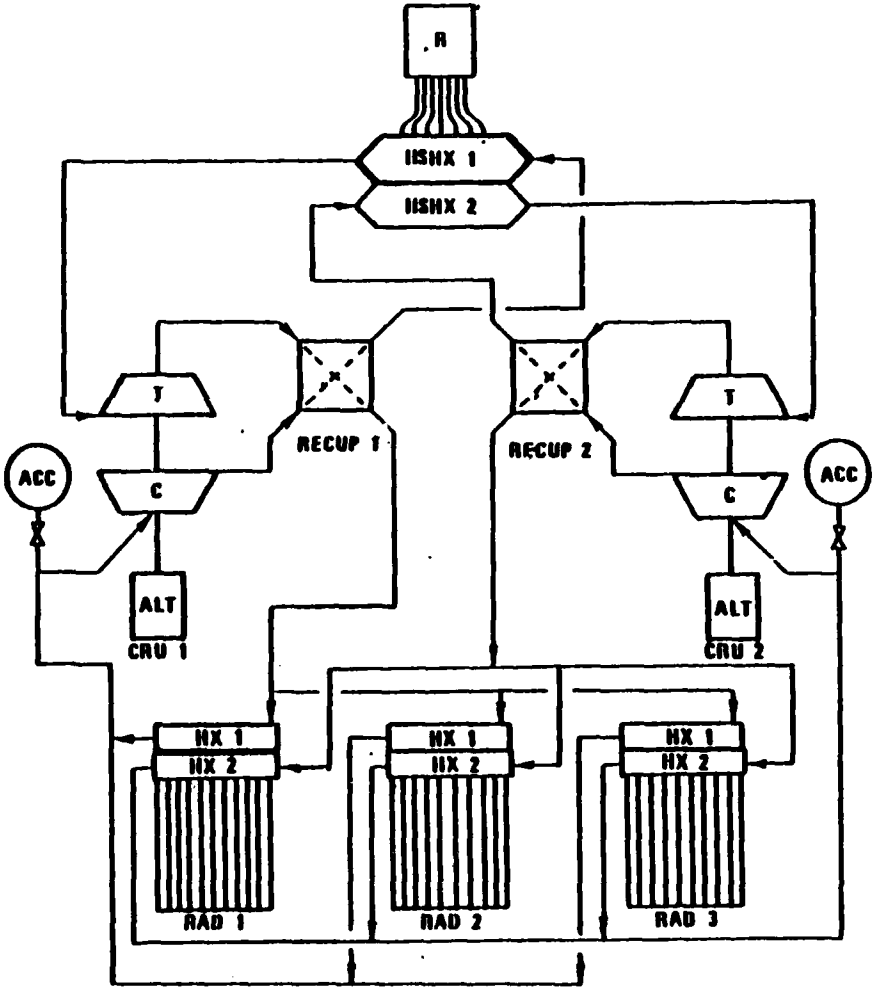

POTASSIUM RANKINE CYCLE TEST TURBINE

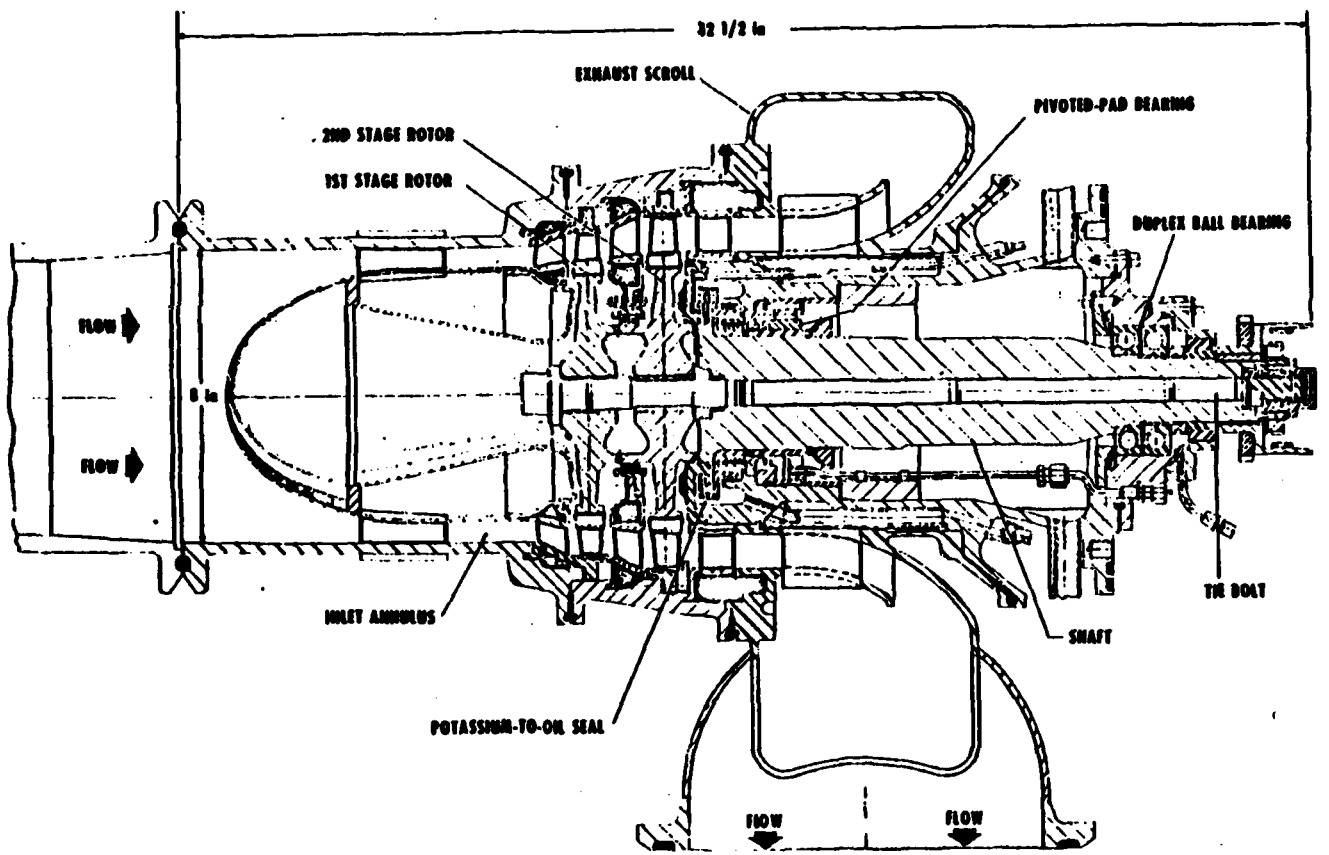

NUCLEAR ELECTRIC ORBITAL TRANSFER VEHICLE

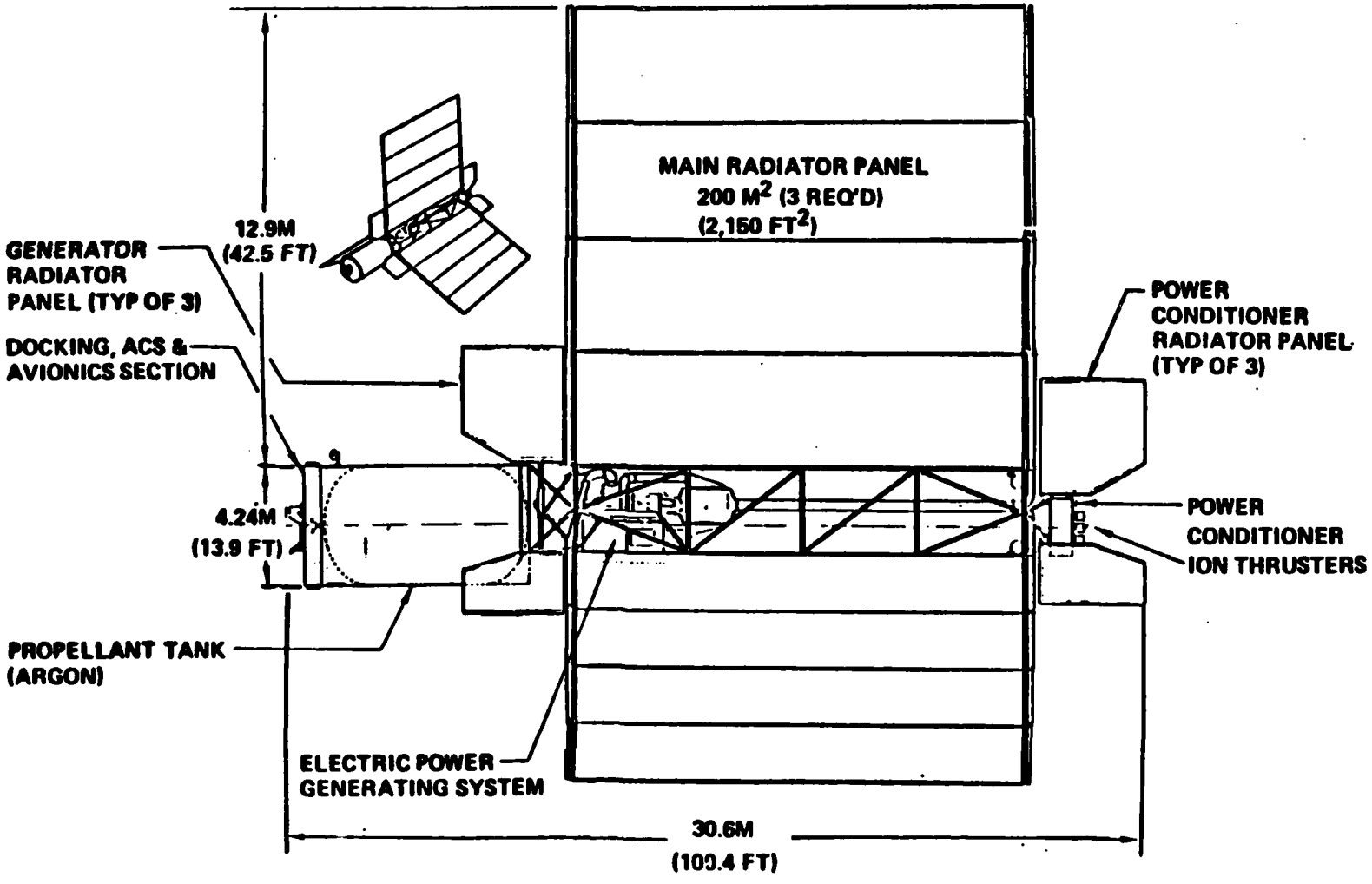

ADVANCED NUCLEAR ELECTRIC ROCKET PROPELLED VEHICLE FOR OUTER SOLAR SYSTEM AND GALACTIC EXPLORATION

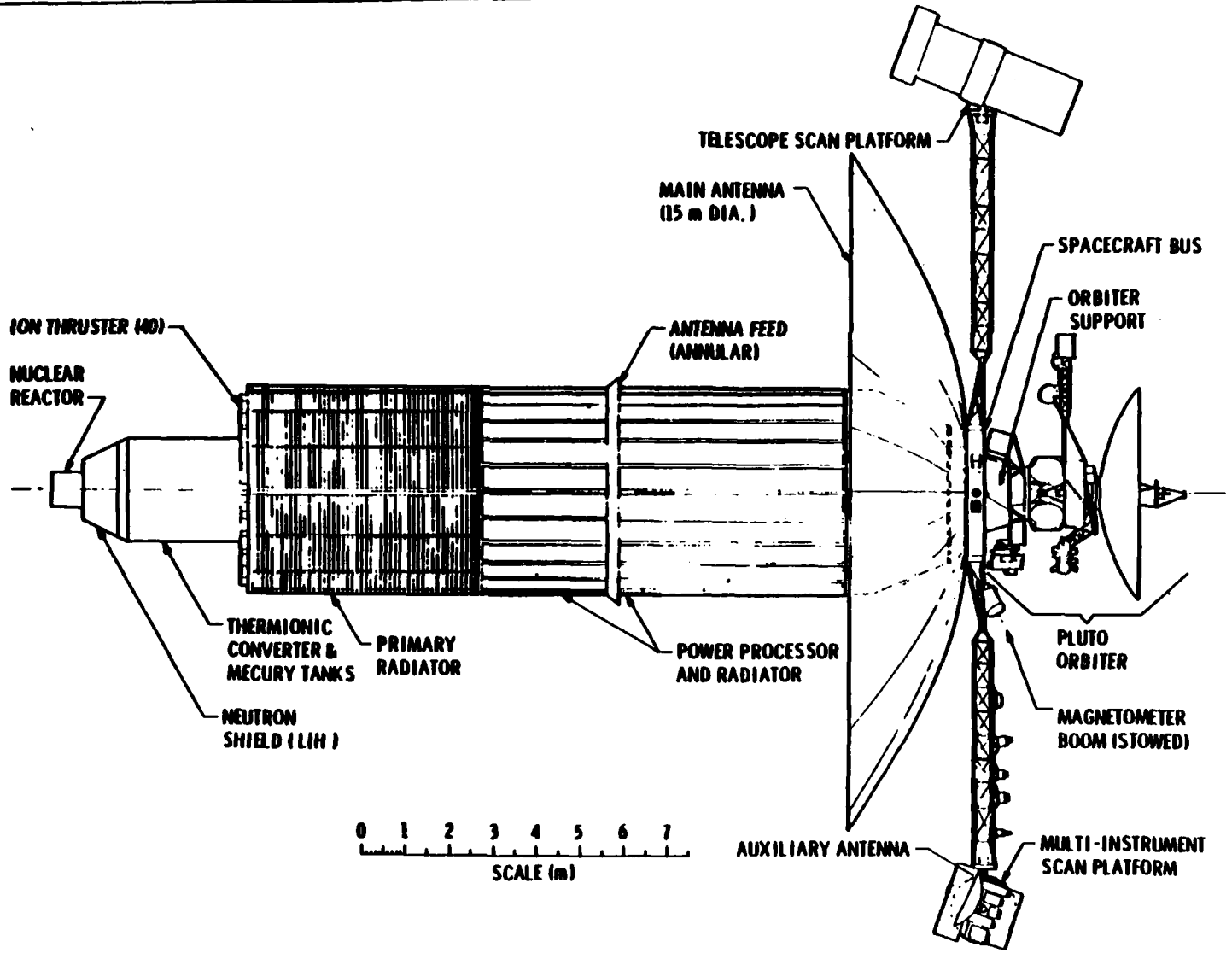

MULTI-MEGAWATT CARBON MONOXIDE LASER POWER SATELLITE

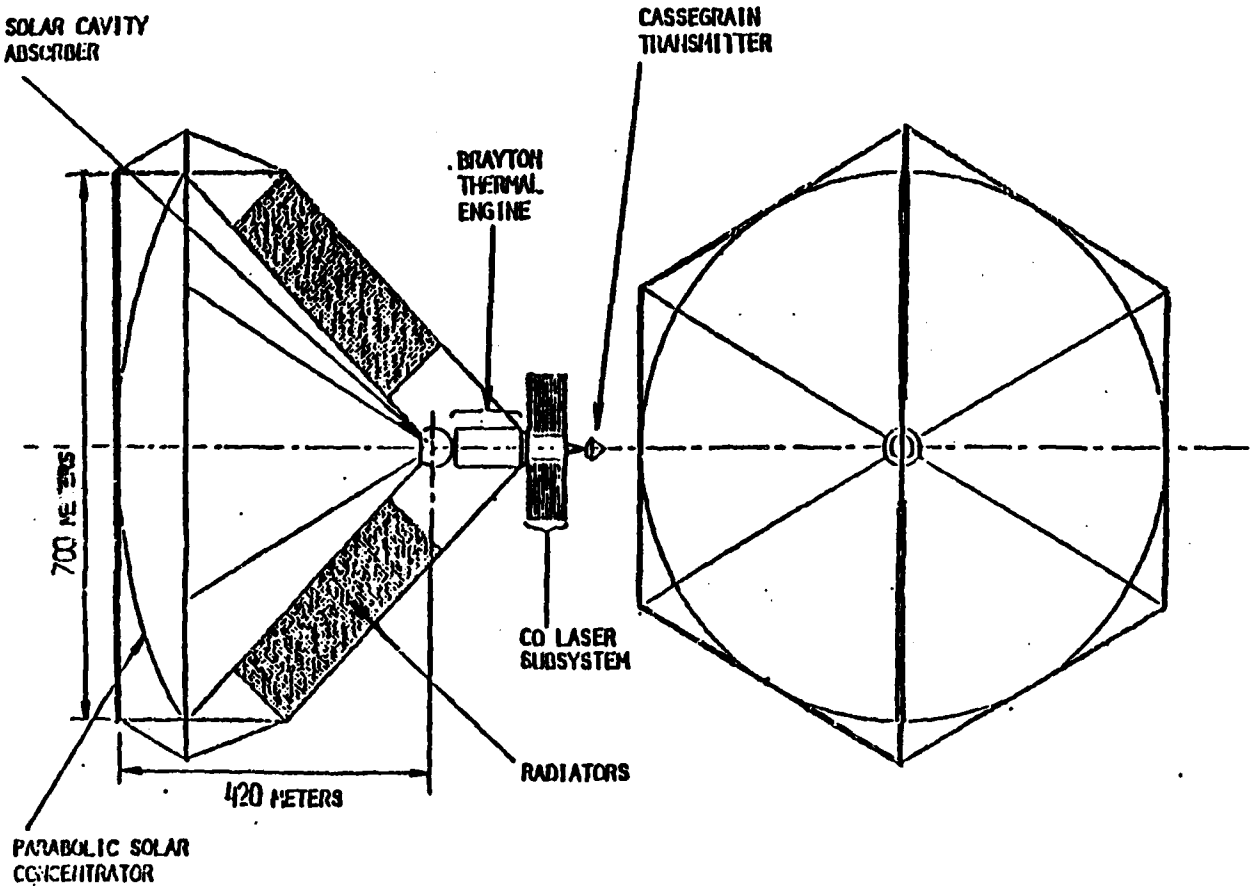

LASER POWER TRANSMISSION IN SPACE

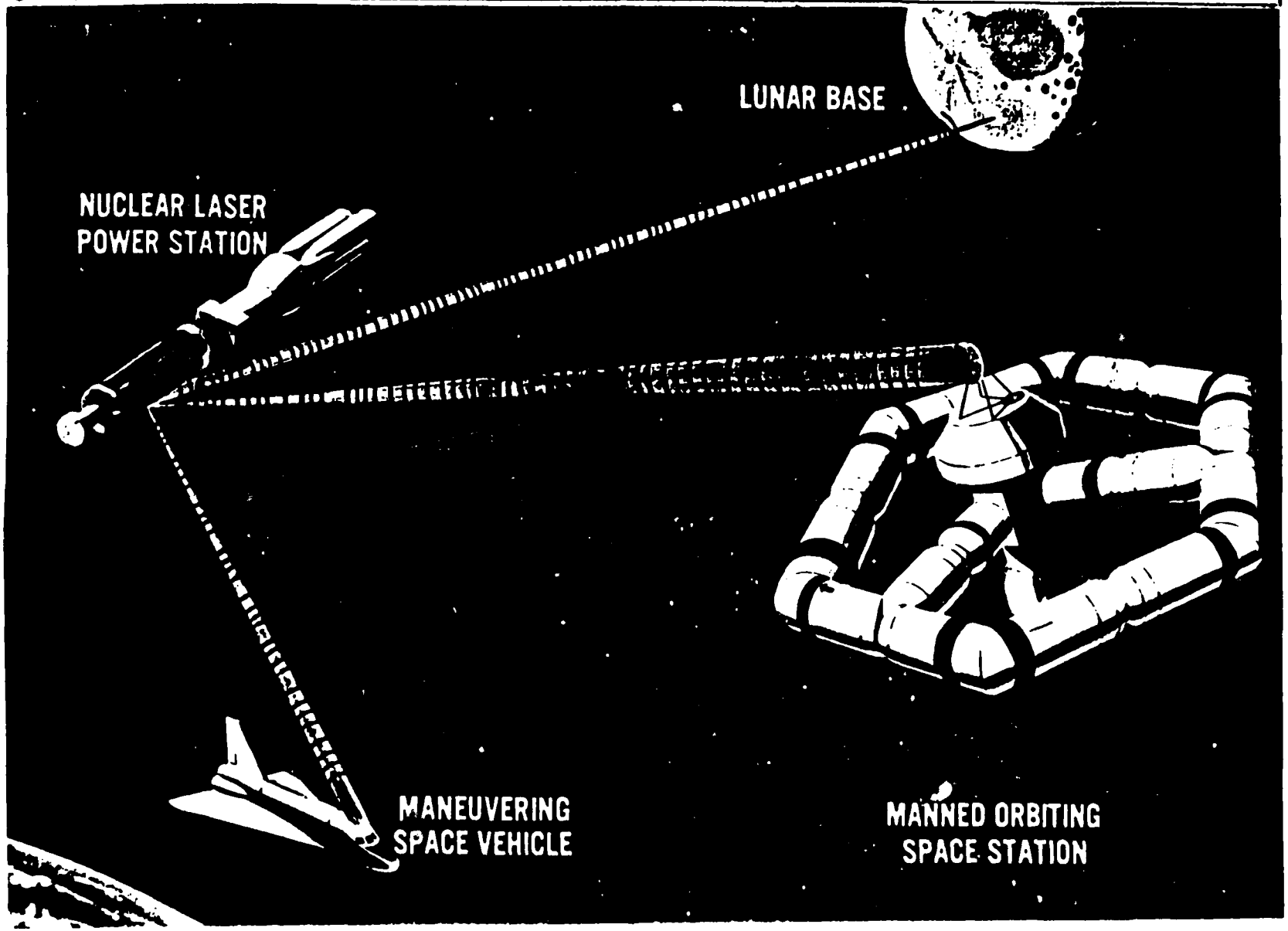

MHD CLOSED CYCLE SPACE POWER SYSTEM

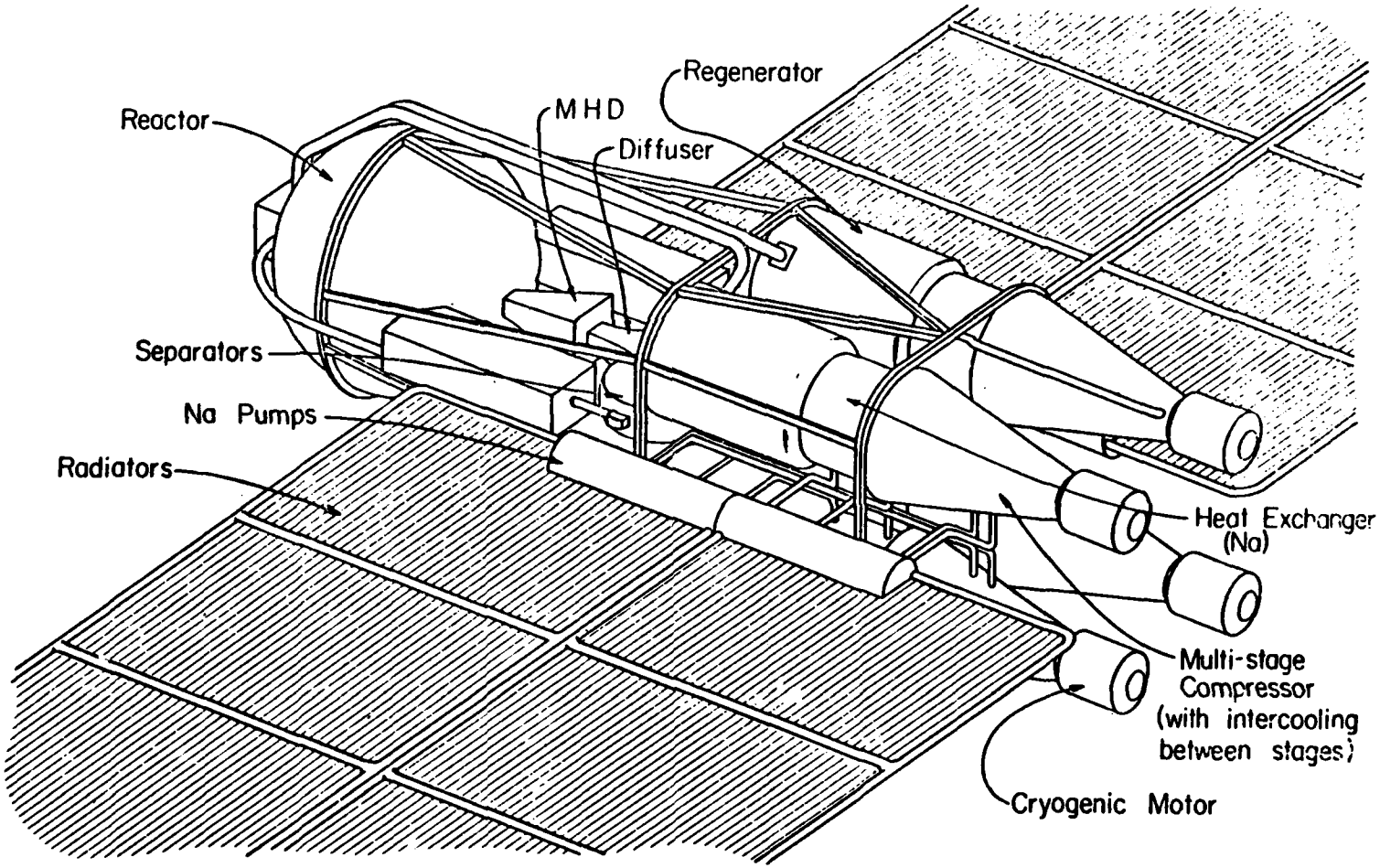

ADVANCED SPACECRAFT POWERED BY A DUAL-MODE, SOLID CORE
SPACE NUCLEAR PROPULSION SYSTEM IN GEOCENTRIC ORBIT

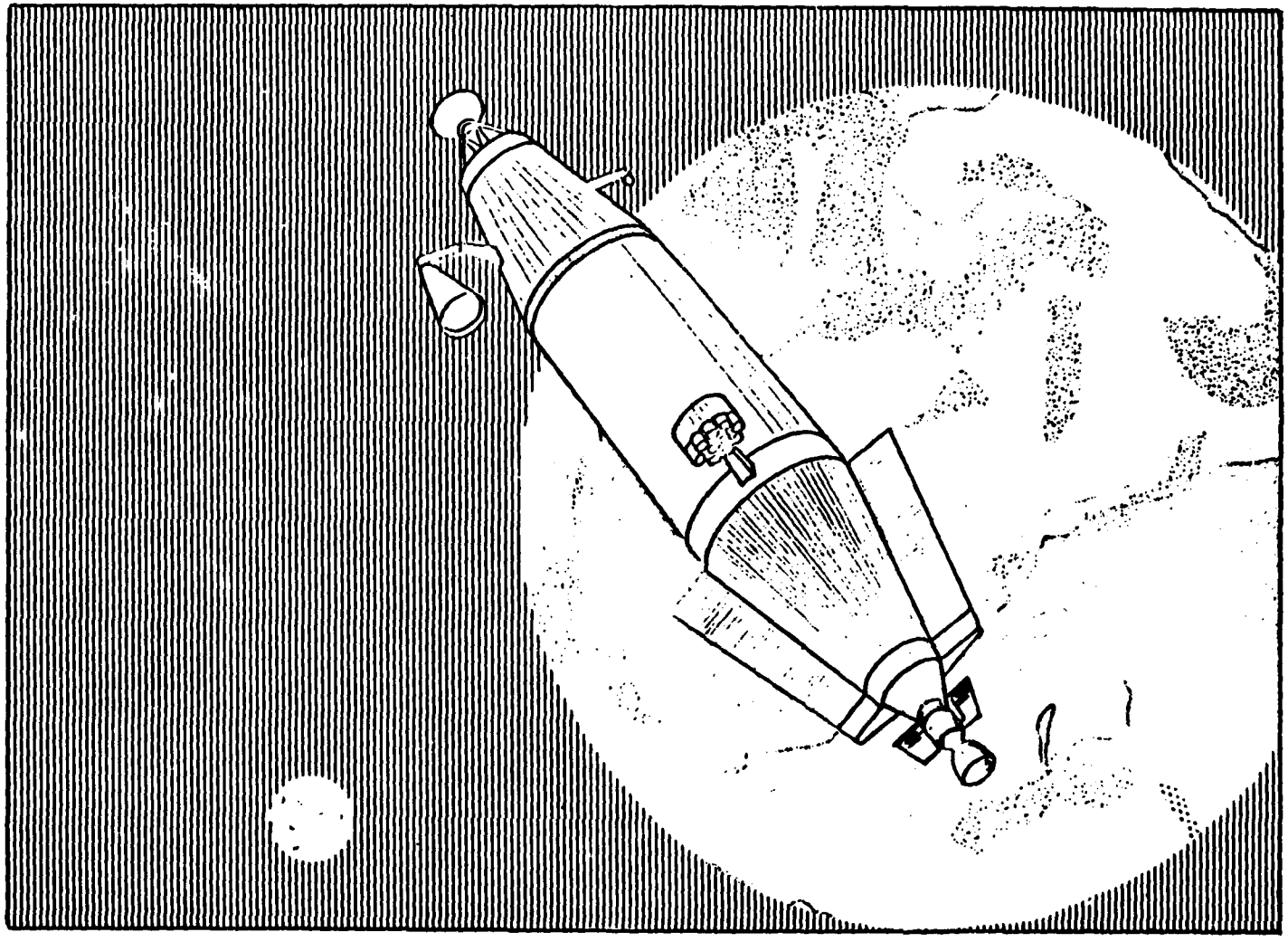

DUAL-MODE SOLID-CORE NUCLEAR POWER/PROPULSION CONCEPT UTILIZING A BRAYTON (OR RANKINE) CYCLE

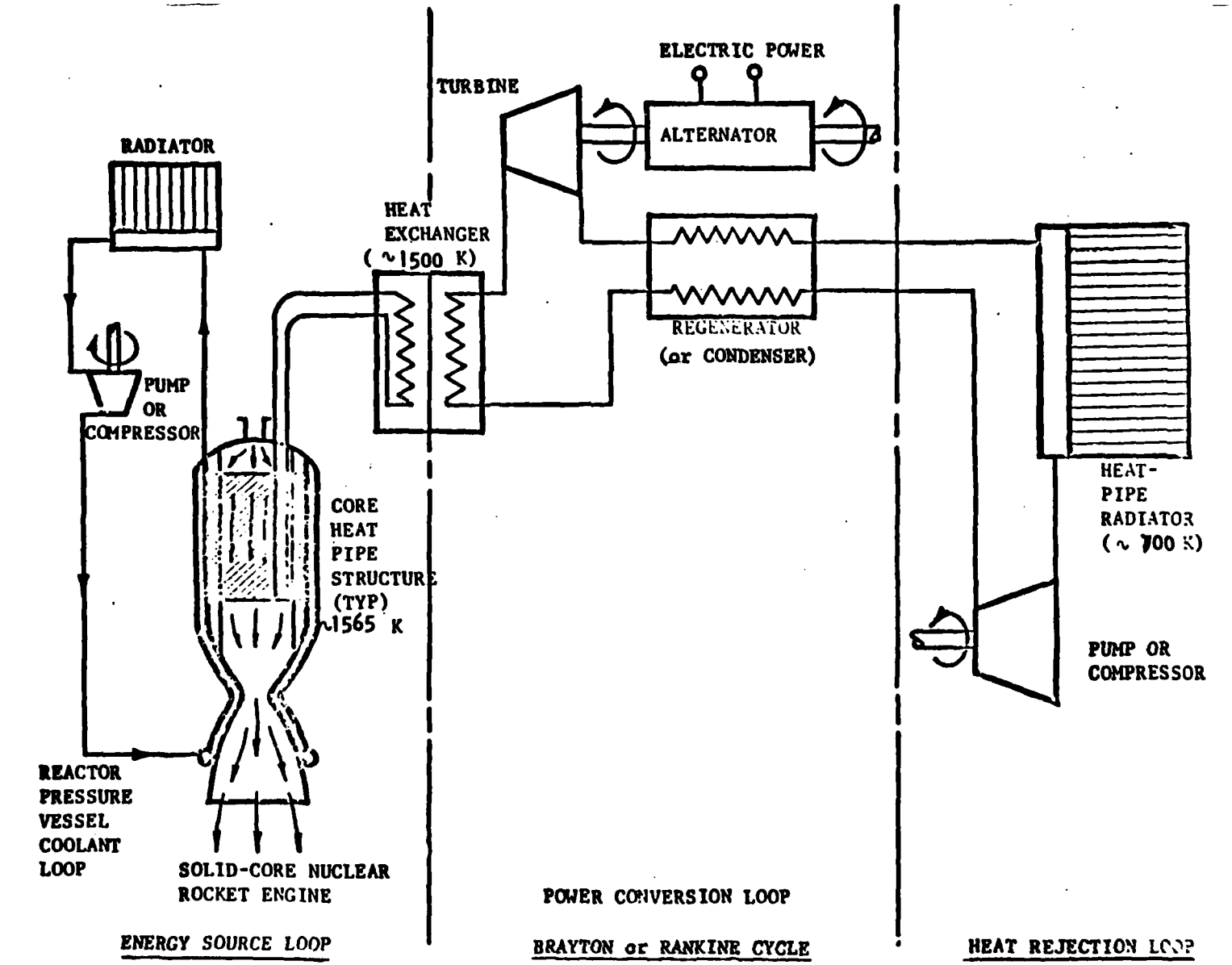

FUEL ELEMENT CONCEPT FOR DUAL MODE SOLID CORE NUCLEAR SPACE POWER AND PROPULSION SYSTEM

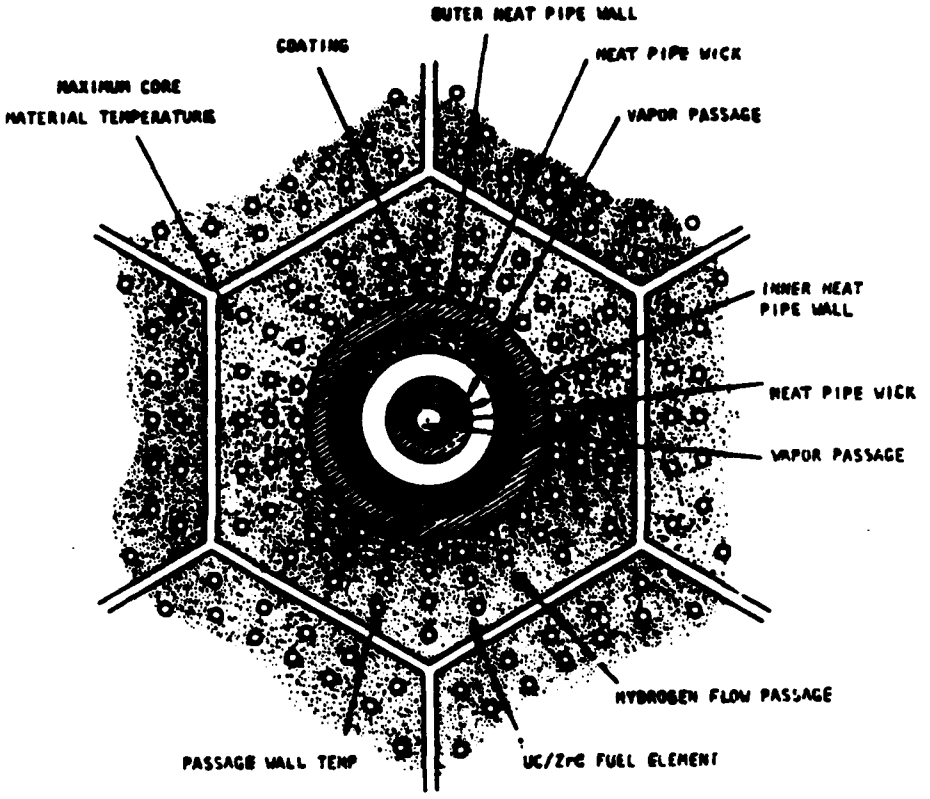

PARAMETRIC SYSTEMS ANALYSIS APPROACH TO ADVANCED MISSIONS

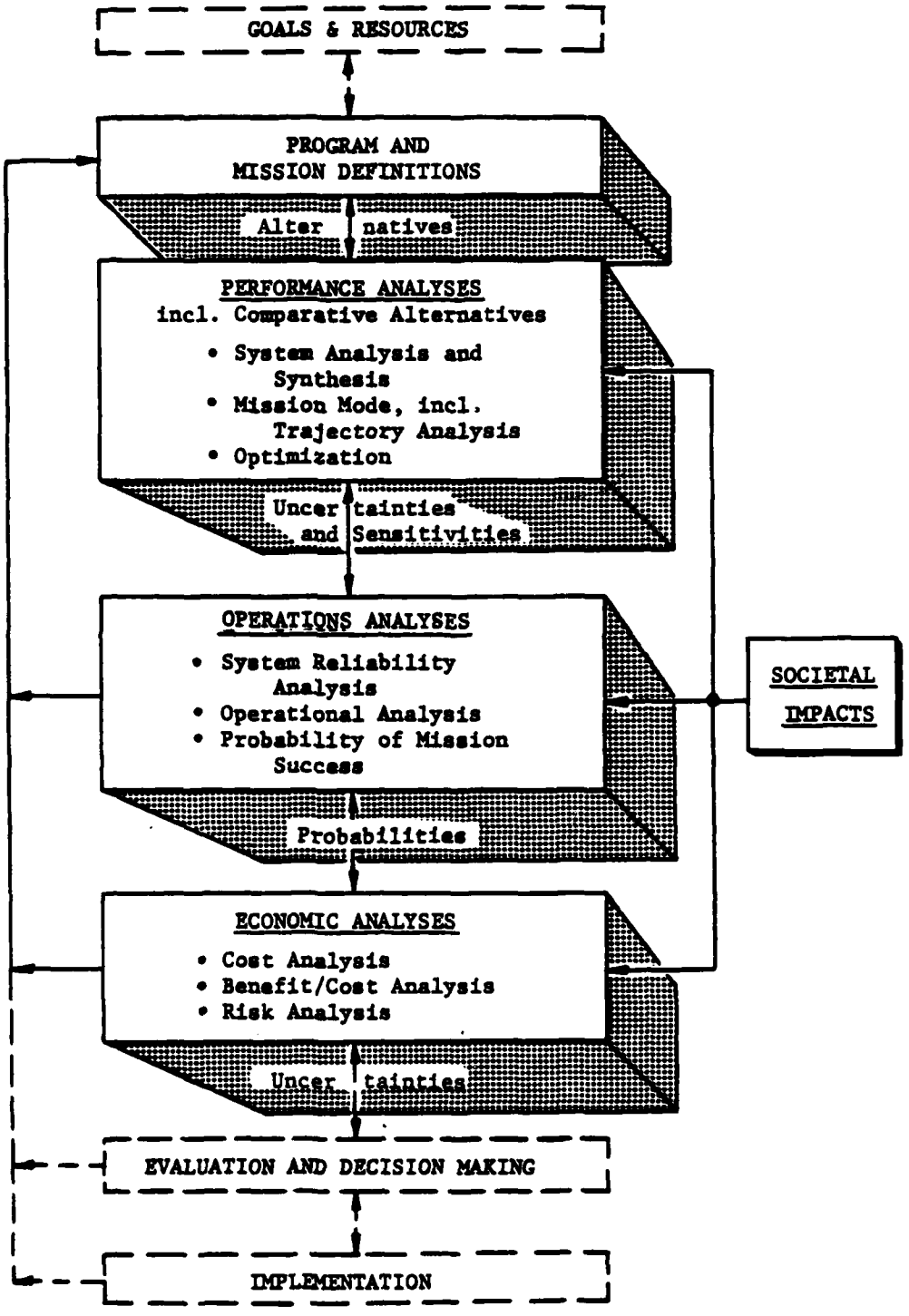

ITERATIVE APPROACH TO THERMODYNAMIC SYSTEMS ANALYSIS CODES

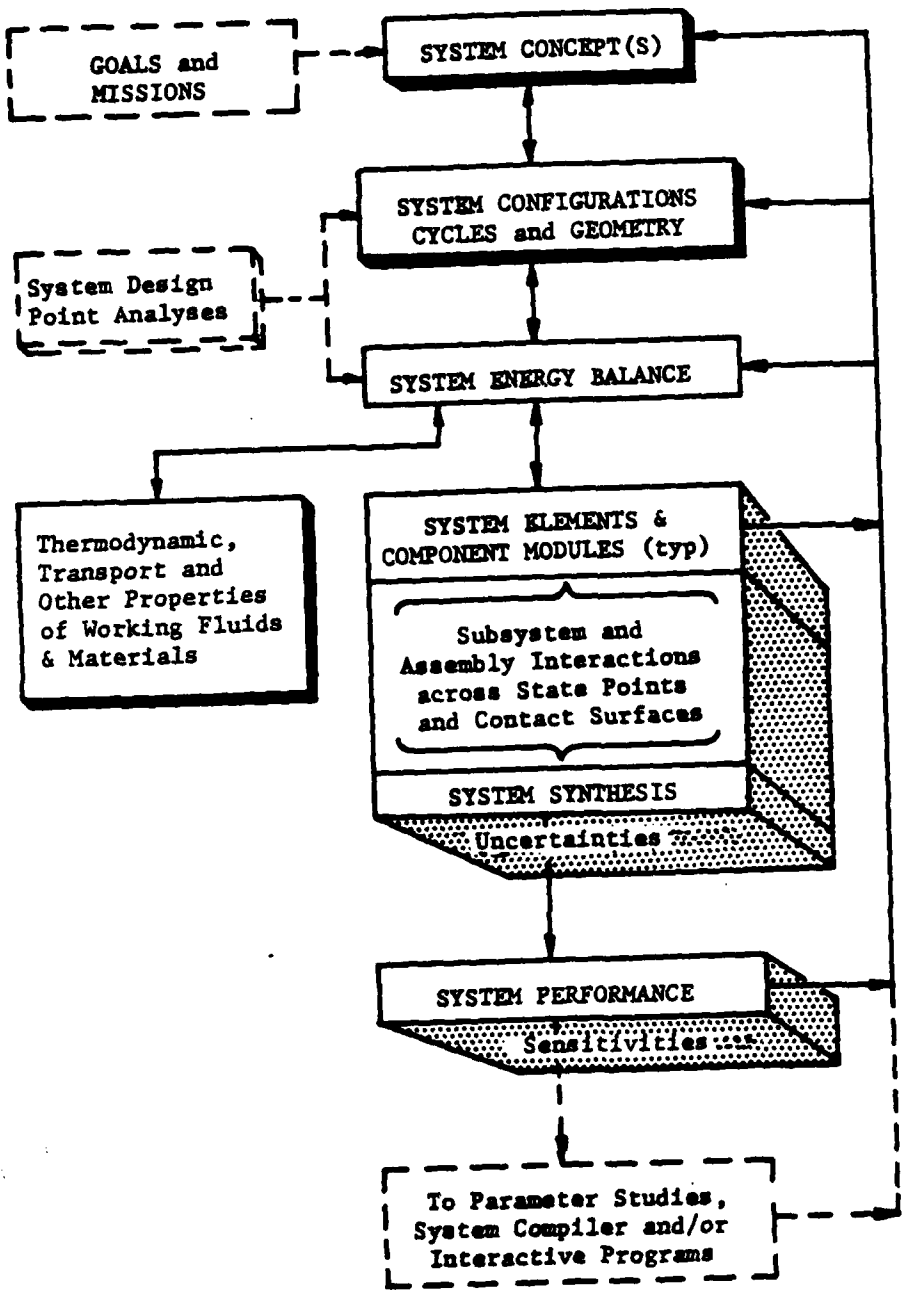

PROBABILISTIC APPROACH TO DETERMINATION OF PRESENT VALUES OF SYSTEMS COSTS AND THEIR STANDARD DEVIATIONS

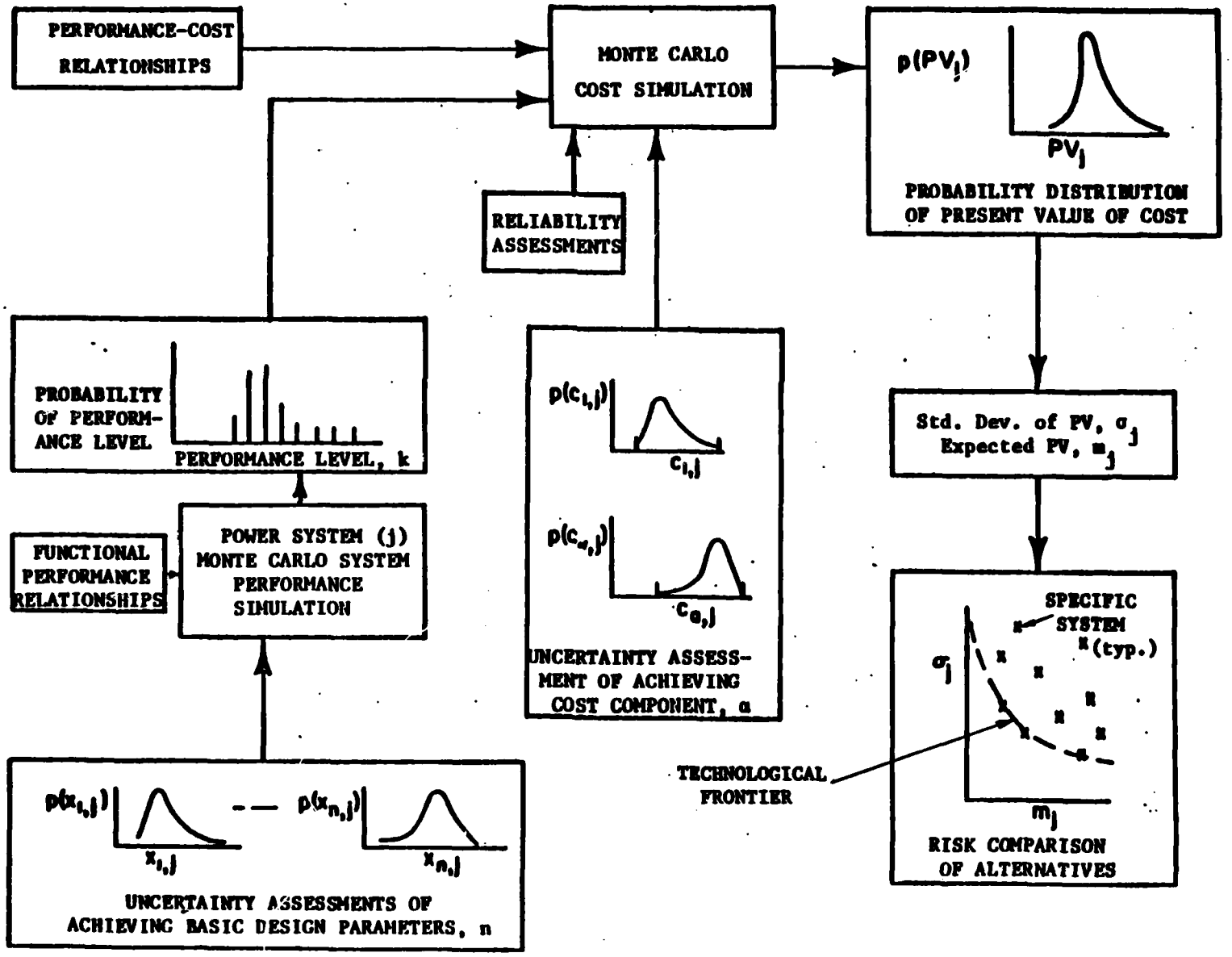

SYSTEMS ANALYSIS PYRAMID

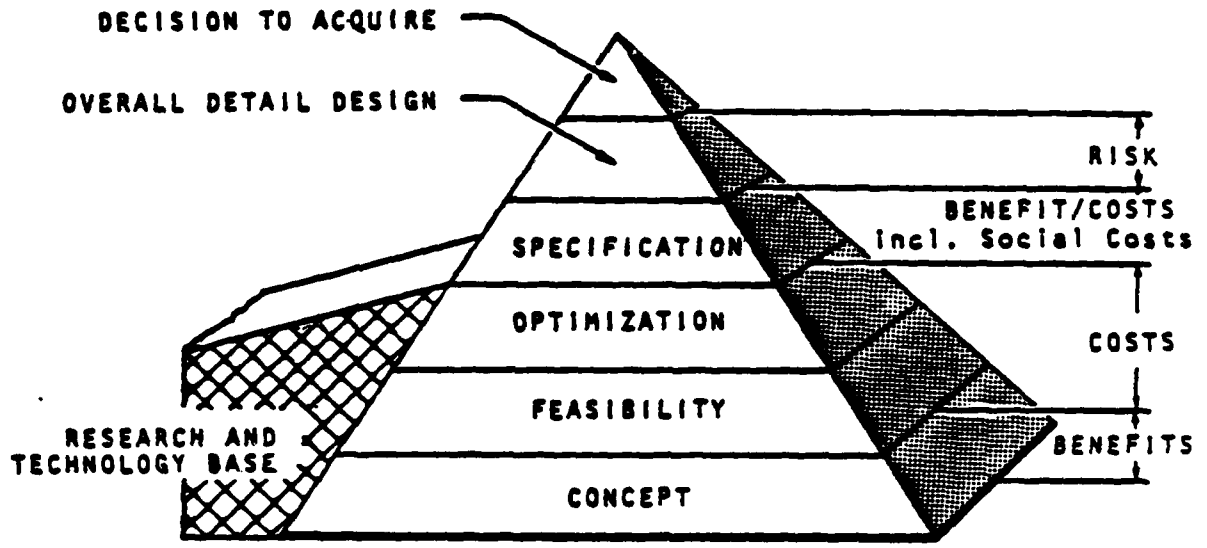

BIBLIOGRAPHY

Space Power Systems in Preliminary System and Mission Analysis, NASA Ames Research Center, circa 1968.

Anon, Brayton Cycle Power Conversion for Space, NASA Literature Search Number 11244, March 16, 1970.

Crane, G. R., et al, DoD/AEC Space Power Study, 30 June 1974.

Layton, J. P., The Evolution of Space Power Systems, Presentation to NASA OSF Advanced Programs, 10 August 1976.

Freitag, R. F. and Kisko, W. A., Evolution of Space Power System, XXIX IAF Congress, Dubrovnik, Yugoslavia, October 1978.

Barthelemy, R. R., The Military Space Power Program, IECEC Paper 799261.

Barthelemy, R. R. and Shelley, V. A., A DoD Space Energy Module, IECEC Paper 799266

Harper, A., Study of Reactor Brayton Power Systems for Nuclear Electric Spacecraft, AiResearch Technical Report 31, 3321, September 28, 1979.

Layton, J. P., Nuclear Reactor Closed Brayton Cycle Space Power Conversion Systems, IECEC Paper 819161.

Cohen, M., Fornoles, E., and Mahafkey, T., Requirements and Technology Trends for Future Military Space Power Systems, IECEC Paper 819182.

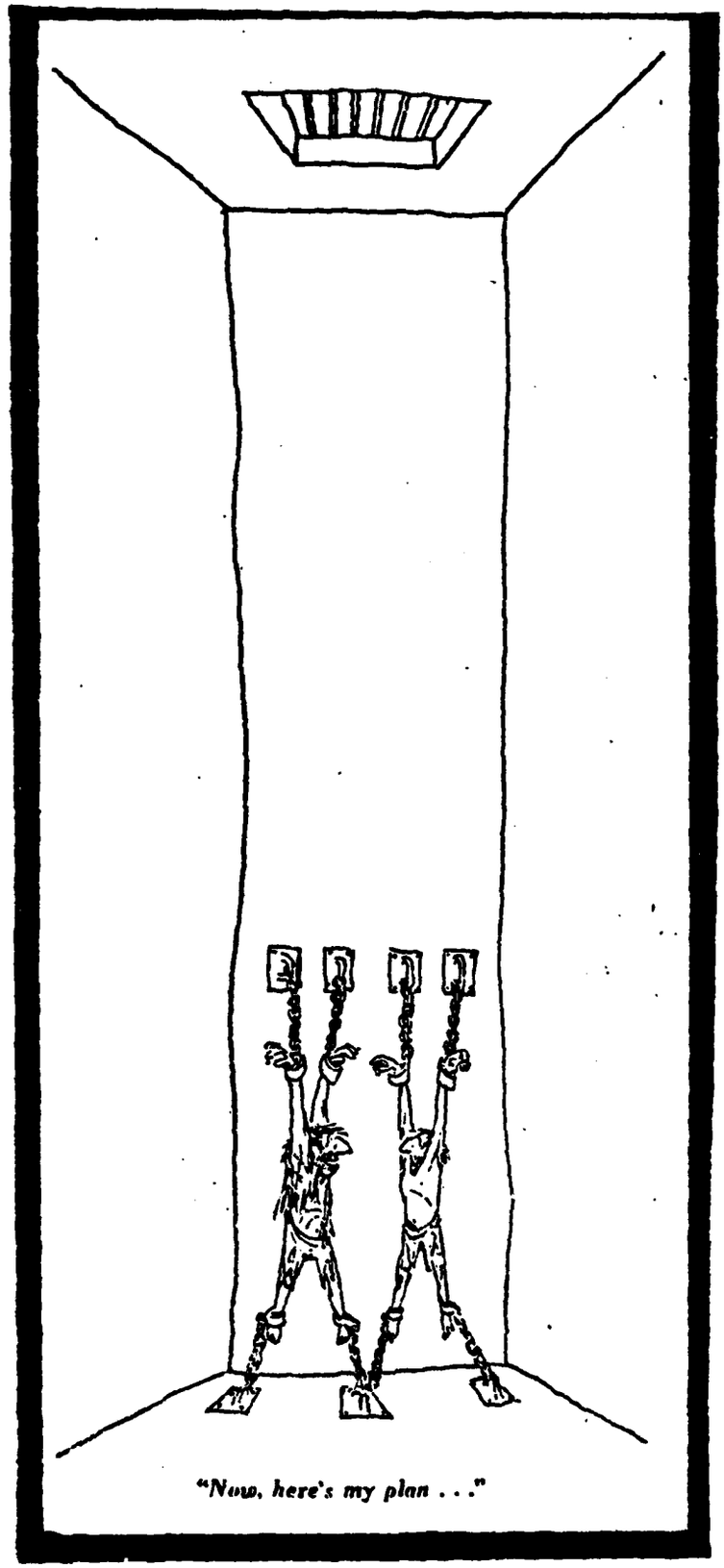

"Now, here's my plan . . ."

Comments on the "Special Conference on Prime-Power for High-Energy Space Systems" and specifically on the "Heat/Systems Session"

I would like to first comment on what I found important and needing further investigation in the section that I chaired. First, it must be emphasized that heat transfer and disposal must be addressed simultaneously with power generation; essentially one watt or more of heat must be disposed of for each watt of power required.

An issue not mentioned in the discussions of power this week has been contamination. Many of the approaches to high continuous or pulse power have a high contamination capability. The problems that this could cause must be considered in any proposed power system.

The session on "Heat/Systems" identified several areas where additional basic understanding would appear to be required:

- Heat pipes, both at high temperatures and at lower temperatures, are critical to many concepts including reactors. The capability to predict the physical properties of some heat transfer fluids would be highly desirable for new fluid development. An understanding of the fundamentals of the operation of heat pipes in zero g. environment could permit more rapid design optimization and increase the confidence in the long life design of these units.

- Papers in this session and in other sessions would suggest that additional work on the fundamentals of two-phase flow with respect to heat transfer might be an important research area.

- Studies of new concepts in heat transfer such as liquid film and droplet radiators must be supported as the concepts are brought forth. However, early systems design must be considered with any new concept to assure proper compatibility can be achieved.

- In the area of large structures that will be required to support these large vehicles and power systems, the need for better data on the on the properties of materials will be critical (as it is in many of the areas covered here). Any properties data study must address the environments appropriate to the use of the materials.

- I might also suggest that analytical techniques, computational procedures, may not be adequate for efficiently predicting the statics and dynamics of such large structures.

- Finally, in the area of reliability, optimization of real-time, on-board management of the thermal, power, and stabilizing systems may require more system dynamics capability than we presently have.

I would like to thank the authors for a most interesting group of presentations.

Overall, I have sought to find themes or basic research needs that might be required in general to efficiently deploy a large long-life power system. Many have already been mentioned, e.g., materials properties and development. One particular general area requiring much work is the study of interfacial processes under conditions that are appropriate to the applications. All power systems require extensive contacting of dissimilar materials such as insulators to conductors and coolant fluids to thermally conductive surfaces. A system must maintain a high reliability for a long time (2 - 10 years). This implies that slow interfacial processes can degrade a system in ways that can only be defined by measuring slow overall rates or by accelerating individual chemical or physical processes and applying these data to an appropriate overall model of the gross interfacial process. Understanding how interfaces change or degrade can directly impact corrosion, heat transfer, and other measures of efficiency. I would urge support in this area.

Finally, I would like to comment on what is trying to be accomplished. I think that "enabling technology" really defines an optimum technology that can be foreseen at a certain time. Unfortunately, the driver for this technology is defined need, generally in terms of a defined system requirement. If tens of kilowatts continuous and/or megawatt pulses were required two years from today, we could do it by several old technologies ...and lots of shuttle and Titan launches. This would be unfortunate for the nation because the immediate cost would be enormous and many of the concepts and research requirements that could lead to a more efficient system would be frozen by

the immediate need. Therefore, we must begin now to provide the basic and applied research inputs and to define the engineering design and development concepts that will provide the technology at the required reliability when high power in space is demanded.

C. C. BADCOCK

SPECIAL CONFERENCE ON PRIME-POWER FOR HIGH-ENERGY SPACE SYSTEMS
AUTHOR INDEX

A

Angelo, J. XI 3

B

Badcock, C. C. XI 9
Bangerter, C. D. III 4
Banks, B. A. VII 12
Barthelemy, R. XI 1
Bartine, D. IV 11
Berry, G. X 8
Bickford, K. J. VII 8
Bland, T. V 3
Blankenship, C. P. VII 14
Botts, T. IV 6
Brandhorst, H. W., Jr. VI 1
Britt, E. J. IV 3, VI 9
Brown, R. A. II 2
Bruckner, A. P. X 3
Bryan, H. R. XI 11
Buden, D. IV 1

C

Caveny, L. I 5
Clark, J. II 1
Cohen, M. I 3
Conway, E. J. VI 5
Cooper, M. H. VII 6

D

Dicks, J. B. III 1
Donovan, T. VIII 3

E

Eastman, G. Y. IX 4,5
El-Genk, M. S. IV 8
Elsner, N. B. IV 5
Engle, W. W., Jr. IV 11
English, R. VI 1, XI 7
Ernst, D. M. X 4,5

F

Finke, R. C. VI 10
Fitzpatrick, G. O. IV 3
Fowle, A. A. X 6
Fraas, A. P. IV 2
Freeman, J. W. VI 11,13

G

Gilardi, R. VII 15
Goswami, A. III 8
Graves, R. D. III 8
Guenther, A. H. XI 6
Gupta, R. VII 8

H

Hartke, K. H. I 1
Haslett, R. X 1
Hertzberg, A. X 2
Holt, J. F. VI 4
Huffman, F. IX 2
Hyder, A. K. XI 10

J

Jackson, W. III 6
Jones, O. C., Jr. IV 9
Junker, B. R. XI 8

K

Koester, J. K. III 11
Kruger, C. H. III 11

L

Laghari, J. R. VII 8
Lawless, J. L. IX 3
Layton, J. P. XI 4
Lee, Ja. H. VI 12
Lee, J. H., Jr. IV 7

L

Levy, P. W. VII 7
Lieb, D. IX 2
Loferski, J. J. VI 2,3
Louis, J. F. III 3

M

Massie, L. D. III 5
Mattick, A. T. X 2
Merrill, O. S. IX 4
Milder, F. L. VII 10,11
Miley, G. H. VI 7
Miskolczy, IX 2
Morris, J. F. VII 2
Mullin, J. I 2
Myrabo, L. IV 6

N

Nahemow, M. VII 5
Nakamura, T. III 1

O

Oberly, C. E. II 4

P

Parker, G. H. IV 4, V 1
Peterson, J. V 2
Phillips, B. R. VI 6
Pierce, B. L. IV 4, V 1
Pierson, E. S. III 7
Powell, J. R. IV 6

R

Rabitz, H. VIII 1
Ranken, W. A. IV 10
Reagan, P. IX 2
Rice, R. W. VII 13
Rosenblatt, G. VIII 2
Rossing, B. R. VII 4

S

Sarjeant, W. J. VII 8
Saunders, N. VII 1
Seikel, G. III 10
Severns, J. G. XI 5
Sheldon, F. III 9
Simons, S. VI 11
Smith, J. M. III 2
Spight, C. III 8
Stapfer, G. V 4
Stedman, J. K. II 3
Sundberg, G. VII 9
Swallom, D. III 9

T

Taussig, R. X 2
Teagan, W. P. X 7
Tenney, D. R. VII 14
Thompson, R. E. IV 4,V 1
Thornton, E. A. X 9

V

Vondra, R. XI 2

W

Walbridge, E. W. VI 8
Wood, C. V 4
Woodall, D. IV 8
Woodcock, G. R. I 4

Y

Yang, L. VII 3, IX

Z

Zauderer, B. III 10

ECIAL CONFERENCE ON PRIME-POWER
FOR HIGH-ENERGY SPACE SYSTEMS
Norfolk, VA
22-25 February 1982

Conference Attendees

A. Warren Adam
Sundstrand ATG
4747 Harrison Ave.
Rockford, IL 61101
(815) 226-6419

Ronald J. Adler
Lockheed Palo Alto Research Lab.
3251 Hanover Street
Palo Alto, CA
(415) 493-4411 X5607

Jack Paxton Aldridge
NSP/WAC MS668
Los Alamos National Laboratory
Los Alamos, NM 87545
(505) 667-8719

David W. Almgren
Arthur D. Little, Inc.
20-531 Acorn Park
Cambridge, MA 02140
(617) 864-5770 X5875

Roy C. Alverson
SRI International
1611 N. Kent Street
Arlington, VA 22209
(703) 524-2053

Allen Andrews
Rockwell International

Dayton, OH
(513) 461-4823

Major Joseph Angelo
AFTAC/TAO
Patrick AFB, FL 32925
(305) 494-2531

Joseph G. Asquith
JAYCOR Engineering
21243 Ventura Blvd. Suite 201
Woodland Hills CA 91364
(213) 716-9666

Charles Badcock
The Aerospace Corp.
P.O. Box 92957 MS A6/2657
Los Angeles, CA 90009
(213) 648-5180

Clinton D. Bangerter
STD, P.O. Box 20007
West Valley City, UT 84120
(801) 255-7791

Bruce Banks
NASA Lewis Research Center MS77-4
21000 Brookpark Road
Cleveland, OH 44135
(216) 433-4000 X491

Robert Barthelemy
AFWAL/POOC
Wright-Patterson AFB, OH 45433
(513) 255-6235

David E. Bartine
Oak Ridge National Laboratory
P.O. Box X
Oak Ridge, TN 37830
(615) 574-6100

J. H. Bechtold
3513 Ridgewood
Pittsburgh, PA 15235
(412) 256-3618

Dr. Robert W. Bercaw
NASA Lewis Research Center
21000 Brookpark Road
Cleveland, OH 44135
(216) 433-4000

Baruch Berman D/793, SLTO
Rockwell International SSD
12214 Lakewood Blvd.
Downey, CA 90241
(213) 594-2945

Hugo W. Bertini
Oak Ridge National Lab
P.O. Box Y Bldg. 9108 MS2
Oak Ridge TN 37830
(615) 483-8785

John Biess
TRW Systems
Bldg. M2-2363
Redondo Beach, CA 90278
(213) 536-1950

Timothy J. Bland
Sundstrand Aviation Dept. 777
4747 Harrison Ave.
Rockford, IL 61101
(815) 226-6771

Ernest Blase
R & D Associates
1401 Wilson Blvd.
Arlington, VA 22209
(703) 522-5400

Howard Bloomberg
Beers Associates, Inc.
P.O. Box 2549
Reston, VA 22090
(703) 435-5750

Thomas E. Botts
Brookhaven National Lab - 820 M
Upton, NY 11973
(516) 282-2473

Henry W. Brandhorst, Jr.
NASA Lewis Research Center
MS 302-1
21000 Brookpark Road
Cleveland, OH 44135
(216) 433-4000 X732

Arthur O. Bridgeforth
Jet Propulsion Lab MS 198-220
4800 Oak Grove Drive
Pasadena, CA 91109
(213) 354-5626

Edward J. Britt
Rasor Associates, Inc.
253 Humboldt Court
Sunnyvale, CA 94080
(408) 734-1622

Robert A. Brown
Eagle-Picher Industries
Joplin, MO 64801
(417)623-8000 X330

Adam P. Bruckner
Aerospace Energetics Research Program
University of Washington FL-10
Seattle, WA 98195
(206) 543-6321

Col. H. R. Bryan USAF
AFOSR/NP
Bolling AFB, DC 20332
(202) 767-4904

David Buden
Los Alamos National Lab MS 576
Los Alamos, NM 81545
(505) 667-5540

Cdr. Larry Burgess
NAVELEXSYSCOM, PME106-49
Washington, D. C. 20360
(202) 692-5793

Brian Burrow
Gould Labs.
40 Gould Center
Rolling Meadows, IL 60008
(312) 640-4411

Leonard H. Caveny
AFOSR/NA
Bolling AFB
Washington, D. C. 20332
(202) 767-4937

A. A. Chilenskas
Argonne National Laboratory
Bldg. 205
Argonne, IL 60439
(312) 972-4552

Sang H. Choi
Information Control Systems, Inc.
28 Research Drive
Hampton, VA 23666
(804) 838-9371

Capt. Jerry Clark
AFWAL/POOS-2
Wright-Patterson AFB, OH 45433
(513) 255-2923

Robert W. Clark
Naval Research Lab
Code 4720
Washington, D. C. 20375
(202) 767-3494

M. E. Cohen
Aerospace Corp.
2350 E. El Segundo Blvd.
El Segundo, CA 90009
(213) 615-4485

William Condit
Westinghouse R & D
1310 Beulah Road
Pittsburgh, PA 15235
(412) 256-7717

Edmund J. Conway
NASA Langley Research Center
MS160 Space Technology Br.
Hampton, VA
(804) 827-3781

Martin H. Cooper
Westinghouse Electric Corp.
Advanced Reactors Div.
P.O. Box 158
Madison, PA 15663
(412) 722-5564

Dr. James Cox
Physics Dept.
Old Dominion University
Norfolk, VA 23508
(804) 440-4613

Oakley H. Crawford
F20, Bldg. 4500N
Oak Ridge National Laboratory
Oak Ridge, TN 37830
(615) 482-7427

Robert Davidson
R & D Associates
1401 Wilson Blvd.
Arlington, VA 22209
(703) 522-5400

Dr. Robert DeWitt
Naval Surface Weapons Center
Code F-12
Dahlgren, VA 22448
(703) 663-8026

John B. Dicks
Applied Energetics
P.O. Box 702
Tullahoma, TN 37388
(619) 455-1629

Norbert Elsner
General Atomic
Box 81608
San Diego, CA 92138
(714) 455-2892

Dr. Raymond C. Elton
Code 6505
Naval Research Lab
Washington, D. C. 20375
(202) 767-2754

Robert English
NASA Lewis Research Center
MS-500-125
21000 Brookpark Road
Cleveland, OH 44135
(216) 433-4000 X6949

Robert A. Englund
Martin Marietta Aerospace
P.O. Box 179
Denver, CO 80201
(303) 977-3908

Donald M. Ernst
Thermacore Inc.
780 Eden Road
Lancaster, PA 17601
(717) 569-6551

G. H. Farbman
Westinghouse Electric
P.O. Box 10864
Pittsburgh, PA 15236
(412) 892-5600 X6292

Robert C. Finke
NASA Lewis Research Center
21000 Brookpark Road
Cleveland, OH 44135
(216) 433-4000 X5232

George P. Fisher
R & D Associates
Box 9695
Marina Del Rey, CA 90291
(213) 822-1715

Gary O. Fitzpatrick
Rasor Associates, Inc.
253 Humboldt Court
Sunnyvale, CA 94086
(408) 734-1622

Arthur A. Fowle
Arthur D. Little, Inc.
20 Acorn Park
Cambridge, MA 02140
(617) 864-5770 X3079

Arthur P. Fraas
Bldg. 9103, Y-12
Oak Ridge, TN 37830
(615) 574-2005

John W. Freeman
Rice University
P.O. Box 1892
Houston, TX 77251
(713) 527-8101 X3524

Richard Gilardi
Naval Research Laboratory
Code 6030
Washington, D. C. 20375
(202) 767-2624

Brendan B. Godfrey
Mission Research Corp.
1400 San Mateo Blvd. S.E. Suite A
Albuquerque, NM 87108
(505) 265-8306

Amit Goswami
AMAF Industries
P.O. Box 1100
Columbia, MD 21044
(301) 995-1919

Dr. Arthur H. Guenther
Chief Scientist
AF Weapons Lab/CA
Kirtland AFB, NM 87117
(505) 844-9856

Major R. L. Gullickson
Defense Nuclear Agency
RAEV
Washington, D. C. 20305
(202) 325-7026

Gregory A. Hagopian
Hughes Aircraft
MS - Bldg. 6-C137
Culver City, CA 90230
(213) 371-0911 X7216

Kwang S. Han
Hampton Institute
Dept. of Physics & Engineering
Hampton, VA 23668
(804) 727-5336

John L. Harrison
Maxwell Laboratories, Inc.
9244 Balboa Ave.
San Diego, CA 92123
(714) 279-5100

Robin Harvey
Hughes Research Labs
3011 Malibu Canyon Road
Malibu, CA 90265
(213) 456-6411

Robert A. Haslett
MS B09-25
Grumman Aerospace Corp.
Bethpage, NY 11714
(516) 575-3924

Dick Henry
Gould Inc.
40 Gould Center
Rolling Meadows, IL 60008
(314) 640-4507

Dr. A. Hertzberg
University of Washington
FL-10
Seattle, WA 98195
(206) 543-6321

James F. Holt
AFWAL/POOC
Wright-Patterson AFB, OH 45433
(513) 255-6235

Capt. N. A. Howard
Office of Naval Research
800 N. Quincy Street
Arlington, VA 22217
(703) 696-4224

Fred Huffman
Thermo Electron
85 First Ave.
Waltham, MA 02254
(617) 890-8700

Robert O. Hutchinson
AFGL/PHK
Hanscom AFB, MA 01731
(617) 861-2933

LTC Anthony Hyder
AFOSR/NP
Bolling AFB
Washington, D. C. 20332
(202) 767-4908

Jay Hyman
Hughes Research Labs
3011 Malibu Canyon Road
Malibu, CA 90265
(213) 456-6411

William D. Jackson
Energy Consultants, Inc.
3509 McKinley Street NW
Washington, D. C. 20015
(202) 686-9141

Prof. Owen C. Jones, Jr.
Rensselaer Polytechnic Institute
Dept. of Nuclear Eng. - NES Bldg.
Troy, NY 12181
(518) 270-6406

Dr. B. R. Junker
Office of Naval Research Code 412
800 N. Quincy Street
Arlington, VA 22217
(202) 696-4219

Gregory F. Knapp (student)
Old Dominion University
Norfolk, VA 23508
(804) 440-3099

Karl Knapp
Astro Research Corp.
6390 Cinoy Lane
Carpinteria, CA 93103
(805) 684-6641

Dr. J. K. Koester
Dept. of Mech. Engineering
Stanford University, CA 94305
(415) 497-1745

Dr. Jerrold Kronenfeld
c/o TASC
One Jacob Way
Reading, MA 01867
(617) 944-6850

S. H. Lam
D-302C Engineering Quad
Princeton University
Princeton, NJ 08544
(609) 924-2191

Alan R. LaRose
Lockheed Missile Space Center
P.O. Box 504
Sunnyvale, CA 94086
(408) 742-9023

Dr. John L. Lawless
Scaife Hall
Carnegie-Mellon University
Pittsburgh, PA 15213
(412) 578-3641

J. Preston Layton
60 Penn-Lyle Road
Princeton Junction, NJ 08550
(609) 799-3094

Ja H. Lee
MS 160
NASA Langley Research Center
Hampton, VA 23665
(804) 827-3781

LTC James Lee
Air Force Weapons Lab
NTE Bldg. 413
Kirtland AFB, NM 87117
(505) 844-0482

Paul W. Levy
Physics Dept.
Brookhaven National Lab
Upton NY 11793
(516) 282-3820

K. S. Ling
Applied Solar Energy Corp.
15251 E. Dow Julian Road
City of Industry, CA 91746
(213) 968-6581

Prof. J. J. Loferski
Div. of Engineering
Brown University
Providence, RI 02412
(401) 863-2640

Prof. J. F. Louis
Bldg. 21-254
Mass. Institute of Technology
Cambridge, MA 02139
(617) 253-1760

Lawrence H. Luessen
Naval Surface Weapons Center
Code F12
Dahlgren, VA 22448
(703) 663-8057

Charles A. Lurio
MIT Rm 33-407
Cambridge, MA 02139
(617) 253-2298

Lahmer Lynds
UTRC
Silver Lane
E. Hartford, CT
(203) 727-7134

Tom Mahefkey
A. F. Wright Aeronautical Labs
AFWAL/POOC
Wright-Patterson AFB, OH 45433
(513) 255-6235

Lynn Marcoux
Hughes Aircraft Bldg. S12 MS V330
P.O. Box 92919 Los Angeles, CA 90009
(213) 615-7220

Prof. Martinez-Sanchez
MIT Rm 37-371
Cambridge, MA 02139
(617) 253-5613

James H. Masson
Martin Marietta Denver Aerospace
P.O. Box 179 Mail #S0550
Denver, CO 80201
(303) 977-4987

Arthur T. Mattick
University of Washington
FL-10
Seattle, WA 98195
(206) 543-6181

Craig D. Maxwell
STD Research Corp.
P.O. Box "C"
Arcadia, CA 91006
(213) 357-2311

Owen S. Merrill
U. S. Dept. of Energy
FE-25 GTN
Washington, D. C. 20545
(301) 353-2816

Fred Milder
Spire Corp.
Patriots Park
Bedford, MA 01730
(617) 275-6000

Frank A. Paparozzi
ANSER
400 Army Navy Dr.
Arlington, VA 22202
(703) 979-0700

G. H. Parker
Westinghouse Electric
Box 10864
Pittsburgh, PA 15236
(412) 892-5600

Nino R. Pereira
Maxwell Labs
8835 Balboa
San Diego, CA 92123
(714) 279-5100

Roy Pettis
Central Intelligence Agency
Washington, D. C. 20505
(703) 351-6846

Dr. Bert Phillips
NASA Lewis Research Center
21000 Brookpark Road
Cleveland, OH 44135
(216) 433-4000

Edward S. Pierson
Argonne National Laboratory
Argonne, IL 60439
(312) 972-5966

A. W. Possner
Westinghouse R & D
1310 Beulah Road
Pittsburgh, PA 15235
(412) 256-3552

James R. Powell
Bldg. 820M
Dept. of Nuclear Energy
Brookhaven National Laboratory
Upton, NY 11973
(516) 282-2440

Mark S. Pronko (student)
Old Dominion University
Norfolk, VA
(804) 440-3099

Neil Puester
Yardney Electric Corp.
82 Mechanic Street
Pawcatuck, CT 02894
(203) 599-1100

Henry Pugh
Dept. of Physics
USAF Academy
USAF Academy, CO 80840
(303) 472-2487

Herschel Rabitz
Princeton University
Dept. of Chemistry
Princeton, NJ 08544
(609) 452-3917

Will Ranken
Los Alamos National Lab
Los Alamos, NM 87544
(505) 667-6578

Bob Reinovsky
AFWL/NTYP
Kirtland AFB, NM 87117
(505) 844-1851

Roy W. Rice
Code 6360
U. S. Naval Research Lab
(202) 767-2131

P. A. Rios
General Electric Co.
P.O. Box 43, Rm 37-363
Schectady, NY 12309
(518) 385-2832

Dr. A. S. Roberts, Jr.
Dept. of Mech. Engineering
Old Dominion University
Norfolk, VA 23508
(804) 440-3720

George H. Miley
214 NEL
University of Illinois
103 S. Goodwin Ave.
Urbana, IL 61801
(217) 333-2294

Dennis F. Miller
National Research Council
Energy Engineering Board
2101 Constitution Ave. NW
Washington, D. C. 20418
(202) 334-3344

Dr. Marshall Molen
Dept. of Elec. Engineering
Old Dominion University
Norfolk, VA 23508
(804) 440-3750

R. E. Morgan
Westinghouse Advanced Reactors Div.
P.O. Box 158
Madison, PA 15663
(412) 722-5508

James F. Morris
Mech. & Energy Sys. Engineering
Arizona State University
Tempe, AZ 85281
(602) 965-4048

Ted S. Mroz
NASA Lewis Research Center
21000 Brookpark Road
Cleveland, OH 44130
(216) 433-4000 X6861

Vernon C. Mueller
McDonnell Douglas Astronautics Co.
P.O. Box 516 Bldg. 106 MS 38
St. Louis, MO 63166
(314) 233-8068

Jerome P. Mullin
NASA Headquarters
Code RTS-6
Washington, D. C. 20546
(202) 755-3278

Leik N. Myrabo
BDM Corp.
7915 Jones Branch Drive
McLean, VA 22102
(703) 821-5000

Martin Nahemow
Westinghouse R & D Center
Pittsburgh, PA 15235
(442) 621-3474

T. Nakamura
Dept. of Mech. Engineering
Stanford University
Stanford, CA 94305
(415) 497-1745

Robert A. Nuttelman
Kaman Sciences Corp.
P.O. Box 7463
Colorado Springs, CO 80933
(303) 599-1945

Charles Oberly
AFWAL/POOS
Wright-Patterson AFB
Dayton, OH 45433
(513) 255-2923

Peter Oettinger
Thermo Electron Corp.
85 First Ave.
Waltham, MA 02154
(617) 890-8700

Ed O'Hair
Texas Tech University
Electrical Eng. Dept.
Lubbock, TX 79409
(806) 742-3441

G. D. O'Kelley
Oak Ridge National Lab.
P.O. Box X
Oak Ridge, TN 37830
(615) 574-5008

Dr. Randall B. Olsen
Chronos Research Labs.
3025 Via De Caballo
Olivenhain, CA 92024
(714) 756-4733

Dr. G. L. Rogoff
Westinghouse R & D Center
1310 Beulah Road
Pittsburgh, PA 15235
(412) 243-5320

M. Frank Rose
NSWC/DL
Code F-04
Dahlgren, VA 22448
(703) 663-8026

Gerd M. Rosenblatt MS-756
Los Alamos National Laboratory
Los Alamos, NM 87545
(505) 666-8270

Barry Rossing
Westinghouse R & D Center
2025 Beulah Road
Pittsburgh, PA 15235
(412) 731-4414

W. J. Sarjeant
4232 Ridge Lea Road
Dept. of Elec. Engineering
State University of NY at Buffalo
Amherst, NY 14226
(716) 831-3164

Neal T. Saunders
NASA-Lewis Research Center
21000 Brookpark Road
Cleveland, OH 44135
(216) 433-4000 X5594

1st Lt. Michael K. Seaton
AFWL/NTEDP
Kirtland AFB, NM 87117
(505) 844-9641

Dick Sederquist
United Technologies
P.O. Box 109
South Windsor, CT 06074
(203) 727-2377

George R. Seikel
SeiTec
P.O. Box 81264
Cleveland, OH 44181
(216) 779-1190

Steven W. Seiler
R & D Associates'
Washington Research Lab
301 A South West Street
Alexandria, VA 22314
(703) 684-0333

William R. Seng
Thermo Electron Corp.
1735 I Street NW Rm 807
Washington, D. C. 20006
(202) 861-0510

James G. Severns
Naval Research Laboratory Code 7710
4555 Overlook Ave.
Washington, D. C. 20375
(202) 767-2635

Fred Sheldon
Avco Everett Research Lab
Revere
Everett MA 02149
(617) 389-3000

Sidney W. Silverman
Boeing Aerospace Co. MS 8C-62
P.O. Box 3999
Seattle, WA 98124

Marshall M. Sluyter
U. S. Dept. of Energy
Div. of MHD FE-26
Germantown, MD 20545
(301) 353-5937

John M. Smith
NASA-Lewis Research Center
MS 500/203
21000 Brookpark Road
Cleveland, OH 44135
(216) 433-4000

Tom Smolinski
General Electric Co. R & D Ctr.
One River Road
Schenectady, NY 12345
(518) 385-7873

Dan G. Soltis
NASA-Lewis Research Center
21000 Brookpark Road
Cleveland, OH 44135
(216) 433-4000

Ronald J. Sovie
NASA Lewis Research Center
21000 Brookpark Road
Cleveland, OH 44135
(216) 433-4000 X5189

Charles G. Spoerer, Jr.
Westinghouse R & D Site
1310 Beulah Road
Pittsburgh, PA 15235
(412) 256-3398

G. Stapfer
Jet Propulsion Lab
4800 Oak Grove Dr.
Pasadena, CA 91103
(213) 354-3922

Dick Statler
Naval Research Laboratory Code 6612
Washington, D. C. 20375
(202) 767-2446

J. K. Stedman
United Technologies Corp.
P.O. Box 109
South Windsor, CT 06074
(203) 727-2211

Dave Straw
AFWL/NTYP
Kirtland AFB, NM 87117
(505) 844-0121

William C. Stwalley
Iowa Laser Facility
University of Iowa
Iowa City, IA 52242
(319) 353-7081

Gale R. Sundberg
NASA-Lewis Research Center
21000 Brookpark Road MS 77-4
Cleveland, OH 44138
(216) 433-4000

Daniel W. Swallom
Avco Everett Research Lab
2385 Revere Beach Parkway
Everett, MA 02149
(617) 389-3000 X384

Robert Taussig
Math Sciences Northwest, Inc.
2755 Northup Way
Bellevue, WA 98004
(206) 827-0460

William R. Terrill
General Electric Co.
GE/AEPD
P.O. Box 527
King of Prussia, PA 19406
(215) 962-4213

J. E. Thompson
College of Engineering
University of South Carolina
Columbia, S. C. 29208
(803) 777-7304

Earl A. Thornton
Mech. Engineering Dept.
Old Dominion University
Norfolk, VA 23508
(804) 440-3735

Peter J. Turchi
R & D Associates
1401 Wilson Blvd.
Arlington, VA 22209
(703) 522-5400

R. P. Turcotte
Battelle, Northwest Div.
P.O. Box 999
Richland, WA 99352
(509) 375-2482

Linda Vahala (student)
Old Dominion University
Norfolk, VA 23508
(804) 440-3000 X4621

A. R. Valentino
Argonne National Laboratory
9700 S. Cass Ave. Bldg. 362
Argonne, IL 60439
(312) 972-5557

David A. Vance
Lockheed Missiles & Space Co.
3251 Hanover Street
Palo Alto, CA 94304
(415) 493-4411

Ihor M. Vitkovitsky
Naval Research Laboratory
Washington, D. C. 20375
(202) 767-2724

Dr. Robert Vondra
AFRPL/OKDH Stop 24
Edwards AFB, CA 93523
(805) 277-5540

C. W. Von Rosenberg, Jr.
Avco Everett Research Lab
2385 Revere Beach Parkway
Everett, MA 02149
(617) 389-3000

Ed Walbridge
Argonne National Laboratory
9700 S. Cass Ave. EES-12
Argonne, IL 60439
(312) 972-3262

Terry C. Wallace
Los Alamos National Laboratory
CMB-3 MS-348
Los Alamos NM 87545
(505) 667-6074

Capt. Steven G. Wax
A. F. Office of Scientific Research
Bolling AFB, DC 20332
(202) 767-4931

Kenneth Whitney
Naval Research Laboratory
Code 6509
Washington, D. C. 20375
(202) 767-2326

H. E. Wilhelm
Physics Div., Code 3814
Naval Weapons Center
China Lake, CA 93555
(714) 939-2857

Charles Wood
Jet Propulsion Lab
9800 Oak Grove Drive
Pasadena, CA 91103
(213) 354-4036

David Woodall
Dept. of Chemical & Nuclear Eng.
University of New Mexico
Albuquerque, NM 87131
(505) 277-5431

Gordon R. Woodcock
Boeing Aerospace Co. MS 8F-03
P.O. Box 3999
Seattle, WA 98124
(206) 773-7984

Paul W. Wren
Sundstrand Corp.
4747 Harrison Blvd.
Rockford, IL 61101
(815) 226-6138

LCDR William E. Wright
DARPA/DEO
1400 Wilson Blvd.
Arlington, VA 22209
(202) 694-1703

Ling Yang
General Atomic Co.
P.O. Box 81603
San Diego, CA 92138
(714) 455-2920

James S. Zimmerman
General Electric
P.O. Box 8661
Philadelphia, PA 19101
(215) 962-2350